Identification, analysis and formulation of natural bio-organic molecules enhanced by nanoparticles for the potential treatment of amyloid disease

Thesis submitted in fulfilment of the requirements for the degree of

Doctor of Philosophy

Department of Chemistry

Lancaster University

By

Bakri Hussain Alaziqi

September 2024

Abstract

Identification, analysis and formulation of natural bio-organic molecules enhanced by nanoparticles for the potential treatment of amyloid disease

By Bakri Alaziqi for the degree of Doctor of Philosophy. September 2024.

The apparent health benefits of a Mediterranean diet have been attributed to the consumption of unprocessed extra virgin olive oil (EVOO), which contains a high content of polyphenols having antioxidant and anti-inflammatory properties. Phenolic compounds from a range of dietary sources have also been found to reduce the rate of protein self-assembly into amyloid fibrils associated with Alzheimer's disease (AD) and other protein misfolding disorders.

Amyloid fibrils are nanoscale fibrous structures formed by the self-assembly of certain proteins into repeating arrays of β-strands stabilized by intermolecular hydrogen bonds. Amyloid is associated with over 30 human diseases and can occur systemically or in localized areas such as around the brain as observed in Alzheimer's disease. AD is associated with the assembly of amyloid-β (Aβ) peptides into β-sheet rich amyloid fibrils and the aggregation of microtubule-associated protein tau into neurofibrillary tangles in the brain. There is a clinical need to find a cure for the disease, or a treatment option which improves the quality of life for patients with Alzheimer's disease. The phenolic compounds oleuropein and oleocanthal from extra virgin olive oil (EVOO) have previously been shown to individually reduce the accumulation of amyloid fibrils associated with Alzheimer's disease (AD), either by inhibiting amyloid formation (oleuropein) or by promoting amyloid clearance (oleocanthal). EVOO contains many other compounds, but as to date, no such evaluation of EVOO phenol mixtures when isolated from the fatty acid component of olive oil has been reported. This thesis aims to examine mixed and individual polyphenols isolated from olive oil and explore their ability to modulate amyloid formation by Aβ and tau.

Chapter 1 focuses on the current literature around natural phenolic compounds derived from EVOO. Also, this chapter discusses the literature around amyloid diseases with a particular focus on Alzheimer's disease including its pathologies and overview of pharmacological and non-pharmacological treatment approaches of AD. **Chapter 2** discusses the main techniques used for analysis and characterisation of polyphenols found in natural products. Also, this chapter illustrates techniques used for investigation and analysis of amyloid β (proteins). **Chapter 3** shows preparation and implementation of a methodology for the expression, purification and characterisation of labelled (^{15}N) and unlabelled, amyloid proteins. **In Chapter 4**, different methods of extraction of phenols from EVOO are evaluated to optimise the yield and range of phenols obtained in the extracted mixture. Mixtures are extracted from Greek and Saudi Arabian EVOO and analysed in detail using chromatographic and magnetic resonance methods. Over 30 different compounds are identified, several of which are quantified and shown to be present in different concentrations in the two EVOO extracts. **Chapter 5** describes a range of methods that are used to test the effects of the phenolic mixtures *in vitro* on the aggregation of the 40-amino acid Aβ40 peptide and a repeat-domain fragment of tau. Thioflavin T fluorescence and circular dichroism measurements show that the Greek extract reduces the rate of tau aggregation only at very high phenolic concentrations (> 100 μg/mL). By comparison, Greek and Saudi extracts exert similar effects on Aβ40 aggregation at much lower concentrations (< 20 μg/mL). Transmission electron microscopy (TEM) indicates that the extracts reduce fibril deposition of Aβ40 after the end-point of aggregation is reached. An HPLC procedure combined with TEM, dynamic light scattering, and solid-state NMR reveals that most compounds in the extracts bind to pre-formed Aβ40 fibrils, which generates soluble Aβ oligomers that are mildly toxic to SH-SY5Y cells. Much higher (500 μg/mL) extract concentrations are required to remodel tau filaments into oligomers and no binding of phenolic compounds to the pre-formed filaments is observed. It is concluded

that the entire phenolic profiles of different EVOO samples are similarly capable of modulating Aβ40 aggregation and fibril morphology *in vitro* at relatively low concentrations but are much less efficient at modulating tau aggregation.

Chapter 6 describes the synthesis and characterization of solid lipid nanoparticles (SLNs) with the aim of enhancing the *in vivo* delivery of polyphenol mixtures in the treatment of amyloid diseases and other pathologies. The method was used to successfully prepare SLNs having a homogeneous size distribution and a high efficiency of polyphenol encapsulation from the mixtures prepared in Chapter 4. Animal experiments are being investigated in future work to increase absorption, bioavailability, and circulation times of EVOO polyphenols *in vivo*.

It is estimated that around 3 M tonnes of olive oil are consumed worldwide annually. The results described in this thesis have increased understanding of the potentially neuroprotective benefits of EVOO consumed in the Mediterranean diet and laid the foundations for future *in vivo* applications of EVOO polyphenol mixtures for disease testing.

Declaration

This thesis has not been submitted in support of an application for another degree at this or any other university. It is the result of my own work and includes nothing that is the outcome of work done in collaboration except where specifically indicated. Many of the ideas in this thesis were the product of discussion with my supervisor Professor. David Middleton.

Excerpts of this thesis have been published in the following conference manuscripts and academic publications:

- Alaziqi, B., Beckitt, L., Townsend, D.J., Morgan, J., Price, R., Maerivoet, A., Madine, J., Rochester, D., Akien, G. and Middleton, D.A., 2024. Characterization of Olive Oil Phenolic Extracts and Their Effects on the Aggregation of the Alzheimer's Amyloid-β Peptide and Tau. ACS omega, 9(30), pp.32557-32578.

- Bakri Alaziqi, David Townsend and David Middleton, 14th World Congress on Polyphenols Applications – September 22 - 24, 2021. Phenolic acid compounds derived from olive oil as potential therapeutic agents against Alzheimer disease.

- Formulation of solid lipid nanoparticles for the delivery and improved bioavailability of phenolic mixtures. (Manuscript in preparation - Chapter 6)

- Effects of formulated polyphenolic mixtures and their metabolites in rat tissues. (Manuscript in preparation - Chapter 6)

Bakri Alaziqi

Lancaster University, UK

Acknowledgements

First of all, I would like to extend my sincere gratitude and deep respect to my academic supervisor, Professor. David Middleton, for his intellectual guidance and support throughout my doctoral research. I am also very grateful to all the current members in Middleton's group. Special thanks should go to Dr David Townsend and Dr Sophie Lau who provided me with a great deal of instructive advice and useful suggestions throughout the project. I also would like to thank all the staff in the School of Chemistry and School of Biomedical and Life Sciences. Special thanks should go to people in the analysis rooms for their help and support with HPLC, LC-MS, NMR and MS *etc*.

I also would like to thank the government of Saudi Arabia and Umm al-Qura University for providing this scholarship with financial support during my studies at Lancaster University.

I also owe my thanks to my father who passed away before this moment, who gave me the strength to keep going, special thanks should go to my mother for her support and blessings. I also would like to thank all my family members, brothers, sisters and all my friends, who have been a huge support to me throughout the doctoral journey.

Table of Contents

Abstract ..... **II**

Chapter 1 (Introduction) **1**

The Mediterranean diet 1

Extra virgin olive oil 2

Polyphenolic compounds in extra virgin olive oil 3

Structure and classification of polyphenols in olive oil 3

Alzheimer's disease 10

Pathogenesis of Alzheimer's Disease 16

Amyloid-β-related pathologies 16

Tau-related pathologies 22

Interaction between amyloid-β- and tau-related pathologies 24

Treatment of Alzheimer's disease 27

Overview of pharmacological and non-pharmacological treatment approaches 27

Antioxidant effect of natural polyphenols and disease 29

Inhibitors of amyloidosis 32

Natural phenolic molecules as inhibitors of amyloidosis 36

Polyphenols from EVOO as potential therapy for Alzheimer's disease 41

Oleocanthal 41

Oleuropein aglycone 43

Hydroxytyrosol and tyrosol 44

Aims of the research 47

Chapter 2 (Experimental Techniques for Analysis) **49**

Overview 49

Chromatography to analyse natural products 49

High-performance liquid chromatography (HPLC) for analysing polyphenols 49

Applications of HPLC in the field of natural products 51

Liquid chromatography-mass spectrometry (LC-MS) for analysing polyphenols 53

Applications of the LC-MS in the field of natural products 56

Nuclear Magnetic Resonance Spectroscopy (NMR) for characterising polyphenols 59

Transmission electron microscopy (TEM) for visualising amyloid fibrils 63

Applications of transmission electron microscopy for visualising amyloid 66

Analysis of amyloid aggregation kinetics using thioflavin T fluorescence 67

Applications of thioflavin T for studying amyloid aggregation 68

Circular Dichroism Spectroscopy (CD) for analysing secondary structures of amyloid 70
Applications of circular dichroism for studying secondary structures of amyloid 71
Chapter 3 (Expression and characterization of proteins) 73
Introduction 73
Expression and characterization of labelled and unlabelled amyloid beta (Aβ40) 73
Tau protein 75
Aims 75
Materials and methods 76
Materials 76
Methods 77
Omit transformation – the MAβ40 vector in *E. coli* strain BL21 cells 77
Preparation of small cultures 78
Protein expression of large cultures 78
Purification of Beta-Amyloid Peptide (MAβ40) - Part 1 78
Sonication and isolation of inclusion bodies 78
DEAE-cellulose purification 79
Gel electrophoresis preparation 80
SDS-PAGE gel electrophoresis and sample runs 81
Purification of Beta-Amyloid Peptide - Part 2 82
Size Exclusion Chromatography (SEC) 82
Determining Protein Concentration 83
Expression of ^{15}N-labelled MAβ40 83
Analysis of mass spectrometer for amyloid beta 84
Mass spectrometry determined amyloid beta protein composition 84
Method of Mass determination 84
Evaluation of aggregation using thioflavin T binding 85
Transmission electron microscopy (TEM) 86
Results 86
Expression of amyloid beta 86
Purification of amyloid beta using size exclusion chromatography (SEC) 88
Amyloid beta identification by mass spectroscopy 91
Yield and reproducibility of MAβ40 expression 92
Analysis of MAβ40 aggregation 92
Transmission electron microscopy of amyloid beta 94
labelled MAβ40 (^{15}N) expression, purification and characterisation 95
Expression of labelled MAβ40 95

Purification of ^{15}N Labelled MAβ40 by SEC 97
Labelled MAβ40 (^{15}N) identification by mass spectroscopy 99
^{15}N labelled MAβ40 expression yield, the number of expressions and yield obtained 101
Discussion 101
Chapter 4 (Extraction and characterization of phenolic compounds from natural olive oil products) 103
Introduction 103
Aims 110
Materials and methods 111
Materials 111
Polyphenol standard solutions 111
Natural olive oil products collection 112
Methods 112
Extraction of polyphenols from extra virgin olive oil using different techniques 112
Extraction of polyphenols from olive oil using solid phase extraction SPE technique 113
Extraction of polyphenols from olive oil using the centrifugation technique 114
Extraction of polyphenols from olive oil using the funnel separation technique 115
Chromatography 117
High-performance liquid chromatography analysis 117
Liquid chromatography–mass spectrometry analysis 117
UV-Vis Spectrophotometer analysis 118
Solution state nuclear magnetic resonance analysis 118
Results 119
Comparison of isolation methods of phenolic compounds from EVOO using LLE and SPE .. 119
Isolation and identification of phenolic compounds from different olive oil sources 124
Isolation of polyphenols 124
UV-Visible absorption spectra of the phenolic extracts 124
Chromatographic analysis 125
Identification and characterisation of polyphenols from both sources using LC-MS 125
Identification and quantification of polyphenols from both sources using HPLC 131
Analysis of polyphenolic compounds from EVOO using solution-state ^{1}H NMR 141
Discussion 147
Chapter 5 (Investigation of the effects of mixed and individual phenolic compounds derived from EVOO on the aggregation of amyloid-β and tau peptides *in vitro*) 152
Introduction 152
Aims 156

Materials and methods 157
Materials 157
Methods 157
Proteins expression 157
Amyloid beta Aβ40 labelled and unlabelled proteins 157
Tau protein 157
Polyphenols 158
Thioflavin T fluorescence assay 158
Circular Dichroism Spectroscopy Analysis 158
Transmission Electron Microscopy Analysis 159
EVOO Extract and individual polyphenol Binding to Protein Aggregates Analysis 159
HPLC Chromatography for Binding Analysis 162
Solid-State NMR for Binding Analysis 162
Cell Viability Assay 163
Dynamic Light Scattering Analysis 163
Computational Molecular Docking Analysis 164
Results 164
EVOO Phenolic Compounds 164
The Effect of EVOO Phenolic Extracts on Aβ40 and Tau Aggregation Kinetics by thioflavin T 164
The Effect of EVOO Phenolic Extracts on Aβ40 Aggregation Kinetics by circular dichroism 169
The Effect of EVOO Phenolic Extracts on Aβ40 and Tau Aggregate Morphologies 171
Summary of the effects of polyphenol extracts on Aβ40 and tau aggregation 174
Effect of EVOO Phenolic Extracts on the size and morphology of pre-formed Aβ40 Aggregates 175
Cellular toxicity of soluble Aβ40 oligomers 181
Binding Investigation of EVOO Compounds to Aβ40 Fibrils 183
Binding Investigation of EVOO Compounds to tau filaments 188
Investigate the Effect of Selected EVOO Polyphenolic Molecules on Aβ40 and Tau Aggregation Kinetics 189
Molecular docking of compounds to fibrillar species 197
Discussion 202
EVOO polyphenol mixtures inhibit Aβ40 aggregation more strongly than tau aggregation 202
Binding of EVOO polyphenols to Aβ40 and tau 203
Mechanisms of inhibition 204
Limitations of the results 204

Chapter 6 (Formulation of solid lipid nanoparticles for the delivery and improved bioavailability of phenolic mixtures extracted from extra virgin natural olive oil) 206
Introduction.....206
Aims and motivation.....212
Materials and methods.....214
Materials.....214
Reagents and equipment.....214
Methods.....215
Polyphenol preparation.....215
Preparation of SLNs loaded with EVOO polyphenol mixtures.....215
Preparation of caffeic acid-SLNs.....216
Preparation of unloaded SLNs.....216
Physicochemical characterization of the prepared SLNs.....218
Solid-state NMR.....218
Transmission Electron Microscopy (TEM) Observations.....220
Dynamic Light Scattering (DLS) measurements.....220
HPLC measurement of entrapment efficiency.....220
EE% measurements with UV-Vis spectrophotometry and liquid-state NMR analysis.....222
Preparation of fluorescence-labelled SLNs for animal experiments.....223
Results.....224
Formulation of caffeic and phenolic mixture-SLNs.....224
Morphological features of the synthesized polyphenol and caffeic acid SLNs.....227
Principle of measurements of entrapment efficiency EE%.....229
Measurement by UV-Vis spectrophotometry.....230
Measurement by HPLC.....232
Characterization of SLNs by solid-state NMR.....234
Measurement of fluorescence in labelled and unlabelled SLNs for animal experiments.....235
Stability of nanoparticles after storage for 8 months.....237
Discussion.....239
Chapter 7 (General discussion and future work) 242
Alzheimer's disease and natural olive oil products.....242
Protein expression.....244
Extraction of phenolic compounds from olive oil products.....245
Investigation of the effects of polyphenol mixtures and individual compounds on Aβ and tau.....247
Nanoparticles formulation.....249
Work in progress.....250

Chapter 8 (References) **252**
Appendix 1 ..... **282**
Appendix 2 ..... **324**
Appendix 3 ..... **333**

List of Figures

Chapter 1

Figure 1.1. Chemical structures of oleuropein, ligstroside and demethyloleuropein phenolic compounds 5
Figure 1.2. Mechanism of the hydrolysis of secoiridoids in olive oil to produce phenolic alcohols 6
Figure 1.3. Chemical structures of tyrosol, hydroxytyrosol and oleocanthal are the main phenolic alcohols in olive oil products. 7
Figure 1.4. Chemical structures of luteolin and apigenin phenolic compounds can be found in olive oil. 7
Figure 1.5. Chemical structures of the most common lignans in EVOO (+)-pinoresinol and (+)-1-acetoxypinoresinol compounds. 8
Figure 1.6. Chemical structures of phenolic acids compounds classified into hydroxybenzoic acid derivatives (A, top) and hydroxycinnamic acid derivatives (B, bottom) can be found in olive oil products 9
Figure 1.7. Chemical structures of hydroxyisochroman compounds in olive oil (left) 1-phenyl-6,7-dihydroxy-isochroman and (right) 1-(3′-methoxy-4′ -hydroxy)-6,7-dihydroxy-isochroman. 10
Figure 1.8. Progression of Alzheimer's brain from diagnosis to advanced stages. (top and bottom) brain structures of typical or healthy brains and brain structures of Alzheimer brains in the mild and advanced stages.. 12
Figure 1.9. Comparison of normal and AD brains associated with the two main pathologies. (a) Normal brain (b) Characterization of Alzheimer disease by the two main pathologies amyloid-β-containing plaques and tau-related pathologies 14
Figure 1.10. Amyloid aggregation kinetics starting from unstructured monomers to end with saturation phase. 18
Figure 1.11. Schematic diagram depicting the structure of amyloid fibre diffraction pattern and the cross-beta steric zipper 19
Figure 1.12. Interactions between Aβ and tau in neuronal pathologies. (a) Aβ causes tau hyperphosphorylation, which leads to toxicity in neurons. (b) Tau mediates Aβ toxicity. (c) Both Aβ and tau exert toxicity by targeting cellular components such as mitochondria 25
Figure 1.13. Chemical structures of available drugs for Alzheimer's disease. (Donepezil, galantamine, rivastigmine and memantine) 28
Figure 1.14. Compound groups known to inhibit tau aggregation: (1) N-phenylamines, (2) 9,10-anthraquinones, (3) phenylthiazolylhydrazides and (4) thioxothiazolidinones 33
Figure 1.15. Scyllo-inositol and derivatives: (A) scyllo-inositol, (B) 1-4-dideoxy-scyllo-inositol, and (C) 1,4,di-O-methyl-scyllo-inositol 35
Figure 1.16. Chemical structures of dopamine (1-left) and levodopa (2-right) 35
Figure 1.17. The mechanism and different pathways of polyphenols to inhibit amyloid formation. Pathways of polyphenols (top left) prevention of native proteins, (top middle) inhibition of amyloidogenic proteins and (top right) disruption of fibrils 38

Figure 1.18. Chemical structures of natural polyphenol compounds that exhibit anti-amyloidogenic activity. 40
Figure 1.19. Chemical structure of oleocanthal 41
Figure 1.20. Chemical structure of oleuropein aglycone 43
Figure 1.21. Chemical structures of tyrosol and hydroxytyrosol 44

Chapter 2

Figure 2.1. Schematic Representation of HPLC 50
Figure 2.2. Medicinal phenolic plant (*Sorbaria tomentosa*) 52
Figure 2.3. Scheme summarises the application of the HPLC to analyse and study natural products such as *Sorbaria*, and that including polyphenols identification, quantification and studies *in vitro* and *vivo* 53
Figure 2.4. Schematic representation showing how the substances are detected in LCMS. 55
Figure 2.5. (a) medicinal phenolic plant (*Caesalpinia crista*), (b) flowers of *Caesalpinia crista*, (c) leaves (d) seed. 57
Figure 2.6. Scheme summarises the application of the LC-MS and shows how this method can be used to analyse and study natural products such as *Caesalpinia crista*, after isolation LC-MS applied for further identification, characterisation, quantification and studies *in vitro* and *vivo* 58
Figure 2.7. Representation of the nuclear magnetic resonance spectroscopy principle 60
Figure 2.8. An example of ^{13}C NMR spectra of a molecule (the flavonoid quercetin) in the solid (top) and solution (bottom) states to illustrate the difference in peak widths 62
Figure 2.9. Transmission electron microscopy principle 65
Figure 2.10. (A) Pathway of amyloid beta aggregation started as monomers, oligomers and finally the formation of fibrils. (B to D) Images were taken by transmission electron microscopy showing (B) Aβ monomers, (C) Aβ oligomers and (D) Aβ fibrils 67
Figure 2.11. (ThT) thioflavin T chemical structure 68
Figure 2.12. Investigation the influence of detergents on Amyloid β $_{1-42}$ fibrils. Thioflavin T (ThT) fluorescence assay used to examine the influence of test substances on fibril production by amyloid beta-$_{1-42}$. (A) circles in the absence of deoxycholate compound and squares in the presence of deoxycholate compound. (B) circles in the absence of the NDSB-211 compound and diamonds in the presence of the compound. (C) circles in the absence of the compound and triangles in the presence of lauryldimethylamine oxide compound (LDAO) 69
Figure 2.13. Examples of secondary structure CD spectra Poly-L-lysine, (1) α-helical at pH 11.1, (2) anti-parallel β-sheet at pH 11.1, and (3) extended conformation (random coil) at pH 5.7. placental collagen, (4) triple-helix native, and (5) denatured 71

Chapter 3

Figure 3.1. The primers and Aβ primary sequence for constructing a synthetic Aβ gene. The M1–M40 amino acid sequence of Aβ is shown, with the amino acid substitutions associated with disease demonstrated above the residues that were replaced 74
Figure 3.2. Tris-tricine SDS-PAGE gel of MAβ40 (E1-E5 and commercial MAβ40 for more confirmation) peptide expression after adding IPTG and incubating for 3-4 hours 88
Figure 3.3. Chromatogram purification of MAβ40 and the UV absorbance for protein using SEC chromatography 89
Figure 3.4. Tris-tricine SDS-PAGE gel of MAβ40 (E1-E4 fractions after SEC) peptide expression after adding IPTG and incubating for 3-4 hours 90

Figure 3.5. Positive electrospray ionization mass spectrometry of MAβ40 obtained mass 4459.2168 Da 91
Figure 3.6. Thioflavin T fluorescence spectroscopy (ThT) assay of monomeric amyloid beta aggregation at 20 μM 93
Figure 3.7. Transmission electron microscopy images of amyloid beta aggregation and fibrils formed at a concentration of 20 μM. Four different regions of the TEM grids scale bar (1.0 μm)..... 95
Figure 3.8. Tris-tricine SDS-PAGE gel of ^{15}N labelled MAβ40 (E1-E5) peptide expression after adding IPTG and incubating for 3-4 hours. The two unmarked lanes on the gel image next to the molecular weight marker and before E1-E5 are some other samples collected during the expression.97
Figure 3.9. Chromatogram purification of ^{15}N labelled MAβ40 and the UV absorbance for protein using SEC chromatography..... 98
Figure 3.10. Tris-tricine SDS-PAGE gel of ^{15}N labelled MAβ40 (E1-E4 fractions after SEC purification) peptide expression after adding IPTG and incubating for 3-4 hours. 99
Figure 3.11. Positive electrospray ionization mass spectrometry of ^{15}N labelled MAβ40 obtained mass 4506.0474 Da..... 100

Chapter 4

Figure 4.1. The diagram showing the steps of solid phase extraction as described in the above section 107
Figure 4.2. The diagram showing the steps of liquid–liquid extraction (a) with funnel separation. (b) with centrifugation..... 109
Figure 4.3. Process of solid phase extraction of phenolic compounds from extra virgin olive oil (EVOO) 114
Figure 4.4. Process of liquid-liquid (Centrifugation) extraction of phenolic compounds from extra virgin olive oil (EVOO) 115
Figure 4.5. Process of liquid-liquid (Funnel separation) extraction of phenolic compounds from extra virgin olive oil (EVOO) 116
Figure 4.6. HPLC chromatograms at three different wavelengths (a) at 240 nm (b) at 275 nm and (c) at 340 nm of polyphenols isolated from extra virgin olive oil using the three different techniques.. 121
Figure 4.7. (a and b) Chromatograms obtained by funnel separation extraction of Greek olive oil samples extracted twice under identical conditions. Phenolic compounds were isolated by extraction of an oil-in-hexane solution with water methanol /water (60/40) to confirm repeatability and reproducibility of results..... 123
Figure 4.8. The UV-Visible absorptances for Greek and Saudi EVOO extracts. (a) the UV–Vis absorption for Greek and Saudi EVOO extracts as stock solutions (10 mg/mL). (b) the UV–Vis absorption for Greek and Saudi EVOO extracts as 10-fold dilutions 125
Figure 4.9. (a) Greek (top) and (b) Saudi (bottom) LC-MS chromatograms of the EVOO extracts. 127
Figure 4.10. LC-MS ion chromatograms for individual phenolic compounds detected from Greek and Saudi EVOOs at identical retention time. 128
Figure 4.11. Greek (black) and Saudi (red) polyphenol extracts' reverse-phase HPLC chromatograms at 240 nm, 275 nm and 340 nm..... 132
Figure 4.12. HPLC chromatograms of phenolic standards at 240 nm, 275 nm and 340 nm.. 136
Figure 4.13. The calibration curves at ten points of some phenolic compounds extracted from Greek and Saudi EVOOs 138
Figure 4.14. The polyphenol extracts (in DMSO-d_6) solution-state ^1H NMR spectra at 700 MHz. Greek EVOO (black) and Saudi EVOO (red) 143
Figure 4.15. Chemical structures of identified phenolic compounds using solution-state ^1H NMR. 146

Chapter 5

Figure 5.1. Structure of oleuropein showing the main chemical parts attached 154
Figure 5.2. Experimental scheme of binding showing the aggregation of protein with polyphenols and without 161
Figure 5.3. A Kinetic analysis of Tau and Aβ40 aggregation in the absence and presence of EVOO polyphenol extracts at discrete concentrations 166
Figure 5.4. Far-UV CD analysis of Aβ40 with and without the presence of polyphenol extract from Greek and Saudi Arabia EVOO 170
Figure 5.5. A morphological analysis of Tau and Aβ40 aggregation in the absence and presence of EVOO polyphenol extracts at discrete concentrations 173
Figure 5.6. Negative-stain TEM images of Aβ40 fibrils (20 μM) were examined following incubation of Aβ40 in isolation (from an initial monomeric state) for 3 days, followed by incubation with a buffer or with 20 μg/mL (≅ 50 μM) EVOO extract for an additional 24 h. Centrifugation was employed to separate the insoluble constituents while the soluble matter was contained within the supernatant . 176
Figure 5.7. Centrifugation was employed to isolate the soluble oligomers (created from pre-formed fibrils exposed to EVOO extracts at 3 concentrations) of Aβ40 in the supernatant 178
Figure 5.8. DLS data for Aβ40 fibrils in isolation and with 740 μg/mL Greek EVOO 179
Figure 5.9. ^{15}N CP-MAS (top) and refocused ^{1}H-^{15}N INEPT spectra of [U-^{15}N] Aβ40 fibrils combined with Greek extract 180
Figure 5.10. Viability results for SH-SY5Y cells, the first two columns are EVOO untreated controls at concentrations of 72 μg/mL and 144 μg/mL following the addition of EVOO extract, Aβ40 fibrils in isolation and followed by the addition of 72 μg/mL and 144 μg/mL Greek EVOO 182
Figure 5.11. UV- Visible and HPLC binding of polyphenolic compounds in Greek and Saudi extracts to pre-formed fibrils of Aβ40 185
Figure 5.12. Binding analysis of polyphenolic compounds in the olive oil extracts to pre-formed fibrils of tau 188
Figure 5.13. The impacts of discrete EVOO phenolic standard compounds on Aβ40 aggregation. ThT analysis of Aβ40 (20 μM) aggregation kinetics in isolation and following the addition of equimolar concentrations of individual polyphenols 190
Figure 5.14. The impacts of discrete EVOO phenolic standard compounds on Aβ fibril binding.. . 194
Figure 5.15. The effects of discrete EVOO phenolic compounds on tau aggregation 195
Figure 5.16. The effects of discrete EVOO phenolic compounds on tau fibril binding 196
Figure 5.17. Interaction of phenolic compounds with β-sheet structures 198
Figure 5.18. Docking sites for EVOO phenols on the solid-state NMR-derived 3-fold symmetry structural model of Aβ40 (PDB 2LMQ), predicted using the ICM Pro software 200
Figure 5.19. Docking sites for EVOO phenols on the cryo-EM structure of heparin-induced 2N4R tau snake filaments (PDB 6QJH), predicted using the ICM Pro software 201

Chapter 6

Figure 6.1. A general diagram representation showing the absorption and metabolism stages of natural polyphenols in the body 208
Figure 6.2. Solid lipid nanoparticle structure and formulations 210
Figure 6.3. Diagram summaries the aim of this study by loading phenolic compounds in nanoparticles to target Alzheimer's disease 213
Figure 6.4. Synthesis of solid lipid nanoparticles in the laboratory. 217
Figure 6.5. Sample preparation steps for solid-state NMR assessment of polyphenol SLNs 219

Figure 6.6. SLN sample preparation steps for measurement of entrapment efficiency using HPLC, UV-Vis and NMR 222
Figure 6.7. Transmission electron microscopy images of caffeic acid and polyphenol SLN formulations 228
Figure 6.8. Centrifugation process for separating nanoparticles from free drug (polyphenols) to determine the EE% of caffeic acid and phenolic mixture SLNs. 230
Figure 6.9. UV-Vis absorbance of entrapment efficiency of caffeic acid SLN to separate nanoparticles from free drug 231
Figure 6.10. UV-Vis absorbance of entrapment efficiency of Greek polyphenols mixture in solid lipid nanoparticles. 231
Figure 6.11. HPLC chromatogram analysis at 275 nm of entrapment efficiency of caffeic acid SLN to separate nanoparticles from free caffeic acid 233
Figure 6.12. HPLC analysis at 240 nm of entrapment efficiency of Greek polyphenols mixture SLN to separate nanoparticles from free polyphenols 233
Figure 6.13. Solid-state NMR spectrum of the nanoparticle residue of polyphenol mixture SLNs . 235

List of Tables

Chapter 4

Table 4.1. The mean yield of phenolic residue extracted from olive oil using liquid-liquid extraction and solid phase extraction methods 120
Table 4.2. Phenolic compounds identified using LC-MS, in Greek (G) and Saudi (S) EVOO 129
Table 4.3. Identification of the main polyphenols in Greek and Saudi EVOO products using available phenolic standards by HPLC (Retention time, Molecular weight and HPLC-DAD) 133
Table 4.4. Phenolic compounds detected and quantified by HPLC from the Greek and Saudi EVOO extracts 139
Table 4.5. Phenolic compounds detected in Greek and Saudi extracts by HPLC, with retention times, linear ranges and regression equations. 140

Chapter 5

Table 5.1. Summary of the impact of EVOO extracts on Aβ40 aggregation kinetics (calculated *via* ThT fluorescence). In the absence of an extract, the highest fluorescence emission, F_{max}, is normalised to Aβ40 167
Table 5.2. A summary of the HPLC binding analysis of phenolic compounds from Greek EVOO binding (20 μg/mL phenolic extract) to pre-formed fibrils of Aβ40 (20 μM monomer equivalent), (n = 1) 186
Table 5.3. A summary of the HPLC binding analysis of phenolic compounds from Saudi EVOO binding (20 μg/mL phenolic extract) to insoluble pre-formed fibrils of Aβ40 (20 μM monomer equivalent), (n = 1) 187
Table 5.4. The impacts of selected EVOO polyphenolic standards on Aβ40 and tau aggregation kinetics (determined *via* ThT) and the binding of tau and Aβ40 aggregates. Maximum fluorescence emission (F_{max}) is expressed as a percentage of the value for Aβ40 or tau (in the isolation of extract). Means and standard errors (in parentheses) are given for ThT data (n = 3). ND = not done. 192

Chapter 6

Table 6.1. Formulations for caffeic acid-SLNs with different lipid weights 218
Table 6.2. Physicochemical properties of synthesized caffeic acid SLNs..... 225
Table 6.3. Physicochemical properties of SLNs carrying the synthesized polyphenol mixture from EVOO..... 226
Table 6.4. Fluorescence of phenolic SLNs (excitation wavelength = 482 nm, emission wavelength = 515 nm)..... 236
Table 6.5. Particle size and PI values of SLNs after 8 months of storage 238

List of Abbreviations

Aβ	Amyloid beta
AD	Alzheimer's disease
AMPK	Adenosine monophosphate-activated protein kinase
ApoE	Apolipoprotein E
ApoJ	Apolipoprotein J
APP	Amyloid precursor protein
APS	Ammonium Persulfate
BBB	Blood-brain barrier
BDNF	Brain derived neurotrophic factor
CAA	Cerebral amyloid angiopathy
CD	Circular dichroism
CP-MAS	Cross-polarization magic-angle spinning
Cryo-EM	Cryo-electron microscopy
CSA	Chemical shift anisotropy
CTF	The contrast transfer function
CV	Column volume
DEAE	Diethylaminoethyl
ΔF	Change in fluorescence intensity
3,4-DHPEA	3,4-Dihydroxyphenylethanol

DLS	Dynamic light scattering
DMEM	Dulbecco's Modified Eagle's Medium
DPPH	2,2-Diphenyl-1-picrylhydrazyl
DQF-COSY	Double quantum filtered COSY
DTT	Dithiothreitol
E. coli	*Escherichia coli*
EDTA	Ethylenediaminetetraacetic acid
EELS	Electron energy loss spectroscopy
EGCG	Epigallocatechin gallate
ERK	Extracellular signal-regulated kinases
ESI	Electrospray ionisation
EVOO	Extra virgin olive oil
GSK-3β	Glycogen synthase kinase 3 beta
HAADF	High-angle annular dark-field
HDL	High-density lipoprotein
HPLC	High-performance liquid chromatography
IAPP	Islet amyloid polypeptide
IC	Ion-exchange chromatography fraction
ICM	Internal coordinate mechanics
IMAC	Immobilised metal ion affinity chromatography
INEPT	Insensitive nuclei enhanced by polarization transfer
IPTG	Isopropyl-β-D- thiogalactoside
$LaB6$	Lanthanum hexaboride
LC-MS	Liquid chromatography–mass spectrometry

LCMS-IT-TOF	Liquid chromatograph mass spectrometer-ion trap (IT)-time of flight (TOF) mass spectrometer
LDAO	Lauryldimethylamine oxide
LDL	Low-density lipoprotein
LLE	Liquid-liquid extraction
MQ	Milli-Q purified water
MS	Mass spectrometry
MW	Molecular weight
NDSB-211	Nondetergent-sulfobetain (Dimethyl-2-hydroxyethylammoniumpropane sulfonate)
NFTs	Neurofibrillary tangles
NMR	Nuclear magnetic resonance
OD600	Optical density at 600 nm
PBS	Phosphate buffered saline
PDB	Protein data bank
p-HPEA	p-Hydroxyphenylethanol
PMSF	Phenylmethylsulphonyl fluoride
SAP	Serum amyloid A protein
SDS	Sodium dodecyl sulfate
SDS- PAGE	Sodium dodecyl sulphate polyacrylamide gel electrophoresis
SEC	Size exclusion chromatography
SLN	Solid lipid nanoparticle
SPE	Solid-phase extraction
SSNMR	Solid-state NMR
TEM	Transmission electron microscopy
TEMED	Tetramethylethylenediamine

ThT	Thioflavin T
T lag	Lag time
UHPLC	Ultra-high performance liquid chromatography
UV-Vis	UV-Visible spectroscopy

Chapter 1 (Introduction)

The Mediterranean diet

The Mediterranean diet is rich in plant-based foods, such as citrus fruit, olive oil, red wine, legumes, whole grains, and nuts, which contain high amounts of polyphenols and are known to have antioxidant and neuroprotective effects. Some other features of the Mediterranean diet are moderate consumption of fish, low to moderate consumption of dairy products, low consumption of poultry and red meat, and moderate consumption of alcohol (reviewed in García-Casares et al., 2021). While there is evidence that a Mediterranean-type diet characterized by high consumption of vegetables and moderate consumption of alcohol is associated with better neuroimaging findings in terms of Aβ deposits (Vassilaki et al., 2018), a more recent meta-analysis and review from 2023 points out that there is still a big gap in our understanding of how this diet alters AD-related structural neuroimaging findings in the brain (Gregory et al., 2023). Despite this lack of neuroimaging evidence, the majority of the studies in the literature do indicate that adhering to a Mediterranean diet lowers the risk of AD (reviewed in García-Casares et al., 2021), so it is expected that this diet and its components will continue to be the subject of research on the prevention and treatment of conditions characterized by cognitive impairment, such as AD.

A specific feature of the Mediterranean diet is that it is rich in extra virgin olive oil, with the dietary consumption ranging from 40 to 50 g/day (Corona et al., 2009). Therefore, the next few sections will focus on polyphenols, the composition of, and metabolites present in olive oil and how they affect cognitive function in AD.

Extra virgin olive oil

Olive oil has long been used for its protective properties and has been shown to prevent and improve conditions such as cardiovascular disease, oxidative stress, obesity, and type 2 diabetes (Bulotta et al., 2014; Amiot-Carlin, 2014). Of all the components of the Mediterranean diet, olive oil may play a particularly important role in the observed preventive and ameliorative effects on AD. In fact, a pilot study conducted in Greece has reported that long-term supplementation with extra virgin olive oil had a better effect on improving cognitive function than just consumption of a typical Mediterranean diet (Tsolaki et al., 2020). Further, a study on the mechanisms of olive oil in cognitive improvement found that extra virgin olive may ameliorate AD-associated neurodegeneration by restoring the activity of the neuroprotective protein BMI1 (Tzekaki et al., 2021). Thus, there is molecular evidence for the cognitive benefits of consuming extra virgin olive oil.

The protective effect of olive oil has been linked to its chemical composition (Wani et al., 2018; Perez-Martinez et al., 2011). Extra virgin olive oil contains about 90-99% glycerol fraction and a 5% non-glycerol fraction or unsaponifiable fraction (Tripoli et al., 2005). The glycerol fraction consists primarily of monounsaturated fatty acids (which account for 55% to 83% of the total fatty acids in olive oil), while the non-glycerol fraction consists of over 230 chemical compounds, including phenolic compounds in the form of oleuropein and its derivatives, phenolic acids such as caffeic acid and vanillic acid, as well as aliphatic alcohols, triterpene alcohols, sterols, hydrocarbons, pigments, and volatile compounds (Caramia et al., 2012; Hadrich et al., 2022; Scoditti et al., 2012). The naturally occurring polyphenol compounds in olive oil consumed as part of the Mediterranean diet have been linked to a decreased incidence of several diseases, including cardiovascular disease, diabetes, certain cancers, and neurodegenerative diseases (Rodríguez Morato et al., 2015; Sofi et al., 2013; Martinez et al., 2013; Scarmeas et al., 2009). In particular, the polyphenol components, which are secondary

metabolites of olive oil, appear to be most promising for the treatment of neurodegenerative diseases.

Polyphenolic compounds in extra virgin olive oil

As secondary metabolites found in olive oil, polyphenols are known for their wide-ranging health benefits, which include their antioxidant, anti-inflammatory, cardioprotective, neuroprotective, anticancer, antidiabetic, and antimicrobial effects; moreover, they are known to play an important role in maintaining the stability and organoleptic characteristics of olive oil (reviewed in Finicelli et al., 2021). Below, we have described their structure and classification.

Structure and classification of polyphenols in olive oil

Polyphenols are low-molecular-weight organic substances that contain an aromatic ring with one or more hydroxyl moieties. They are found in both simple and complex forms and are classified into several classes and subclasses according to their chemical structure, the number of aromatic rings, the positions of various functional groups, and the carbon skeleton (reviewed in Zagoskina et al., 2023). More than 10,000 polyphenolic compounds have been discovered so far, and their numbers continue to increase with advancements in isolation and analytical methods (Singla et al., 2019).

The amyloid architecture is believed to incorporate π-stacking, wherein the aromatic amino acids assemble through stabilizing π–π interactions and through hydrophobic interactions. It has been proposed that the aromatic rings of polyphenol compounds interfere with the π-stacking in amyloids, thus inhibiting the stabilization of the amyloid core structure (Ahmad et al., 2011). Further, through interaction with the hydroxyl moieties, these compounds can

disrupt the hydrophobic core of the amyloid structure and increase its solubility (Casamenti and Stefani, 2017; Wu et al., 2006).

Olive oils can contain upwards of 30 polyphenol compounds, and many of these have been shown to inhibit the formation of amyloid of Aβ or tau, in isolation. According to their structure, they are categorized into secoiridoids, phenolic alcohols, flavonoids, lignins, phenolic acids, and hydroxy-isocromans (reviewed in Finicelli et al., 2021).

Secoiridoids: These compounds are composed of a phenyl ethyl alcohol (3,4-DHPEA or *p*-HPEA) linked to elenolic acid or its derivates, and they are glycosylated in most cases. They are considered to be responsible for the bitter taste of olive oil. The secoiridoids demethyloleuropein, oleuropein, and ligstroside are the main glycosides in olive fruit and comprise 90% of the phenolic compounds in extra virgin olive oil. The secoiridoids oleuropein, ligstroside and demethyloleuropein chemical structures are shown in **Figure 1.1** (Finicelli et al., 2021).

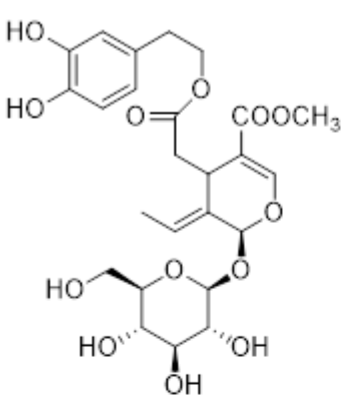

Oleuropein

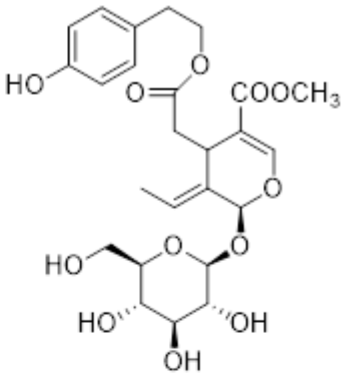

Ligstroside

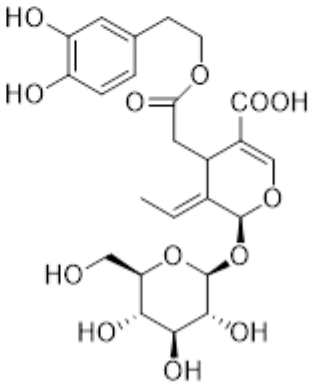

Demethyloleuropein

Figure 1.1. Chemical structures of oleuropein, ligstroside and demethyloleuropein phenolic compounds.

Phenolic alcohols: They are also referred to as phenylethanoids and feature a hydroxyl group linked to an aromatic hydrocarbon group. While their concentrations in fresh olive oil are low, their concentrations increase with storage as a result of the hydrolysis of secoiridoids **Figure 1.2** the mechanism of secoiridoids hydrolysis to produce phenolic alcohols (Johnson and Mitchell, 2018). The main phenolic alcohols found in olive oil are hydroxytyrosol (3,4-dihydroxyphenyl ethanol), tyrosol (*p*-hydroxyphenyl ethanol), and oleocanthal. Their chemical structures are shown in **Figure 1.3** (Finicelli et al., 2021).

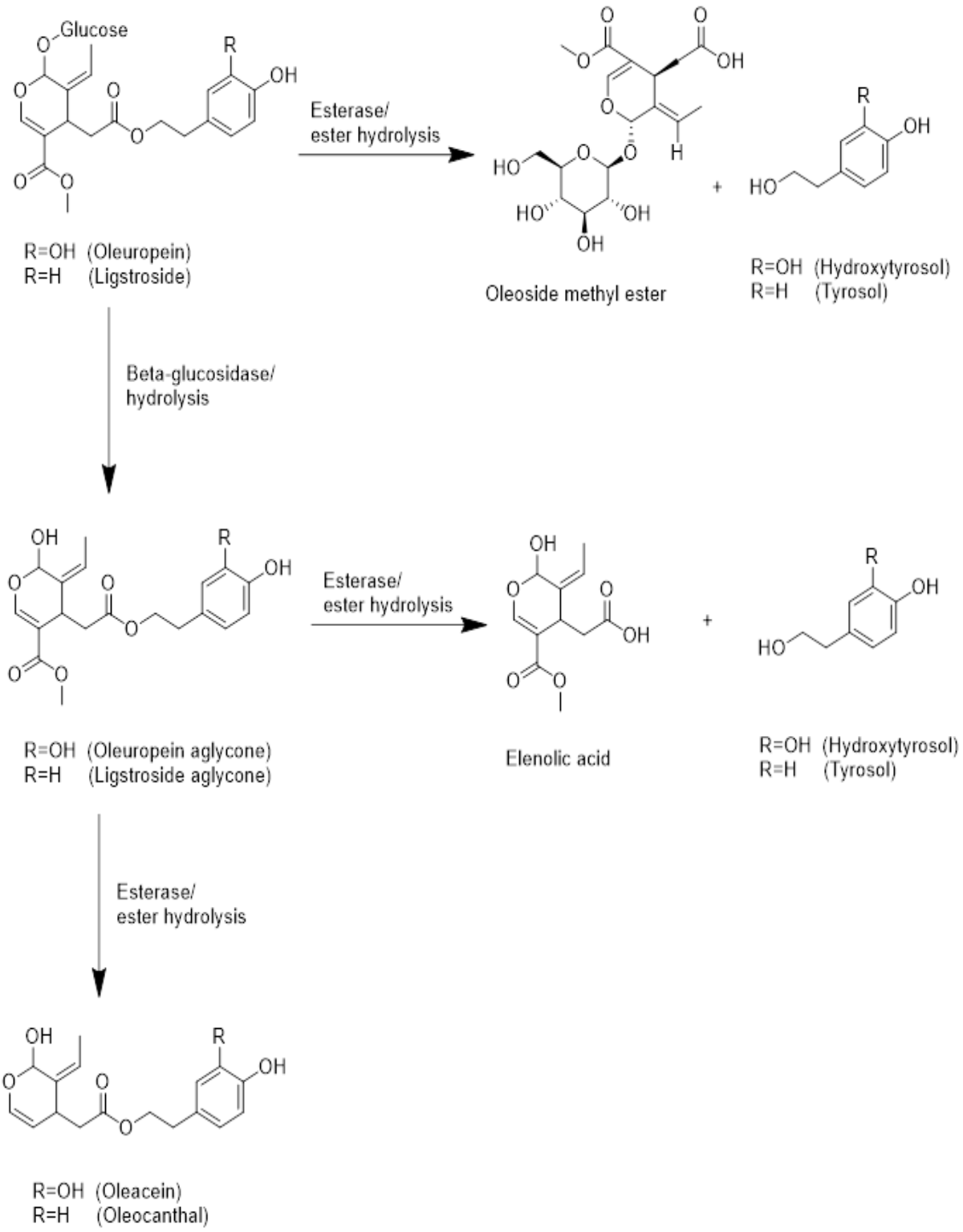

Figure 1.2. Mechanism of the hydrolysis of secoiridoids in olive oil to produce phenolic alcohols (Johnson and Mitchell, 2018). Another name of elenolic acid is 2-[(2S,3S,4S)-3-formyl-5-methoxycarbonyl-2-methyl-3,4-dihydro-2H-pyran-4-yl] acetic acid (Pubchem, accessed in 2025).

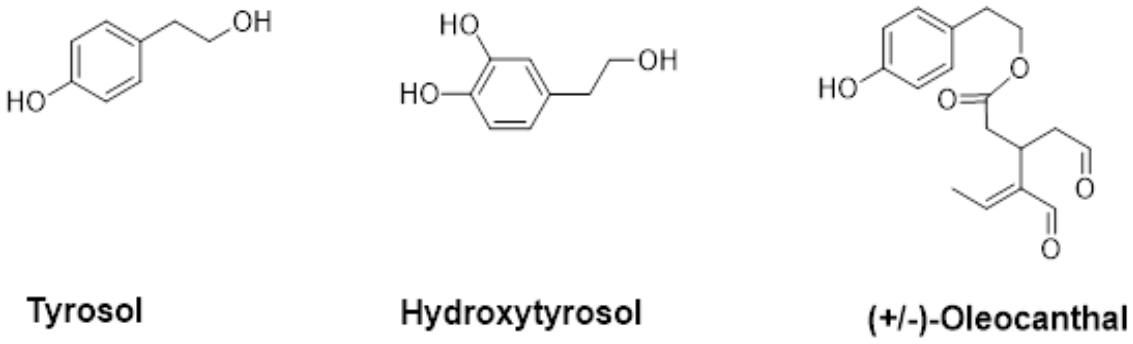

Figure 1.3. Chemical structures of tyrosol, hydroxytyrosol and oleocanthal are the main phenolic alcohols in olive oil products.

Flavonoids: They are composed of two benzene rings attached by three linear carbon chains. Flavonoids undergo further modifications to form other compounds such as flavones, flavonols, flavanones, and flavanols. Luteolin and apigenin are the flavonoids found in the highest concentrations in olive oil see **Figure 1.4** for their chemical structures (Finicelli et al., 2021).

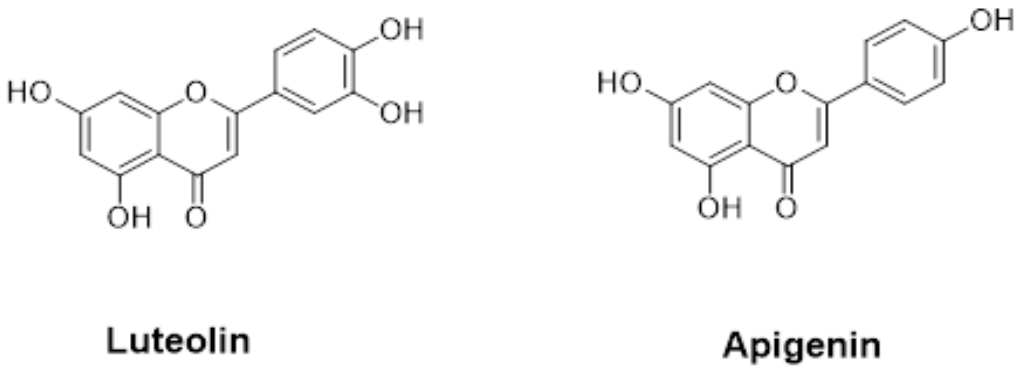

Figure 1.4. Chemical structures of luteolin and apigenin phenolic compounds can be found in olive oil.

Lignans: These phenolic compounds are formed as a result of the condensation of aromatic aldehydes, and they are found in the woody component of the olive seed. They are released into the oil during the extraction process in their original form, without biochemical modifications. (+)-Pinoresinol and (+)-1-acetoxypinoresinol are the most common lignans found in extra virgin olive oil. Their chemical structures are shown in **Figure 1.5** (Finicelli et al., 2021).

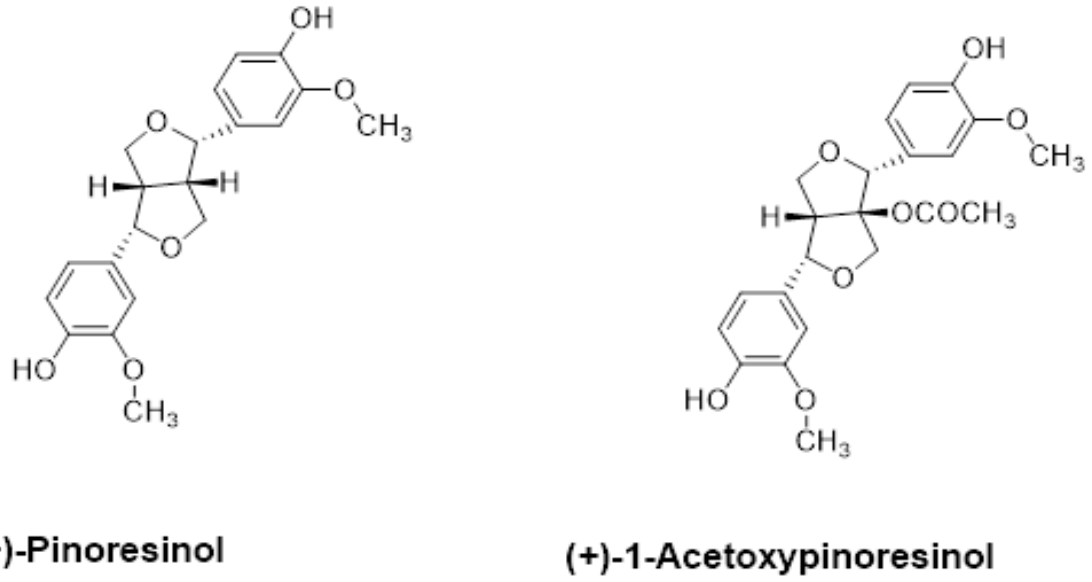

Figure 1.5. Chemical structures of the most common lignans in EVOO (+)-pinoresinol and (+)-1-acetoxypinoresinol compounds.

Phenolic acids: They are classified into hydroxybenzoic acid derivatives (*e.g.*, *p*-hydroxybenzoic, protocatechuic, and gallic acid) and derivatives of hydroxycinnamic acid (*e.g.*, *p*-coumaric acid, cinnamic acid, caffeic acid, and synapinic acid). The chemical structures are shown in **Figure 1.6** (Finicelli et al., 2021).

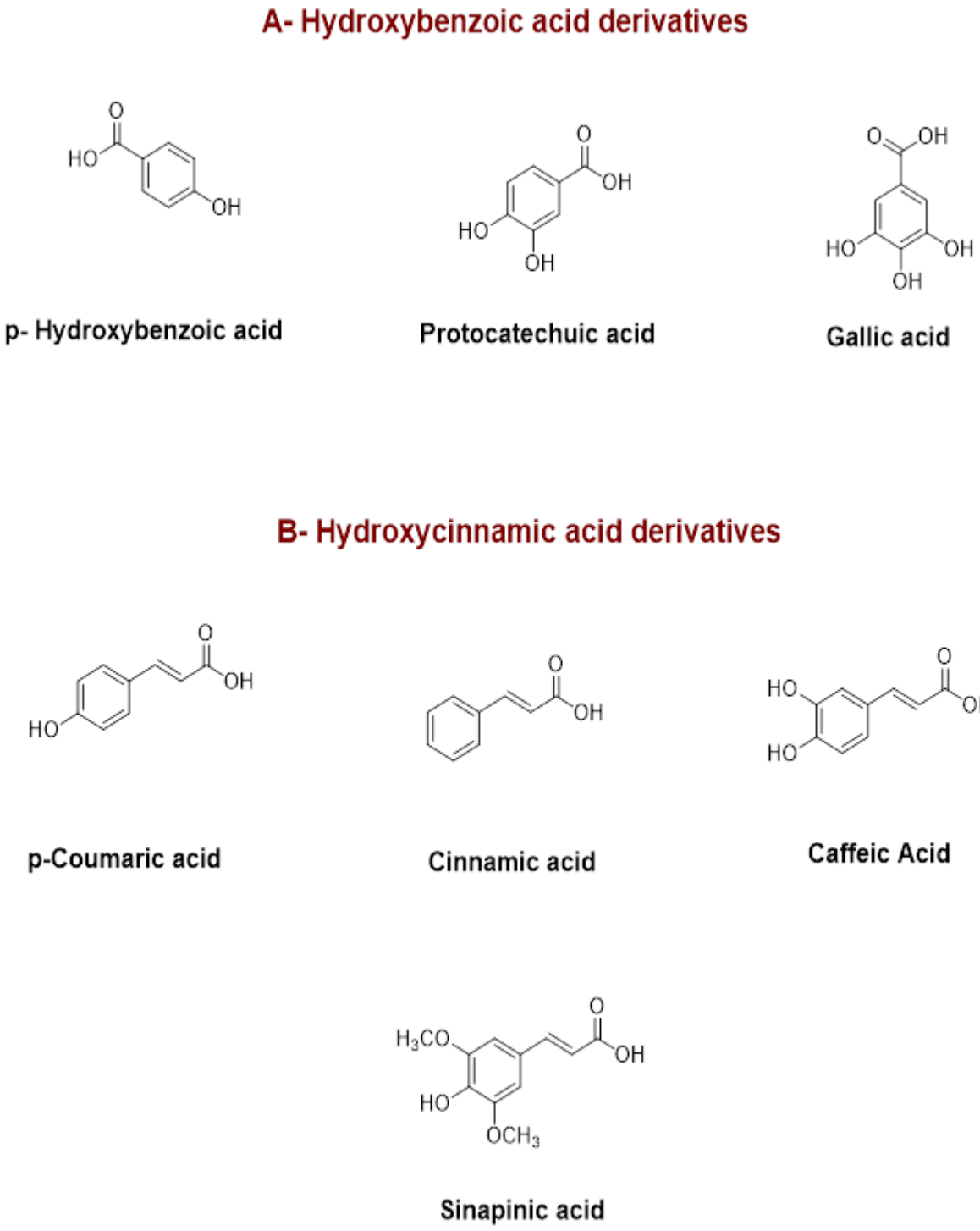

Figure 1.6. Chemical structures of phenolic acids compounds classified into hydroxybenzoic acid derivatives (A, top) and hydroxycinnamic acid derivatives (B, bottom) can be found in olive oil products.

Hydroxyisochromans: Only two hydroxyisochromans are found in commercially available olive oil: 1-phenyl-6,7-dihydroxy-isochroman and 1-(3′-methoxy-4′ -hydroxy)-6,7-dihydroxy-isochroman (**Figure 1.7**), which are formed when hydroxytyrosol reacts with benzaldehyde and vanillin, respectively (Finicelli et al., 2021).

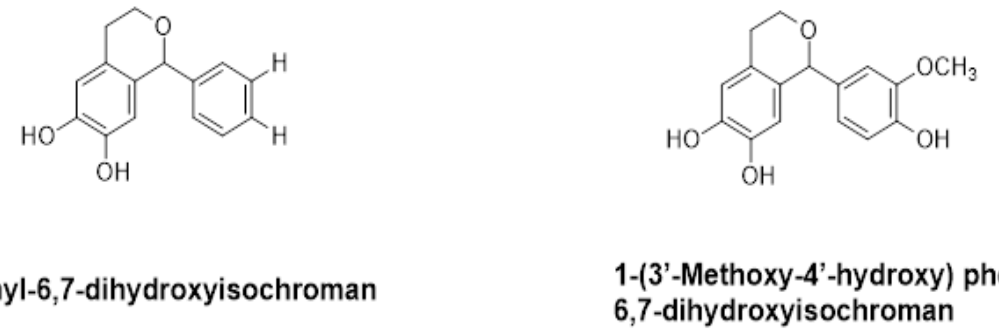

Figure 1.7. Chemical structures of hydroxyisochroman compounds in olive oil (left) 1-phenyl-6,7-dihydroxy-isochroman and (right) 1-(3′-methoxy-4′ -hydroxy)-6,7-dihydroxy-isochroman.

Alzheimer's disease

Alzheimer's disease (AD) is defined as a progressive neurodegenerative disease that generally worsens with age (Citron, 2010). AD was first described by Alois Alzheimer in 1906 (Hippius & Neundörfer, 2003). Early symptoms of the disease include problems in recalling recent events, and as the condition worsens, individuals can experience increasing memory loss, become disorientated, and experience mood swings and behavioral problems, until they are eventually unable to live independently as a result of deterioration of bodily functions (Cummings et al., 2016). These main signs are often preceded by problems in vision and language (Schachter & Davis, 2000). This condition can eventually lead to the death of patients,

and the average time for progression from diagnosis to death varies between three and ten years (Zanetti et al., 2009), depending on the severity of neurodegeneration, as shown in **Figure 1.8**. The management of Alzheimer's disease is becoming a major societal challenge. Furthermore, a cure for the disease is lacking and the current treatment options are only modest in treating selected symptoms and that all depend on early and precise diagnosis, reducing the symptoms and decreasing the rate of disease progressions (Cummings et al., 2016).

AD is associated with multiple risk factors that range from environmental factors, such as exposure to pollution, toxic heavy metals, and stress (Chen et al., 2017; Justice, 2018; Neri & Hewitt, 1991), to metabolic risk factors such as diabetes mellitus, poor nutrition, and cardiovascular disease (Akbaraly et al., 2019; de Bruijn & Ikram, 2014; Butterfield et al., 2014). Importantly, the risk of AD is 60% to 80% dependent on heritable risk factors, and about 40 genetic loci associated with the risk of AD have been identified (Scheltens et al., 2021). Examples include recombinants of the amyloid precursor protein (*APP*) gene (Goate et al., 1991; Sheppard and Coleman, 2020), missense mutations of the Alzheimer disease 3 (*AD3*) gene (Sherrington et al., 1995), a point mutation in the presenilin 2 (*STM2*) gene (Levy-Lahad et al., 1995), and mutations in apolipoprotein E (*APOE*) (Corder et al., 1993). However, it should be noted that autosomal dominant AD accounts for only about 1% of all AD cases. This implies that AD can be prevented in the majority of the cases by management of the risk factors, but there is no clear evidence to indicate this. Despite extensive research on this disease, there are still many gaps in our understanding of its etiology.

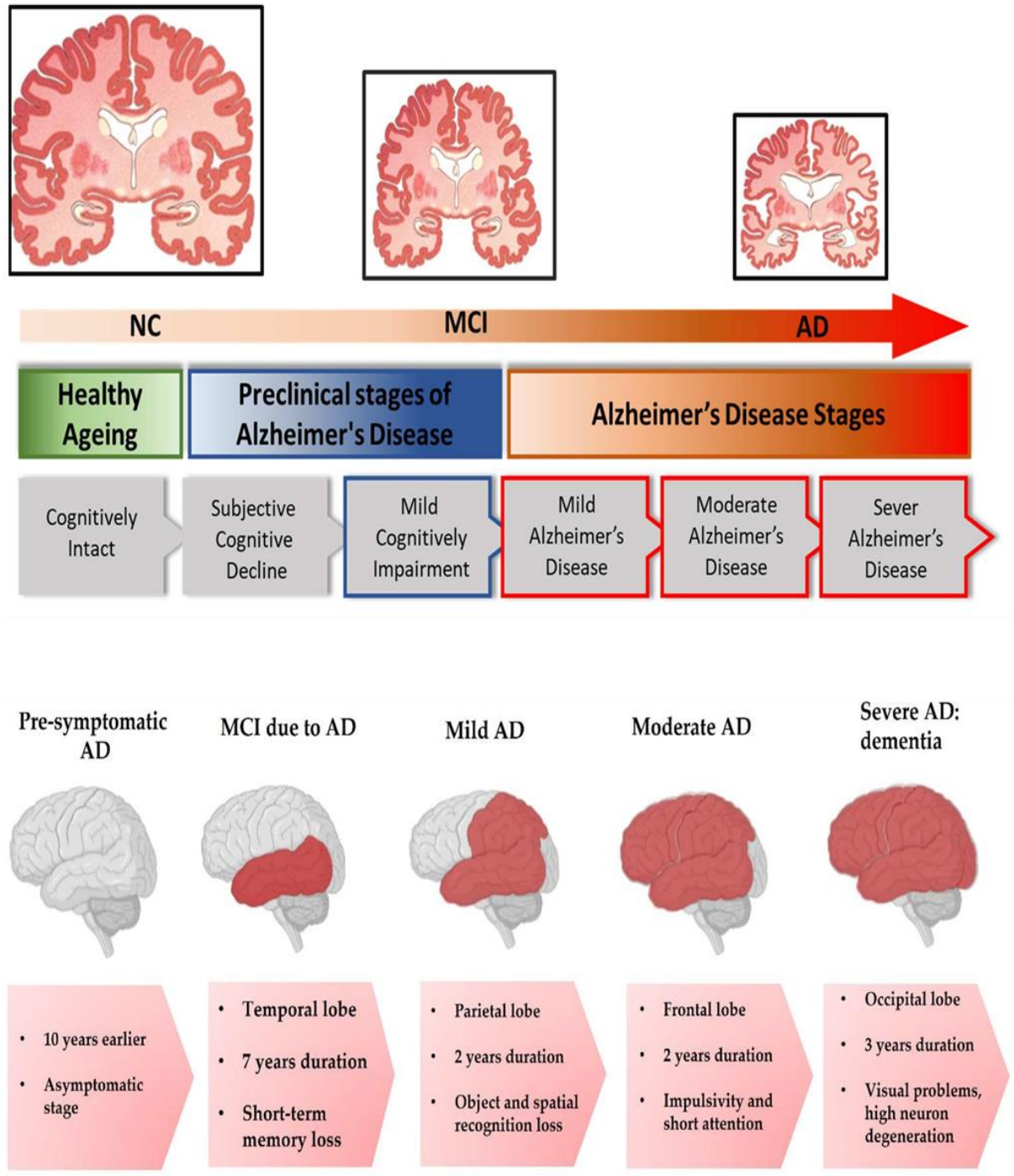

Figure 1.8. Progression of Alzheimer's brain from diagnosis to advanced stages. (top and bottom) brain structures of typical or healthy brains and brain structures of Alzheimer brains in the mild and advanced stages (Adapted from Malik et al., 2024; Pinto-Hernandez et al., 2023). The figure is reproduced under a Creative Common CC BY license (Copyright 2024, MDPI and copyright 2023, MDPI).

AD is characterized by loss of synapses and atrophy of neurons, both of which are largely concentrated in the hippocampus and cerebral cortex (Sheppard & Coleman, 2020). Recently, brainstem atrophy was also detected in the early phase of AD (Ji et al., 2021). Synaptic loss and neuronal atrophy are associated with the two main pathologies of AD (**Figure 1.9**), namely, plaques containing fibrillar amyloid-β-containing and tau-related pathologies (that is, neurofibrillary tangles [NFTs] composed of tau proteins) (Ittner and Götz, 2011). Amyloid-β (Aβ) is a peptide byproduct of cellular metabolism derived from the APP protein, and the tau protein family plays a role in microtubule formation and stability in nerve cells. Aβ deposition is an extracellular pathology, while NFT formation is an intracellular pathology. Cases in which only both these pathologies are observed are rare, as they are commonly accompanied by a host of other pathologies, including Lewy body pathology (the intracellular aggregation of misfolded alpha-synuclein protein in neurons), aggregates of other proteins (such as TAR DNA-binding protein 43 [TDP-43] proteinopathy and hyperphosphorylated-τ proteinopathy), inflammatory pathology, and various vascular pathologies (Abner et al., 2017; Elobeid et al., 2016; Kapasi et al., 2017; Kovacs et al., 2013; Robinson et al., 2018; Spires-Jones et al., 2017; White et al., 2016). In addition, there are some more recently discovered pathologies that still need to be validated through larger scale studies, for example, limbic-predominant age-related TDP-43 encephalopathy, chronic traumatic encephalopathy, and aging-related tau astrogliopathy (Trejo-Lopez et al., 2022; Stein and Crary, 2020). Despite the presence of this wide spectrum of association pathologies, it should be noted that Aβ and tau are the prominent pathologies of AD that have been consistently documented in the majority of AD cases worldwide, and therefore, they remain the focus of research on AD.

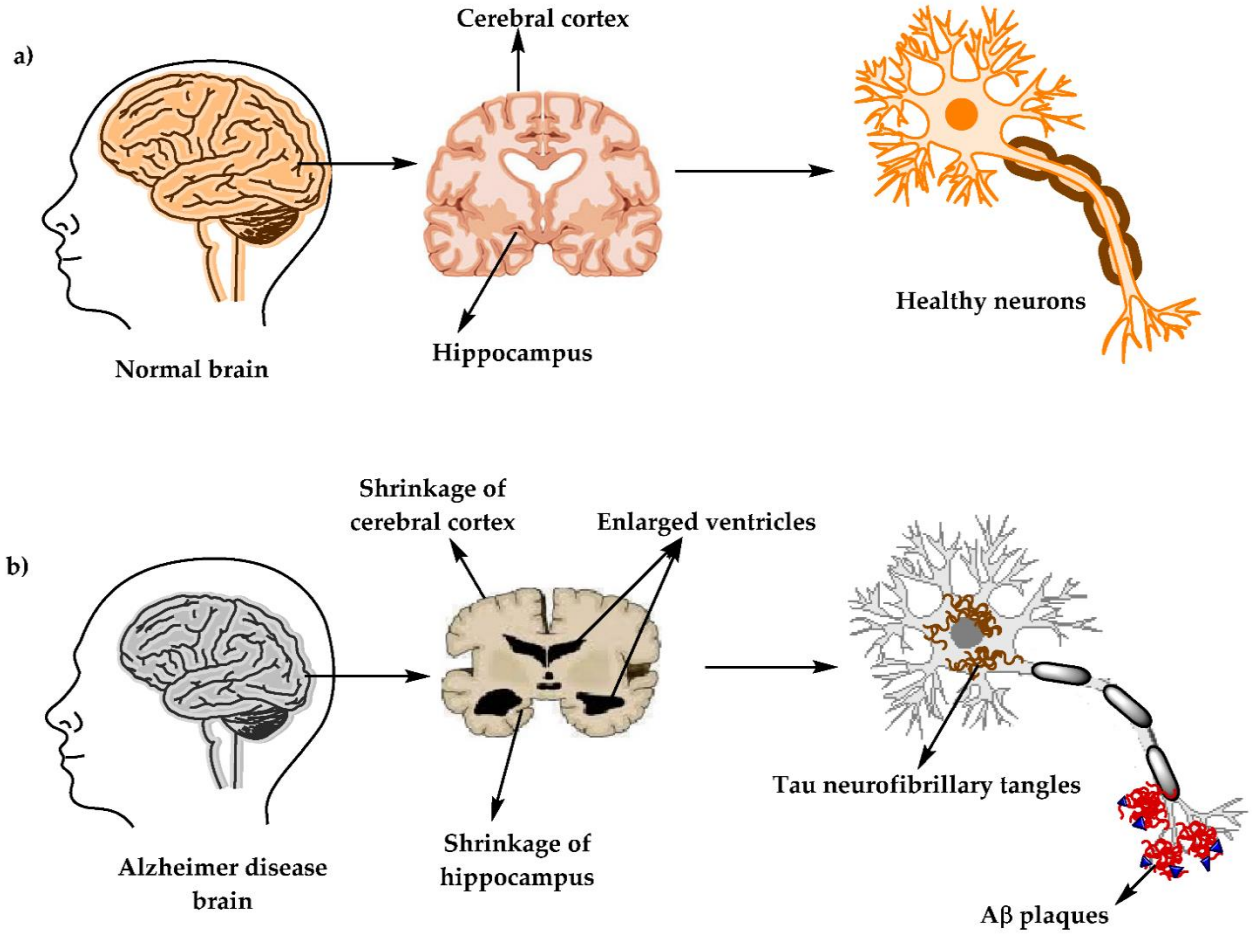

Figure 1.9. Comparison of normal and AD brains associated with the two main pathologies. (a) Normal brain (b) Characterization of Alzheimer disease by the two main pathologies amyloid-β-containing plaques and tau-related pathologies (Adapted from Breijyeh and Karaman, 2020). The figure is reproduced under a Creative Common CC BY license (Copyright 2020, MDPI).

Alzheimer's disease (AD) predominantly affects individuals aged above 65 years, with those below the age of 65 accounting for only 3% of AD cases (Alzheimer's Association, 2019). Further, the risk of developing the disease increases with age: one in 14 people over the age of 65 years are at risk of developing the disease, whereas this increases to one in six for people over the age of 80 years (Alzheimer's Research UK, 2018). It is estimated that the number of people living with AD globally will increase from 50 million in 2018 to 152 million in 2050, which equates to a 204% increase (Alzheimer's Research UK, 2018). In the UK alone, the number of people living with AD is set to rise to one million by 2025 and to two million by 2050 (Alzheimer's Research UK, 2018). Because of the aging population, the management of AD is becoming a major societal challenge that may be exacerbated in the future. Currently, AD is managed by symptomatic treatment, and there are no therapeutic strategies for halting the progression of the disease or reversing it. Thus, there is a need for curative strategies or, at least, treatments that can significantly improve the quality of life for patients with AD (Cummings et al., 2016). Further, researchers have discovered that the processes are triggered several decades before symptoms are manifested (Trejo-Lopez et al., 2022). Therefore, the ability to detect AD in its preclinical stages may aid in the identification of high-risk patients, in whom the pathologies could be prevented or controlled through the management of modifiable risk factors such as diet and lifestyle.

In relation to dietary modifications, in recent years, phenolic compounds derived from olive oil have been receiving attention for their strong neuroprotective effects in various neurodegenerative and inflammatory diseases, including AD. Given that these compounds are found in a variety of plant-derived foods, such as olive oil, nuts, berries, cacao, vegetables, and spices, consumption of these foods or supplements derived from these foods may present a basis for the prevention and alleviation of neurodegenerative conditions.

This introduction chapter focuses on the two main pathologies of AD, namely, amyloid plaques and NFTs composed of tau-related proteins, and the benefits of phenolic compounds in the prevention and treatment of this condition.

Pathogenesis of Alzheimer's Disease

Amyloid-β-related pathologies

Aβ has been shown to have a critical role in the progression of AD (Sadigh-Eteghad et al., 2015). Aβ containing 39 to 42 amino acids is derived from cleavage of the APP protein by the enzyme β-secretase in pathological conditions (LaFerla et al., 2007). In contrast, in normal conditions, APP is cleaved by α-secretase to form a soluble APPα fragment. Recent research has revealed that Aβ may actually have important physiological roles that are evolutionarily conserved but are lost with AD progression or administration of Aβ-targeting therapies (reviewed in Kent et al., 2020). According to the review by Kent et al. (2020), the roles of Aβ range widely, and it may be involved in the regulation of learning and memory, blood vessel formation, neuron formation, repair of the blood–brain barrier, response to injury, antimicrobial activities, and antitumor responses. Certain physiological concentrations of Aβ appear to be necessary for various physiological activities, but the same activities can be disrupted if the concentrations are above or below the optimal level required for those activities. In other words, Aβ may play a hormetic role in the human body (Kent et al., 2020).

The predominant Aβ peptides are $A\beta_{40}$ and $A\beta_{42}$, which accumulate within the parenchymal tissue of the brain to form oligomeric species that are toxic to neuron synapses (Kumar and Singh, 2015; Kurz and Perneczky, 2011; Viola and Klein, 2015; Ferreira and Klein, 2011; Hayden and Teplow, 2013; Hefti et al., 2013; Nisbet et al., 2015) and disrupt

cholesterol-based membranes (Jang et al., 2013; Subasinghe et al., 2003). It is widely accepted that the postsynaptic compartment within synapses is the target of Aβ toxicity (Selkoe, 2002), and several postsynaptic receptors might play a role in Aβ binding, including a7-nicotinergic receptors and metabotropic glutamate receptors (Laurén et al., 2009). However, it is unlikely that the toxicity results from direct binding of Aβ with the receptors, and it is more likely to be the result of indirect contact, such as membrane associations (Kessels et al., 2010). In addition, Aβ-induced hyperexcitation of neurons may be another mechanism responsible for the neuronal hyperactivation and associated circuit dysfunction that occur in the early stages of AD (Zott et al., 2019).

Figure 1.10 the oligomeric forms of Aβ undergo spontaneous aggregation to form β-sheet-rich amyloid fibrils. These insoluble fibrils are referred to as amyloids and are present within tissues as well as within extracellular spaces in organs (Townsend et al., 2018; Race et al., 2017). Within the fibrils, the protein aggregates form a folded shape, which allows the addition of more proteins and the formation of larger aggregates (Rambaran and Serpell, 2008). They consist of long unbranched fibers that are characterized by a cross-β-sheet quaternary structure in which antiparallel chains of β-stranded peptides are organized in an orientation perpendicular to the axis of the fiber, as shown in **Figure 1.11** (Race et al., 2017).

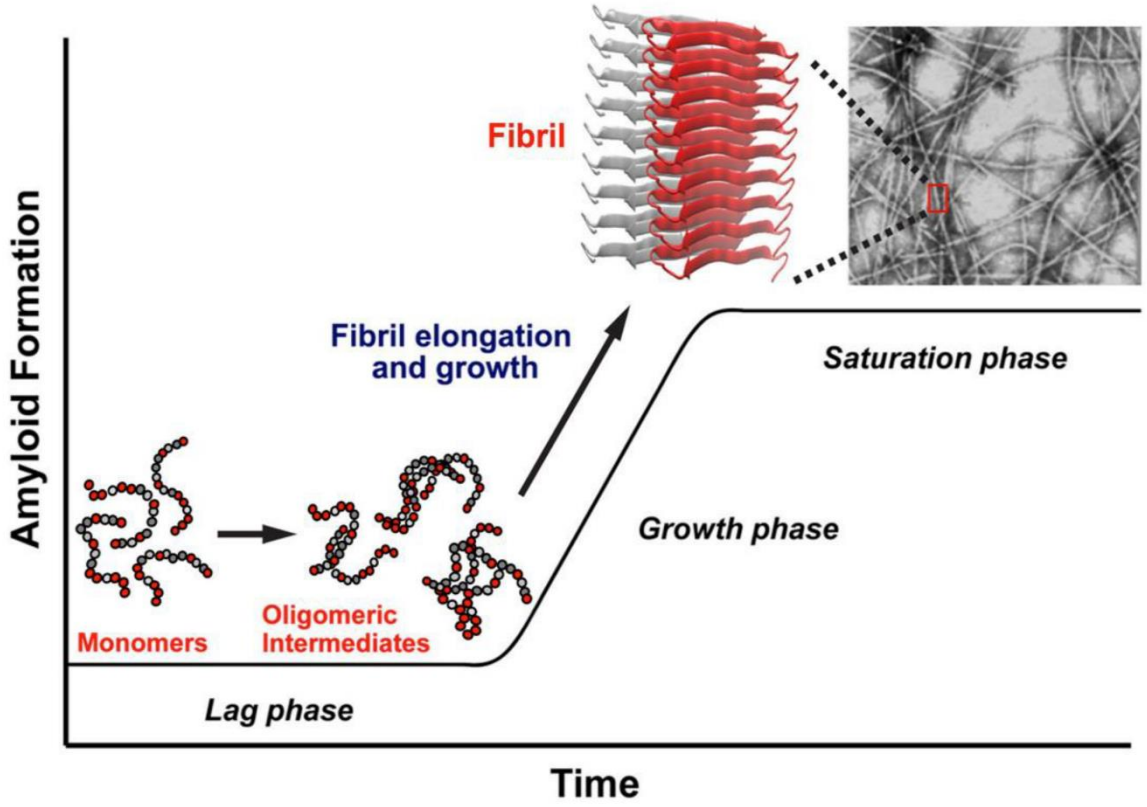

Figure 1.10. Amyloid aggregation kinetics starting from unstructured monomers to end with saturation phase (Adapted from Moore et al., 2018; Abedini et al., 2016). The figure is reproduced under a Creative Common CC BY license (Copyright 2018, MDPI).

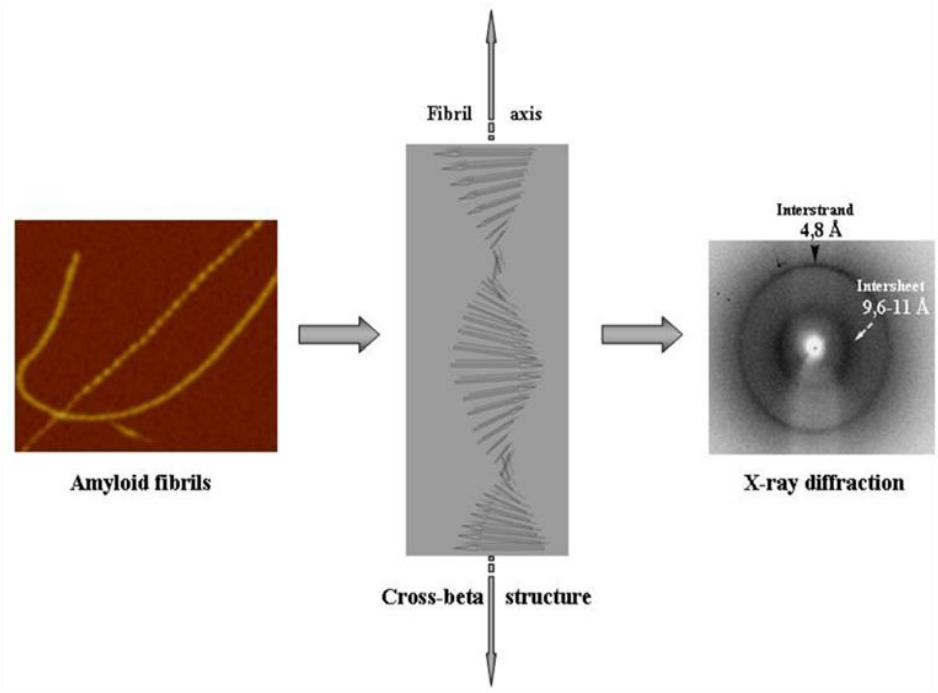

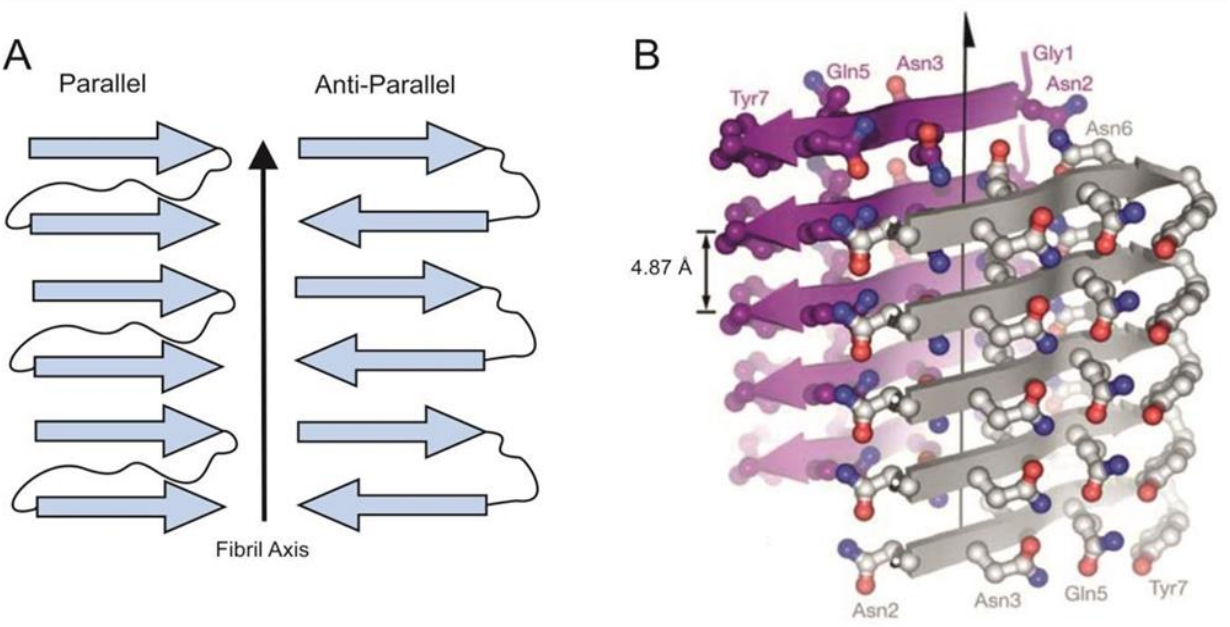

Figure 1.11. Schematic diagram depicting the structure of amyloid fibre diffraction pattern and the cross-beta steric zipper (Nelson et al., 2005; Townsend, 2016; Stefani, 2008). The figure is reproduced with permission (Copyright 2005, Nature and copyright 2008, MDPI).

The structure of amyloids progresses from a cross-β-sheet structure to a protofilament structure and, finally, the complete fibril form (Nelson et al., 2005; Townsend, 2016; Race et al., 2017).

Amyloids form fibrous deposits in the form of plaques, which surround cells and, consequently, hinder normal cell function. The extent of Aβ plaque spread is one of the main clinical indicators based on which dementia pathologies are diagnosed and scored, but it should be noted that this plaque pathology is also associated with the normal process of aging. Aβ plaques are found in a range of different forms—from diffuse plaques to coarse-grained and cored plaques (reviewed in Walker, 2020). Under normal aging conditions, the diffused form is more common, while the cored form is more commonly observed in conditions associated with cognitive decline (Dickson et al., 1992).

Thal et al. (2002) classified amyloid pathologies by defining the spread of Aβ plaques in different regions of the brain according to the phase of dementia, as follows: phase 1 (early phase): neocortex; phase 2: entorhinal cortex, subiculum, amygdala, and cingulate gyrus; phase 3: basal ganglia, thalamus, and other subcortical areas; phase 4: parts of the brainstem, including the midbrain, pons, and medulla oblongata; phase 5 (end stage): cerebellar cortex. Phases 1 and 2 are not associated with any symptoms and can be considered as the preclinical phase in younger patients or the normal aging pathology in older patients, whereas phases 4 and 5 are associated with clinical signs of dementia (Thal et al., 2002). Based on this classification, imaging studies could be used to detect AD early on or determine the stage of progression. This line of investigation is important, as the symptomatic presentation may start appearing only from phase 3 onwards and varies widely between patients.

Another common amyloid pathology observed in patients with AD is cerebral amyloid angiopathy (CAA), which is characterized by Aβ deposits in cerebral and leptomeningeal blood vessels (Bergeron et al., 1987; Haussmann et al., 2023). CAA is associated with the destruction of blood vessels and the likelihood of cerebral hemorrhage, either microhemorrhages or large lobar hemorrhages (McCarron & Nicoll, 1998), and even infarct (Thal et al., 2002). However, it should be noted that in aged patients with AD, CAA may not be the most important, or the

only, risk factor for hemorrhage, given the presence of other risk factors such as hypertension (Jellinger et al., 2007).

All these Aβ-related pathologies in AD are collectively referred to as the Aβ hypothesis, and more recent studies exploring this hypothesis of AD have revealed that the starting point of the pathology may be an imbalance between the production and clearance of $A\beta_{42}$ and related Aβ peptides (reviewed in Selkoe & Hardy, 2016). In this regard, three isoforms of the ApoE protein, namely, ApoE2, ApoE3, and ApoE4, have been linked with the dyshomeostasis of Aβ (Castellano et al., 2011). ApoE is a major transporter of lipids in the human brain and is necessary for neural repair and regeneration. Importantly, ApoE mutations have been identified as the strongest genetic risk factor for AD (Musiek & Holtzman, 2015). The Aβ pathologies are supported by several other lines of genetic evidence. For example, a link has been reported between mutations in *APP* genes and changes in Aβ metabolism that subsequently affect Aβ aggregation and cognitive function in patients with AD (Godbolt et al., 2006; Lan et al., 2014). Further, there is also genetic evidence for a link between mutations in the β- and γ-secretase genes and AD (Citron et al., 1992; Levy-Lahad et al., 1995; Sherrington et al., 1995; Rogaev et al., 1995).

Finally, it should be noted that Aβ deposits are complex structures that also include several other co-aggregating proteins, such as ApoE, APOJ, and midkine, as well as hundreds of other co-localizing proteins, such as proteins involved in metabolism, endocytosis, and other cellular processes (Bastrup, 2019; Martin-Rehrmann et al., 2005; Namba et al., 1991; Yasuhara et al., 1993) and proteins involved in immune responses (e.g., immunoglobulins), complement and inflammatory response, blood coagulation, hemostasis, and molecular transport, among others (Rahman & Lendel, 2021). Overall, the pathologies related to Aβ are myriad and highly complex, and there is a huge amount of research on all of these pathological mechanisms that goes beyond the scope of this review. Nonetheless, the findings unanimously point to Aβ as

the starting point of the AD pathologies that further leads to other pathologies related to tau and other proteins, inflammation, oxidative stress, and various metabolic dysfunctions.

Tau-related pathologies

The tau protein consists of three major domains—an amino-terminal projection domain, a carboxyl-terminal domain, and a short tail sequence (Ittner and Götz, 2011). Tau proteins are synthesized by neuronal cells and associate with microtubules to provide strength and polarity to, and support the growth of, neurons (Kumar and Singh, 2015). Tau proteins are encoded by the *MAPT* gene located on chromosome 17 (Neve et al., 1986). The human brain contains six tau isoforms, which form as a result of alternative splicing of exons 2, 3, and 10 (Ittner and Götz, 2011). Tau is found in its highest concentration within axons, but it has also been detected in dendrites at lower concentrations (Sotiropoulos et al., 2017). Tau proteins are thought to play a role in the stabilization of microtubules and the regulation of motor-driven axonal transport (Sotiropoulos et al., 2017). However, like Aβ, the tau protein is evolutionarily conserved, and its role in the human body is extensive and includes myelination, pathways for glucose metabolism, iron homeostasis, learning and memory, and neuron formation and neuronal excitability, among others (reviewed in Kent et al., 2020).

Tau is highly phosphorylated during the development of neurons, and lower levels of phosphorylation are observed in mature neurons. Analysis of patients with AD indicates that tau is highly phosphorylated even in mature neurons (Khan and Bloom, 2016). The hyperphosphorylation leads to tau detaching from the microtubules at these phosphorylation sites (Schneider et al., 2004). Consequently, the ability to stabilize microtubules and axonal transport regulation is lost or severely compromised, and this mechanism could contribute to

the development of AD. Studies have indicated that the hyperphosphorylated form of tau can also compromise mitochondrial respiration and axonal transport (Ittner et al., 2009).

Hyperphosphorylated tau accumulates within the somatodendritic compartment of neurons and gradually leads to the formation of NFTs, which are observed as paired helical filaments. The spread of NFTs in the brain is characteristic of the progression of AD (Querfurth and LaFerla, 2010; Braak and Braak, 1995). However, as observed for Aβ plaques, age-related tau pathologies that are not associated with any major cognitive impairment are common (Crary et al., 2014), although their distribution in the brain appears to differ in comparison to AD-related tau pathologies (Walker, Fudym, et al., 2021; Walker, Richardson, et al., 2021). The accumulation of aggregated tau in the NFTs begins in the allocortex of the medial temporal lobe and spreads to the isocortex. This is similar to the pattern of spread of Aβ plaques, which also first accumulate in the isocortex before spreading to the enthorhinal cortex and hippocampus (Lane et al., 2018).

Similar to the classification of Aβ spread in the progressive phases of AD described by Thal et al. (2002), Braak and colleagues (1991) proposed the progressive stages of the spread of NFTs in AD: stage I: transentorhinal region of the hippocampal formation; stage II: subiculum region of the hippocampal pyramidal cell layer; stage III: entorhinal cortex and the entire hippocampal pyramidal cell layer; stage IV: inferior temporal cortex and neocortical areas such as the superior temporal cortex and the frontal cortex; stage V: peristriate area of the occipital cortex; stage VI: striate area. Stages I and II are asymptomatic, and stages V and VI are strongly associated with clinical signs of dementia (similar to the staging for Aβ) (Braak et al., 1991). Based on the spread of tau in neurons across adjacent connected areas of the brain, it has been proposed that tau may have a prion-like spreading mechanism (Dujardin & Hyman, 2020). Further, extracellular vesicles in the brain may play a role in this mechanism of spread, as demonstrated by a recent study on a mouse model (Ruan et al., 2021).

In addition to the pathologies of NFTs composed of hyperphosphorylated tau, some other pathologies associated with tau have been reported. For example, a higher ratio of 4R (a tau isoform with four microtubule-binding repeats) to 3R (a tau isoform with three microtubule-binding repeats) has been linked to transcriptional changes in the Wnt signaling pathway (Chen et al., 2011). Further, higher levels of tau were found to be associated with inhibited vesicle and organelle transport and lead to an increase in oxidative stress (Stamer et al., 2002), as well as affect axonal transport (Dixit et al., 2008). In addition, mislocalization of tau to the dendritic spine can affect cognition and synapses *in vivo* (Hoover et al., 2010; Miller et al., 2014). With regard to the genetic basis of these tau pathologies in AD, in mouse models, tau mutations have been linked with severe neurotoxicity and neuropathologies (Allen et al., 2002; Yoshiyama et al., 2007). Further, somatic mutations of *PIN1* and various other genes in the brain have been associated with increased tau phosphorylation and aggregation, as well as the progression of tau pathologies (Downey et al., 2022; Park et al., 2019).

Given that both amyloids and NFTs originate in the same location of the brain, there is evidence that the hyperphosphorylation of tau is caused by the oxidative damage induced by Aβ oligomers (Kurz and Perneczky, 2011; Ma et al., 2009; De Felice et al., 2008). Moreover, considering that age-related Aβ and tau pathologies (in isolation) are not associated with major cognitive impairment (Crary et al., 2014; Dickson et al., 1992), understanding the interaction between both pathologies in the context of AD is important.

Interaction between amyloid-β- and tau-related pathologies

Although it has been well documented that both Aβ and tau can cause toxicity through their own distinct pathways, there is also evidence for their interactions in dementia pathologies. Specifically, it is believed that Aβ has the ability to drive tau pathology **(Figure 1.12)**. Studies

on mice with APP mutations have demonstrated that the formation of Aβ leads to tau hyperphosphorylation, while these were not observed in mice with tau mutations (Götz et al., 2004). This was confirmed by a study on a three-dimensional human stem-cell-derived culture system in which hyperphosphorylated tau and tau aggregates were observed only after Aβ deposition (Choi et al., 2014). In addition, when synthetic Aβ was injected intracranially into mutant tau-transgenic mice, the NFT pathology was disrupted (Götz et al., 2001). One of the proposed mechanisms by which Aβ drives the tau pathology is the dysregulation of exon splicing of the tau protein, which leads to the formation of tau isoforms that are more prone to hyperphosphorylation (Lagunes et al., 2014). In addition, Aβ may also exacerbate the tau pathology at later disease stages, as it has been found that misfolding of the tau protein may be mediated by both newly forming amyloid plaques and older and more mature deposits of Aβ (Xu et al., 2022).

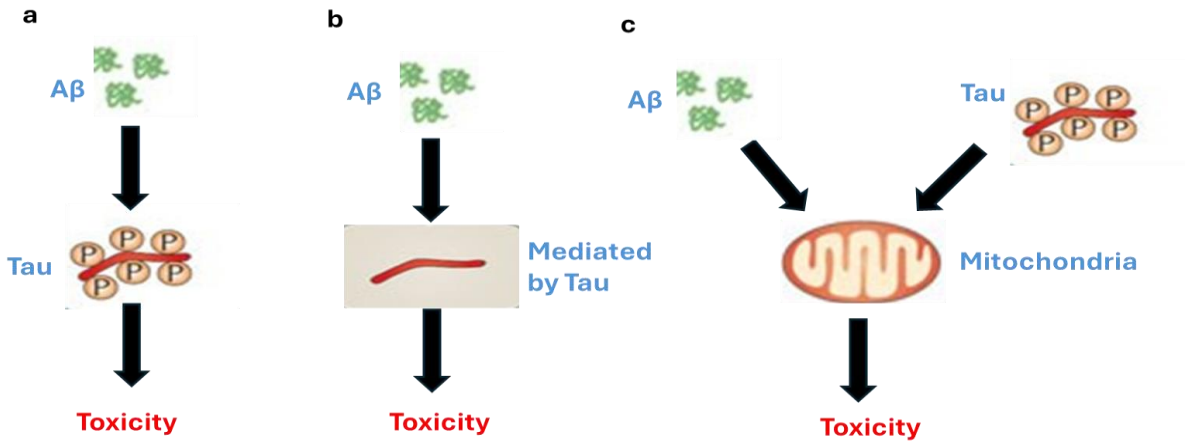

Figure 1.12. Interactions between Aβ and tau in neuronal pathologies. (a) Aβ causes tau hyperphosphorylation, which leads to toxicity in neurons. (b) Tau mediates Aβ toxicity. (c) Both Aβ and tau exert toxicity by targeting cellular components such as mitochondria (Ittner and Götz, 2011). The figure is reproduced with permission (Copyright 2011, Nature Reviews Neuroscience).

Neuritic plaques, also referred to as senile plaques, might be the key to understanding the interaction between the two pathologies in AD, because dystrophic neurites have been found to be associated with both Aβ deposits and tau proteins in animal models (He et al., 2018). However, there is no evidence of direct binding between tau and Aβ (Chaudhary et al., 2020). Despite this, metformin treatment has been found to ameliorate both pathologies by increasing the phagocytosis of tau and Aβ plaques in dystrophic neurons (Chen, Zhao, et al., 2021). Thus, neuritic plaques comprising both protein bodies could be an important target for the treatment of AD, as the induction of immune responses against these plaques could result in the reduction of the two major mediators of AD pathogenesis.

Aβ and tau have been found to work synergistically to cause several behavioral and transcriptional deficits in mouse models of AD (Pickett et al., 2019). Research into the mechanisms has shown that the tau protein is required for Aβ-mediated disruption of long-term potentiation in the hippocampus (Shipton et al., 2011). Importantly, the synaptic pathology of AD is believed to be the result of both Aβ and tau proteins (Crimins et al., 2013). Despite the observed synergistic interactions, evidence from imaging and cognitive function studies indicates that tau proteins, and not amyloid, are the major drivers of structural and cognitive abnormalities in AD (Rubinski et al., 2020; Dubbelman et al., 2023). In fact, positron emission tomography imaging of Tau is considered the main marker of AD, especially in more advanced disease stages.

With regard to the underlying molecular pathways, it has been suggested that Aβ and tau may interact *via* intermediate molecules such as kinases, *e.g*., GSK-3β and ERK (Zheng et al., 2002). In fact, a genetic link has been reported between the *GSK3β* and *APBB2* genes, and it is argued that *GSK3β* is involved in both these primary pathologies of AD (Hohman et al., 2015). Overall, research so far indicates that the two proteins may not have a strictly hierarchical

relationship, but rather, they may co-localize and exert synergistic effects by amplifying each other's toxicities (reviewed in Zhang et al., 2021).

Treatment of Alzheimer's disease

Overview of pharmacological and non-pharmacological treatment approaches

Because of the complex and multifactorial pathogenesis of AD, treatments that target single factors or only one aspect of the disease are unlikely to yield successful results. Instead, multipronged treatments that target several pathologies over a period of time might be more promising. Accordingly, therapies are focused on early and precise diagnosis, reduction of the symptoms, and decrease in the rate of disease progression.

As discussed above, Aβ and tau exist in toxic species that contribute to the spread of the disease, and, therefore, the main focus of research has been to block aggregation of these peptides to halt disease progression (Nelson and Tabet, 2015). The anti-β-amyloid monoclonal antibody lecanemab has shown promising results in this regard and recently received first approval from the US Food and Drug Administration (FDA) (Hoy, 2023). In addition, aducanumab, which targets the clearing of Aβ deposits, has also received approval from the FDA (Pardo-Moreno et al., 2022). Therapies that target tau clearance and aggregation have mostly focused on immunotherapies, but none of these trials has yet reached phase 3 (reviewed in Vaz & Silvestre, 2020). Another treatment approach is the correction of synaptic dysfunction and promotion of neural regeneration, for which several trials are ongoing. The trials on the quinolone derivative cilostazol report particularly promising results in terms of reducing Aβ and tau levels and ameliorating memory deficits (reviewed in Ju & Tam, 2022). Targeting loss of cholinergic innervation, which is associated with cognitive decline in AD, is another therapeutic strategy, and three cholinesterase inhibitors, namely, donepezil, galantamine, and rivastigmine, have so

far received approval from the FDA **(Figure 1.13)** (reviewed in Ju & Tam, 2022). In addition, agents that target glutamatergic, GABAergic, and monoaminergic neurotransmission, as well as other modes of neurotransmission related to the decline in cognitive function in AD, have been under research (reviewed in Ju & Tam, 2022). Therapy such as cholinesterase inhibitors and N-methyl-D-aspartate receptor antagonists are used in order to reduce the progress of the disease however these approaches still have varied results and its success is often dependent on the severity of the disease (Anand and Singh, 2013; Shi et al., 2016). However, despite the extensive research on therapeutic modalities for AD, their efficacy has been limited and an optimal multipronged approach is still lacking.

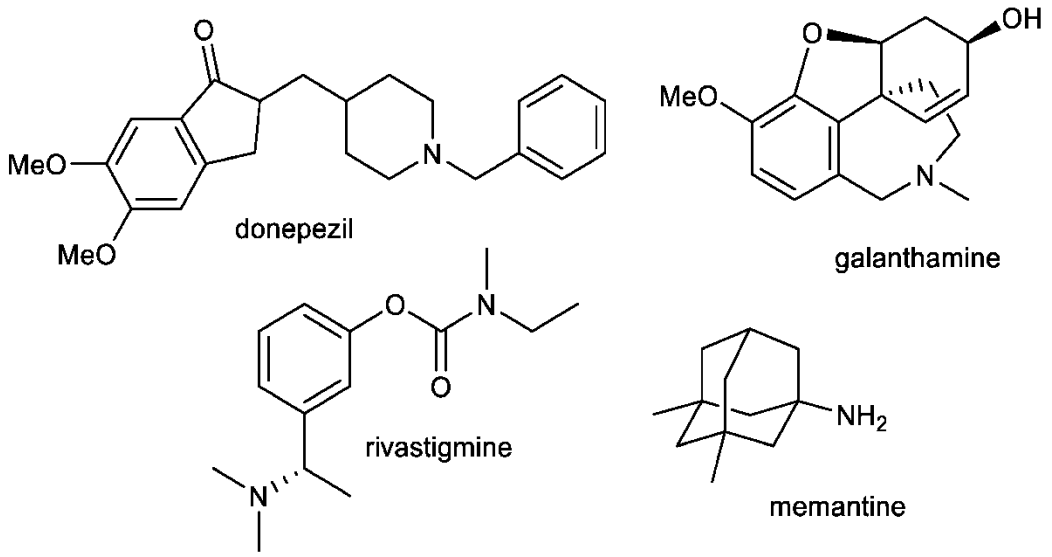

Figure 1.13. Chemical structures of available drugs for Alzheimer's disease. (Donepezil, galantamine, rivastigmine and memantine) (Vrabec et al., 2023).

As currently there is no cure for Alzheimer's disease, and instead therapies are focused on early and precise diagnosis, reducing the symptoms and decreasing the rate of disease progressions. Studies have also suggested that non-pharmacological approaches, such as nutrition supplementation, changes in lifestyle, and dietary changes, can influence the onset and progression of AD. Compounds that prevent or disrupt the formation of amyloid fibrils and filaments *in vivo*, known as anti-aggregation drugs, remain the focus of research for degenerative diseases like AD where amyloid aggregation is thought to play a significant role (Habchi et al., 2017; Saunders et al., 2016). Most notably, the Mediterranean diet has been found to improve cognitive function as well as reduce the progression of the disease. Naturally occurring polyphenols consumed as part of a normal diet, have therapeutic potential as some have been shown to impede Aβ and tau aggregation and destabilize fibrils, whilst having little if any toxicity at dietary levels (Porat et al., 2006; Casamenti and Stefani, 2017; Omar, 2019). These aspects are discussed in detail in the next sections.

Antioxidant effect of natural polyphenols and disease

Polyphenols have been found to have strong inhibitory effects against oxidative stress and inflammatory mechanisms in a range of diseases. The antioxidant effects of polyphenols are mediated by their ability to scavenge peroxyl radicals, act as metal chelators and prevent copper sulphate-induced oxidation of low-density lipoprotein (LDL), promote the transcription and activity of various antioxidant enzymes such as superoxide dismutase, and regulate AMPK signalling (reviewed in Bucciantini et al., 2021). While research on these antioxidant molecular mechanisms of polyphenols has its limitations and still requires a lot of work, a large number of studies in the literature have demonstrated how these antioxidant effects, in combination with anti-inflammatory and other mechanisms, ameliorate the risk of several aging- and lifestyle-related diseases.

In vitro studies on human and rat cardiomyocytes have shown that polyphenols may have cardioprotective effects that are mediated by its anti-inflammatory, antioxidant, antithrombotic, and vasodilatory properties (Otręba et al., 2021). It has also been reported that the polyphenols in olive oil may exert beneficial cardiovascular effects through their ability to lower LDL cholesterol levels by binding to LDL cholesterol and reducing its oxidation (Castañer et al., 2012). In addition, their cardioprotective effects may be linked to their ability to increase the level of HDL cholesterol (Hernáez et al., 2014) and promote the anti-inflammatory activity of HDL (Loued et al., 2013). In fact, each 10 g/d increase in the consumption of extra virgin olive oil was found to decrease the risk of cardiovascular disease and mortality by 10% and 7%, respectively (Guasch-Ferré et al., 2015).

There is considerable evidence from *in vitro* and animal studies to show that polyphenols could also be useful for treating non-alcoholic fatty liver disease based on the inhibition of hepatic fat accumulation *via* anti-inflammatory, antioxidant, and insulin resistance modification mechanisms (reviewed in Abenavoli et al., 2021). While there is a lack of conclusive evidence from clinical trials on non-alcoholic fatty liver disease, studies on the effect of polyphenols on the features of metabolic syndrome, such as diabetes and obesity, may point to potential benefits in the case of non-alcoholic fatty liver disease, too. For example, consumption of polyphenols has been linked to a reduction in obesity based on measurements of weight, BMI, and hip and waist circumference in several studies (Guo et al., 2017; Marranzano et al., 2018; Wang et al., 2014). Moreover, consumption of olive oil with a high polyphenol content has been found to be linked to a decrease in both fasting blood glucose and HbA1c levels (Santangelo et al., 2016). Finally, it is possible that polyphenols present in olive oil also reduce the risk of cancer through mechanisms that include decreasing the bioavailability of carcinogens, protecting against oxidative stress, inhibiting cancer-promoting and metastasis-

related enzymes, and regulating tumor cell cycle progression and gene expression (reviewed in Bucciantini et al., 2021).

In terms of AD, considerable research has been carried out on the inhibition of amyloid-related diseases by small synthetic or natural molecules. The discovery of anti-aggregation drugs that impede the formation of fibrils and filaments *in vivo* continues to be a major therapeutic goal (Pokrzywa et al., 2017; Coelho et al., 2016; Saunders et al., 2016; Habchi et al., 2017; Konijnenberg et al., 2016; Joshi et al., 2016; Porat et al., 2006; Ono et al., 2003). Anti-aggregation agents obtained from natural products are attractive from a therapeutic perspective because they can be consumed as part of a normal diet, are readily available, and have low toxicity. In this regard, aromatic-rich compounds, including natural polyphenols such as flavonoids, phenolic acids and some vitamins have been shown to alter the aggregation kinetics or restructure many amyloidogenic proteins into nontoxic species and have an affinity for the cross-β-structure, rather than the sequence of the protein (Konijnenberg et al., 2016; Porat et al., 2006; Ono et al., 2003; Townsend et al., 2018; Stefani and Rigacci, 2014). The majority of current *in vitro* studies focus on the main three or four polyphenol compounds in olive oil, namely, oleocanthal and oleuropein and its hydrolytic products tyrosol and hydroxytyrosol (Casamenti and Stefani, 2017; Daccache et al., 2011; Monti et al., 2012; Pitt et al., 2009; Ladiwala et al., 2011); few groups have addressed the potential combined neuroprotective effects of other olive oil polyphenols in attenuating both Aβ and tau amyloidosis. In a recent study, luteolin and elenolic acid emerged as the most potent compounds in olive oil in terms of their effects on several AD pathologies (Hachani et al., 2023). Another emerging olive oil compound is ligstroside, which has been found to alleviate mitochondrial dysfunction in mouse models of AD (Grewal et al., 2020).

Inhibitors of amyloidosis

The design of anti-aggregation molecules that act on amyloidogenic proteins is a particularly difficult area in drug design, in part because how typical proteins aggregate is only poorly understood. As a result, the majority of the small molecules that have been found to have antiamyloid effects have tended to be broad spectrum amyloidogenic protein inhibitors, rather than having protein-specific inhibitory activity (Härd and Lendel, 2012; Townsend, 2016). Such molecules, which are often found by screening extensive libraries/databases of known compounds, have the disadvantage that they often interact with the fluorescent marker molecules used to determine the extent of amyloid deposits. For example, in research on islet amyloid polypeptide (IAPP) amyloidosis, the small molecule rifampicin, which can inhibit amyloidosis, interacts with both ThT and Congo Red (Meng et al., 2008; Buell et al., 2010). Bulic et al. (2009) surveyed research into the inhibition of tau aggregation and found that of 200,000 screened compounds, 77 had been identified as having inhibitory action on tau aggregation. These compounds could be categorized into four groups: the N-phenylamines, anthraquinones, phenylthiazolylhydrazides, and thioxothiazolidinones, all of which share certain structural properties or functional groups (Bulic et al., 2009; Townsend, 2016). Specifically, such research stressed the importance of both ring structures and hydrophobic loci on candidate molecules (**Figure 1.14**), to maximize the potential for hydrogen bonding to the target protein (Bulic et al., 2009; Townsend, 2016).

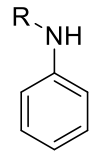

(1) N-phenylamines

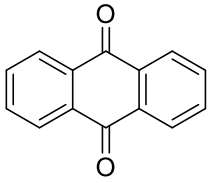

(2) 9,10-anthraquinones

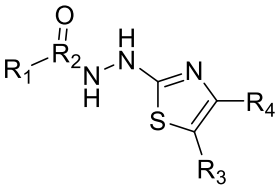

(3) Phenylthiazolylhydrazides

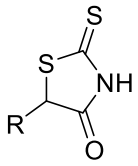

(4) Thioxothiazolidinones

Figure 1.14. Compound groups known to inhibit tau aggregation: (1) N-phenylamines, (2) 9,10-anthraquinones, (3) phenylthiazolylhydrazides (Townsend, 2016; Pickhardt et al., 2007), and (4) thioxothiazolidinones (Townsend, 2016; Bursavich et al., 2007).

Altering compounds of small molecular size in order that they possess specific properties, such as disrupting fibril formation, is a much less complex task than it is with larger molecules. For example, by modifying the specific orientation of the hydroxyl groups of inositol compounds, they can be made to inhibit or promote the aggregation of Aβ into β-sheet structures (Townsend, 2016).

Research indicates that scyllo-inositol (**Figure 1.15 A**) can stabilise small sized soluble Aβ complexes, resulting in an inhibitory effect on Aβ aggregation, with no TEM-detectable fibrils remaining. The key mechanism is the same as it is with the tau compounds – the hydrogen

bonding between the inhibitor and the soluble Aβ monomer – and thus the key molecular sites are hydrophilic ones. For example, unlike scyllo-inositol, 1,4-dideoxy-scyllo-inositol (**Figure 1.15 B**) contains less hydroxyl groups and its inhibitory effect is much less pronounced, with TEM capable of detecting the presence of intermediate length fibrils. Thus, the hydroxyl groups appear to be essential for the compound's inhibitory action. However, increasing the hydrophobicity of the compound by attaching two methyl groups (**Figure 1.15 C**) at the same time stops fully-elongated fibrils from forming, by stabilising the (usually cytotoxic oligomeric) proto-filament intermediate (Townsend, 2016; Hawkes et al., 2010). The reason the hydroxylation of the inhibitor is important for its anti- aggregation effects is likely attributable to the hydrogen bonding it promotes between its hydroxyl groups and the peptide's amides (Churches et al., 2014; Hudson et al., 2009; Porat et al., 2006; Townsend, 2016). Once this bound species is formed, it may stabilize small oligomeric species or Aβ monomers. Another possibility is that it alters the aggregation pathway of Aβ, in a similar manner to that proposed for the green tea polyphenolic compound EGCG. Their activity is thought to be in part dependent on the coplanarity of the aromatic substructures within the molecule, plausibly by promoting interactions related to π -stacking and hydrophobicity (Churches et al., 2014; Carver et al., 2010). The cross-β sheets typical of Aβ aggregates also allows rigid planar molecules to intercalate within them (Townsend, 2016; Churches et al., 2014; Convertino et al., 2009).

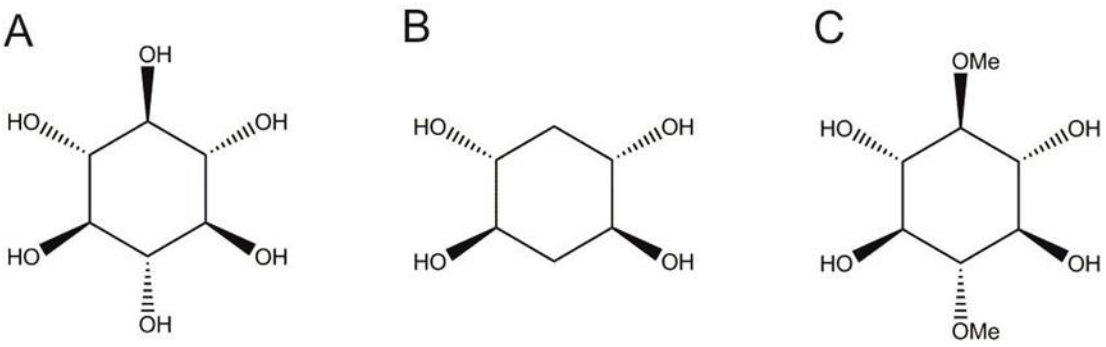

Figure 1.15. Scyllo-inositol and derivatives: (A) scyllo-inositol, (B) 1,4-dideoxy-scyllo-inositol, and (C) 1,4-di-O-methyl-scyllo-inositol (adapted from Townsend, 2016).

Further, fifteen out of 169 screened compounds, one of which was dopamine, have been found (*in vitro*) to have anti-aggregation activity on α-synuclein. However, while both dopamine and levodopa (**Figure 1.16** demonstrated their chemical structures) have an inhibitory effect on α-synuclein, such inhibitory action brings with it an increase in cytotoxic protofibrils (Townsend, 2016; Conway et al., 2001). Such interactions illustrate the challenge drug designers face creating molecules that have minimal adverse effects when used pharmacologically as well as inhibitory actions on amyloid aggregation (Townsend, 2016). In the next section will be discussed the ability of natural phenols to inhibit amyloid.

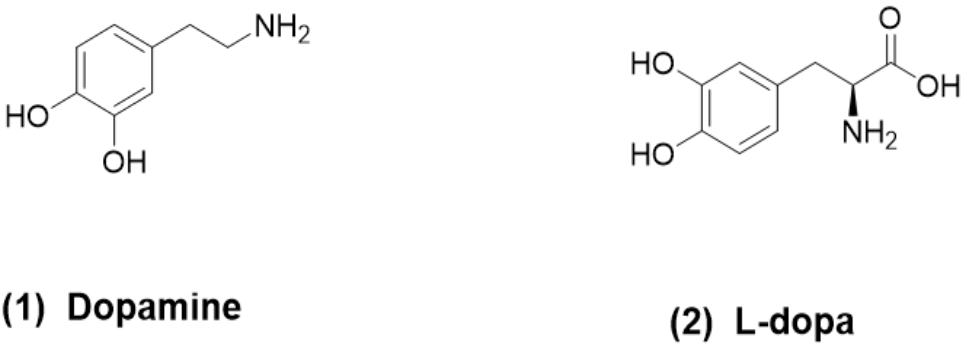

Figure 1.16. Chemical structures of dopamine (1-left) and levodopa (2-right) (Conway et al., 2001).

Natural phenolic molecules as inhibitors of amyloidosis

In this section will be discussed the mechanism and biochemistry of natural polyphenol-mediated amyloid fibril inhibition.

Attention has recently focused on naturally occurring polyphenols' inhibitory effect on the formation of amyloid fibrils, as well as their ability to destabilize or disaggregate already formed fibrils (Ngoungoure et al., 2015; Stefani and Rigacci, 2013). Alzheimer's disease (AD) is one of several human diseases, not all of which are neurological, which have been linked to amyloid fibril aggregation. Natural polyphenols' ability to disrupt protein self-assembly, and to do so in many of those proteins found in the fibrillar assemblies linked to diseases like AD, gives them great potential in the treatment of this class of human diseases (Ngoungoure et al., 2015). The fact that these compounds are quite widely distributed in edible plants is an added advantage, as their intake can be controlled relatively simply by changes in dietary habits. Currently some naturally occurring polyphenols that appear to have anti-amyloid effects are already undergoing clinical trials as treatments for AD or for its progression (Velander et al., 2017). These include curcumin (found in turmeric), resveratrol (found in red grape skin) and epigallocatechin-3-gallate (EGCG) (found in tea).

The major mechanism responsible for amyloid disease is thought to be the self-assembly of amyloid proteins into toxic oligomeric and fibrillary aggregates. Consequently, developing therapeutic compounds that prevent or disrupt amyloid protein aggregation is seen as a promising research strategy. The diverse biochemical activity of natural polyphenols, which has been studied extensively, includes antioxidant, anti-inflammatory, and neuroprotective actions, that makes them potentially important compounds for preventing the pathological tissue reactions related to deposits of amyloidogenic proteins (Ngoungoure et al., 2015).

Finding means to inhibit Aβ aggregation is, therefore, one of the goals of research on AD and its prevention or retardation (Hamaguchi et al., 2009). Currently, 44 natural polyphenolic compounds have been found to have inhibitory or modulating effects on Aβ aggregation, some of which play a crucial role in amyloid fibrillogenesis. The search for more inhibitors of amyloid aggregation continues, with more polyphenols being discovered to have potentially inhibitory effects (Phan et al., 2019; Velander et al., 2017; Ngoungoure et al., 2015).

Naturally occurring polyphenols exert their inhibitory effect on amyloid formation through several different mechanisms and on different pathways involved in assembly. They also exert the inhibitory action on a range of amyloid structures, from monomeric to oligomeric and fibrillar. Some have an inhibitory effect on oligomer formation, but a promoting one on fibril formation, while others inhibit fibril formation but have no effect on oligomers, and so forth **Figure 1.17**. A further example of the diversity and complexity of polyphenolic activity can be seen with epigallocatechin gallate (EGCG), which alters the way oligomers are constructed in such a way as to favour the formation of non-fibrillogenic types over fibrillogenic ones (Ngoungoure et al., 2015).

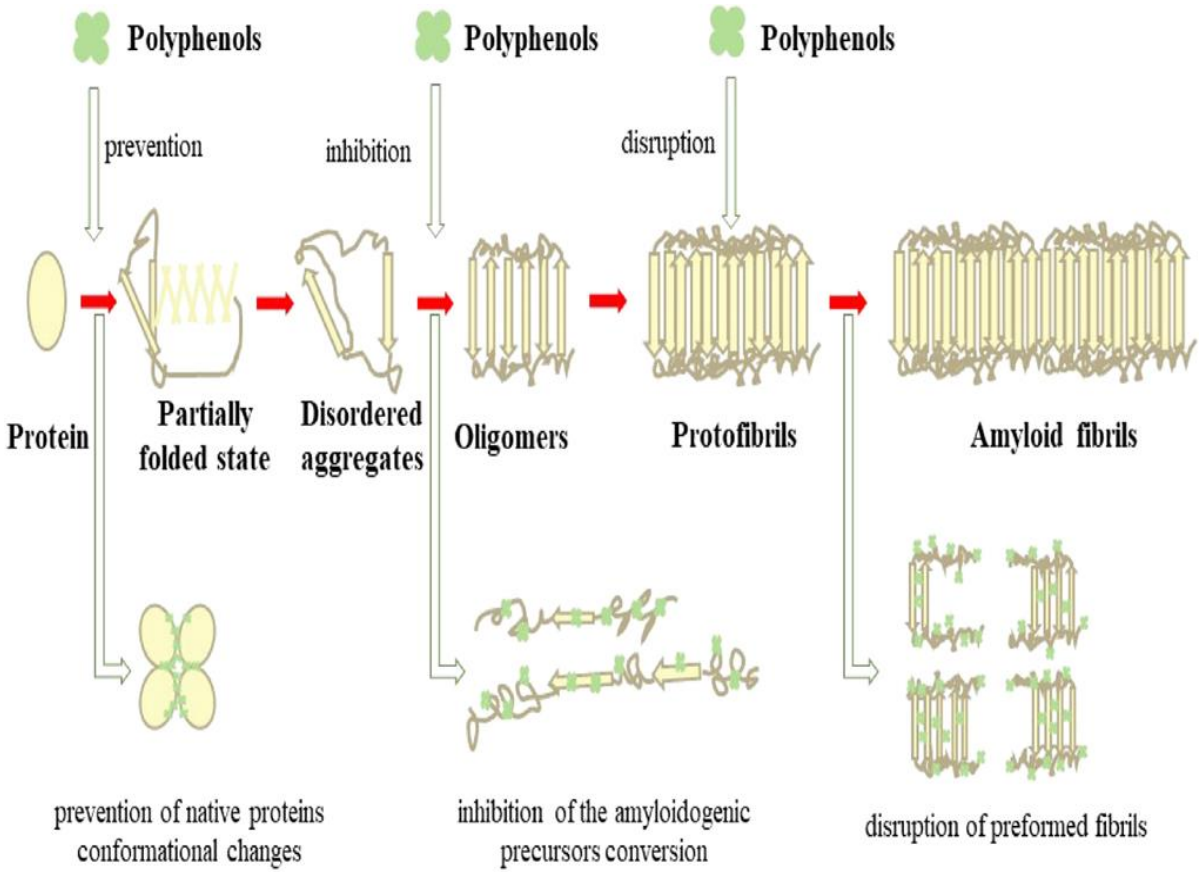

Figure 1.17. The mechanism and different pathways of polyphenols to inhibit amyloid formation. Pathways of polyphenols (top left) prevention of native proteins, (top middle) inhibition of amyloidogenic proteins and (top right) disruption of fibrils (adapted from Ruan et al., 2022). The figure is reproduced under a Creative Common CC BY license (Copyright 2022, Maximum Academic Press).

Naturally occurring polyphenols have aromatic rings and one or more singly or multiply hydroxylated phenolic rings which can interact with amyloidogenic proteins' aromatic residue. This interaction impedes the self-assembly of the protein into amyloid fibrils. Examples of these plant-based compounds include oleuropein, resveratrol, silybin, curcumin, rosmarinic acid, tannic acid, baicalein, piceid, ferulic acid, EGCG, salvianolic acid B, kaempferol, myricetin, quercetin, morin, catechin, and epicatechin their chemical structures shown in **Figure 1.18**. These polyphenols contain one or more phenolic rings whose hydroxyl groups

account for their hydrophobic interaction with proteins. The interaction of the phenol rings in the polyphenols and the aromatic components of the amyloidogenic proteins, is thought by some authors to be the inhibitory mechanism. This interaction prevents the $\pi - \pi$ interaction, and in consequence the β-structure's protein units can no longer stack, which in turn prevents the self-assembly that results in amyloid fibril formation (Ngoungoure et al., 2015).

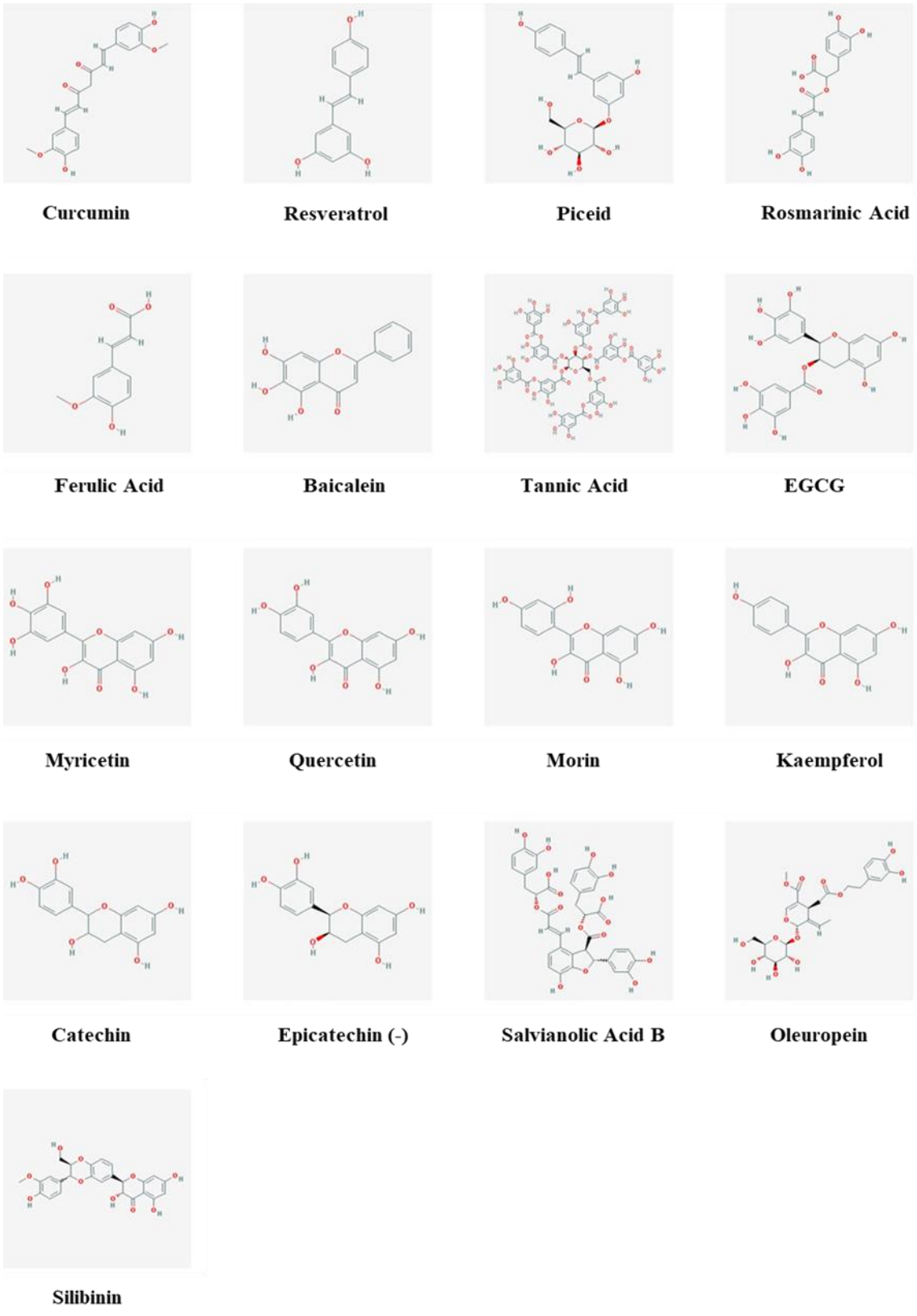

Figure 1.18. Chemical structures of natural polyphenol compounds that exhibit anti-amyloidogenic activity (Ngoungoure et al., 2015). The figure is reproduced with permission (Copyright 2015, Wiley Online Library).

In conclusion the number of polyphenols found in plants is very large, but their abilities to bind to amyloid has rarely been the focus of research. Those where this property has been studied, however, show highly potent effects in preclinical models. The availability of high throughput screens makes it very likely that further natural polyphenols will be found to possess significant anti-amyloidogenic effects. The identification of such compounds will provide a pipeline of candidate molecular structures for the design of new pharmaceutical drugs, formulations, or imaging agents. Increasing the intake of polyphenols in an individual's daily diet may therefore be an important factor in the prevention of amyloidosis and could be a target of nutraceutical methods to reduce Alzheimer disease and other amyloid diseases (Ngoungoure et al., 2015). The next sections will discuss the most significant polyphenol components of olive oil that have shown promise in the treatment of AD.

Polyphenols from EVOO as potential therapy for Alzheimer's disease

Oleocanthal

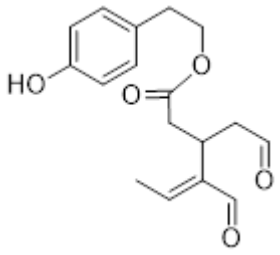

Figure 1.19. Chemical structure of oleocanthal.

One of the most researched phenolic components is oleocanthal (**Figure 1.19**), which has been shown to have anti-inflammatory and antioxidant properties that are comparable to those of the widely used as anti-inflammatory drug ibuprofen (Rigacci, 2015). More interestingly, it was

found to have potential neuroprotective properties that could prevent cognitive decline in diseases such as AD (Daccache et al., 2011). This notion has been supported by population-based studies that have compared the prevalence of AD between populations consuming Mediterranean and non-Mediterranean diets (Qosa et al., 2015). For example, a study conducted in the USA reported a 40% reduction in the prevalence of AD when subjects consumed a Mediterranean diet (Scarmeas et al., 2009). Various mechanisms that lead to this decrease in incidence have been proposed. Li et al. (2009) suggested that oleocanthal inhibits NFT formation. It is believed that oleocanthal acts directly on tau proteins and prevents NFT formation (Li et al., 2009). Other researchers have suggested that oleocanthal actually acts on Aβ plaques. For example, Pitt et al. (2009) demonstrated that oleocanthal has the ability to interact with Aβ and is able to change its oligomerization state, converting it to a nontoxic form and, thereby, conferring a neuroprotective effect (Pitt et al., 2009). A recent study by Abuznait et al. (2013) reported that oleocanthal has the ability to increase the capacity of the brain to clear substances. The study found that oleocanthal lead to upregulation of Aβ-degrading enzymes, which led to a higher rate of degradation and clearance of Aβ (Abuznait et al., 2013). In addition, a recent study on a mouse model of AD demonstrated that the therapeutic effects of oleocanthal may also be related to its ability to target multiple inflammatory mechanisms and reduce inflammation (Abdallah et al., 2023). Further, another study on a mouse model revealed that oleocanthal may alleviate mitochondrial damage in the brain associated with AD (Grewal et al., 2020). Oleocanthal has also been found to counter oxidative stress and improve cell metabolism in neurons (Angeloni et al., 2019). Improving blood–brain barrier function though inhibition of the NLRP3 inflammasome might be yet another mechanism *via* which oleocanthal improves cognitive function (Al Rihani et al., 2019). The mechanistic studies on oleocanthal are extensive, and some of the other suggested mechanisms underlying its neuroprotective effects include a decrease in interleukin-1β, increase in BDNF, and promotion

of neurogenesis and synapse formation in the hippocampus (reviewed in Kothawade et al., 2023).

Oleuropein aglycone

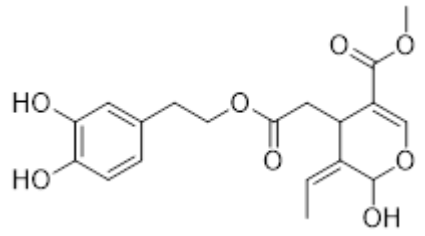

Figure 1.20. Chemical structure of oleuropein aglycone.

Oleuropein aglycone (OLE) its chemical structure is shown in **Figure 1.20** is a well-characterized polyphenol found in extra virgin olive oil. OLE is associated with a number of health benefits, including antioxidant, antidiabetic, antimicrobial, antiviral, cardioprotective, neuroprotective, and anti-inflammatory characteristics (Carrera-González et al., 2013; Fuentes & Palomo, 2014; Rubió et al., 2014; Sepporta et al., 2014). Further, antiatherogenic effects mediated through inhibition of endothelial activation have also been reported for OLE (Carluccio et al., 2003). With regard to its beneficial cognitive mechanisms, it has been found to improve synaptic activity and long-term plasticity in the hippocampus (Pu et al., 2005), as well as improve hippocampal post-tetanic potentiation and long-term potentiation (Luccarini et al., 2015).

Recent *in vivo* studies have suggested that OLE reduces cognitive impairment as well as improves synaptic function. These positive outcomes have been attributed to the inhibition of tau and Aβ aggregation and the stimulation of autophagy (Daccache et al., 2011; Diomede et al., 2013). Daccache et al (2011) investigated the anti-aggregation effect of OLE on tau protein *in vitro* and demonstrated that it could inhibit fibrillization of low-molecular-weight tau. Another study reported that OLE can inhibit Aβ aggregation in an animal model: OLE led to a

decrease in Aβ plaque deposition and reduced levels of toxic Aβ oligomers, and this was responsible for a reduction in the level of paralysis and an increase in life expectancy (Diomede et al., 2013). Further, OLE has been found to specifically inhibit S100A9 (Leri et al., 2021), which is both a proinflammatory and amyloidogenic protein, and this mechanism may explain the overall protective effect of OLE against neurodegeneration.

Studies have suggested that OLE can promote autophagy, the ability to clear substances from the body, which consequently leads to cognitive improvement *in vivo*. In a study using wild-type and TgCRND8-transgenic mice, supplementation of their diet with OLE led to an increase in the number of autophagic vesicles that was suggestive of an increase in the breakdown of Aβ and subsequent clearance from the body (Grossi et al., 2013). In addition to the increased breakdown and clearance of Aβ, OLE has also been found to improve blood–brain barrier function, and these two mechanisms may together contribute to its effect on improving memory function in AD (Abdallah et al., 2022).

Hydroxytyrosol and tyrosol

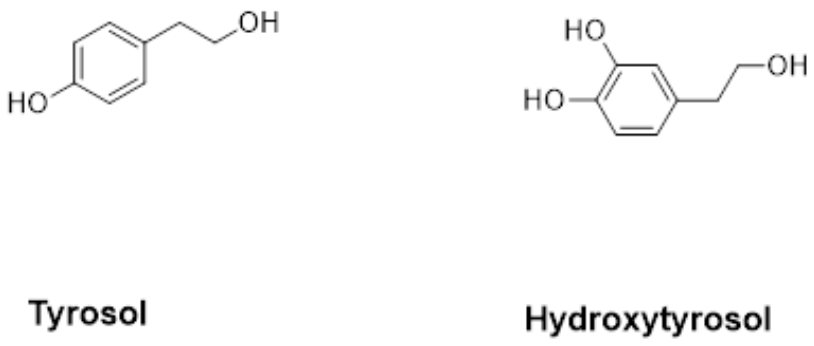

Figure 1.21. Chemical structures of tyrosol and hydroxytyrosol.

Hydroxytyrosol is an antioxidant phenolic found in olive oil. Its chemical structure can be seen in **Figure 1.21** on the right side. Beneficial effects of hydroxytyrosol on cognitive function have been demonstrated in a mouse model of AD (Qin et al., 2021). With regard to the

underlying mechanism, hydroxytyrosol was found to improve the metallomics profile (that is, the cellular distribution of metal ions) in a rat model (Tabanez et al., 2023). Further, it has been shown to be effective in reducing oxidative stress, mitochondrial dysfunction, and neural toxicity in specific disease states (Zheng et al., 2015). Specifically, hydroxytyrosol was found to increase mitochondrial activity in a cellular model of AD (Visioli et al., 2020). Further, it was found to directly interfere with the seeding and aggregation of Aβ oligomers in human neuroblastoma cells (Leri et al., 2019). In addition, a synergistic effect of hydroxytyrosol and OLE has been suggested that involves activation of autophagic flux and prevention of cellular damage by Aβ oligomers (Leri, Bertolini, et al., 2021). It has been suggested that because hydroxytyrosol can cross the blood–brain barrier, it can directly act to improve mitochondrial function, as well as decrease oxidative stress and inflammation in the brain (Liu et al., 2014; Peng et al., 2016). In addition to these effects, hydroxytyrosol has been found to exert antiatherogenic effects, mediated through inhibition of endothelial activation (Carluccio et al., 2003). Overall, hydroxytyrosol appears to have a wide range of potent neurological effects on multiple neurological conditions, including AD, and could have potential as a novel drug or functional ingredient for the prevention and treatment of such diseases (reviewed in Chen, Ai, et al., 2021).

Tyrosol is another polyphenol found in olive oil. Its chemical structure is shown in **Figure 1.21** on the left side. It has been hypothesized that tyrosol has protective effects against Aβ-induced toxicity. In this regard, both hydroxytyrosol and tyrosol have been found to protect *in vitro* neuroblastoma cells against Aβ-induced toxicity (St-Laurent-Thibault et al., 2011). Their mechanism is related to the reduction of the activity of the transcription factor NF-kB, which is responsible for mediating some neurotoxic effects of Aβ deposits (St-Laurent-Thibault et al., 2011). Thus, the anti-inflammatory effect of both hydroxytyrosol and tyrosol may hold the key to their neuroprotective effects.

EVOO is rich in phytochemicals, some of which, particularly the polyphenols, have potentially beneficial pharmacological effects. Given that EVOO is also a natural part of many people's diet, understanding how its polyphenols influence the aggregation of both Aβ peptide and tau proteins, is of great interest. To date, however, there has been no reported comprehensive assessment of the phenolic fraction (mixture) of EVOO fatty acids.

In summary, AD is a neurodegenerative disease with a complex pathology that mainly involves Aβ and tau deposits in the brain, among several other co-pathologies. Extra virgin olive oil has the potential to be used in the treatment of AD. The polyphenol components within olive oil hold the most promise in the treatment of neurodegenerative diseases. In particular, oleocanthal and oleuropein, both polyphenols found in extra virgin olive oil, have attracted attention over the last decade. Both are believed to reduce the progression and symptoms of AD through their action on both Aβ-containing plaques and tau-related pathologies. It is hypothesized that the polyphenols within olive oil can reduce Aβ production, enhance the clearance of toxic substances such as Aβ oligomers, and reduce tau hyperphosphorylation. Because of the aging of the population, the management of AD is becoming a major societal challenge. Current treatment options have only shown modest effects in treating selected symptoms, and there are no treatments that can completely cure or reverse this condition. There is evidence to suggest that the active components of olive oil could be advantageous in the treatment of AD, but more research is required on the details of their underlying mechanisms. As discussed above, the most extant reports of in-vitro studies of the polyphenolics in EVOO have targeted oleuropein, oleocanthal, and hydroxytyrosol. As far as we are aware, there have been no published evaluations of the phenolic mixtures isolated from the fatty acid component of EVOO. In this research project, we investigate the ability of these mixtures, and other individual polyphenols found in EVOO that have not been studied in detail for their ability to modulate amyloid formation by Aβ peptides and tau proteins.

Aims of the research:

The aims of the research in this thesis were firstly to investigate and understand the effects of mixtures and individual phenolic compounds derived from natural olive oil products on the aggregation of the Alzheimer's amyloid-β peptide and tau. Secondly, this research aimed to synthesise solid lipid nanoparticle to enhance the therapeutic viability of these polyphenols. Finally, we aimed to apply a range of techniques in this work to obtain a good understanding.

The objectives of the research were to:

- Find a suitable and the most effective method for extracting the polyphenolic components of EVOO. This work will be shown in **Chapter 4**.
- Prepare water soluble extracts of olive oil from different sources. This will be outlined in **Chapter 4**.
- Analyse the composition of different olive oil preparations to separate, identify, quantify, and characterize the main polyphenolic compounds that are considered to be biologically active in a mixture or individual phenol at preventing amyloid formation for treating AD. A range of techniques will be used including chromatography, mass spectrometry and NMR spectroscopy. This will be shown in **Chapter 4**.
- Prepare and implement a methodology for the expression and characterization of labelled (^{15}N) and unlabelled, amyloid proteins. This will be shown in **Chapter 3**.
- Investigate and determine how a mixture of polyphenols isolated from Greek and Saudi Arabia EVOOs, and individual phenolic compounds affects the aggregation propensity of Aβ40 and tau and/or the properties of the aggregates. The binding of polyphenols to protein aggregates will be determined using a co-sedimentation experiment, and the effects of polyphenols on Aβ40 and tau aggregation will be examined using a range of techniques including ThT fluorescence, circular dichroism, transmission electron

microscopy, HPLC, UV-Vis and dynamic light scattering. Additionally, the structure of Aβ40 aggregates formed in the presence of polyphenols, and with polyphenols added (after aggregation has ceased) will be determined *via* SSNMR and compared to Aβ40 aggregates alone. Finally, to apply computational modelling of individual polyphenol compounds to fibrillar structural models of amyloid β and tau using Molsoft ICM Pro software. This will be shown and discussed in **Chapter 5**.

- Synthesis of nanoparticles and use of different techniques for characterization of the polyphenols in solid lipid nanoparticles. This will be shown in **Chapter 6**.

Chapter 2 (Experimental Techniques for Analysis)

Overview

This chapter aims to give a background and introduction to some of the main techniques used for analysis of polyphenols found in natural products. Also, this chapter will show techniques used for analysis of amyloid β (proteins). These techniques will be performed in the experimental chapters 3,4,5 and 6 to examine polyphenols ability to modulate amyloid formation.

Chromatography to analyse natural products

High-performance liquid chromatography (HPLC) for analysing polyphenols

Relative to chemistry and biochemistry, one potent analytical tool for component separation, identification, and quantification is high-performance liquid chromatography or HPLC (Ali, 2022). The adsorption-separation concept is the bedrock of HPLC. The chemicals to be separated are delivered in a mixed form into the HPLC column. Still, different components move at different rates due to their varying affinities for the stationary phase. A slower rate of movement is seen for components with a higher affinity for the stationary phase, as compared to a faster rate of movement for components with a lower affinity. The components are separated because no two compounds have the same affinity for the stationary phase. **Figure 2.1** shows the main parts of the HPLC system (Bhati et al., 2022).

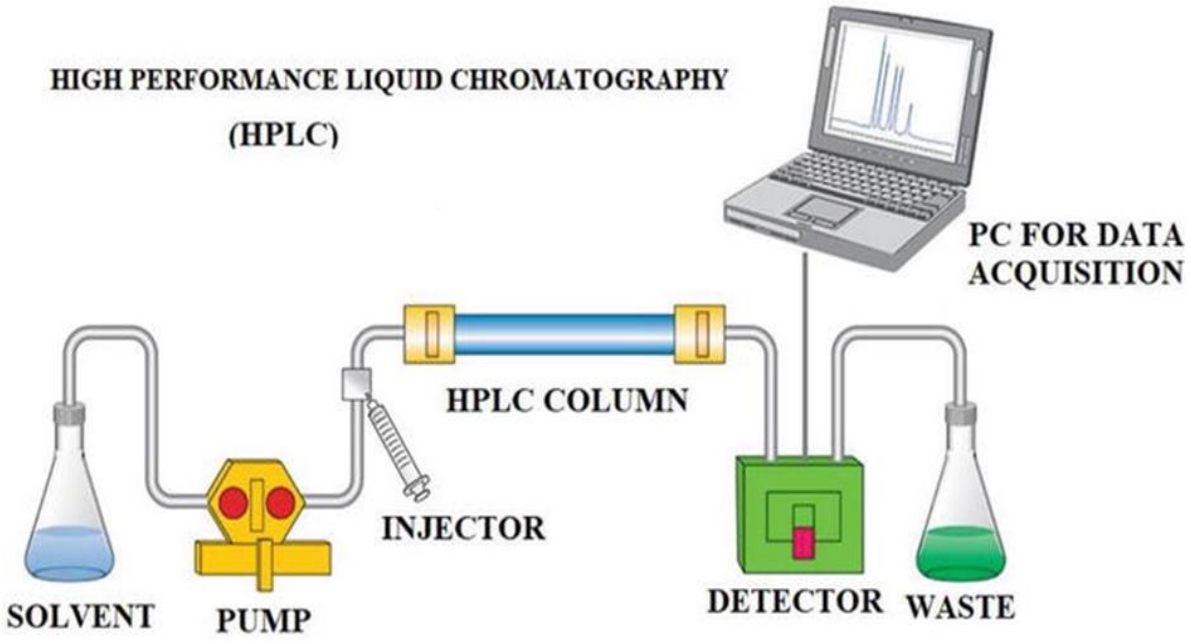

Figure 2.1. Schematic Representation of HPLC (Deshpande, 2020; Bhati et al., 2022)**.** The figure obtained with permission (Copyright 2020, IntechOpen).

The liquid chromatography method uses high-pressure pumps to transfer the sample-containing solvent through a stationary phase-packed column. The mobile phase describes the liquid solvent that moves the sample from one location in the column to another. Its selection depends on the analytes' separation characteristics (Ali, 2022). Mobile phases often consist of a combination of water and organic solvents, such as methanol or acetonitrile. A solid or densely packed bed of particles is the usual stationary phase in these columns. A variety of compounds must be considered while deciding on a stationary phase. Besides, an autosampler is used to inject the sample into the system. An accurately measured and controlled sample quantity may be introduced into the mobile phase by regulating the injection volume (Ali, 2022).

Moreover, compound separation occurs in the column **Figure 2.1**, an essential component. It contains a stationary phase that separates the sample components by interacting with them differently. Eluted components are detected when they travel through a detector. The most common detectors are mass spectrometers, fluorescence detectors, and ultraviolet-visible

spectrophotometers. Chromatograms, which show the concentration of various components with time, are created from signals recorded by the detector. Also, the components in the sample are identified and quantified by analysing the data collected from the detector. The concentration of each analyte is determined by generating chromatograms and then analysing the peak regions or heights (Ali, 2022).

Applications of HPLC in the field of natural products

HPLC's great sensitivity, efficiency, and accuracy make it a popular tool in many industries, including medicine, environmental science, food and drink testing, and clinical research. Combine it with other analytical methods, such as mass spectrometry, to characterize compounds in more depth, and it separates complicated mixtures with high resolution. Many examples can be found in the literature such as medicinal plants from the Rosaceae family have a lengthy historical record of traditional use in treating neurological diseases. *Sorbaria tomentosa* Lindl. Rehder comprises polyphenolic compounds with antioxidant and neuroprotective properties **Figure 2.2** (Mahnashi et al., 2023).

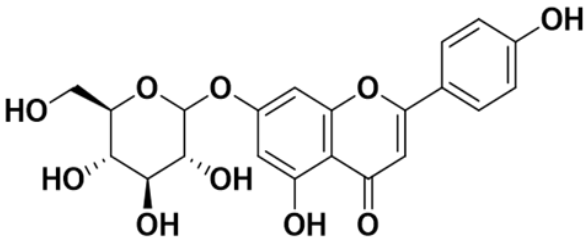

Apigenin-7-glucoside

Figure 2.2. Medicinal phenolic plant (*Sorbaria tomentosa*) the plant image was adapted from (Flickr, accessed online in 2025). The figure is reproduced under a Creative Common CC BY license (Copyright 2025, Flickr online).

The purpose of the study by Mahnashi et al. (2023) was to investigate the phenolics profile using a high-performance liquid chromatography-photodiode array detector (HPLC-DAD) and to confirm the neuroprotective and anxiolytic properties of S. tomentosa using *in vitro* and *in vivo* experimental studies. **Figure 2.3** summarises the application of the HPLC in the field of natural products such as this study. The HPLC-DAD analysis detected significant levels of phenolic chemicals. In the case of St.Cr (*Sorbaria tomentosa* crude), a total of 21 phenolics were measured, including apigenin-7-glucoside (291.6 mg/g), quercetin (122.1 mg/g), quercetin-3-feruloylsophoroside-7-glucoside (52.6 mg/g), quercetin-7-glucoside (51.8 mg/g), ellagic acid (42.7 mg/g), luteolin (45.0 mg/g), kaempferol (40.5 mg/g), and 5-feruloylquinic acid (43.7 mg/g), which were found in higher concentrations; finally, the effects of identified compounds were studied *in vitro* and vivo (Mahnashi et al., 2023).

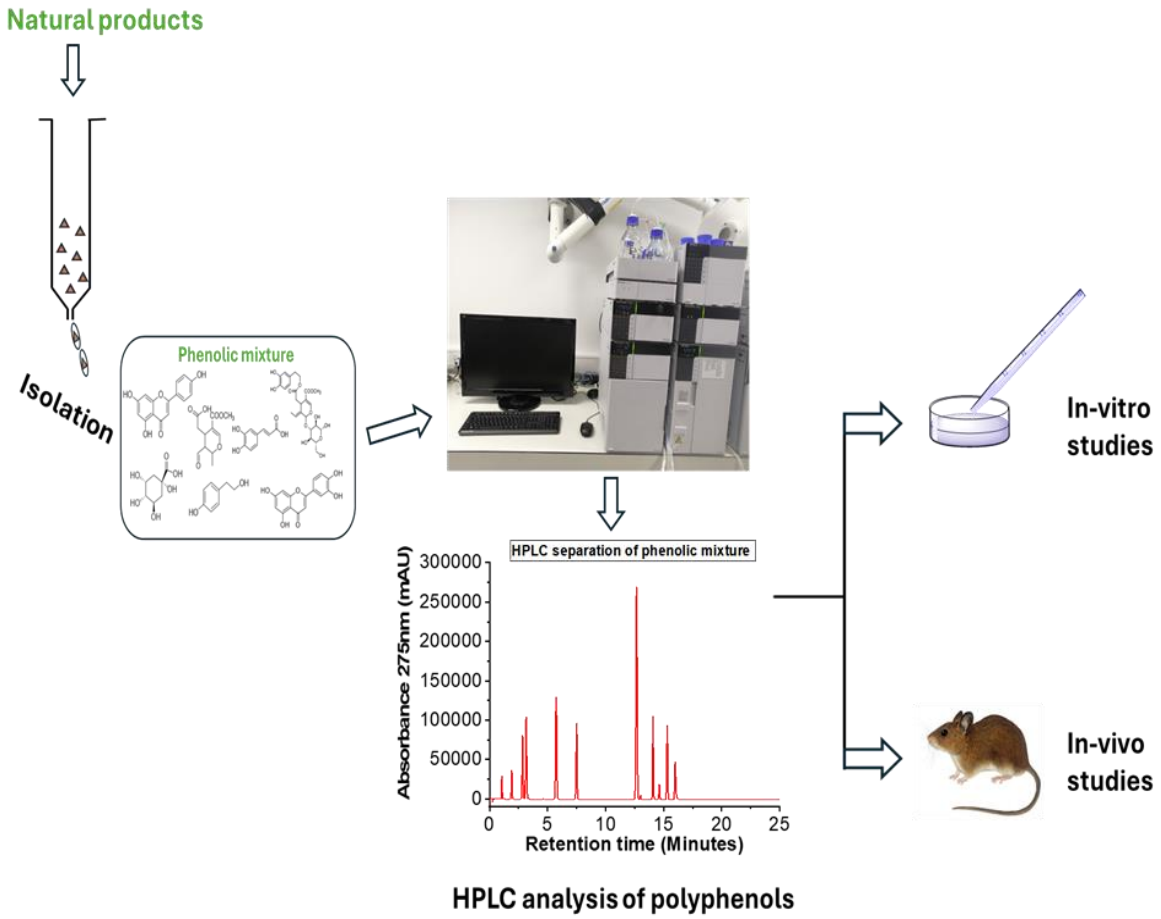

Figure 2.3. Scheme summarises the application of the HPLC to analyse and study natural products such as from *Sorbaria*, and that including polyphenols identification, quantification and studies *in vitro* and *in vivo*, © Bakri A.

Liquid chromatography-mass spectrometry (LC-MS) for analysing polyphenols

One technique that allows for the individual examination of chemicals is liquid chromatography (LC), which separates them in solution. The LC process starts with a chromatographic column, usually filled with a stationary phase. The stationary phase selection is contingent upon the characteristics of the compounds under examination. LC employs a liquid mobile phase, a solvent, to transport the sample through the column. The mobile phase composition can be modified to enhance separation efficiency (López-Fernández et al., 2020).

In LC-MS, the substances that the liquid chromatography column has separated are injected into the mass spectrometer. Ionization sources, such as electrospray ionization (ESI) or air pressure chemical ionization (APCI), transform the analyte molecules into ions. The mass analyser segregates ions according to their mass-to-charge ratio (*m/z*). Quadrupole, time-of-flight (TOF), and ion trap are often encountered types of mass analysers. The detector measures the relative amount of ions at various *m/z* values, producing a mass spectrum. The provided information is essential for the identification and quantification of the chemicals present in the sample as shown in **Figure 2.4** (Kiani et al., 2023).

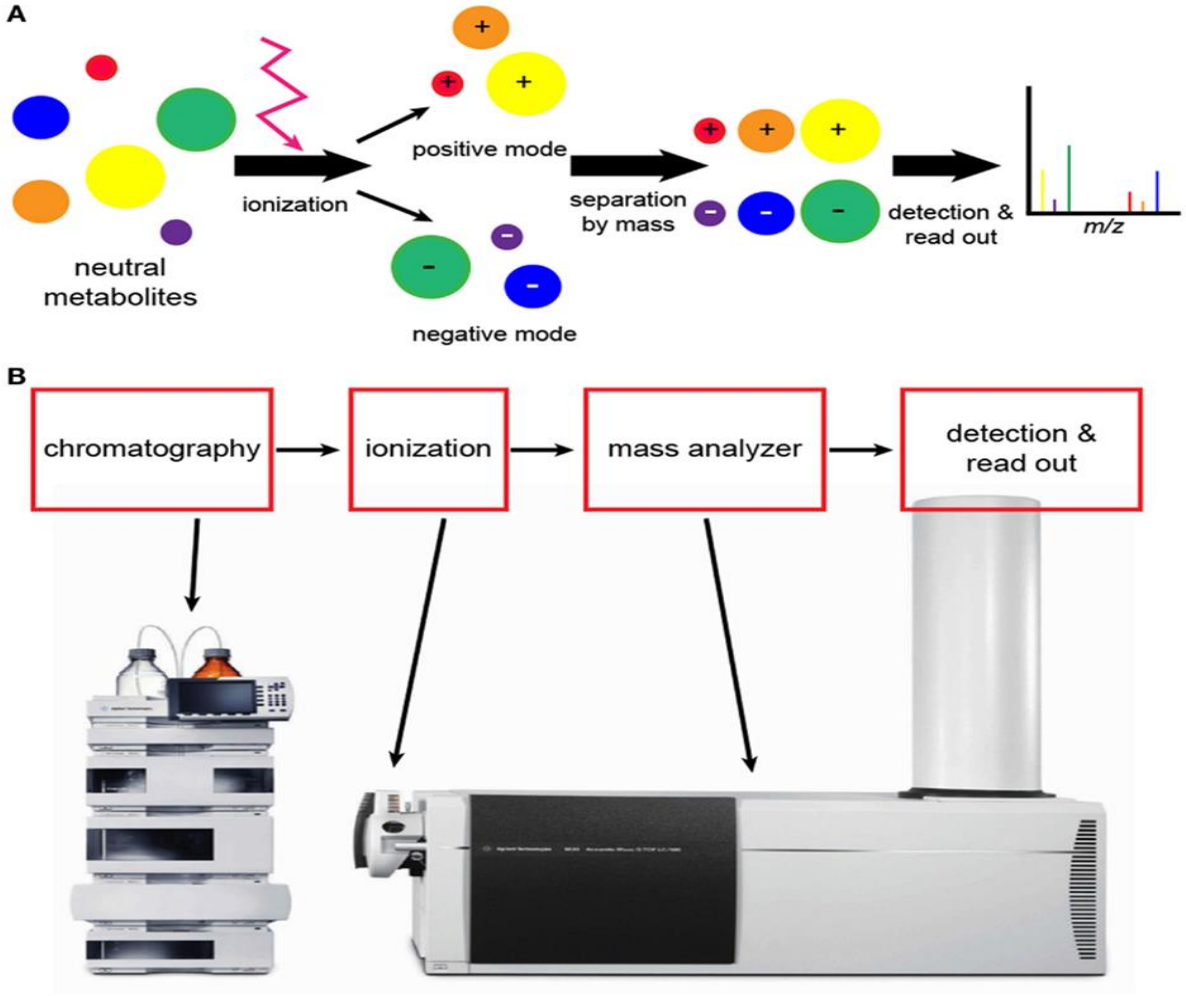

Figure 2.4. Schematic representation showing how the substances are detected in LCMS. Adapted from (Stringer et al., 2016).

The figure reproduced with permission (Copyright 2016, Frontiers in immunology).

Dedicated software is employed to interpret and evaluate the data produced by the mass spectrometer. These tasks encompass peak identification, deconvolution, and spectral matching. Mass spectra can be cross-referenced with databases of established chemicals to facilitate identification. LC-MS provides exceptional sensitivity and specificity, enabling the identification of substances present at deficient concentrations. It facilitates the examination of a broad spectrum of substances, spanning from diminutive molecules to substantial macromolecules. Integrating chromatographic separation with mass spectrometric detection amplifies the capacity to separate and characterize intricate mixtures. Optimizing the LC conditions is essential for attaining the most favourable separation. Accurate quantification requires the use of proper calibration and standardization procedures. Also, precise sample preparation is necessary to eliminate interference (Li and Zhu, 2020).

The MS identifies various molecules at various retention durations, which occur after injection when they depart the column. Chromatograms, which show the MS response *vs.* retention time, are generated from this. All the ions measured at a given retention period constitute this MS response. However, the MS keeps track of the *m/z* values, so it's possible to extract this data and create a chromatogram for a particular *m/z*. In that manner, a chromatogram of each molecule could be integrated separately (Van der Lee & Van den Pol, 2015).

Applications of the LC-MS in the field of natural products

Liquid chromatography–mass spectrometry is a powerful technique that has been widely used in the field of natural products to analyse and characterise molecules. There are many examples to show and below a recent application of the LC-MS used to identify phenolic compounds derived from *Caesalpinia crista* product.

The study by Chethana et al. (2018) aims to analyse plant extract fractions from *Caesalpinia crista* (C. crista) leaves **Figure 2.5** in order to identify the specific components contributing to their cholinergic and anti-amyloidogenic effects.

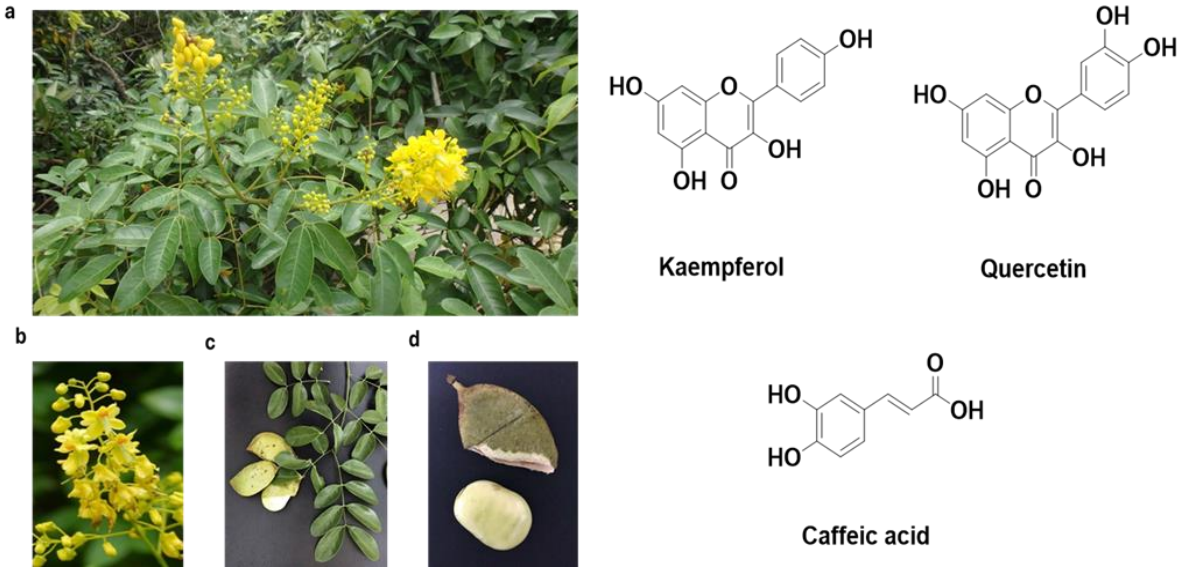

Figure 2.5. (a) medicinal phenolic plant (*Caesalpinia crista*), (b) flowers of *Caesalpinia crista*, (c) leaves (d) seed. Images were taken from (Chan et al., 2018; Flickr, accessed online in 2025). The figure is reproduced under a Creative Common CC BY license (Copyright 2025, Flickr online image (a) and copyright 2018, Japsonline images (b, c and d)).

This research explores the potential of these components for treating Alzheimer's disease. The study investigated the effects of C. crista extracts on the suppression of oxidative stress, cholinergic activity, and amyloidosis across various solvents with varying polarities. The DPPH total antioxidant test examined the antioxidant activity. The cholinergic assay was conducted using Ellman's technique, while the anti-amyloidogenic assay was performed using thioflavin-T fluorescence and transmission electron microscopy (TEM). The measurement of polyphenols was conducted using the HPLC fingerprinting method with the methanolic extract of C. crista (CCMeOH), in addition to LC-MS analysis and identification using the MS

LAMPS database a range of active phenolic compounds and their derivatives were detected such as quercetin, myricitin and kaempferol *etc*. The inclusion of polyphenols as the active components further corroborates these findings. **Figure 2.6** summarises the application and the use of the LC-MS in natural products such as this study. As a result, utilizing multi-potent target medication therapy has excellent potential in the treatment of Alzheimer's disease. The methanolic extract of *Caesalpinia crista* has promising efficacy against cholinergic enzymes and amyloid-β42 aggregation, along with antioxidant properties (Chethana et al., 2018).

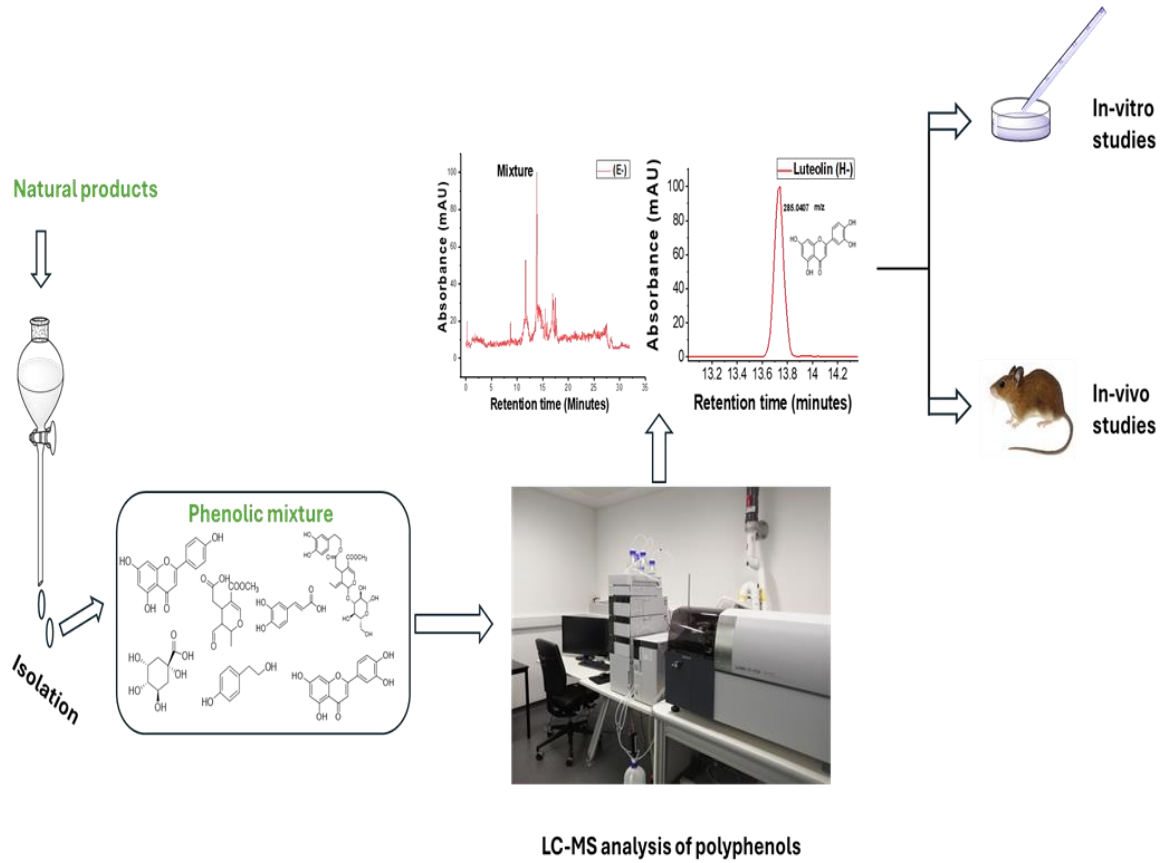

Figure 2.6. Scheme summarises the application of the LC-MS and shows how this method can be used to analyse and study natural products such as *Caesalpinia crista*, after isolation LC-MS applied for further identification, characterisation, quantification and studies *in vitro* and *in vivo*, © Bakri A.

Nuclear Magnetic Resonance Spectroscopy (NMR) for characterising polyphenols

Nuclear magnetic resonance (NMR) spectroscopy and imaging employ nuclear spins to investigate nearby atomic and electronic structures. Solution-state NMR is a widely used and well-established method for determining molecular structure in biochemistry, organic chemistry, and pharmaceutical research. In recent decades, there has been a significant advancement in solid-state NMR. While solution NMR and solid-state NMR share the same principles, solid-state NMR does not average out anisotropic and through-space NMR interactions like chemical shifts and dipolar, quadrupolar, and paramagnetic couplings (Li et al., 2021).

Solid-state SSNMR is a sophisticated analytical method that finds many uses in pharmaceutical research and development (R&D). The technique is well-acknowledged in structural biology for its ability to reveal intricate molecular information about biomacromolecular systems. Its primary objective is comprehending the basic chemical and biological mechanisms. Pharmaceutical interests encompass several areas, such as identifying the structure of ion channels and transporters as potential targets for drugs, studying the binding of ligands for drug development, investigating how drugs interact with cellular membranes, understanding the process of fibrilization in human amyloid disorders, and exploring supermolecular assembly (Li et al., 2021).

The NMR signal arises from the disparity in the total spin number between different energy states. For nuclei with a nuclear spin quantum number, I of ½, two spin states with distinct energy levels are denoted as $|\alpha\rangle$ and $|\beta\rangle$. The spin states of a nucleus are degenerate in the absence of a magnetic field but attain different energies. Upon applying an external magnetic field, B_0, the spins precess and the Zeeman interaction separates the energies of the different spin states according to their alignment with the magnetic field. The initial magnetization (M_0) at equilibrium is the disparity in magnetism between the two states, $|\alpha\rangle$

and |β>, which signifies NMR intensity (Li et al., 2021). The spin states are brought into resonance by applying electromagnetic radiation at radio frequencies (Rf) and the spins nutate about the B_0 to produce an oscillating signal. An NMR spectrum for the relevant nucleus is obtained by measuring and processing the signal by applying Fourier transformation. A schematic of the NMR principle is shown in the **Figure 2.7** below (Borisov et al., 2010).

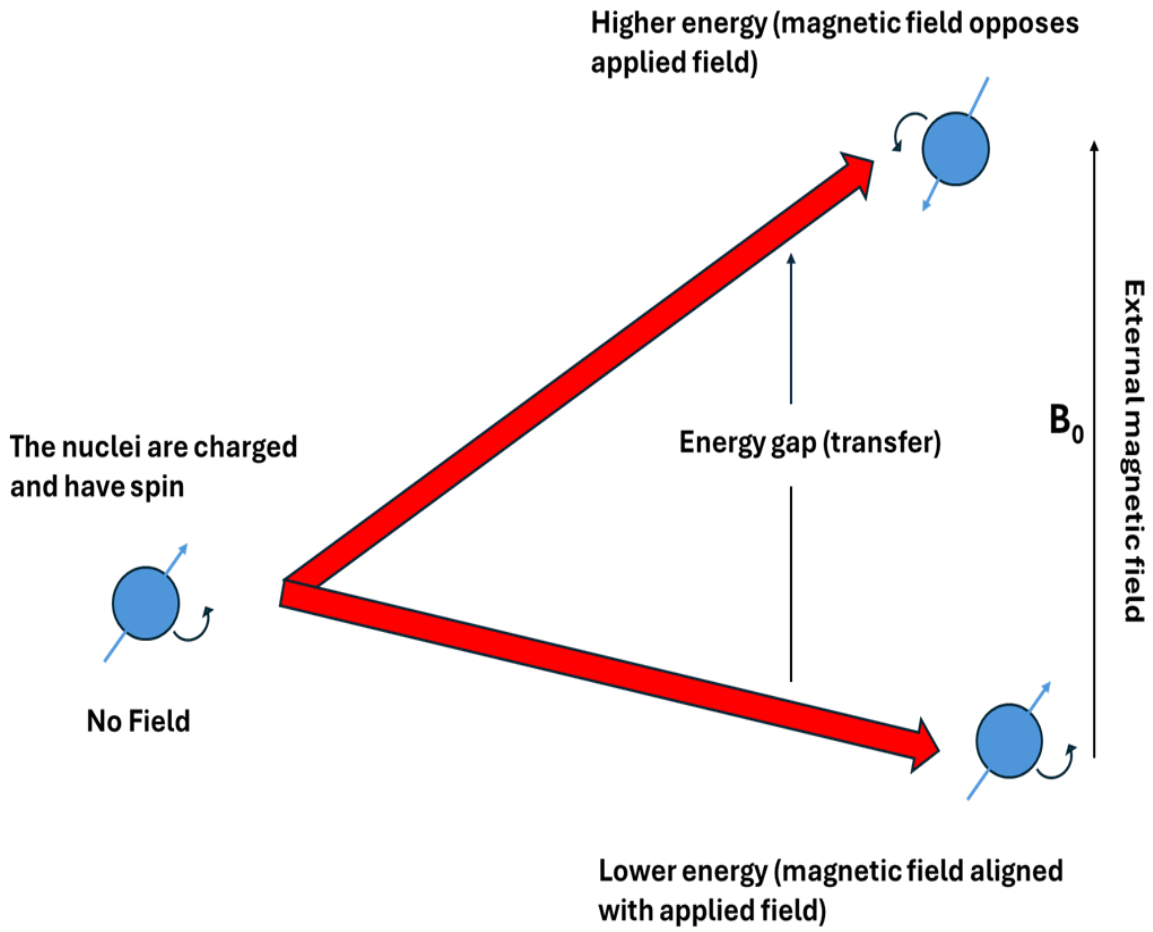

Figure 2.7. Representation of the nuclear magnetic resonance spectroscopy principle.

Equations (Li et al., 2021).

$$M_0 = -(1/2) * (N_{(\beta)} - N_{(\alpha)}) * \gamma\hbar B_0 = [n(\gamma\hbar)^2 B_0] / [4kT] \quad [\mathbf{2.1}]$$

S/N is the signal-to-noise ratio describing the sensitivity as shown below.

$$S/N = \sqrt{\omega_0} * M_0 \propto [n*(\gamma)^{\wedge} (5/2) * (B_0)^{\wedge} (3/2)] / T, \text{ considering } N \propto \sqrt{\omega_0} \quad [\mathbf{2.2}]$$

Equation [**2.1**] states that the bulk nuclear magnetization is directly proportional to the number of spins being considered. The integrated peak areas of NMR spectra are directly proportional to the number of nuclei or molecules that give rise to the peaks and is commonly used to identify a mixture's composition accurately. Hence, NMR quantification does not require a calibration curve constructed from samples with varying analyte percentages, commonly employed in spectroscopic, diffraction, and calorimetric techniques. Due to its quantitative character, SSNMR is frequently employed for calibrating other solid-state quantification methods, such as powder X-ray diffraction (PXRD), differential scanning calorimetry (DSC), and Raman spectroscopy (Li et al., 2021).

The spectrum of NMR in a solution exhibits narrow peaks from magnetically-inequivalent nuclei due to the fast-random tumbling that averages anisotropic NMR interactions (dipole-dipole and chemical shielding). In contrast, the spectrum of a solid-state NMR experiment will show the full range of interactions, including isotropic and orientation-dependent ones and consequently the peaks may be very broad. An example of ^{13}C NMR spectra of molecules in their solid and solution states are shown in **Figure 2.8** Dipolar interactions between coupled nuclei —which do not cancel each other out in a solid state—and Chemical Shift Anisotropy (CSA) are mainly responsible for the signal's wide shape in **Figure 2.8** (Borisov et al., 2010; Pranitha et al., 2011).

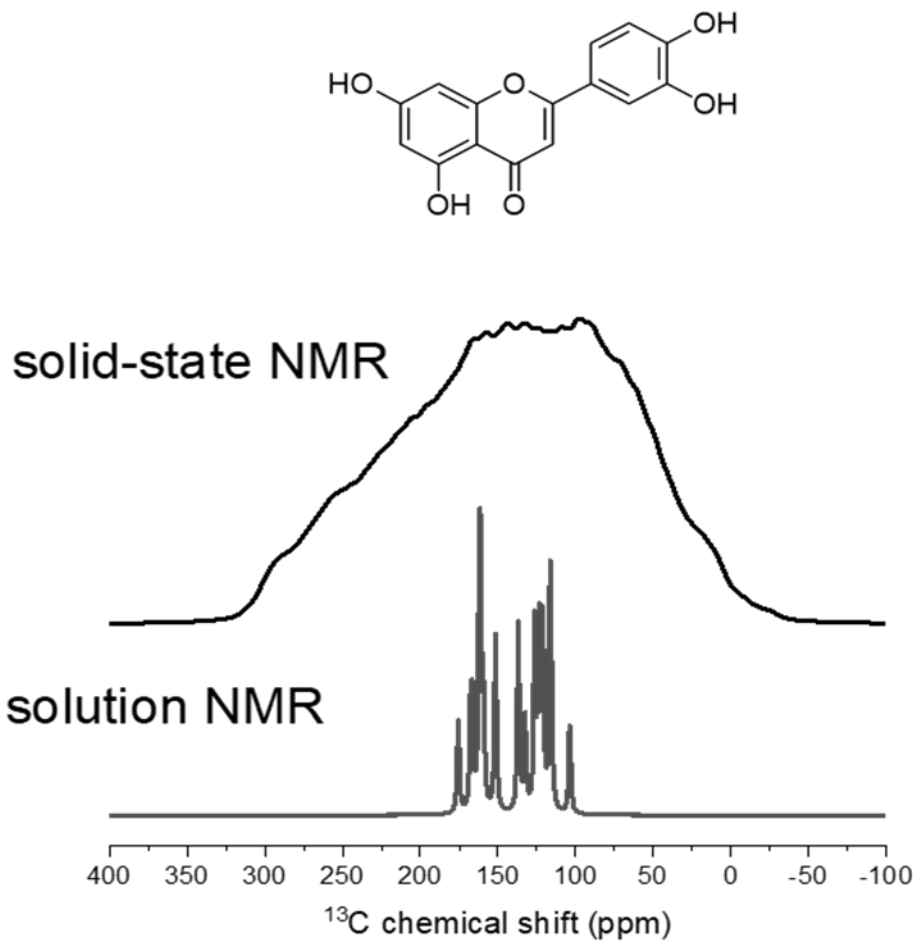

Figure 2.8. An example of ^{13}C NMR spectra of a molecule (the flavonoid quercetin) in the solid (top) and solution (bottom) states to illustrate the difference in peak widths. This figure was produced by Professor. D. Middleton.

Anisotropic interactions in immobile media (such as crystals, powders, big membrane vesicles, and molecular aggregates) significantly affect a system of nuclear spins. Both homo- and hetero-nuclear couplings are possible. When two nuclear spins are dipolar coupled, they experience the effects of each other's small magnetic field, which depends on the orientation of the through-space vector joining the two nuclei relative to B_0 (Borisov et al., 2010; Pranitha et al., 2011). Chemical shielding, whereby the magnetic field is generated by electrons surrounding the nuclei, is also orientationally dependent. These broadening effects can be

eliminated in solids by applying magic-angle spinning (MAS), in which the sample is rotated at an angle of 54.7° relative to B_0.

Transmission electron microscopy (TEM) for visualising amyloid fibrils

Transmission Electron Microscopy (TEM) is an advanced imaging method that employs a focused stream of electrons to investigate the intricate details of materials at an exceptionally high level of detail. Although TEM cannot be used to analyse polyphenols directly, it may be utilized to see the structure and arrangement of polyphenols within natural products at the subcellular or nanoscale level. The TEM can be used to study the effects of polyphenols on fibrils formation. A beam of high-energy electrons in TEM passes through a thin object, allowing for both elastic and inelastic scattering of part of the electrons (Pu, Gong and Robertson, 2020). The resulting beam can be gathered and examined using various methods, such as employing high-angle annular dark-field detectors (HAADF) to produce images that are sensitive to atomic number or measuring the energy loss of electrons that are scattered inelastically to obtain a distinctive spectrum known as electron energy loss spectroscopy (EELS). Using low-vapour-pressure liquids is the most direct method, as these liquids can withstand the extreme vacuum conditions of the TEM. Liquids can be seen using the same method as solid specimens in a transmission electron microscope (TEM) by directly applying the ionic liquid over a regular specimen grid (Pu et al., 2020).

Figure 2.9 the TEM consists primarily of an electron source known as a gun or electron cannon. This gun typically contains a V-shaped filament made of $LaB6$ (lanthanum hexaboride) or tungsten. An electric potential, positive to the anode, is applied to the filament (cathode), causing it to heat up and generate an electron current. The De Broglie equation [**2.3**] determines the wavelength of these electrons (Sierra, 2019).

$$\lambda = h / [2m_0 eV (1 + eV / 2m_0 c^2)] \wedge (1/2) \qquad [\mathbf{2.3}]$$

The variables in the equation are as follows: λ represents the wavelength, h represents the Planck constant, m_0 represents the residual mass of the electron, e represents the charge of the electron, V represents the potential difference, and c represents the speed of light. Before reaching the sample, the electron beam undergoes modifications through the condenser and aperture lenses to enhance the coherence of the light. The waves remain in the same direction with a consistent phase difference. Subsequently, the electron beam interacts with the sample, undergoing various processes. During these processes, the electrons that impact the sample are scattered in a way that prevents energy loss (elastic scattering) (Sierra, 2019).

Additionally, there are other processes in which electrons transfer some of their energy to internal electrons within the sample (inelastic scattering). Next, the objective lens focuses the dispersed beams to create the first picture through a diffraction process facilitated by the projection lens, which enlarges the electron beam and reflects it onto the phosphor screen. The idea of image resolution is closely linked to the changes in amplitude and phase of electron beams resulting from the effects of the objective lens. These changes are governed by the contrast transfer function (CTF), which may be expressed by equation [**2.4**] (Sierra, 2019).

$$CTF = A(q) \cdot exp\,[iX(q)] \qquad [\mathbf{2.4}]$$

The function $A(q)$ represents the diffraction diagram truncation caused by the aperture of the objective lens, whereas $\exp[iX(q)]$ represents the phase function that characterizes the distortion of the output wave caused by the objective lens. Based on this value, the contrast can vary. If the CTF is negative, the atoms will be displayed with a black contrast against a white backdrop. Conversely, they will appear with a white contrast against a black background (Sierra, 2019).

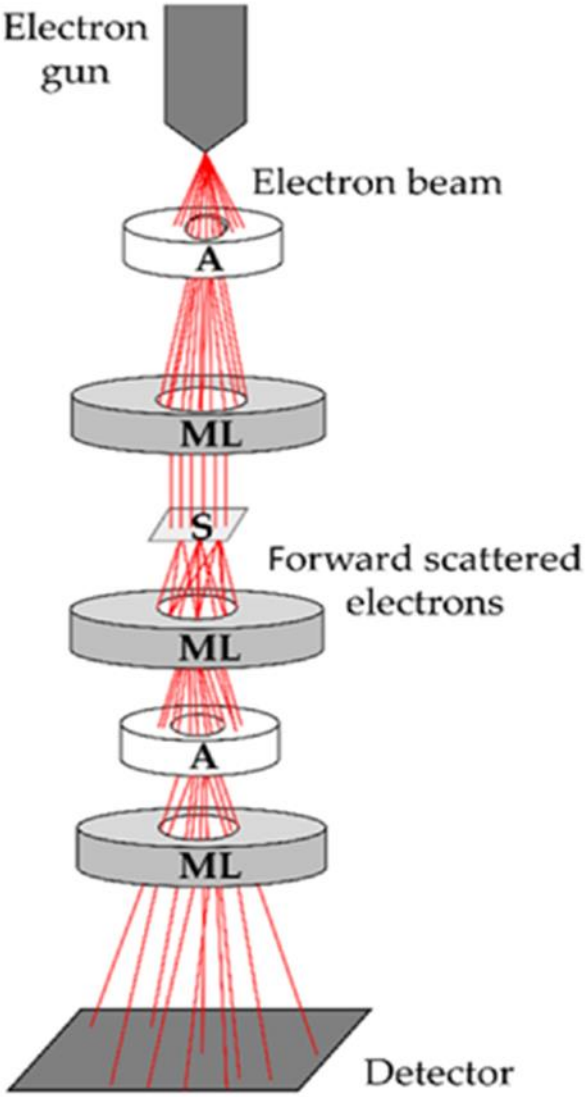

Figure 2.9. Transmission electron microscopy principle. Aperture (A), magnetic lens (ML) and sample (S) (Malenica et al., 2021). The figure is reproduced under a Creative Common CC BY license (Copyright 2021, MDPI).

Applications of transmission electron microscopy for visualising amyloid

Transmission electron microscopy is a powerful method, and it can be used to study proteins such as amyloid. Amyloid is defined as a protein which is deposited in the form of insoluble fibrils present within tissues as well as within extracellular spaces in organs (Townsend et al., 2018; Race et al., 2017). They can occur systemically or in localized areas such as around the brain as observed in Alzheimer's disease. Amyloid β has been shown to have a critical role in the progression of AD (Sadigh-Eteghad et al., 2015). Amyloid peptides, predominantly, Amyloid-β40 and Amyloid-β42 accumulate within the parenchymal tissue of the brain and assemble to form insoluble plaques which is a major characteristic of Alzheimer's disease. The cleavage of amyloid precursor protein (APP) lead to the creation of 39 to 42 amino acid peptide amyloid-β (LaFerla et al., 2007). This form of amyloid is prone to aggregation and folding which leads to the formation of plaques and leads to the formation of toxic species such as dimers, oligomers and fibrils (TEM images are shown in **Figure 2.10**). However, currently it is not understood which of these species is the toxic species. Despite limited knowledge of what species contribute toxicity, it is widely accepted that the postsynaptic compartment within synapses is the target of amyloid-β toxicity (Selkoe, 2002) (see **Chapter 1** for more detail).

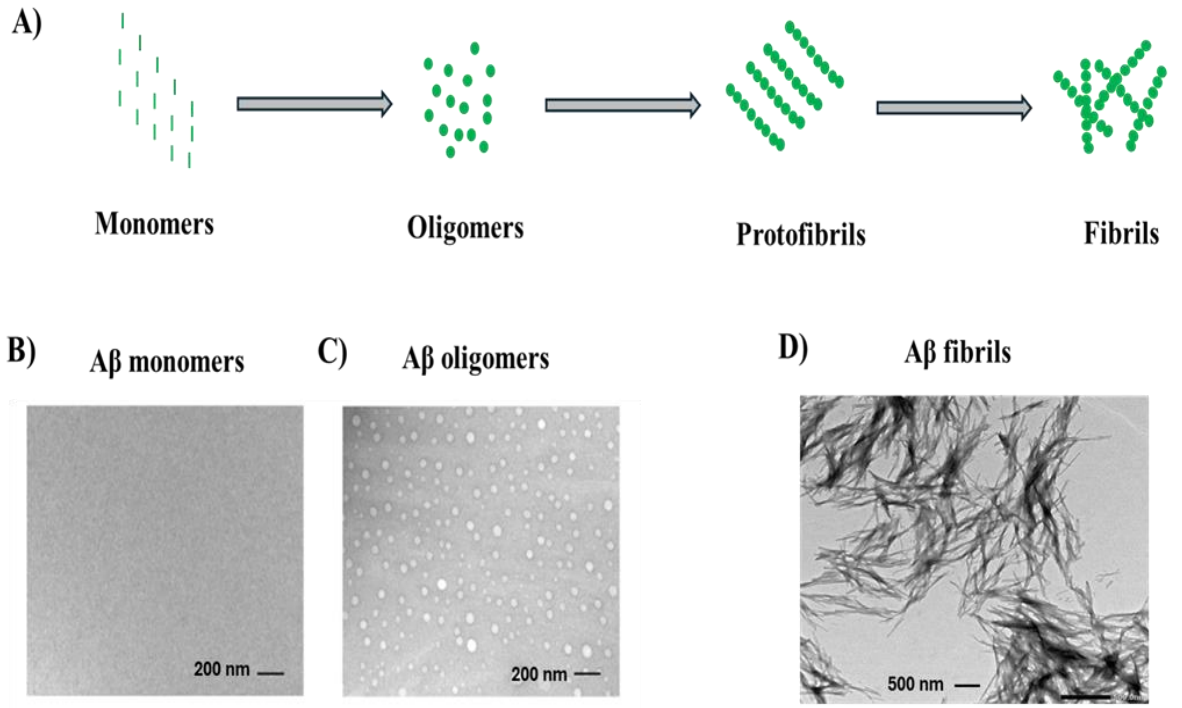

Figure 2.10. (A) Pathway of amyloid β aggregation started as monomers, oligomers and finally the formation of fibrils. (B to D) images were taken by transmission electron microscopy showing (B) Aβ monomers, (C) Aβ oligomers and (D) Aβ fibrils (images B and C adapted from Chunhui et al., 2018). Images A and D, © Bakri A and images B and C reused with permission (Copyright 2018, JoVE).

Analysis of amyloid aggregation kinetics using thioflavin T fluorescence

Plate reader enables researchers to conduct diverse tests utilizing a solitary device. The system is intended to accept microplates, extensively utilized in high-throughput screening and several other applications such as ThT fluorescence (Luo et al., 2011). **Figure 2.11** shows Thioflavin T (ThT), an important amyloid staining dye used in biochemical research on fibril formation. The compound has played a key part in understanding the kinematic details of the inhibition of fibril formation (Gade Malmos et al., 2017).

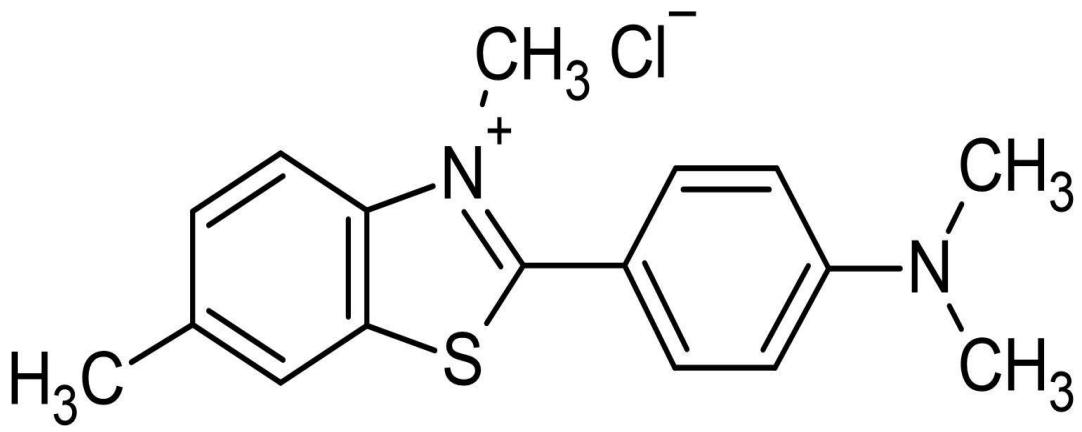

Figure 2.11. (ThT) thioflavin T chemical structure (Peña et al., 2023). The figure is reproduced under a Creative Common CC BY license (Copyright 2023, MDPI).

Applications of thioflavin T for studying amyloid aggregation

Ryan et al. (2012) used a 96-well plate to examine the influence of test substances on fibril production by amyloid $\beta_{1\text{-}42}$ using a continuous thioflavin T (ThT) fluorescence assay **Figure 2.12**. A 1 X PBS solution containing 30 μM thioflavin T (ThT) was used to dilute the detergents at a 1:20 ratio, creating an ultimate concentration equal to 50% of the mentioned critical micelle concentration. Before measuring the ThT fluorescence intensity (444-nm excitation and 485-nm emission) using a Flexstation Plate reader (Molecular Devices), the plate incubated at 37 °C with shaking every 7 minutes for 3 seconds after adding $A\beta_{1\text{-}42}$. It was found that 36 of the compounds stimulate fibril formation, whereas 30 of the chemicals prevent aggregation using electron microscopy and thioflavin T fluorescence tests (Ryan et al., 2012).

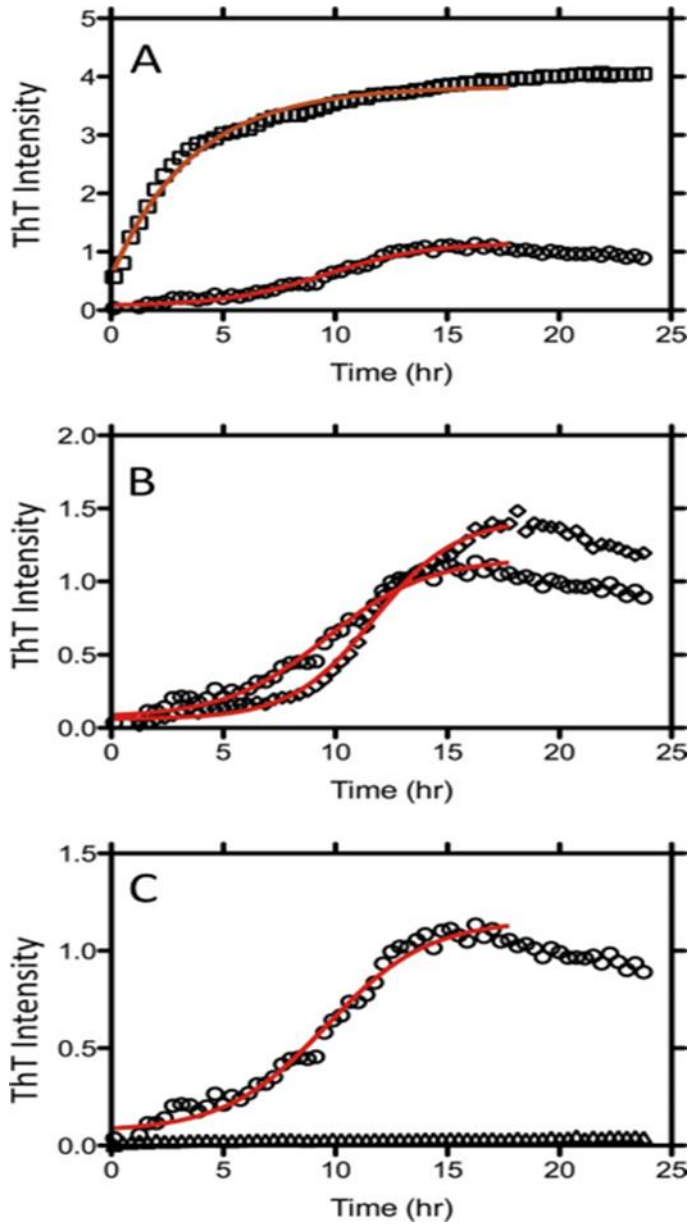

Figure 2.12. Investigation the influence of detergents on Amyloid β $_{1\text{-}42}$ fibrils. Thioflavin T (ThT) fluorescence assay used to examine the influence of test substances on fibril production by amyloid beta-$_{1\text{-}42}$. (A) circles in the absence of deoxycholate compound and squares in the presence of deoxycholate compound. (B) circles in the absence of the NDSB-211 compound and diamonds in the presence of the compound. (C) circles in the absence of the compound and triangles in the presence of lauryldimethylamine oxide compound (LDAO) (Ryan et al., 2012). The figure is reproduced under a Creative Common CC BY license (Copyright 2012, Journal of Biological Chemistry (JBC)).

Circular Dichroism Spectroscopy (CD) for analysing secondary structures of amyloid

Circular Dichroism Spectroscopy (CD) is an effective analytical method for investigating compounds' chiral characteristics. It is highly beneficial for examining the secondary structure of biomolecules, including proteins, nucleic acids, and other chiral compounds. Circular dichroism quantifies the discrepancy in absorption between left-handed (L-circularly polarized) and right-handed (R-circularly polarized) light when it traverses optically active specimens. This method offers insights into chiral compounds' structural and conformational characteristics (Gu et al., 2023; Hirschmann et al., 2021; Sreerama and Woody, 2000; Sreerama and Woody, 2004). The CD is caused by the unequal absorption of left- and right-circularly polarized light resulting from the interaction between chiral molecules and circularly polarized light, which may be expressed by equation [**2.5**] (Gu et al., 2023; Hirschmann et al., 2021; Sreerama and Woody, 2000; Sreerama and Woody, 2004; Greenfield, 2006b). CD spectrum is a graphical representation of the variation in absorbance between left and right circularly polarized light concerning wavelength. A conventional CD spectrometer has a UV lamp as the light source, a monochromator or a set of filters for wavelength selection, a sample container, and a detector. The sample compartment houses the optically active substance within a cuvette, such as a protein or DNA solution (Gu et al., 2023; Hirschmann et al., 2021; Sreerama and Woody, 2000; Sreerama and Woody, 2004).

Circular dichroism = $\Delta A(\lambda) = A(\lambda)LCPL - A(\lambda)RCPL$, where λ is the wavelength [**2.5**].

Applications of circular dichroism for studying secondary structures of amyloid

The chromophores in proteins form secondary structures that are aligned in specific arrangements such as α-helices or β-sheets (Greenfield, 2006b; Greenfield and Fasman, 1969; Holzwarth and Doty, 1965), and result in characteristic circular dichroism (CD) spectra **(Figure 2.13)** during analysis.

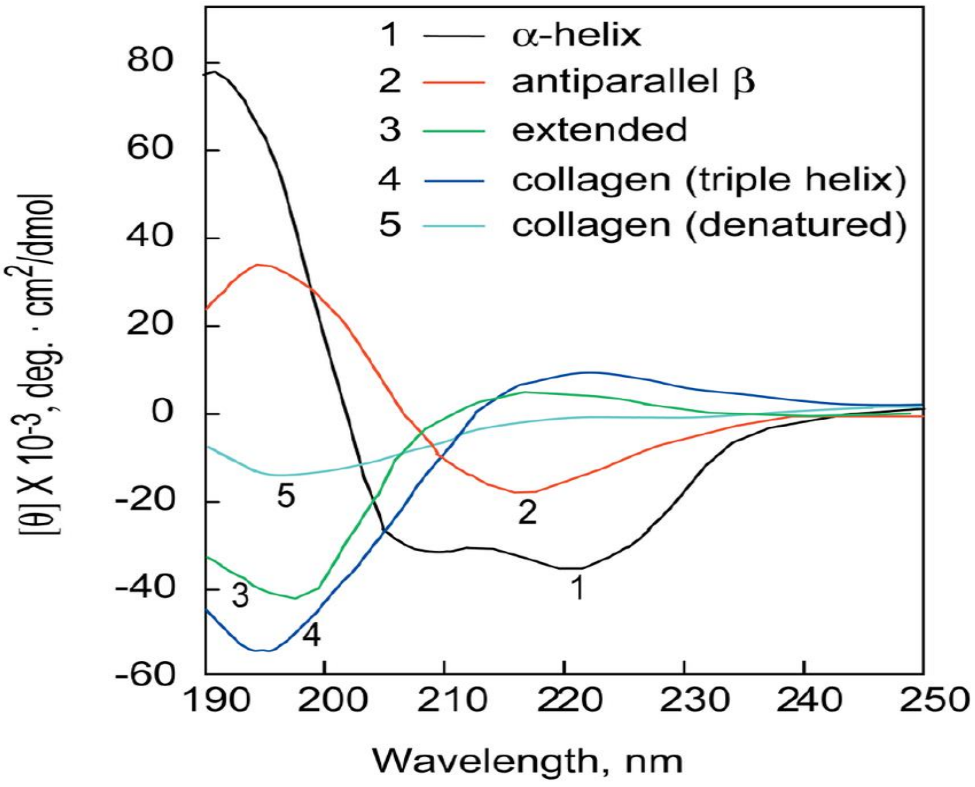

Figure 2.13. Examples of secondary structure CD spectra Poly-L-lysine, (1) α-helical at pH 11.1, (2) anti-parallel β-sheet at pH 11.1, and (3) extended conformation (random coil) at pH 5.7. placental collagen, (4) triple-helix native, and (5) denatured (Greenfield, 2006b). The figure is reproduced with permission (Copyright 2007, Springer Nature).

Several deconvolution algorithms can be used to estimate the secondary structures in a protein sample with and a match sought for in a reference data set of proteins with known structures (Greenfield and Fasman, 1969; Greenfield, 2006b; Sreerama and Woody, 2000; Sreerama and

Woody, 2004; Wallace and Janes, 2009; Whitmore and Wallace, 2008). The protein's CD spectra thus facilitate the characterization of their molecular structure, and changes to the spectra can be informative about their thermal stability and denaturation (Greenfield and Fasman, 1969; Greenfield, 2006a).

Chapter 3 (Expression and characterization of proteins)

Introduction

Expression and characterization of labelled and unlabelled amyloid beta (Aβ40)

The peptide component of amyloid precursor protein (APP), known as amyloid beta 40 (Aβ40), plays a vital role in the neurodegenerative process of Alzheimer's disease. The cleavage of amyloid precursor protein (APP) leads to the creation of 39 to 42 amino acid peptide amyloid-β (LaFerla et al., 2007) (described in **Chapter 1**). The misfolding and aggregation of amyloid into fibrillar deposits in the neuronal milieu lead to synaptic dysfunction and neuronal death. Over 20 different Aβ sequences have been observed in human cerebrospinal fluid and brain, although single molecules of Aβ do not occur naturally. The most commonly found isoform of Aβ is Aβ1–40, a 40-residue peptide starting at Asp1 and terminating at Val40 as can be seen in **Figure 1** (Walsh et al., 2009). It is of utmost importance to have a comprehensive understanding of the different biochemical and structural properties of Aβ40 in order to develop viable treatments for this fatal form of Alzheimer's disease (Bigi et al., 2022) (see **Chapter 1** for detail).

This thesis describes, in part, research into effects of olive oil polyphenol mixtures on Aβ aggregation. It was necessary, therefore, to implement a reliable, flexible and cost-effective method for producing Aβ40. Many published studies of Aβ40 have utilized synthetic peptides, which incurs high manufacturing costs and/or costs of peptide-synthesis instrumentation. Further, analysis of Aβ40 by solution-state or solid-state nuclear magnetic resonance often requires isotope-labelled peptides (Pastore et al., 2007). A cheaper and more flexible option for

protein production is to use bacterial expression systems to express the target protein, principally *Escherichia coli*.

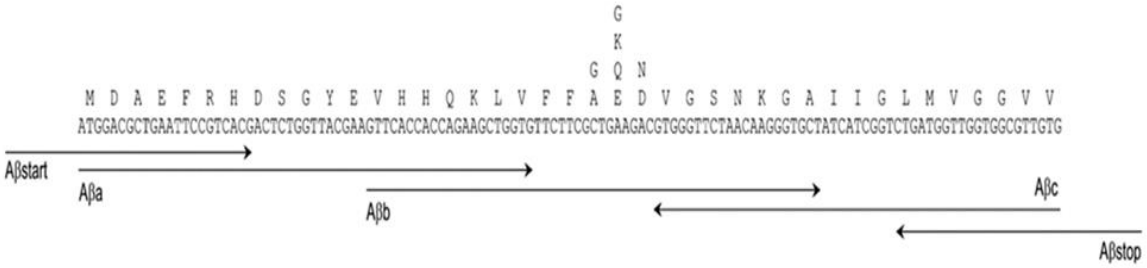

Figure 3.1. The primers and Aβ primary sequence for constructing a synthetic Aβ gene. The M1– M40 amino acid sequence of Aβ is shown, with the amino acid substitutions associated with disease demonstrated above the residues that were replaced. Figure obtained from (Walsh et al., 2009). The figure is reproduced under a Creative Common CC BY license (Copyright 2009, Wiley).

Traditional heterologous expression systems, such as *E. coli*, for the purpose of Aβ production, are attractive because of their rapid growth and the ease with which they may be modified. High protein yields are also achievable, which is important for many biophysical studies, including those described in this thesis. This Chapter describes the methodology for expression and analysis of the unlabelled Aβ40 for characterization by thioflavin T fluorescence, CD spectroscopy and transmission electron microscopy, and for expression of ^{15}N labelled Aβ40 for NMR. The plasmid construct employed (obtained from University of Leeds) expresses Aβ40 with a non-native N-terminal methionine residue, which improves solubility for purification. Many studies, including from the Middleton group, have used this variant of Aβ40 and have shown that it aggregates virtually identically to the authentic Aβ40 (Stewart et al., 2016; Walsh et al., 2009). To distinguish this variant from the authentic Aβ40, it will be referred to as MAβ40 henceforth.

Tau protein

The tau related pathology in the absence of amyloid-β containing plaques is characterized as frontotemporal dementia which is considered to be the second most common type of dementia occurring amongst people below the age of 65 (Querfurth and LaFerla, 2010). The spreading of NFTs in the brain is characteristic of Alzheimer's disease advancement (Querfurth and LaFerla, 2010; Braak and Braak, 1995). In this work it was interesting to investigate the effects of phenolic mixtures on tau as well. This research utilised a tau construct consisting of residues 255-441 of human tau from cDNA clone htau46; the protein was expressed and purified *via* the aforementioned methodologies (Hasegawa et al., 1998). The resultant isoform consists of 4 microtubule binding (MTB) repeat units (tau 4R), but with the removal of the aggregation impeding the N terminus isolated which leaves the second and third MTB with the extremely amyloidogenic sequences VQIINK and VQIVYK, respectively (Eschmann et al., 2017). Any experiments pertaining to tau were executed in 30 mM Tris, 1 mM DTT, and pH 7.5. Tau used in this thesis was kindly provided by Dr David Townsend as described above following the previous established methods (Hasegawa et al., 1998; Eschmann et al., 2017).

Aims

The primary objective of the work described in this chapter was to establish a functional methodology for the expression and purification of amyloid beta to obtain a pure and high sample yield, following the previous protocol obtained from (Stewart et al, 2016 and Walsh et al, 2009). The expression system was further employed to enable the expression of uniformly labelled MAβ40 with ^{15}N, facilitating its analysis using solid-state NMR.

Materials and methods

Materials

All chemical reagents used were obtained from Sigma-Aldrich. These include: ampicillin; chloramphenicol; isopropyl β-D-1-thiogalactopyranoside (IPTG); LB agar; LB media; tris base; EDTA; urea; NaCl; MeOH; ammonium bicarbonate, a protease inhibitor(EDTA-free tablets); DEAE-cellulose; acetic acid; coomassie G250; phenylmethylsulphonyl fluoride (PMSF); DNase; guanidine; NaOH; EtOH; tricine; SDS; 2X sample buffer; 40 % bis-acrylamide solution; glycerol; tetramethylethylenediamine (TEMED); APS; 96-well black; thioflavin T; carbon coated former grids; 2 % phosphotungstic acid) and Milli-Q purified water was provided from the system available in the lab at (Biomedical and Life Sciences, Lancaster University).

Equipment such as autoclave, shaking incubator, pH meter, sonicator, centrifuges, nanodrop™ 2000c, chemidoc imager, AKTA chromatography, plate reader, freeze dryer, thermoshaker, vortexer, vacuum pump, and transmission electron microscopy were used for this experimental work.

Methods

This technique is designed for a 4-liter scale. The method used was adapted from previous established methods (Stewart et al., 2016; Walsh et al., 2009).

Omit transformation – the MAβ40 vector in *E. coli* strain BL21 cells

Solutions were prepared of 2 g ampicillin (10% w/v) in 10 mL Milli-Q purified water (H_2O), 500 mg chloramphenicol in 20 mL of 100% EtOH, and 1 M IPTG 4.8 g in 20 mL dH_2O. These were all sterile filtered (0.22 μm pore).

One packet of plates was prepared using autoclaved 500 mL LB agar. After cooling to approximately 55 °C, 0.5 mL ampicillin and 0.5 mL chloramphenicol were added to the LB agar then transferred to plate. 500 mL and 2-3 L LB media were prepared in dH_2O, autoclaved, and 1 mL ampicillin and 1 mL chloramphenicol per litre of LB media added after cooling.

The following inoculation procedures were conducted under sterile conditions: 10 – 20 mL LB, 100 μg/mL ampicillin, and 25 μg/mL chloramphenicol were transferred to small sterile flasks or 50 mL sterile falcon tubes (x2). One pipette scraping of frozen (-80 °C) MAβ40 glycerol cell stock was transferred to the LB antibiotic media and incubated at 37 °C for 12 hours while mixing at 180 rpm. The cultures were then removed from the incubator and stored at 4 °C for 10 hours, before being streaked onto LB agar plates (x3) using a sterile loop and incubated overnight for ≤ 16 hours at 37 °C (together with 1 uninoculated control plate).

Preparation of small cultures

Under sterile conditions, the plates were checked for single-cell colonies, covered with parafilm to seal, and stored at 4 °C. The LB cultures were each inoculated with a single colony and allowed to grow overnight (starting no later than around 4 pm for a total night's growth). Single colonies were then transferred to the flasks containing the LB media and antibiotics and incubated overnight at 37 °C with mixing at 180 - 200 rpm.

Protein expression of large cultures

Under sterile conditions, the OD_{600} of the starter cultures were confirmed to be between 1.0 and 1.5, and 5 mL added to each 500 mL LB media + antibiotics. 500 mL of the inoculated media was then added to each 2 L flask and incubated at 37 °C at 180-200 rpm. The OD_{600} was checked every 2-3 hours until it equalled 0.5, at which point 0.5 mL of 1 M IPTG was added to each 500 mL of cell culture to give final IPTG concentration of 1 mM. The cells were incubated for 3 – 4 hours at 37 °C and at 180 – 200 rpm, before being cooled to 4 °C and centrifuged at 8000 rpm. After resuspension in lysis buffer, they were frozen at -20 °C and 12.5 mL lysis buffer added to each 1 L pellet. The pellets were scraped into 50 mL conical tubes, paraffin wrapped, and frozen at -20 °C.

Purification of Beta-Amyloid Peptide (MAβ40) - Part 1

Sonication and isolation of inclusion bodies

The lysate was thawed on ice for 24 hours and purified using the following procedure: 300 µL of 200 mM PMSF (a protease inhibitor) and 0.5 mg DNase were added to the lysate, stirred, and stored at 4 °C for 12 hours. 25 mL Q Sepharose Fast Flow resin (DEAE-cellulose) was equilibrated with Buffer A. 100 mL of Buffer A was mixed with approximately 35 mL

suspended resin in a 250 mL flask, stirred, allowed to settle for approximately 1 hour and then the buffer poured off and replaced. The buffer washing process was repeated four times. After 12 hours the solution was pulled through a 50 mL syringe with a 1.5" mixing needle and stirred for 30 minutes at 4 °C, while the lysate remained on ice. The suspension was sonicated for 30 s at 10 μm, transferred to tubes and centrifuged at 4 °C for 15 minutes at 18,000 rpm. The supernatant was collected, labelled as "S1" and stored on ice, before being resuspended in 10 mL of Buffer A and stirred at 4 °C for 1-2 hours to homogenize. The sonication and centrifugation steps were repeated to give the supernatant "S2" (S1 and S2 should contain *E. coli*., proteins, with Aβ in the IC fraction). The last pellet was then sonicated for 30 s, centrifuged at 4 °C for 15 min at 18,000 rpm, and the supernatant collected and labelled as "IC". 25 μL samples were retained to prepare a gel. "IC" means ion-exchange chromatography fraction as the supernatant is combined with the DEAE-cellulose anion exchange resin.

DEAE-cellulose purification

Each part of the supernatant IC was diluted with 4 parts of Buffer A. The sample was combined with 35 mL equilibrated DEAE-cellulose. Some Buffer A with resin was combined with the diluted IC and transferred to a 50 mL falcon tube, placed sideways on a rocker for a minimum 30 minutes to batch bind the resin. The mixture was added to a Buchner funnel with Whatman 70 mm circle filter paper "1" attached to a 500 mL flask with a side arm, stirred with a glass rod and allowed to settle for 5 minutes. The vacuum was applied, and fractions collected in 50 mL disposable tubes. The first fractions were saved as flow through (FT). 50 mL Buffer A was then stirred into the resin, allowed to settle for 5 minutes, vacuumed, and collected as Wash 1 (W1). This process was repeated to produce Wash 2 (W2). The peptide was eluted with 50 mL fractions of elution buffer five times, with each fraction recovered and saved as E1 to E4, and the final fraction, E5, which could contain more contaminants than the lower salt elutions. The

resin was then first washed with 50 mL 1 M NaCl + Buffer A and collected as Hs (high salt), and second washed with 1 M NaCl + Buffer A + 8 M urea and collected as HsU (high salt + urea). The fractions E1-E5 were then checked for protein concentration. The same blank was used for each fraction.

Gel electrophoresis preparation

Gel Tris-tricine SDS-PAGE :

The purity of MAβ40 during the amyloid beta 40 protein expressions was determined at several stages with sodium dodecyl sulphate polyacrylamide gel electrophoresis (SDS-PAGE). The anionic detergent SDS was added to the samples to dismantle the proteins 'tertiary structure. At the same time the proteins were linearized and denatured by applying a 90 °C heat shock. The negatively charged proteins move towards the anode when a constant voltage is applied and can then be evaluated against a chart of proteins with molecular weights already established. Tris-tricine SDS-PAGE was reported to separate proteins between 1–100 kDa (Schägger and Von Jagow, 1987).

Tris gel buffer of pH 8.45 was prepared using 500 mL 3 M tris base to which 181.5 g SDS was added. A 0.3% (w/v) SDS solution was prepared. The stacking gel was prepared by mixing 1 mL of 40% bis-acrylamide solution, 2.5 mL of the tris gel buffer (pH 8.45), and 6.5 mL dH_2O. The separating gel was prepared with 4.125 mL 40% bis-acrylamide solution, 3.3 mL of the tris gel buffer, 1 mL glycerol, and 1.575 mL dH_2O. 7.5 µL TEMED and 75 µL of 10 % APS was added just prior to pouring the gel plates consisted of a 4% (1-2 cm) stacking gel layer (4%) and 16.5% stacking layer capable of separating 1.5-30 kDa. The end of each layer was marked. Before layering the gels, the plates were cleaned with methanol. Water-saturated butanol was used between each layer and washed off with dH_2O when the gel had set.

For 40 % acrylamide solution. 1 mL volume of gel solution, 40 %* x = 16.5 %, x = 0.4125. For 10 mL = 4.125 mL.

SDS-PAGE gel electrophoresis and sample runs

Ten 1 L solutions of tris-tricine running buffer (BioRad Manual) were prepared with a pH of 8.3, by combining 1 M tris, 1 M tricine, and 1% SDS, in 1 L dH_2O. Two 10 mL sample buffer solutions were prepared by combining 0.8 g 8% (w/v) SDS, 2.4 mL 24% (v/v) glycerol, 0.4 mL 4% mercaptoethanol, 2 mg 0.02% Coomassie brilliant blue G, and 100 mM tris base adjusted to pH 6.8 with HCl. 1 mL aliquots of the sample buffer was transferred to 1.5 mL Eppendorf tubes and stored at -20 °C.

Samples were prepared by vortexing, heating for 5 minutes at 90 °C, and syringing into the wells up to 20 μL. The marker used was an ultra-low range protein ladder previously stored at 20 °C and neither vortexed nor heated.

Samples were run at 150 V for 2 – 3 hours using the BioRad system, and the gel carefully removed. The plastic layers were separated with a gel wedge and stained using 40% (v/v) EtOH, 10% (v/v) acetic acid, and 0.1% (w/v) Coomassie G250. They were stained again with InstantBlue for 45 minutes on a rotary shaker, checked, and left for 12 h, destained, and rinsed with dH_2O. Where necessary, gels were further destained using 40% (v/v) MeOH and 10% (v/v) acetic acid in dH_2O. The gels were then imaged using ChemiDoc imager to check that the protein had eluted from resins E1 to E4 and E5. On confirmation of protein elution, the dialysis and lyophilization (freeze-drying) stage commenced.

Dialysis and lyophilisation of the protein began by cutting snakeskin tubing (cutoff of 3500 MW) into lengths sufficient to hold the protein samples. The tubing was wetted with dH_2O and equilibrated by immersion in 5 L Dialysis Buffer (diluted to contain $6.25x10^6$ fraction salts).

The elution fractions (E1-E4 and E5) that had been confirmed to contain proteins by electrophoresis, were dialyzed for two days (at least one full night) in 5 L buffer, which was changed 3-5 times over two days. After dialysis, 25-30 mL of the peptides were lyophilised for 2-3 days in 50 mL falcon tubes, to give a total yield of approximately 200 mL – 300 mL of solution.

Purification of Beta-Amyloid Peptide - Part 2

Size Exclusion Chromatography (SEC)

The ÄKTA Start chromatography system and UNICORN™ Start 1.0 software (GE Healthcare) were used to separate the MAβ40 monomer. All solutions were filtered and degassed for 20 – 30 minutes using a high vacuum pump. A Superdex 75 pg 16/600 column (120 mL CV, max 0.5 mPa, 5 mL sample loop) was used for the SEC.

All manual runs were carried out at 0.3 mPa. The SEC column was prepared by running 1-2 CV H_2O at 2 mL/min. Immediately before running the tubes, the column was cleaned by running 1 CV of 1 M NaOH at 0.5-1.5 mL/min followed by 1 CV of H_2O at 0.5-1.5 mL/min. The sample loop was then cleaned with water and buffer in a 5 mL syringe and the column equilibrated with a minimum of 1 CV ammonium carbonate buffer at 0.5 mL/min and the fraction collector loaded with a minimum of 78 tubes.

For any of these equilibrations, the column could be run overnight at 0.1-0.2 mL/min.

The lyophilized protein (4-6 falcon tubes) was dissolved in 1-1.25 mL cold solubilization buffer to give a total volume of 5.1 mL on each of two SEC runs. The solubilized aliquots were transferred to clean microfuge tubes and centrifuged for 10 minutes at 14000 rpm at 4 °C to remove particulates (small dark pellets). 35 µL of the protein was reserved for gel. The samples

were first loaded into a single 5 mL syringe with a blunt needle, and then loaded into the column and run at a flow rate of 1.5 mL/min.

Protein-containing fractions were removed and saved during the run, with fractions 33-39 containing the eluted monomeric MAβ40. The fractions were collected, and their concentration measured with Nanodrop™ 2000c, and pooled based on the gel results. 500 µL and 1 mL aliquots were transferred into microfuge tubes with holes in the lids, and one accurately measured 2 mL aliquot was transferred to disposable tubes with holes in the lids. The samples were then lyophilized for 24-48 hours.

Determining Protein Concentration

The samples were removed from the freeze drier, their caps changed, sealed with parafilm, and stored at -20 °C. The sample protein concentration was checked by solubilizing 1 mL sample in 200 µL solubilization buffer (20 mM sodium phosphates pH 7.4). Absorption was checked and the A_{260}, A_{280}, and A_{340} values recorded. Absorbance values were corrected for dilution and the molar concentration (M) of MAβ40 calculated using the molecular coefficient of 1490 M^{-1} cm^{-1}. Protein concentration was calculated as: A_{280} / 5-fold dilution = absorbance – correction = corrected absorbance.

The total protein was calculated as mg/mL taking account of the number of aliquots, the prep size, and the molar weight of Aβ (4459 g/mol). The extracted MAβ40 was stored at -20 °C.

Expression of ^{15}N-labelled MAβ40

Isotopically labelled MAβ40 was produced for analysis by solid-state NMR. Labelling was achieved by expressing MAβ40 in a minimal bacterial growth medium using ^{15}N-labelled

ammonium chloride (CortecNet) as the sole nitrogen source. Expression was carried out on a 4-liter scale. The cells were cultivated according to the previously mentioned method. Briefly, BL21 cells with the appropriate MAβ40 plasmid were cultured overnight and then used to inoculate 2 L of LB media. The culture was incubated at 37 °C until reaching an optical density at 600 nm (OD_{600}) of 0.5. The cells were subsequently collected by centrifugation at 5000 g at room temperature and suspended in 2 L of pre-warmed minimum medium and antibiotics, along with 20 mL of a solution containing 2 g of ^{15}N ammonium chloride, 200 µL of 1 M $CaCl_2$, and 4 mL of 1 M $MgSO_4$ in Milli-Q purified water. The cells were allowed to acclimatise to the new media for a duration of 30 minutes prior to being stimulated with 2 mL of 1 mM IPTG. The cells were incubated for an additional 4-5 hours in order to promote protein expression.

Analysis of mass spectrometer for amyloid beta

Mass spectrometry determined amyloid beta protein composition

Samples were analyzed by outsourcing. After processing the protein samples, the Centre for Proteome Research's analytical support team used ESI-TOF MS with the Q-ToF Micro mass spectrometer to examine the data. The ^{15}N-labelled MAβ40 was supplied at a concentration of 10 µM in a 20 µL solution. The dissolved proteins were buffered by 20 mM sodium phosphates at pH 7.4.

Method of Mass determination

The analysis of the mass spectra of MAβ40 (unlabelled and ^{15}N-labelled) was performed using electrospray ionisation mass spectrometry. The samples were sent to the Institute of Integrative

Biology (the Centre for Proteome Research's analytical support team) at Liverpool University to be run and analysed by Dr Brownridge as described below.

A 10 µM sample of MAβ40 was diluted to 1 pmol/µL with 97% HPLC Water, 3% Acetonitrile, and 0.1% Trifluoroacetic acid (TFA). Mass analysis was conducted using a Nano-Aquity UPLC (Waters, Manchester) attached to a Synapt G2-Si. For the final analysis, a 1 µL sample (1 picomole) was deposited on a C4 Trap column. The column was washed for 6 minutes with 90% A (99.9% H_2O 0.1% formic acid) and 10% B (99.9% ACN 0.1% formic acid). After washing, the material was eluted using a gradient from 95% A and 5% B to 10% A and 90% B. The gradient was applied for 90 seconds at 25 µL/min. The mass spectrum from *m/z* 500 to 3000 was scanned at 1 scan per second.

Before running the samples, 250 femtomoles of 16951.49 Daltons Myoglobin were injected as a control protein of known mass. The recorded mass of 16951.44 represented an error of 2.9 ppm, which was considered to be acceptable within the measurements limits of the instrument.

The analysis of the mass spectra of MAβ40 (unlabelled and ^{15}N-labelled) was carried out as follows. Deconvolution with MaxEnt 3 accounted for isotopic peaks. This technique used *m/z* 700-15000 intensities, 7 charges, and peptide isotope distribution. MaxEnt was used to estimate the peptide's mass using the mass spectrum of positive ions, which comprised ions with multiple charges.

Evaluation of aggregation using thioflavin T binding

The accumulation of amyloid was quantified using an intensified fluorescence signal in the presence of the amyloid-specific dye Thioflavin T (ThT). The MAβ40 peptide, at a concentration of 20 µM, was subjected to incubation in the presence of Thioflavin T at a concentration of 20 µM. Fluorescence measurements were obtained from 12 well samples

using a Molecular Devices Flexstation 3 Microplate Reader. The excitation wavelength was set at 450 nm, and the emission wavelength at 482 nm. Measurements were collected every 2 minutes for a duration of 72 hours. The samples were continuously agitated at a temperature of 37 °C throughout the incubation process.

Transmission electron microscopy (TEM)

Negative-stain TEM was used to study the morphology and density of MAβ40 aggregates formed after incubation with shaking for 24 hours at 37 °C using eppendorf mixer. The sample was prepared for TEM as follow 10 µL suspension of 20 µM MAβ40 aggregates was deposited onto carbon-coated formar grids. The surplus liquid was eliminated by blotting after a duration of 5 minutes. To perform negative staining, apply 10 µL of a 2% solution of phosphotungstic acid onto the prepared grids. The grids were left for 3 minutes, then excess liquid was removed, and the grid was left in a glass petri dish to dry naturally. The grids were observed using a Jeol JEM-1010 electron microscope, and photographs were taken to portray the whole grid accurately.

Results

Expression of amyloid beta

In accordance with the procedures outlined in the Methods section, the MAβ40 clone was introduced into the *E. coli* strain BL21 expression host and induced with IPTG. For the purpose of collecting the inclusion bodies, the cells were lysed and washed thoroughly. The overexpressed target protein was predominantly found in the inclusion bodies associated with the insoluble fraction. Subsequently, the insoluble fraction was dissolved in a buffer that

contained urea in order to denature the inclusion body. The solubilized protein was subjected to DNAse treatment in order to eliminate any interactions with DNA that could have resulted in DNA contamination in the final protein. Following this, the solubilized protein was introduced onto a DEAE cellulose column filter. The column was washed with buffer in order to remove undesired proteins that were loosely bound *via* the process. The desired protein fractions were then eluted with buffer that had a high concentration of sodium chloride. Fractions 50 mL per Elution were collected and numbered E1 to E5.

Figure 3.2 shows a tris-tricine SDS PAGE gel of fractions E1 to E5 after elution. Across these fractions, a distinct band with a molecular weight of roughly the target size of 4 kDa can be seen. The band runs to a similar position to that of commercially sourced MAβ40 the same gel picture (**Figure 3.2**). The photograph of the gel shows that lanes E-1, E-2, and E-5 contain high-molecular weight impurities. The next step was to eliminate the undesired protein by using size exclusion chromatography.

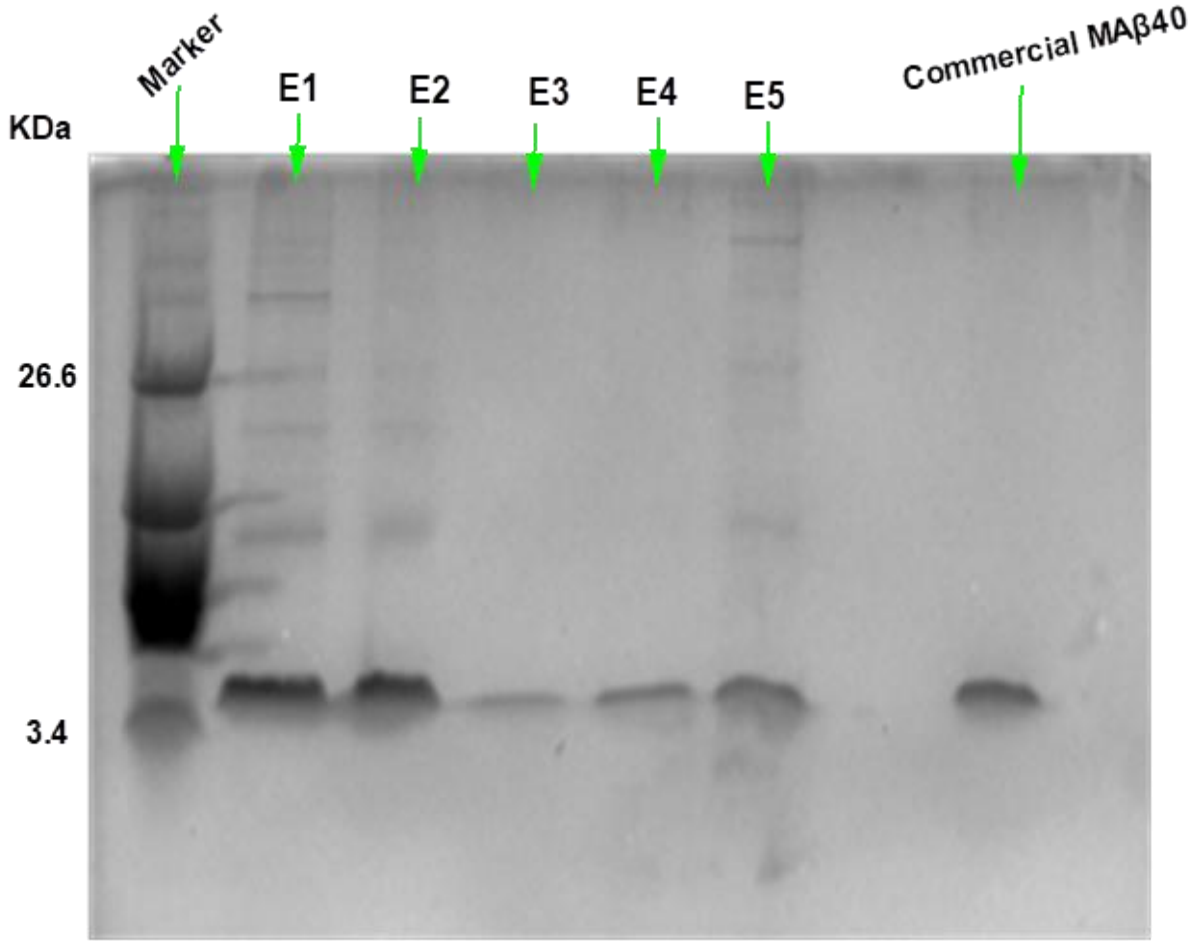

Figure 3.2. Tris-tricine SDS-PAGE gel of MAβ40 (E1-E5 and commercial MAβ40 for more confirmation) peptide expression after adding IPTG and incubating for 3-4 hours.

Purification of amyloid beta using size exclusion chromatography (SEC)

Using the buffer system that was provided in the Materials and Methods section, the eluted fractions E1-E4 were combined and injected onto ab ÄKTA Start FPLC system that was equipped with a Superdex 75 pg SEC 16/600 column. The chromatographic trace exhibited two prominent peaks, labelled as peak 1 and peak 2, as well as several minor peaks at longer elution times (**Figure 3.3**). In the ÄKTA Start chromatography the maximum sample loading volume is about 5 mL because of this loading limitations the MAβ40 sample was loaded into

the column three times separately and they called here as run 1, run 2 and run 3 as result we obtained the same outcome for all runs as shown in **Figure 3.3**.

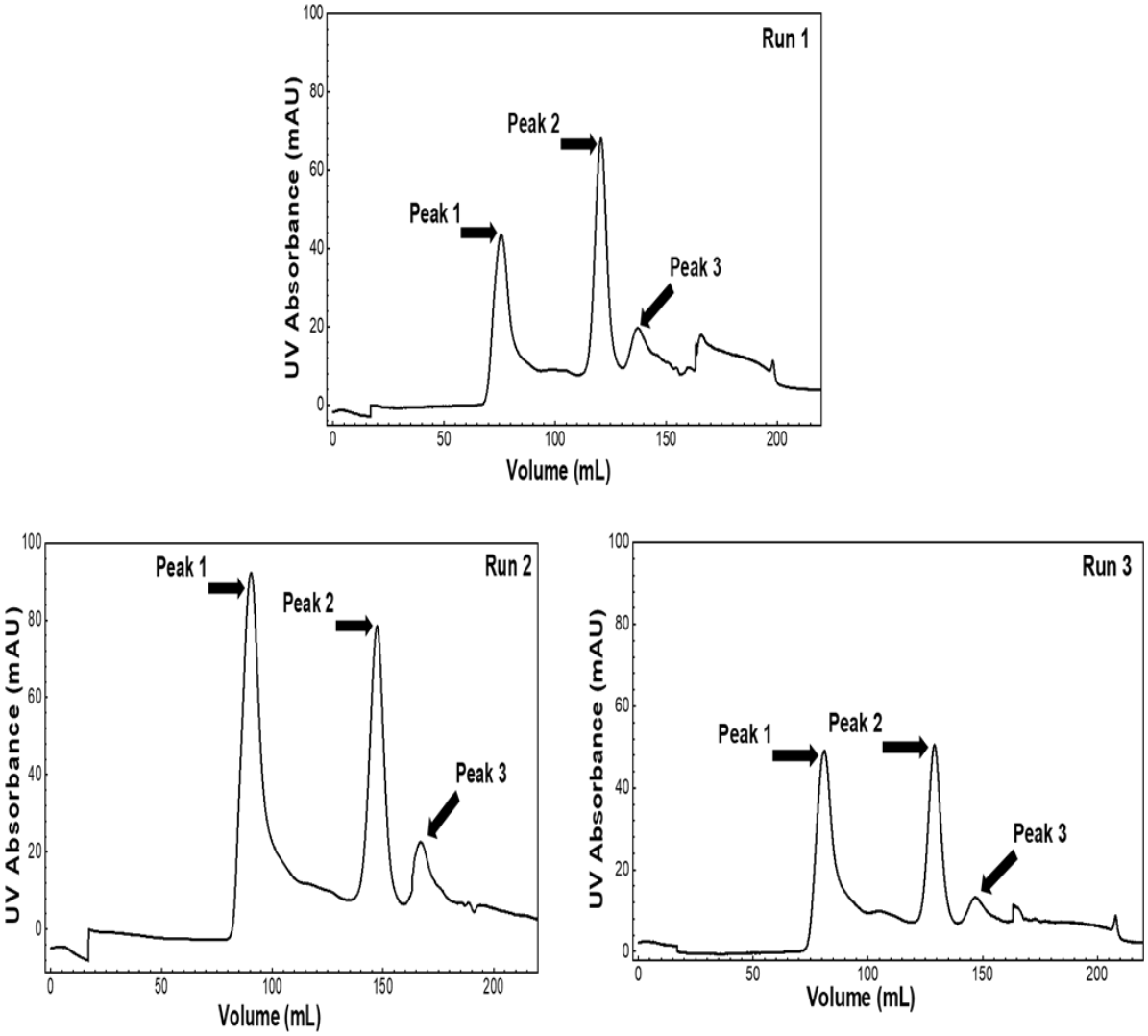

Figure 3.3. Chromatogram purification of MAβ40 and the UV absorbance for protein using SEC chromatography.

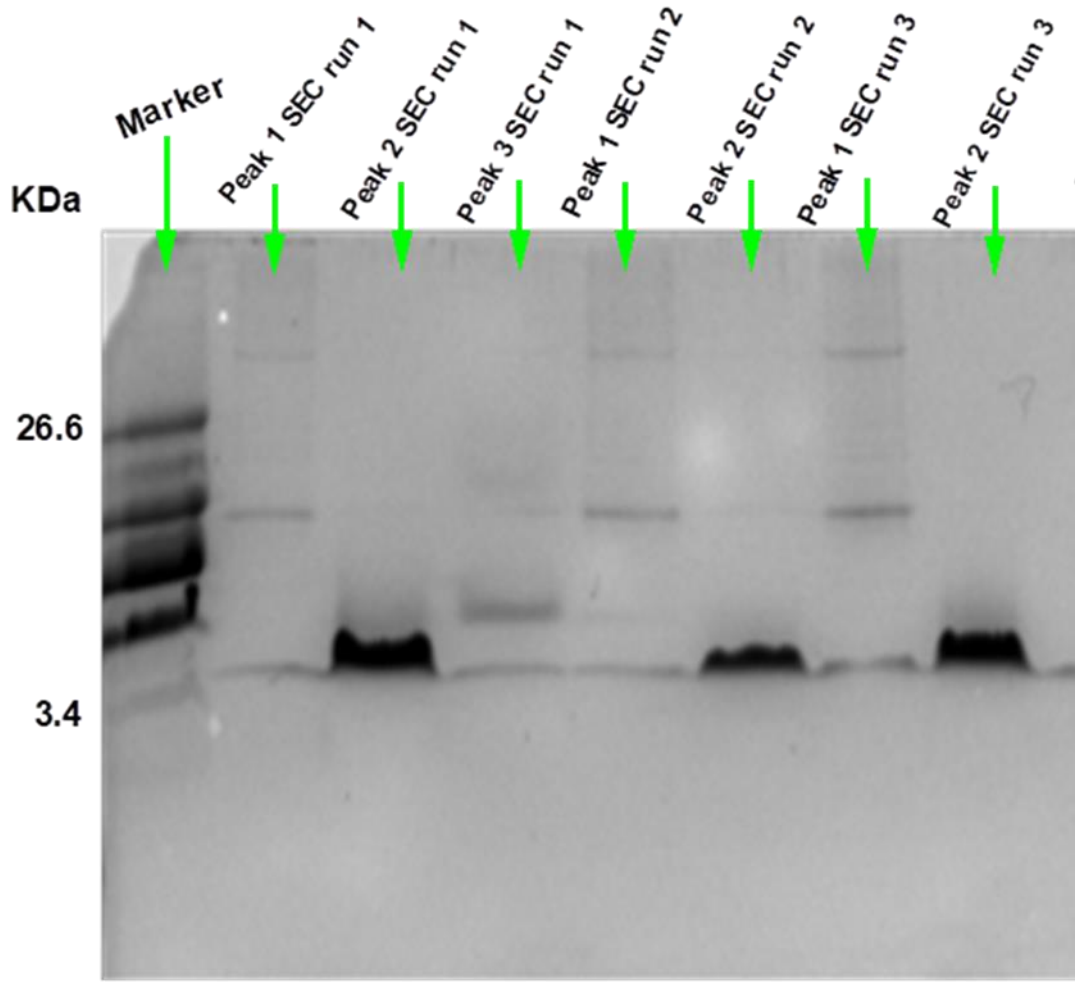

Figure 3.4. Tris-tricine SDS-PAGE gel of MAβ40 (E1-E4 fractions after SEC) peptide expression after adding IPTG and incubating for 3-4 hours.

Following the above step each peak was run on Tris-tricine SDS-PAGE gel along with molecular weight marker. As depicted by **Figure 3.4** (lower panel), MAβ40 of high purity can be observed under peak 2 SEC run 1, peak 2 SEC run 2, and peak 2 SEC run 3, corresponding to the band observed at the commercial MAβ40 lane **Figure 3.2**. The concentration of peak 2 obtained from elution fraction is of the highest concentration, which was confirmed by observing with a UV spectrophotometer.

Amyloid beta identification by mass spectroscopy

The fractions corresponding to peak 2 were combined and submitted for mass spectroscopic analysis to confirm the identity of the purified protein using ESI-TOF MS. **Figure 3.5** shows a peak with molecular weight of 4459.2168 Da accurately validates the identity of Aβ40, compared with the expected mass of Aβ40 4459.21 Da, also the mass detected here is closer to the expected mass when it compared with the mass reported by Walsh et al, 2009 of 4459.19 Da (Walsh et al., 2009; Stewart et al., 2016).

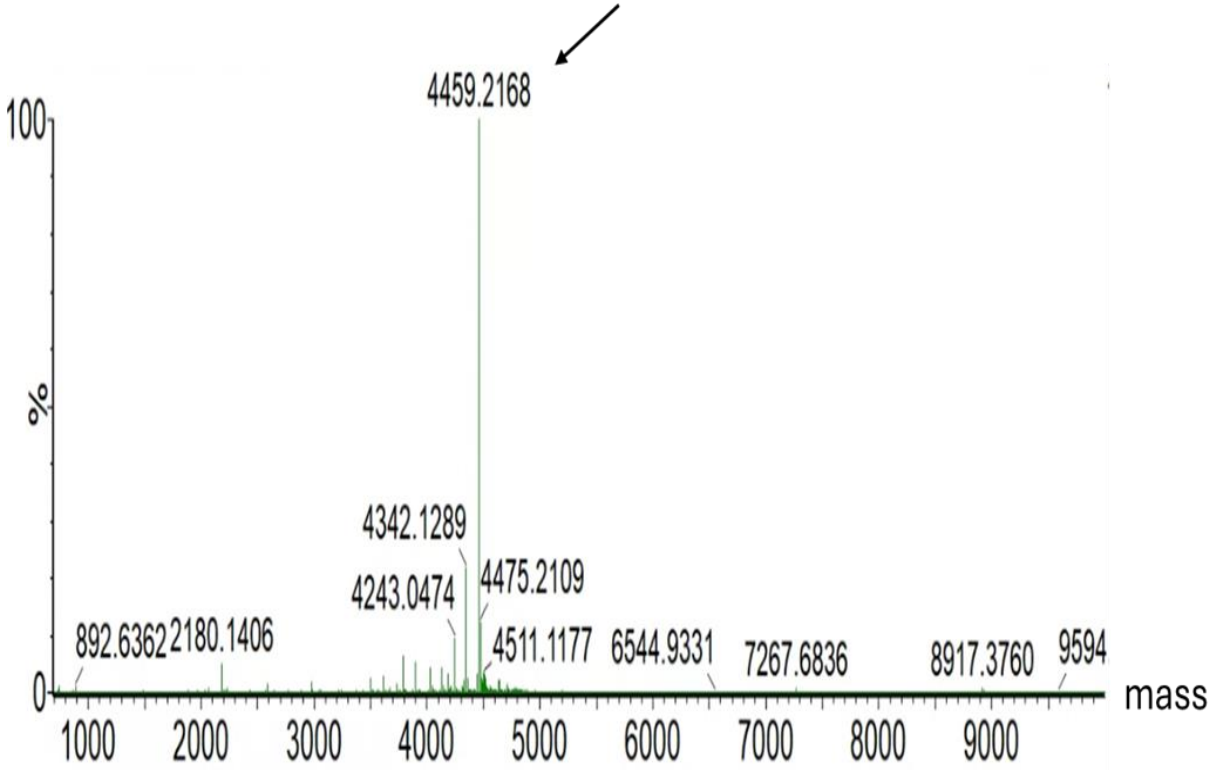

Figure 3.5. Positive electrospray ionization mass spectrometry of MAβ40 obtained mass 4459.2168 Da.

Yield and reproducibility of MAβ40 expression

Three rounds of expression and purification of MAβ40 were carried out throughout the project and resulted in a consistent yield. The quantity of unlabelled MAβ40 obtained from expression on rich (LB) media was 4.49 mg in the initial iteration, 4.44 mg in the subsequent iteration, and 4.52 mg in the final iteration, each from 4 L of growth media. These three expressions demonstrate the ability of the expression system to be replicated and emphasize its strength in generating MAβ40. The expression technique exhibits high stability and repeatability, as seen by the minimal change in yields observed after successive expressions. The amounts of protein produced are comparable to previously reported yields (Stewart et al., 2016).

Analysis of MAβ40 aggregation

Various fluorescent probes and methods are employed to detect amyloid aggregation of proteins, including Aβ40. ThT assay is one of the well-established and tested methods to establish the amyloid kinetics of a protein or peptide. Proteins undergoing amyloid aggregation gradually convert to a β sheet structure. ThT binds specifically to the cross-β sheet structure of amyloid fibers and fluoresces more intensely once bound, which indirectly correlates with ThT fluorescence intensity and the growth of the amyloid fibril (Ratha et al., 2016).

Figure 3.6 shows a fibril growth curve for MAβ40 20 μM with ThT. The aggregation follows a typical sigmoidal growth profile (**Figure 3.6**) as expected for Aβ40 (Walsh et al., 2009; Stewart et al., 2016). The kinetics of MAβ40 fibrillation exhibit the three distinct stages commonly observed in fibrillation processes that depend on nucleation. These stages include a period of inactivity known as the lag phase, a rapid increase in fibre production during the elongation phase, and a saturation phase characterized by a drop in the concentration of free peptides.

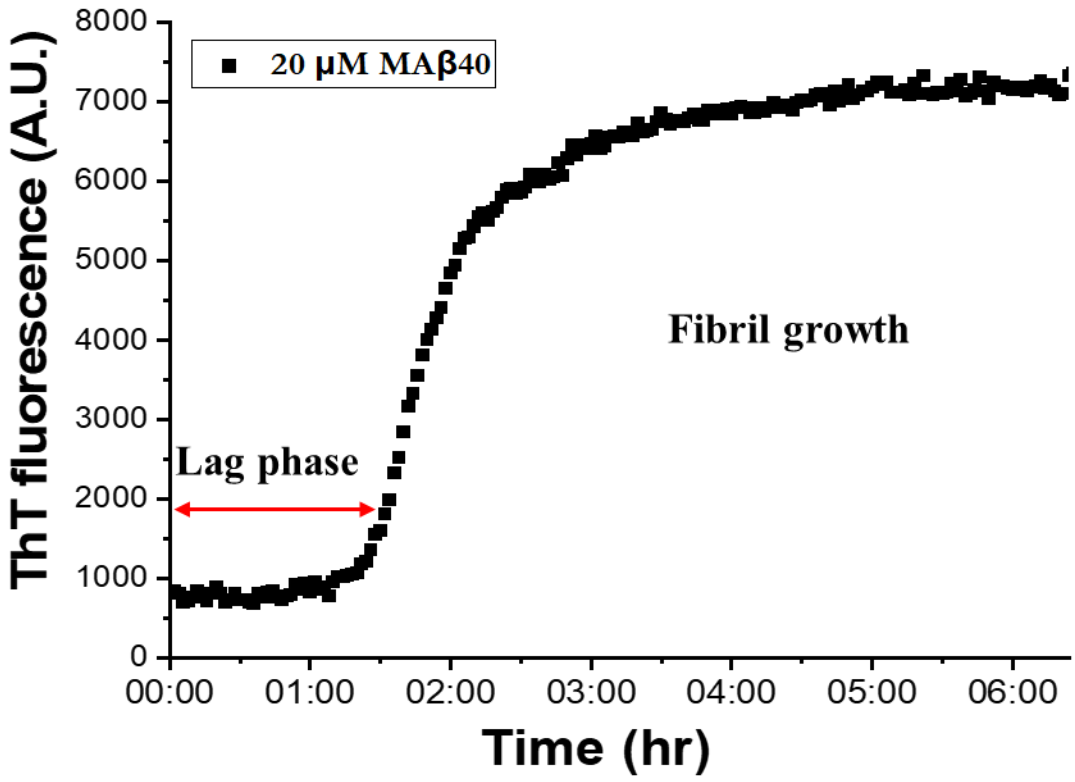

Figure 3.6. Thioflavin T fluorescence spectroscopy (ThT) assay of monomeric amyloid beta aggregation at 20 µM.

Following the sigmoidal curve, the kinetic parameters estimated are a t_{lag} of roughly 90 minutes and a $t_{1/2}$ of approximately 115 minutes. The t_{lag} is a precise measurement that indicates the exact amount of time required for the initial formation of the main nucleus in the aggregation of MAβ40 (Ratha et al., 2016). As shown by the curve, the $t_{1/2}$ represents the amount of time that must pass before the fluorescence intensity reaches half of its maximum setting. Before entering the log phase, a population of MAβ40 peptide molecules typically assumes a β sheet structure, forming stacks of β sheet peptides.

Transmission electron microscopy of amyloid beta

TEM was performed to verify the presence of amyloid fibrils visually. This was done after it was established that the recombinant MAβ40 produced in this work possessed the ability to aggregate into ThT -reactive structures. Monomeric MAβ40 20 μM was incubated with shaking for 24 hours at 37 °C using an Eppendorf mixer. For TEM imaging, an aliquot of 10 μL sample was placed on a carbon-coated formar transmission electron microscopy (TEM) grid in accordance with the procedure given in the methods section. The TEM images indicated that MAβ40 had assembled into the expected distinctive pattern of interconnected fibrillar structures (Gulisano, 2018; Vrancx et al., 2021). **Figure 3.7** indicates a network of fibrous filaments; here, these fibers seem to be branched and clumped aggregates. The aggregates with a width in the nanometer range (100 nm-1000 nm). The fibrillar morphology visualized by TEM is visually similar to previously reported studies. There is no evidence of smaller, oligomeric aggregates that are typically spherical, and which are associated with toxicity to neuronal cells. Oligomers are typically more prevalent in the early stages of aggregation and during the lag phase, so their absence here (after incubation for 24 hours) is unsurprising.

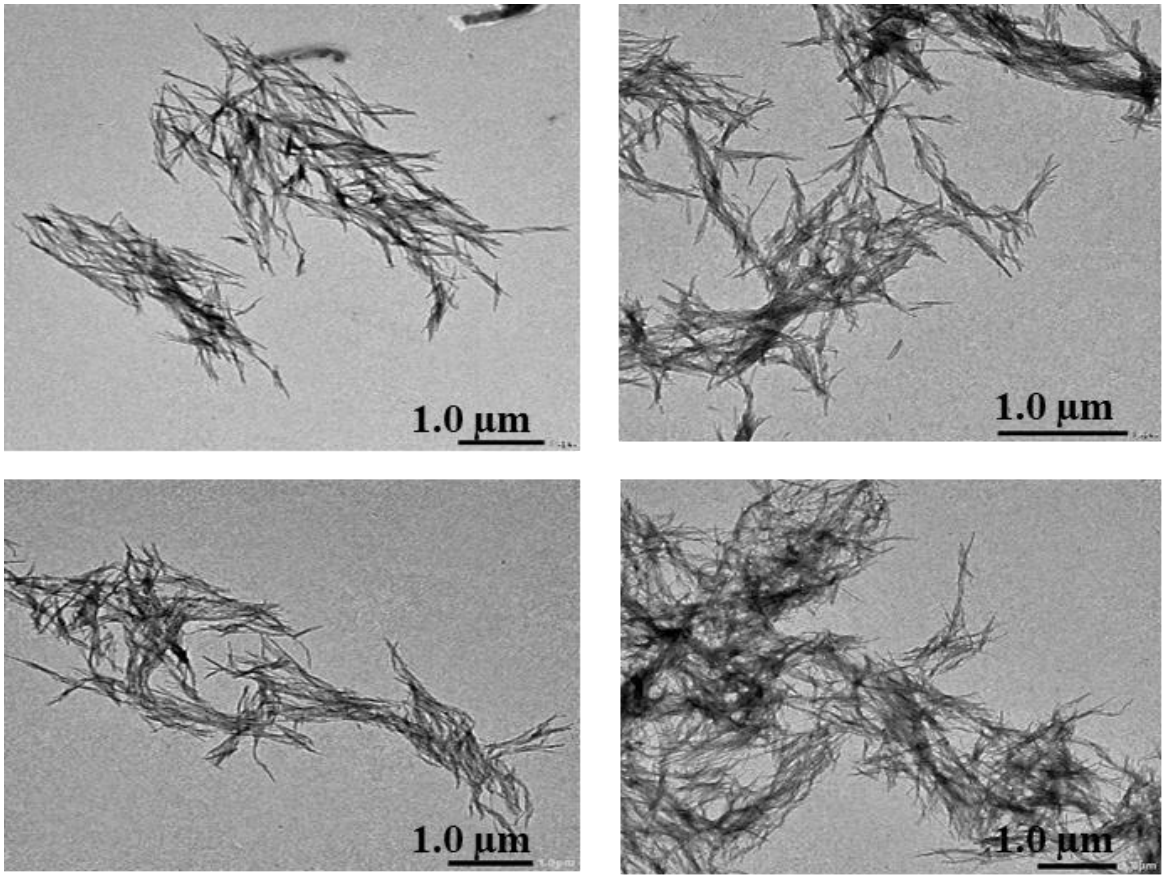

Figure 3.7. Transmission electron microscopy images of amyloid beta aggregation and fibrils formed at a concentration of 20 µM. Four different regions of the TEM grids scale bar (1.0 µm).

labelled MAβ40 (^{15}N) expression, purification and characterisation

Expression of labelled MAβ40

Recombinant protein expression enables the incorporation of stable isotope labels, specifically ^{13}C and ^{15}N, which can be evenly or sparsely dispersed across the protein sequence. These are crucial for solid-state nuclear magnetic resonance (SSNMR) investigations, since they provide enhanced sensitivity and resolution while simplifying the intricacies of the spectra. Uniform labelling enhances the precision of residue assignment, particularly when aided by multi-

dimensional triple resonance tests (Lian and Middleton, 2001; Townsend, 2016). To accomplish this, MAβ40 was produced in *E. coli* using a simplified growing medium that included either ^{13}C glucose or ^{15}N NH_4Cl as the only sources of carbon and nitrogen or both for expressing dual-labelled [^{13}C,^{15}N]-protein. The results of expression on minimal growth medium are shown separately from the previous results of expression on LB (rich) media. This is because yields and purity are usually affected detrimentally by the minimal growth conditions.

For the first purification steps involving elution with NaCl buffer, the steps were repeated as described above and elution fractions E1-E5 collected as before. **Figure 3.8** Gels show a 4 kDa band for each elution E-1 to E-3. Unlike the unlabelled protein purification, E-4 and E-5 lanes do not show the MAβ40 protein band on the gel image. Also, the bands are much fainter, consistent with much lower yields when compared to the unlabelled protein. The minimal media has hindered bacterial growth, resulting in lower cell mass at the time of harvest. Nevertheless, the band confirms the presence of a protein similar to the one being examined by comparing it to the unlabelled MAβ40 protein purification gel image (**Figure 3.2**). In the gel image, lanes E-1, E-2, and E-5 contain higher molecular weight contaminants.

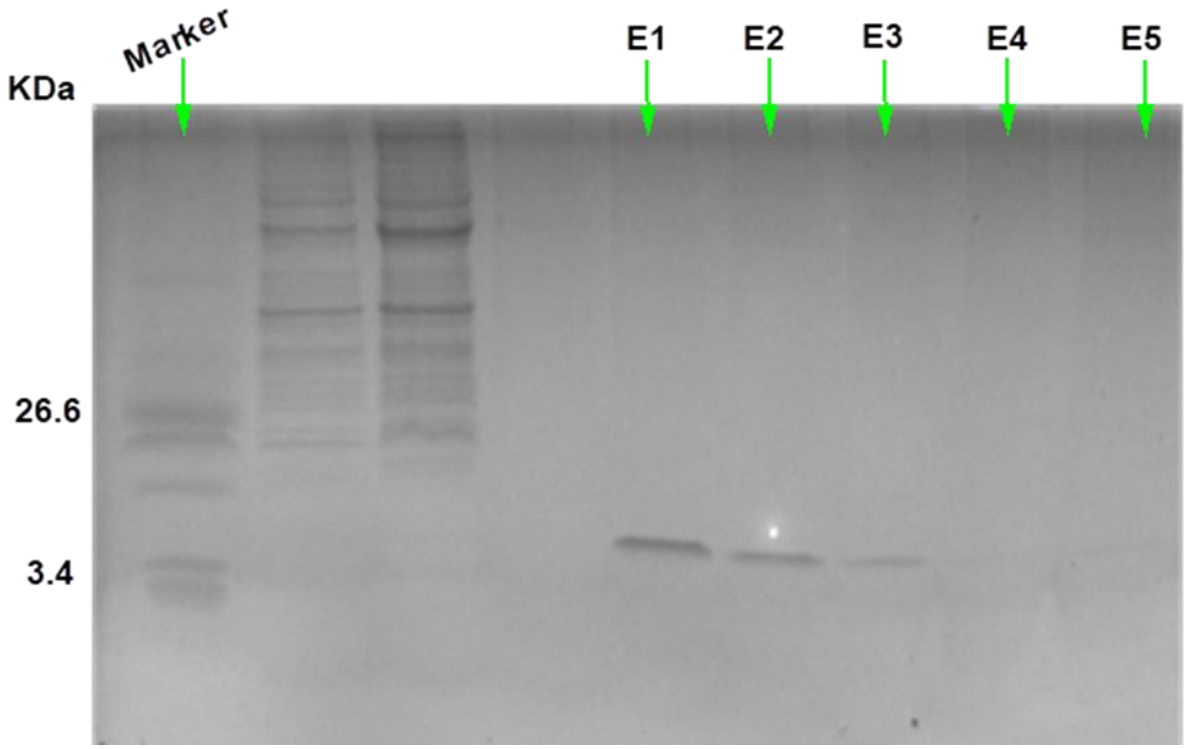

Figure 3.8. Tris-tricine SDS-PAGE gel of ^{15}N labelled MAβ40 (E1-E5) peptide expression after adding IPTG and incubating for 3-4 hours. The two unmarked lanes on the gel image next to the molecular weight marker and before E1-E5 are some other samples collected during the expression.

Purification of ^{15}N Labelled MAβ40 by SEC

SEC was again used to remove impurities as per the established protocol followed in the unlabelled protein purification. Again, due to the capacity limitation of loading the sample, ^{15}N Labelled MAβ40 was loaded into the column two times separately and they called here as run 1 and run 2. Both runs showed the same outcome as shown in (**Figure 3.9**), fraction FPLC chromatograms showed four peaks, with peak 1 and peak 4 being most prominent (**Figure 3.9**). The size of peak 4 contrasted with the chromatogram of the unlabelled protein and reflects an altered expression profile. The bacterium may have overexpressed survival proteins due to growth in a minimal medium. Tris-tricine SDS-PAGE gel analysis of each peak from both runs.

Figure 3.10 (bottom panel) shows high purity MAβ40 under peak 1 SEC run 1 and run 2 of 15 labelled MAβ40. None of the other peaks gave rise to bands on the gel consistent with MAβ40. Peak 1 also contains the highest protein concentration, as validated by a UV absorbance at 280 nm.

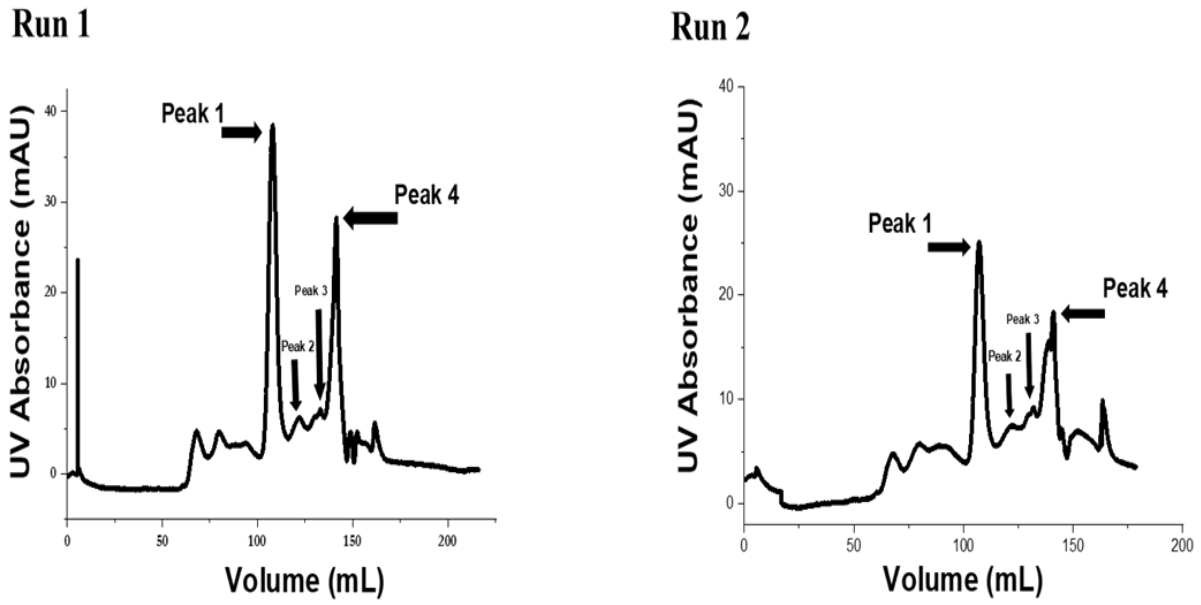

Figure 3.9. Chromatogram purification of ^{15}N labelled MAβ40 and the UV absorbance for protein using SEC chromatography.

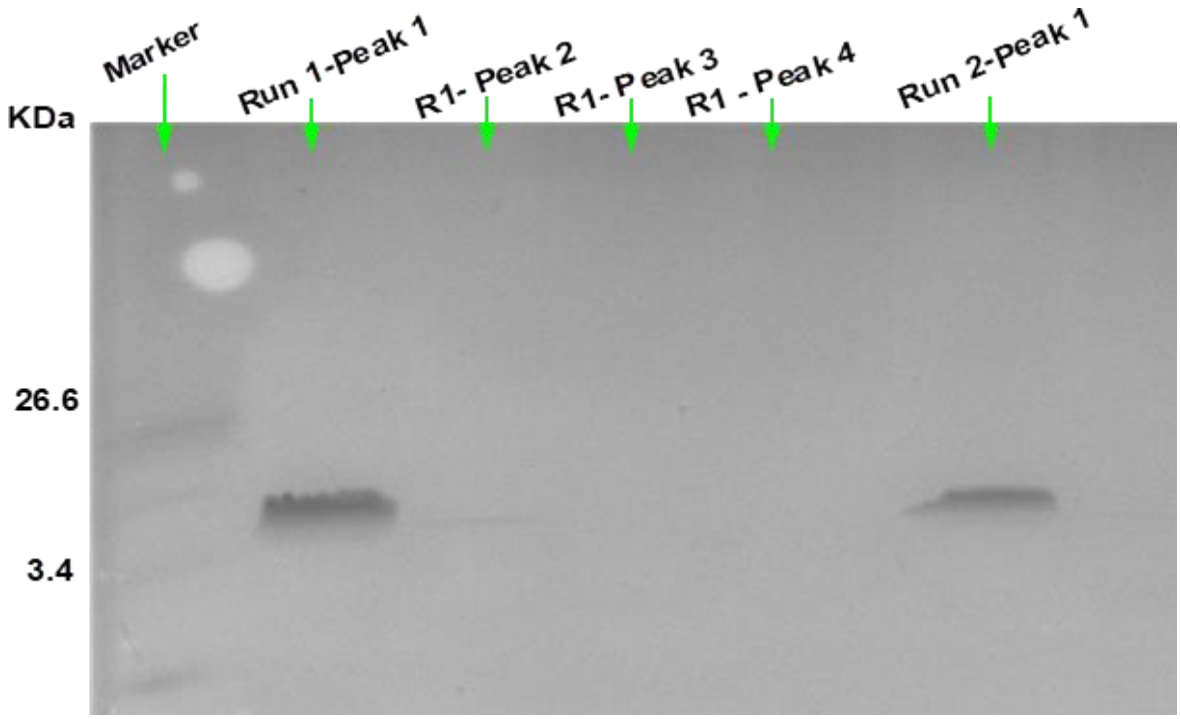

Figure 3.10. Tris-tricine SDS-PAGE gel of ^{15}N labelled MAβ40 (E1-E4 fractions after SEC purification) peptide expression after adding IPTG and incubating for 3-4 hours.

Labelled MAβ40 (^{15}N) identification by mass spectroscopy

In a similar fashion to the analysis of the unlabelled protein ESI-MS mass spectroscopy was used to determine the mass of the protein collected in Peak 1.

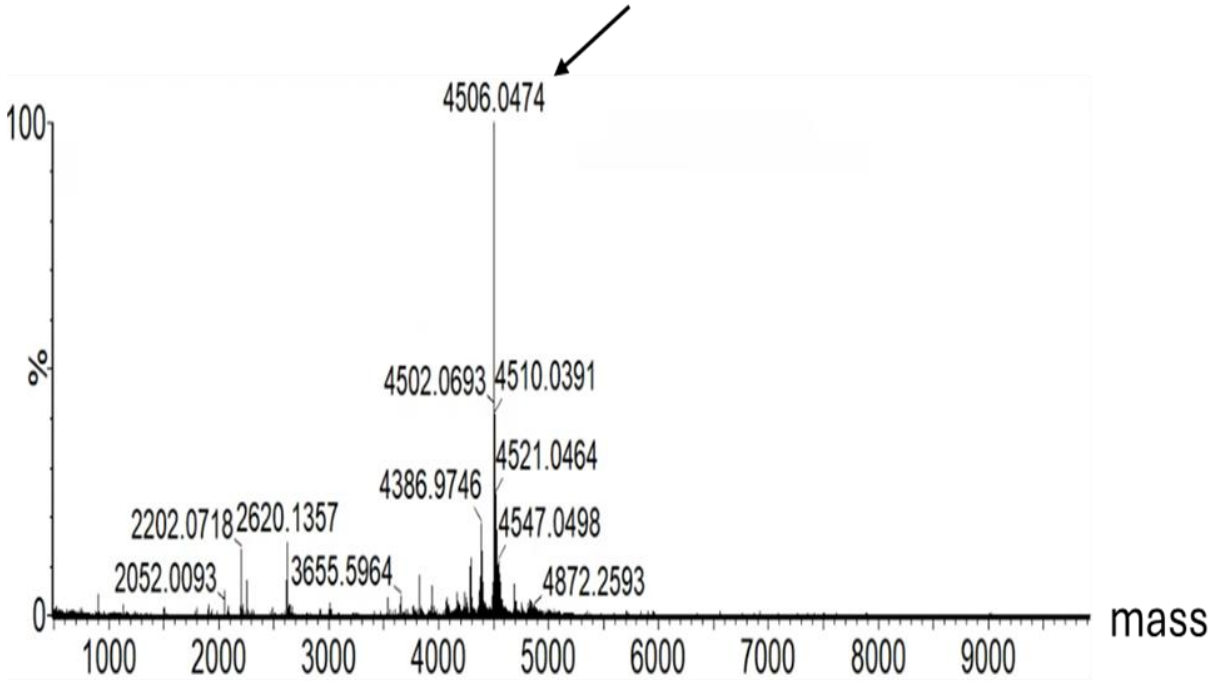

Figure 3.11. Positive electrospray ionization mass spectrometry of ^{15}N labelled MAβ40 obtained mass 4506.0474 Da.

Mass spectrometry was able to detect the molecular weight accurately, which established and measured the molecular weight with a precision of 4506.0474 Daltons (**Figure 3.11**). The determined molecular weight for the ^{15}N labelled protein is higher than compared to the unlabelled protein of 4459.2168 Da (**Figure 3.5**). The gain in molecular weight confirms the incorporation of ^{15}N-labelled amino acids in MAβ40. Correlating the observed on the tris-tricine PAGE gel proves that the expression and purification of ^{15}N labelled MAβ40 were successful.

^{15}N labelled MAβ40 expression yield, the number of expressions and yield obtained

After carrying out two independent iterations of ^{15}N labelled MAβ40 expression and purification, the production profile of MAβ40 shows a remarkable and consistent yield. The quantity of MAβ40 obtained from the consecutive ^{15}N labelled expressions was 1.30 mg in the initial iteration and 1.36 mg in the subsequent iteration. Hence, the ^{15}N labelled yield is about 30 percent of that of the unlabelled MAβ40 protein. Though it is three-fold lower than the yield of unlabelled protein, it can be justified by the lower bacterial mass growing under minimal media. The expression technique is both replicable and effective in producing ^{15}N labelled MAβ40.

Discussion

The work performed in this part of the thesis demonstrates that sufficient (i.e., milligram) quantities of MAβ40 could be produced to enable analysis of the interactions of the polyphenolic mixture with the insoluble protein fibres, as will be described in the following chapters. Also, labelled MAβ40 with ^{15}N was achieved for SSNMR analysis. The protein aggregates according to sigmoidal growth kinetics on a timescale consistent with that reported previously. The aggregates formed after 24 hours consist of fibrillar structures and no evidence of oligomers was observed.

This experimental chapter aimed to efficiently create a cost-effective and productive procedure for expressing and purifying amyloid beta 40 (MAβ40) peptide from *E. coli*, both before and after ^{15}N labelling. Using a small amount of medium for ^{15}N-labeling significantly reduced production costs while providing a large amount of pure protein for future research.

Through the use of SDS-PAGE gel, mass spectrometry, and a ThT aggregation experiment, it was confirmed that the updated procedure produced exceptionally pure unlabelled MAβ40.

Transmission electron microscopy verified the presence of discrete fibrous structures, providing additional support for the functional integrity of the separated peptide. The fact that the yield achieved from iterative overexpression of MAβ40 in *E. coli* remains consistent demonstrates the procedure's scalability and reliability. Although bacterial growth was reduced due to the use of a minimum media regimen, we could extract sufficient amounts of ^{15}N-labelled MAβ40 for further applications (Papaneophytou & Kontopidis, 2014). The presence of the ^{15}N isotope was detected using mass spectrometry. Establishment of this experimental procedure will allow future nuclear magnetic resonance (NMR) studies to reveal the structural dynamics and interactions of MAβ40. Because ^{15}N-labelled MAβ40 was successfully expressed and purified, there are opportunities to investigate its complicated interactions with inhibitors, cellular partners and disease-related mutations using solution and solid-state nuclear magnetic resonance (SSNMR) techniques.

Chapter 4 (Extraction and characterization of phenolic compounds from natural olive oil products)

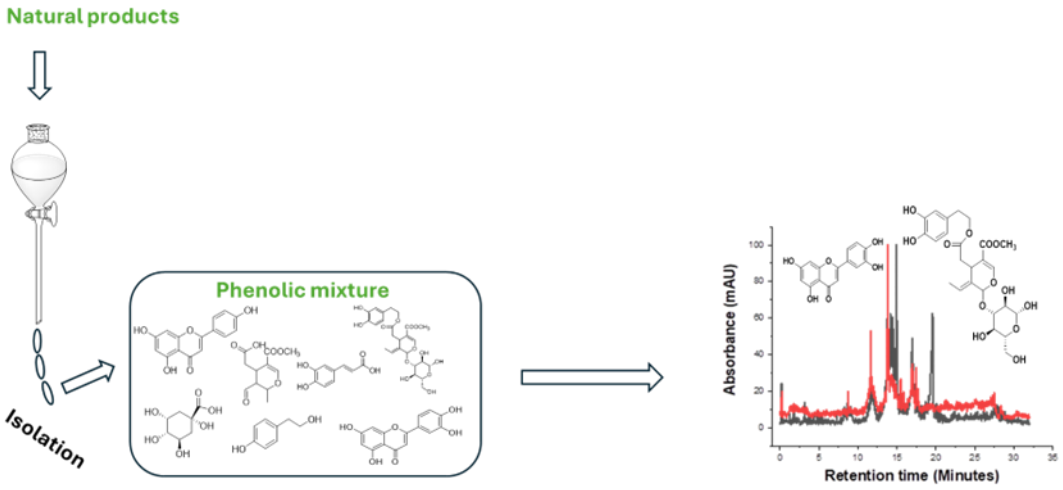

Introduction

The polar polyphenolic compounds contained in the fruits and oil of olive trees have powerful antioxidant properties (Dais and Boskou, 2009). Structurally, polyphenols all possess one or more hydroxylated benzene rings and their functional derivatives (Dey and Harborne, 1989; Pizarro et al., 2013). The antioxidant and free radical-scavenging activity of phenolic derivatives derives from the hydroxyl group(s) attached to the benzene rings. These compounds can give up the hydrogen atom of one of the phenolic hydroxyl groups to free radicals, thereby halting the cascade of electron transfer involved in oxidation (Pizarro et al., 2013). Polyphenols also have significant structural functions in protective and supportive tissues and have important roles in defensive and signalling mechanisms (Garcia-Salas et al., 2010). The antioxidant properties of these compounds also protect the olive fruit itself (and the oils it contains) from atmospheric oxygen.

While many of the nutraceutical effects of olives and olive oil are thought to arise from the antioxidant activity of the polyphenols they contain, as, for example, in their protective effect against degenerative diseases like cancer and heart disease (Dais and Boskou, 2009), polyphenols are also known to modify protein aggregation into amyloid fibrils associated with diseases. The latter property of EVOO polyphenols has received considerable recent attention as it suggests these compounds can be protective against neurodegenerative diseases caused by the build-up of protein aggregates, and which include Alzheimer's Disease (see **Chapter 1** and Rodríguez-Morató et al., 2015; Farré et al., 2019 for a detailed discussion of this aspect of their function). The anti-aggregation properties of EVOO polyphenols are part of the subject of this thesis. The chemical composition of EVOO contains different components which constitutes approximately 98% of the total weight of EVOO including glycerols (García-Villalba et al., 2009; Aparicio and Alonso, 1994; Holman et al., 1952; Fedeli et al., 1997; Pérez-Camino et al., 1996). However, it is the remaining 2% of the oil, particularly the phenolic part, that contains the antioxidant and anti-aggregation properties (García-Villalba et al., 2009; Vázquez-Roncero et al., 1976; Owen et al., 2000). Olive oils contain different classes of phenolic compounds, from simple phenols (hydroxytyrosol and tyrosol) to polyphenols. The latter include cinnamic derivatives, such as caffeic acid and *p*-coumaric acid, and benzoic acid derivatives, such as vanillic acid, as well as flavones (e.g., apigenin and luteolin), and secoiridoids (e.g., oleuropein and ligtroside derivatives) (Finicelli et al., 2021; de Fernandez et al., 2014). Summary of their chemical structures can be seen in **Chapter 1**. The phenolic fraction contains a multiplicity of subtypes, many of which have only recently been identified and about which only limited research exists (García-Villalba et al., 2009). In this thesis the results of an intensive review made of most of the detected components in olive oil are summarised in **Table S4.1 Appendix 1**.

The exact phenolic of the phenolic fraction of the compounds found in olive oils is dependent on several factors, including the variety, environmental conditions (soil type, climate, *etc*.), the time of harvest, and the method of oil extraction (e.g. malaxation temperature and oil extraction technique), making it of great interest to identify and quantify these compounds. Over the last ten years many analytical procedures have been proposed for determining the complete phenolic profile of EVOO (Hrncirik and Fritsche, 2004; Brenes et al., 1999; Montedoro et al., 1993; Rovellini et al., 1997; Brenes et al., 2000), but variations in extraction methods, chromatographic techniques, and quantification standards have all contributed to inconsistent reports about the levels of phenolic components in olive oil (Tasioula-Margari and Tsabolatidou, 2015; Hrncirik and Fritsche, 2004; Montedoro et al., 1992; Pirisi et al., 2000). Determining the levels of specific phenolics in EVOO requires three analytical stages – extracting the phenolic fraction from the oil sample, separation by chromatography, and quantification. The phenolics in EVOO exhibit diverse molecular sizes, polarities, and stabilities, making their complete extraction and subsequent isolation a challenging analytical procedure (Hrncirik and Fritsche, 2004).

Extraction is a critical first step and usually involves separating the phenolics by taking advantage of their weak polarity, compared to the non-polar lipids, and the effect this has on their solubility in various organic solvents or aqueous organic solvents. One common technique is solid-phase extraction (SPE) where the differential affinity of the phenolic and non-phenolic components of the oil for a particular solid sorbent is used as the separation mechanism (Pizarro et al., 2013; Servili et al., 1999; Favati et al., 1994; Favati et al., 1995; Andreoni and Fiorentini, 1995; Mateos et al., 2001). The oil is passed through a sorbent matrix (typically referred to as a cartridge) in which the sorbent used preferentially adsorb the phenolics. Subsequently the matrix is washed with a suitable solvent to remove interferents and a final solvent used to elute the phenolics from the sorbent matrix. The optimal choices of initial carrier solvent, washing

solvent, and elution solvent, are therefore critical aspects of SPE (Targuma et al., 2021; Badawy et al., 2018; Rosero-Moreano, 2018). The most commonly used sorbents for extracting the phenolic components of EVOO is the C_{18} cartridge (Pizarro et al., 2013; Servili et al., 1999; Favati et al., 1994; Favati et al., 1995), but anionic exchange cartridges (Pizarro et al., 2013; Andreoni and Fiorentini, 1995), amino phase cartridges, and diol-bond phase SPE cartridges (Pizarro et al., 2013; Mateos et al., 2001) are also used. One advantage of this method is that it minimizes or eliminates the need for expensive and environmentally toxic solvents. But one of the major disadvantages of this method is that samples need to be thoroughly prepared to remove particulates that could cause clogging of the sorbent cartridges, and some compounds of interest may also attach to the sorbent more strongly than others which can distort the subsequent analytical results (Targuma et al., 2021; Zdravkovic, 2017; Narenderan et al., 2020). **Figure 4.1** shows the SPE method.

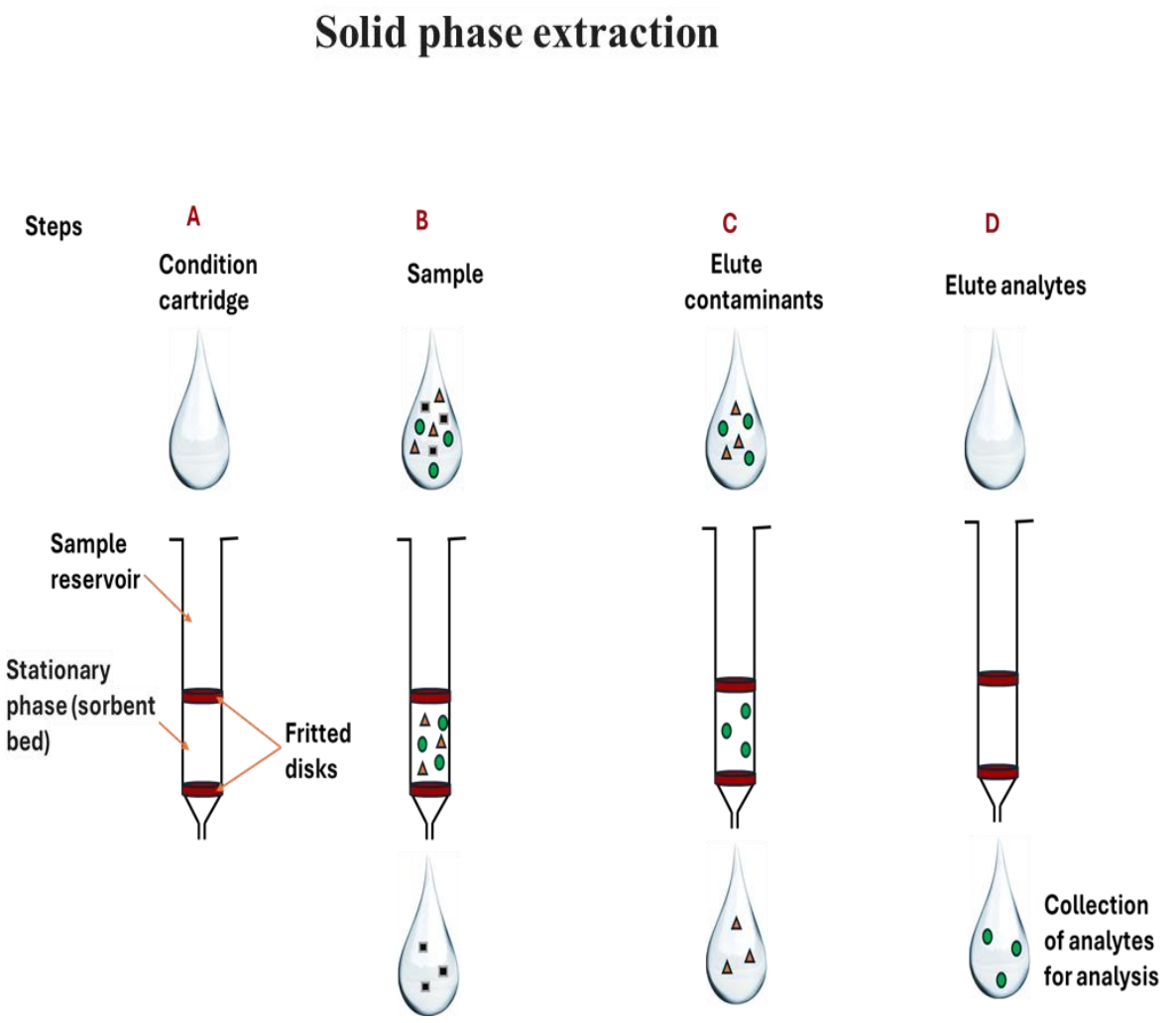

Figure 4.1. The diagram showing the steps of solid phase extraction as described in the above section, © Bakri A.

Another commonly used method is liquid-liquid extraction (LLE), where two immiscible liquid solvents are used to extract the phenolics based on the latter's greater solubility, and consequent migration into, one solvent. This requires determination of the partition (or distribution) coefficient of the phenolics (the solute of interest, or analyte) between both liquids (Garcia-Salas et al., 2010; Dobiáš et al., 2010; Pizarro et al., 2013; Brenes et al., 2000; Owen et al., 2000a; Owen et al., 2000b; Vázquez Roncero, 1978; Cortesi and Fedeli, 1983; Cortesi et al., 1995). The analyte is first dissolved into one solvent and placed in a funnel or centrifugation tube and the other immiscible solvent is added and mechanically shaken or

mixed at the optimal temperature and for the optimal time before being centrifuged (Targuma et al., 2021; Marsousi et al., 2019; Nichols, accessed online in 2024). The analyte migrates from the first solvent to the second solvent and after the two phases are separated in the centrifuge and funnel, can be collected and analysed **Figure 4.2** depicts the LLE process (Targuma et al., 2021; Nichols, accessed online in 2024). In the case of EVOO, the ideal choice of solvents would be such that the phenolics were highly soluble in both, and the non-phenolics or interferents having very little solubility in the second solvent. Literature reported that many different solvents are used in liquid-liquid extraction (LLE) of polyphenols such as lipophilic solvents containing methanol (Pizarro et al., 2013; Owen et al., 2000a; Owen et al., 2000b), aqueous organic solvents like methanol/water (Pizarro et al., 2013; Vázquez Roncero, 1978; Cortesi and Fedeli, 1983), and tetrahydrofuran/water (Pizarro et al., 2013; Cortesi et al., 1995), as well as N,N-dimethylformamide (Pizarro et al., 2013; Brenes et al., 2000).

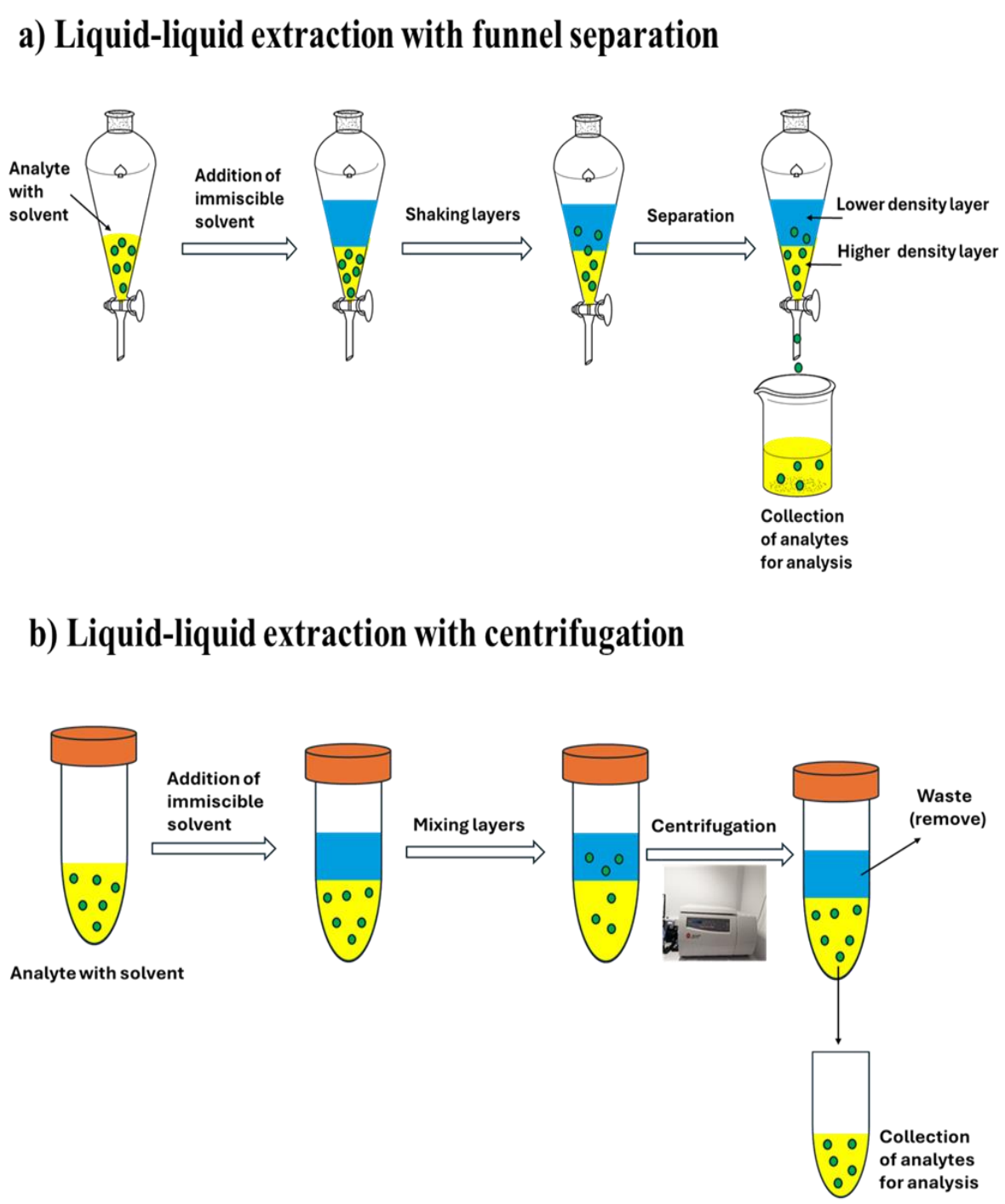

Figure 4.2. The diagram showing the steps of liquid–liquid extraction (a) with funnel separation. (b) with centrifugation, © Bakri A.

In addition to the types of solvent/sorbents used, the extraction process is sensitive to many factors including time, temperature, pressure, and sample-solvent dilution. Furthermore, it may be necessary to repeat the extraction procedure several times to attain satisfactory yields. These methods may also be enhanced by combining them with other techniques such as sonification or microwave radiation. It is important to note that the distribution of phenolics within any sample of EVOO can show marked variations, and this will affect which extraction method, and solvents need to be used to obtain optimal extraction (Khoddami et al., 2013). The characterization (compound identification and quantification) of the extracted phenolic fraction of the oil is carried out with techniques such as spectrophotometry, high performance liquid chromatography (HPLC), liquid chromatography–mass spectrometry (LC-MS), gas chromatography–mass spectrometry (GC-MS) and nuclear magnetic resonance (NMR) techniques (Khoddami et al., 2013; Garcia-Salas et al., 2010; Targuma et al., 2021; Badawy et al., 2018; Rosero-Moreano, 2018).

Aims

As will be described in **Chapter 5**, the effects of individual phenolic compounds from EVOO on protein aggregation into amyloid has been studied extensively. However, the collective anti-aggregation properties of polyphenol mixtures extracted directly from EVOO has not been studied and is part of the aim of the work in this thesis. To understand the effects of EVOO polyphenol mixtures on amyloid, and the variability of the effects from different EVOO sources, it is first necessary to (i) develop a suitable extraction procedure and (ii) gain a comprehensive understanding of the composition of the extracts. This chapter aims to analyse the composition of different olive oil preparations to separate, identify, quantify, and characterise the main polyphenolic compounds that are considered to be biologically active as mixture or individual phenol at preventing amyloid formation for treating AD. The difference

in the polyphenol content from EVOO obtained from two different sources (Greece and Saudi Arabia) was also analysed. The first step is to find a suitable and the most effective method for extracting the polyphenolic components of EVOO.

Materials and methods

Materials

All chemicals, including methanol (99.9% analytical reagent grade), hexane (95% HPLC grade) and acetonitrile (99.9% HPLC Gradient grade) were purchased from Fisher Scientific. Ethyl acetate (99.5+%) was purchased from Acros Organics Chemicals. DMSO-d_6 for NMR (99.9 atom %D) was obtained from ThermoScientific. Formic acid 98% was purchased from Honeywell Fluka. Milli-Q water was provided by the in-house purification system (Milli-Q purified water, Q-POD IQ 7000 Biomedical and Life Sciences, Lancaster University).

The equipment used for this experimental work involves using various state-of-the-art analytical and spectroscopic techniques, including HPLC and tandem mass spectrometry, UV-Vis, NMR in solution and solid state, centrifuge, sonicator, rotary evaporator and freeze dryer.

Polyphenol standard solutions

These were a range of polyphenol compounds already identified in EVOO and made up to 500 µM solutions of methanol/water. These included (with percentage purities) tyrosol (98%), hydroxytyrosol (98%), vanillic acid (97%), syringic acid (98%), cinnamic acid (99%), ferulic acid (99%), p-coumaric acid (98%), caffeic acid (98%) and oleuropein (98%), were purchased from Sigma Aldrich; Luteolin (97%), apigenin (97%), naringenin (97%), were obtained from

Alfa Aesar; and (+)-pinoresinol (95%) was purchased from Cayman Chemical Cambridge Bioscience.

Stock solutions of each polyphenol were made by dissolving the specified quantity of the pure solid in 25 mL of methanol/water (50:50). Standardized solutions were prepared at various concentrations in 10 mL volumetric flasks by dilution and stored in the dark at 4 °C. All solutions were passed through a 0.22 µm filter before injection into the ultra-high-performance chromatograph (UHPLC) and LC-MS.

Natural olive oil products collection

In this thesis work the two different sources of the extra virgin olive oils used are commercial products available in Saudi Arabia (Buseita Al Jouf Early Harvest Extra Virgin Olive Oil first and cold press) and Greece (Yannis Fresh Greek Early Harvest Extra Virgin Olive Oil cold extraction), both products covered with foil and stored in the dark at 4 °C.

Methods

Extraction of polyphenols from extra virgin olive oil using different techniques

For extraction of polyphenols, three distinct techniques of funnel separation, LLE centrifugation and SPE were performed to extract polyphenols from olive oils, in order to test their effectiveness and to identify the technique providing a promising result. The aim of this section is to find a suitable extraction method.

Extraction of polyphenols from olive oil using solid phase extraction SPE technique

A diol-phase cartridge was employed to perform solid phase extractions under the conditions specified by Mateos et al. (2001) (see **Figure 4.3**). The first step was dissolving 10 ± 0.001 g olive oil into hexane, followed by 5-minuted sonication at 20 microns of the solution using a tip sonicator. Pre-equilibration and conditioning of 6 mL (1g) Discovery DSC-Diol SPE cartridge (Sigma) were performed by passing 15 mL methanol and 15 mL hexane to avoid column drying. The next step was loading the oil solution onto the column. 15 mL hexane and 15 mL 90:10 hexane:ethyl acetate were used to wash the column before elution of the polyphenols with 20 mL methanol. The methanolic phases were collected and kept in the fridge for 24 hours to remove the oil droplets. After overnight drying in a vacuum oven, the subsequent step was weighing and redissolution of the solids in 50:50 methanol water to a final concentration of 10 mg/mL.

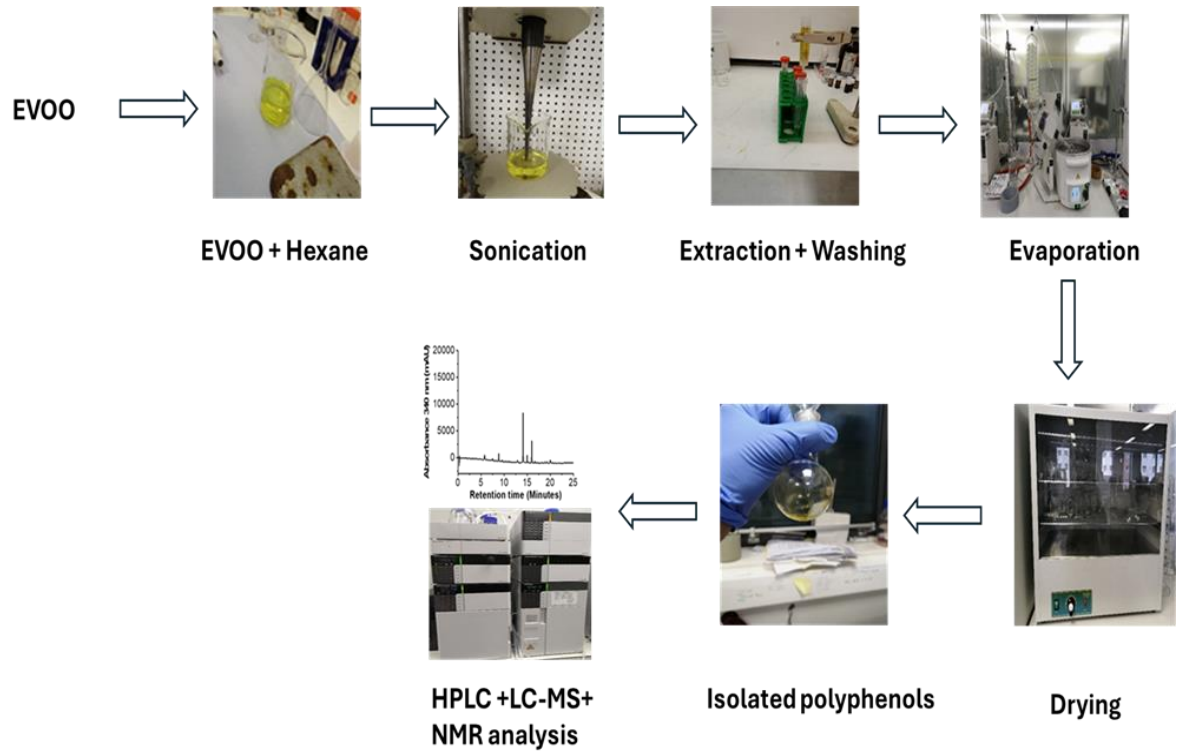

Figure 4.3. Process of solid phase extraction of phenolic compounds from extra virgin olive oil (EVOO), © Bakri A.

Extraction of polyphenols from olive oil using the centrifugation technique

The protocol outlined by Ferro et al. (2019) was implemented with some modifications to extract olive oil polyphenols through centrifugation, as described below (see **Figure 4.4**). The first step was dissolution of 10 ± 0.003 g EVOO in hexane and the solution was sonicated at 20 microns for 5 minutes followed by addition of 20 mL methanol/water (60:40 v/v). A vortex device was used to shake the solution for a minute before 10-minute centrifugation at 4000 rpm. The next step was extraction of the methanolic phase. The process of extraction was conducted in triplicate and washed twice with hexane. The oil droplets were eliminated by gathering and storing the methanolic phase in the fridge for 24 hours, followed by methanol removal through evaporation at 40 °C. Last but not least, water removal was performed by

freeze-drying the solution at -70 °C and 0.0026 mbar pressure, followed by weighing and redissolution of the solid in 50:50 methanol/water to a final concentration of 10 mg/mL.

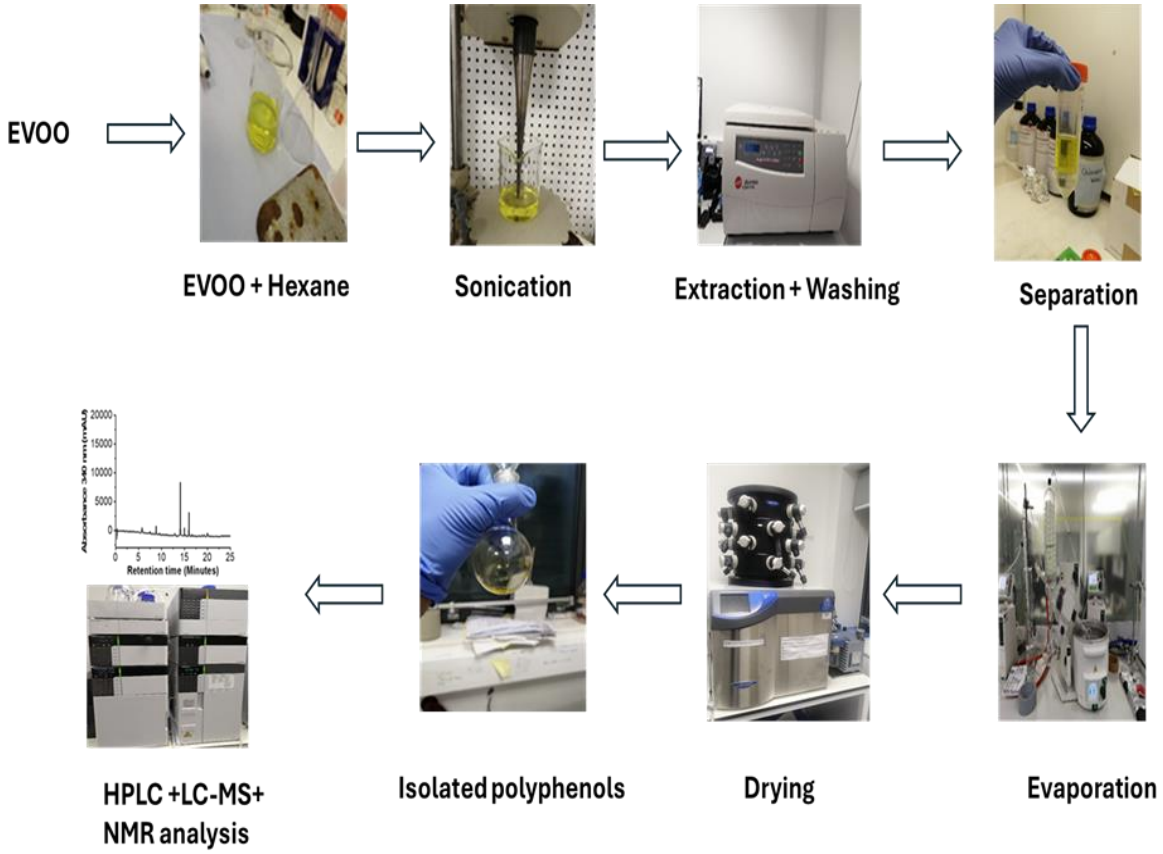

Figure 4.4. Process of liquid-liquid (Centrifugation) extraction of phenolic compounds from extra virgin olive oil (EVOO), © Bakri A.

Extraction of polyphenols from olive oil using the funnel separation technique

The protocol used to perform funnel separation was derived from (Pizarro et al., 2013; Gutfinger, 1981; Vázquez, 1973) with some modifications as described below (see **Figure 4.5**). The olive oil (10 ± 0.003 g) was dissolved in hexane and the solution sonicated at 20 microns for 5 minutes, then loaded into the separating funnel, and shaken for 2 minutes before three-

fold extraction with 20 mL of methanol/water (60:40, v/v). The methanolic fraction contained the polar polyphenol compounds and after collection was washed with hexane two times before being refrigerated for 24 hours, following which the methanol was evaporated off at low pressure at 40 °C. It was then lyophilised at 0.0026 mbar for 24 hours at -70 °C, followed by weighing and redissolution of the solid in 50:50 methanol/water to a final concentration of 10 mg/mL.

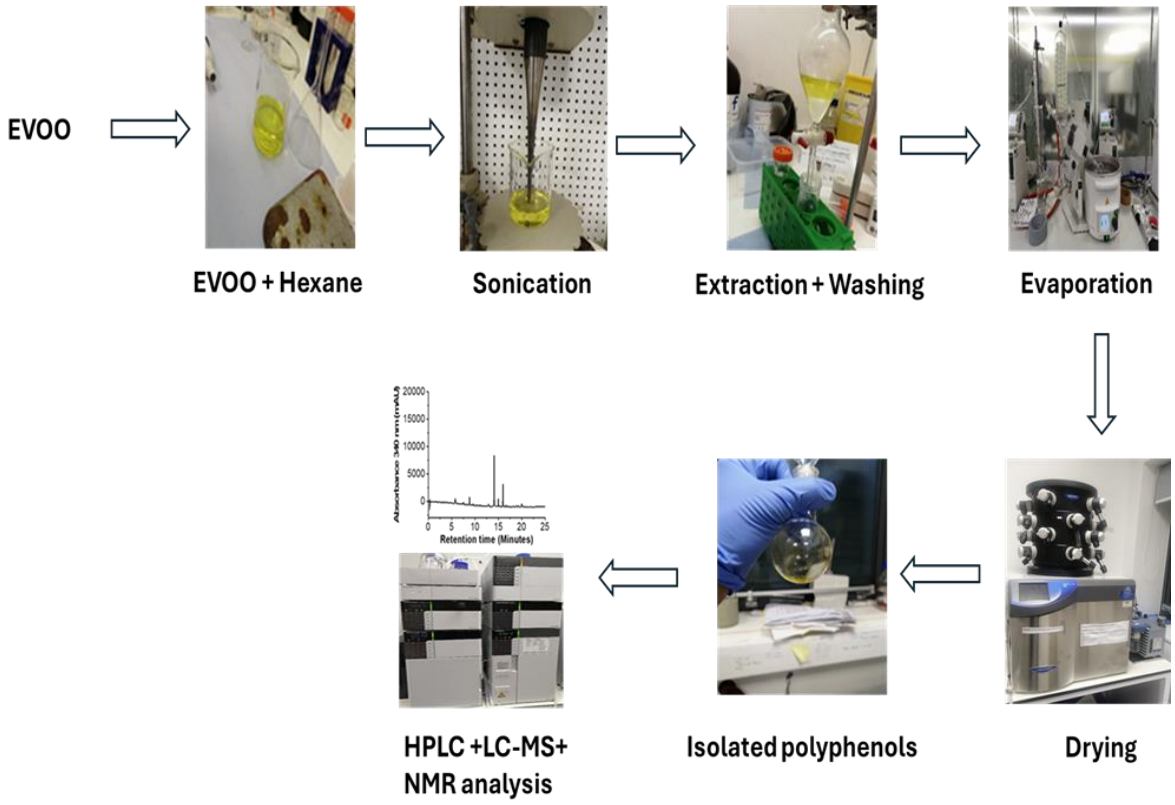

Figure 4.5. Process of liquid-liquid (Funnel separation) extraction of phenolic compounds from extra virgin olive oil (EVOO), © Bakri A.

Chromatography

High-performance liquid chromatography analysis

Separation of the unknown compounds was developed and carried out by HPLC on a NexeraX2 UHPLC (Shimadzu) system, this process was performed at a temperature of 40 °C with a mobile phase consisting of 0.1% formic acid in either ultrapure water (Buffer A) or acetonitrile (Buffer B). The solid phase comprised a Shim-pack XR-ODS 2.2 µm (3.0 mm x 50 mm) column. The system was loaded with 10 µL of the 1 mg/mL dilution from stock 10 mg/mL olive oil extract and the system run at a flow rate of 1 mL/min, with the gradient elution comprised 5% Buffer B for 0-3 minutes, 40% Buffer B for 3-26 minutes, 50% Buffer B for 26-27 minutes, and 5% Buffer B for 27-32 minutes. Absorbance intensity was measured at 240 nm, 275 nm, and 340 nm, with a bandwidth of 4 nm.

Liquid chromatography–mass spectrometry analysis

The extract mixtures were analysed by liquid chromatography–mass spectrometry (LC-MS), using a Shimadzu LCMS-IT-TOF coupled with a NexeraX2 UHPLC. The latter comprised a DGU-20A5R degassing unit, two LC-30AD LC pumps, a SIL-30AC autosampler, and a CTO-20AC column oven. Separation was attained with the same Shim-pack XR-ODS column, and optimum separation ensured by using a binary mobile phase gradient elution of 1 mL/min flow rate. The column temperature was kept at 40 °C and with a 20 µL injection volume. The solvent buffers and elution profile were identical to those used for the HPLC analysis. The data was acquired in positive and negative ionizations with polarity switching. The acquisition range for both positive and negative was from 100 *m/z* to 700 *m/z* with ion accumulation at 40 ms. The data was analysed with Shimadzu LC-MS solution software. Sample peak areas were

calculated from the predicted *m/z* value of $[M + H]^+$, $[M - H]^-$ and $[M + Na]^+$ ions in positive and negative ionization scan modes.

UV-Vis Spectrophotometer analysis

UV-Visible spectroscopy was used to analyse the phenolic samples extracted from each of the EVOOs. UV–Visible spectra were acquired at room temperature (25 °C) using a NanoDrop 2000/2000c spectrophotometer equipment, (Supplied and serviced by Labtech Biomedical and Life Sciences, Lancaster University) in the 200 nm to 500 nm range. The transmittance signal was adjusted with a blank sample (Alves et al., 2019; Milanez et al., 2017).

Solution state nuclear magnetic resonance analysis

The polyphenols were extracted from 20 g of EVOO using the method described earlier, to produce a mixture sufficiently high in polyphenols to obtain an accurate NMR spectrum. For solution state NMR experiment 40 mg of Greek and Saudi phenolic extracts dissolved in 0.6 mL DMSO-d_6 and the acidity adjusted by stepwise addition of DMSO-d_6 stock solutions of trifluoroacetic acid (TFA) or triethylamine while monitoring the linewidth of the hydroxyl peaks of the 1D proton spectra. Too much triethylammonium trifluoroacetate can catalyse proton transfer and provide unwanted line-broadening, and together with the fact that the optimal acidity was in quite a narrow concentration range, can make overshooting a potential problem. This required the incremental addition of 10-20 µL of a 100 mM TFA stock, to give polyphenol hydroxyl linewidths of 1-2 Hz. Magnitude-mode DQF-COSY spectra were obtained with a 5.5 ppm offset and direct and indirect dimension spectral widths of 4 kHz using the *cosygpmfppqf* Bruker library sequence and 256 two-transient t1 increments.

Results

Comparison of isolation methods of phenolic compounds from EVOO using LLE and SPE

Three different extraction techniques, LLE with funnel separation, LLE with centrifugation, and SPE, were evaluated for their ability to extract polyphenol compounds from the EVOO. The LLE and SPE methods were compared in terms of the number of different polyphenols extracted and their quantities. To ensure the methods were reliable, the extraction procedures were replicated 3 times, and the consistency of the results across replications assessed statistically. This evaluation step was important in determining the most suitable method for our future work on the potential of polyphenolic extracts from EVOO to mitigate the protein aggregation processes involved in Alzheimer's disease. Both LLE techniques gave higher yields than SPE, as shown in **Table 4.1** below. The extracted compounds were then separated using HPLC and the chromatograms generated at 240 nm, 275 nm and 340 nm wavelengths were examined. The results obtained from HPLC analysis confirmed the finding that the LLE techniques were more effective than SPE, with the former generating more peaks (see **Figure 4. 6**). Moreover, Capriotti et al., 2014 reported that increasing the concentration 2.25 times of SPE did not improve the outcome compared with LLE. These results agree with previous studies that also found SPE problematic because it extracts particular phenolic compounds, particularly the aglycone types, less well than others. For example, the reactive dialdehydic forms of the oleuropein and ligstroside aglycones have previously been reported to be poorly recovered using SPE method (Tasioula-Margari and Tsabolatidou, 2015; Capriotti et al., 2014; Hrncirik and Fritsche, 2004; Montedoro et al., 1992; Pirisi et al., 2000). This is unfortunate as it has advantages as an isolation technique in terms of speed, cost, and solvent usage (Suárez et al., 2008).

Table 4.1. The mean yield of phenolic residue extracted from olive oil using liquid-liquid extraction and solid phase extraction methods.

Method	Total average of phenolic residue (mg)
SPE (Diol-phase cartridge)	17.6 ± 0.04
LLE (Funnel separation)	25.3 ± 0.02
LLE (Centrifugation)	25.5 ± 0.05

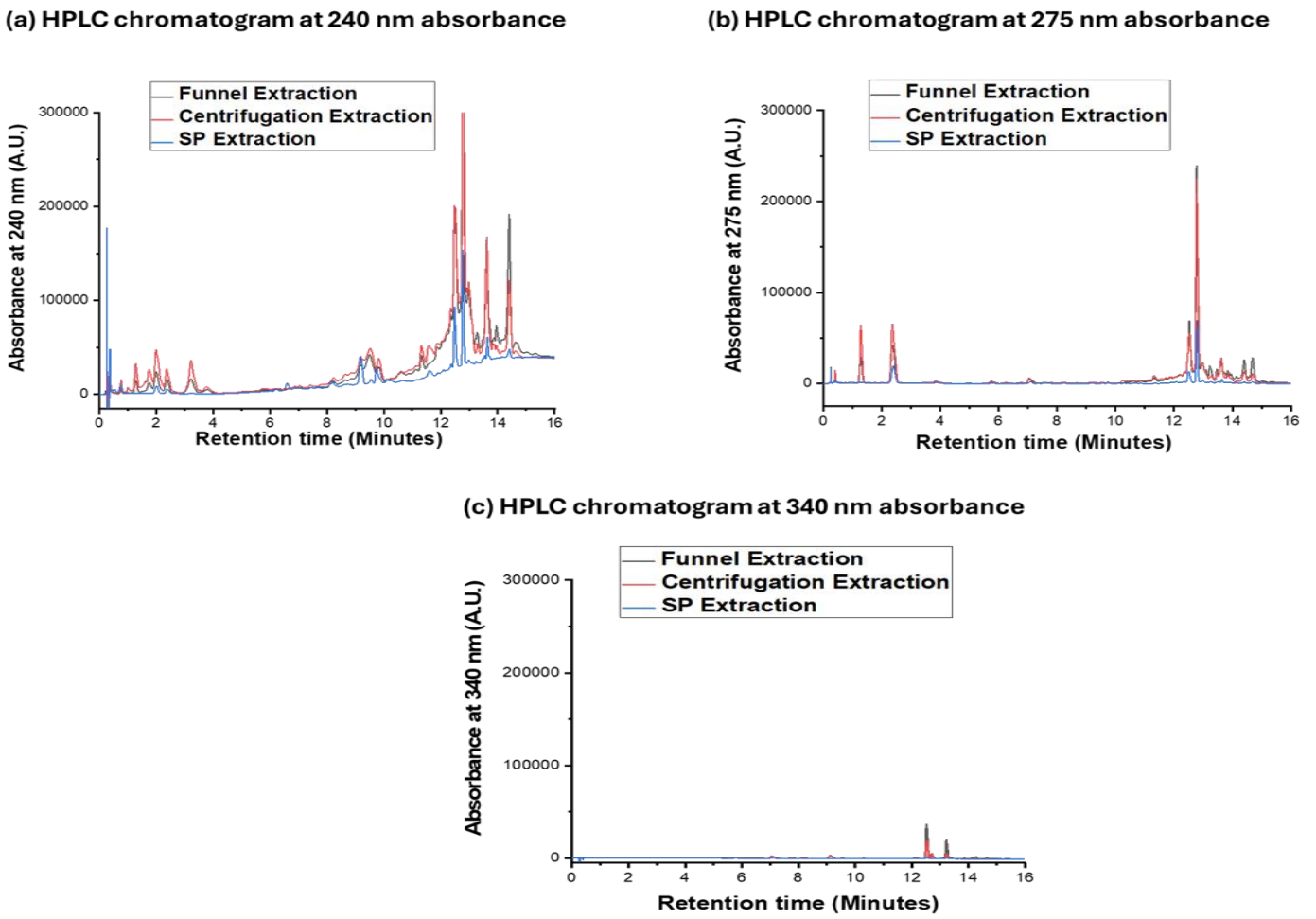

Figure 4.6. HPLC chromatograms at three different wavelengths (a) at 240 nm, (b) at 275 nm and (c) at 340 nm of polyphenols isolated from extra virgin olive oil using the three different techniques. Peak assignments will be described later in this chapter.

In the LLE extraction methods, particularly with centrifugation, the stage where the aqueous methanol/hexane mixture separates into layers is critical. Great care is needed at this stage, as even very minor deviations in the procedure can lead to widely different results, a difficulty also recognized in previous work (Pirisi et al., 2000). Based on our results, LLE Funnel Extraction was chosen as the best method to isolate polyphenolic compounds from olive oil, and subsequently enhanced by adding sonication, washing steps and improving the HPLC separation particularly in the area after 12 mins. To establish the reliability of the method, the extraction technique was replicated twice with samples from the same EVOO and under identical conditions. No significant differences were observed in the HPLC results for the two replications, which confirms the reproducibility of the findings and thus the reliability of this technique (see **Figure 4.7**).

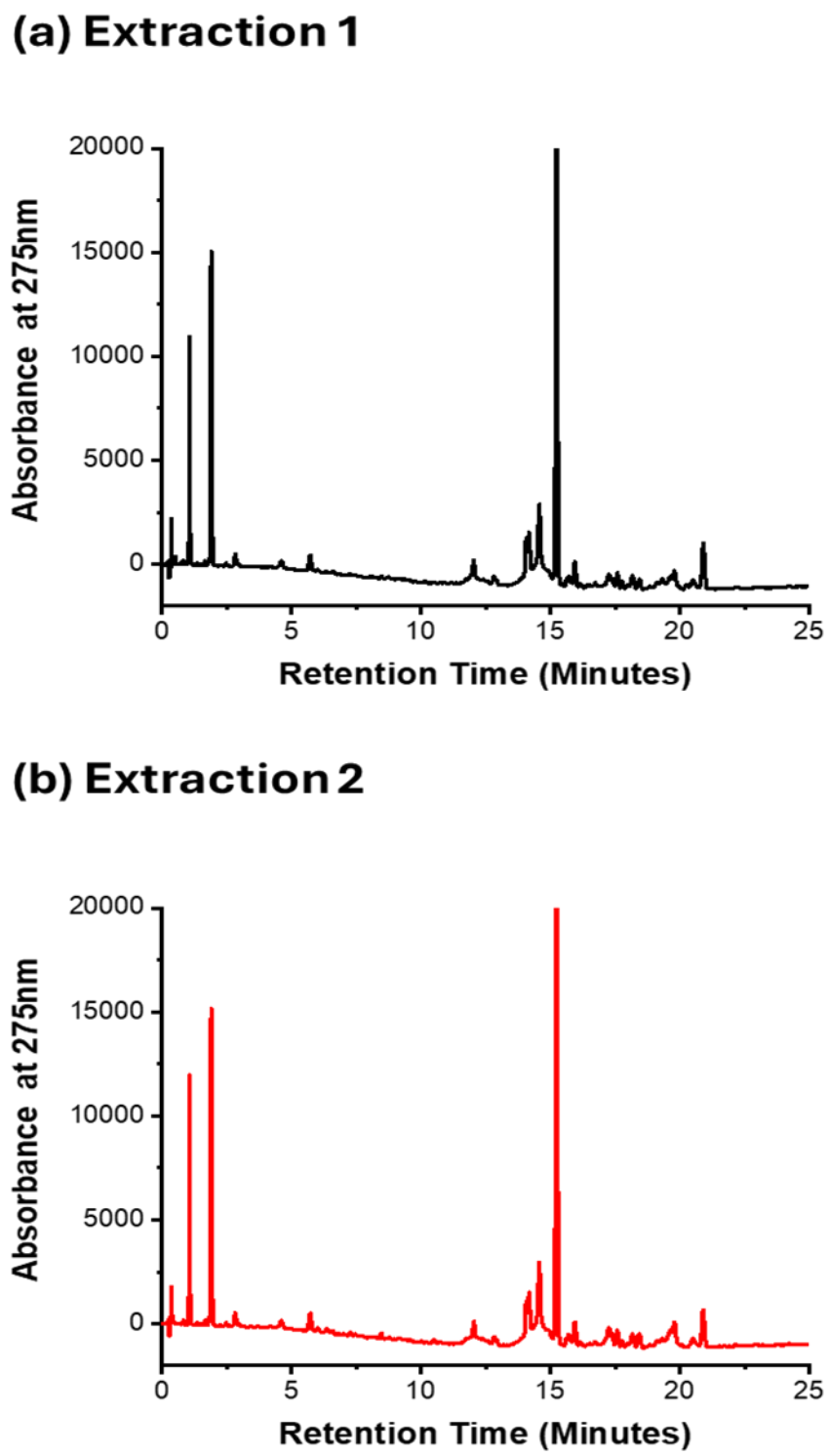

Figure 4.7. (a and b) Chromatograms obtained by funnel separation extraction of Greek olive oil samples extracted twice under identical conditions. Phenolic compounds were isolated by extraction of an oil-in-hexane solution with water methanol /water (60/40) to confirm repeatability and reproducibility of results.

In the present work, optimal outcomes for extracting the phenolic compounds from olive oil, were attained using LLE with funnel separation and methanol/water as the polar solvent, which is in agreement with previous studies (Carrasco Pancorbo et al., 2004; Hrncirik and Fritsche, 2004; Montedoro et al., 1978; Vazquez Roncero, 1978; Vazquez Roncero et al., 1976; Vázquez, 1973).

Isolation and identification of phenolic compounds from different olive oil sources

Isolation of polyphenols

The polyphenols were first isolated from Greek and Saudi Arabian EVOO using the enhanced LLE polar phase extraction method described above. Using hexane/methanol as solvents gave the highest yield of 25.3 mg solid extract per 10 g EVOO from both the Greek and Saudi oils.

UV-Visible absorption spectra of the phenolic extracts

The UV–Vis absorption spectra between 200 nm and 500 nm from both Greek and Saudi EVOO samples were obtained (Fuentes et al., 2012). This was done to identify the wavelengths of the main bands for detection in the HPLC chromatograms, and also to give an approximate comparative method for quantifying the extract concentrations. The spectral region between 240 nm and 400 nm, has previously been reported as characteristic of hydroxycinnamic acids, hydroxybenzoic acids, flavonoids, secoiridoids and their derivatives in methanol/water solution (Fuentes et al., 2012; Shahidi and Naczk, 1996). Moreover, it has been identified that the absorption of phenolic compounds at 240 nm are attributed to elenolic acid and its derivatives, and the absorption at 280 nm is characteristic of most phenolic compounds, while the absorption between 310 nm and 320 nm could be indicative of flavonoids such as apigenin

and luteolin. The UV-Visible absorptances for Greek and Saudi EVOO extracts were recorded at higher and lower concentrations as shown in **Figure 4.8** (Fuentes et al., 2012; Lerma-García et al., 2009).

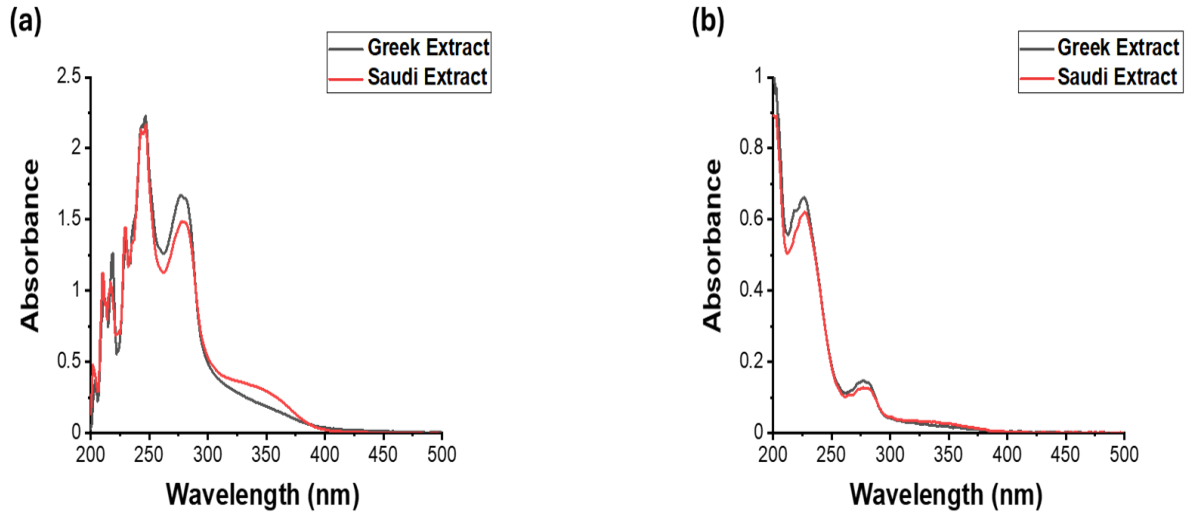

Figure 4.8. The UV-Visible absorptances for Greek and Saudi EVOO extracts. (a) the UV–Vis absorption for Greek and Saudi EVOO extracts as stock solutions (10 mg/mL). (b) the UV–Vis absorption for Greek and Saudi EVOO extracts as 10-fold dilutions.

Chromatographic analysis

Identification and characterisation of polyphenols from both sources using LC-MS

We next sought to identify the molecular composition of the extracts. Chromatography was used to identify and characterize individual phenolic components of extra virgin olive oil from the different sources. Liquid chromatography–mass spectrometry (LC-MS) was applied as the first method. The HPLC-MS coupling concerning atmospheric pressure ionization methods, time-of-flight (TOF), as well as electrospray ionization (ESI) are robust and appropriate tools for determining the natural products in crude extracts, as they have soft ionization (Tasioula et

al., 2015). In this work it was ensured that LC-MS performed with the same column and the same mobile phase solvent gradient that was used in the HPLC separation technique. HPLC will be described later in this section.

LC-MS chromatograms for both Greek and Saudi EVOO identification are shown in **Figure 4.9** the outcome showed that both sources containing almost the same phenolic compounds but at different concentrations and the difference can be seen when the peak heights compared in both sources for examples peak at 19.5 min is higher in Greek extract than Saudi extract while peaks at 11.6 and 15.65 mins are higher in Saudi EVOO than Greek EVOO. This finding has also been reported previously when the composition of different olive oils was analysed by LC-MS (Gatt et al., 2021). The two mixtures' MS profiles were examined for the presence of polyphenol masses H^+, H^- and Na^+, which are frequently found in olive oil (see **Figure 4.10**). **Figure 4.15** of the NMR section shows the chemical structures of these compounds and **Table 4.2** shows their empirical formulae. More than 40 chromatographic peaks were observed in the LC-MS analysis, which could be assigned to 20 polyphenols or their isomers. Each mixture contained many of the polyphenols that have already been reported to be contained in EVOO, such as elenolic acid, oleuropein, tyrosol and derivatives of hydroxytyrosol (e.g., glucosides, aglycones, *etc*.) and derivatives of oleocanthal. The oleocanthal derivatives are the polyphenols responsible for the pronounced, bitter taste of EVOO made from olives harvested early in the season. Also present were flavonoids, such as apigenin, lignans, vanillic and other dihydroxybenzoic acids, and the phenolic acids, including caffeic, coumaric, and ferulic acids. Of particular relevance, is that *in vitro* experiments have demonstrated the inhibitory effect of apigenin, ferulic acid, oleuropein, and tyrosol, on fibril formation and Aβ aggregation. Overall, the chemical profiles of the Greek and Saudi olive oils were similar, with nearly all of the detected compounds present in both samples.

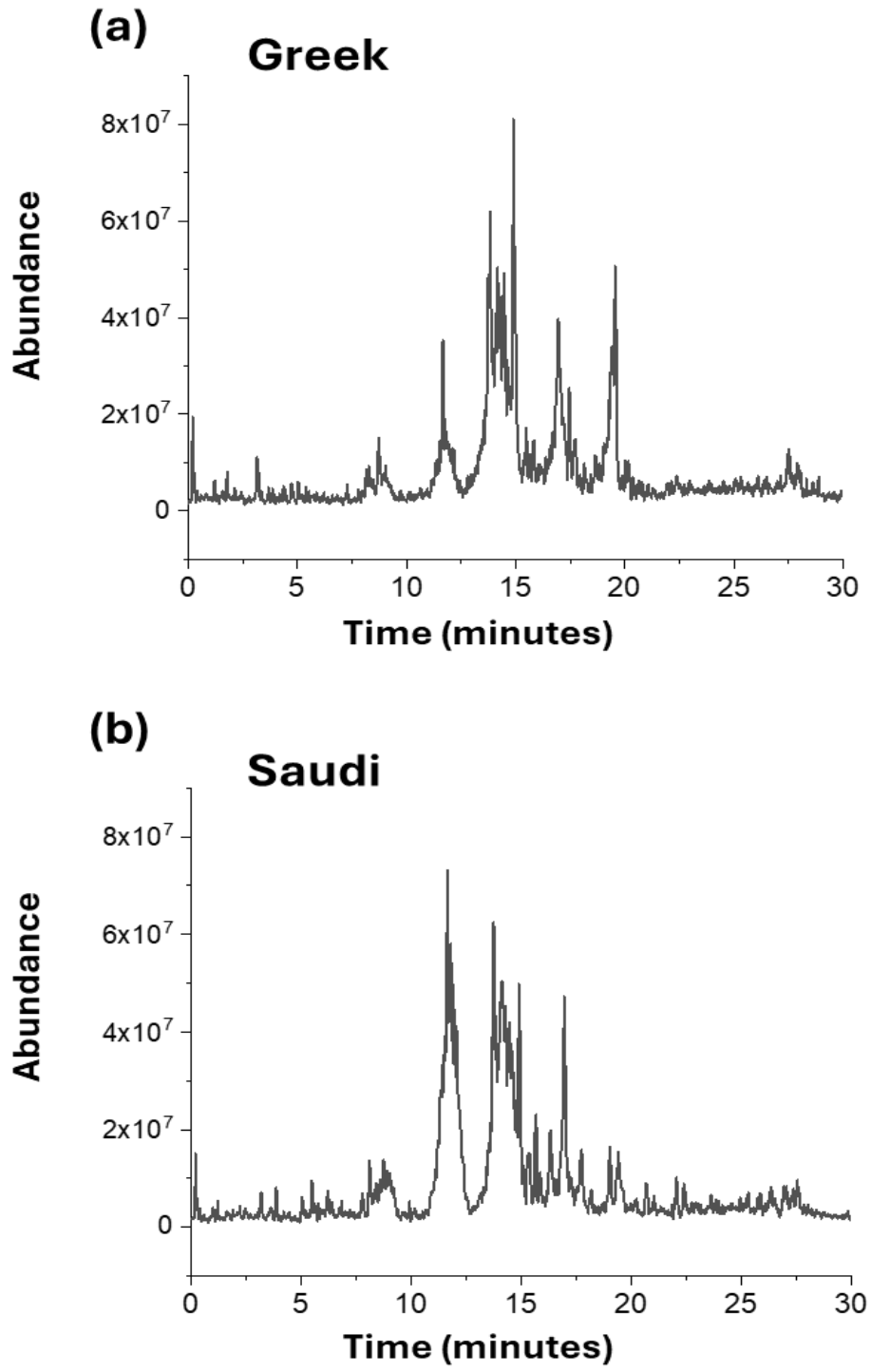

Figure 4.9. (a) Greek (top) and (b) Saudi (bottom) LC-MS chromatograms of the EVOO extracts.

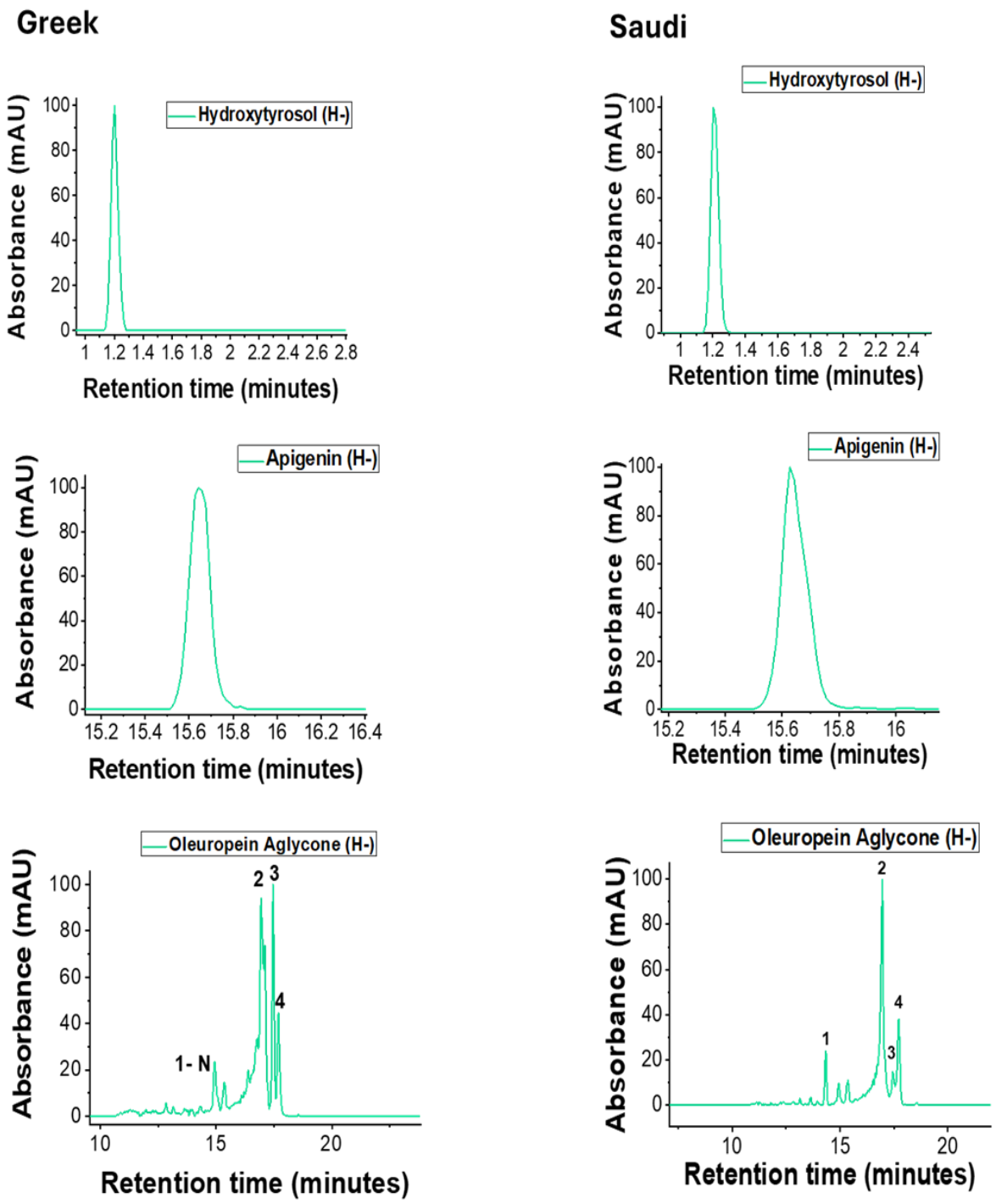

Figure 4.10. LC-MS ion chromatograms for individual phenolic compounds detected from Greek and Saudi EVOOs at identical retention time, here we are showing some of them including hydroxytyrosol, apigenin and oleuropein aglycone (Greek individual compounds in the left side and Saudi individual compounds in the right side of the figure shown above focusing on individual peak detection and retention time of each compound). The rest of

individual detected compounds and their retention times are given in **Appendix 1 Figure S4.1** for Greek extract and **Figure S4.2** for Saudi extract.

Table 4.2. Phenolic compounds identified using LC-MS, in Greek (G) and Saudi (S) EVOO.

Name	RT (min)	H (+)	H (-)	Na (+)	G	S
Quinic Acid	0.31		191.0567		Y	Y
Hydroxytyrosol	1.20		153.0585		Y	Y
Vanillic Acid	3.19	169.0846			Y	Y
Caffeic acid	3.64		179.0323		Y	Y
Hydroxyelenoic Acid (Isomer 1)	6.91		257.0655		Y	N
Hydroxyelenoic Acid (Isomer 2)	7.41		257.0664		Y	Y
Hydroxyelenoic Acid (Isomer 3)	8.74	259.0777	257.0660		Y	Y
Elenolic Acid	9.00	243.0820	241.0722		Y	Y
Hydroxyelenoic Acid (Isomer 4)	9.57		257.0657		Y	Y
Hydroxydecarboxymethyl-oleuropein aglycone	11.63	337.1235	335.1113	359.1068	Y	Y
Dihydroxyoleuropein Aglycone (Isomer 1)	11.70		409.1074		Y	N
Hydroxytyrosol Acetate	11.72		195.0677		Y	Y
Dihydroxyoleuropein Aglycone (Isomer 2)	11.79		409.1077		Y	N
Luteolin	13.74	287.0508	285.0407		Y	Y
Decarboxymethyl-oleuropein aglycone	13.83	321.1300	319.1179	343.1103	Y	Y
Pinoresinol (+)-	14.20		357.1105		Y	Y
Oleuropein aglycone (Isomer 1)	14.34		377.1225	401.1185	N	Y
Naringenin	14.91		271.0633		Y	Y

Hydroxyoleuropein aglycone (Isomer 1)	15.13	395.1309	393.1184	417.1399	Y	Y
Hydroxyoleuropein aglycone (Isomer 2)	15.48	395.1320	393.1174	417.1181	Y	Y

Table 4.2 continued.

Name	**RT (min)**	**H (+)**	**H (-)**	**Na (+)**	**G**	**S**
Apigenin	15.65	271.0562	269.0448		Y	Y
Hydroxyoleuropein aglycone (Isomer 3)	15.84	395.1319	393.1158	417.1237	Y	Y
Tyrosol glucoside (Salidroside)	16.32	301.0673	299.0551		N	Y
Oleuropein aglycone (Isomer 2)	16.95	379.1363	377.1230	401.1179	Y	Y
Ligstroside aglycone (Isomer 1)	17.24	363.1430	361.1302	385.1244	Y	Y
Oleuropein aglycone (Isomer 3)	17.44	379.1344	377.1230	401.1189	Y	Y
Oleuropein aglycone (Isomer 4)	17.70	379.1381	377.1230	401.1201	Y	Y
Keto oleuropein aglycone	17.95	393.1196	391.1028		Y	N
Ligstroside aglycone (Isomer 2)	19.41	363.1389		385.1238	Y	Y
Ligstroside aglycone (Isomer 3)	19.59	363.1409		385.1208	Y	Y
Ligstroside aglycone (Isomer 4)	20.20	363.1439		385.1243	Y	N

Identification and quantification of polyphenols from both sources using HPLC

HPLC was therefore performed for more identification and characterization of individual compounds in the extracts. To isolate and identify particular compounds in each extract, we used reverse-phase high-performance liquid chromatography. The Greek and Saudi extracts' UV-Vis spectra both show peaks (3 bands) with different relative absorbances, at 240 nm, 275 nm and 340 nm and the corresponding HPLC chromatograms are shown for these wavelengths in **Figure 4.11**. HPLC was able to separate over 40 peaks of individual compounds in the extracts. The retention time and areas for all detected peaks can be found in (**Appendix 1 Tables S4.2** for Greek EVOO and **S4.3** for Saudi EVOO). HPLC was able to detect some compounds by matching retention time and UV absorption (**Table 4.3**) using the commercially available phenolic standards hydroxytyrosol, tyrosol, vanillic acid, caffeic acid, *p*-coumaric acid, ferulic acid, cinnamic acid, oleuropein, luteolin, (+)-pinoresinol, naringenin and apigenin.

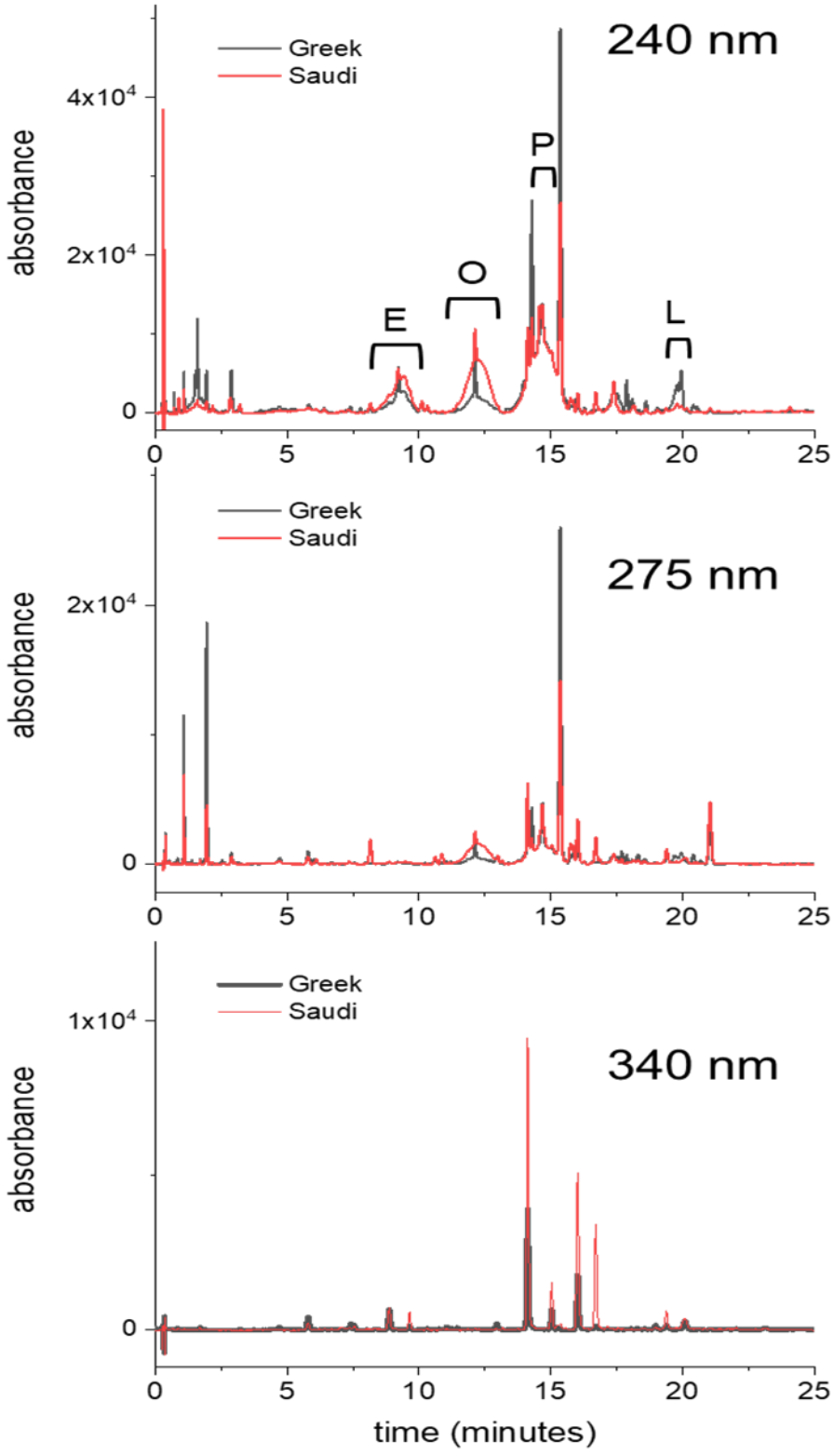

Figure 4.11. Greek (black) and Saudi (red) polyphenol extracts' reverse-phase HPLC chromatograms at 240 nm, 275 nm and 340 nm. The analysis was conducted using samples

made from a 10 mg/mL methanol/water (50:50 v/v) stock solution after diluting in water to 1 mg/mL. **Tables 4.2** and **4.4** show the polyphenol content for the two EVOO extracts, together with some of the compounds' concentrations. The 240 nm peaks correspond to derivatives of (E) elenolic acid, (L) ligstroside, (O) oleuropin, and (P) pinoresinol.

Table 4.3. Identification of the main polyphenols in Greek and Saudi EVOO products using available phenolic standards by HPLC (Retention time, Molecular weight and HPLC-DAD).

Phenolic Compounds	Retention time (minute)	Molecular weight	HPLC-DAD (nm)
Hydroxytyrosol	1.0	154.16	275 nm
Tyrosol	1.9	138.17	275 nm
Vanillic acid	2.9	168.14	275 nm
Caffeic acid	3.0	180.16	275 nm
p-Coumaric acid	5.7	164.16	275 nm
Ferulic acid	7.4	194.18	275 nm
Oleuropein	13.0	540.51	275 nm
Luteolin	14.1	286.24	340 nm
(+)-Pinoresinol	14.6	358.38	275 nm
Naringenin	15.3	272.25	275 nm
Apigenin	16.0	270.24	340 nm
Cinnamic acid	n.d	148.16	-

n.d: not detected.

Due to the wide range of polyphenol compounds that are known to be present in EVOO, and of which many are heterogeneously glycosylated, few HPLC reference standards were available with which to identify the individual compounds based on retention time matching.

Further analyses of both mixtures were carried out using the same reverse-phase HPLC. The phenols were quantified at 240 nm, 275 nm, and 340 nm wavelengths (corresponding to the band maxima identified in the UV/Vis spectra), and the corresponding chromatograms are shown in **Figure 4.11**. Retention times up to 25 minutes show several sharp peaks as well as several less distinct broad peaks. In earlier analyses, the broader peaks have been attributed to derivatives of elenolic acid (9.4 min), of oleuropein (12.3 min), and of (+)-pinoresinol (14.6 min), and to ligstrosides at 19.8 min (Tasioula-Margari and Tsabolatidou, 2015; De la Torre-Carbot et al., 2005; Mateos et al., 2001; Mateos et al., 2004). For these wavelengths the two mixtures' HPLC profiles indicate clear differences in the relative proportions of the components. Most of the well-defined narrow peaks of the Greek extract at 240 nm are higher than the Saudi extract at the same wavelength, while the broader, less defined peaks in the chromatogram of the Saudi sample at 9.4 min and 12.3 min are larger than the corresponding ones in the Greek extract. Conjugated aromatic compounds like flavonoids, are most strongly absorbing at 340 nm, and most of the observed peaks at this wavelength show greater intensities in the Saudi EVOO extract. While the phenolic compounds identified in the Greek and Saudi extracts were similar, their concentration profiles are easily distinguishable.

HPLC analysis of the reference compounds at different concentrations enables estimation of their concentrations in each extract. **Figure 4.12** shows an example of HPLC chromatograms at three wavelengths of the standardized compound concentrations used for quantification. These reference standards were used to assign some of the sharp peaks in the chromatograms to specific compounds and determine their concentrations. Standard calibration graphs (curves) prepared for each compound at UV wavelengths of 240 nm, 275 nm, and 340 nm. Linear ranges were established through serial dilution of stock solutions of the studied compounds. All the calibration curves (based on the peak area integrals) were linear over the range studied and calculated from ten linearly spaced concentrations the calibration curves for

hydroxytyrosol and tyrosol are shown in **Figure 4.13** (**Figure S4.5** in **Appendix 1** gives all the calibration curves for other compounds). The correlation coefficients (R^2), regression equations and linear ranges μg/mL, are shown in **Tables 4.4** and **4.5**.

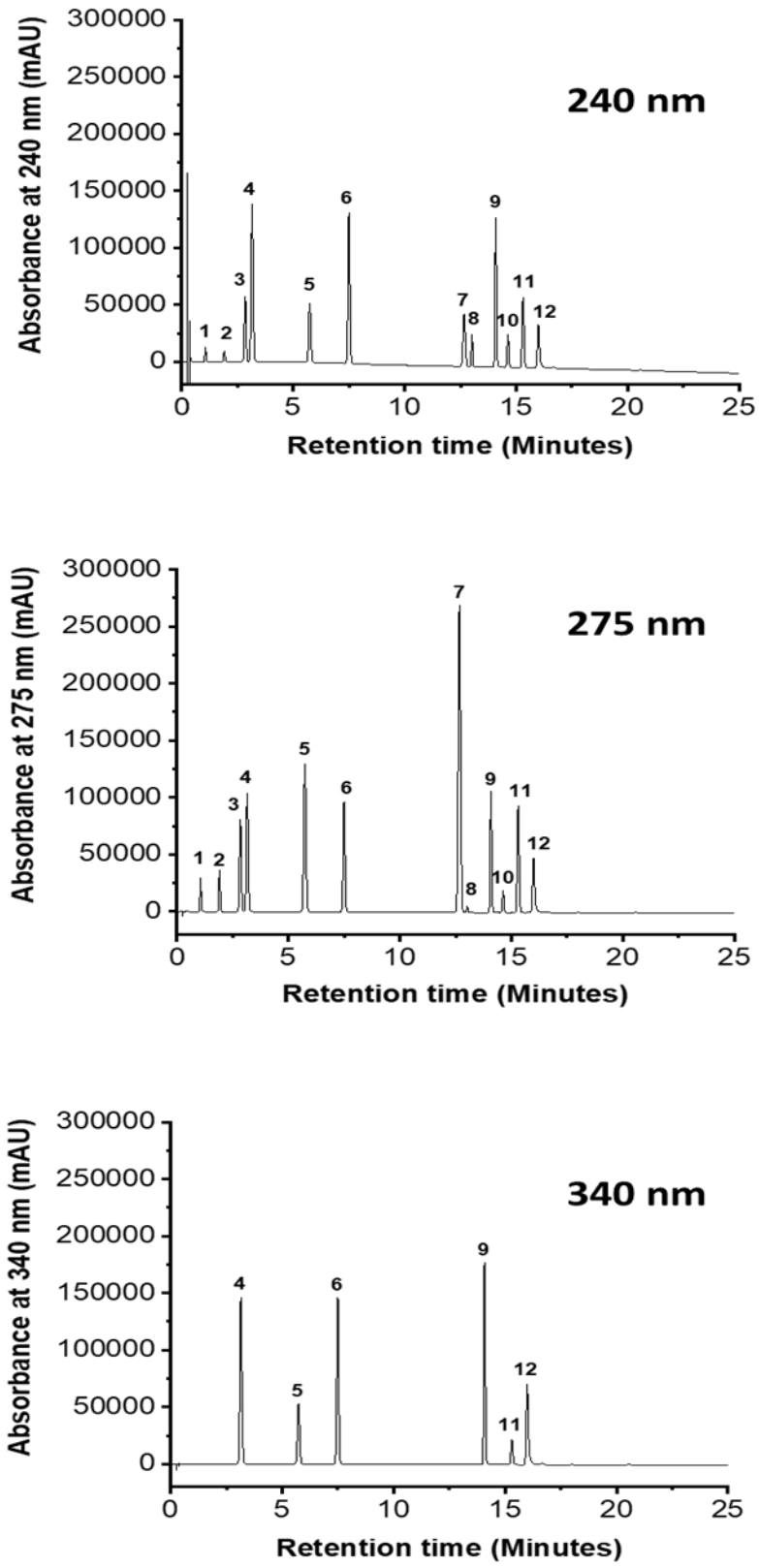

Figure 4.12. HPLC chromatograms of phenolic standards at 240 nm, 275 nm and 340 nm. Peaks 1: Hydroxytyrosol, 2: Tyrosol, 3: Vanillic acid, 4: Caffeic acid, 5: *p*-Coumaric acid, 6:

Ferulic acid, 7: Cinnamic acid, 8: Oleuropein, 9: Luteolin, 10: (+)-Pinoresinol, 11: Naringenin and 12: Apigenin.

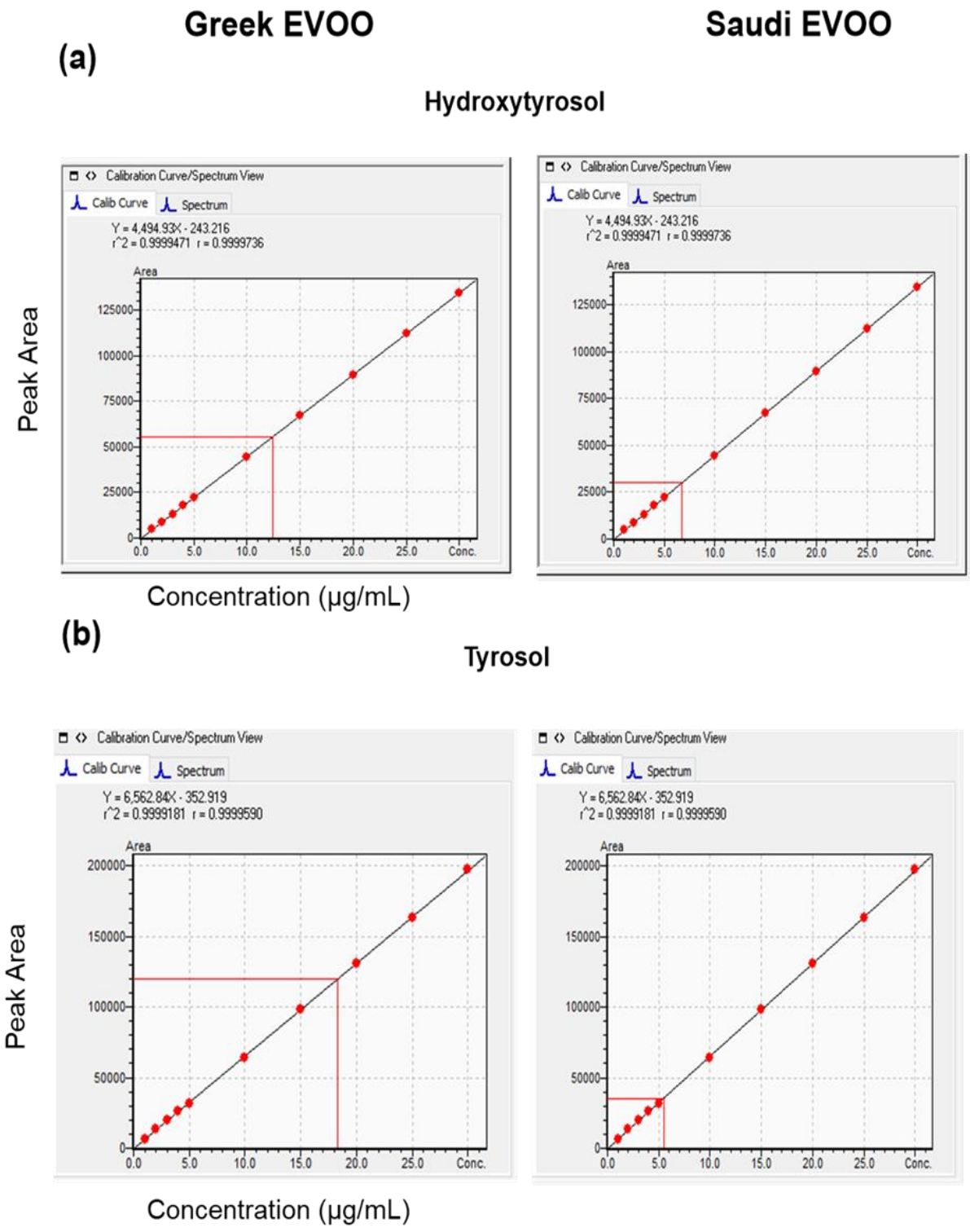

Figure 4.13. The calibration curves at ten points of some phenolic compounds extracted from Greek and Saudi EVOOs. The calibration curves of hydroxytyrosol isolated from both sources are presented in (a). The calibration curves of tyrosol isolated from both sources are presented in (b).

Table 4.4. Phenolic compounds detected and quantified by HPLC from the Greek and Saudi EVOO extracts. The wavelengths are displayed for peaks that could be most accurately determined.

Polyphenolic compounds	Retention time (min)	EVOO extract concentration (µg/g EVOO)	
		Greek	Saudi
Hydroxytyrosol	1.0	15.70	8.52
Tyrosol	1.9	23.11	6.92
Vanillic acid	2.9	0.51	0.52
Caffeic acid	3.0	0.07	0.09
p-Coumaric acid	5.7	0.50	0.32
Ferulic acid	7.4	0.10	0.18
Oleuropein aglycone	13.0	10.42	3.55
Luteolin	14.1	1.84	4.72
(+)-Pinoresinol	14.6	10.78	14.53
Naringenin	15.3	15.68	10.19
Apigenin	16.0	1.05	3.76

Table 4.5. Phenolic compounds detected in Greek and Saudi extracts by HPLC, with retention times, linear ranges and regression equations.

Phenolic Compound	Retention time (min)	Linearity range µg/mL	R	R^2	Regression equation
Hydroxytyrosol	1.0	1-30	0.999	0.999	4494.9x – 243.216
Tyrosol	1.9	1-30	0.999	0.999	6562.8x – 352.919
Vanillic acid	2.9	0.05-0.5	0.997	0.994	17900.0x + 307.488
Caffeic acid	3.0	0.05-0.5	0.987	0.974	25926.8x + 222.960
p-Coumaric acid	5.7	0.05-0.5	0.997	0.995	36462.7x + 235.056
Ferulic acid	7.4	0.05-0.5	0.999	0.999	22615.9x – 35.2171
Oleuropein	13.0	1-30	0.999	0.999	918.1x – 132.863
Luteolin	14.1	1-30	0.999	0.999	34492.4x – 4,138.65
(+)-Pinoresinol	14.6	1-30	0.998	0.997	4384.1x – 1,434.26
Naringenin	15.3	1-30	0.999	0.999	22711.6x – 3,923.09
Apigenin	16.0	0.1-20	0.999	0.998	2,442.6x + 3,054.90

R: The coefficient of correlation. R^2: The coefficient of determination.

The peaks and corresponding concentrations of the flavonoids apigenin, luteolin and naringenin, and tyrosol and hydroxytyrosol, caffeic acid, and oleuropein aglycone, were then determined. Compared to the Saudi extract, the Greek extract had higher concentrations of oleuropein and its tyrosol metabolites, but lower concentrations of the flavonoids luteolin and apigenin. Most of the narrow peaks not common to both extracts, and all the poorly defined peaks, could not be attributed to specific compounds with a reasonable level of certainty.

Chromatography is a powerful method for identification and characterisation natural products, but in order to recover the limitation of each technique it is useful to use different chromatographic techniques for example here we applied both HPLC and LC-MS (this is discussed in detail in the discussion section below).

Analysis of polyphenolic compounds from EVOO using solution-state ^{1}H NMR

Further analyses were performed using solution-state ^{1}H NMR **Figure 4.14**. Complete assignment of the spectra was not attempted because the main aim here was to investigate whether the extracts contained of phenolic glucosides, but some peaks could be detected as particular compounds by referring to previous work. The chemical structures of the identified phenolic compounds provided in **Figure 4.15**, enabled the compounds in **Figure 4.14** to be identified as (A) apigenin, (B) luteolin, (C) (+)-pinoresinol, (D) syringaresinol, (E) 1-acetoxypinoresinol, (F) tyrosol, (G) hydroxytyrosol, (H) elenolic acid, (I) (+/-) oleocanthal, (J) oleuropein glucoside, (K) ligstroside glucoside, (L) oleuropein aglycone, (M) ligstroside aglycone, (N) hydrated dialdehydic form of oleuropein, (O) aldehydic form of oleuropein, (P) aldehydic form of ligstroside and (Q-U) unknown (Alaziqi et al., 2024; Olmo-Cunillera et al., 2020; Ruiz-Aracama et al., 2017; Christophoridou and Dais, 2009; Charisiadis et al., 2011).

Oleocanthal, elenoic acid and the dialdehydic form of oleuropein all contain aldehydic protons, and resonances from these are evident in the 8-10 ppm range (Alaziqi et al., 2024; Mateos et al., 2001; Servili et al., 1999). Resonances from glucosyl groups can be seen within the 3.3 – 5 ppm range, and are also distinguishable in the 2DCOSY spectrum. This would be useful to identify polyphenols with the O-glucoside forms for example here we found pinoresinol, oleuropein and others attached with the O-glucoside, and this may impact and limit their interactions with tau and Aβ40 (Alaziqi et al., 2024; Mateos et al., 2001; Servili et al., 1999).

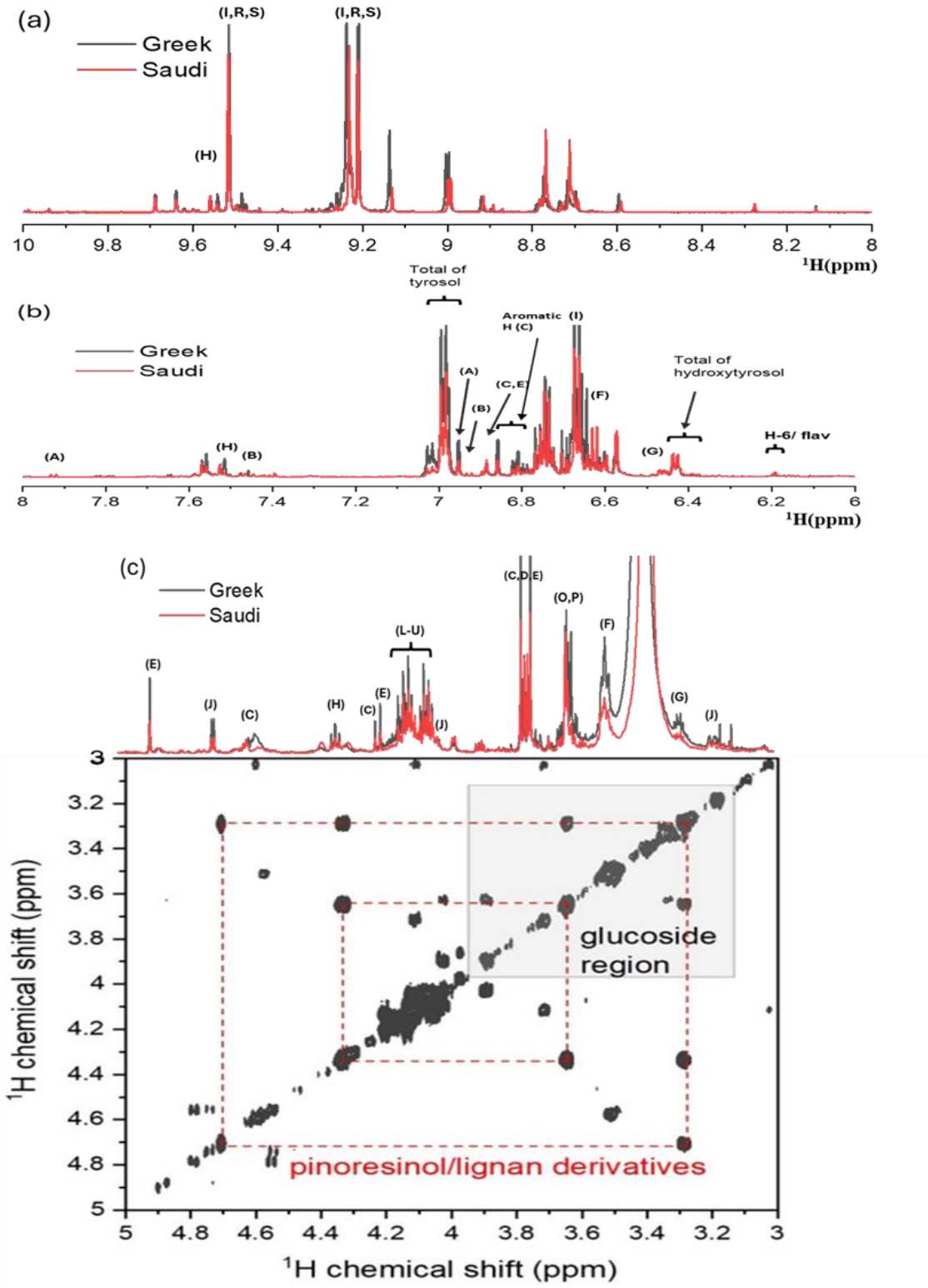

Figure 4.14. The polyphenol extracts (in DMSO-d_6) solution-state ^{1}H NMR spectra at 700 MHz. Greek EVOO (black) and Saudi EVOO (red). (a) Aldehydic proton resonances in the low-field region. (b) Aromatic region. (c) Cross-peaks of glucosyl groups in the mid-field region (1D spectra and 2D COSY spectrum).

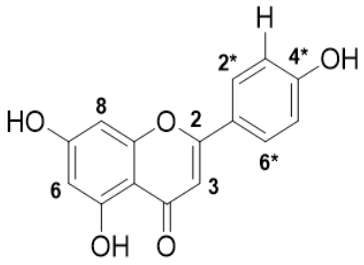

Apigenin (A)

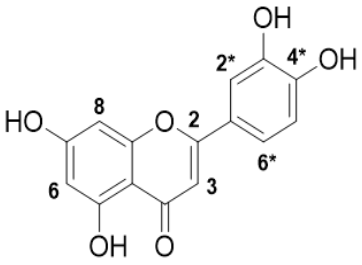

Luteolin (B)

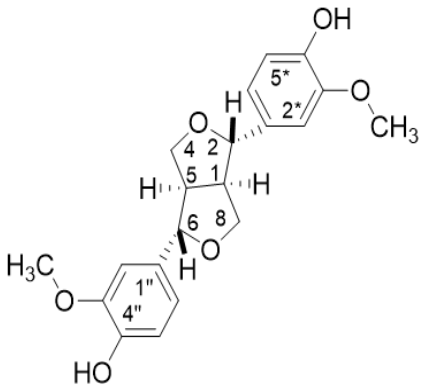

(+)-pinoresinol (C)

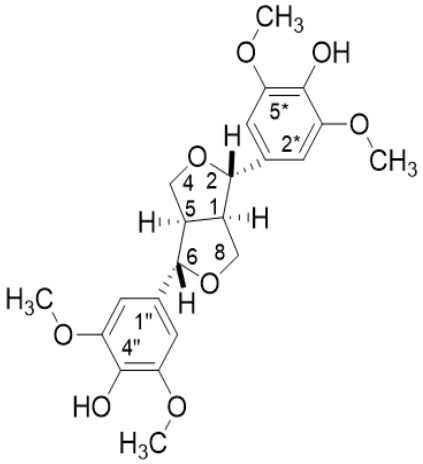

Syringaresinol (D)

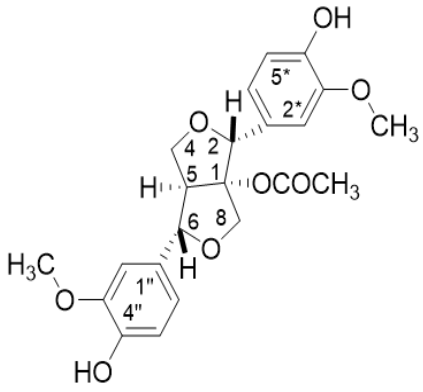

1-Acetoxypinoresinol (E)

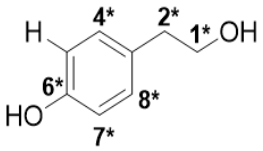

Tyrosol (F)

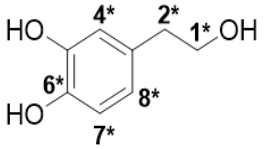

Hydroxytyrosol (G)

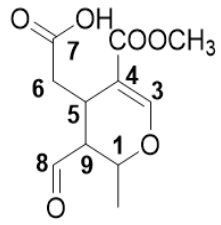

Elenolic acid (H)

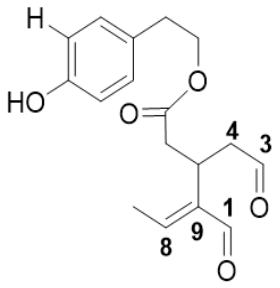

(+/-) Oleocanthal (I)

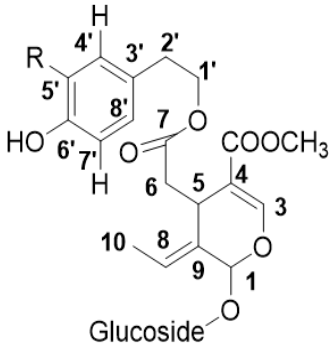

R = OH, oleuropein glucoside (J)
R = H, ligstroside glucoside (K)

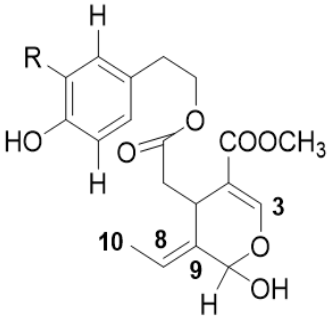

R = OH, oleuropein aglycone (L)
R = H, ligstroside aglycone (M)

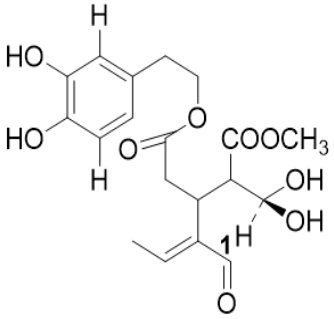

Hydrated dialdehydic form of oleuropein (N)

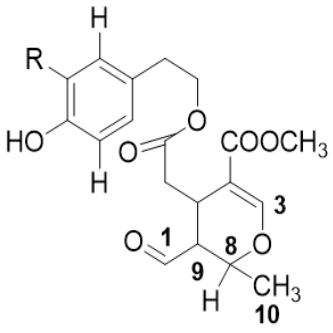

R = OH, aldehydic form of oleuropein (O)
R = H, aldehydic form of ligstroside (P)

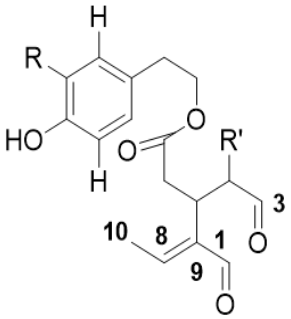

R = OH, R' = $COOCH_3$ (Q)
R = OH, R' = H (R)
R = R' = H (S)

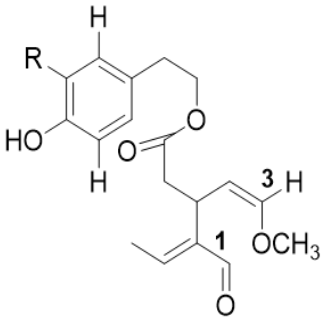

R = OH (T)
R = H (U)

Figure 4.15. Chemical structures of identified phenolic compounds using solution-state ^{1}H NMR adapted from (Alaziqi et al., 2024; Olmo-Cunillera et al., 2020; Ruiz-Aracama et al., 2017; Christophoridou and Dais, 2009; Charisiadis et al., 2011).

Finally, as the NMR spectra were in close agreement with the LC-MS HPLC profiles, the major differences between the samples can be characterized as not being in the particular polyphenols detected (most were present in both the Greek and Saudi EVOO samples), but in their relative contributions to the total phenolic profiles.

Discussion

One of the major reasons the Mediterranean is associated with a lower occurrence heart disease, diabetes, and some cancers and neurodegenerative disorders, is thought to be the high consumption of EVOO, which ranges from 40 to 50 g/day (Corona et al., 2009; Martinez-Lapiscina et al., 2013; Rodríguez-Morató et al., 2015; Scarmeas et al., 2009; Sofi et al., 2010). Like most fruits and vegetables, unprocessed EVOO contains many polyphenols, many of which are known for their anti-inflammatory and antioxidant properties (Pizarro et al., 2013; Weinbrenner et al., 2004; Gilbert-López, 2014; Bayram et al., 2012; Jiménez et al., 2007; Bianco et al., 2003). Certain phenolic compounds can cross the blood-brain barrier, a property which is essential for their protective effect against neurodegenerative diseases like AD. Polyphenols are thought to protect neurons from oxidative damage, particularly by radical oxygen species. However, *in vitro* data suggest that phenolic compounds may also directly inhibit amyloid fibril formation (Stefani and Rigacci, 2013) – a property discussed in more detail in the next chapter. How the Mediterranean diet affects the structural changes in the brain that occur in neurodegenerative disease and that have been observed in neuroimaging studies is still largely unknown (Gregory et al., 2023). Nonetheless, this diet does appear to lower the risk of diseases such as AD, or at least delay their onset (reviewed in García-Casares et al. 2021), and so this diet and the specific compounds it is richer in than other diets, will continue to be the subject of research on the prevention and treatment of neurodegenerative diseases. In particular, the phenolic compounds, which are secondary metabolites in the oil, seem likely to be the compounds responsible for the observed protective effects against neurodegenerative diseases.

To recover and isolate the bioactive phytochemicals such as phenolic compounds from plant materials or oils first requires their extraction (Stalikas, 2007). The most commonly used phenolic extraction procedures for olive oil are LLE and SPE, largely because of their ease of

use, efficiency, and wide-ranging applicability (Tasioula-Margari and Tsabolatidou, 2015; Hrncirik and Fritsche, 2004; Montedoro et al., 1992; Pirisi et al., 2000; Dais and Boskou, 2009; Stalikas, 2007). The results presented here show the enhanced (with sonication and washing steps) LLE method coupled with chromatography, to be a highly suitable technique for determining the major phenolic compounds of these oils. Although SPE has advantages as an isolation step in terms of speed, cost, and solvent use, its analytic accuracy is questionable as the process extracts certain polyphenols more reliably than others, a problem that has led to inconsistent findings in the literature (Tasioula-Margari and Tsabolatidou, 2015; Hrncirik and Fritsche, 2004; Montedoro et al., 1992; Pirisi et al., 2000; Dais and Boskou, 2009; Stalikas, 2007). In this research project we aimed first to identify the technique that reliably extracts the greatest quantity of polyphenols from EVOOs, as well as isolating most of the individual phenolic compounds present in these oils. Both LLE and SPE methods were examined, and in agreement with the literature, we found SPE to lose some components during the extraction. LLE Funnel Extraction was selected as the best procedure to extract the phenolic fraction from the EVOOs as this technique gave a higher yield and HPLC data that were more consistent across replications, than LLE Centrifugation and SPE.

As mentioned earlier, selecting a suitable method is an important step in extracting polyphenols, and several different LLE or SPE procedures are reported in the literature with the one chosen in part depending on the purpose of the research. However, it is important to point out that SPE has a limited ability for recovering secoiridoid aglycones. Specifically, SPE does not extract the reactive dialdehydic forms of the oleuropein and ligstroside aglycones very well (Tasioula-Margari and Tsabolatidou, 2015; Hrncirik and Fritsche, 2004; Montedoro et al., 1992; Pirisi et al., 2000). In addition, the step where the aqueous layers are separated in the LLE centrifugation technique is extremely sensitive, and if not applied well can give different results – an aspect of the process which has been noted by other researchers (Pirisi et al., 2000).

For the analysis and characterization of the phenolic compounds isolated from Greek and Saudi olive oils using LLE funnel extraction, a range of analytical techniques were applied, including UV-Visible absorption, LC-MS, HPLC chromatography, and NMR spectroscopy. UV-Visible absorption spectra were first examined in both extracts at the same concentration, enabling us to determine the particular absorption curves of the phenolic compounds from both sources. The results showed that some compounds absorbed at 240 nm and 275 nm were present in greater amount in Greek EVOO than Saudi EVOO. However, the flavonoid compounds absorbed at 340 nm were higher in the Saudi extract and this outcome will be clarified and confirmed when chromatographic analyses were applied. The extracts were then examined using LC-MS, through which over 30 compounds were identified, including simple phenolic acids, cinnamic and benzoic acids and derivatives, flavones, and secoiridoids (oleuropein and ligtroside derivatives). Additionally, many of the polyphenol compounds previously reported to be contained in EVOO were identified, including oleocanthal derivatives at relatively high concentrations (de Fernandez et al., 2014). However**,** LC-MS failed to identify some peaks with retention times below 5 minutes, that were detected by HPLC. This early elution is often associated with the smaller polyphenolic compounds, such as phenolic acid, with molecular weights below 200 Da, and is routinely reported in studies of EVOO extracts (Suárez et al., 2008). The concentration of phenolic compounds in virgin olive oil varies dramatically depending on both the variety of olive and the brand of oil. Due to the low signal to noise ratio arising from the complexity of the polyphenolic profile of EVOO, LCMS' lower sensitivity to compounds with molecular weights below 200 Da, might result in missing peaks corresponding to smaller and lighter compounds. For more characterization, some commercial reference polyphenols, including the smaller molecules tyrosol, hydroxytyrosol, caffeic acid, vanillic acid, ferulic acid and coumaric acid were analysed using HPLC with the same column and conditions. By matching retention time and UV absorption we managed to detect most of the

standards present in the extracts - hydroxytyrosol, tyrosol, vanillic acid, caffeic acid, p-coumaric acid, ferulic acid, cinnamic acid, oleuropein, luteolin, (+)-pinoresinol, naringenin and apigenin. Moreover, employing solution-proton NMR helped to assign some phenolic compounds by elucidating their structures through comparison with the data of previous work.

Both extracts were then subject to a partially quantitative analysis using reverse-phase HPLC. Peaks and their corresponding concentrations were studied using available polyphenolic standards including ferulic acid, *p*-coumaric acid, caffeic acid, vanillic acid, tyrosol, hydroxytyrosol, oleuropein aglycone, (+)-pinoresinol and the flavonoids apigenin, luteolin and naringenin. The main difference between the two oils was that a higher proportion of oleuropein and its tyrosol metabolites were found in the Greek extract compared to the Saudi extract, while the latter was richer in the flavonoids luteolin and apigenin, thereby confirming the primary data obtained from UV-Vis.

The phenolic profiles revealed by NMR, LC-MS, HPLC and UV-Visible were in agreement and indicated that Greek and Saudi EVOO extracts contained almost the same variety of compounds but in different relative proportions.

In conclusion, to quantify phenolics precisely, it is essential to prepare samples and eliminate undesirable substances effectively. However, regarding the extraction and isolation of phenolics, the method of extraction remains the factor of greatest importance. Sample preparation, type of solvents, and the method itself, are the major factors determining how the extraction process unfolds. Choosing an appropriate method and solvents to extract phenolics from olive oil is critical, as attested to by the outcomes of the extractions presented here. The NMR spectra, chromatography and UV-Vis profiles reported in this chapter were in close agreement, which reinforces our confidence in the finding that the Greek and Saudi EVOO extracts contained almost the same phenolic compounds, differing only in their relative

proportions. The detailed characterization of the phenolic extracts of EVOO from two different geographical regions, has enabled us to show that these oils have distinct compositions, including different concentrations of oleuropein and its metabolites, phenolic acids, and flavonoids. In the next chapter, both phenolic extracts and their constituent compounds, will be examined for their potentially protective effect against AD.

Chapter 5 (Investigation of the effects of mixed and individual phenolic compounds derived from EVOO on the aggregation of amyloid-β and tau peptides *in vitro*)

Introduction

Numerous contemporary studies (Martinez-Lapiscina et al., 2013; Rodríguez-Morató et al., 2015; Scarmeas et al., 2009; Sofi et al., 2010) have identified a correlation between the systematic consumption of olive oil in the Mediterranean diet and a reduced prevalence of neurodegenerative disorders, diabetes, cardiovascular disease, diabetes, and some varieties of cancer. Unprocessed extra virgin olive oil (EVOO), alongside numerous plant-based foods, is comprised of phenolic compounds which are well-recognised for their antioxidant and anti-inflammatory qualities (Pizarro et al., 2013; Weinbrenner et al., 2004; Gilbert-López et al., 2014; Bayram et al., 2012; Jiménez et al., 2007; Bianco et al., 2003). Due to their ability to cross the blood-brain barrier (BBB), phenolic compounds derived from plants are currently a primary source of research regarding their ability to inhibit the onset of the pathological traits of Alzheimer's disease (AD). The primary therapeutic mechanism indicates that phenolic compounds can scavenge free radicals and prevent neuronal oxidative impairment; however, *in vitro,* the data indicates an additional function: the ability to inhibit amyloid fibril formation (Stefani and Rigacci, 2013; Henríquez et al., 2020).

As described earlier in this thesis, Alzheimer's disease (AD) is linked with the 39-42 residue amyloid-β (Aβ) peptides which construct β-sheet rich, insoluble amyloid fibrils and accumulate within heterogeneous plaques in the extracellular spaces of brain tissue (Selkoe and Hardy, 2016). Amyloid fibrils are fibrous insoluble nanoscale constructs, with a diameter of approximately 10 nm and a length of micrometres, distinguished by the cross-β pattern displayed under X-ray fibre diffraction and the green birefringence exhibited upon binding to

Congo red (Sipe et al., 2016; Sipe et al., 2010; Westermark, 2012). The fibrils are formed when transitory oligomeric species (which are toxic to neuron synapses) disrupt the membrane of a cell (Jang et al., 2013; Hefti et al., 2013; Ferreira and Klein, 2011; Viola and Klein, 2015; Kumar and Singh, 2015; Kurz and Perneczky, 2011). An additional trait of AD concerns the hyperphosphorylation of microtubule-associated protein tau (MAPT, or tau; UniProtKB P10636), by glycogen synthase kinase enzymes. This process initiates aggregation into neurofibrillary tangles related to neurodegeneration which succeeds the Aβ aggregation and the associated inflammatory response (Nisbet et al., 2015; Spires-Jones and Hyman, 2014; Ballatore et al., 2007; Augustinack et al., 2002). Current research regarding AD (and other amyloid disorders) is focused on the implementation of anti-aggregation medications which inhibit the development of amyloid fibrils and filaments *in vitro* (Habchi et al., 2017; Joshi et al., 2016; Saunders et al., 2016). Certain compounds, such as the phenolic compounds found in olive oil, are a promising area for research because they possess minimal toxicity, can reduce the rate of Aβ and tau aggregation, and destabilize fibrils (Porat et al., 2006; Stefani and Rigacci, 2014; Casamenti and Stefani, 2017) (**Chapters 1** and **3** covered the above in detail).

Olive oil is a naturally occurring source of oleuropein (a catechol-containing compound) that, in its aglycone form, inhibits Aβ, tau and other protein aggregation *in vitro* and can improve amyloid pathologies *in vivo* (Casamenti et al., 2015; Diomede et al., 2013; Grossi et al., 2013; Luccarini et al., 2014; Daccache et al., 2011; Leri et al., 2021). Oleuropein is an ester of elenolic acid and hydroxytyrosol and is linked to glucose *via* a glycosidic bond or extant (in the aglycone form) (**Figure 5.1**) (Casamenti et al., 2015; Diomede et al., 2013; Grossi et al., 2013; Luccarini et al., 2014; Rigacci et al., 2011). Oleuropein and its metabolic products (hydroxytyrosol and tyrosol) are the most prevalent phenolic compounds in EVOO (Tasioula-Margari and Tsabolatidou, 2015; Lesage-Meessen et al., 2001) and numerous studies have analysed the amyloid-inhibiting and clearing attributes of each compound (Rigacci et al.,

2011; Lesage-Meessen et al., 2001; Ferhat et al., 2017; Owen et al., 2000; Brenes et al., 2000) (see **Chapter 1** for detail).

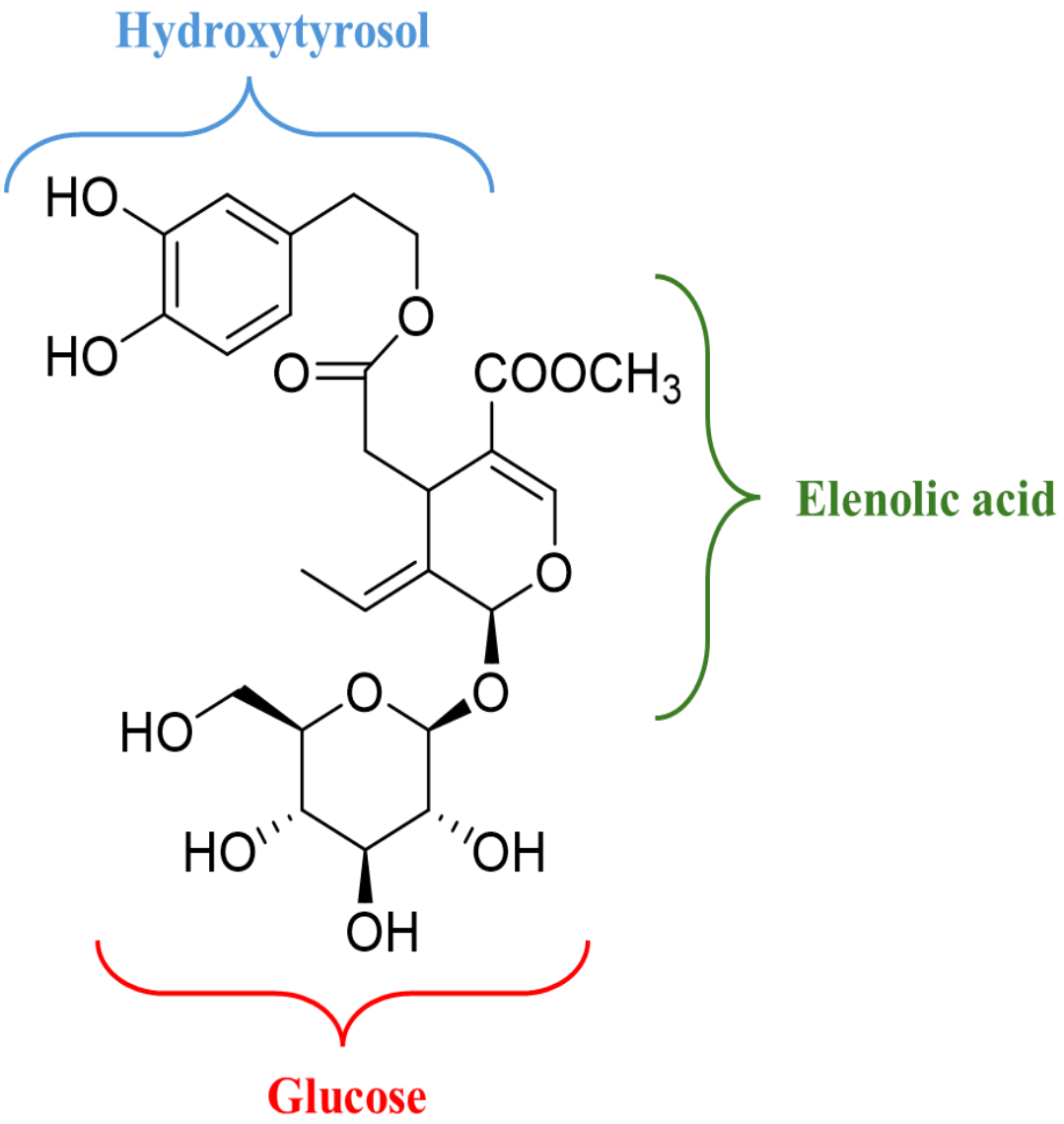

Figure 5.1. Structure of oleuropein showing the main chemical parts attached.

Due to its medicinal capabilities, oleuropein (and its metabolites) are of great interest; however, it is often overlooked that olive oil contains an abundant supply of numerous other phenolic compounds including flavonoids (Ferhat et al., 2017), lignans (Owen et al., 2000; Brenes et al., 2000), hydroxybenzoic acids (Erol-Dayi et al., 2012; Brenes et al., 1999), and phenolic acids (Nergiz and Ünal, 1991; Ocakoglu et al., 2009; Carrasco Pancorbo et al., 2004). Various compounds such as ferulic acid (Ono et al., 2005; Yan et al., 2001), and hydroxycinnamic (coumaric) acids (Hao et al., 2020), alongside the flavonoids quercetin (Chiang et al., 2021) and apigenin (Lozano-Castellon et al., 2020), have demonstrated the ability to inhibit Aβ and/or tau aggregation, disrupt fibrils, and relieve AD-like pathologies in animal test subjects (Yan et al., 2013). A key polyphenol (oleocanthal) found in olive oil augments the eradication of Aβ fibrils from the brain (Abuznait et al., 2013) and modulates tau fibrilization (Monti et al., 2012). When compared with oleuropein in EVOO, several of these compounds exist in lower levels of concentration; however, bioavailability varies between phenols and the most abundant compounds may not present the highest concentrations of active metabolites in the intended tissues (Manach et al., 2005). The metabolism of secoiridoid aglycones (such as oleuropein) releases hydroxytyrosol or tyrosol and elenolic acid by enzymatic hydrolysis in the gastrointestinal tract; therefore, the concentrations of circulating oleuropein may be minimal (Miro-Casas et al., 2003).

Due to the extensive Mediterranean intake of extra virgin olive oil and the potential of its pharmacologically active classes of compounds, the phenolic profile of EVOO and its impact on the aggregation properties of Aβ peptide and tau proteins warrants further investigation. No research to date has assessed the efficacy of EVOO phenol mixtures (following isolation from the fatty acid component) and their impact on the symptoms of AD. To address this knowledge gap, this study extracted phenolic mixtures from early harvest Greek and Saudi Arabia EVOO then analysed and evaluated their effects on the aggregation of Aβ40

(residues 672-711 of the amyloid precursor protein; UniProtKB P05067) and a recombinant tau fragment Δtau187, comprising residues 255-441 of the C-terminal microtubule-binding domain (Townsend et al., 2020).

In **Chapter 4** it was shown that LC-MS and HPLC analysis identified more than thirty compounds including flavonoids, oleuropein derivatives, and simple phenolic acids in extracts from Greek and Saudi olive oils. In this chapter, work is presented that has established that the extract mixtures from the two sources influence Aβ40 aggregation and destabilization of Aβ40 fibrils to a greater extent than they do upon tau. As such, this work provides justification for further investigation of olive oil as a potential dietary protection against AD.

Aims

This chapter will determine how a mixture of polyphenols isolated from Greek and Saudi Arabia EVOO, and individual phenolic compounds affects the aggregation propensity of Aβ40 and tau and/or the properties of the aggregates. The binding of polyphenols to protein aggregates will be determined using a co-sedimentation experiment, and the effects of polyphenols on Aβ40 and tau aggregation will be examined using a range of techniques including ThT fluorescence, circular dichroism, transmission electron microscopy and dynamic light scattering. The structure of Aβ40 aggregates formed in the presence of polyphenols, and with polyphenols added (after aggregation has ceased) will be determined *via* SSNMR and compared to Aβ40 aggregates alone. Finally, potential amyloid interaction sites for polyphenols are explored by computational docking analysis using Molsoft ICM Pro software with structural models of Aβ40 and tau fibrils.

Materials and methods

Materials

Chemical reagents used were purchased from Sigma-Aldrich. These include heparin, tris, dithiothreitol (DTT), sodium phosphate, sodium hydroxide (NaOH), hydrochloric acid (HCl), 96-well black plate fluorescence, thioflavin T, carbon coated former grids, 2 % phosphotungstic acid. Polyphenolic standards and all chemical reagents used for HPLC, NMR, UV-Vis and CD detail described in **Chapter 4**. Milli-Q purified water was also provided from the system available in the lab at (Biomedical and Life Sciences, Lancaster University).

Methods

Proteins expression

Amyloid beta Aβ40 labelled and unlabelled proteins

Human Aβ40 (consisting of amyloidogenic 1-40 residues containing an additional N-terminal methionine residue) was decontaminated and extracted using the aforementioned methodology (Stewart et al., 2016) (**Chapter 3** described expression and purification of Aβ40 proteins). Each experiment involving Aβ40 was conducted in 25 mM phosphate, 0.1 % NaN_3, pH 7.4.

Tau protein

This research utilised a tau construct consisting of residues 255-441 of human tau from cDNA clone htau46; the protein was expressed and purified *via* the aforementioned methodologies (Hasegawa et al., 1998). The resultant isoform consists of 4 microtubule binding (MTB) repeat units (tau 4R), but with the removal of the aggregation impeding the N terminus isolated which

leaves the second and third MTB with the extremely amyloidogenic sequences VQIINK and VQIVYK, respectively (Eschmann et al., 2017). Any experiments pertaining to tau were executed in 30 mM Tris, 1 mM DTT, and pH 7.5.

Polyphenols

The isolation and characterisation of the phenolic compounds derived from natural extra virgin olive oil products are detailed in **Chapter Four**.

Thioflavin T fluorescence assay

The enhanced fluorescence of Thioflavin T (an amyloid-specific dye) was used to monitor the kinetics of amyloid formation in the presence and absence of olive oil extracts. Aβ40 (20 μM) or tau with heparin (20 and 5 μM respectively) were incubated in 20 μM Thioflavin T and included the addition of a variety of concentrations of EVOO extracts or 20 μM of each polyphenol reference compound (including caffeic acid, *trans*-cinnamic acid, *p*-coumaric acid, ferulic acid, tyrosol, vanillic acid, syringic acid, oleuropein, luteolin, apigenin and naringenin). A Molecular Devices Flexstation 3 Microplate Reader (Molecular Devices) measured fluorescence in triplicate samples (excitation at 450 nm and emission at 482 nm) every 2 minutes for 50 hours. Throughout incubation, the samples were shaken constantly at a temperature of 37 °C. Heparin was required to induce tau aggregation, as well documented elsewhere (Townsend et al., 2020).

Circular Dichroism Spectroscopy Analysis

20 μM of Aβ40 was incubated at 37 °C in isolation (or in the presence of EVOO extracts or with 20 μM of each polyphenol compound). Spectra were measured and recorded at three intervals: immediately following preparation, after two hours, and after twenty-four hours. A

Chirascan Plus CD spectrometer (calibrated between 180 and 260 nm with a bandwidth of 1 nm, using a path length of 0.1 mm) was used to record spectra. Additionally, background signals from the buffer and the relevant compound were eliminated from the spectra.

Transmission Electron Microscopy Analysis

Aβ40 (20 μM) and tau with heparin (20 and 5 μM, respectively) were incubated in isolation (or in the presence of phenolic extracts/an individual component). At the beginning of incubation (or following fibril formation), phenolic extracts were amalgamated with the protein (compound bound to the fibrils). A 10 μL suspension was spotted onto formvar and carbon-coated copper grids and, five minutes later, any surplus liquid was removed *via* blotting. For the negative staining process, 10 μL of 2 % phosphotungstic acid was added to the loaded grids, left for 3 minutes, and blotted to eradicate any surplus liquid. A JEOL JEM-1010 or JEOL 1400 Flash transmission electron microscope was employed to examine each grid and capture a series of representative images.

EVOO Extract and individual polyphenol Binding to Protein Aggregates Analysis

HPLC analysis using UV spectrophotometry was employed to measure any binding between the extracts and the Aβ40 and tau aggregates. Aggregates of Aβ40 or tau (20 μM monomer equivalent) were initially constructed following incubation of the proteins in 500 μL phosphate buffer at 37 °C for 3 days. Bench-top centrifugation was employed to sediment the insoluble fibrils and the top 480 μL of supernatant was extracted.

The residual pellet was resuspended in 480 µL phosphate buffer containing 20 µg/mL EVOO extract, homogenised, incubated with agitation at 37 °C for 24 hours, and centrifuged. The resultant supernatants were conserved for further examination.

EVOO extract control samples were prepared *via* the same methodology (although the fibrils were omitted) (see **Figure 5.2**).

Reverse phase HPLC was utilised to examine the centrifuged solutions (with and without fibrils), and this process is detailed in the subsequent section. 10 µL of each solution was injected into the column and from each resolved peak in the HPLC chromatogram the percentage of the corresponding compound bond to the fibrils was calculated *via* the intensity ratio $100(1-I_f)/I_c$ (where I_f is the peak intensity for the fibril-treated sample and I_c is the peak intensity for the control sample) (Alaziqi et al., 2024). Existing reference samples were used to identify individual compounds (as described previously).

A UV spectrophotometric analysis of binding was conducted *via* the following approach: all of the samples previously prepared for HPLC binding were analysed using NanoDrop 2000/2000c Spectrophotometric equipment (Supplied and serviced by Labtech Biomedical and Life Sciences, Lancaster University) which utilised UV–Visible spectra in the range 200-500 nm. The transmittance signal was modified by using a blank.

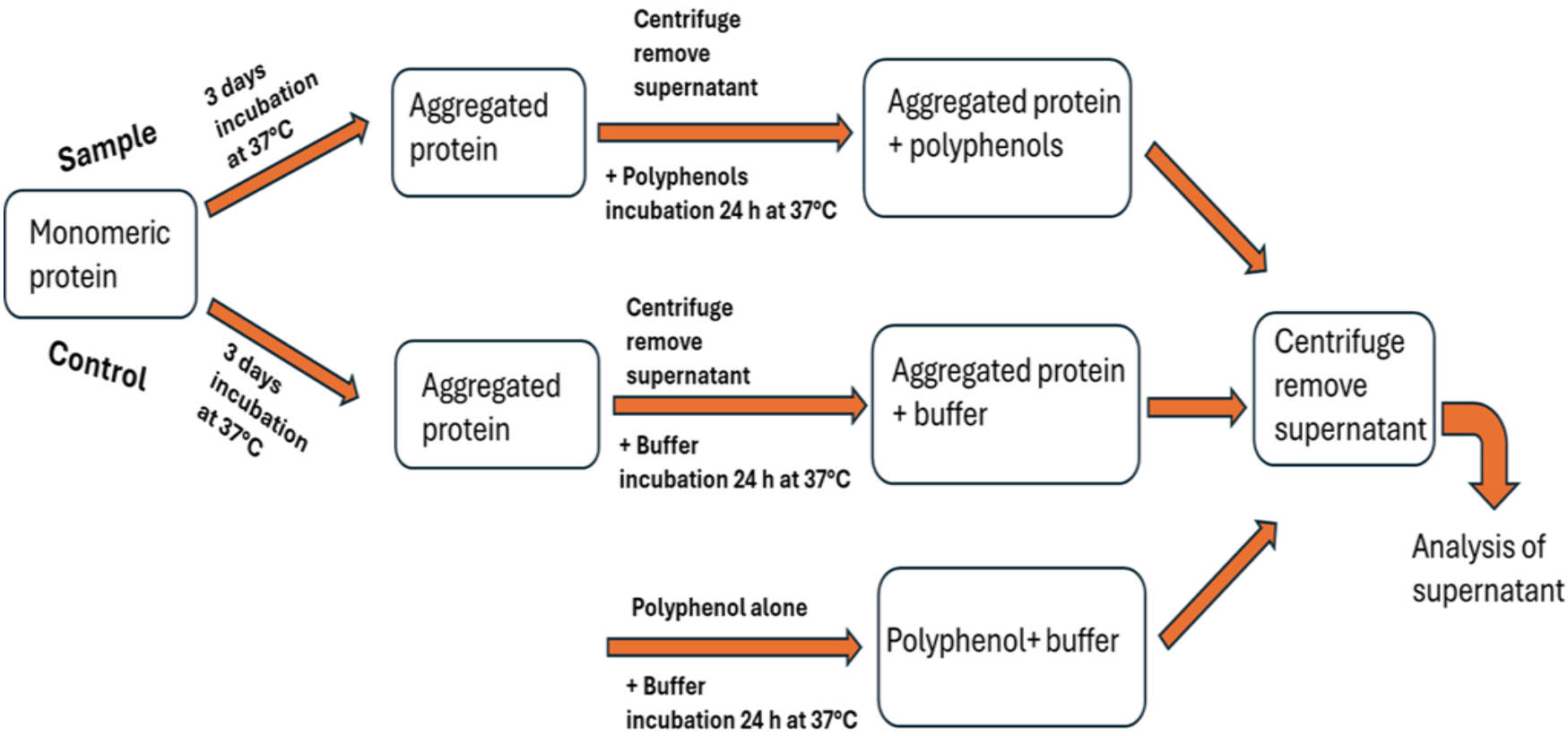

Figure 5.2. Experimental scheme of binding showing the aggregation of protein with polyphenols and without.

HPLC Chromatography for Binding Analysis

This process involved the use of a NExeraX2 UHPLC (Shimadzu) system at 40 °C with a mobile phase consisting of 0.1% formic acid in either ultrapure water (buffer A) or acetonitrile (buffer B), while the solid phase utilised a Shim-pack XR-ODS 2.2 μm (3.0 x 50 mm) column.10 μL was loaded and the system functioned at a flow rate of 1 mL/min, with an elution profile of 5% buffer B for 0-3 mins; 40% buffer B for 3-25 mins; 40% buffer B for 25-26 mins; 50% buffer B for 26-27 mins; 5% buffer B for 27-27.10 mins; and 5% buffer B for 27.10-32 mins. Measurements of absorbance intensity were recorded at 240 nm, 275 nm and 340 nm with 4 nm bandwidth.

Solid-State NMR for Binding Analysis

For this process (solid-state NMR), 740 μg of Greek extra virgin olive oil was thoroughly mixed with sedimented fibrils in a small volume of phosphate buffer and incubated for 24 hours at 37 °C. Any remaining liquid was extracted *via* centrifugation and the pellet was transferred to a 3.2 mm magic angle spinning (MAS) rotor. ^{15}N cross-polarization (CP-MAS) SSNMR spectra of uniformly ^{15}N ([U-^{15}N]) Aβ40 fibrils in the absence and presence of Greek EVOO extract were obtained at a ^{1}H Larmor frequency of 700.13 MHz on a Bruker Avance 700 spectrometer. Following 3 days of incubation at 37 °C, any insoluble fibrils were isolated *via* centrifugation. A proton-decoupled ^{15}N CP-MAS NMR spectrum was obtained at 10 kHz MAS with the following parameters: excitation of ^{1}H magnetization was achieved with a 3 μs π/2 pulse, followed by a 2 ms contact time during which a ramped proton field of 63 kHz was matched to a ^{15}N field to achieve the Hartmann-Hahn condition. A SPINAL-64 sequence was employed to acquire the signal *via* a 63 kHz proton decoupling. A ^{1}H – ^{15}N refocused INEPT spectrum was acquired (at a matching MAS frequency) *via* π/2 and π pulses of 3 μs and 6 μs

at the ^{1}H frequency and 4 μs and 8 μs at the ^{15}N frequency, with inter-pulse delays of 1 ms. An ambient temperature was required to record the relevant spectra.

Cell Viability Assay

The viability of the SH-SY5Y cells was sustained by Dulbecco's Modified Eagle's Medium (DMEM) with 1% non-essential amino acids, 1% Penicillin-Streptomycin, and 10% foetal bovine serum (FBS). 8000 cells were deposited in each of 96 well plates in 80 μL and incubated at 37 °C for 24 hours with 5% CO_2. Pre-prepared samples (20 μM Aβ40 fibrils alone and following addition of 72 μg/mL and 144 μg/mL Greek EVOO for 24 h, and EVOO alone controls) were added in 20 μL per well and incubated for an additional 48 hours. 10 μL of Cell Counting Kit-8 (CCK-8, Stratech) was added to each well, and the absorbance was recorded at 450 nm/650 nm over 3 h. As per the CCK-8 dye guidelines, a 650 nm reference wavelength was employed to compensate for the insoluble fibrillar material. Graph Pad was employed to process and analyse the data by reporting on % viability *via* an evaluation against the live (buffer alone) and dead (1% triton final concentration) controls using one-way ANOVA with Tukey multiple comparison correction. This work was carried out by collaborators at Liverpool University (Dr Jillan Madine, Rebecca Price).

Dynamic Light Scattering Analysis

A Malvern Panalytical Zetasizer Nano ZSP at room temperature was employed to conduct dynamic light scattering. Following this, averaged profiles were calculated by conducting 12 measurements (in triplicate) for each sample (unaccompanied Aβ40 fibrils and after the addition of 144 μg/mL of Greek EVOO for 24 h). This work was carried out by collaborators at Liverpool University (Dr Jillan Madine, Rebecca Price).

Computational Molecular Docking Analysis

Molsoft ICM-Pro (version 3.9-1a) was used to generate fibrillar structural models of tau (PDB 6QJH) and Aβ (PDB 2LMQ) and run docking simulations. The PDB files were first converted into ICM files with optimized residues of histidine, hydrogen, cysteine, glutamate, glycine, and proline, leaving strongly bound molecules of H_2O. The ICM Pro Pocket Finder algorithm (tolerance = 3) was used to determine initial binding sites. After ordering by volume, the files were made ready for docking without changing the location of the ligand from its starting place. Chemical structures from ChEMBL were selected for each of the target compounds and entered in the Chemical Table and the docking simulations run with conformation lengths of 10 and 3 nm.

Results

EVOO Phenolic Compounds

The principal objective was to prepare EVOO extracts with distinctive phenolic profiles for evaluation against Aβ40 and tau aggregation. The polyphenols were extracted from Greek and Saudi Arabia natural extra virgin olive oil products and characterised (the data regarding this process is located in the previous chapter).

The Effect of EVOO Phenolic Extracts on Aβ40 and Tau Aggregation Kinetics by thioflavin T

The principal am of the work in this chapter was to establish whether or not the EVOO polyphenol extracts inhibit the rate of amyloid formation by Aβ40 and tau, and/or reduce the final yield of the amyloid aggregates produced. Analysis of the aggregation kinetics of these proteins in the absence and presence of the extracts using ThT fluorescence is a convenient

method for assessing the ability of the polyphenol mixtures to inhibit amyloid formation. Effective inhibition of the rate is observed as an increase in the time $t_{1/2}$ taken for half maximum fluorescence to be attained. A reduction in the maximum fluorescence, Fmax, in the presence of the polyphenols, may suggest a reduction of the yield of fibrils produced.

Following Xue et al. (2017), the aggregation of Aβ40 at 37 °C under agitating conditions was observed by the amyloid reactive dye thioflavin T (ThT) which exhibits enhanced fluorescence emission at ~480 nm upon binding to amyloid structures and correlates linearly with the fibril concentration. When exposed to increasing concentrations of the Greek EVOO, tau aggregation experienced a progressive reduction of ThT fluorescence at the end-point measurement of 12 hours (see **Figure 5.3a**).

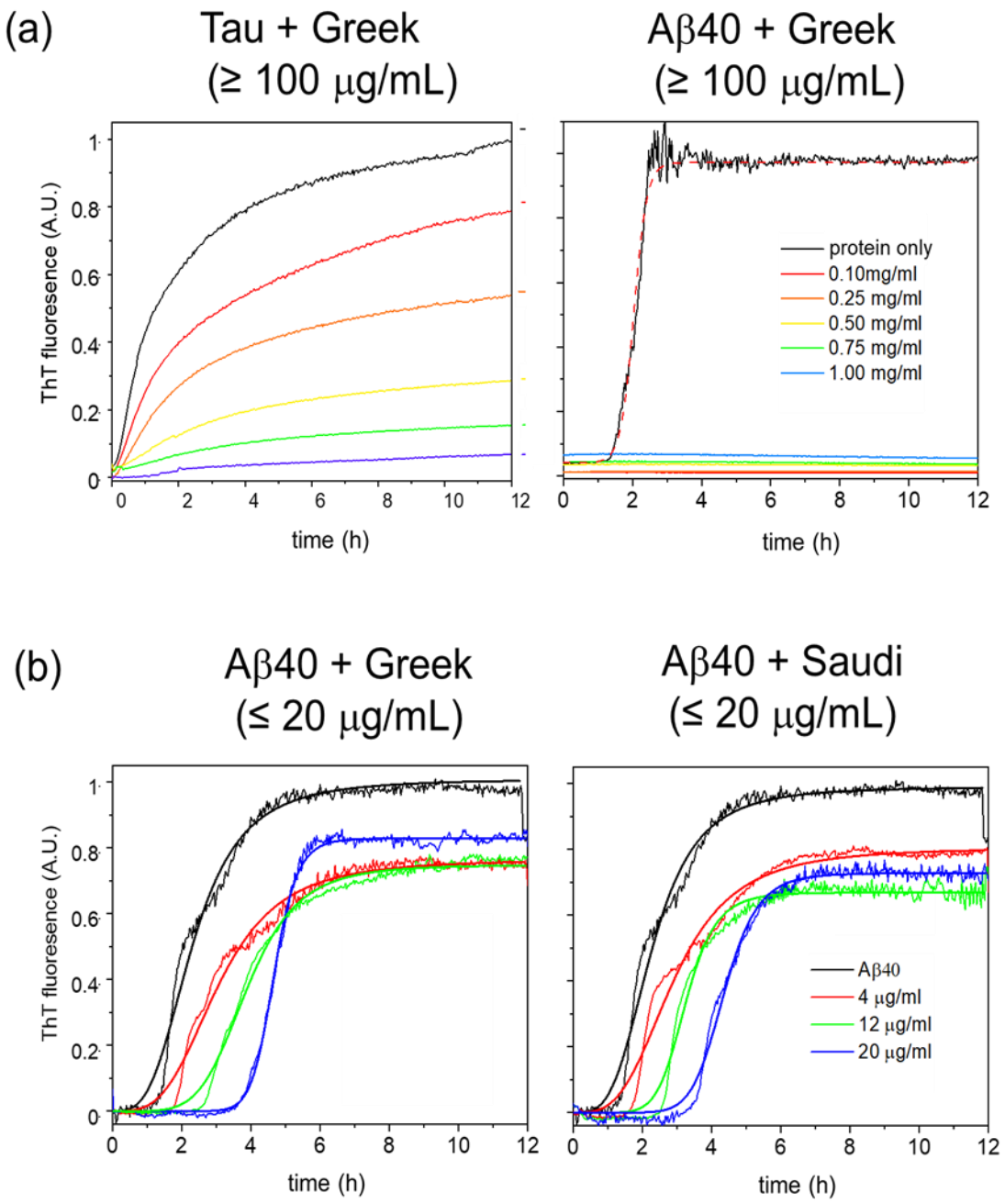

Figure 5.3. A Kinetic analysis of Tau and Aβ40 aggregation in the absence and presence of EVOO polyphenol extracts at discrete concentrations. The dry weight of the extracts dissolved in a solvent is expressed in mg/mL. (a) ThT analysis of Tau and Aβ40 aggregation with and without elevated concentrations (0.1 – 1.0 mg/mL) of the Greek EVOO extracts. The mean values of n = 3 measurements are displayed. (b) ThT analysis of Aβ40 aggregation with and without reduced concentrations of the Greek and Arabian EVOO extracts. The values included in **Table 5.1** were used to create lines of best fit (using a standard Hill function).

Table 5.1. Summary of the impact of EVOO extracts on Aβ40 aggregation kinetics (calculated *via* ThT fluorescence). In the absence of an extract, the highest fluorescence emission, F_{max}, is normalised to Aβ40.

Extract	**Extract concentration**							
	Aβ40 only		4 μg/mL		12 μg/mL		20 μg/mL	
	F_{max}	$t_{1/2}$ (h)	F_{max}	$t_{1/2}$ (h)	F_{max}	$t_{1/2}$ (h)	F_{max}	$t_{1/2}$ (h)
Greek	1.00 (0.15)	2.31 (0.20)	0.76 (0.18)	3.06 (0.22)	0.75 (0.13)	3.90 (0.32)	0.83 (0.15)	4.67 (0.25)
Saudi	1.00 (0.15)	2.31 (0.20)	0.80 (0.19)	2.90 (0.25)	0.67 (0.19)	3.25 (0.23)	0.73 (0.16)	4.37 (0.13)

[a]The maximum fluorescence emission, F_{max}, is expressed normalized to Aβ40 in the absence of extract. [b]Means (standard errors) are given from measurements on $n = 3$ samples per group.

A detailed analysis of the data signifies that increased concentrations of EVOO extract lengthen the lag time and decrease the rate of filament elongation (**Appendix 2 Figure S5.1**). However, any observable effect required an elevated concentration of the extract (≥ 100 μg/mL); if the average molecular weight of compounds in the extract is assumed to be that of oleuropein aglycone (M_r ~ 384), 100 μg/mL would equate to a concentration of 250 μM. Sub-equimolar concentrations of compounds relative to the protein concentration (20 μM in this case) are generally considered to be required for an effective inhibitor (Porat et al., 2006). Although the phenolic mixture in the extract does decrease the tau aggregation rates, it requires concentration levels to be ten times higher than is currently considered appropriate for an inhibitory compound.

Aβ40 alone aggregates with a time to half completion of aggregation, $t_{1/2}$, of 2.3 h. Following the addition of Greek EVOO extract at identical concentrations employed for tau inhibition (≥ 100 μg/mL), the ThT fluorescence is effectively eradicated (**Figure 5.3a**, right); therefore, under these conditions, it was unfeasible to measure the kinetics. It was possible to discern a concentration effect on the aggregation of Aβ40 (see **Figure 5.3b**) following a reduction of the concentration of the Greek EVOO extract (to ≤ 20 μg/mL ≅ 50 μM). Following an increase in the extract concentration (from 4 μg/mL to 20 μg/mL), it was possible to observe a progressive shift of $t_{1/2}$ from 2.1 h to 4.7 h alongside a minor decrease in the end-point fluorescence (**Table 5.1**).

Notably, despite possessing a different phenolic profile to the Greek extract, the Arabian extract exhibited almost identical results at lower concentrations (see **Figure 5.3b**). The concentration range of the extract required to stimulate Aβ40 inhibition (assuming the average M_r as above) is equimolar with the protein. Hudson et al. (2009) note that reduced fluorescence can be falsely ascribed to a reduction in fibril yield since some polyphenols

compete with ThT for fibrillar binding sites. Therefore, an independent methodology should be employed to confirm the existence of any inhibitory effects.

The Effect of EVOO Phenolic Extracts on Aβ40 Aggregation Kinetics by circular dichroism

Far-UV circular dichroism spectroscopy was employed to oversee the alterations of Aβ40 secondary structures throughout aggregation (see **Figure 5.4**). Amyloid formation typically progresses from an initial unfolded or partially folded protein to β-sheet rich species, culminating in insoluble amyloid fibrils with the characteristic cross-β structure. CD is sensitive to the initial structural transition of the soluble proteins, and loss of signal may be observed later on when the fibrils precipitate from solution.

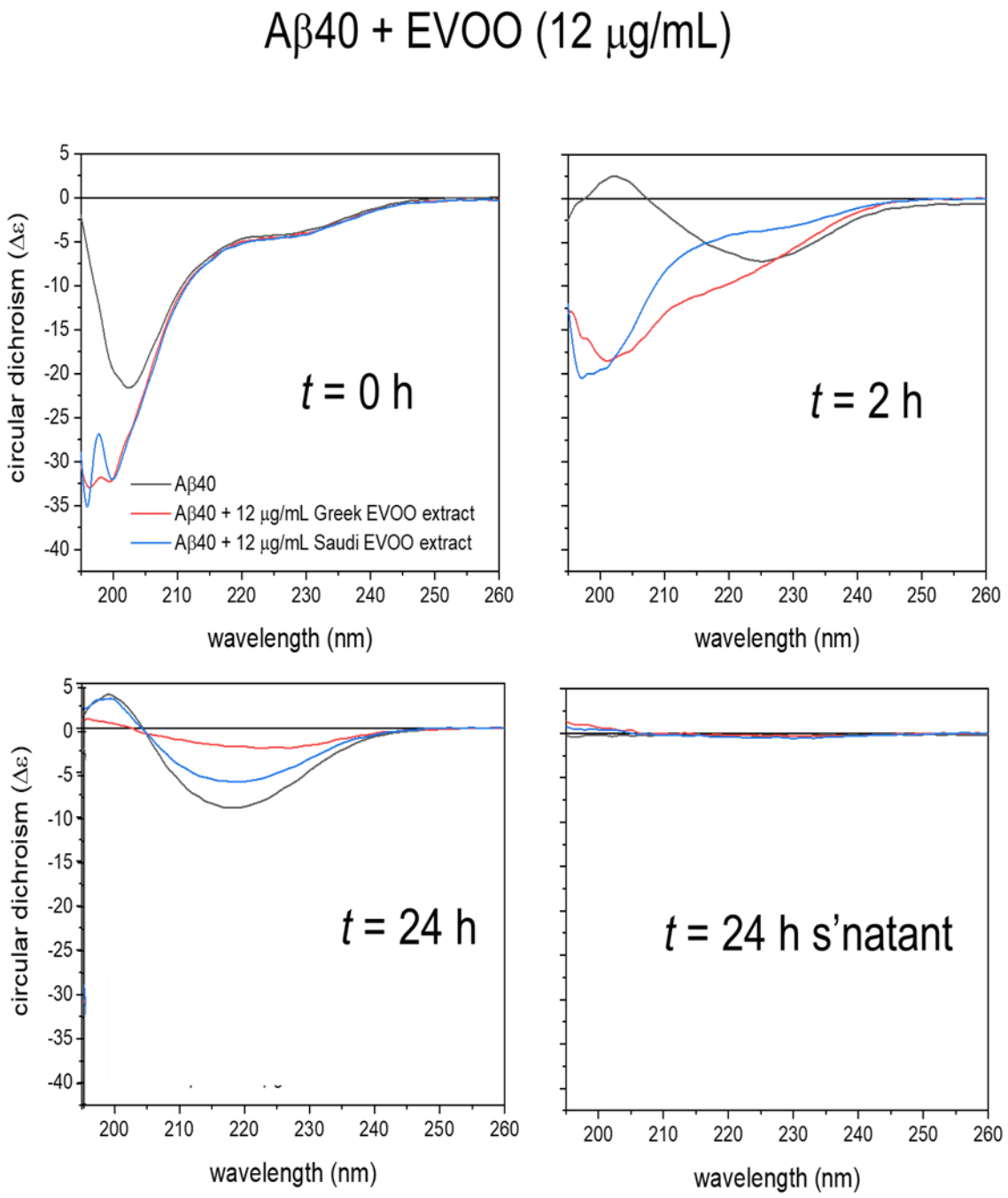

Figure 5.4. Far-UV CD analysis of Aβ40 with and without the presence of polyphenol extract from Greek and Saudi Arabia EVOO at *t* = 0 h, 2 h and 24 h. The supernatant at 24 h was assessed following sedimentation of the insoluble matter (right in the bottom).

The spectrum of Aβ40 in isolation exhibits the expected features of an unfolded protein at $t = 0$ (a large negative lobe at ~200 nm) and is in agreement with a conformational transition to a β-sheet-containing state (positive lobe at 200 nm and negative lobe at ~222 nm) at $t = 2$ h and $t = 24$ h. When exposed to the Greek and Saudi Arabia EVOO extracts (12 μg/mL), the β-sheet transition is visibly inhibited and, following 2 hours of incubation, the spectra maintain the features of an unfolded state. The CD spectra are in agreement with the shift to longer $t_{1/2}$ values observed in the ThT curves of Aβ40 combined with the extracts. Following a 24-hour incubation, all of the spectra display a negative lobe at ~220 nm and no negative lobe at ~200 nm, which, in all cases, correlates with a total loss of the initial unfolded state and the formation of β-sheet rich structures. The spectra of the three samples (Aβ40 with and without the presence of polyphenol extracts) diverge in the $\Delta_{\mathcal{E}}$ observed at 220 nm, which implies that the aggregates possess different β-sheet contents. Following the removal of the insoluble aggregates (*via* centrifugation), there is minimal to no signal from the supernatant (see **Figure 5.4** right in the bottom).

The Effect of EVOO Phenolic Extracts on Aβ40 and Tau Aggregate Morphologies

Visualisation of the morphology and magnitude of tau deposition and Aβ40 aggregates created following the addition of the EVOO extracts (**Figure 5.5, a, and b**) was determined *via* negative-stain transmission electron microscopy (TEM). A fresh solution consisting of monomeric Aβ40 (20 μM) was incubated alone (or with the addition of Greek or Saudi extracts at 20 μg mL ≅ 50 μM) for 24 h. Aggregation of the solution consisting solely of Aβ40 produced fibrillar species with a width of 17.7 (± 0.4) nm and length of 396 (± 25) nm, clustered together in dense networks (See **Figure 5.5a**). Conversely, in the samples containing Greek and Arabian EVOO extracts, the fibrils present as short and slender and are distributed sparingly (see **Figure 5.5a** – middle and right). In the presence of the two extracts (Greek and Saudi Arabia), there

are no noteworthy populations of non-fibrillar structures and no detectible difference between the extent of fibril deposition or morphology.

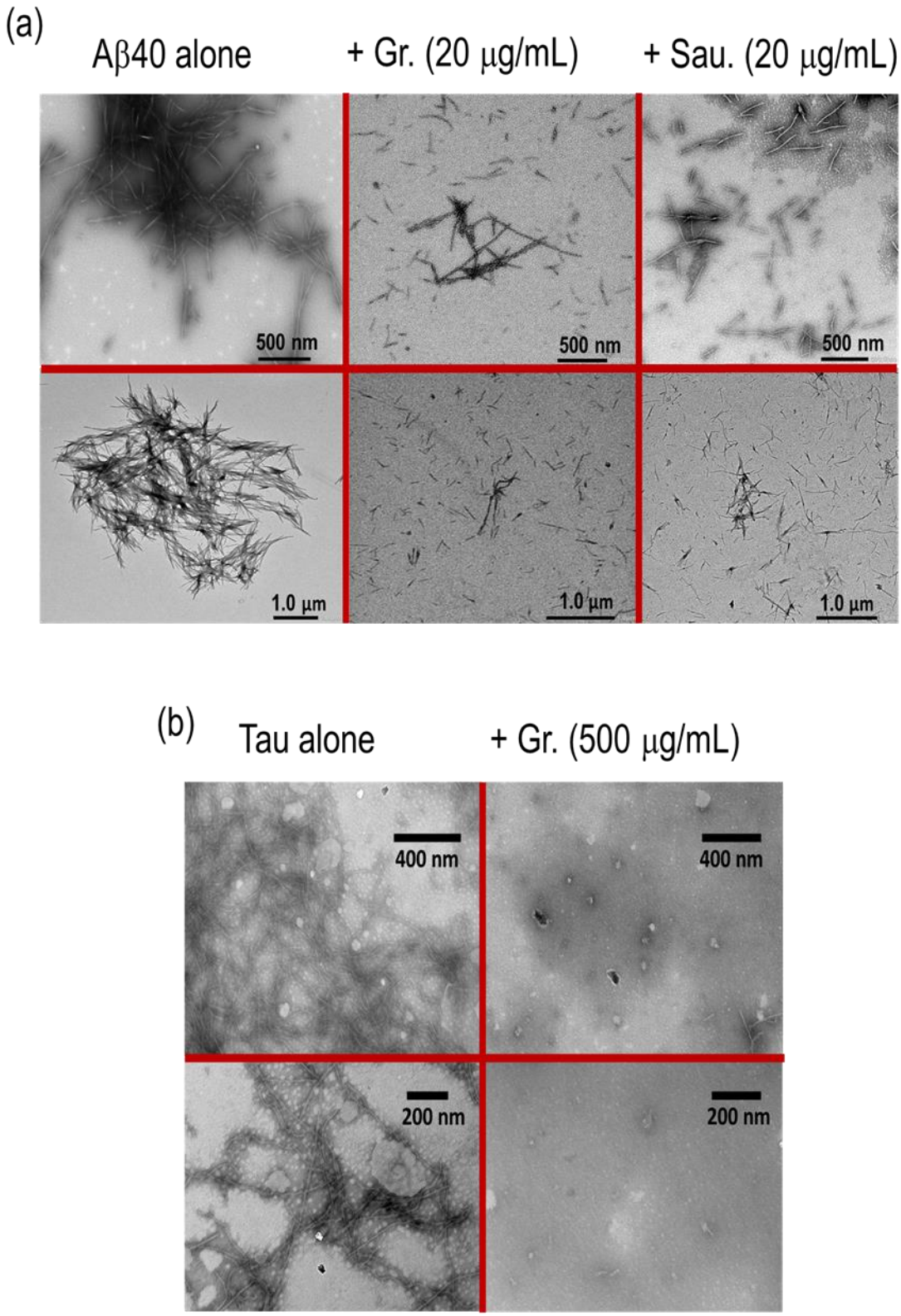

Figure 5.5. A morphological analysis of Tau and Aβ40 aggregation in the absence and presence of EVOO polyphenol extracts at discrete concentrations. (a) Negative-stain TEM images of Aβ40 aggregates (20 μM monomer equivalent) isolated following incubation alone

or with 20 μg/mL (≅ 50 μM) Greek or 20 μg/mL Saudi EVOO extract for 3 days. (b) Negative-stain TEM images of tau aggregates (20 μM monomer equivalent) isolated following incubation in isolation or with 500 μg/mL (≅ 1.25 mM) Greek EVOO extract for 3 days. Two distinct magnifications and views are presented (top and bottom).

Over a comparable period, the incubation of tau gave rise to fibrillar structures (see **Figure 5.5b**) whose density and morphology were indistinguishable from fibrils obtained with 20 μg/mL EVOO (data not presented). However, when incubated with 0.5 mg/mL EVOO extract, the tau morphology was altered and elicited a reduced ThT fluorescence in response to its presence (see **Figure 5.3a**). The utilisation of an extract with a higher concentration initiated the formation of spherical oligomers with filaments of comparable size and morphology to those of tau alone.

Summary of the effects of polyphenol extracts on Aβ40 and tau aggregation

In summary, the Greek and Saudi EVOO extracts reduced the rate of Aβ40 aggregation (as determined *via* ThT and CD spectroscopy) in the concentration range approximating that of Aβ. Contrastingly, a minimum of a 10-fold concentration of the extracts is required to inhibit tau aggregation. Despite having a lower concentration of oleuropein aglycone, tyrosol, and hydroxytyrosol than the Greek extract, the Saudi Arabia extract exhibited similar effects on Aβ40 suggesting that the Arabian extract contains other phenolic compounds which compensate for deficiencies in the aforementioned inhibitory compounds.

Effect of EVOO Phenolic Extracts on the size and morphology of pre-formed Aβ40 Aggregates

The next phase of this research concerned the ability of phenolic mixtures to modify pre-formed Aβ40 fibrillar aggregates into alternative morphologies. As noted by Townsend et al. (2018) and Ehrnhoefer et al. (2008), amyloid-remodelling behaviour has been detected in specific individual phenolic compounds such as EGCG (the polyphenol found in green tea). These observations are interesting because the polyphenols may have the ability to reduce the pathological plaques associated with amyloid diseases, including AD.

In this experiment, monomeric Aβ40 (20 μM) was incubated under aggregating conditions for three days to allow fibrils to fully form, and afterwards the insoluble aggregates were isolated from the bulk solution by centrifugation. Following this process, EVOO extract solutions were added to the sedimented aggregates to a final concentration of 20 μg mL (≅ 50 μM), 72 μg mL or 740 μg mL. The samples were incubated for a further 24 h and then the soluble and insoluble fractions were separated *via* centrifugation. Control samples were prepared following the same procedure but omitting the polyphenols. Analysis of the insoluble and soluble fractions was carried out using negative stain TEM to determine whether the polyphenol extracts change the morphology of the insoluble aggregates and/or release smaller soluble species (e.g. oligomers) into the aqueous phase.

TEM images of Aβ40 in isolation revealed the accumulation of a condensed network of insoluble fibrils (see **Figure 5.6a (top)** and **Figure 5.5a (left)**) and there was an evident lack of visible species remaining in the supernatant following centrifugation (**Figure 5.6a, bottom**). The pre-formed fibrils treated with 20 μg/mL of the EVOO extract solutions (Greek and Saudi Arabia) and sedimented by centrifugation (insoluble fraction) were observed to remodel into slender insoluble fibrils (see **Figure 5.6b** and **c**). In the supernatant of the same sample (soluble

fraction), minor populations of soluble annular (or spherical) structures, averaging ~30 nm in diameter, and reminiscent of oligomers (Kayed et al., 2003) were observed at a few positions on the TEM grid. These species constitute a very small fraction of the total aggregate mass (at this concentration of extract) and were non-existent when extracts were added at concentrations < 20 µg/mL (data not shown).

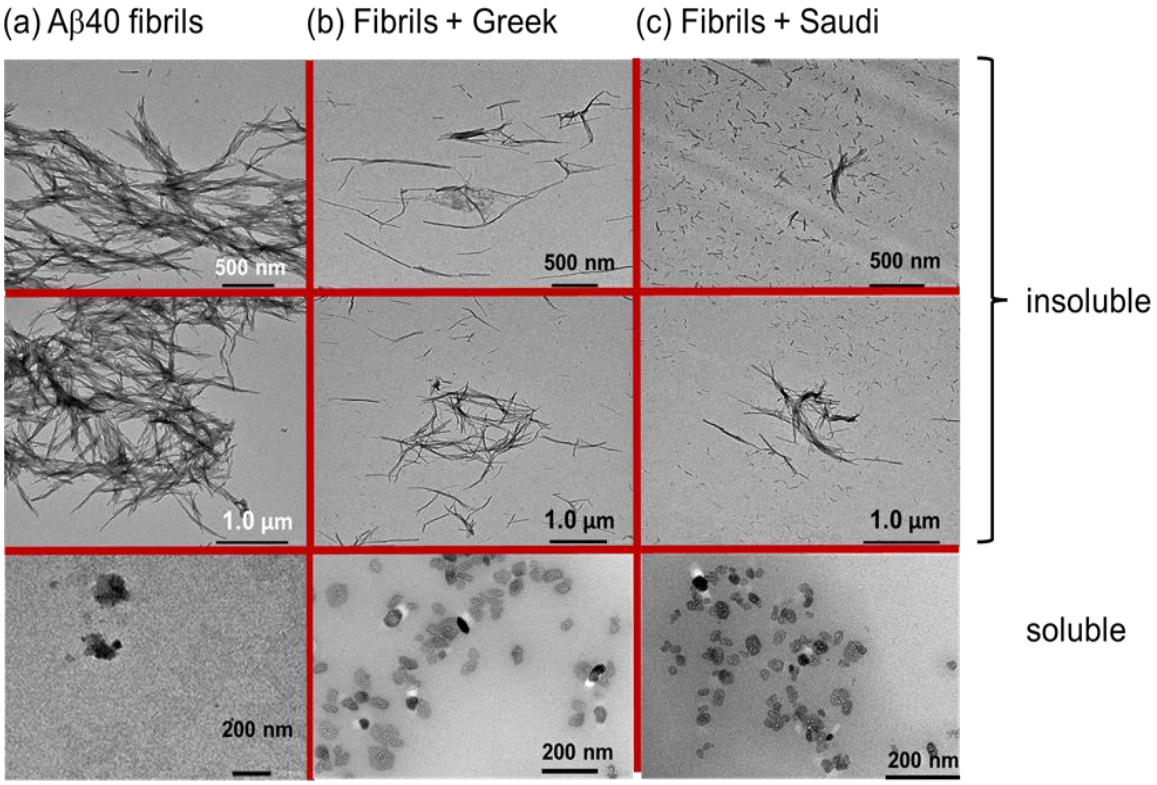

Figure 5.6. Negative-stain TEM images of Aβ40 fibrils (20 µM) were examined following incubation of Aβ40 in isolation (from an initial monomeric state) for 3 days, followed by incubation with a buffer or with 20 µg/mL (≅ 50 µM) EVOO extract for an additional 24 h. (a) Buffer incubated Aβ40 fibrils. (b) Aβ40 following the addition of Greek EVOO extract. (c) Aβ40 following the addition of Saudi EVOO extract. Centrifugation was employed to separate the insoluble constituents while the soluble matter was contained within the supernatant.

Following the addition of 72 µg/mL of the Greek extract solution, there was a notable increase in the number of soluble oligomers. Upon adding 740 µg/mL of the same solution, all of the detectable aggregates had remodelled into the oligomeric morphology characterised with a smaller average diameter (see **Figure 5.7** (1 top)). In the absence of the extracts, tau forms dense filaments following a three-day incubation period. Adding concentrations of the Greek extract solution (up to 500 µg/mL) to the pre-formed tau filaments made almost no impact on the morphology of the aggregates (see **Figure 5.7** (2 bottom)).

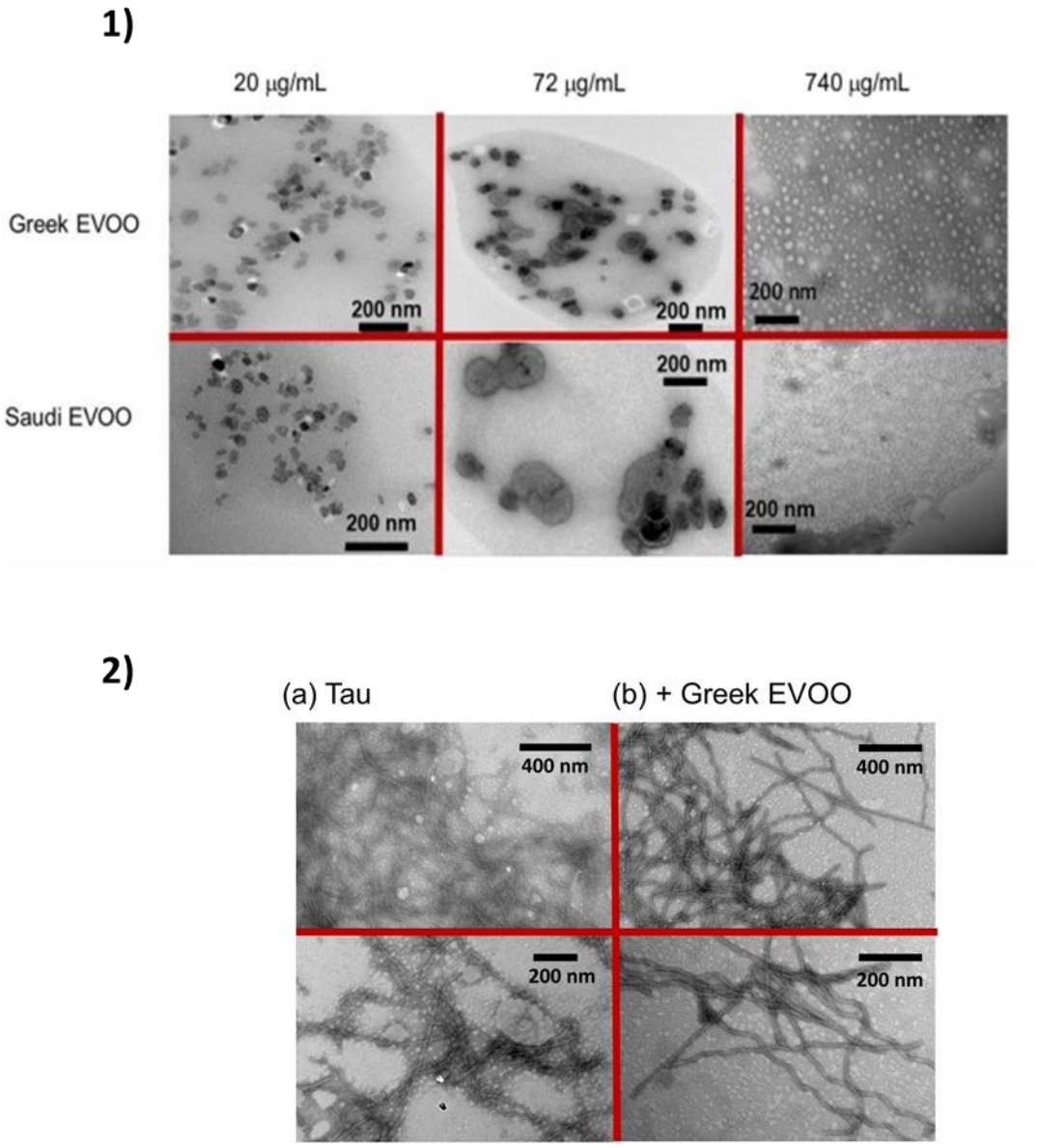

Figure 5.7. (1 top) Centrifugation was employed to isolate the soluble oligomers (created from pre-formed fibrils exposed to EVOO extracts at 3 concentrations) of Aβ40 in the supernatant. (2 bottom) (a) Negative-stain TEM images of tau filaments formed in isolation (after 3 days) and (b) subsequent to the addition of 500 µg/mL of Greek EVOO extract.

Measurements were conducted on the pre-formed Aβ40 aggregates after the addition of the Greek extract using dynamic light scattering (DLS) to measure the size distribution of the species formed. The highest concentration of Greek extract (740 µg/mL) decreased the mean diameter of the aggregates by nearly an order of magnitude (see **Figure 5.8**).

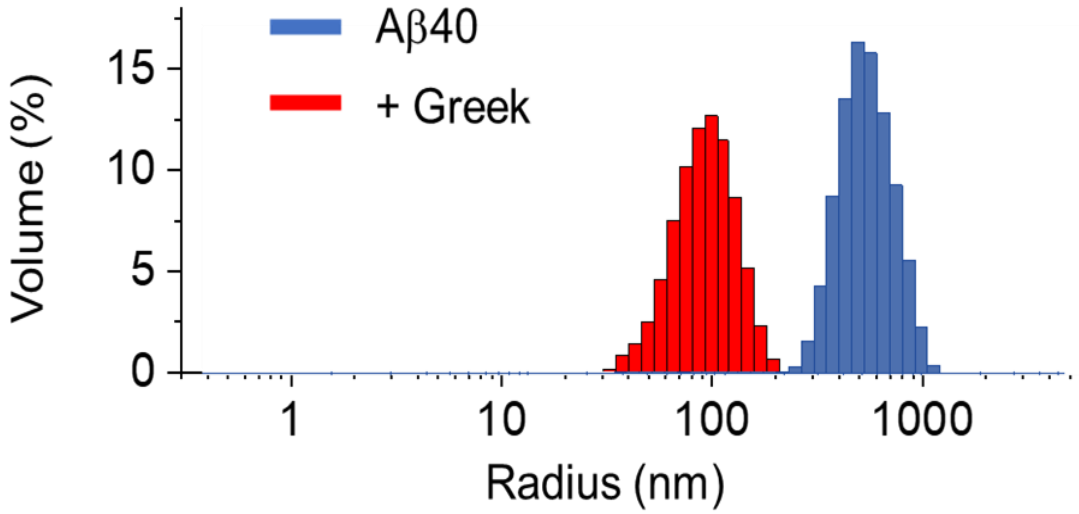

Figure 5.8. DLS data for Aβ40 fibrils in isolation and with 740 µg/mL Greek EVOO.

^{15}N cross-polarization magic-angle spinning solid-state NMR of uniformly ^{15}N-labelled Aβ40 fibrils before treatment with the extract exhibits characteristic peaks from the backbone amine (100-125 ppm) and arginine, lysine, and histidine sidechains (see **Figure 5.9 - top**). The CP-MAS spectrum shows peaks from dynamically restricted sites which are indicative of intact fibrils. A ^{1}H-^{15}N refocused INEPT SSNMR test on the identical sample (not shown) failed to reveal any signals; however, following the addition of the EVOO extract (20 µg/mL), selective peaks from the backbone and arginine ^{15}N sites emerge in the INEPT spectrum (see **Figure 5.9 - bottom**).

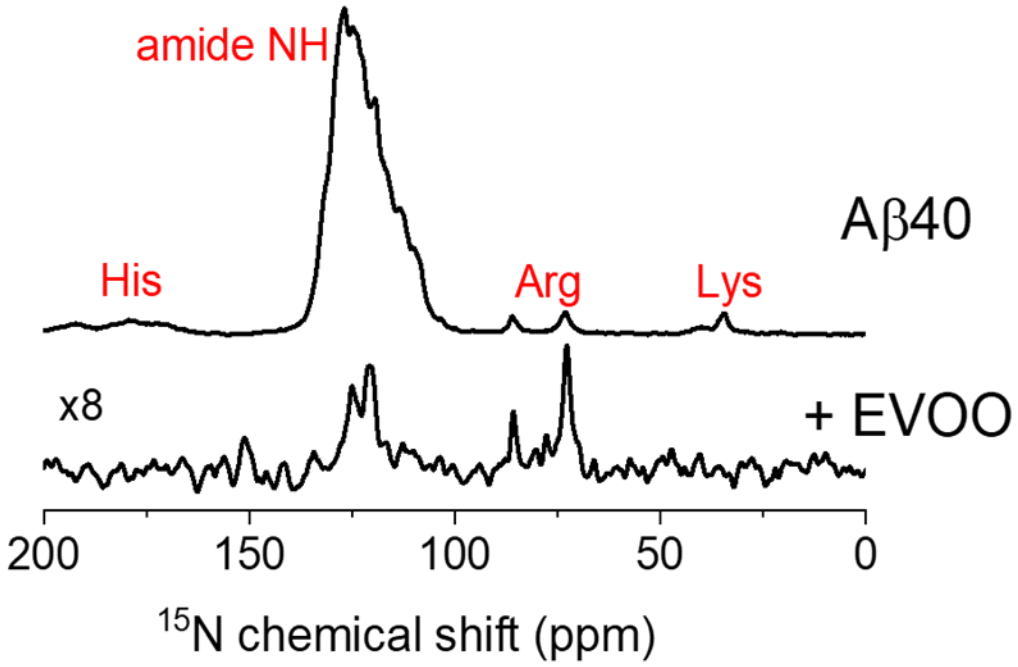

Figure 5.9. ^{15}N CP-MAS (top) and refocused ^{1}H-^{15}N INEPT spectra of [U-^{15}N] Aβ40 fibrils combined with Greek extract.

The INEPT methodology only detects resonances from mobile groups and the observed results are consistent with a partial mobilisation of the fibrils following the addition of the extract. The combined results of the TEM, DLS and SSNMR data signify that the phenolic extracts mobilise the Aβ40 fibrils, form soluble oligomers, and remodel the residual fibrils into a more slender configuration.

Cellular toxicity of soluble Aβ40 oligomers

Selkoe & Hardy. (2016) and numerous others have reported that soluble oligomers of Aβ40 that form on-pathway to the mature fibrils have a direct correlation with toxicity and may be the pathological culprits in the progression of AD. Formation of the oligomeric-like species of Aβ40 after the addition of the polyphenol extracts could therefore be potentially pathogenic and counter the beneficial anti-aggregation effects seen earlier. To test this hypothesis, SH-SY5Y neuroblastoma cells were used in a cell viability assay to assess the cytotoxicity of the oligomer-like species produced by Aβ40 following the addition of the Greek phenolic extract.

The experiment was designed to assess the effects of the extract at various concentrations (specifically 72 μg/mL and 144 μg/mL) which were selected for three reasons: firstly, the concentration levels are high enough to stimulate the formation of oligomers; secondly, the concentrations are higher than required to completely eradicate aggregation, finally, but the levels of concentration are not so high that they risk solubilisation of the fibrils. The two levels of concentration of the extract solutions selected for this experiment had no impact on cell viability (see **Figure 5.10**).

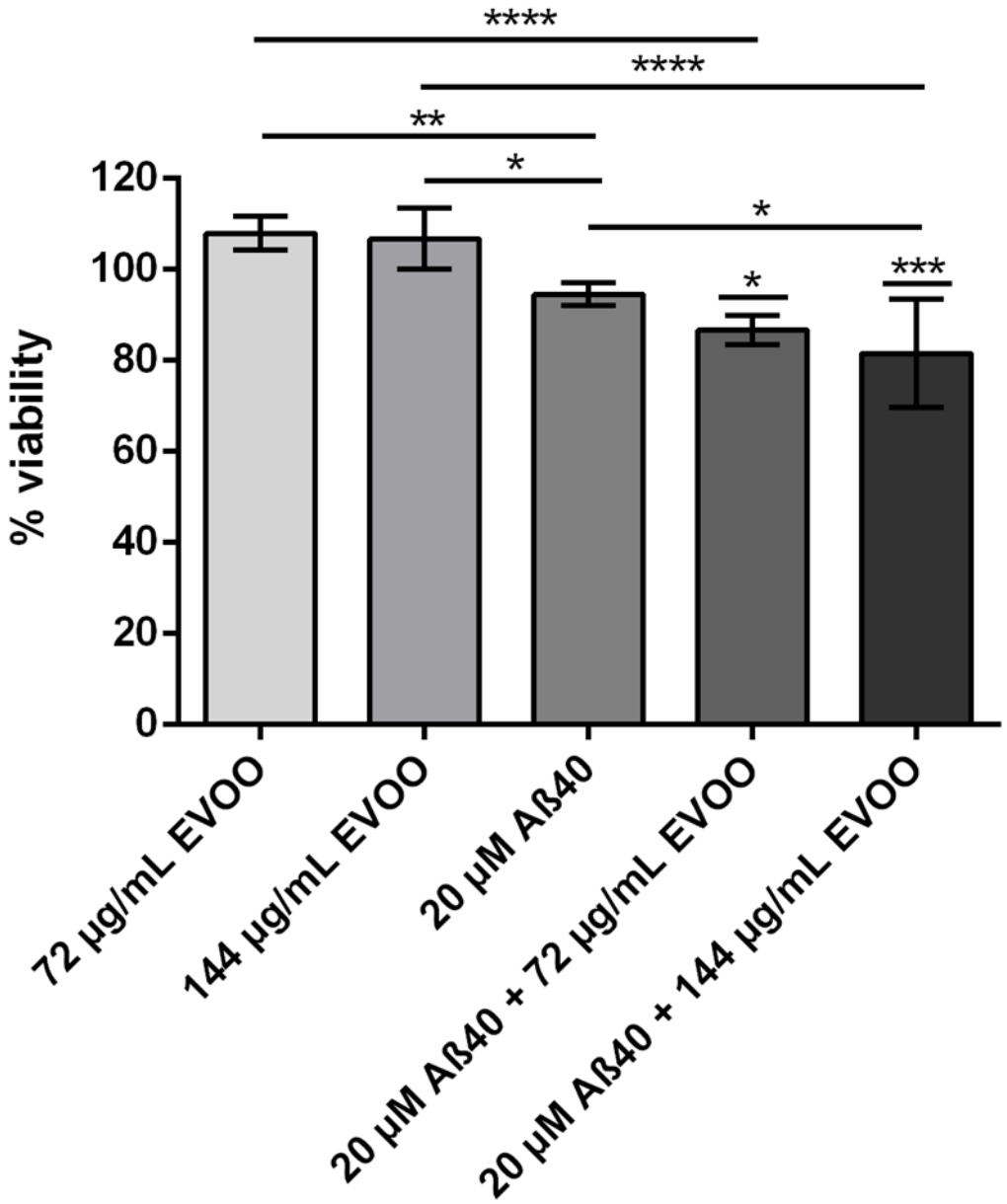

Figure 5.10. Viability results for SH-SY5Y cells, the first two columns are EVOO untreated controls at concentrations of 72 µg/mL and 144 µg/mL following the addition of EVOO extract, Aβ40 fibrils in isolation and followed by the addition of 72 µg/mL and 144 µg/mL Greek EVOO as shown in the last three columns, n = 6 per condition. ANOVA with Tukey multiple correction comparison between the live and Aβ40-treated cells in the presence of EVOO at both concentrations and between comparison groups (*p<0.05, **p<0.01, ****p<0.001, ****p<0.0001) was utilised to calculate p values.

The Aβ40 aggregates (total soluble and insoluble fractions) in the absence of the extract solutions had a minimal effect on the cells, reducing viability by less than 10% relative to the untreated cell controls. When the Aβ40 aggregates were treated with the extract solutions for 24 h before being added to the cells cell viability was reduced by a further 5 to 10%. This additional reduction in viability is small but statistically significant. These results demonstrate that the addition of extracts at the specified concentrations to Aβ40 aggregates stimulate the creation of mildly cytotoxic species (consistent with the observations of TEM regarding oligomer remodelling).

Binding Investigation of EVOO Compounds to Aβ40 Fibrils

The remodelling of Aβ40 fibrils into short, slender structures and soluble oligomers in the presence of EVOO extracts suggests an interaction between the aggregates and some of the polyphenols in the extracts. Therefore, the research aimed to determine which of the phenolic compounds found in the EVOO extracts binds to the insoluble Aβ40 species. To identify the relevant phenolic compounds, the extracts (20 μg/mL) and pre-formed insoluble fibrils (20 μM monomer equivalent) were incubated for 24 h and sedimentation was employed to extract the insoluble material. This procedure replicated the method used to prepare the TEM samples. The fibrils and any bound polyphenols were then sedimented by centrifugation. The concentration of polyphenols remaining in the supernatant was compared with the initial concentration to give a measure of how much had bound to the fibrils. Hence, binding of polyphenols to the fibrils will be observed as a reduction in the supernatant concentration. The reduction of the overall polyphenol concentration in the supernatant was measured by UV/Visible spectrophotometry, and the reduction of individual polyphenols was resolved by reverse-phase HPLC.

Figure 5.11a and **b** shows the UV/Visible spectra of the Greek and Saudi extract solutions before and after the addition of Aβ40 fibrils and their subsequent extraction *via* sedimentation. The spectra reveal that absorption across the entire spectra is reduced by >50% following the addition and removal of the fibrils. These results indicate that a substantial percentage of the species in the extracts bind to the insoluble fibril fraction, although the spectra do not indicate which species are removed. Reverse-phase HPLC was employed to resolve the binding species in the Greek and Arabian extracts (see **Figure 5.11c** for Greek EVOO and **d** for Saudi EVOO, **Table 5.2** for Greek EVOO and **Table 5.3** for Saudi EVOO). This process determined that a significant majority of the compounds (detectable at 240 nm, 275 nm, and 340 nm, these 3 wavelengths enabling us to determine the particular absorption of the phenolic compounds) had bound with the fibrils (to some degree) and, in some instances, were completely removed from the solution.

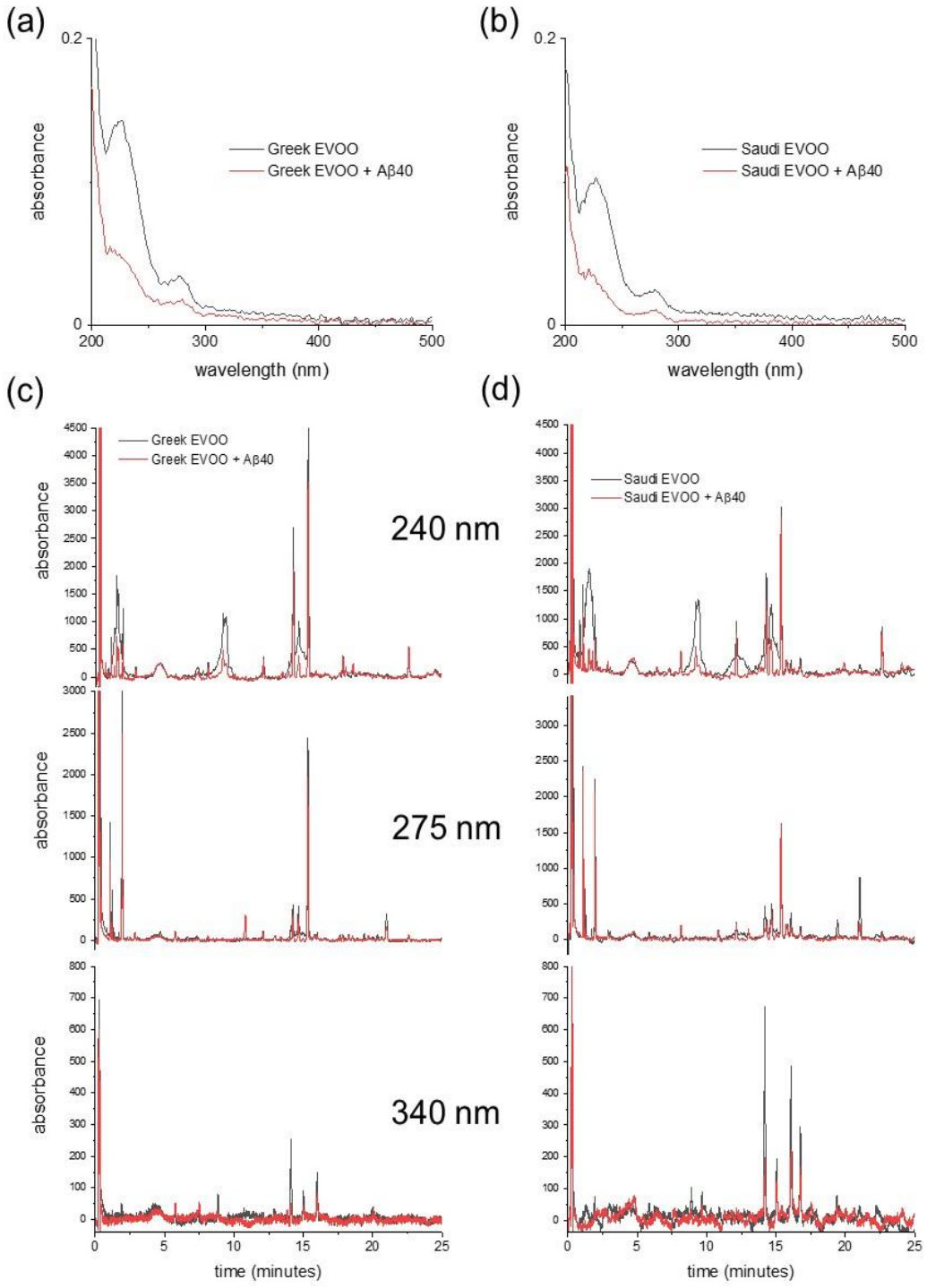

Figure 5.11. UV- Visible and HPLC binding of polyphenolic compounds in Greek and Saudi extracts to pre-formed fibrils of Aβ40. (a and b) UV/Visible absorption spectra of both extracts (20 µg/mL) in isolation (black lines) and of the supernatant obtained following the addition of 20 µM Aβ40 fibrils, incubation for 24 h, and the use of centrifugation to extract the insoluble material (red lines). (c and d) Reverse-phase HPLC chromatograms at 3 different wavelengths

of the Greek and Arabian extracts in isolation (black) and following the addition and extraction of Aβ40 fibrils (red). **Tables 5.2** and **5.3** below contain the primary peaks, retention times, and some assignments.

Table 5.2. A summary of the HPLC binding analysis of phenolic compounds from Greek EVOO binding (20 μg/mL phenolic extract) to pre-formed fibrils of Aβ40 (20 μM monomer equivalent), (*n* = 1).

Retention time (min)	Compound	Normalized peak intensity[a]		% Bound	λ (nm)[b]
		- fibril	+fibril		
1.0	Hydroxytyrosol	12.9	3.8	71	275
1.2	Unknown	11.7	1.7	86	275
1.7	Unknown	1.3	0.0	100	275
1.9	Tyrosol	93.1	8.4	91	275
2.9	Vanillic acid	2.2	0.0	100	275
3.0	Caffeic acid	1.6	0.0	100	275
5.7	*p*-Coumaric acid	3.8	0.0	100	275
8.1	Unknown	7.2	6.3	12	240
8.9	Unknown	1.4	0.0	100	340
9.2	Unknown	100.0	14.4	86	240
9.4	Unknown	96.5	6.3	93	240
12.1	Unknown	6.5	5.5	16	240
14.1	Luteolin	3.6	1.2	66	340
14.3	Unknown	11.8	7.2	39	275
14.6	(+)-Pinoresinol	12.9	8.9	31	275
15.0	Unknown	2.1	0.0	100	340
15.3	Naringenin	70.3	55.5	21	275
15.8	Unknown	2.4	0.0	100	275
16.0	Apigenin	3.1	0.0	100	340
17.7	Unknown	1.5	0.0	100	275
17.8	Unknown	1.6	1.2	24	275
18.3	Unknown	2.5	2.0	25	275
19.7	Unknown	3.2	0.0	100	275
19.9	Unknown	1.1	0.0	100	275
20.4	Unknown	1.4	0.0	100	275
22.6	Unknown	20.2	14.6	28	240

[a]Normalised to the maximum peak intensity (at 9.2 min) without Aβ40 fibrils.

[b]Wavelength of quantification selected to provide the strongest absorbance.

Table 5.3. A summary of the HPLC binding analysis of phenolic compounds from Saudi EVOO binding (20 μg/mL phenolic extract) to insoluble pre-formed fibrils of Aβ40 (20 μM monomer equivalent), (*n* = 1).

Retention time (min)	Compound	Normalized peak intensity[a]		% bound
		-fibril	+fibril	
1.0	Hydroxytyrosol	21.9	21.7	1
1.2	Unknown	7.9	1.6	80
1.7	Unknown	2.0	0.0	100
1.9	Tyrosol	37.1	31.5	15
2.9	Vanillic acid	2.9	0.0	100
3.0	Caffeic acid	2.4	0.0	100
8.1	Unknown	9.6	11.6	0
8.9	Unknown	2.1	0.0	100
9.2	Unknown	65.9	9.7	85
9.4	Unknown	100.0	0.0	100
12.1	Unknown	15.9	15.9	0
14.1	Luteolin	16.1	4.1	74
14.3	Unknown	6.0	5.3	12
14.5	Unknown	24.2	15.4	36
14.6	(+)-Pinoresinol	15.9	13.9	13
15.0	Unknown	4.3	3.4	21
15.3	Naringenin	40.7	41.7	0
15.7	Unknown	5.0	4.4	12
15.8	Unknown	4.5	2.7	39
16.0	Apigenin	13.1	4.7	64
16.7	Unknown	7.5	4.0	47
19.4	Unknown	9.4	0.0	100
21.0	Unknown	31.6	8.5	73
22.6	Unknown	28.1	23.6	16

[a]Normalised to the maximum peak intensity (at 9.4 min) without Aβ40 fibrils.

Reduced intensity peaks include the broad peaks associated with elenoic acid, oleuropein isomers and derivatives, pinoresinol and ligstrosides, and sharper peaks, prominent at the longer wavelengths, from tyrosol and flavonoids (see **Figure 4.11 Chapter 4**). All of the peaks assigned to the reference standards (and the unassigned peaks) were reduced in intensity (see **Tables 5.2** and **5.3** – shaded rows). It should be pointed out the percentage reduction of the peaks does not necessarily indicate the affinity of the corresponding components for the fibrils;

the complexities of competitive binding must be acknowledged. However, it can be concluded that the majority of the phenolic compounds in the Greek and Saudi extracts bind to the Aβ40 fibrils (to a greater or lesser extent).

Binding Investigation of EVOO Compounds to tau filaments

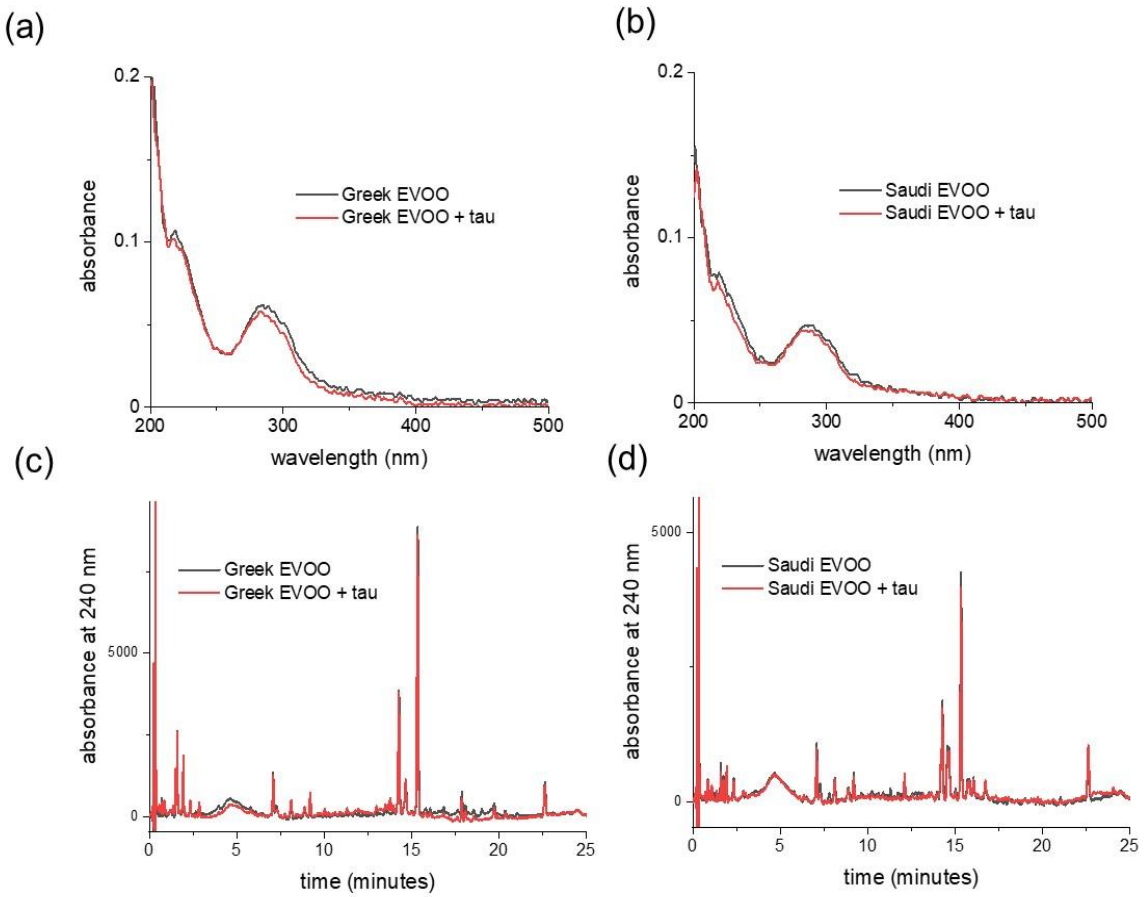

Figure 5.12. Binding analysis of polyphenolic compounds in the olive oil extracts to pre-formed fibrils of tau. (a and b) Greek and Saudi extracts (20 µg/mL): UV/Visible absorption spectra alone (black lines) and the supernatant acquired following the addition of 20 µM tau fibrils, 24 h incubation, and the employment of centrifugation to extract the insoluble material (red lines). (c and d) Reverse-phase HPLC chromatograms at 240 nm of the Greek and Saudi

Arabia extracts alone (black) and following the addition and extraction of insoluble tau fibrils (red).

The UV/Vis and HPLC analysis of the Greek extract revealed little or no binding to tau aggregates, as evidenced by the similarity in the profiles before and after removal of the aggregates (see **Figure 5.12**). This result contrasts with the extensive binding of the polyphenol mixtures to Aβ40 aggregates. However, this adverse outcome is consistent with the observed lack of effect of the extract solution on tau morphology and its diminished ability to impede tau aggregation. Notably, the difference in polyphenol binding to the Aβ40 and tau aggregates argue against nonspecific binding to amyloid fibrils in general and suggest that Aβ40 fibrils possess specific recognition sites for polyphenols while tau filaments do not. This possibility is explored later in the chapter with computational docking analysis. However, it should also be noted that tau requires the presence of a polyanionic species (heparin in this instance) which may repel the binding of polyphenols.

Investigate the Effect of Selected EVOO Polyphenolic Molecules on Aβ40 and Tau Aggregation Kinetics

Kim et al. (2005) note that, *in vitro*, individual dietary compounds of the flavonoid, phenolacrylic acid, hydroxybenzoic acid, and secoiridoid classes can inhibit Aβ aggregation. Here, it was investigated whether selected compounds of these classes that were identified in EVOO can individually affect Aβ40 and tau aggregation and bind to pre-formed Aβ40 and tau fibrils. The compounds selected for this comparison were apigenin, naringenin, luteolin, caffeic acid, vanillic acid, coumaric acid, ferulic acid, oleuropein, tyrosol, and hydroxytyrosol. Cinnamic acid and syringic acid were included but were not conclusively identified in the extracts used in this study; however, research conducted by Yorulmaz et al. (2012), indicates

that EVOO contains cinnamic acid at a concentration of 2-9 mg/kg (comparable to tyrosol) and syringic acid at a concentration of <1 mg/kg (comparable to coumaric acid).

The discrete compounds were combined with the monomeric protein in equimolar concentration (20 μM) and ThT fluorescence was employed to examine aggregation kinetics over 10 hours (see **Figure 5.13** and **Table 5.4**). Oleuropein and its metabolite, tyrosol, increased the $t_{1/2}$ of the sigmoidal aggregation curves of Aβ40, whereas hydroxytyrosol

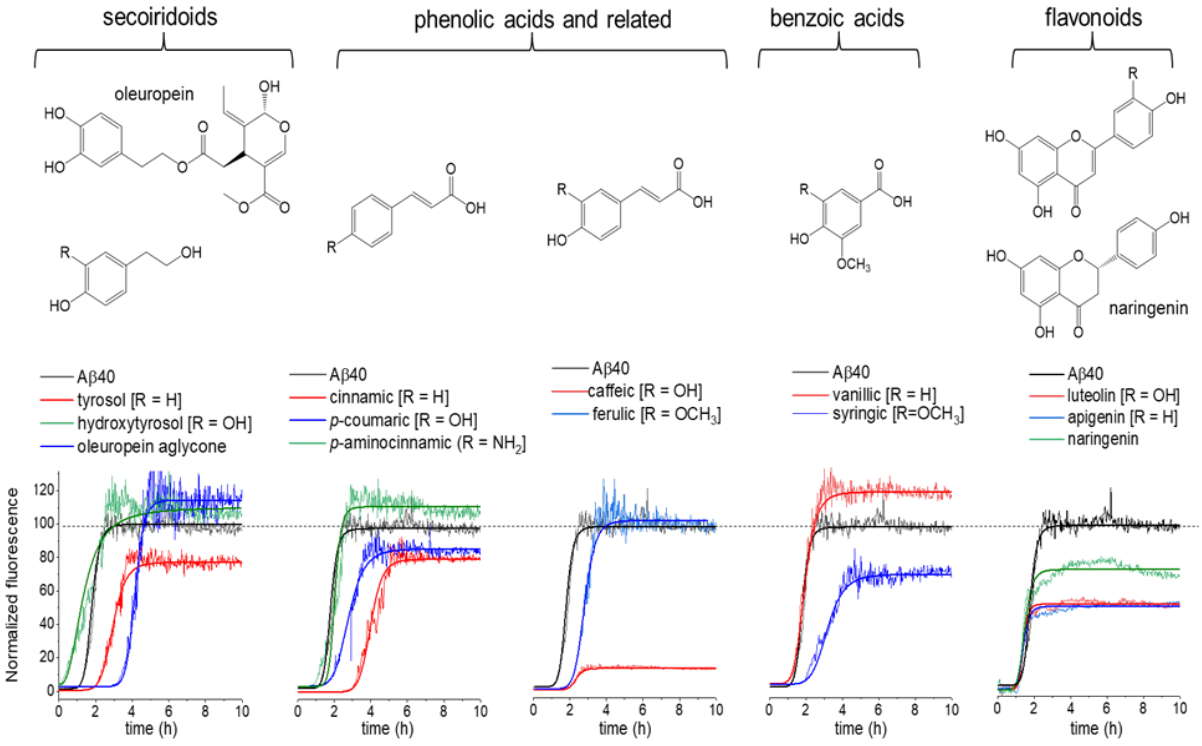

Figure 5.13. The impacts of discrete EVOO phenolic standard compounds on Aβ40 aggregation. ThT analysis of Aβ40 (20 μM) aggregation kinetics in isolation and following the addition of equimolar concentrations of individual polyphenols (chemical structures detailed above). Means are derived from n = 3 values per group.

caused a minimal reduction in $t_{1/2}$ (**Figure 5.13**). The phenolacrylic acids (caffeic acid, *p*–coumaric acid and ferulic acid) modified the $t_{1/2}$ of aggregation to extended durations, as did cinnamic acid (which lacks the catechol hydroxyl groups). It should be noted that only caffeic acid produced a significant diminution of F_{max}.

Table 5.4. The impacts of selected EVOO polyphenolic standards on Aβ40 and tau aggregation kinetics (determined *via* ThT) and the binding of tau and Aβ40 aggregates. Maximum fluorescence emission (F_{max}) is expressed as a percentage of the value for Aβ40 or tau (in the isolation of extract). Means and standard errors (in parentheses) are given for ThT data (n = 3). ND = not done.

	ThT F_{max} (%)		ThT $t_{1/2}$ (h)		% bound	
	A*β*40	**tau**	**A*β*40**	**tau**	**A*β*40**	**tau**
A*β*40 only	100.0 (9.2)		1.53 (0.23)			
tau only		100.0 (13.2)		2.23 (0.25)		
oleuropein	118.1 (12.3)	84.5 (12.1)	4.18 (0.26)	0.66 (0.14)	ND	ND
tyrosol	80.2 (8.1)	85.9 (9.2)	3.15 (0.22)	0.74 (0.31)	32.0	0.0
hydroxytyrosol	109.4 (11.3)	ND	1.32 (0.33)	ND	ND	ND
cinnamic acid	80.8 (12.9)	62.2 (11.3)	4.25 (0.21)	0.53 (0.27)	23.0	8.0
p-coumaric acid	86.6 (9.4)	100.3 (9.2)	2.96 (0.28)	2.03 (0.26)	12.0	0.0
ferulic acid	107.0 (9.9)	100.2 (14.3)	2.76 (0.29)	2.44 (0.34)	23.0	0.0
caffeic acid	12.8 (3.3)	47.7 (8.4)	2.34 (0.21)	1.90 (0.13)	49.0	16.0
vanillic acid	121.2 (11.0)	137.2 (0.0)	1.54 (0.22)	3.66 (0.13)	5.0	0.0
syringic acid	74.2 (9.3)	58.8 (19.2)	3.31 (0.34)	3.02 (0.34)	ND	ND
luteolin	50.5 (9.4)	ND	1.48 (0.17)	ND	41.0	ND
apigenin	49.2 (8.2)	ND	1.49 (0.13)	ND	38.0	ND
naringenin	71.3 (9.3)	ND	1.47 (0.1)	ND	4.0	ND

Notably, *p*-amino cinnamic acid (an amino analogue of *p*-coumaric acid) was not identified in olive oil but was analysed as a model compound. It had no discernible effect on $t_{1/2}$ (1.48 h +/- 0.32 h) compared to Aβ40 alone (1.53 h +/- 0.23 h) and produced a minor increase in F_{max} (to 111.5 % +/- 9.8 %) in comparison to Aβ40 in isolation. The dissimilar responses of *p*-aminocinnamic acid and *p*-coumaric acid imply that substituting the -OH group with -NH_2 modifies the dimensions or hydrogen bonding capacity and nullifies the inhibitory effect. Hydroxybenzoic acid and vanillic acid did not affect $t_{1/2}$ and increased F_{max}, whereas syringic acid increased $t_{1/2}$ and reduced F_{max}. The flavonoids apigenin, luteolin and naringenin all reduced F_{max} relative to Aβ40 alone but had minimal effect on $t_{1/2}$.

The reverse-phase HPLC approach was employed on an equimolar mixture of certain compounds (20 μM each) mixed with pre-formed Aβ40 fibrils (20 μM monomer equivalent) to determine the degree of fibril binding. The peak intensities for each compound reduced (to different extents) after the addition and removal of Aβ40 fibrils. Some compounds such as caffeic acid, exhibited a higher affinity than others (see **Figure 5.14a** and **Table 5.4**). The peak intensity reductions in the chromatogram are an indicator of competitive binding between the mixed compounds and the fibrils. By analysing this restricted group of compounds, it is evident that the phenolic compounds in EVOO exert different inhibitory effects on Aβ40 aggregation and fibril binding occurs at diverse levels. There is a moderate to strong linear correlation between the effect of the individual compounds on F_{max} for Aβ40 aggregation and the estimated percentage of binding of each compound in the mixture to pre-formed Aβ40 fibrils (**Figure 5.14b**). These results suggest the existence of a commonality between the effect of the phenolics on the fibril yield of Aβ40 and their affinity for Aβ40 aggregates; however, confirmation of this hypothesis will require additional systematic investigation. Contrastingly, when considering F_{max}, there is no distinct relationship between fibril binding and the effects of the compounds on $t_{1/2}$ of Aβ40 aggregation.

(a)

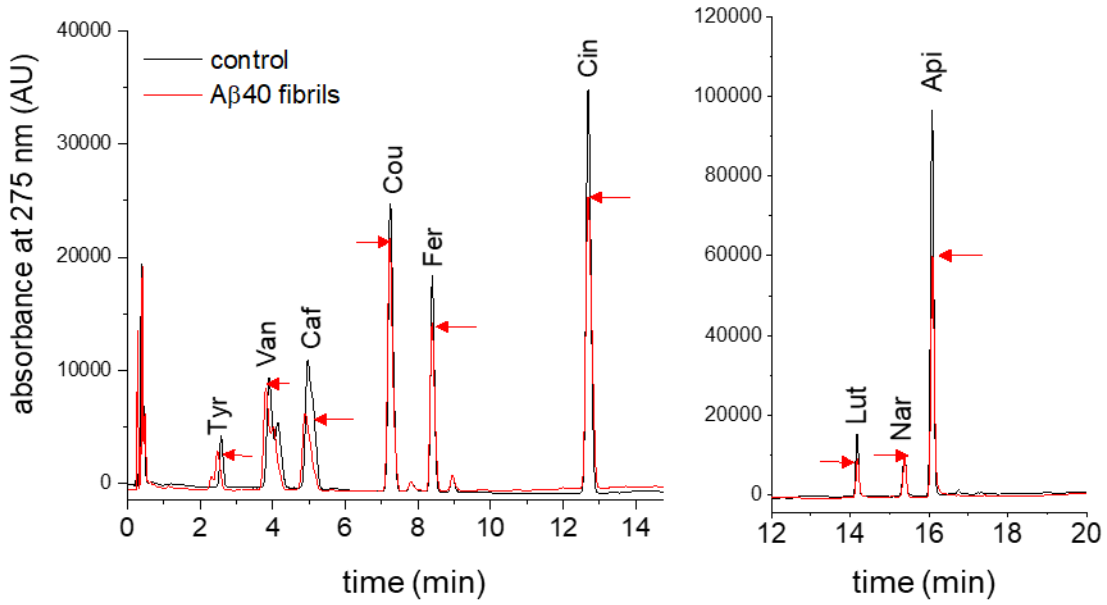

(b)

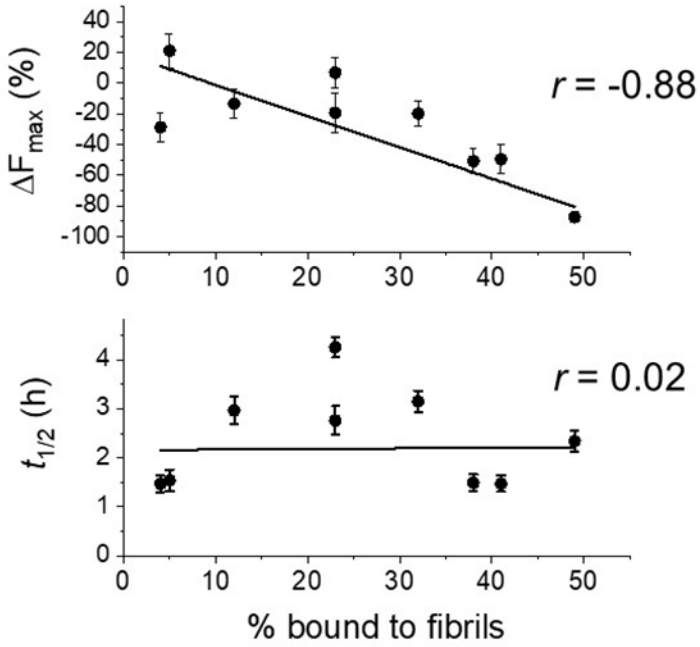

Figure 5.14. The impacts of discrete EVOO phenolic standard compounds on Aβ fibril binding. (a top) HPLC binding analysis of a combination of EVOO phenolic compounds in the

presence of Aβ40 fibrils. Chromatograms are presented for two solutions of 20 μM standard compounds alone (black) and following the addition and extraction of 20 μM Aβ40 by sedimentation (red). (b bottom) Relationship of the extent of binding to fibrils and the impacts on aggregation. ΔF_{max} is the percentage reduction of F_{max} in the presence of each phenolic compound relative to F_{max} of Aβ40 in isolation.

During testing of the aforementioned compounds against tau aggregation, it was evident that none of them produced a significant reduction in the rate of tau aggregation; however, some compounds (such as oleuropein, tyrosol, and caffeic acid) had the inverse effect and shortened $t_{1/2}$ (see **Figure 5.15** and **Table 5.4**).

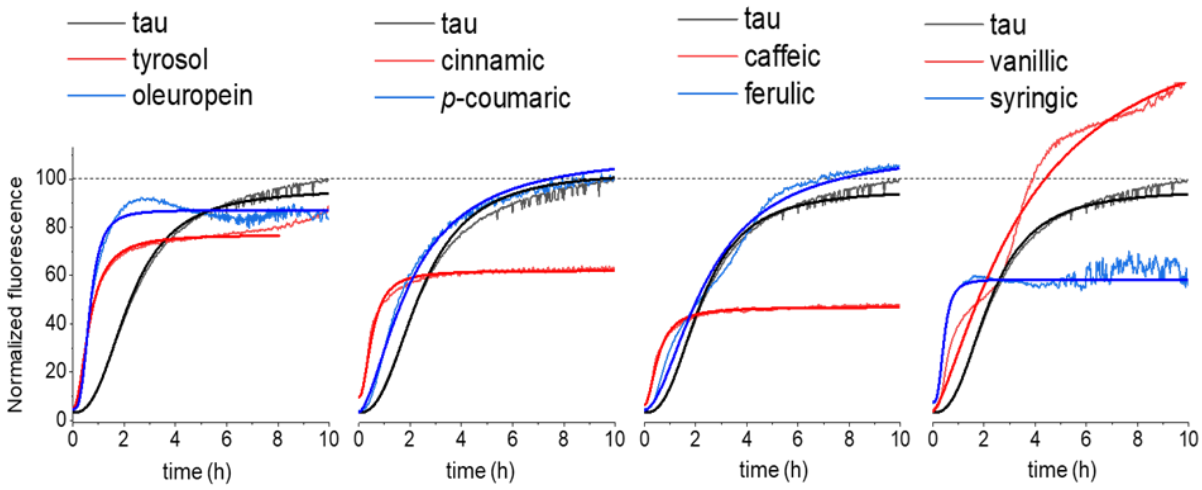

Figure 5.15. The effects of discrete EVOO phenolic compounds on tau aggregation. ThT appraisal of tau (20 μM) aggregation in isolation and when exposed to equimolar concentrations of singular polyphenols (see **Figure 5.13** for chemical structures). Means were calculated from $n = 3$ measurements per group.

This research concludes that an equimolar concentration of the phenolic compounds is ineffectual at reducing the tau aggregation rates which is in agreement with observations regarding the EVOO mixture. The reduced HPLC peak intensities following removal of the fibrils indicate that the compounds exhibit minimal binding to the insoluble filaments (see **Figure 5.16**).

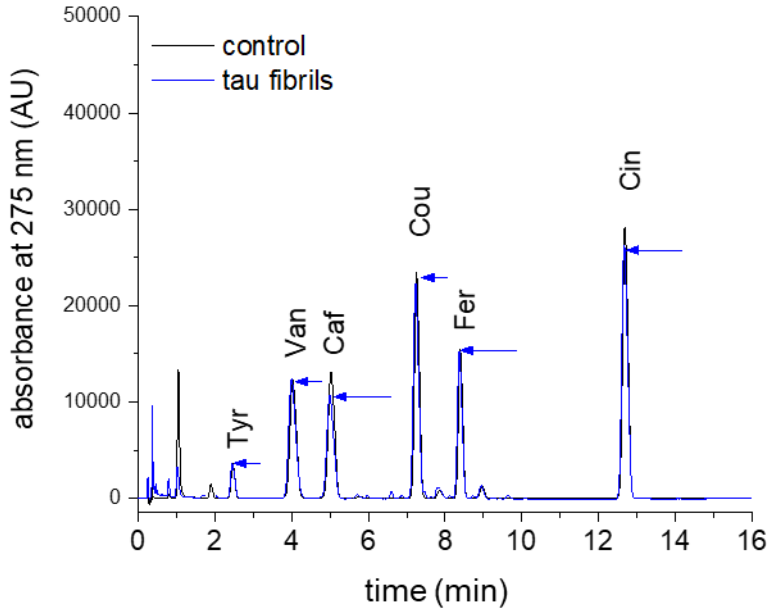

Figure 5.16. The effects of discrete EVOO phenolic compounds on tau fibril binding. HPLC binding analysis of a conglomeration of EVOO polyphenolic compounds with tau filaments. The chromatograms displayed refer to a solution of 20 µM compounds alone (black) and following addition and extraction by sedimentation of 20 µM tau (blue).

Molecular docking of compounds to fibrillar species

Inspection of the structures of phenolic compound-binding proteins in the Protein Structural Databank reveals that this class of molecule frequently associates with β-sheet regions (e.g., **Figure 5.17 (a)**). The ligands may be sandwiched between two β-sheets, a β-sheet and an α-helix or bound to the surface of a single β-sheet. The binding sites tend to encompass hydrophilic residues forming polar contacts or hydrogen bonds with the ligand, plus aromatic residues in positions capable of forming π-π interactions with the ligand phenolic ring. It is possible that the phenolic compounds also recognise nascent β-sheet assemblies formed during the early stages of Aβ and tau aggregation and participate in polar and aromatic interactions that impede or accelerate fibril elongation.

Flexible docking of the phenolic compounds to tau and Aβ40 fibrils was performed computationally using the internal coordinate mechanics (ICM) method. The software (ICM Pro, Molsoft) calculates a grid of potential maps representing one or more binding pockets and performs Monte Carlo simulations to dock the ligands optimally within the binding pockets. Interaction sites were predicted from the structural models of fibrillar tau (PDB 6QJH) (Zhang et al., 2019) and Aβ (2LMQ) (Paravastu et al., 2008).

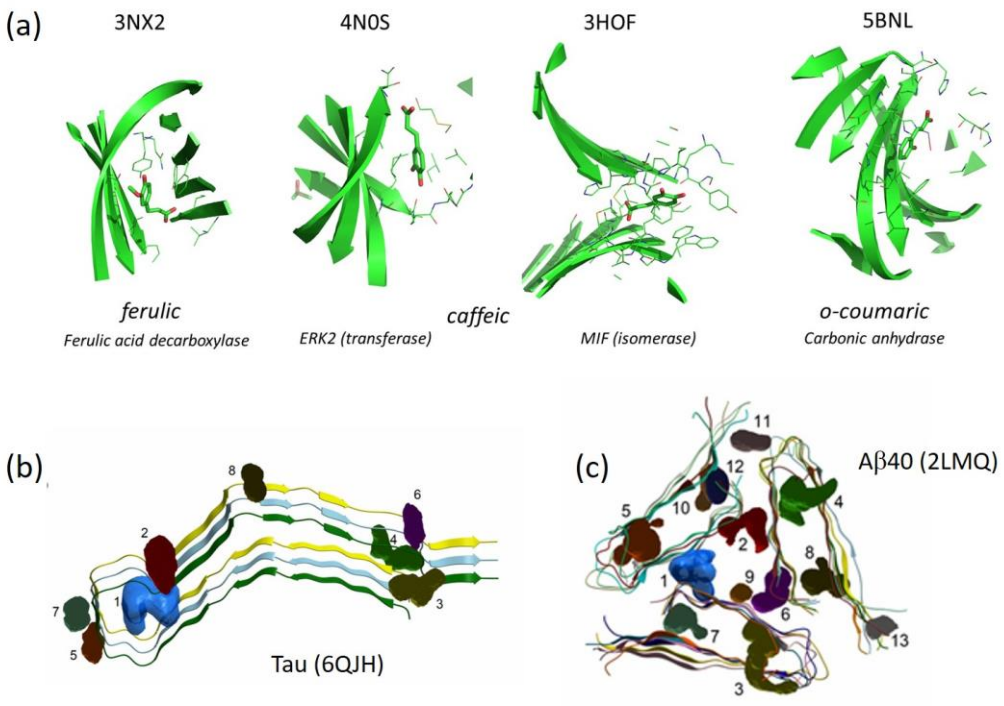

Figure 5.17. Interaction of phenolic compounds with β-sheet structures. (a) Examples of enzyme crystal structures in which phenolic acids (ferulic acid, caffeic acid and o-coumaric acid) interact with β-sheet regions. (b) ICM Pro Pocket Finder algorithm highlighting the 8 most probable binding pockets in tau (PDB 6QJH). (c) The 13 most probable binding pockets in Aβ40 (3-fold symmetry model; PDB 2LMQ).

Initially, binding pockets were identified on these models, which are detailed in **Appendix 2 Tables S5.1** and **S5.2**, respectively and displayed in **Figure 5.17** (b and c). The model of tau produced 8 binding regions (see **Figure 5.17 (b)**), with only the largest pocket by volume, pocket 1, having a Merck's score above the cut off. A total of 13 possible binding regions were identified in the Aβ model (**Figure 5.17 (c)**), 3 of which (numbers 4, 5, and 12) were deemed druggable with Merck's scores > 0.5 (Sheridan et al., 2010). In both models, the binding regions identified as druggable correspond to the most hydrophobic and buried pockets. The software was then used to dock the phenolic compounds extracted from EVOO, alongside

thioflavin T and oleocanthal as comparators. A binding score of below -32 is deemed a strong binding affinity.

In the Aβ model, oleuropein aglycone, cinnamic acid and vanillic acid are predicted to interact most strongly with the druggable pocket 5, producing a moderate ICM Grid Docking Energy of -45.05 kcal/mol, -25.27 kcal/mol and -17.2 kcal/mol, respectively all docking energy demonstrated in **Appendix 2 Table S5.3**, suggesting that despite associating with a druggable region of Aβ fibrils, they are unable to affect its self-assembly. Caffeic acid is predicted to bind in pocket 6 with hydrogen bonds forming with residue G27, with a considerably stronger grid score of -28.42 kcal/mol. Other compounds with high binding scores (coumaric acid, -28.21 kcal/mol; oleocanthal, -44.2 kcal/mol; tyrosol, -30.64 kcal/mol) also bind to this same pocket. Compounds bind to pockets are shown in **Figure 5.18**.

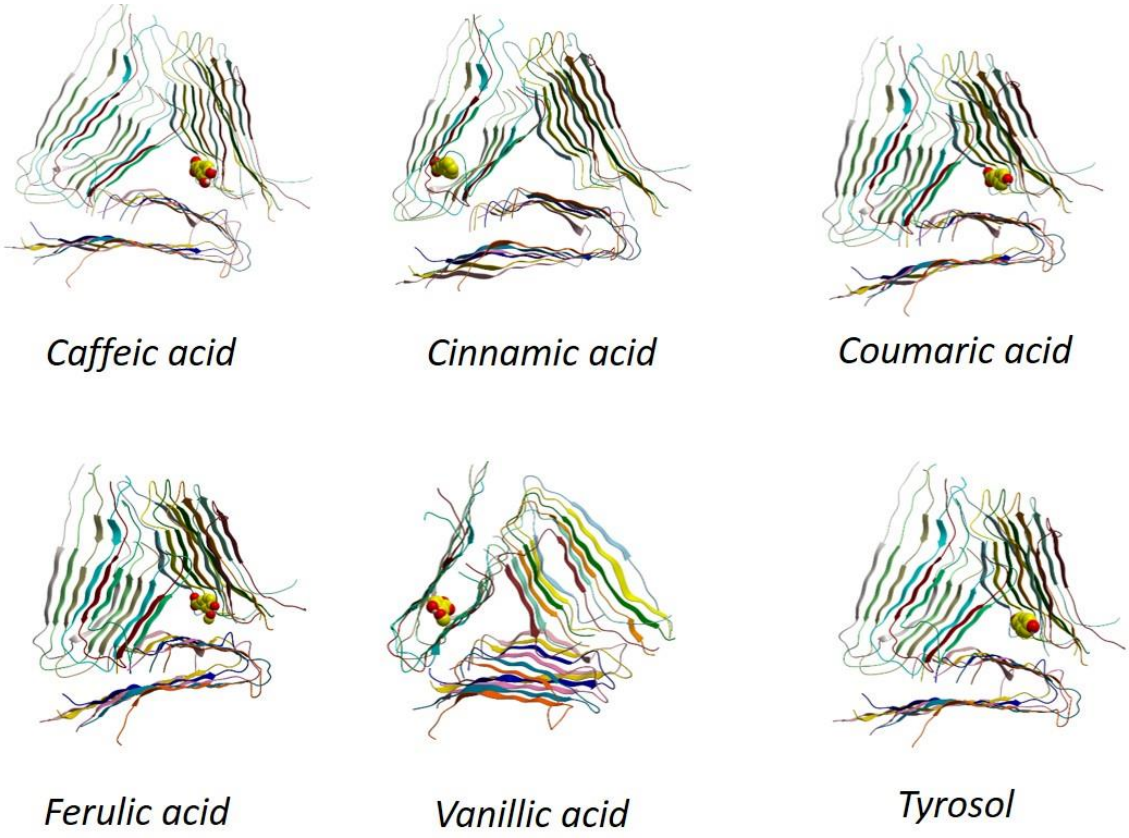

Figure 5.18. Docking sites for EVOO phenols on the solid-state NMR-derived 3-fold symmetry structural model of Aβ40 (PDB 2LMQ), predicted using the ICM Pro software. The ligands are represented by spheres (See **Appendix 2 Figure S5.2** for all compounds bind to pockets).

In the tau model, compounds bind to pockets are shown in **Figure 5.19** many compounds bind to pocket 2, including caffeic acid with a higher binding energy of -19.9 kcal/mol, cinnamic acid (-19.09 kcal/mol), coumaric acid (-20.39 kcal/mol) and oleuropein (-24.93 kcal/mol) all docking energy can be found in **Appendix 2 Table S5.4**. Most of these compounds, apart from oleuopein form hydrogen bonds with residue S305. However, none shows an ability to reduce the kinetics of tau aggregation by thioflavin T fluorescence. Both tyrosol (-20.91 kcal/mol) and coumaric acid (-20.39 kcal/mol) bind to tau with increased affinity, but also do not impede amyloid formation.

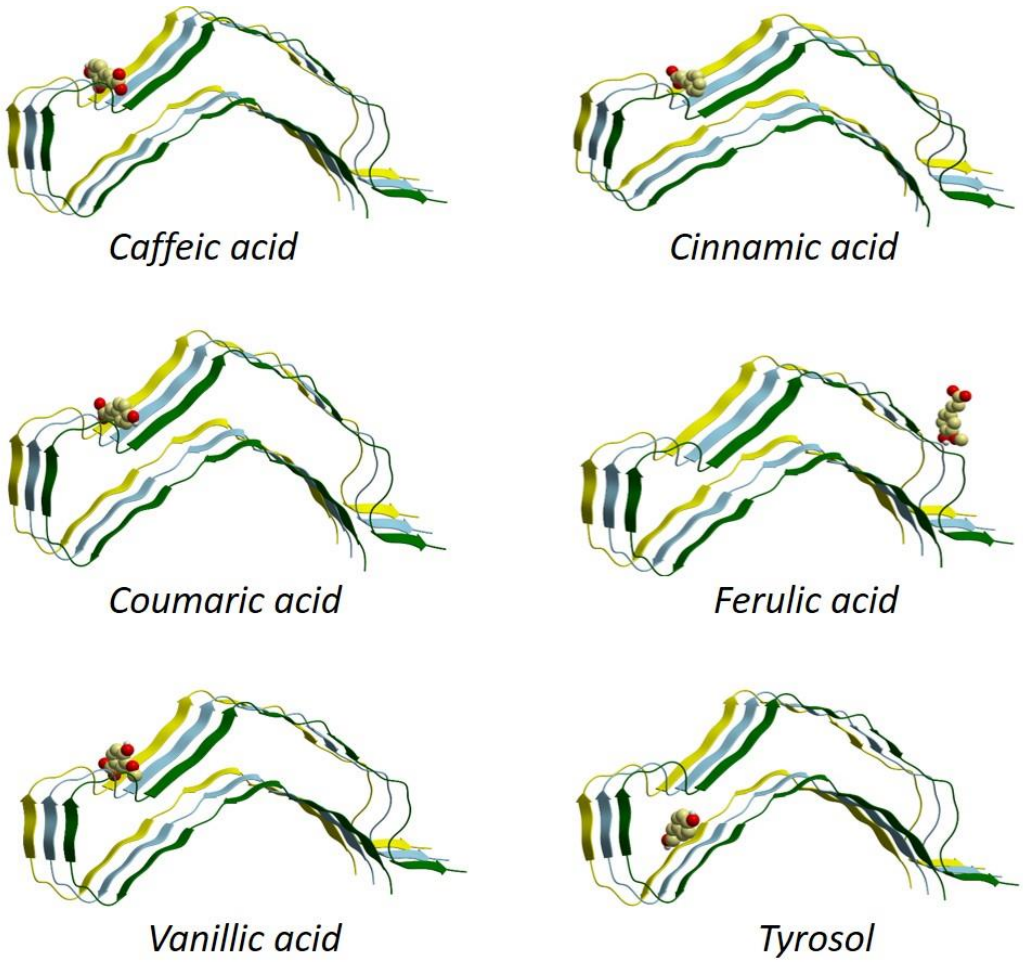

Figure 5.19. Docking sites for EVOO phenols on the cryo-EM structure of heparin-induced 2N4R tau snake filaments (PDB 6QJH), predicted using the ICM Pro software. The ligands are represented by spheres (See **Appendix 2 Figure S5.3** for all compounds binding).

Finally, a comparison of docking energies of all phenolic compounds demonstrated in **Appendix 2 Tables S5.3** and **S5.4** suggesting that most of phenolic compounds bind to Aβ (2LMQ) with considerably stronger grid score when it compared to tau (PDB 6QJH).

Discussion

EVOO polyphenol mixtures inhibit Aβ40 aggregation more strongly than tau aggregation

The work in **Chapter 4** analysed phenolic extracts prepared from Greek and Saudi Arabia EVOO sources and determined that they were composed of flavonoids, phenolic acids, and different concentrations of oleuropein and its metabolites. The work in **Chapter 4** also confirmed that the EVOO extracts from the two sources have slightly different polyphenol compositions, as would be expected according to their different geographies, harvesting and processing. However, the work in this chapter showed that the Greek and Saudi extracts were comparably successful at inhibiting Aβ40 aggregation *in vitro*, despite their different compositions. At concentrations up to 20 μg/mL, both mixtures shift the $t_{1/2}$ for Aβ40 aggregation to extended times and higher concentrations (> 100 μg/mL) eradicate aggregation (see **Figure 5.3a** and **b**). The inhibitory properties of the extracts against Aβ40 can be partially explained by the presence of oleuropein, tyrosol, and hydroxytyrosol which, as indicated by ThT fluorescence, individually impede Aβ40 aggregation (see **Figure 5.13**). This research has identified that additional compounds in the extracts (such as caffeic acid, ferulic acid, and specific flavonoids) are also effective at inhibiting Aβ40 aggregation, although at higher concentrations than those found in EVOO.

It may be appropriate to consider the cumulative effect of the total EVOO phenolic pool on Aβ40 aggregation, rather than attributing the effects to individual compounds. Deficiencies in some phenols in an EVOO extract (e.g., oleuropein) may be compensated by increases in other compounds (e.g., tyrosol), so that extracts of different compositions possess similar anti-aggregation properties. This was confirmed *via* an HPLC binding analysis which revealed that the majority of EVOO compounds bind to Aβ40 fibrils. Additional research on individual EVOO compounds suggests a relationship between binding to the mature fibrils and the yield

of aggregates formed. For more investigation from monomers in the presence of those compounds. Additional study is required to confirm the details of this association.

One notable result of this research concerns the fact that the EVOO extract mixtures were noticeably less effective at reducing tau aggregation than Aβ40 aggregation: elevated concentration levels were required to observe an effect on tau aggregation kinetics than is considered acceptable for an inhibitory compound. The insignificant inhibitory effect on tau is comparable with the weak binding of the EVOO phenolics to tau filaments exhibited by several EVOO compounds (**Figures 5.12** and **5.16**). There is an evident discrepancy between binding and the subsequent tau and Aβ40 inhibition which argues against non-specific interactions of the phenolic mixture with the proteins in their various stages of aggregation. Additionally, this data suggests that the specialised binding sites observed in the Aβ40 aggregates are non-existent in tau.

Binding of EVOO polyphenols to Aβ40 and tau

The work in this chapter revealed that the EVOO mixtures bind to pre-formed Aβ40 fibrils and, at higher extract concentrations, remodel them into soluble oligomers. Amyloid remodelling is a feature of several polyphenols derived from food sources, including the flavonoid kaempferol, EGCG from green tea and resveratrol from grapes (Bieschke et al., 2010; Sharoar et al., 2012; Wang et al., 2015). Unlike the amyloid oligomers promoted by the aforementioned compounds, the EVOO phenol-indued Aβ40 oligomers are mildly cytotoxic to SH-SY5Y cells while EGCG and resveratrol modify fibrils and oligomers into non-toxic, off-pathway species.

Although comparatively minimal concentrations of the extracts are needed to produce Aβ40 oligomers, these represent extremely low populations of the overall amyloid species at

the concentrations (20 μg/mL). Remodelling of the tau filaments into oligomers demands increasingly higher concentrations (500 μg/mL). Further study in *vivo* would be important for more investigation and understanding.

Mechanisms of inhibition

The inhibition of amyloid formation by small phenolic molecules normally involves stabilising the interactions between phenolic and protein aromatic groups, possibly enabled by the ability of planar aromatic groups to insert between, or align with, β-sheet layers (Porat et al., 2006; Ono et al., 2003). Leri et al. (2021) propose that the phenolic rings of polyphenol compounds interfere with π-stacking and inhibit the stabilisation of the amyloid core structure, with the hydroxyl groups contributing to the disruption of the hydrophobic core and increasing solubility (Rigacci et al., 2011; Tasioula-Margari and Tsabolatidou, 2015). Many of the compounds extracted from EVOO possess these properties and may possess a preference for β-sheet structures. To confirm the theory, this research used the Protein Data Bank (PDB) to inspect protein structures containing the bound phenolic compounds detected in EVOO. In over 70 structures, the phenolic compounds were observed to predominantly bind to β-sheet regions of the proteins, even though the same proteins possess a superior α-helical content.

Limitations of the results

This *in vitro* research does not address the bioavailability of EVOO phenols or the *in vivo* reproducibility of their anti-aggregation effects: as noted by Figueira et al. (2017), dietary phenolic compounds are absorbed from the gastrointestinal tract which allows microbiota to degrade the complex polyphenols into low molecular weight phenolics and cause other

biotransformation. Polyphenols (esters, glycosides, or polymers) cannot be directly absorbed and must first undergo hydrolysis. Additional hepatic transformations of the absorbed phenolic compounds result in a complex distribution of unmodified, fragmented and partially methylated, sulphated and glucuronidated compounds (Manach et al., 2005). To be effective, the circulating phenolics must then traverse the highly regulated, selectively permeable endothelial BBB (Figueira et al., 2017).

When considering flavonoids, Youdim et al. (2003) propose that the transmembrane diffusion of phenols across the BBB correlates with their lipophilicity, such that the brain uptake of less polar derivatives such as methylated derivatives is higher than the uptake of more polar (e.g. sulfated) metabolites. The EVOO flavonoids apigenin (Yang et al., 2014), naringenin (Sarkar et al., 2012), and secoiridoids including oleuropein (Dinda et al., 2019) traverse the BBB and exert neuroprotection.

The results of this study serve as a baseline for future studies (see later in this thesis) regarding the effects of EVOO phenolic compounds on Aβ40 and tau aggregation *in vivo* and the effects of known metabolic transformations of polyphenols by gut microbiota and the liver on these activities.

Chapter 6 (Formulation of solid lipid nanoparticles for the delivery and improved bioavailability of phenolic mixtures extracted from extra virgin natural olive oil)

Introduction

The Mediterranean diet, which refers to the diet consumed in regions surrounding the Mediterranean Sea, is known to have tremendous health benefits. While the diet is varied and typically comprises high amounts of lentils, whole grains, fish, nuts, fruits, and vegetables, the use of virgin olive oil is a common feature across the region. In particular, extra virgin olive oil (EVOO) is well known for its health benefits, which include anti-inflammatory, antioxidant, antiangiogenic, and antiatherogenic effects (Bucciantini et al., 2021; Marrero et al., 2024), as well as the maintenance of lipid metabolism (Zupo et al., 2023). In addition, consumption of EVOO is linked with a reduced risk of type 2 diabetes (Guasch-Ferré et al., 2015) and neurodegenerative diseases such as Alzheimer disease (Salis et al., 2020). The beneficial effects of olive oil are mainly linked to its bioactive phenol components, even though they only account for about 2% of the total compounds (see **Chapter 1** for more detail) (Finicelli et al., 2021; Rodríguez-López et al., 2020).

The phenolic content of virgin olive oil is dependent on geographic conditions, cultivar, ripeness of the fruit, and the method used for extraction, and the concentration can range widely from 50 to 940 mg/kg, with the typical concentration range being 100 to 300 mg/kg (as reviewed in Marrero et al., 2024). Notably, EVOO, which has been the focus of studies on the health properties of olive oil, is extracted through mechanical, low-temperature methods such as crushing, pressing, decantation, and filtration, and is typically not extracted through solvent- or chemical-based methods (Jiménez-López et al., 2020). Typically, a Mediterranean diet includes 25 to 50 mL of olive oil per day, which corresponds to consumption of approximately

9 mg of phenols daily (De la Torre, 2008). In addition to the extraction method used and the phenolic contents, the benefits of consuming EVOO are also dependent on the bioavailability of its active ingredients in target tissues/organs after ingestion.

Bioavailability refers to the absorption and metabolism of a compound within an organism **Figure 6.1**. The bioavailability of phenolic compounds is dependent on several physiochemical properties such as polarity, polymerization or glycosylation ability, and solubility (Cicerale et al., 2010). While most polyphenols in EVOO can reach the colon and small intestine without any modifications, their absorption rates vary widely beyond this point, with the phenolic compounds hydroxytyrosol and tyrosol having the highest absorption rates at 40%–95% and secoiridoids (the most abundant phenolic compound in EVOO) having duodenal recovery rates as low as 7%–34% (as reviewed in Rodríguez-López et al., 2020). Importantly, their absorption and metabolism in the body seem to be associated with the food matrix. That is, their intake in the liquid form seems to have better results than intake in capsule form, and their delivery as a natural component of olive oil seems to be better than delivery through aqueous solutions or refined oil (as reviewed in Rodríguez-López et al., 2020). Phenols that are not absorbed in the intestine or colon are fermented by the gut microbiota, and the products of microbial fermentation of polyphenols have been found to promote intestinal homeostasis and exert prebiotic-like effects (de Bock et al., 2013; Pinto et al., 2011). Given the known health benefits of phenolic compounds in EVOO (as studied in detail in **Chapter 5**) and the challenges with their absorption and metabolism in the human body, research on delivery strategies that can improve their bioavailability is currently receiving a lot of attention. Among these strategies, nanoformulations in the form of liposomes, polymeric nanoparticles, nano-structured lipid carriers, and solid lipid nanoparticles have been the focus.

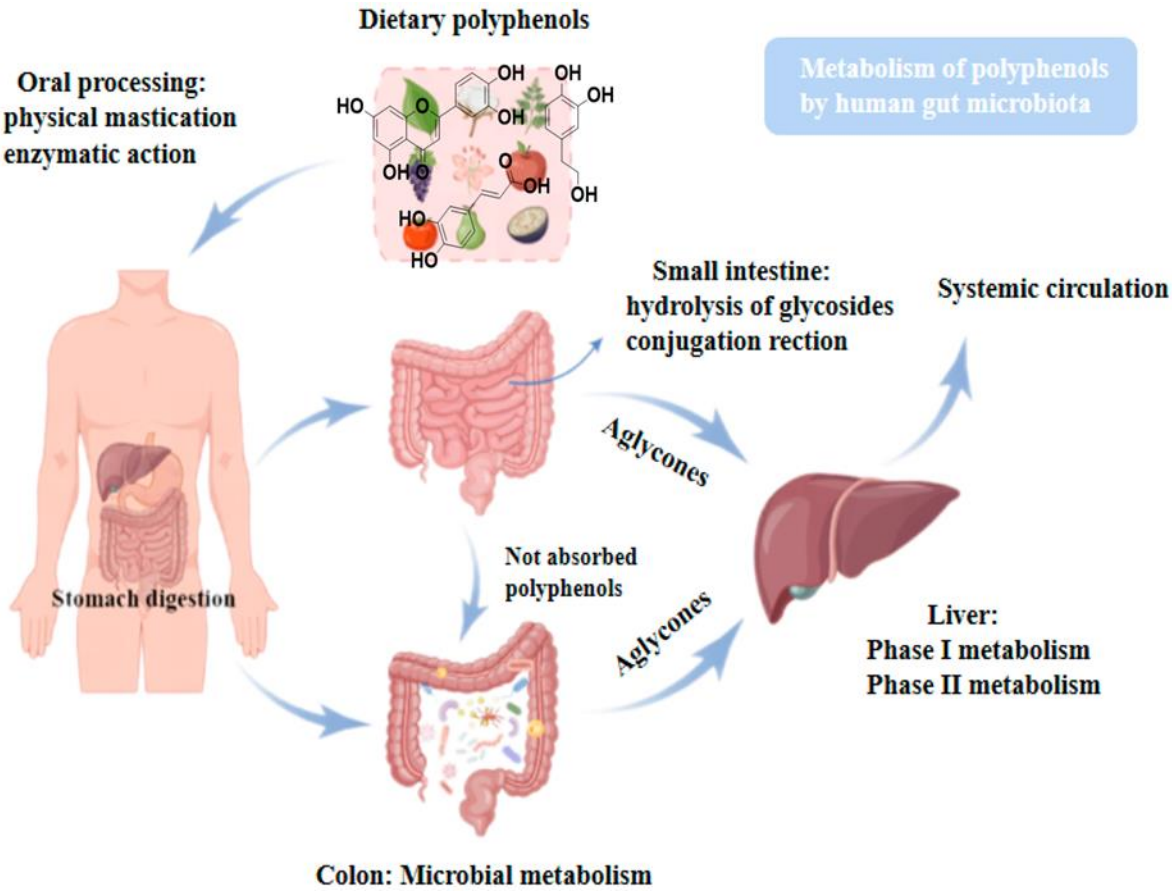

Figure 6.1. A general diagram representation showing the absorption and metabolism stages of natural polyphenols in the body (Wang et al., 2022). The figure is reproduced under a Creative Common CC BY license (Copyright 2022, MDPI).

Solid lipid nanoparticles (SLNs) have become popular as drug delivery systems on account of their nontoxicity, stability, biodegradability, ability to deliver both hydrophilic and lipophilic compounds (as well as compounds that have been traditionally difficult to deliver such as biomolecules), and ease of large-scale manufacturing (Duan et al., 2020; Mehnert & Mäder, 2012). In particular, their stability at both room temperature and the temperature of human body makes them suitable for the controlled release of drugs (Borges et al., 2020). In fact, it has been reported that unmodified SLNs of size 50–1000 nm can be adequately absorbed into lymphatic pathways (Florence, 1997) and can also be taken up by the intestine *via* the

intracellular or paracellular way and subsequently transported to lymphatic organs in particulate form (Kreuter, 1991).

SLNs are typically spherical and have a diameter of 50 to 1000 nm as shown in **Figure 6.2**, which means that they can carry a wide range of molecules. **Figure 6.2** shows SLN formulations contain lipids (that are in the solid state at both room temperature and physiological temperature) that comprise 0.1% to 30% (w/v) of the nanoparticle, emulsifiers that comprise 0.5% to 5% (w/v), active pharmaceutical agents, and a solvent for carrying the active ingredients (Duan et al., 2020; Viegas et al., 2023). The use of a lipid component is pertinent because the lipids are believed to improve the oral absorption of ingredients in a similar way to the lipids found in a typical diet (Souto and Müller, 2006). The lipids typically used in SLN formulations include fatty acids, fatty alcohols, triglycerides, fatty esters, and partial glycerides, and the emulsifiers used include ionic and nonionic polymers, surfactants, and organic salts (Duan et al., 2020). The function of the emulsifiers is to ensure optimal mixing of the lipid/oil phase and the aqueous phase. Some of the methods used for the production of SLNs are high-pressure homogenization, solvent-emulsion diffusion, ultrasonication, solvent injection, and electrospray (Duan et al., 2020). The choice of method depends on the experimental conditions, target cell/tissue/model, the nature of the pharmaceutical agent being delivered (that is, its stability, solubility, hydrophilicity, lipophilicity, and so on), and availability of equipment. The efficiency of SLNs is dependent on their physicochemical properties such as particle size, zeta potential, crystallinity, drug release pharmacokinetics, encapsulation efficiency, surface morphological characteristics, polydispersity index, and charge (Duan et al., 2020).

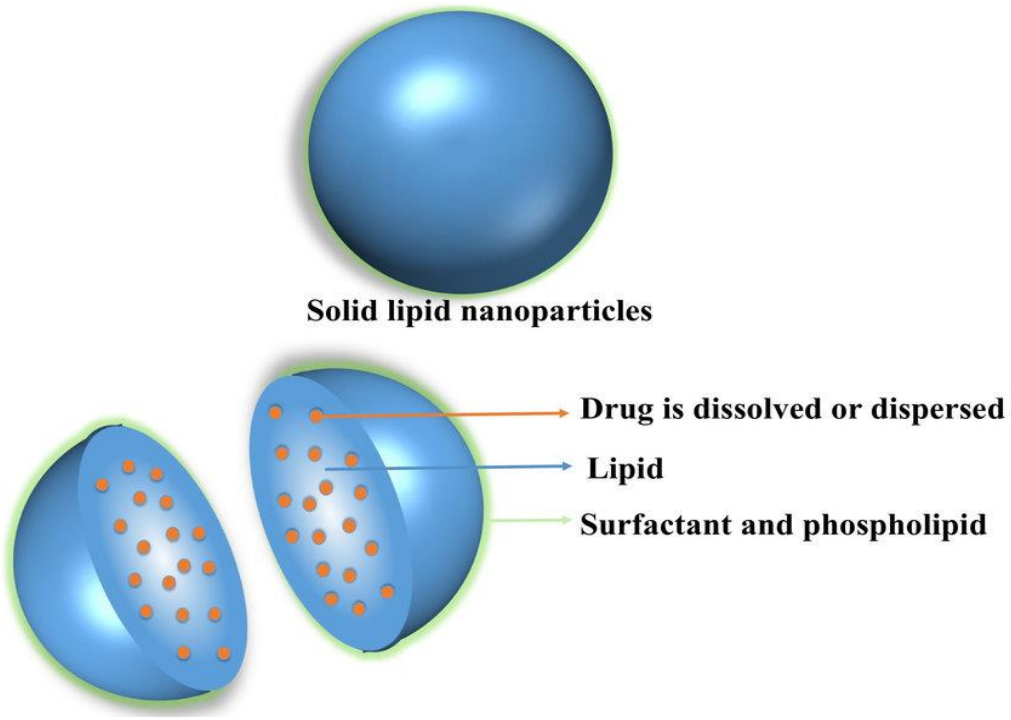

Figure 6.2. Solid lipid nanoparticle structure and formulations, (**lipid** such as fatty acids, fatty alcohols and triglycerides, they are in the solid state at both room temperature and physiological temperature comprise 0.1% to 30% (w/v) of SLNs), (**emulsifiers** such as surfactant that comprise 0.5% to 5% (w/v) of SLNs), (**drug** or active pharmaceutical agents, and a solvent for carrying the active ingredients) (adapted from Mishra et al., 2018). (The figure is reproduced under a Creative Common CC BY license (Copyright 2018, MDPI).

SLNs are potentially beneficial for the treatment of neurodegenerative diseases such as Alzheimer's due to their ability to cross the blood–brain barrier. SLNs carrying a wide range of both synthetic and naturally derived bioactives have been investigated for their ability to encapsulate these compounds and cross the blood–brain barrier through *in vivo* models and have shown promising results (as reviewed in Fernandes et al., 2021). For example, andrographolide, the main bioactive found in the medicinal herb Andrographis paniculata that is known for its anti-inflammatory, antioxidative, and antineoplastic effects, showed better

permeability against the blood–brain barrier when it was delivered *via* SLNs than in its free form (Graverini et al., 2018).

With regard to phenolic compounds, SLNs have been reported as carriers for ferulic acid, a common phenolic acid found in plant cells. For example, ferulic acid-loaded SLNs were found to have higher antioxidant action than its free form in neurons; thus, these ferulic acid nanocarriers could be useful for the treatment of Alzheimer disease (Bondi et al., 2009). Moreover, curcumin was found at 16 times higher concentrations in the brain when delivered *via* SLNs compared to oral administration in *in vivo* mouse models (Kakkar et al., 2013). Some modifications that can further improve the ability of SLNs to cross the blood–brain have also been reported. For example, Loureiro et al. (2017) found that coupling resveratrol-loaded SLNs with an OX-26 monoclonal antibody improved its ability to affect target tissues and compounds in the brain and ensured stability in cranial tissue for at least one month. This slow release could ensure the sustained inhibition of Aβ (1–42) aggregate formation and could, thus, have potential implications in the treatment of Alzheimer disease. Thus, there is much evidence in the literature to demonstrate the potential of SLNs in treating neurodegenerative diseases on account of their ability to permeate the blood–brain barrier and to remain stable in cranial tissue.

With regard to EVOO-derived polyphenol SLNs, oleuropein-loaded SLNs have been found to have good physiochemical properties and also strong antioxidative effects in lung epithelial cells (Huguet-Casquero et al., 2020; Monteiro et al., 2021). Further, the formulation of tyrosol-loaded nanoparticles and their optimization were recently reported (Telmoudi et al., 2024).

Some studies have also attempted the delivery of more than one bioactive compound through SLNs. For example, co-encapsulation of both curcumin and resveratrol in lipid nanoparticles was found to have an improved combined antioxidant effect (Coradini et al., 2014). Thus,

combining more than one phenolic compound within SLNs could result in improved health benefits.

Aims and motivation

Considering the positive effects of EVOO polyphenol mixtures on Aβ40 aggregation *in vitro* reported in the previous chapter, alongside the known antioxidant activities of these compounds, there is incentive to find ways to improve the therapeutic profile of these compounds *in vivo*. The aim of this work is to synthesize and characterize for the first time SLNs for a mixture of polyphenols isolated from EVOO of Greek origin. Most previous studies on the combined effects of polyphenols have attempted the synthesis of SLNs with only two isolated bioactive compounds. This chapter describes the first attempt to isolate a mixture of several polyphenols from any natural source and then load the mixture into SLNs, so the findings will have significant implications in the field. The steps are summarised as follows:

1. EVOO polyphenols were extracted as described in **Chapter 4**.

2. The solvent diffusion–solvent evaporation method was used for engineering EVOO polyphenol-loaded SLNs with stearic acid as the lipid core, poloxamer 188 as the emulsifying agent, and methanol used to dissolve polyphenols.

3. The size and morphology of the generated SLNs were assessed by electron microscopic and dynamic light scattering.

4. The polyphenol loading of the SLNS was assessed by using spectrophotometric and magnetic resonance.

5. Preliminary *in vivo* studies of the SLN preparations were conducted.

The work also focused on the production of caffeic acid-containing SLNs, as described in previous publications (Alaziqi et al., 2024; Andrade et al., 2023; Alam et al., 2022). For comparison with the results on EVOO polyphenol-loaded SLNs. Beneficial effects of caffeic acid-containing nanoparticles in the treatment and management of cancer and neurological diseases, especially Alzheimer disease have been reported (Alam et al., 2022; Andrade et al., 2023).

The SLN formulations prepared here will be useful for future research into the benefits of these phenolic compounds in the treatment of Alzheimer disease given their ability to cross the blood–brain barrier. To this end, we plan to carry out further *in vivo* experiments with mouse models to determine the effects of the SLN formulations **Figure 6.3**.

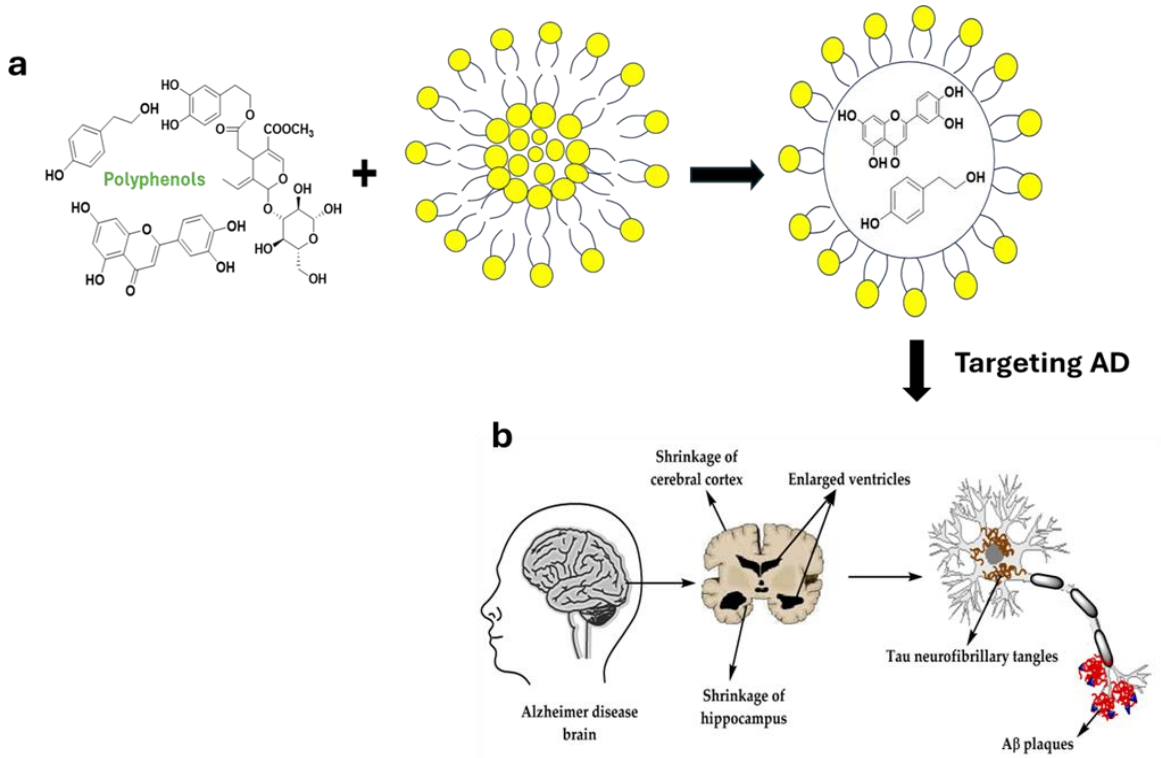

Figure 6.3. Diagram summaries the aim of this study by loading phenolic compounds in nanoparticles (a) to target Alzheimer's disease (b). Image (a) prepared by © Bakri A. Image (b) adapted from (Breijyeh and Karaman, 2020). The image reproduced with permission (Copyright 2020, MDPI).

Materials and methods

Materials

Reagents and equipment

The chemical reagents used for the preparation of SLNs were purchased from Sigma-Aldrich, and included stearic acid, poloxamer 188, caffeic acid (purity 98%), BODIPY™ FL C16 (4,4-difluoro-5,7-dimethyl-4-bora-3a,4a-diaza-s-indacene-3-hexadecanoic acid), and 2% phosphotungstic acid. The solvents methanol (99.9% analytical reagent grade), hexane (95% high-performance liquid chromatography [HPLC] grade), acetonitrile (99.9% HPLC gradient grade), and EtOH were obtained from Fisher Scientific. DMSO-d_6 for NMR (99.9 atom %D) was obtained from Thermo Scientific. Formic acid (98%) was purchased from Honeywell Fluka, and Milli-Q purified water was provided by the laboratory.

The equipment used for this study included 96-well black, carbon-coated Formar grids, (HPLC), UV-Visible spectroscopy (UV-Vis), nuclear magnetic resonance (NMR) in the liquid and solid state, centrifuges, sonicator, rotary evaporator, freeze dryer, autoclave, shaking incubator, pH meter, Nanodrop™ 2000c, plate reader, thermoshaker, vortexer, vacuum pump, hot plate, and magnetic stirrer. Nanoparticle size and morphology were determined by dynamic light scattering (DLS) and transmission electron microscopy (TEM).

Methods

Polyphenol preparation

EVOO used in the experiments was a commercially available product from Greece (Yannis Fresh Greek Early Harvest Extra Virgin Olive Oil, cold extraction) and was stored in its original glass bottle, covered with foil, and kept away from light at 4°C. Polyphenols were isolated using the selective extraction method described previously in Chapter 4, following a modified version of the protocol used in previous reports (Gutfinger, 1981; Pizarro et al., 2013; Vázquez, 1973). The olive oil (20 g) was dissolved in hexane, and the solution was sonicated at 20 mm for 5 min. It was then loaded into the separating funnel and shaken for 2 min before three-fold extraction with methanol/water (60:40, v/v). The methanolic fraction contained the polar polyphenol compounds and after collection was washed with hexane two times before being refrigerated for 24 hours, following which the methanol was evaporated off at low pressure at 40 °C. It was then lyophilised at 0.0026 mbar for 24 hours at -70 °C. The solid extract that remained was weighed. The polyphenol yield was 42 mg.

Preparation of SLNs loaded with EVOO polyphenol mixtures

Polyphenol-SLNs were prepared using a modified version of the solvent diffusion–solvent evaporation method reported previously (Borges et al., 2020; Hashem et al., 2014; Pandita et al., 2014; Patel et al., 2011). Synthesis of solid lipid nanoparticles in the laboratory described in **Figure 6.4**. The stearic acid (100 mg) was melted at 75 °C and mixed in 1 mL of methanol containing 3.3 mM of the dissolved polyphenols and once thoroughly mixed, injected into an aqueous solution (1% w/v in Milli-Q purified water) of the nonionic surfactant, poloxamer 188, at the same temperature as the stabilizing agent. Formation of dispersed SLNs could be seen by the solution immediately turning opaque. The solvent was then evaporated for 30 min with

the dispersion being continuously stirred at 700 rpm on a magnetic stirrer. Re-crystallization took place for 1 h at 4 °C, and the dispersed nanoparticles extracted from the solvent by centrifugation for 40 min at 4 °C and 15,000 rpm. The nanoparticles were then twice resuspended in distilled water and centrifuged to wash any free drug (polyphenols) remaining in the voids between them (This process was repeated twice to ensure that no free polyphenols remained in the void between the nanoparticles).

Preparation of caffeic acid-SLNs

Three different formulations of caffeic acid SLNs containing 50, 100, and 200 mg of stearic acid were prepared to determine the optimal lipid content for the preparation of polyphenol SLNs. The steps were the same as described above, except that the polyphenol component was replaced with caffeic acid. **Table 6.1** gives the composition formulae for the various caffeic acid-SLNs.

Preparation of unloaded SLNs

Blank SLNs carrying no cargo were prepared using the same procedure as described above, but in the first step, the methanol mixed with the stearic acid contained no dissolved polyphenols.

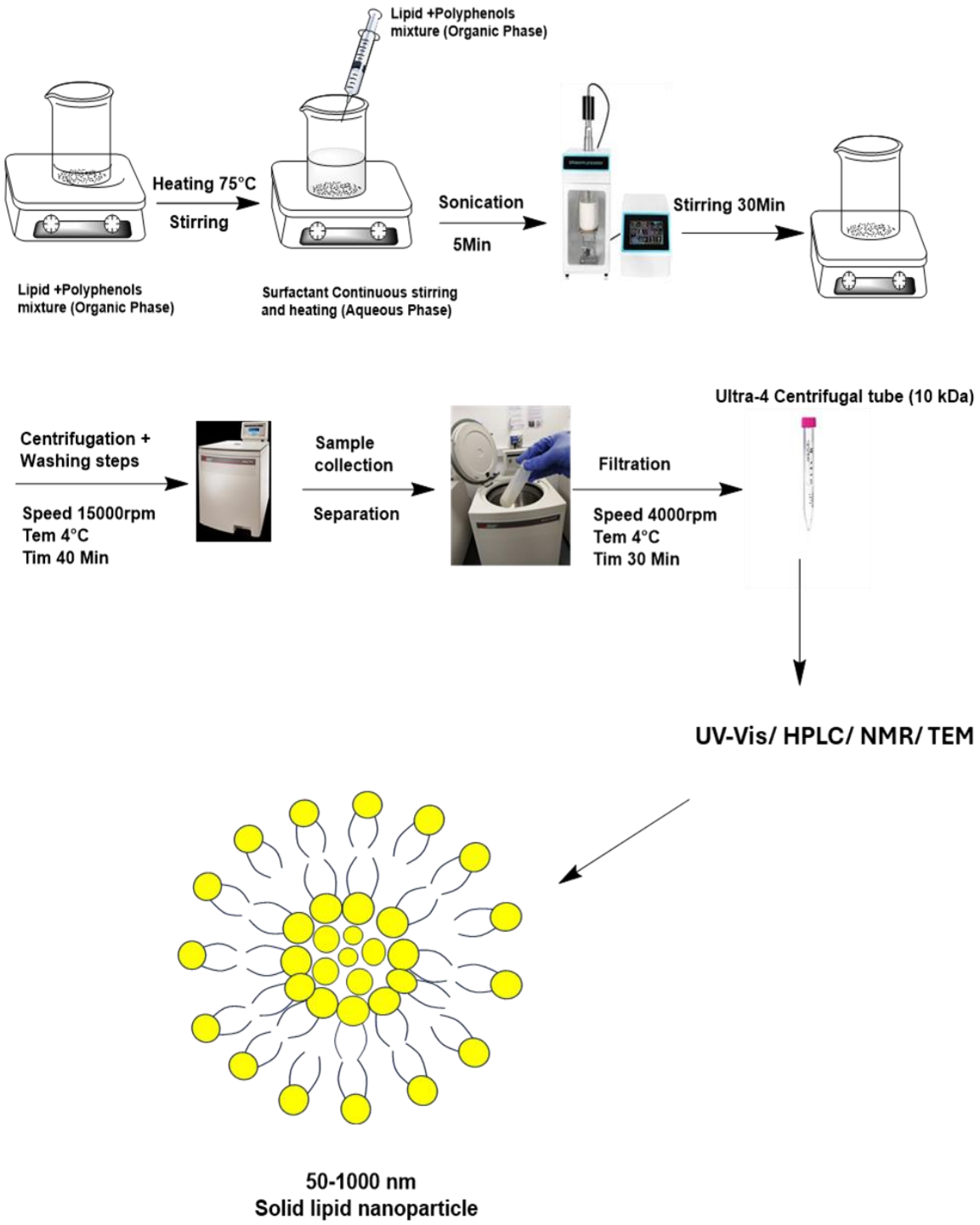

Figure 6.4. Synthesis of solid lipid nanoparticles in the laboratory, © Bakri A.

Table 6.1. Formulations for caffeic acid-SLNs with different lipid weights (note F1, F2 and F3 are abbreviations of different formulations).

Formulation	F1	F2	F3
Drug	3.3 mM	3.3 mM	3.3 mM
Lipid (SA)	50 mg	100 mg	200 mg
Surfactant (poloxamer 188)	1%	1%	1%

F: Formulation of SLN

Physicochemical characterization of the prepared SLNs

Solid-state NMR

In order to analyse the composition of the insoluble fraction obtained from the above experimental to investigate and confirm if all polyphenols are presented in the nanoparticle solution or could be detected some in the insoluble fraction.

For this investigation SSNMR was used to characterise the insoluble fraction of the preparation. The washed nanoparticle solid residues were transferred to a 3.2 mm rotor with a Kel-F cap (Bruker, U.K) **Figure 6.5**. Refocused 1D and 2D INEPT ^{13}C–^{13}C SSNMR spectra (Townsend et al., 2018; Elena et al., 2005) at a magnetic field strength of 16.3 T were obtained using a 3.2 mm HXY probe operating in double-resonance mode with a Bruker Avance III 700 spectrometer and a magic angle spinning of 14 kHz. During signal acquisition, 100 kHz proton decoupling with SPINAL-64 was applied for a contact time of 2 ms to attain Hartmann-Hahn cross-polarization. ^{1}H nutation frequency was reduced to 14 kHz during the 20 ms mixing time to facilitate dipolar-assisted rotational resonance (DARR) mixing. The States-TPPI method for

phase sensitivity with 256 transients per increment was then employed to record a total of 256 t1 increments.

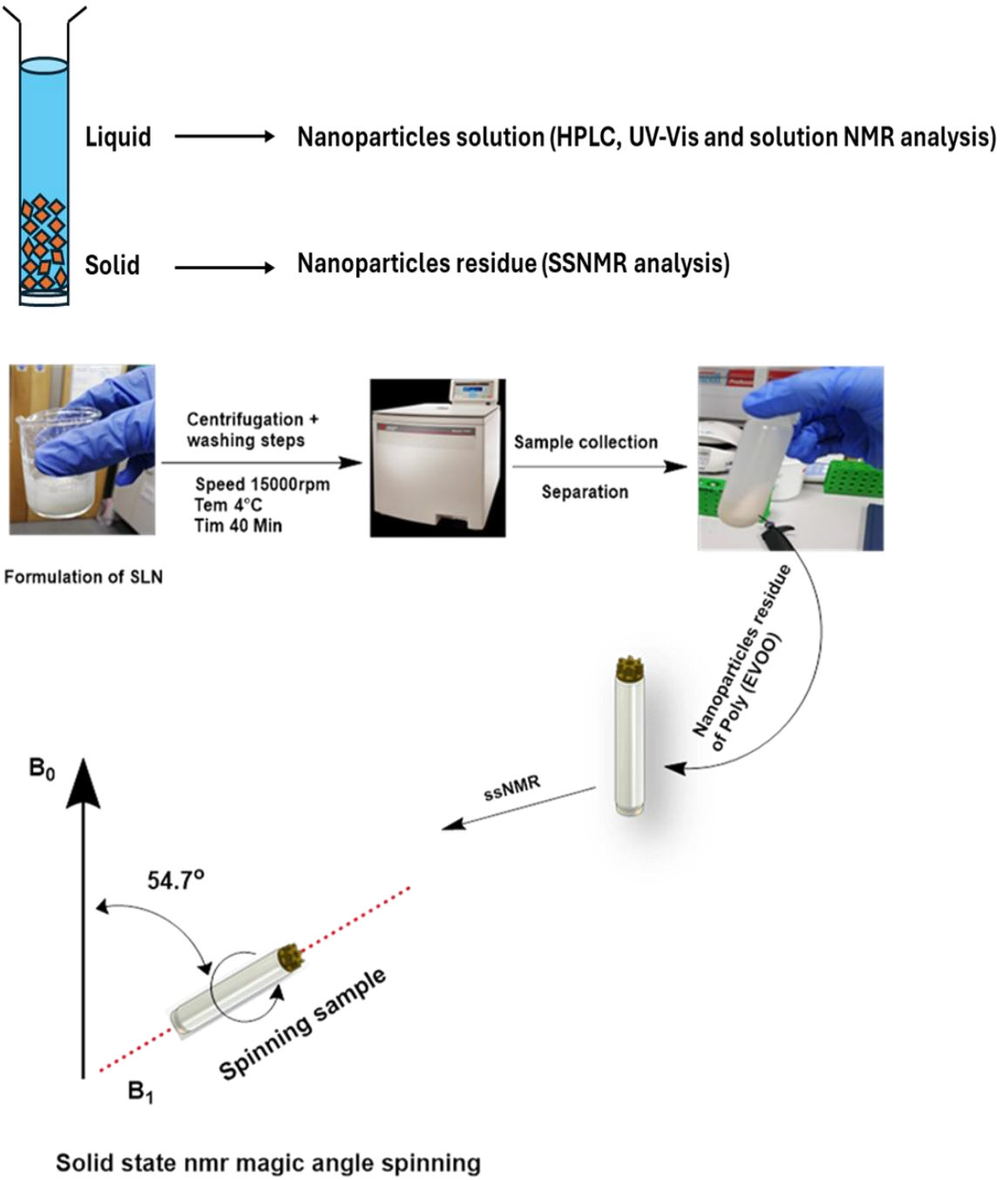

Figure 6.5. Sample preparation steps for solid-state NMR assessment of polyphenol SLNs, © Bakri A.

Transmission Electron Microscopy (TEM) Observations

The morphology of the SLNs was characterized using TEM. A 10 µL suspension of SLN samples diluted in Milli-Q purified water was spotted onto carbon-coated Formar grids. After 2 min, the excess liquid was removed by blotting. For negative staining, 10 µL of 2% phosphotungstic acid (pH 7) was spotted onto the loaded grids and left for 2 min before blotting the excess. The grids were then kept for 24 h in the glass petri dish to air dry. Grids were viewed on a JEOL JEM-1010 electron microscope, and representative images were captured.

Dynamic Light Scattering (DLS) measurements

The average particle size, polydispersity index (PDI) and zeta potential of SLNs were measured by dynamic light scattering using a Zetasizer Nano ZS (Malvern Instruments Ltd, Malvern, UK) with a 4mW 632.8 nm laser and 173º detection angle. All DLS measurements were conducted at 25 °C and all formulated SLN samples including caffeic and phenolic mixture in dH_2O were diluted 1:20 in 1 mM HEPES buffer prior to DLS analysis.

HPLC measurement of entrapment efficiency

Controls for all the entrapment efficiency (EE) measurement experiments (including UV-Visible spectrophotometry and liquid-state NMR) were prepared using a modified version of the solvent diffusion–solvent evaporation method reported previously (Borges et al., 2020; Hashem et al., 2014; Pandita et al., 2014; Patel et al., 2011). Polyphenols at a concentration of 3.3 mM were dissolved in 1 mL of methanol and injected into the column (1% w/v in Milli-Q purified water) at the same temperature with stirring. The resulting dispersion was continuously stirred at 700 rpm for 30 min on a magnetic stirrer to evaporate the solvent and stored at 4 ℃ for 1 h. The resulting dispersion was then centrifuged at 15,000 rpm for 40 min at 4 ℃.

To measure entrapment efficiency, the SLN sample was prepared and then ultrafiltered with Amicon® Ultra-4 Centrifugal filter tubes (Millipore) with a molecular cut-off of 10 kDa (Pandita et al., 2014; Hashem et al., 2014; Neves et al., 2013) to determine the amount of unentrapped aqueous free drug. One mL of the polyphenol nanoparticle suspension was then placed in tubes and centrifuged for 40 min at 4000 rpm and 4 °C, followed by three washings with Millli-Q water to remove all traces of free drug from the voids between the nanoparticles. The supernatant fractions recovered were then diluted 10-fold (Huguet-Casquero et al., 2020; Pandita et al., 2014; Hashem et al., 2014; Neves et al., 2013). A NexeraX2 UHPLC (Shimadzu) system operating at 40 °C with a mobile phase consisting of 0.1% formic acid in either ultrapure water (Buffer A) or acetonitrile (Buffer B) was used to determine amount of unentrapped drug in the filtrate. To measure the solid phase, 10 µL of the diluted sample was loaded into a Shim-pack XR-ODS 2.2 µm (3.0 mm x 50 mm) column running at a 1 mL/min flow rate. The elution profile was 5% Buffer B for minutes 0 to 3, 40% Buffer B for minutes 3 to 25, 40% Buffer B for minutes 25 to 26, 50% Buffer B for minutes 26 to 27, 5% Buffer B for minutes 27 to 27.10, and 5% Buffer B for minutes 27.10 to 32 (steps as shown in **Figure 6.6**). Absorbance intensity at 240 nm, 275 nm, and 340 nm was measured with 4 nm bandwidths. For the control setting, the total drug solution (with a drug concentration of 3.3 mM) was prepared following an identical procedure. EE% was calculated using the following formula:

EE% = (total added drug – unentrapped drug / total added drug) × 100 [**6.1**] (Pandita et al., 2014).

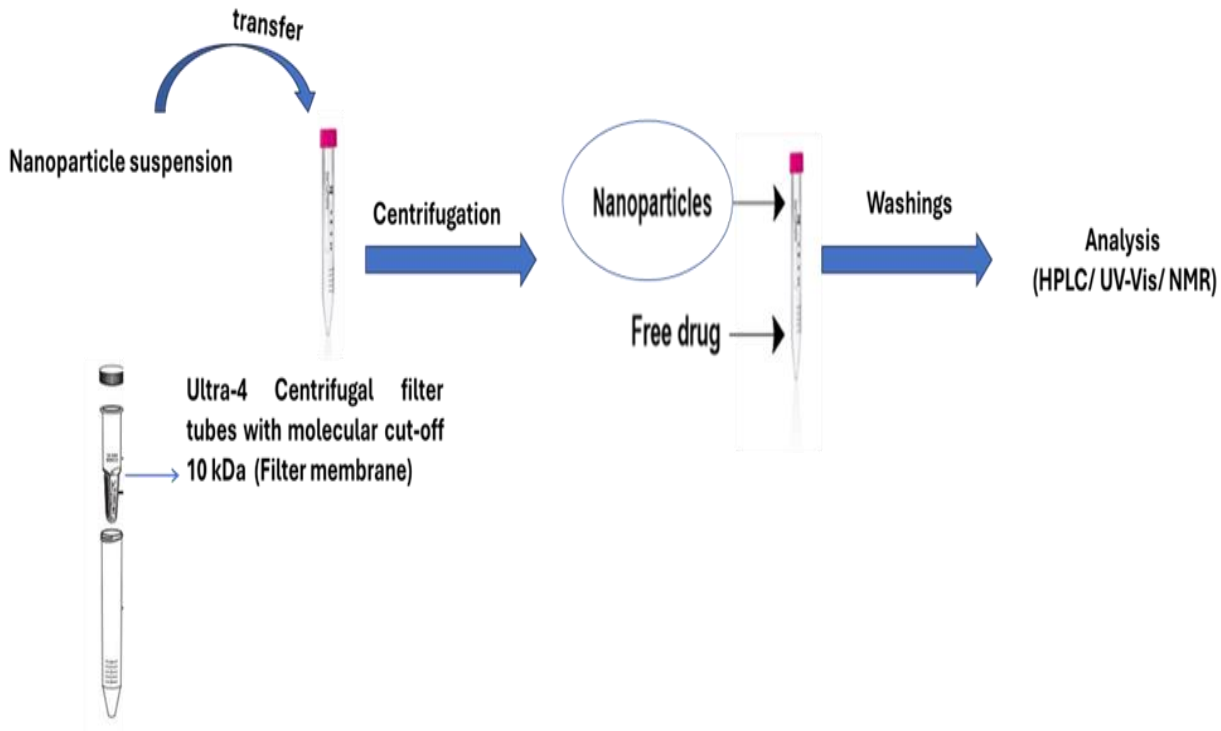

Figure 6.6. SLN sample preparation steps for measurement of entrapment efficiency using HPLC, UV-Vis and NMR, © Bakri A.

EE% measurements with UV-Vis spectrophotometry and liquid-state NMR analysis

For greater characterization of the separated free drug from the nanoparticles, the centrifugation procedures described above were used to collect supernatant fractions from the control and polyphenols SLNs that were then assessed with UV-Visible spectrophotometry and liquid-state NMR.

The polyphenol SLN samples were analyzed by UV-Vis spectroscopy at room temperature (25 °C). UV-Vis spectra in the 200–500 nm range were obtained with a NanoDrop 2000/2000c spectrophotometer after the transmittance signal was adjusted with a blank (Alves et al., 2019; Milanez et al., 2017). EE was calculated using the same formula as that used for HPLC.

The polyphenol SLN samples were characterized by obtaining their ^{1}H NMR spectra (Milli-Q purified water) through solution NMR using a Bruker 700 spectrometer at 700 MHz. Chemical

shifts as δ_H (ppm), number of protons, multiplicity, coupling constant, and *J* (Hz), are reported and couplings indicated by "s" (singlet), "br s" (broad singlet), "d" (doublet), "t" (triplet), "q" (quartet), "quint" (quintet), sextet, septet, and "m" (multiplet). Observed apparent multiplicities of proton resonances are given where coincidental S-3 coupling constants in the NMR spectra were observed.

Preparation of fluorescence-labelled SLNs for animal experiments

Nanoparticles that would be suitable for animal experiments were prepared following a modified version of the procedure described earlier in the section "Preparation of polyphenol SLNs." The procedure was modified by adding the fluorescent probe BODIPY FL C16 at a concentration of 1% (with respect to stearic acid lipid), the C16 was added in stearic acid lipid at the stage where the methanol-polyphenol solution (or pure methanol for blank SLNs) and lipid were mixed.

Results

Formulation of caffeic and phenolic mixture-SLNs

As explained in the methods section, caffeic acid SLNs containing three different lipid concentrations were first used as a reference to determine the optimal stearic acid concentration for preparing the polyphenol-loaded SLNs. When 50 mg of stearic acid (formulation F1 **Table 6.2**) was added, the SLNs fell below the detection limits of the TEM and DLS analyses. When 100 and 200 mg stearic acid (formulations F2 and F3 respectively **Table 6.2**) were compared, the increase in lipid content was found to increase the particle size and EE without any significant changes in PI or zeta potential **Table 6.2**. Therefore, we chose the F2 formulation for its lower lipid content and smaller particle size as it has been reported that smaller particle size would have a better ability to enter inside the membrane compared with larger particle (Duan et al., 2020; Viegas et al., 2023; Mishra et al., 2018).

Table 6.2. Physicochemical properties of synthesized caffeic acid SLNs.

Formulation	Particle size (nm)	PI	Zeta potential (mV)	EE (%) UV-Vis	EE (%) HPLC
F1	n.d.	-	-	-	-
F2	219.0	0.171	- 8.50 ± 0.30	63	62.4
F3	336.9	0.162	- 8.20 ± 0.08	64.8	64.7

n.d.: Not detected; F: Formulation of SLN; PI: Polydispersity index; EE: Entrapment efficiency. Average and standard deviation for particle size, polydispersity index and entrapment efficiency can be found in **Appendix 3** (**Figure S6.1** and **table S6.1**).

Based on the comparison of the caffeic acid SLN formulations, the EVOO-derived polyphenol SLNs were formulated with 100 mg of stearic acid (F2 formulation). As shown in **Table 6.3** the mean particle size was bigger than that of the corresponding caffeic acid SLNs. There was no significant difference in zeta potential, which refers to the degree of attraction or repulsion between nanoparticles in a suspension. High positive or negative values indicate that the particles repel each other and have a lower likelihood of forming aggregates. Values between -10 mV and +10 mV mean that the charge between particles is neutral (Clogston & Patri, 2010). The PI values of the caffeic acid and polyphenol SLNs were also similar. PI refers to the uniformity of the size of SLNs in suspension, and values less than 0.2 are considered to indicate uniformity (Eccleston, 1994; Swarbrick, 2013).

Table 6.3. Physicochemical properties of SLNs carrying the synthesized polyphenol mixture from EVOO.

Formulation	Particle size (nm)	PI	Zeta potential (mV)	EE (%) UV-Vis	EE (%) HPLC
F2 poly- EVOO	387.8	0.177	- 12.93 ± 0.32	85.6 %	From 11% to 100%

F: Formulation of SLN; Poly: Polyphenols; PI: Polydispersity index; EE: Entrapment efficiency. Average and standard deviation for particle size, polydispersity index and entrapment efficiency can be found in **Appendix 3** (**Figure S6.1** and **table S6.2**).

In summary of physicochemical characterization of the synthesized caffeic acid and polyphenol mixture SLNs using DLS to measure particle size, PI, and zeta potential as shown in the above **Tables 6.2** and **6.3**, and **Appendix 3 Figure S6.1** , chromatograms obtained from DLS, the PI values of caffeic acid and polyphenol SLNs following formulation **F2** with 100 mg stearic acid indicated that the SLN particles were fairly uniform in size, as PI values less than 0.2 are considered to indicate good uniformity in the size of colloidal/lipid droplets (Eccleston, 1994;

Swarbrick, 2013). The zeta potential indicated a high negative charge, which is indicative of fairly good stability. The particle size fell in the moderate range for SLNs, although the polyphenol particles were larger than caffeic acid particles. For more characterisation morphological analysis was applied and will be discussed in the next section.

Morphological features of the synthesized polyphenol and caffeic acid SLNs

SLNs were imaged at the Edge Hill JEOL Imaging Centre using a JEOL 1400-Flash Transmission Electron Microscope (TEM) at 100kV. Grids were scanned and representative images of each sample captured. Area of SLNs were measured from representative TEM images using ImageJ (Schneider et al., 2012). A manual threshold was first applied to each image then particles were analysed, and their area measured. Only particles with sufficient contrast to enable effective thresholding were measured. TEM imaging of the synthesized SLNs showed that they were spherical and uniform in shape, had diameters in the nano-range, and showed no signs of crystallization as presented in **Figure 6.7**.

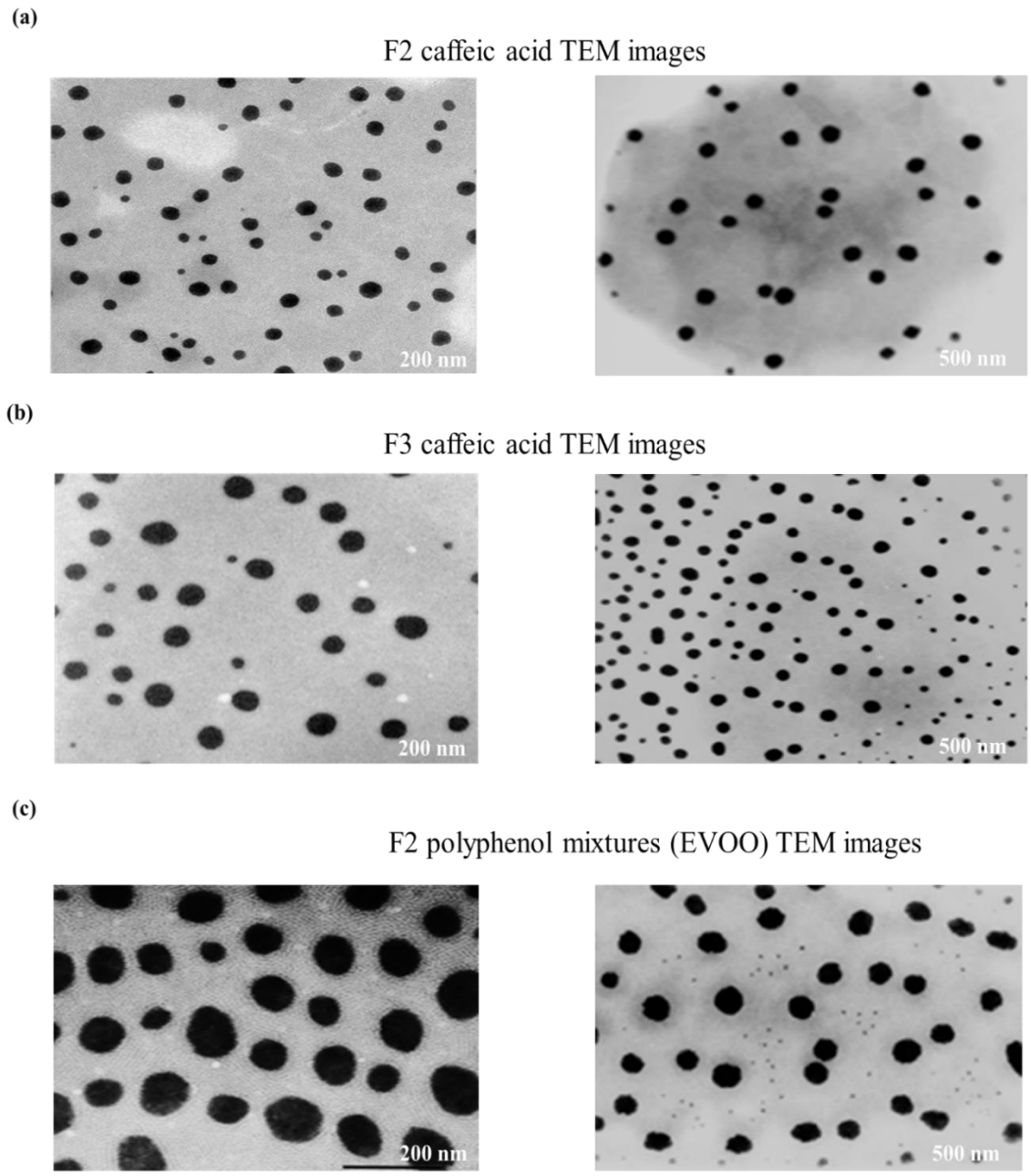

Figure 6.7. Transmission electron microscopy images of caffeic acid and polyphenol SLN formulations, (a) the formulation F2 of caffeic acid SLN using 100 mg of stearic acid, (b) the formulation F3 of caffeic acid SLN using 200 mg of stearic acid, (c) the formulation F2 of polyphenolic mixtures SLN using 100 mg of stearic acid. Two regions of the TEM grids, with two different magnifications, the TEM scale bars are (200 nm and 500 nm), are shown for each sample (left and right).

Principle of measurements of entrapment efficiency EE%

Entrapment efficiency % is defined as the percentage weight of the added drug entrapped by the system. To measure entrapment efficiency, the nanoparticles were isolated and then ultrafiltered with Amicon® Ultra-4 Centrifugal filter tubes (Millipore) with a molecular cut-off of 10 kDa (molecular cut-off (MWCO) can be described as a filter membrane with specific pore size that can be used in many applications such as biological purification and separation *etc*) (Singh, 2014). **Figure 6.8** shows the process for separating nanoparticles from free polyphenols to determine the EE (Pandita et al., 2014; Hashem et al., 2014; Neves et al., 2013). The method assumes that exchange of the polyphenols between the SLNs and aqueous phase is slow.

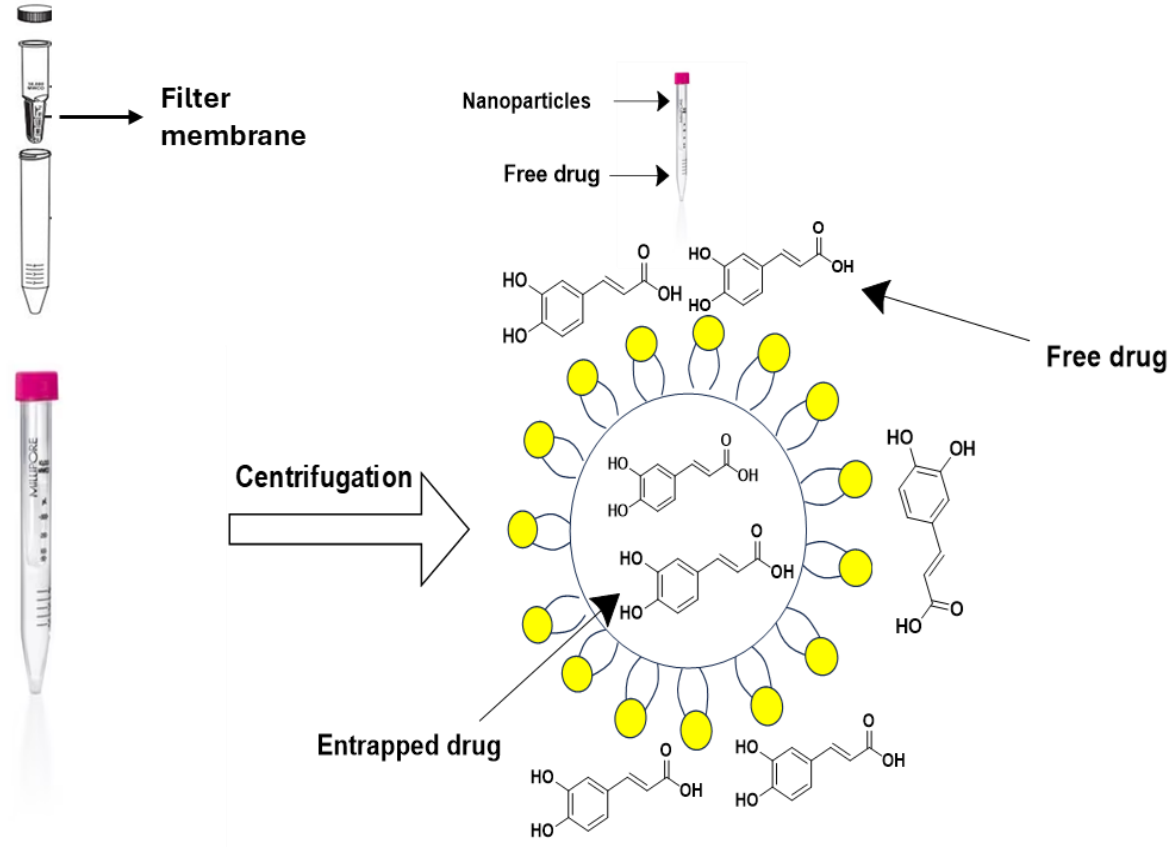

Figure 6.8. Centrifugation process for separating nanoparticles from free drug (polyphenols) to determine the EE% of caffeic acid and phenolic mixture SLNs, © Bakri A.

Measurement by UV-Vis spectrophotometry

UV-Vis spectrophotometric analysis was used to determine the EE values of the different SLN preparations. As shown in **Figures 6.9** and **6.10** below and the basic data summarised previously in **Tables 6.2** and **6.3** above section, the EE value of the formulation F2 (using 100 mg of stearic acid) with polyphenol mixture SLNs was much higher (85.6%) than the EE value of the formulation F2 (using 100 mg of stearic acid lipid) with caffeic acid SLNs (63%). The EE percentages here describe that 85.6% of polyphenolic mixture could be inside the particles and 63% for caffeic SLN sample. (Calculations of entrapment efficiencies are given in **Appendix 3 Tables S6.1** and **S6.2**).

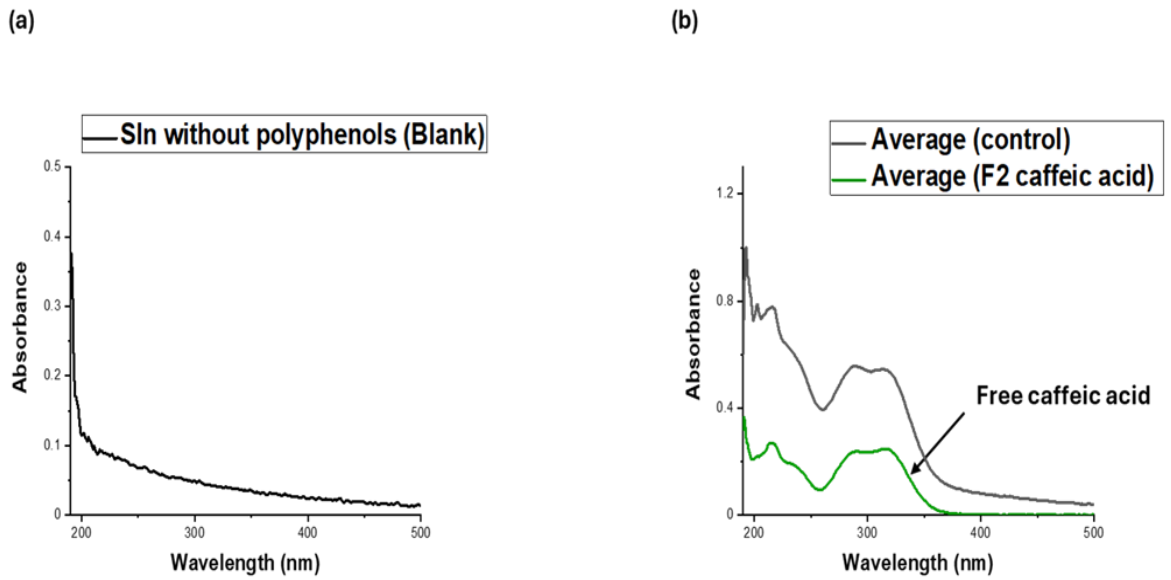

Figure 6.9. UV-Vis absorbance of entrapment efficiency of caffeic acid SLN to separate nanoparticles from free drug (a) blank SLN formulation without polyphenols, (b) the caffeic acid SLN formulation F2 using 100 mg of stearic acid.

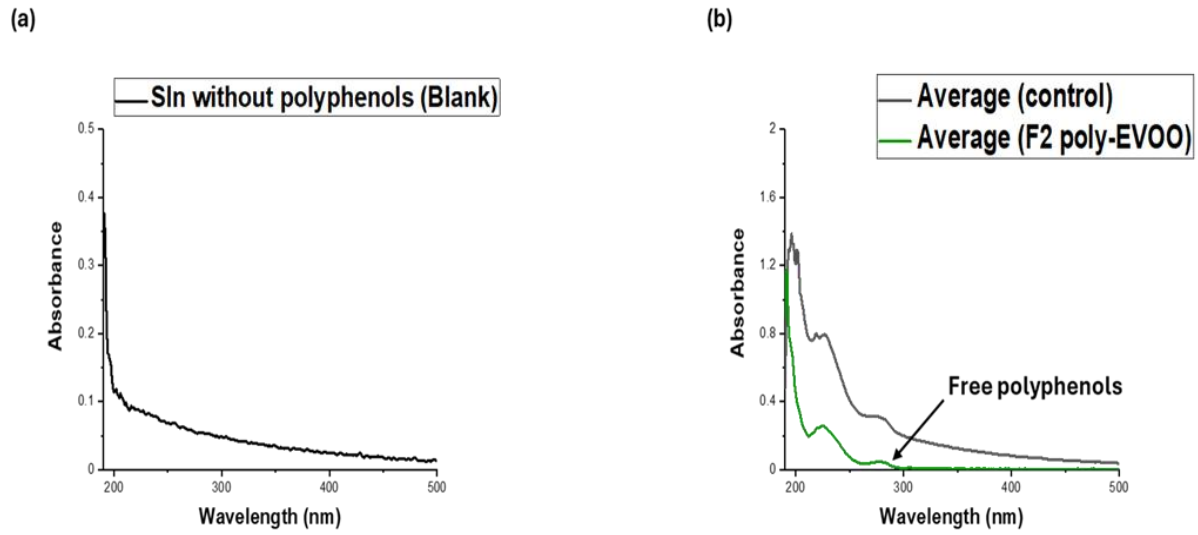

Figure 6.10. UV-Vis absorbance of entrapment efficiency of Greek polyphenols mixture in solid lipid nanoparticles using F2 formulation (100 mg of stearic acid), (a) blank SLN formulation without polyphenols, (b) the phenolic mixture SLN formulation F2 using 100 mg of stearic acid.

Measurement by HPLC

For further and specific characterisation HPLC was performed as we are dealing with mixture of polyphenols so HPLC will help to separate compounds and analyse them individually. HPLC is powerful method to resolve individual compounds.

Entrapment efficiency was also analysed by HPLC for the caffeic acid SLNs as presented in **Figures 6.11**. HPLC chromatogram analysis of the EE of caffeic acid SLNs was performed after separation of nanoparticles from free caffeic. The EE% of caffeic acid SLN formulation F2 using 100 mg of stearic acid was measured and obtained 62.4% data described previously in the above **Table 6.2** (Calculation of entrapment efficiency in **Appendix 3 Table S6.3**). However, as shown in the above **Table 6.3**, the EE values of individual compounds in the polyphenol mixture SLNs varied widely and ranged from 11% to 100% and that is because we are dealing with a mixture of compounds as shown in **Figure 6.12** HPLC analysis of EE of phenolic mixture SLNs using the F2 formulation at 240 nm (chromatograms for HPLC at 275 and 340 nm can be found in **Appendix 3** (**Figure S6.4** and **Table S6.4** summarised EE% calculation from 11% to 100%). For more characterization and investigation solution NMR was used and the polyphenol SLN samples were characterized by obtaining their ^{1}H NMR spectra (Milli-Q purified water) through solution NMR using a Bruker 700 spectrometer data not shown. Entrapment efficiency (EE %) was not calculated directly, but the observations were used to confirm the results of HPLC and UV-Vis spectrophotometry. As a result, the difference in the EE values obtained by HPLC and UV-Vis can probably be explained by the separation of the components in HPLC.

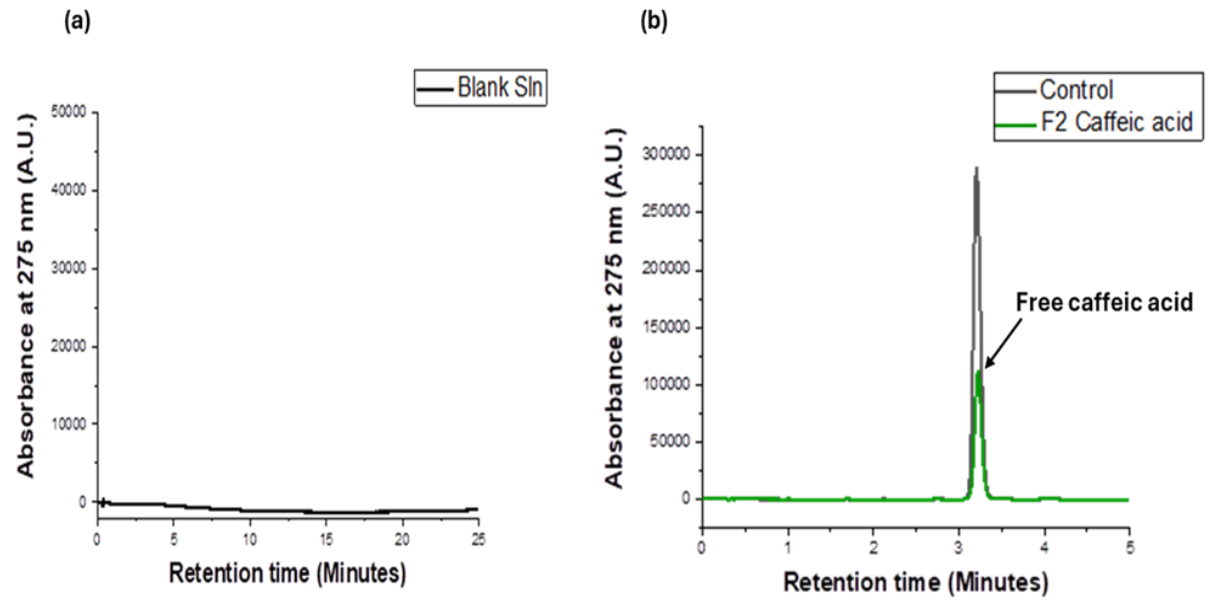

Figure 6.11. HPLC chromatogram analysis at 275 nm of entrapment efficiency of caffeic acid SLN to separate nanoparticles from free caffeic acid (a) blank SLN formulation without caffeic acid, (b) the formulation F2 of caffeic acid SLN using 100 mg of stearic acid.

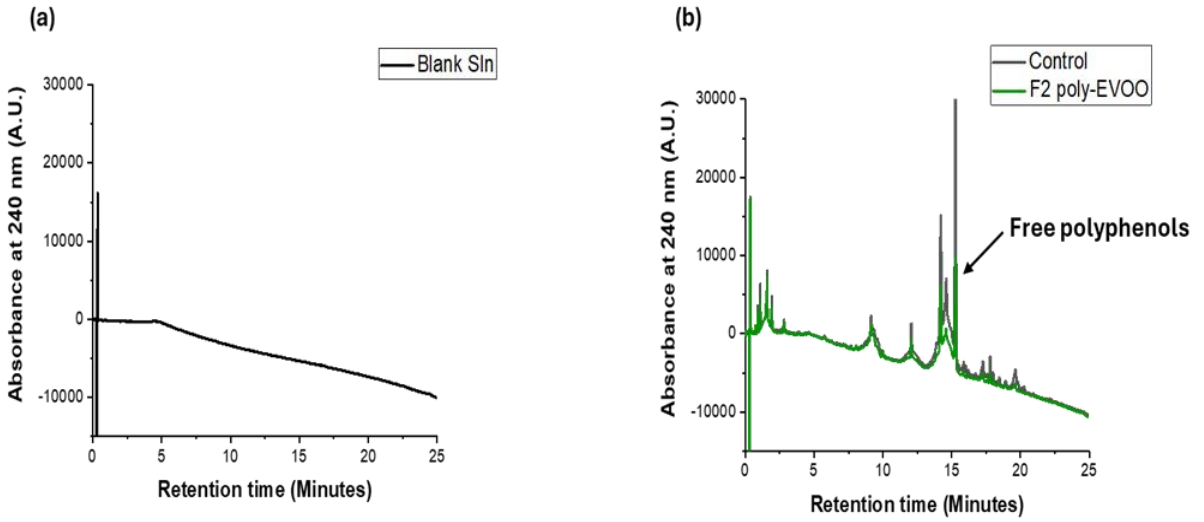

Figure 6.12. HPLC analysis at 240 nm of entrapment efficiency of Greek polyphenols mixture SLN to separate nanoparticles from free polyphenols (a) blank SLN formulation without phenolic mixture, (b) the formulation F2 of phenolic mixture SLN using 100 mg of stearic acid.

Characterization of SLNs by solid-state NMR

After preparation of SLNs, the final centrifugation step results in the sedimentation of insoluble material that is discarded to leave the described soluble nanoparticles. The insoluble fraction has not been considered in previous publication yet could contain a significant quantity of the cargo and carrier components. To optimise the preparation, it is therefore desirable to minimise the amount of polyphenol mixture that is discarded as insoluble waste product. To analyse the composition of the insoluble fraction, ^{13}C MAS SSNMR was used. The spectrum is consistent with the presence of stearic acid as the main component of the insoluble material, and no peaks were detected in the region from 100-150 ppm where the aromatic groups of polyphenols are expected to appear. The conclusion is that little or none of the polyphenol payload was discarded with the insoluble fraction at this stage of the preparation and so no further optimisation in this regard was necessary as shown in **Figure 6.13**.

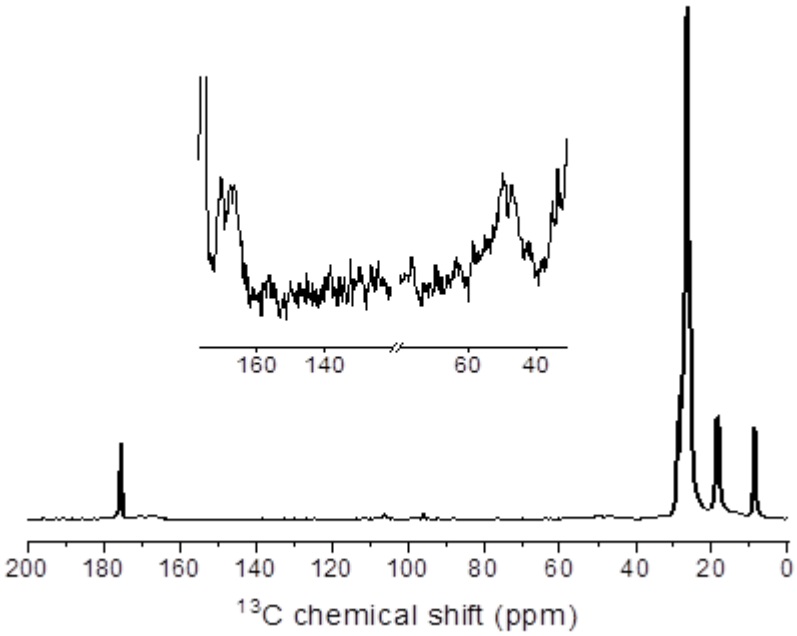

Figure 6.13. Solid-state NMR spectrum of the nanoparticle residue of polyphenol mixture SLNs (F2 formulation using 100 mg stearic acid). When ^{13}C SSNMR was applied, the spectrum only shows the presence of stearic acid. This confirms that all the polyphenols were concentrated in the nanoparticle solution.

Measurement of fluorescence in labelled and unlabelled SLNs for animal experiments

For future study and investigation, the SLNs for animal experiments were prepared as described in the method section. The aim was to monitor the distribution of the nanoparticle components in tissue after daily oral ingestion for 1 week. In the longer term, it is intended to detect the distribution and nature of the polyphenols delivered in the SLNs. However, the preliminary experiments were designed to detect the stearic acid component of the SLNs, which were tagged with a fluorescent probe. Imaging of the animal gut and other tissue post mortem would give an indication of whether the nanoparticles had been absorbed from the gut.

The first step towards these aims was to characterise the fluorescently-tagged SLNs *in vivo*, to ensure that the emission quantum yield could be suitable for *in vivo* detection. **Table 6.4** indicates that the fluorescence intensity of labelled SLNs in the absence of polyphenols is relatively strong, but decreases with the incorporation of EVOO polyphenols. This observation suggests that fluorescence quenching occurs resulting from the interaction of polyphenol particles with the fluorescent probe within the core of the particles. This interesting result needs to be further investigated to understand the nature of these molecular interactions and whether they could interfere with the effectiveness and bioavailability of the polyphenols contained with the SLNs in animal models.

Table 6.4. Fluorescence of phenolic SLNs (excitation wavelength = 482 nm, emission wavelength = 515 nm).

Samples	Mean (nm)	Standard deviation
SLNs labelled with fluorescent probe C16 - mixture polyphenols (EVOO)	5351.1	72.2
SLNs labelled with fluorescent probe C16 + mixture polyphenols (EVOO)	2021.8	34.8
SLNs unlabelled + mixture polyphenols (EVOO)	32.6	1.1

Stability of nanoparticles after storage for 8 months

In preparation for animal studies, it may be necessary to store the nanoparticles for days, weeks or months in advance of commencing dosing. The stability of SLN samples was therefore investigated and as shown in **Table 6.5**, the PI increased substantially, as did the mean particle size, after 8 months of storage in the room temperature. These values imply that the size of the nanoparticles changed over time and their uniformity decreased with time.

Table 6.5. Particle size and PI values of SLNs after 8 months of storage.

	Particle size _(nm)		Polydispersity index (PI)	
Sample Name	**Mean**	**Standard deviation**	**Mean**	**Standard deviation**
F2- Caffeic acid	628.96	5.58957	0.27	0.00814
F3- Caffeic acid	594.36	8.40555	0.29	0.02214
F2- Polyphenol mixtures (EVOO)	674.16	24.5329	0.39	0.02055

F: Formulation of SLN

Discussion

In the present study, we have formulated for the first time SLNs containing a mixture of polyphenols derived from EVOO. The synthesized SLNs showed fairly uniform size, based on PI values that were below 0.2, as well as good stability, based on zeta potential values of −12.93 mV. With regard to the ability to encapsulate the phenolic compounds, UV-Vis spectrometry revealed an EE of 85.6%. These values look promising given that we have attempted to load SLNs with the entire polyphenol contents of EVOO. Animal experiments with these SLNs will be conducted to determine the bioavailability of these SLNs under *in vivo* conditions. The mean size of the polyphenol SLNs was 387.8 nm, which means that they fell in the normal range for SLNs (50 to 1000 nm). Moreover, nanoparticles falling within this range have shown good absorption in the body (Florence, 1997; Kreuter, 1991). Further, TEM analysis of the surface morphology showed that the particles were uniformly spherical and had no signs of crystal formation.

In this study, before the polyphenol mixture was loaded onto the SLNs, we determined the optimal lipid content of the SLN formulation by using caffeic acid as a reference. We found that using 100 mg stearic acid led to the generation of SLNs of good size, stability, and uniformity. Therefore, the final polyphenol SLNs were synthesized with 100 mg stearic acid as the lipid core, methanol as the solvent phase in which the active ingredients were dissolved, and poloxamer 188 as the emulsifying agent. A previous study that combined two phenolic compounds, namely resveratrol and curcumin, in lipid core nanocapsules reported a particle size of 200 nm and an EE close to 100% (Coradini et al., 2014). Further, another study used nanolipid carriers to improve the bioavailability of oleuropein, which has poor stability and low bioavailability in its natural state, and reported a particle size of 150 nm, a zeta potential of −21 mV, and an EE of 99.12% (Huguet-Casquero et al., 2020). It should be noted that these studies used nanostructured lipid carriers, which also contain a liquid lipid component in the

core. It is believed that the addition of the liquid lipid to the core allows for the encapsulation of a greater amount of active drugs, better drug release, and better stability (Viegas et al., 2023). This may explain the values reported. In addition, as the previous studies used only one or two active components, this may explain the smaller size of the nanoparticles. However, both SLNs and nanostructured lipid carriers are similar in terms of their ability to improve the bioavailability of drugs, their ability for controlled release of drugs, and their ability for targeted delivery to the required tissues/cells. High-pressure homogenization is considered the most effective and efficient method for the synthesis of lipid nanoparticles (Müller et al., 2000). However, we chose the solvent diffusion–solvent evaporation method based on the findings of a previous study that synthesized resveratrol-loaded SLNs and reported that the SLNs had a smooth surface with a size of 134 ± 7.6 nm, a zeta potential of −34.3 ± 2.5 mV, and an EE of 88.9 ± 3.1% (Pandita et al., 2014). Again, considering that we used the same method to load a mixture containing the entire polyphenol content of EVOO, the particle size, zeta potential, and EE values we have reported look promising.

The research described here lays some important groundwork for future investigations into SLNs that can carry a mixture of different polyphenols. Achieving an EE of about 85% on this first attempt is a promising result that warrants more efforts into optimizing SLNs containing a complex mixture of polyphenols. Moreover, we used a whole array of methods to characterize the synthesized SLNs, and the data will serve as an important foundation for further improvements to the formulation. In particular, our solid-state NMR findings demonstrate that all the polyphenols had been extracted into the soluble fraction of the nanoparticles. SLNs have been found to have the ability to cross the blood–brain barrier (Satapathy et al., 2021), and curcumin-loaded SLNs have been proposed as an innovative tool for the management of Alzheimer disease based on the results of experimental cellular and animal models of the disease (Campisi et al., 2022; Loureiro et al., 2017). Further, as discussed in the introduction

section, SLNs have shown strong ability to cross the blood–brain barrier and, thus, improve the concentration of the active ingredients in the brain. Thus, the polyphenol SLNs synthesized here could have immense potential in the future for the treatment of neurodegenerative disease such as Alzheimer disease. In the future, the formulations prepared here can be further modified to optimize their stability and bioavailability. That is, the EE could be improved further given the variations in the absorption and metabolism of EVOO compounds *in vivo*. Further, preserving the stability and characteristics of these SLNs in storage is another area of focus for the future. Finally, the fluorescence-labeled probes need to be examined in animal models to determine their *in vivo* bioavailability and their ability to cross the blood–brain barrier. We have created a plan to formulate these SLNs to observe their effects on animal models of such neurodegenerative diseases. The proposed experiments are explained briefly in **Chapter 7**.

Chapter 7 (General discussion and future work)

The overall aims of the research in this thesis have been to investigate and understand the effects of polyphenolic mixtures derived from natural EVOO on the aggregation of the Alzheimer's amyloid-β peptide and tau. Potential drug delivery formulations of polyphenol mixtures have also been developed. Many types of human disease are associated with so-called amyloid fibrils, which are fibrous deposits of insoluble protein material that accumulate in human tissue including the brain, heart, and kidneys. The most famous of these amyloid diseases is Alzheimer's disease (AD). In particular we have been interested to find molecules that occur in natural olive oil products and test them as a mixture or individually to find which either prevent the formation of amyloid plaques, or else break them up into soluble harmless fragments. Such mixtures could be used to supplement other medications for therapeutic treatment. This work involved using a range of state-of-the-art techniques to do this investigation, including HPLC, tandem mass-spectrometry, circular dichroism spectroscopy, ultraviolet–visible spectroscopy, dynamic light scattering, transmission electron microscopy, Thioflavin T fluorescence and NMR in solution and solid state.

Alzheimer's disease and natural olive oil products

Literature on Alzheimer's disease focuses on the two main pathologies of AD, namely, amyloid plaques and NFTs composed of tau-related proteins (Abner et al., 2017; Elobeid et al., 2016; Kapasi et al., 2017; Kovacs et al., 2013; Robinson et al., 2018; Spires-Jones et al., 2017; White et al., 2016; Ittner and Götz, 2011). The management of Alzheimer's disease is becoming a major societal challenge. Furthermore, a cure for the disease is lacking and the current

treatment options are only modest in treating selected symptoms and that all depend on early and precise diagnosis, reducing the symptoms and decreasing the rate of disease progressions (Cummings et al., 2016). Aβ and tau exist in toxic species that contribute to the spread of the disease, and, therefore, the main focus of research has been to block aggregation of these peptides to halt disease progression (Nelson and Tabet, 2015).

A wealth of literature indicates that extra virgin olive oil has the potential to be used in the treatment of Alzheimer's disease. Significantly, it is the polyphenol component within olive oil that poses the most promise in the treatment of neurodegenerative diseases. Oleocanthal and oleuropein aglycone are both polyphenols found in extra virgin olive oil and have attracted the most attention over the last decade. Both are believed to act to reduce the progression and symptoms of Alzheimer's disease through action on both amyloid-β containing plaques and tau-related pathologies. It is hypothesized that the polyphenols within olive oil can reduce amyloid-β production, enhance the clearance of toxic substances such as amyloid-β oligomers as well as reducing tau hyperphosphorylation but more research is required. Most in-vitro studies have focused on the three main types of polyphenols found in olive oil: oleocanthal, oleuropein and hydroxytyrosol, tested individually. To date, however, there have been no reported evaluations of EVOO phenol mixtures isolated from the fatty acid component of olive oil. As polyphenol mixtures are normally consumed in the diet, it is important to determine whether the mixtures can affect amyloid aggregates. Here, we examine the impact of phenolic mixtures isolated from olive oil, also study individual olive oil polyphenol that have not been studied in detail for their ability to modulate amyloid formation by Aβ peptides and tau proteins.

Protein expression

The peptide component of amyloid precursor protein (APP), known as amyloid beta 40 (Aβ40) has been shown to have a critical role in the progression of Alzheimer's disease (Sadigh-Eteghad et al., 2015).

Expression is a primary step in our research in order to use these proteins to investigate the interactions of phenolic mixtures with amyloid beta and determine what effects they have on the structure of the fibrils.

Aβ40 was expressed and characterized following the expression procedure adapted from previous established methods (Stewart et al., 2016; Walsh et al., 2009). In this work the aim was to efficiently create a cost-effective and productive procedure for expressing and purifying amyloid beta 40 (MAβ40) peptide from *E. coli*, including ^{15}N labelled peptide for NMR studies. Using a small amount of medium for ^{15}N-labeling significantly reduced production costs while providing a large amount of pure protein for future research.

The significant step in the expression of unlabelled and labelled MAβ40 was identification and characterization of proteins, this was confirmed by using SDS-PAGE gel, electrospray ionisation mass spectrometry, and thioflavin T (ThT) aggregation experiment. Moreover, transmission electron microscopy (TEM) was used to verify the presence of amyloid fibrils visually. In terms of labelled MAβ40 labelling was performed by expressing Aβ40 in a minimal bacterial growth medium containing ^{15}N-labelled ammonium chloride (CortecNet) as the sole nitrogen source. Labelled MAβ40 with ^{15}N ammonium chloride was produced and confirmed to allow studying the effect of polyphenol mixtures on amyloid using SSNMR for the first time experiments shown in **Chapter 5**. Finally, it was confirmed that the updated procedure produced exceptionally pure unlabelled and ^{15}N labelled MAβ40.

Extraction of phenolic compounds from olive oil products

The Mediterranean diet is rich in extra virgin olive oil with the dietary consumption ranging from 40-50 g/day. Phenol components within olive oil pose the most promise in the treatment of neurodegenerative diseases. The polar polyphenolic compounds in EVOO are known to modify protein aggregation into amyloid fibrils associated with diseases such as Alzheimer's disease (**Chapter 1** and **4**). Another aim of this thesis was to analyse the composition of different olive oil obtained from Greece and Saudi Arabia, preparations to separate, identify and characterize the main polyphenol compounds that are biologically active at preventing amyloid formation for treating AD and exam their ability to inhibit protein aggregation into amyloid and to break up the amyloid fibres (**Chapter 5**).

Here the first objective was to develop a suitable procedure to extract polyphenolic compounds from EVOO. Three different extraction methods, namely, LLE with funnel separation, LLE with centrifugation and SPE were compared systematically in order to determine the most effective technique to maximise the yield and diversity of polyphenols extracted. A direct comparative study of this type has not been reported in the literature. In summary the result obtained for SPE method agreed with the previous studies and indicated that the reactive dialdehydic forms of the oleuropein and ligstroside aglycones were poorly recovered using SPE technique (Tasioula-Margari and Tsabolatidou, 2015; Capriotti et al., 2014; Hrncirik and Fritsche, 2004; Montedoro et al., 1992; Pirisi et al., 2000). Also, when LLE with centrifugation method was tested in this work, we found the separation step of the aqueous methanol/hexane layers is very sensitive and critical, which may cause widely different results. This issue was also reported by other researchers (Pirisi et al., 2000). The LLE with funnel technique was most promising in terms of its reproducibility, yield and range of extraction, so this technique was selected to be used to isolate polyphenolic compounds from olive oil. This method was refined further by adding sonication and washing steps that have not been reported previously.

Phenolic compounds from Greek and Saudi olive oils were isolated using LLE with funnel method and then a range of analytical techniques including UV-Visible absorption, HPLC, LC-MS chromatography and NMR spectroscopy were used for identifying, quantifying and characterizing phenolic compounds. LC-MS identified over 30 compounds in the extracts, including some simple phenolic acids and their derivatives, flavones and secoiridoids (oleuropein and ligtroside derivatives). One limitation of LC-MS was its inability to identify some peaks with retention times below 5 minutes. This limitation of LC-MS was due to the low signal to noise ratio arising from the complexity of the polyphenolic profile of EVOO. Further, LC-MS had lower sensitivity to compounds with molecular weights below 200 Da, resulting in missing peaks corresponding to smaller and lighter compounds. HPLC was therefore applied for further characterization. HPLC enable the concentrations of some polyphenols to be quantified with the use of commercial reference polyphenols, including the smaller molecules tyrosol, hydroxytyrosol, caffeic acid, vanillic acid, ferulic acid and coumaric acid. By matching retention time and UV absorption we managed to detect and quantify most of the standards present in the extracts. Moreover, employing solution-proton NMR helped to assign some phenolic compounds by elucidating their structures through comparison with the data of previous work but the particular aim of using NMR was to investigate glucosyl groups in both extracts (**Figure 4.14 Chapter 4**).

To conclude, the work described in **Chapters 4** enabled the efficient extraction of polyphenol mixtures from EVOO and quantified and/or identified the vast majority of the main compounds in the mixture. A key finding was that the polyphenol profiles of EVOO obtained from two sources (Greek and Saudi) were quite different, which enabled comparisons of their activities against amyloid in **Chapter 5**.

Further work would be interesting to investigate and characterize some unknown peaks in both extracts **Figure 4.11 Chapter 4** some of these peaks have not been reported in the literature,

applying solution NMR would be a powerful technique for depth characterization also due to the chemical complexity of the obtained extracts GC-MS would be helpful in drug screening to identify, characterize and cover a wide range of unknown compounds particularly small and volatile molecules. Further work in which olive oil polyphenols are combined into nanoparticles with hydrogenated olive fatty acids is being explored as a potential novel strategy for oil recycling.

Investigation of the effects of polyphenol mixtures and individual compounds on Aβ and tau

A multitude of studies (Martinez-Lapiscina et al., 2013; Rodríguez-Morató et al., 2015; Scarmeas et al., 2009; Sofi et al., 2010), have hypothesised that a typically Mediterranean diet improves resistance against several pathological diseases including Alzheimer's disease which impacts 44 million people globally and will cost the USA alone approximately $600 billion by 2050 (Lane et al., 2018). The Mediterranean diet is rich in olive oil which contains oleuropein and tyrosol which are capable of disrupting the formation of Aβ and tau amyloid species, which present in the AD brain as plaques and neurofibrillary tangles, respectively (Sipe et al., 2016; Sipe et al., 2010; Kumar and Singh, 2015). However, Augustinack et al. (2002) emphasise the current lack of understanding regarding how these pathological manifestations influence the disease phenotype or how abrogation of these pathologies is beneficial for those with AD. The search for molecules which can inhibit the rate of tau and Aβ aggregation *in vivo* is currently being investigated as a new therapeutic paradigm (Doig and Derreumaux, 2015). Dietary sources that contain such molecules are considered to be a viable option as they are inexpensive, safe for consumption, and easily available. Oleuropein adheres to these criteria and its anti-aggregation properties have been well documented. However, the collective effects of phenolic compounds on amyloid aggregation kinetics and morphology remain unexplored.

The focus of this chapter was to investigate the biological effects of mixture, and individual phenolic compounds already isolated from Greek and Saudi sources and compared their impacts on the aggregation of amyloid-β and tau peptides *in vitro*. To do this investigation, we applied a rang of methods including HPLC, UV-Vis for binding, ThT, CD, TEM, DLS, SSNMR and molecular docking in order to gain better understanding.

The result in this thesis chapter showing that when the two mixtures of water-soluble phenolic extracted from Greek and Saudi EVOO sources were quantified and characterized as described in **Chapter 4** then we aimed here to do comparative studies of their effects on Aβ and tau aggregation as have not been reported. In term of their effects both Greek and Saudi extracts were shown to be similarly effective at inhibiting Aβ40 aggregation *in vitro*. At concentrations up to 20 μg/mL, the mixtures shift the $t_{1/2}$ for Aβ40 aggregation to longer times and at higher concentrations abolish aggregation completely. The effects can be attributed in part to the presence of oleuropein, tyrosol and hydroxytyrosol in the extracts, each of which individually impedes Aβ40 aggregation according to ThT fluorescence. We confirm, however, that other compounds in the extract, such as caffeic acid, ferulic acid and certain flavonoids are also effective at inhibiting Aβ40 aggregation, albeit at higher concentrations than are found in EVOO. It is appropriate to consider the cumulative effect of the entire phenolic pool on Aβ40 aggregation rather than attributing the effects to individual compounds. Deficiencies in certain phenolics in a sample may be buffered by higher, compensatory concentrations of others such that extracts of different composition can have similar anti-aggregation properties. A HPLC binding experiment was developed to confirm the above outcome using the same concentrations, the HPLC data showed that most of EVOO compounds in both extracts bind to Aβ40 fibrils. Furthermore, at lower concentrations (< 20 μg/mL) transmission electron microscopy, circular dichroism dynamic light scattering, and solid-state NMR reveals that most compounds in the extracts bind to pre-formed Aβ40 fibrils, which generates soluble Aβ

oligomers that are mildly toxic to SH-SY5Y cells. Tau was then examined but it was interesting that less effects were observed, and it required higher concentration of extracts (> 100 μg/mL) to be remodelled. Finally, computational analysis was applied and many of the compounds extracted from EVOO possess these properties and may be expected to have a preference for β-sheet structures. This was confirmed by inspecting protein structures from the Protein Data Bank (PDB) that contained bound phenolic compounds identified in EVOO. From a total of over 70 structures, the phenolic compounds were seen to bind predominantly to β-sheet regions of the proteins, despite the same proteins having an overall higher α-helical content. The competition between active and nonactive phenolic components in the mixtures may play a critical role in their activity as inhibitors against Aβ and tau.

Nanoparticles formulation

The mixture of polyphenols has been isolated and characterised from extra virgin olive oil (**Chapter 4**) and tested for their ability to bind to amyloid fibrils associated with AD. Compounds that bind to the fibrils also inhibit the formation of fibrils from the monomeric protein and are potentially able to prevent AD, as shown in **Chapter 5**. The therapeutic viability of these polyphenols is limited by their poor absorption from the gut and rapid metabolism in the bloodstream, which restricts their bioavailability and pharmacokinetics. New formulations of the polyphenols in solid lipid nanoparticles, which protect them from metabolism and degradation *in vivo*, were developed in this thesis. Here, we successfully formulated for the first time SLNs containing a mixture of polyphenols derived from EVOO. The synthesized SLNs showed fairly uniform size, based on PI values that were below 0.2, as well as good stability, based on zeta potential values of −12.93 mV. With regard to the ability to encapsulate the phenolic compounds, UV-Vis spectrometry revealed an EE of 85.6%. These values look promising given that we have attempted to load SLNs with the entire polyphenol contents of

EVOO. Animal experiments with these SLNs will be conducted to determine the bioavailability of these SLNs under *in vivo* conditions. The size of the polyphenol SLNs was 387.8 nm, which means that they fell in the normal range for SLNs (50 to 1000 nm). Moreover, nanoparticles falling within this range have shown good absorption in the body (Florence, 1997; Kreuter, 1991). Further, TEM analysis of the surface morphology showed that the particles were uniformly spherical and had no signs of crystal formation.

Work in progress

The following SLNs were prepared for animal experiments: SLNs containing the polyphenol mixture extracted from EVOO and labelled with fluorescent probe C16, SLNs not containing the polyphenol mixture labelled with fluorescent probe C16, and SLNs containing the polyphenol mixture that were not labelled with the fluorescent probe. SLN samples were prepared with 8.8 mM of SLN-polyphenol mixture, and fluorescence measurements were made at room temperature with a plate reader at an excitation wavelength of 482 nm and an emission wavelength of 515 nm (Molecular Devices Flexstation 3 Microplate Reader, Molecular Devices). All measurements were performed in triplicate.

Animal experiment: mice litters housed for 7 weeks prior to be treated. After this period of time, different groups of four mice each has been treated once a day for 7 days with a 100 µL solution containing 250 µg SLNs: fluorescence-labelled polyphenol SLNs, fluorescence-labelled SLNs not containing polyphenols, unlabelled polyphenol SLNs, and using water as a control (see **Appendix 3 Figure S7.1)**. Currently the experimental work is in the stage of monitoring weight and collecting faecal samples 7 of days prior to, and during, the week of treatment. At the end, we will collect small and large intestine, blood and liver to study the effects using analytical methods.

Further work to the current findings which need to be discussed and investigated for the future. The first is the wide variation in the encapsulation efficiency of different compounds within the mixture that was observed by using HPLC. Further study into identifying compounds with poor EE and strategies to improve the EE of the poorly encapsulated compounds would be useful in the future, especially given the variations in the absorption and metabolism of EVOO compounds *in vivo*. Another limitation is the lack of experimental models. Work is in progress to test these SLNs in animal experimental models, as explained in the last part of this thesis (see part **work in progress**), and the data will be collected and analysed in the future. An additional work should be planned to investigate the increase in particle size and decrease in their uniformity with time (as observed after storage in the room temperature for 8 months). We did not measure zeta potential after 8 months of storage, so we currently cannot comment on the stability of these SLNs with time. This is an important parameter to evaluate in the future also would be interesting to test the storage stability at 4 ºC and -20 ºC in order to obtain a better understanding. Finally, fluorescence labelling of the SLNs for animal experiments showed a decrease in fluorescence with the addition of the polyphenol mixture. This points to molecular interactions between the probes and the phenolic compounds that probably led to fluorescence quenching—a phenomenon that needs to be investigated further to determine its potential effects on the bioavailability of the phenols in the animal experimental models.

Chapter 8 (References)

Abdallah, I.M., Al-Shami, K.M., Alkhalifa, A.E., Al-Ghraiybah, N.F., Guillaume, C. and Kaddoumi, A., 2023. Comparison of oleocanthal-low EVOO and oleocanthal against amyloid-β and related pathology in a mouse model of Alzheimer's disease. *Molecules*, *28*(3), p.1249.

Abdallah, I.M., Al-Shami, K.M., Yang, E., Wang, J., Guillaume, C. and Kaddoumi, A., 2022. Oleuropein-rich olive leaf extract attenuates neuroinflammation in the Alzheimer's disease mouse model. *ACS Chemical Neuroscience*, *13*(7), pp.1002-1013.

Abedini, A., Plesner, A., Cao, P., Ridgway, Z., Zhang, J., Tu, L.H., Middleton, C.T., Chao, B., Sartori, D.J., Meng, F. and Wang, H., 2016. Time-resolved studies define the nature of toxic IAPP intermediates, providing insight for anti-amyloidosis therapeutics. *Elife*, *5*, p.e12977.

Abenavoli, L., Larussa, T., Corea, A., Procopio, A.C., Boccuto, L., Dallio, M., Federico, A. and Luzza, F., 2021. Dietary polyphenols and non-alcoholic fatty liver disease. *Nutrients*, *13*(2), p.494.

Abner, E.L., Kryscio, R.J., Schmitt, F.A., Fardo, D.W., Moga, D.C., Ighodaro, E.T., Jicha, G.A., Yu, L., Dodge, H.H., Xiong, C. and Woltjer, R.L., 2017. Outcomes after diagnosis of mild cognitive impairment in a large autopsy series. *Annals of neurology*, *81*(4), pp.549-559.

Abuznait, A.H., Qosa, H., Busnena, B.A., El Sayed, K.A. and Kaddoumi, A., 2013. Olive-oil-derived oleocanthal enhances β-amyloid clearance as a potential neuroprotective mechanism against Alzheimer's disease: In vitro and in vivo studies. *ACS chemical neuroscience*, *4*(6), pp.973-982.

Adoni, M., Yadam, M., Gaddam, S.A., Rayalacheruvu, U. and Kotakadi, V.S., 2020. Antimicrobial, antioxidant, and dye degradation properties of biosynthesized silver nanoparticles from Artemisia annua L. *Lett. Appl. NanoBioScience*, *10*, pp.1981-1992.

Ahmad, E., Ahmad, A., Singh, S., Arshad, M., Khan, A.H. and Khan, R.H., 2011. A mechanistic approach for islet amyloid polypeptide aggregation to develop anti-amyloidogenic agents for type-2 diabetes. *Biochimie*, *93*(5), pp.793-805.

Akbaraly, T.N., Singh-Manoux, A., Dugravot, A., Brunner, E.J., Kivimäki, M. and Sabia, S., 2019. Association of midlife diet with subsequent risk for dementia. *Jama*, *321*(10), pp.957-968.

Aksenov, A.A., da Silva, R., Knight, R., Lopes, N.P. and Dorrestein, P.C., 2017. Global chemical analysis of biology by mass spectrometry. *Nature Reviews Chemistry*, *1*(7), p.0054.

Al Rihani, S.B., Darakjian, L.I. and Kaddoumi, A., 2019. Oleocanthal-rich extra-virgin olive oil restores the blood–brain barrier function through NLRP3 inflammasome inhibition simultaneously with autophagy induction in TgSwDI mice. *ACS chemical neuroscience*, *10*(8), pp.3543-3554.

Alam, M., Ahmed, S., Elasbali, A.M., Adnan, M., Alam, S., Hassan, M.I. and Pasupuleti, V.R., 2022. Therapeutic implications of caffeic acid in cancer and neurological diseases. *Frontiers in oncology*, *12*, p.860508.

Alaziqi, B., Beckitt, L., Townsend, D.J., Morgan, J., Price, R., Maerivoet, A., Madine, J., Rochester, D., Akien, G. and Middleton, D.A., 2024. Characterization of Olive Oil

Phenolic Extracts and Their Effects on the Aggregation of the Alzheimer's Amyloid-β Peptide and Tau. *ACS omega*, *9*(30), pp.32557-32578.

Ali, A.H., 2022. High-performance liquid chromatography (HPLC): A review. *Annals of advances in chemistry*, *6*(1), pp.010-020.

Allen, B., Ingram, E., Takao, M., Smith, M.J., Jakes, R., Virdee, K., Yoshida, H., Holzer, M., Craxton, M., Emson, P.C. and Atzori, C., 2002. Abundant tau filaments and nonapoptotic neurodegeneration in transgenic mice expressing human P301S tau protein. *Journal of Neuroscience*, *22*(21), pp.9340-9351.

Alves, F.C., Coqueiro, A., Março, P.H. and Valderrama, P., 2019. Evaluation of olive oils from the Mediterranean region by UV–Vis spectroscopy and Independent Component Analysis. *Food chemistry*, *273*, pp.124-129.

Alzheimer's Research Uk. 2018. Statistics about Dementia [Online]. Available: https://www.dementiastatistics.org/statistics-about-alzheimers-research-uk/ [Accessed 1st August 2019].

Alzheimer's Association, 2019. 2019 Alzheimer's disease facts and figures. *Alzheimer's & dementia*, *15*(3), pp.321-387.

Amiot-Carlin, M.J., 2014. Olive oil and health effects: from epidemiological studies to the molecular mechanisms of phenolic fraction. *OCL Oilseeds and fats crops and lipids*, *21*(5), pp.1-8.

Anand, P. and Singh, B., 2013. A review on cholinesterase inhibitors for Alzheimer's disease. *Archives of pharmacal research*, *36*, pp.375-399.

Andrade, S., Pereira, M.C. and Loureiro, J.A., 2023. Caffeic acid loaded into engineered lipid nanoparticles for Alzheimer's disease therapy. *Colloids and Surfaces B: Biointerfaces*, *225*, p.113270.

Andreoni, N. and Fiorentini, R., 1995. Determiazione di composti fenolici in oli di oliva. *Rivista Italiana delle Sostanze Grasse*, *72*(4), pp.163-164.

Angeloni, C., Giusti, L. and Hrelia, S., 2019. New neuroprotective perspectives in fighting oxidative stress and improving cellular energy metabolism by oleocanthal. *Neural regeneration research*, *14*(7), pp.1217-1218.

Aparicio, R. and Alonso, V., 1994. Characterization of virgin olive oils by SEXIA expert system. *Progress in lipid research*, *33*(1-2), pp.29-38.

Augustinack, J.C., Schneider, A., Mandelkow, E.M. and Hyman, B.T., 2002. Specific tau phosphorylation sites correlate with severity of neuronal cytopathology in Alzheimer's disease. *Acta neuropathologica*, *103*, pp.26-35.

Badawy, M.E., El-Nouby, M.A. and Marei, A.E.S.M., 2018. Development of a Solid-Phase Extraction (SPE) Cartridge Based on Chitosan-Metal Oxide Nanoparticles (Ch-MO NPs) for Extraction of Pesticides from Water and Determination by HPLC. *International journal of analytical chemistry*, *2018*(1), p.3640691.

Ballatore, C., Lee, V.M.Y. and Trojanowski, J.Q., 2007. Tau-mediated neurodegeneration in Alzheimer's disease and related disorders. *Nature reviews neuroscience*, *8*(9), pp.663-672.

Bamberger, M.E., Harris, M.E., McDonald, D.R., Husemann, J. and Landreth, G.E., 2003. A cell surface receptor complex for fibrillar β-amyloid mediates microglial activation. *Journal of Neuroscience*, *23*(7), pp.2665-2674.

Bastrup, J., 2019. Molecular Complexity of Senile Plaques in Alzheimer's Disease: Can it be Modulated by a Targeted Antibody?.

Bayram, B., Esatbeyoglu, T., Schulze, N., Ozcelik, B., Frank, J. and Rimbach, G., 2012. Comprehensive analysis of polyphenols in 55 extra virgin olive oils by HPLC-ECD and their correlation with antioxidant activities. *Plant Foods for Human Nutrition*, *67*, pp.326-336.

Bergeron, C., Ranalli, P.J. and Miceli, P.N., 1987. Amyloid angiopathy in Alzheimer's disease. *Canadian journal of neurological sciences*, *14*(4), pp.564-569.

Bhati, C., Minocha, N., Purohit, D., Kumar, S., Makhija, M. and Saini, S., 2022. High performance liquid chromatography: Recent patents and advancement. *Biomedical and Pharmacology Journal*, *15*(2), pp.729-746.

Bianco, A., Buiarelli, F., Cartoni, G., Coccioli, F., Jasionowska, R. and Margherita, P., 2003. Analysis by liquid chromatography-tandem mass spectrometry of biophenolic compounds in virgin olive oil, Part II. *Journal of Separation Science*, *26*(5), pp.417-424.

Bieschke, J., Russ, J., Friedrich, R.P., Ehrnhoefer, D.E., Wobst, H., Neugebauer, K. and Wanker, E.E., 2010. EGCG remodels mature α-synuclein and amyloid-β fibrils and reduces cellular toxicity. *Proceedings of the National Academy of Sciences*, *107*(17), pp.7710-7715.

Bigi, A., Cascella, R., Chiti, F. and Cecchi, C., 2022. Amyloid fibrils act as a reservoir of soluble oligomers, the main culprits in protein deposition diseases. *BioEssays*, *44*(11), p.2200086.

Bondi, M.L., Montana, G., Craparo, E.F., Picone, P., Capuano, G., Carlo, M.D. and Giammona, G., 2009. Ferulic acid-loaded lipid nanostructures as drug delivery systems for Alzheimer's disease: Preparation, characterization and cytotoxicity studies. *Current Nanoscience*, *5*(1), pp.26-32.

Borges, A., de Freitas, V., Mateus, N., Fernandes, I. and Oliveira, J., 2020. Solid lipid nanoparticles as carriers of natural phenolic compounds. *Antioxidants*, *9*(10), p.998.

Borisov, A.S., Hazendonk, P. and Hayes, P.G., 2010. Solid-state nuclear magnetic resonance spectroscopy: A review of modern techniques and applications for inorganic polymers. *Journal of Inorganic and Organometallic Polymers and Materials*, *20*, pp.183-212.

Braak, E., Strotkamp, B. and Braak, H., 1991. Parvalbumin-immunoreactive structures in the hippocampus of the human adult. *Cell and tissue research*, *264*(1), pp.33-48.

Braak, H. & Braak, E. 1995. Staging of alzheimer's disease-related neurofibrillary changes. *Neurobiology of Aging*, *16*, 271-278.

Braak, H. and Braak, E., 1991. Demonstration of amyloid deposits and neurofibrillary changes in whole brain sections. *Brain pathology*, *1*(3), pp.213-216.

Braak, H. and Braak, E., 1991. Neuropathological stageing of Alzheimer-related changes. *Acta neuropathologica*, *82*(4), pp.239-259.

Breijyeh, Z. and Karaman, R., 2020. Comprehensive review on Alzheimer's disease: causes and treatment. *Molecules*, *25*(24), p.5789.

Brenes, M., García, A., García, P. and Garrido, A., 2000. Rapid and complete extraction of phenols from olive oil and determination by means of a coulometric electrode array system. *Journal of agricultural and food chemistry*, *48*(11), pp.5178-5183.

Brenes, M., García, A., García, P., Rios, J.J. and Garrido, A., 1999. Phenolic compounds in Spanish olive oils. *Journal of Agricultural and Food Chemistry*, *47*(9), pp.3535-3540.

Brenes, M., Hidalgo, F.J., García, A., Rios, J.J., García, P., Zamora, R. and Garrido, A., 2000. Pinoresinol and 1-acetoxypinoresinol, two new phenolic compounds identified in olive oil. *Journal of the American Oil Chemists' Society*, *77*, pp.715-720.

Brody, D.L. and Esparza, T.J., 2014. P4-260: AMYLOID-BETA OLIGOMERS FROM HUMAN ALZHEIMER'S DISEASE BRAIN LYSATES. *Alzheimer's & Dementia*, *10*, pp.P880-P881.

Bucciantini, M., Leri, M., Nardiello, P., Casamenti, F. and Stefani, M., 2021. Olive polyphenols: Antioxidant and anti-inflammatory properties. *Antioxidants*, *10*(7), p.1044.

Buell, A.K., Dobson, C.M., Knowles, T.P. and Welland, M.E., 2010. Interactions between amyloidophilic dyes and their relevance to studies of amyloid inhibitors. *Biophysical journal*, *99*(10), pp.3492-3497.

Bulic, B., Pickhardt, M., Schmidt, B., Mandelkow, E.M., Waldmann, H. and Mandelkow, E., 2009. Development of tau aggregation inhibitors for Alzheimer's disease. *Angewandte Chemie International Edition*, *48*(10), pp.1740-1752.

Bulotta, S., Celano, M., Lepore, S.M., Montalcini, T., Pujia, A. and Russo, D., 2014. Beneficial effects of the olive oil phenolic components oleuropein and hydroxytyrosol: focus on protection against cardiovascular and metabolic diseases. *Journal of translational medicine*, *12*, pp.1-9.

Bunu, S.J., Otele, D., Alade, T. and Dodoru, R.T., 2020. Determination of serum DNA purity among patients undergoing antiretroviral therapy using NanoDrop-1000 spectrophotometer and polymerase chain reaction. *Biomedical and Biotechnology Research Journal (BBRJ)*, *4*(3), pp.214-219.

Bursavich, M.G., Gilbert, A.M., Lombardi, S., Georgiadis, K.E., Reifenberg, E., Flannery, C.R. and Morris, E.A., 2007. Synthesis and evaluation of aryl thioxothiazolidinone inhibitors of ADAMTS-5 (Aggrecanase-2). *Bioorganic & medicinal chemistry letters*, *17*(5), pp.1185-1188.

Butterfield, D.A., Di Domenico, F. and Barone, E., 2014. Elevated risk of type 2 diabetes for development of Alzheimer disease: a key role for oxidative stress in brain. *Biochimica et Biophysica Acta (BBA)-Molecular Basis of Disease*, *1842*(9), pp.1693-1706.

Campisi, A., Sposito, G., Pellitteri, R., Santonocito, D., Bisicchia, J., Raciti, G., Russo, C., Nardiello, P., Pignatello, R., Casamenti, F. and Puglia, C., 2022. Effect of unloaded and curcumin-loaded solid lipid nanoparticles on tissue transglutaminase isoforms expression levels in an experimental model of Alzheimer's disease. *Antioxidants*, *11*(10), p.1863.

Capriotti, A.L., Cavaliere, C., Crescenzi, C., Foglia, P., Nescatelli, R., Samperi, R. and Laganà, A., 2014. Comparison of extraction methods for the identification and quantification of polyphenols in virgin olive oil by ultra-HPLC-QToF mass spectrometry. *Food Chemistry*, *158*, pp.392-400.

Caramia, G., Gori, A., Valli, E. and Cerretani, L., 2012. Virgin olive oil in preventive medicine: From legend to epigenetics. *European Journal of Lipid Science and Technology*, *114*(4), pp.375-388.

Carluccio, M.A., Siculella, L., Ancora, M.A., Massaro, M., Scoditti, E., Storelli, C., Visioli, F., Distante, A. and De Caterina, R., 2003. Olive oil and red wine antioxidant polyphenols inhibit endothelial activation: antiatherogenic properties of Mediterranean diet phytochemicals. *Arteriosclerosis, thrombosis, and vascular biology*, *23*(4), pp.622-629.

Carrasco Pancorbo, A., Cruces-Blanco, C., Segura Carretero, A. and Fernández Gutiérrez, A., 2004. Sensitive determination of phenolic acids in extra-virgin olive oil by capillary zone electrophoresis. *Journal of Agricultural and Food Chemistry*, *52*(22), pp.6687-6693.

Carrera-González, M.P., Ramírez-Expósito, M.J., Mayas, M.D. and Martínez-Martos, J.M., 2013. Protective role of oleuropein and its metabolite hydroxytyrosol on cancer. *Trends in food science & technology*, *31*(2), pp.92-99.

Carver, J.A., Duggan, P.J., Ecroyd, H., Liu, Y., Meyer, A.G. and Tranberg, C.E., 2010. Carboxymethylated-κ-casein: A convenient tool for the identification of polyphenolic inhibitors of amyloid fibril formation. *Bioorganic & medicinal chemistry*, *18*(1), pp.222-228.

Casamenti, F. and Stefani, M., 2017. Olive polyphenols: New promising agents to combat aging-associated neurodegeneration. *Expert Review of Neurotherapeutics*, *17*(4), pp.345-358.

Casamenti, F., Grossi, C., Rigacci, S., Pantano, D., Luccarini, I. and Stefani, M., 2015. Oleuropein aglycone: a possible drug against degenerative conditions. In vivo evidence of its effectiveness against Alzheimer's disease. *Journal of Alzheimer's Disease*, *45*(3), pp.679-688.

Castaner, O., Covas, M.I., Khymenets, O., Nyyssonen, K., Konstantinidou, V., Zunft, H.F., de la Torre, R., Munoz-Aguayo, D., Vila, J. and Fito, M., 2012. Protection of LDL from oxidation by olive oil polyphenols is associated with a downregulation of CD40-ligand expression and its downstream products in vivo in humans. *The American journal of clinical nutrition*, *95*(5), pp.1238-1244.

Castellano, J.M., Kim, J., Stewart, F.R., Jiang, H., DeMattos, R.B., Patterson, B.W., Fagan, A.M., Morris, J.C., Mawuenyega, K.G., Cruchaga, C. and Goate, A.M., 2011. Human apoE isoforms differentially regulate brain amyloid-β peptide clearance. *Science translational medicine*, *3*(89), pp.89ra57-89ra57.

Chan, E.W.C., Tangah, J., Baba, S., Chan, H.T., Kainuma, M. and Inoue, T., 2018. Caesalpinia crista: A coastal woody climber with promising therapeutic values. *Journal of Applied Pharmaceutical Science*, *8*(3), pp.133-140.

Charisiadis, P., Primikyri, A., Exarchou, V., Tzakos, A. and Gerothanassis, I.P., 2011. Unprecedented ultra-high-resolution hydroxy group 1H NMR spectroscopic analysis of plant extracts. *Journal of natural products*, *74*(11), pp.2462-2466.

Charoenprasert, S. and Mitchell, A., 2012. Factors influencing phenolic compounds in table olives (Olea europaea). *Journal of agricultural and food chemistry*, *60*(29), pp.7081-7095.

Chaudhary, H., Meister, S.W., Zetterberg, H., Löfblom, J. and Lendel, C., 2020. Dissecting the structural organization of multiprotein amyloid aggregates using a bottom-up approach. *ACS chemical neuroscience*, *11*(10), pp.1447-1457.

Chen, C., Ai, Q.D. and Wei, Y.H., 2021. Potential role of hydroxytyrosol in neuroprotection. *Journal of Functional Foods*, *82*, p.104506.

Chen, H., Kwong, J.C., Copes, R., Tu, K., Villeneuve, P.J., Van Donkelaar, A., Hystad, P., Martin, R.V., Murray, B.J., Jessiman, B. and Wilton, A.S., 2017. Living near major roads and the incidence of dementia, Parkinson's disease, and multiple sclerosis: a population-based cohort study. *The Lancet*, *389*(10070), pp.718-726.

Chen, S., Townsend, K., Goldberg, T.E., Davies, P. and Conejero-Goldberg, C., 2011. MAPT isoforms: differential transcriptional profiles related to 3R and 4R splice variants. *Journal of Alzheimer's disease*, *22*(4), pp.1313-1329.

Chen, Y., Zhao, S., Fan, Z., Li, Z., Zhu, Y., Shen, T., Li, K., Yan, Y., Tian, J., Liu, Z. and Zhang, B., 2021. Metformin attenuates plaque-associated tau pathology and reduces amyloid-β burden in APP/PS1 mice. *Alzheimer's research & therapy*, *13*, pp.1-13.

Chethana, K.R., Sasidhar, B.S., Naika, M. and Keri, R.S., 2018. Phytochemical composition of Caesalpinia crista extract as potential source for inhibiting cholinesterase and β-amyloid aggregation: Significance to Alzheimer's disease. *Asian pacific journal of tropical biomedicine*, *8*(10), pp.500-512.

Chiang, N.N., Lin, T.H., Teng, Y.S., Sun, Y.C., Chang, K.H., Lin, C.Y., Hsieh-Li, H.M., Su, M.T., Chen, C.M. and Lee-Chen, G.J., 2021. Flavones 7, 8-DHF, quercetin, and apigenin against Tau toxicity via activation of TRKB signaling in ΔK280 TauRD-DsRed SH-SY5Y cells. *Frontiers in Aging Neuroscience*, *13*, p.758895.

Choi, S.H., Kim, Y.H., Hebisch, M., Sliwinski, C., Lee, S., D'Avanzo, C., Chen, H., Hooli, B., Asselin, C., Muffat, J. and Klee, J.B., 2014. A three-dimensional human neural cell culture model of Alzheimer's disease. *Nature*, *515*(7526), pp.274-278.

Christophoridou, S. and Dais, P., 2009. Detection and quantification of phenolic compounds in olive oil by high resolution 1H nuclear magnetic resonance spectroscopy. *Analytica Chimica Acta*, *633*(2), pp.283-292.

Chunhui, H., Dilin, X., Ke, Z., Jieyi, S., Sicheng, Y., Dapeng, W., Qinwen, W. and Wei, C., 2018. A11-positive β-amyloid oligomer preparation and assessment using dot blotting analysis. *Journal of Visualized Experiments: JoVE*, (135), p.57592.

Churches, Q.I., Caine, J., Cavanagh, K., Epa, V.C., Waddington, L., Tranberg, C.E., Meyer, A.G., Varghese, J.N., Streltsov, V. and Duggan, P.J., 2014. Naturally occurring polyphenolic inhibitors of amyloid beta aggregation. *Bioorganic & medicinal chemistry letters*, *24*(14), pp.3108-3112.

Cicerale, S., Lucas, L. and Keast, R., 2010. Biological activities of phenolic compounds present in virgin olive oil. *International journal of molecular sciences*, *11*(2), pp.458-479.

Citron, M., 2010. Alzheimer's disease: strategies for disease modification. *Nature reviews Drug discovery*, *9*(5), pp.387-398.

Citron, M., Oltersdorf, T., Haass, C., McConlogue, L., Hung, A.Y., Seubert, P., Vigo-Pelfrey, C., Lieberburg, I. and Selkoe, D.J., 1992. Mutation of the β-amyloid precursor protein in familial Alzheimer's disease increases β-protein production. *Nature*, *360*(6405), pp.672-674.

Clogston, J.D. and Patri, A.K., 2010. Zeta potential measurement. In *Characterization of nanoparticles intended for drug delivery* (pp. 63-70). Totowa, NJ: Humana press.

Coelho, T., Merlini, G., Bulawa, C.E., Fleming, J.A., Judge, D.P., Kelly, J.W., Maurer, M.S., Planté-Bordeneuve, V., Labaudinière, R., Mundayat, R. and Riley, S., 2016. Mechanism of action and clinical application of tafamidis in hereditary transthyretin amyloidosis. *Neurology and therapy*, *5*, pp.1-25.

Convertino, M., Pellarin, R., Catto, M., Carotti, A. and Caflisch, A., 2009. 9, 10-Anthraquinone hinders β-aggregation: How does a small molecule interfere with Aβ-peptide amyloid fibrillation?. *Protein Science*, *18*(4), pp.792-800.

Conway, K.A., Rochet, J.C., Bieganski, R.M. and Lansbury Jr, P.T., 2001. Kinetic stabilization of the α-synuclein protofibril by a dopamine-α-synuclein adduct. *Science*, *294*(5545), pp.1346-1349.

Coradini, K., Lima, F.O., Oliveira, C.M., Chaves, P.S., Athayde, M.L., Carvalho, L.M. and Beck, R.C.R., 2014. Co-encapsulation of resveratrol and curcumin in lipid-core nanocapsules improves their in vitro antioxidant effects. *European journal of pharmaceutics and biopharmaceutics*, *88*(1), pp.178-185.

Corder, E.H., Saunders, A.M., Strittmatter, W.J., Schmechel, D.E., Gaskell, P.C., Small, G., Roses, A.D., Haines, J.L. and Pericak-Vance, M.A., 1993. Gene dose of apolipoprotein E type 4 allele and the risk of Alzheimer's disease in late onset families. *Science*, *261*(5123), pp.921-923.

Corona, G., Spencer, J.P. and Dessi, M.A., 2009. Extra virgin olive oil phenolics: absorption, metabolism, and biological activities in the GI tract. *Toxicology and industrial health*, *25*(4-5), pp.285-293.

Cortesi, N. and Fedeli, E., 1983. I composti polari di oli di oliva vergine. I. *Rivista Italiana delle Sostanze Grasse*, *60*(6), pp.341-351.

Cortesi, N., Azzolini, M., Rovellini, P. and Fedeli, E., 1995. I componenti minori polari degli oli vergini di oliva: ipotesi di struttura mediante LC-MS. *Rivista Italiana delle Sostanze Grasse*, *72*(6), pp.241-251.

Crary, J.F., Trojanowski, J.Q., Schneider, J.A., Abisambra, J.F., Abner, E.L., Alafuzoff, I., Arnold, S.E., Attems, J., Beach, T.G., Bigio, E.H. and Cairns, N.J., 2014. Primary age-related tauopathy (PART): a common pathology associated with human aging. *Acta neuropathologica*, *128*, pp.755-766.

Crimins, J.L., Pooler, A., Polydoro, M., Luebke, J.I. and Spires-Jones, T.L., 2013. The intersection of amyloid beta and tau in glutamatergic synaptic dysfunction and collapse in Alzheimer's disease. *Ageing research reviews*, *12*(3), pp.757-763.

Cummings, J., Aisen, P.S., DuBois, B., Frölich, L., Jack, C.R., Jones, R.W., Morris, J.C., Raskin, J., Dowsett, S.A. and Scheltens, P., 2016. Drug development in Alzheimer's disease: the path to 2025. *Alzheimer's research & therapy*, *8*, pp.1-12.

Daccache, A., Lion, C., Sibille, N., Gerard, M., Slomianny, C., Lippens, G. and Cotelle, P., 2011. Oleuropein and derivatives from olives as Tau aggregation inhibitors. *Neurochemistry international*, *58*(6), pp.700-707.

Dais, P. and Boskou, D., 2009. Detection and quantification of phenolic compounds in olive oil, olives, and biological fluids. *Detect. Quantif. Phenol. Compd*, pp.55-107.

Dal Prà, I., Chiarini, A., Gui, L., Chakravarthy, B., Pacchiana, R., Gardenal, E., Whitfield, J.F. and Armato, U., 2015. Do astrocytes collaborate with neurons in spreading the "infectious" Aβ and Tau drivers of Alzheimer's disease?. *The Neuroscientist*, *21*(1), pp.9-29.

De Bock, M., Thorstensen, E.B., Derraik, J.G., Henderson, H.V., Hofman, P.L. and Cutfield, W.S., 2013. Human absorption and metabolism of oleuropein and hydroxytyrosol ingested as olive (O lea europaea L.) leaf extract. *Molecular nutrition & food research*, *57*(11), pp.2079-2085.

de Bruijn, R.F. and Ikram, M.A., 2014. Cardiovascular risk factors and future risk of Alzheimer's disease. *BMC medicine*, *12*, pp.1-9.

De Felice, F.G., Wu, D., Lambert, M.P., Fernandez, S.J., Velasco, P.T., Lacor, P.N., Bigio, E.H., Jerecic, J., Acton, P.J., Shughrue, P.J. and Chen-Dodson, E., 2008. Alzheimer's disease-type neuronal tau hyperphosphorylation induced by Aβ oligomers. *Neurobiology of aging*, *29*(9), pp.1334-1347.

de Fernandez, M.D.L.A., SotoVargas, V.C. and Silva, M.F., 2014. Phenolic compounds and antioxidant capacity of monovarietal olive oils produced in Argentina. *Journal of the American Oil Chemists' Society*, *91*(12), pp.2021-2033.

de la Torre, R., 2008. Bioavailability of olive oil phenolic compounds in humans. *Inflammopharmacology*, *16*(5), pp.245-247.

De la Torre-Carbot, K., Jauregui, O., Gimeno, E., Castellote, A.I., Lamuela-Raventós, R.M. and López-Sabater, M.C., 2005. Characterization and quantification of phenolic compounds in olive oils by solid-phase extraction, HPLC-DAD, and HPLC-MS/MS. *Journal of agricultural and food chemistry*, *53*(11), pp.4331-4340.

Deshpande, M.M., 2020. Analytical, Bioanalytical, Stability-Indicating Methods: Key Part of Regulatory Submissions. In *Analytical Chemistry-Advancement, Perspectives and Applications*. IntechOpen.

Dey, P.M. and Harborne, J.B., 1989. Methods in plant biochemistry: Plant phenolics. *Academic Press Ltd, London*, *1*, p.552.

Di Gaspero, M., Ruzza, P., Hussain, R., Honisch, C., Biondi, B., Siligardi, G., Marangon, M., Curioni, A. and Vincenzi, S., 2020. The secondary structure of a major wine protein is modified upon interaction with polyphenols. *Molecules*, *25*(7), p.1646.

Dickson, D.W., Crystal, H.A., Mattiace, L.A., Masur, D.M., Blau, A.D., Davies, P., Yen, S.H. and Aronson, M.K., 1992. Identification of normal and pathological aging in prospectively studied nondemented elderly humans. *Neurobiology of aging*, *13*(1), pp.179-189.

Dinda, B., Dinda, M., Kulsi, G., Chakraborty, A. and Dinda, S., 2019. Therapeutic potentials of plant iridoids in Alzheimer's and Parkinson's diseases: A review. *European Journal of Medicinal Chemistry*, *169*, pp.185-199.

Diomede, L., Rigacci, S., Romeo, M., Stefani, M. and Salmona, M., 2013. Oleuropein aglycone protects transgenic C. elegans strains expressing Aβ42 by reducing plaque load and motor deficit. *PLoS one*, *8*(3), p.e58893.

Dixit, R., Ross, J.L., Goldman, Y.E. and Holzbaur, E.L., 2008. Differential regulation of dynein and kinesin motor proteins by tau. *Science*, *319*(5866), pp.1086-1089.

Dobiáš, P., Pavlíková, P., Adam, M., Eisner, A., Beňová, B. and Ventura, K., 2010. Comparison of pressurised fluid and ultrasonic extraction methods for analysis of plant antioxidants and their antioxidant capacity. *Central European Journal of Chemistry, 8*(1), pp.87-95.

Doig, A.J. and Derreumaux, P., 2015. Inhibition of protein aggregation and amyloid formation by small molecules. *Current opinion in structural biology*, *30*, pp.50-56.

Downey, J., Lam, J.C., Li, V.O. and Gozes, I., 2022. Somatic mutations and Alzheimer's disease. *Journal of Alzheimer's Disease*, *90*(2), pp.475-493.

Duan, Y., Dhar, A., Patel, C., Khimani, M., Neogi, S., Sharma, P., Kumar, N.S. and Vekariya, R.L., 2020. A brief review on solid lipid nanoparticles: Part and parcel of contemporary drug delivery systems. *RSC advances*, *10*(45), pp.26777-26791.

Dubbelman, M.A., Mimmack, K.J., Sprague, E.H., Amariglio, R.E., Vannini, P. and Marshall, G.A., 2023. Decline in everyday functioning in relation to cerebral tau burden across the clinical spectrum of Alzheimer's disease. *Alzheimer's & Dementia*, *19*, p.e075056.

Dujardin, S. and Hyman, B.T., 2020. Tau prion-like propagation: state of the art and current challenges. *Tau Biology*, pp.305-325.

Eccleston, J., Microemulsions, in J, Swarbrick, J.C. Boylan (Eds)., 1994. Encyclopedia of Pharmaceutical Technology. *NewYork; Marcel Dekker*, pp. 375-421.

Ehrnhoefer, D.E., Bieschke, J., Boeddrich, A., Herbst, M., Masino, L., Lurz, R., Engemann, S., Pastore, A. and Wanker, E.E., 2008. EGCG redirects amyloidogenic polypeptides into unstructured, off-pathway oligomers. *Nature structural & molecular biology*, *15*(6), pp.558-566.

Elena, B., Lesage, A., Steuernagel, S., Böckmann, A. and Emsley, L., 2005. Proton to carbon-13 INEPT in solid-state NMR spectroscopy. *Journal of the American Chemical Society*, *127*(49), pp.17296-17302.

Elobeid, A., Libard, S., Leino, M., Popova, S.N. and Alafuzoff, I., 2016. Altered proteins in the aging brain. *Journal of Neuropathology & Experimental Neurology*, *75*(4), pp.316-325.

Erol-Dayi, Ö., Arda, N. and Erdem, G., 2012. Protective effects of olive oil phenolics and gallic acid on hydrogen peroxide-induced apoptosis. *European journal of nutrition*, *51*, pp.955-960.

Eschmann, N.A., Georgieva, E.R., Ganguly, P., Borbat, P.P., Rappaport, M.D., Akdogan, Y., Freed, J.H., Shea, J.E. and Han, S., 2017. Signature of an aggregation-prone conformation of tau. *Scientific Reports*, *7*(1), p.44739.

Farré, M., Picó, Y. and Barceló, D., 2019. Direct analysis in real-time high-resolution mass spectrometry as a valuable tool for polyphenols profiling in olive oil. *Analytical Methods*, *11*(4), pp.472-482.

Favati, F., Caporale, G. and Bertuccioli, M., 1994. Rapid determination of phenol content in extra virgin olive oil. *Grasas y Aceites*, *45*(1-2), pp.68-70.

Favati, F., Carporale, G., Monteleone, E. and Bertuccioli, M., 1995. Food flavors: generation, analysis and process influence. Charalamous G (ed), *Elsevier, Amsterdam*, pp. 429-438.

Fedeli, E., in: Ralph, E., Holman, T. (Eds.)., 1997. Progress on Chemistry of fats and other lipids, *Pergamon Press, Paris*, pp. 15–74.

Ferhat, R., Lekbir, A., Ouadah, H., Kahoul, M.A., Khlalfa, L., Laroui, S. and Alloui-Lombarkia, O., 2017. Effect of extraction solvent on total phenolic content, total flavonoid content, and antioxidant activities of Algerian pomace olive oil. *International Food Research Journal*, *24*(6).

Fernandes, F., Dias-Teixeira, M., Delerue-Matos, C. and Grosso, C., 2021. Critical review of lipid-based nanoparticles as carriers of neuroprotective drugs and extracts. *Nanomaterials*, *11*(3), p.563.

Ferreira, S.T. and Klein, W.L., 2011. The Aβ oligomer hypothesis for synapse failure and memory loss in Alzheimer's disease. *Neurobiology of learning and memory*, *96*(4), pp.529-543.

Ferro, M.D., Santos, S.A., Silvestre, A.J. and Duarte, M.F., 2019. Chromatographic separation of phenolic compounds from extra virgin olive oil: Development and validation of a new method based on a biphenyl HPLC column. *International journal of molecular sciences*, *20*(1), p.201.

Figueira, I., Menezes, R., Macedo, D., Costa, I. and Nunes dos Santos, C., 2017. Polyphenols beyond barriers: a glimpse into the brain. *Current neuropharmacology*, *15*(4), pp.562-594.

Finicelli, M., Squillaro, T., Galderisi, U. and Peluso, G., 2021. Polyphenols, the healthy brand of olive oil: Insights and perspectives. *Nutrients*, *13*(11), p.3831.

Florence, A.T., 1997. The oral absorption of micro-and nanoparticulates: neither exceptional nor unusual. *Pharmaceutical research*, *14*, pp.259-266.

Freyssin, A., Page, G., Fauconneau, B. and Bilan, A.R., 2018. Natural polyphenols effects on protein aggregates in Alzheimer's and Parkinson's prion-like diseases. *Neural regeneration research*, *13*(6), pp.955-961.

Fuentes, E. and Palomo, I., 2014. Antiplatelet effects of natural bioactive compounds by multiple targets: Food and drug interactions. *Journal of Functional Foods*, *6*, pp.73-81.

Fuentes, E., Báez, M.E., Bravo, M., Cid, C. and Labra, F., 2012. Determination of total phenolic content in olive oil samples by UV–visible spectrometry and multivariate calibration. *Food Analytical Methods*, *5*, pp.1311-1319.

Gade Malmos, K., Blancas-Mejia, L.M., Weber, B., Buchner, J., Ramirez-Alvarado, M., Naiki, H. and Otzen, D., 2017. ThT 101: a primer on the use of thioflavin T to investigate amyloid formation. *Amyloid*, *24*(1), pp.1-16.

García-Casares, N., Gallego Fuentes, P., Barbancho, M.Á., López-Gigosos, R., García-Rodríguez, A. and Gutiérrez-Bedmar, M., 2021. Alzheimer's disease, mild cognitive impairment and Mediterranean diet. A systematic review and dose-response meta-analysis. *Journal of clinical medicine*, *10*(20), p.4642.

Garcia-Salas, P., Morales-Soto, A., Segura-Carretero, A. and Fernández-Gutiérrez, A., 2010. Phenolic-compound-extraction systems for fruit and vegetable samples. *Molecules*, *15*(12), pp.8813-8826.

García-Villalba, R., Carrasco-Pancorbo, A., Vázquez-Martín, A., Oliveras-Ferraros, C., Menéndez, J.A., Segura-Carretero, A. and Fernández-Gutiérrez, A., 2009. A 2-D-HPLC-CE platform coupled to ESI-TOF-MS to characterize the phenolic fraction in olive oil. *Electrophoresis*, *30*(15), pp.2688-2701.

Gatt, L., Lia, F., Zammit-Mangion, M., Thorpe, S.J. and Schembri-Wismayer, P., 2021. First profile of phenolic compounds from maltese extra virgin olive oils using liquid-liquid extraction and liquid chromatography-mass spectrometry. *Journal of Oleo Science*, *70*(2), pp.145-153.

Gilbert-López, B., Valencia-Reyes, Z.L., Yufra-Picardo, V.M., García-Reyes, J.F., Ramos-Martos, N. and Molina-Díaz, A., 2014. Determination of polyphenols in commercial extra virgin olive oils from different origins (Mediterranean and South American countries) by liquid chromatography–electrospray time-of-flight mass spectrometry. *Food Analytical Methods*, *7*, pp.1824-1833.

Goate, A., Chartier-Harlin, M.C., Mullan, M., Brown, J., Crawford, F., Fidani, L., Giuffra, L., Haynes, A., Irving, N., James, L. and Mant, R., 1991. Segregation of a missense mutation in the amyloid precursor protein gene with familial Alzheimer's disease. *Nature*, *349*(6311), pp.704-706.

Godbolt, A.K., Beck, J.A., Collinge, J.C., Cipolotti, L., Fox, N.C. and Rossor, M.N., 2006. A second family with familial AD and the V717L APP mutation has a later age at onset. *Neurology*, *66*(4), pp.611-612.

Gotz, J., Chen, F.V., Van Dorpe, J. and Nitsch, R., 2001. Formation of neurofibrillary tangles in P301L tau transgenic mice induced by Aβ42 fibrils. *Science*, *293*(5534), pp.1491-1495.

Götz, J., Streffer, J.R., David, D., Schild, A., Hoerndli, F., Pennanen, L., Kurosinski, P. and Chen, F., 2004. Transgenic animal models of Alzheimer's disease and related disorders: histopathology, behavior and therapy. *Molecular psychiatry*, *9*(7), pp.664-683.

Grasse, E.K., Torcasio, M.H. and Smith, A.W., 2016. Teaching UV–Vis spectroscopy with a 3D-printable smartphone spectrophotometer. *Journal of Chemical Education*, *93*(1), pp.146-151.

Graverini, G., Piazzini, V., Landucci, E., Pantano, D., Nardiello, P., Casamenti, F., Pellegrini-Giampietro, D.E., Bilia, A.R. and Bergonzi, M.C., 2018. Solid lipid nanoparticles for delivery of andrographolide across the blood-brain barrier: in vitro and in vivo evaluation. *Colloids and Surfaces B: Biointerfaces*, *161*, pp.302-313.

Greenfield, N.J. and Fasman, G.D., 1969. Computed circular dichroism spectra for the evaluation of protein conformation. *Biochemistry*, *8*(10), pp.4108-4116.

Greenfield, N.J., 2006. Using circular dichroism collected as a function of temperature to determine the thermodynamics of protein unfolding and binding interactions. *Nature protocols*, *1*(6), pp.2527-2535.

Greenfield, N.J., 2006. Using circular dichroism spectra to estimate protein secondary structure. *Nature protocols*, *1*(6), pp.2876-2890.

Gregory, S., Pullen, H., Ritchie, C.W., Shannon, O.M., Stevenson, E.J. and Muniz-Terrera, G., 2023. Mediterranean diet and structural neuroimaging biomarkers of Alzheimer's and cerebrovascular disease: a systematic review. *Experimental gerontology*, *172*, p.112065.

Grewal, R., Reutzel, M., Dilberger, B., Hein, H., Zotzel, J., Marx, S., Tretzel, J., Sarafeddinov, A., Fuchs, C. and Eckert, G.P., 2020. Purified oleocanthal and ligstroside protect against mitochondrial dysfunction in models of early Alzheimer's disease and brain ageing. *Experimental neurology*, *328*, p.113248.

Grossi, C., Rigacci, S., Ambrosini, S., Ed Dami, T., Luccarini, I., Traini, C., Failli, P., Berti, A., Casamenti, F. and Stefani, M., 2013. The polyphenol oleuropein aglycone protects TgCRND8 mice against Aß plaque pathology. *PloS one*, *8*(8), p.e71702.

Gu, Y., Du, Y., Wang, W., Fang, X., Li, Z. and Zhao, L., 2023. Enantioselective inorganic nanomaterials with near-infrared circular-polarized-activated photothermal response. *Chemical Engineering Journal*, *472*, p.144873.

Guasch-Ferré, M., Hruby, A., Salas-Salvadó, J., Martínez-González, M.A., Sun, Q., Willett, W.C. and Hu, F.B., 2015. Olive oil consumption and risk of type 2 diabetes in US women. *The American journal of clinical nutrition*, *102*(2), pp.479-486.

Gulisano, W., 2018. A renewed vision for Amyloid beta and tau in Alzheimer s disease pathophysiology.

Guo, X., Tresserra-Rimbau, A., Estruch, R., Martínez-González, M.A., Medina-Remón, A., Fitó, M., Corella, D., Salas-Salvadó, J., Portillo, M.P., Moreno, J.J. and Pi-Sunyer, X., 2017. Polyphenol levels are inversely correlated with body weight and obesity in an elderly population after 5 years of follow up (the randomised PREDIMED study). *Nutrients*, *9*(5), p.452.

Gutfinger, T., 1981. Polyphenols in olive oils. *Journal of the American Oil Chemists' Society*, *58*(11), pp.966-968.

Habchi, J., Chia, S., Limbocker, R., Mannini, B., Ahn, M., Perni, M., Hansson, O., Arosio, P., Kumita, J.R., Challa, P.K. and Cohen, S.I., 2017. Systematic development of small molecules to inhibit specific microscopic steps of Aβ42 aggregation in Alzheimer's disease. *Proceedings of the National Academy of Sciences*, *114*(2), pp.E200-E208.

Hachani, K., Othmani, F., Essam, M., Akhtar, M.J. and Khan, S.A., 2023. In silico studies on olive oil polyphenolic natural products to identify neuroprotective lead compounds beneficial in the treatment of Alzheimer's disease. *Arabian Journal of Medicinal and Aromatic Plants*, *9*(1), pp.61-83.

Hadrich, F., Chamkha, M. and Sayadi, S., 2022. Protective effect of olive leaves phenolic compounds against neurodegenerative disorders: Promising alternative for Alzheimer and Parkinson diseases modulation. *Food and Chemical Toxicology*, *159*, p.112752.

Hamaguchi, T., Ono, K., Murase, A. and Yamada, M., 2009. Phenolic compounds prevent Alzheimer's pathology through different effects on the amyloid-β aggregation pathway. *The American journal of pathology*, *175*(6), pp.2557-2565.

Han, X., Xing, Z., Si, S., Yao, Y. and Zhang, Q., 2014. Electrospun grape seed polyphenols/gelatin composite fibers contained silver nanoparticles as biomaterials. *Fibers and Polymers*, *15*, pp.2572-2580.

Hao, S., Li, X., Han, A., Yang, Y., Luo, X., Fang, G., Wang, H., Liu, J. and Wang, S., 2020. Hydroxycinnamic acid from corncob and its structural analogues inhibit Aβ40 fibrillation and attenuate Aβ40-induced cytotoxicity. *Journal of Agricultural and Food Chemistry*, *68*(33), pp.8788-8796.

Härd, T. and Lendel, C., 2012. Inhibition of amyloid formation. *Journal of molecular biology*, *421*(4-5), pp.441-465.

Hasegawa, M., Smith, M.J. and Goedert, M., 1998. Tau proteins with FTDP-17 mutations have a reduced ability to promote microtubule assembly. *FEBS letters*, *437*(3), pp.207-210.

Hashem, F.M., Nasr, M. and Khairy, A., 2014. In vitro cytotoxicity and bioavailability of solid lipid nanoparticles containing tamoxifen citrate. *Pharmaceutical development and technology*, *19*(7), pp.824-832.

Haussmann, R., Homeyer, P., Sauer, C., Grey, A., Krukowski, P., Brandt, M.D., Donix, M. and Linn, J., 2023. Comorbid cerebral amyloid angiopathy in dementia and prodromal stages—Prevalence and effects on cognition. *International journal of geriatric psychiatry*, *38*(10), p.e6015.

Hawkes, C.A., Deng, L.H., Shaw, J.E., Nitz, M. and McLaurin, J., 2010. Small molecule β-amyloid inhibitors that stabilize protofibrillar structures in vitro improve cognition and pathology in a mouse model of Alzheimer's disease. *European Journal of Neuroscience*, *31*(2), pp.203-213.

Hayden, E.Y. and Teplow, D.B., 2013. Amyloid β-protein oligomers and Alzheimer's disease. *Alzheimer's research & therapy*, *5*, pp.1-11.

He, Z., Guo, J.L., McBride, J.D., Narasimhan, S., Kim, H., Changolkar, L., Zhang, B., Gathagan, R.J., Yue, C., Dengler, C. and Stieber, A., 2018. Amyloid-β plaques enhance

Alzheimer's brain tau-seeded pathologies by facilitating neuritic plaque tau aggregation. *Nature medicine*, *24*(1), pp.29-38.
Hefti, F., Goure, W.F., Jerecic, J., Iverson, K.S., Walicke, P.A. and Krafft, G.A., 2013. The case for soluble Aβ oligomers as a drug target in Alzheimer's disease. *Trends in Pharmacological Sciences*, *34*(5), pp.261-266.
Henríquez, G., Gomez, A., Guerrero, E. and Narayan, M., 2020. Potential role of natural polyphenols against protein aggregation toxicity: in vitro, in vivo, and clinical studies. *ACS Chemical Neuroscience*, *11*(19), pp.2915-2934.
Hernáez, Á., Fernández-Castillejo, S., Farràs, M., Catalán, Ú., Subirana, I., Montes, R., Solà, R., Muñoz-Aguayo, D., Gelabert-Gorgues, A., Díaz-Gil, Ó. and Nyyssönen, K., 2014. Olive oil polyphenols enhance high-density lipoprotein function in humans: a randomized controlled trial. *Arteriosclerosis, Thrombosis, and Vascular Biology*, *34*(9), pp.2115-2119.
Hippius, H. and Neundörfer, G., 2003. The discovery of Alzheimer's disease. *Dialogues in clinical neuroscience*, *5*(1), pp.101-108.
Hirschmann, M., Merten, C. and Thiele, C.M., 2021. Treating anisotropic artefacts in circular dichroism spectroscopy enables investigation of lyotropic liquid crystalline polyaspartate solutions. *Soft Matter*, *17*(10), pp.2849-2856.
Hohman, T.J., Chibnik, L., Bush, W.S., Jefferson, A.L., De Jaeger, P.L., Thornton-Wells, T.A., Bennett, D.A. and Schneider, J.A., 2015. GSK3β interactions with amyloid genes: an autopsy verification and extension. *Neurotoxicity research*, *28*, pp.232-238.
Holman, R.T., Lundberg, W.O. and Malkin, T. eds., 1952. Progress in the Chemistry of Fats and Other Lipids, vol. 1.
Holzwarth, G. and Doty, P., 1965. The ultraviolet circular dichroism of polypeptides1. *Journal of the American Chemical Society*, *87*(2), pp.218-228.
Hoover, B.R., Reed, M.N., Su, J., Penrod, R.D., Kotilinek, L.A., Grant, M.K., Pitstick, R., Carlson, G.A., Lanier, L.M., Yuan, L.L. and Ashe, K.H., 2010. Tau mislocalization to dendritic spines mediates synaptic dysfunction independently of neurodegeneration. *Neuron*, *68*(6), pp.1067-1081.
Hoy, S.M., 2023. Lecanemab: first approval. *Drugs*, *83*(4), pp.359-365.
Hrncirik, K. and Fritsche, S., 2004. Comparability and reliability of different techniques for the determination of phenolic compounds in virgin olive oil. *European journal of lipid science and technology*, *106*(8), pp.540-549.
https://link.springer.com/article/10.1007/s42250-022-00520-3 [Accessed 14 March 2024].
https://pubchem.ncbi.nlm.nih.gov/compound/Elenolic-acid [Accessed 2 May 2025].
https://www.google.com/search?q=caesalpinia+crista+plant+&sca_esv=a8da63474d091aac&udm=2&biw=1536&bih=703&tbs=sur%3Acl&ei=kXngZ5XoNNP97_UP4r286Qc&ved=0ahUKEwjV9Ie4j6GMAxXT_rsIHeIeL30Q4dUDCBE&uact=5&oq=caesalpinia+crista+plant+&gs_lp=EgNpbWciGWNhZXNhbHBpbmlhIGNyaXN0YSBwbGFudCAyBBAAGB5IliVQwg1Ymh9wAXgAkAEAmAG6AaAByQmqAQMwLje4AQPIAQD4AQGYAgigAvIJwgIKEAAYgAQYQxiKBcICBRAAGIAEmAMAiAYBkgcDMS43oAf8CrIHAzAuN7gH6Ak&sclient=img#vhid=HAyJ7AMkdMXjAM&vssid=mosaic [Accessed 13 February 2025].
https://www.google.com/search?q=Sorbaria+tomentosa&sca_esv=a8da63474d091aac&udm=2&source=lnt&tbs=sur:cl&sa=X&ved=2ahUKEwjHwp_dlKGMAxVVVaQEHbPwIjQQpwV6BAgBECA&biw=1536&bih=703&dpr=1.25#vhid=7aqqpMu9f0vy-M&vssid=mosaic [Accessed 13 February 2025].
https://www.thelancet.com/journals/lancet/article/PIIS0140-6736(20)32205-4/fulltext, [Accessed 12 January 2024].

Hudson, S.A., Ecroyd, H., Dehle, F.C., Musgrave, I.F. and Carver, J.A., 2009. (−)-Epigallocatechin-3-gallate (EGCG) maintains κ-casein in its pre-fibrillar state without redirecting its aggregation pathway. *Journal of molecular biology*, *392*(3), pp.689-700.

Hudson, S.A., Ecroyd, H., Kee, T.W. and Carver, J.A., 2009. The thioflavin T fluorescence assay for amyloid fibril detection can be biased by the presence of exogenous compounds. *The FEBS journal*, *276*(20), pp.5960-5972.

Huguet-Casquero, A., Moreno-Sastre, M., López-Méndez, T.B., Gainza, E. and Pedraz, J.L., 2020. Encapsulation of oleuropein in nanostructured lipid carriers: Biocompatibility and antioxidant efficacy in lung epithelial cells. *Pharmaceutics*, *12*(5), p.429.

Ittner, L.M. and Götz, J., 2011. Amyloid-β and tau—a toxic pas de deux in Alzheimer's disease. *Nature Reviews Neuroscience*, *12*(2), pp.67-72.

Ittner, L.M., Ke, Y.D. and Götz, J., 2009. Phosphorylated Tau interacts with c-Jun N-terminal kinase-interacting protein 1 (JIP1) in Alzheimer disease. *Journal of Biological Chemistry*, *284*(31), pp.20909-20916.

Jang, H., Connelly, L., Teran Arce, F., Ramachandran, S., Kagan, B.L., Lal, R. and Nussinov, R., 2013. Mechanisms for the Insertion of Toxic, Fibril-like β-Amyloid Oligomers into the Membrane. *Journal of chemical theory and computation*, *9*(1), pp.822-833.

Jellinger, K.A., Lauda, F. and Attems, J., 2007. Sporadic cerebral amyloid angiopathy is not a frequent cause of spontaneous brain hemorrhage. *European journal of neurology*, *14*(8), pp.923-928.

Ji, X., Wang, H., Zhu, M., He, Y., Zhang, H., Chen, X., Gao, W., Fu, Y. and Alzheimer's Disease Neuroimaging Initiative, 2021. Brainstem atrophy in the early stage of Alzheimer's disease: a voxel-based morphometry study. *Brain imaging and behavior*, *15*, pp.49-59.

Jiménez, M.S., Velarte, R. and Castillo, J.R., 2007. Direct determination of phenolic compounds and phospholipids in virgin olive oil by micellar liquid chromatography. *Food chemistry*, *100*(1), pp.8-14.

Jimenez-Lopez, C., Carpena, M., Lourenço-Lopes, C., Gallardo-Gomez, M., Lorenzo, J.M., Barba, F.J., Prieto, M.A. and Simal-Gandara, J., 2020. Bioactive compounds and quality of extra virgin olive oil. *Foods*, *9*(8), p.1014.

Johnson, R.L. and Mitchell, A.E., 2018. Reducing phenolics related to bitterness in table olives. *Journal of food quality*, *2018*(1), p.3193185.

Josephs, K.A., Dickson, D.W., Tosakulwong, N., Weigand, S.D., Murray, M.E., Petrucelli, L., Liesinger, A.M., Senjem, M.L., Spychalla, A.J., Knopman, D.S. and Parisi, J.E., 2017. Rates of hippocampal atrophy and presence of post-mortem TDP-43 in patients with Alzheimer's disease: a longitudinal retrospective study. *The Lancet Neurology*, *16*(11), pp.917-924.

Josephs, K.A., Whitwell, J.L., Tosakulwong, N., Weigand, S.D., Murray, M.E., Liesinger, A.M., Petrucelli, L., Senjem, M.L., Ivnik, R.J., Parisi, J.E. and Petersen, R.C., 2015. TAR DNA-binding protein 43 and pathological subtype of Alzheimer's disease impact clinical features. *Annals of neurology*, *78*(5), pp.697-709.

Joshi, P., Chia, S., Habchi, J., Knowles, T.P., Dobson, C.M. and Vendruscolo, M., 2016. A fragment-based method of creating small-molecule libraries to target the aggregation of intrinsically disordered proteins. *ACS combinatorial science*, *18*(3), pp.144-153.

Ju, Y. and Tam, K.Y., 2022. Pathological mechanisms and therapeutic strategies for Alzheimer's disease. *Neural regeneration research*, *17*(3), pp.543-549.

Justice, N.J., 2018. The relationship between stress and Alzheimer's disease. *Neurobiology of stress*, *8*, pp.127-133.

Kakkar, V., Mishra, A.K., Chuttani, K. and Kaur, I.P., 2013. Proof of concept studies to confirm the delivery of curcumin loaded solid lipid nanoparticles (C-SLNs) to brain. *International journal of pharmaceutics*, *448*(2), pp.354-359.

Kapasi, A., DeCarli, C. and Schneider, J.A., 2017. Impact of multiple pathologies on the threshold for clinically overt dementia. *Acta neuropathologica*, *134*, pp.171-186.

Kapasi, A., Yu, L., Boyle, P.A., Barnes, L.L., Bennett, D.A. and Schneider, J.A., 2020. Limbic-predominant age-related TDP-43 encephalopathy, ADNC pathology, and cognitive decline in aging. *Neurology*, *95*(14), pp.e1951-e1962.

Kayed, R., Head, E., Thompson, J.L., McIntire, T.M., Milton, S.C., Cotman, C.W. and Glabe, C.G., 2003. Common structure of soluble amyloid oligomers implies common mechanism of pathogenesis. *Science*, *300*(5618), pp.486-489.

Kent, S.A., Spires-Jones, T.L. and Durrant, C.S., 2020. The physiological roles of tau and Aβ: implications for Alzheimer's disease pathology and therapeutics. *Acta neuropathologica*, *140*(4), pp.417-447.

Kessels, H.W., Nguyen, L.N., Nabavi, S. and Malinow, R., 2010. The prion protein as a receptor for amyloid-β. *Nature*, *466*(7308), pp.E3-E4.

Khan, S.S. and Bloom, G.S., 2016. Tau: the center of a signaling nexus in Alzheimer's disease. *Frontiers in Neuroscience*, *10*, p.31.

Khoddami, A., Wilkes, M.A. and Roberts, T.H., 2013. Techniques for analysis of plant phenolic compounds. *Molecules*, *18*(2), pp.2328-2375.

Kiani, H.S., Ali, B., Al-Sadoon, M.K., Al-Otaibi, H.S. and Ali, A., 2023. Lc-ms/ms and gc-ms identification of metabolites from the selected herbs and spices, their antioxidant, anti-diabetic potential, and chemometric analysis. *Processes*, *11*(9), p.2721.

Kim, H., Park, B.S., Lee, K.G., Choi, C.Y., Jang, S.S., Kim, Y.H. and Lee, S.E., 2005. Effects of naturally occurring compounds on fibril formation and oxidative stress of β-amyloid. *Journal of agricultural and food chemistry*, *53*(22), pp.8537-8541.

Kola, A., Vigni, G., Baratto, M.C. and Valensin, D., 2023. A combined NMR and UV–Vis approach to evaluate radical scavenging activity of rosmarinic acid and other polyphenols. *Molecules*, *28*(18), p.6629.

Konijnenberg, A., Ranica, S., Narkiewicz, J., Legname, G., Grandori, R., Sobott, F. and Natalello, A., 2016. Opposite structural effects of epigallocatechin-3-gallate and dopamine binding to α-synuclein. *Analytical chemistry*, *88*(17), pp.8468-8475.

Kothawade, S.M., Buttar, H.S., Tuli, H.S. and Kaur, G., 2023. Therapeutic potential of flavonoids in the management of obesity-induced Alzheimer's disease: an overview of preclinical and clinical studies. *Naunyn-Schmiedeberg's Archives of Pharmacology*, *396*(11), pp.2813-2830.

Kovacs, G.G., Milenkovic, I., Wöhrer, A., Höftberger, R., Gelpi, E., Haberler, C., Hönigschnabl, S., Reiner-Concin, A., Heinzl, H., Jungwirth, S. and Krampla, W., 2013. Non-Alzheimer neurodegenerative pathologies and their combinations are more frequent than commonly believed in the elderly brain: a community-based autopsy series. *Acta neuropathologica*, *126*, pp.365-384.

Kreuter, J., 1991. Peroral administration of nanoparticles. *Advanced drug delivery reviews*, *7*(1), pp.71-86.

Kumar, A. and Singh, A., 2015. A review on Alzheimer's disease pathophysiology and its management: an update. *Pharmacological reports*, *67*(2), pp.195-203.

Kumar, C.S., Thangam, R., Mary, S.A., Kannan, P.R., Arun, G. and Madhan, B., 2020. Targeted delivery and apoptosis induction of trans-resveratrol-ferulic acid loaded chitosan coated folic acid conjugate solid lipid nanoparticles in colon cancer cells. *Carbohydrate Polymers*, *231*, p.115682.

Kurz, A. and Perneczky, R., 2011. Novel insights for the treatment of Alzheimer's disease. *Progress in Neuro-Psychopharmacology and Biological Psychiatry*, *35*(2), pp.373-379.

Ladiwala, A.R.A., Mora-Pale, M., Lin, J.C., Bale, S.S., Fishman, Z.S., Dordick, J.S. and Tessier, P.M., 2011. Polyphenolic glycosides and aglycones utilize opposing pathways to selectively remodel and inactivate toxic oligomers of amyloid β. *ChemBioChem*, *12*(11), pp.1749-1758.

LaFerla, F.M., Green, K.N. and Oddo, S., 2007. Intracellular amyloid-β in Alzheimer's disease. *Nature Reviews Neuroscience*, *8*(7), pp.499-509.

Lagunes, T., Herrera-Rivero, M., Hernández-Aguilar, M.E. and Aranda-Abreu, G.E., 2014. Abeta (1-42) induces abnormal alternative splicing of tau exons 2/3 in NGF-induced PC12 cells. *Anais da Academia Brasileira de Ciências*, *86*(04), pp.1927-1934.

Lan, M.Y., Liu, J.S., Wu, Y.S., Peng, C.H. and Chang, Y.Y., 2014. A novel APP mutation (D678H) in a Taiwanese patient exhibiting dementia and cerebral microvasculopathy. *Journal of Clinical Neuroscience*, *21*(3), pp.513-515.

Lane, C.A., Hardy, J. and Schott, J.M., 2018. Alzheimer's disease. *European journal of neurology*, *25*(1), pp.59-70.

Laurén, J., Gimbel, D.A., Nygaard, H.B., Gilbert, J.W. and Strittmatter, S.M., 2009. Cellular prion protein mediates impairment of synaptic plasticity by amyloid-β oligomers. *Nature*, *457*(7233), pp.1128-1132.

Leri, M., Bertolini, A., Stefani, M. and Bucciantini, M., 2021. EVOO polyphenols relieve synergistically autophagy dysregulation in a cellular model of Alzheimer's disease. *International Journal of Molecular Sciences*, *22*(13), p.7225.

Leri, M., Chaudhary, H., Iashchishyn, I.A., Pansieri, J., Svedruzic, Z.M., Gómez Alcalde, S., Musteikyte, G., Smirnovas, V., Stefani, M., Bucciantini, M. and Morozova-Roche, L.A., 2021. Natural compound from olive oil inhibits S100A9 amyloid formation and cytotoxicity: Implications for preventing Alzheimer's disease. *ACS Chemical Neuroscience*, *12*(11), pp.1905-1918.

Leri, M., Natalello, A., Bruzzone, E., Stefani, M. and Bucciantini, M., 2019. Oleuropein aglycone and hydroxytyrosol interfere differently with toxic Aβ1-42 aggregation. *Food and Chemical Toxicology*, *129*, pp.1-12.

Lerma-García, M.J., Simo-Alfonso, E.F., Chiavaro, E., Bendini, A., Lercker, G. and Cerretani, L., 2009. Study of chemical changes produced in virgin olive oils with different phenolic contents during an accelerated storage treatment. *Journal of agricultural and food chemistry*, *57*(17), pp.7834-7840.

Lesage-Meessen, L., Navarro, D., Maunier, S., Sigoillot, J.C., Lorquin, J., Delattre, M., Simon, J.L., Asther, M. and Labat, M., 2001. Simple phenolic content in olive oil residues as a function of extraction systems. *Food Chemistry*, *75*(4), pp.501-507.

Levy-Lahad, E., Wasco, W., Poorkaj, P., Romano, D.M., Oshima, J., Pettingell, W.H., Yu, C.E., Jondro, P.D., Schmidt, S.D., Wang, K. and Crowley, A.C., 1995. Candidate gene for the chromosome 1 familial Alzheimer's disease locus. *Science*, *269*(5226), pp.973-977.

Li, J. and Zhu, H.J., 2020. Liquid chromatography-tandem mass spectrometry (LC-MS/MS)-based proteomics of drug-metabolizing enzymes and transporters. *Molecules*, *25*(11), p.2718.

Li, M., Xu, W. and Su, Y., 2021. Solid-state NMR spectroscopy in pharmaceutical sciences. *TrAC Trends in Analytical Chemistry*, *135*, p.116152.

Li, W., Sperry, J.B., Crowe, A., Trojanowski, J.Q., Smith III, A.B. and Lee, V.M.Y., 2009. Inhibition of tau fibrillization by oleocanthal via reaction with the amino groups of tau. *Journal of neurochemistry*, *110*(4), pp.1339-1351.

Li, X.W., Chen, H.P., He, Y.Y., Chen, W.L., Chen, J.W., Gao, L., Hu, H.Y. and Wang, J., 2018. Effects of rich-polyphenols extract of Dendrobium loddigesii on anti-diabetic, anti-inflammatory, anti-oxidant, and gut microbiota modulation in db/db mice. *Molecules*, *23*(12), p.3245.

Lian, L.Y. and Middleton, D.A., 2001. Labelling approaches for protein structural studies by solution-state and solid-state NMR. *Progress in Nuclear Magnetic Resonance Spectroscopy*, *39*(3), pp.171-190.

Liu, J., Peng, Y., Feng, Z., Shi, W., Qu, L., Li, Y., Liu, J. and Long, J., 2014. Reloading functionally ameliorates disuse-induced muscle atrophy by reversing mitochondrial dysfunction, and similar benefits are gained by administering a combination of mitochondrial nutrients. *Free Radical Biology and Medicine*, *69*, pp.116-128.

López-Fernández, O., Domínguez, R., Pateiro, M., Munekata, P.E., Rocchetti, G. and Lorenzo, J.M., 2020. Determination of polyphenols using liquid chromatography–tandem mass spectrometry technique (LC–MS/MS): A review. *Antioxidants*, *9*(6), p.479.

Loued, S., Berrougui, H., Componova, P., Ikhlef, S., Helal, O. and Khalil, A., 2013. Extra-virgin olive oil consumption reduces the age-related decrease in HDL and paraoxonase 1 anti-inflammatory activities. *British Journal of Nutrition*, *110*(7), pp.1272-1284.

Loureiro, J.A., Andrade, S., Duarte, A., Neves, A.R., Queiroz, J.F., Nunes, C., Sevin, E., Fenart, L., Gosselet, F., Coelho, M.A. and Pereira, M.C., 2017. Resveratrol and grape extract-loaded solid lipid nanoparticles for the treatment of Alzheimer's disease. *Molecules*, *22*(2), p.277.

Lozano-Castellón, J., López-Yerena, A., Rinaldi de Alvarenga, J.F., Romero del Castillo-Alba, J., Vallverdú-Queralt, A., Escribano-Ferrer, E. and Lamuela-Raventós, R.M., 2020. Health-promoting properties of oleocanthal and oleacein: Two secoiridoids from extra-virgin olive oil. *Critical reviews in food science and nutrition*, *60*(15), pp.2532-2548.

Luccarini, I., Dami, T.E., Grossi, C., Rigacci, S., Stefani, M. and Casamenti, F., 2014. Oleuropein aglycone counteracts Aβ42 toxicity in the rat brain. *Neuroscience Letters*, *558*, pp.67-72.

Luccarini, I., Grossi, C., Rigacci, S., Coppi, E., Pugliese, A.M., Pantano, D., la Marca, G., Dami, T.E., Berti, A., Stefani, M. and Casamenti, F., 2015. Oleuropein aglycone protects against pyroglutamylated-3 amyloid-ß toxicity: biochemical, epigenetic and functional correlates. *Neurobiology of aging*, *36*(2), pp.648-663.

Luo, J., Zhu, Y., Zhu, M.X. and Hu, H., 2011. Cell-based calcium assay for medium to high throughput screening of TRP channel functions using FlexStation 3. *Journal of Visualized Experiments: JoVE*, (54), p.3149.

Ma, Q.L., Yang, F., Rosario, E.R., Ubeda, O.J., Beech, W., Gant, D.J., Chen, P.P., Hudspeth, B., Chen, C., Zhao, Y. and Vinters, H.V., 2009. β-amyloid oligomers induce phosphorylation of tau and inactivation of insulin receptor substrate via c-Jun N-terminal kinase signaling: suppression by omega-3 fatty acids and curcumin. *Journal of Neuroscience*, *29*(28), pp.9078-9089.

Mahnashi, M.H., Ayaz, M., Alqahtani, Y.S., Alyami, B.A., Shahid, M., Alqahtani, O., Kabrah, S.M., Zeb, A., Ullah, F. and Sadiq, A., 2023. Quantitative-HPLC-DAD polyphenols analysis, anxiolytic and cognition enhancing potentials of Sorbaria tomentosa Lindl. Rehder. *Journal of Ethnopharmacology*, *317*, p.116786.

Maiuolo, J., Musolino, V., Gliozzi, M., Carresi, C., Oppedisano, F., Nucera, S., Scarano, F., Scicchitano, M., Guarnieri, L., Bosco, F. and Macrì, R., 2022. The employment of genera Vaccinium, Citrus, Olea, and Cynara polyphenols for the reduction of selected anti-cancer drug side effects. *Nutrients*, *14*(8), p.1574.

Maji, S.K., Wang, L., Greenwald, J. and Riek, R., 2009. Structure–activity relationship of amyloid fibrils. *FEBS letters*, *583*(16), pp.2610-2617.

Malenica, M., Vukomanović, M., Kurtjak, M., Masciotti, V., Dal Zilio, S., Greco, S., Lazzarino, M., Krušić, V., Perčić, M., Jelovica Badovinac, I. and Wechtersbach, K., 2021. Perspectives of microscopy methods for morphology characterisation of extracellular vesicles from human biofluids. *Biomedicines*, *9*(6), p.603.

Malik, I., Iqbal, A., Gu, Y.H. and Al-Antari, M.A., 2024. Deep learning for Alzheimer's disease prediction: a comprehensive review. *Diagnostics*, *14*(12), p.1281.

Manach, C., Williamson, G., Morand, C., Scalbert, A. and Rémésy, C., 2005. Bioavailability and bioefficacy of polyphenols in humans. I. Review of 97 bioavailability studies. *The American journal of clinical nutrition*, *81*(1), pp.230S-242S.

Marranzano, M., Ray, S., Godos, J. and Galvano, F., 2018. Association between dietary flavonoids intake and obesity in a cohort of adults living in the Mediterranean area. *International journal of food sciences and nutrition*, *69*(8), pp.1020-1029.

Marrero, A.D., Quesada, A.R., Martínez-Poveda, B. and Medina, M.Á., 2024. Anti-cancer, anti-angiogenic, and anti-atherogenic potential of key phenolic compounds from virgin olive oil. *Nutrients*, *16*(9), p.1283.

Marsousi, S., Karimi-Sabet, J., Moosavian, M.A. and Amini, Y., 2019. Liquid-liquid extraction of calcium using ionic liquids in spiral microfluidics. *Chemical Engineering Journal*, *356*, pp.492-505.

Martinez-Lapiscina, E.H., Clavero, P., Toledo, E., San Julian, B., Sanchez-Tainta, A., Corella, D., Lamuela-Raventos, R.M., Martinez, J.A. and Martinez-Gonzalez, M.A., 2013. Virgin olive oil supplementation and long-term cognition: the PREDIMED-NAVARRA randomized, trial. *The Journal of nutrition, health and aging*, *17*(6), pp.544-552.

Martin-Rehrmann, M.D., Hoe, H.S., Capuani, E.M. and Rebeck, G.W., 2005. Association of apolipoprotein J-positive β-amyloid plaques with dystrophic neurites in alzheimer's disease brain. *Neurotoxicity research*, *7*, pp.231-241.

Mateos, R., Cert, A., Pérez-Camino, M.C. and García, J.M., 2004. Evaluation of virgin olive oil bitterness by quantification of secoiridoid derivatives. *Journal of the American Oil Chemists' Society*, *81*, pp.71-75.

Mateos, R., Espartero, J.L., Trujillo, M., Ríos, J.J., León-Camacho, M., Alcudia, F. and Cert, A., 2001. Determination of phenols, flavones, and lignans in virgin olive oils by solid-phase extraction and high-performance liquid chromatography with diode array ultraviolet detection. *Journal of Agricultural and Food Chemistry*, *49*(5), pp.2185-2192.

McCarron, M.O. and Nicoll, J.A., 1998. High frequency of apolipoprotein E ϵ2 allele is specific for patients with cerebral amyloid angiopathy-related haemorrhage. *Neuroscience letters*, *247*(1), pp.45-48.

McDonald, C.R., McEvoy, L.K., Gharapetian, L., Fennema-Notestine, C., Hagler Jr, D.J., Holland, D., Koyama, A., Brewer, J.B. and Dale, A.M., 2009. Regional rates of neocortical atrophy from normal aging to early Alzheimer disease. *Neurology*, *73*(6), pp.457-465.

Mehnert, W. and Mäder, K., 2012. Solid lipid nanoparticles: production, characterization and applications. *Advanced drug delivery reviews*, *64*, pp.83-101.

Meng, F., Marek, P., Potter, K.J., Verchere, C.B. and Raleigh, D.P., 2008. Rifampicin does not prevent amyloid fibril formation by human islet amyloid polypeptide but does inhibit fibril thioflavin-T interactions: implications for mechanistic studies of β-cell death. *Biochemistry*, *47*(22), pp.6016-6024.

Michno, W., Blennow, K., Zetterberg, H. and Brinkmalm, G., 2021. Refining the amyloid β peptide and oligomer fingerprint ambiguities in Alzheimer's disease: Mass

spectrometric molecular characterization in brain, cerebrospinal fluid, blood, and plasma. *Journal of Neurochemistry*, *159*(2), pp.234-257.
Milanez, K.D.T.M., Nóbrega, T.C.A., Nascimento, D.S., Insausti, M., Band, B.S.F. and Pontes, M.J.C., 2017. Multivariate modeling for detecting adulteration of extra virgin olive oil with soybean oil using fluorescence and UV–Vis spectroscopies: A preliminary approach. *LWT-Food Science and Technology*, *85*, pp.9-15.
Miller, E.C., Teravskis, P.J., Dummer, B.W., Zhao, X., Huganir, R.L. and Liao, D., 2014. Tau phosphorylation and tau mislocalization mediate soluble Aβ oligomer-induced AMPA glutamate receptor signaling deficits. *European Journal of Neuroscience*, *39*(7), pp.1214-1224.
Miro-Casas, E., Covas, M.I., Farre, M., Fito, M., Ortuno, J., Weinbrenner, T., Roset, P. and De La Torre, R., 2003. Hydroxytyrosol disposition in humans. *Clinical chemistry*, *49*(6), pp.945-952.
Mishra, V., Bansal, K.K., Verma, A., Yadav, N., Thakur, S., Sudhakar, K. and Rosenholm, J.M., 2018. Solid lipid nanoparticles: Emerging colloidal nano drug delivery systems. *Pharmaceutics*, *10*(4), p.191.
Montedoro, G., Bertuccioli, M. and Anichini, F., 1978. Aroma analysis of virgin olive oil by head spce (volatiles) and extraction (polyphenols) techniques. In *Flovor of foods and berages. Chemistry and techmology* (pp. 247-281). G. Charalambous, GE Inglett.
Montedoro, G., Servili, M., Baldioli, M. and Miniati, E., 1992. Simple and hydrolyzable phenolic compounds in virgin olive oil. 1. Their extraction, separation, and quantitative and semiquantitative evaluation by HPLC. *Journal of agricultural and food chemistry*, *40*(9), pp.1571-1576.
Montedoro, G., Servili, M., Baldioli, M., Selvaggini, R., Miniati, E. and Macchioni, A., 1993. Simple and hydrolyzable compounds in virgin olive oil. 3. Spectroscopic characterizations of the secoiridoid derivatives. *Journal of Agricultural and Food Chemistry*, *41*(11), pp.2228-2234.
Monteiro, M., Silva, A.F., Resende, D., Braga, S.S., Coimbra, M.A., Silva, A.M. and Cardoso, S.M., 2021. Strategies to broaden the applications of olive biophenols oleuropein and hydroxytyrosol in food products. *Antioxidants*, *10*(3), p.444.
Monti, M.C., Margarucci, L., Riccio, R. and Casapullo, A., 2012. Modulation of tau protein fibrillization by oleocanthal. *Journal of natural products*, *75*(9), pp.1584-1588.
Moore, S.J., Sonar, K., Bharadwaj, P., Deplazes, E. and Mancera, R.L., 2018. Characterisation of the structure and oligomerisation of islet amyloid polypeptides (IAPP): a review of molecular dynamics simulation studies. *Molecules*, *23*(9), p.2142.
Müller, R.H., Mäder, K. and Gohla, S., 2000. Solid lipid nanoparticles (SLN) for controlled drug delivery–a review of the state of the art. *European journal of pharmaceutics and biopharmaceutics*, *50*(1), pp.161-177.
Namba, Y., Tomonaga, M., Kawasaki, H., Otomo, E. and Ikeda, K., 1991. Apolipoprotein E immunoreactivity in cerebral amyloid deposits and neurofibrillary tangles in Alzheimer's disease and kuru plaque amyloid in Creutzfeldt-Jakob disease. *Brain research*, *541*(1), pp.163-166.
Narenderan, S.T., Meyyanathan, S.N. and Babu, B.J.F.R.I., 2020. Review of pesticide residue analysis in fruits and vegetables. Pre-treatment, extraction and detection techniques. *Food Research International*, *133*, p.109141.
Nediani, C., Ruzzolini, J., Romani, A. and Calorini, L., 2019. Oleuropein, a bioactive compound from Olea europaea L., as a potential preventive and therapeutic agent in non-communicable diseases. *Antioxidants*, *8*(12), p.578.
Nelson, L. and Tabet, N., 2015. Slowing the progression of Alzheimer's disease; what works?. *Ageing research reviews*, *23*, pp.193-209.

Nelson, P.T., Dickson, D.W., Trojanowski, J.Q., Jack, C.R., Boyle, P.A., Arfanakis, K., Rademakers, R., Alafuzoff, I., Attems, J., Brayne, C. and Coyle-Gilchrist, I.T., 2019. Limbic-predominant age-related TDP-43 encephalopathy (LATE): consensus working group report. *Brain*, *142*(6), pp.1503-1527.

Nelson, R., Sawaya, M.R., Balbirnie, M., Madsen, A.Ø., Riekel, C., Grothe, R. and Eisenberg, D., 2005. Structure of the cross-β spine of amyloid-like fibrils. *Nature*, *435*(7043), pp.773-778.

Nergiz, C. and Ünal, K., 1991. Determination of phenolic acids in virgin olive oil. *Food Chemistry*, *39*(2), pp.237-240.

Neri, L. and Hewitt, D., 1991. Aluminium, Alzheimer's disease, and drinking water. *The Lancet*, *338*(8763), p.390.

Neve, R.L., Harris, P., Kosik, K.S., Kurnit, D.M. and Donlon, T.A., 1986. Identification of cDNA clones for the human microtubule-associated protein tau and chromosomal localization of the genes for tau and microtubule-associated protein 2. *Molecular Brain Research*, *1*(3), pp.271-280.

Neves, A.R., Lúcio, M., Martins, S., Lima, J.L.C. and Reis, S., 2013. Novel resveratrol nanodelivery systems based on lipid nanoparticles to enhance its oral bioavailability. *International Journal of Nanomedicine*, pp.177-187.

Ngoungoure, V.L.N., Schluesener, J., Moundipa, P.F. and Schluesener, H., 2015. Natural polyphenols binding to amyloid: A broad class of compounds to treat different human amyloid diseases. *Molecular nutrition & food research*, *59*(1), pp.8-20.

Nichols, L. Overview of Extraction. Available online: https://chem.libretexts.org/Bookshelves/Organic_Chemistry/Book%3A_Organic_Chemistry_Lab_Techniques_(Nichols)/04%3A_Extraction/4.02%3A_Overview_of_Extraction [Accessed 6 January 2024].

Nisbet, R.M., Polanco, J.C., Ittner, L.M. and Götz, J., 2015. Tau aggregation and its interplay with amyloid-β. *Acta neuropathologica*, *129*, pp.207-220.

Ocakoglu, D., Tokatli, F., Ozen, B. and Korel, F., 2009. Distribution of simple phenols, phenolic acids and flavonoids in Turkish monovarietal extra virgin olive oils for two harvest years. *Food Chemistry*, *113*(2), pp.401-410.

Olmo-Cunillera, A., López-Yerena, A., Lozano-Castellón, J., Tresserra-Rimbau, A., Vallverdú-Queralt, A. and Pérez, M., 2020. NMR spectroscopy: A powerful tool for the analysis of polyphenols in extra virgin olive oil. *Journal of the Science of Food and Agriculture*, *100*(5), pp.1842-1851.

Omar, S.H., 2019. Mediterranean and MIND diets containing olive biophenols reduces the prevalence of Alzheimer's disease. *International journal of molecular sciences*, *20*(11), p.2797.

Ono, K., Hirohata, M. and Yamada, M., 2005. Ferulic acid destabilizes preformed β-amyloid fibrils in vitro. *Biochemical and biophysical research communications*, *336*(2), pp.444-449.

Ono, K., Yoshiike, Y., Takashima, A., Hasegawa, K., Naiki, H. and Yamada, M., 2003. Potent anti-amyloidogenic and fibril-destabilizing effects of polyphenols in vitro: implications for the prevention and therapeutics of Alzheimer's disease. *Journal of neurochemistry, 87*(1), pp.172-181.

Otręba, M., Kośmider, L. and Rzepecka-Stojko, A., 2021. Polyphenols' cardioprotective potential: Review of rat fibroblasts as well as rat and human cardiomyocyte cell lines research. *Molecules*, *26*(4), p.774.

Owen, R.W., Mier, W., Giacosa, A., Hull, W.E., Spiegelhalder, B. and Bartsch, H., 2000. Identification of lignans as major components in the phenolic fraction of olive oil. *Clinical Chemistry*, *46*(7), pp.976-988.

Owen, R.W., Mier, W., Giacosa, A., Hull, W.E., Spiegelhalder, B. and Bartsch, H., (2000 b). Phenolic and lipid components of olive oils: Identification of lignans as major components of the phenolic fraction of olive oil. *Clinical Chemistry*, *46*(7), pp.976-988.

Owen, R.W., Mier, W., Giacosa, A., Hull, W.E., Spiegelhalder, B. and Bartsch, H., 2000. Phenolic compounds and squalene in olive oils: the concentration and antioxidant potential of total phenols, simple phenols, secoiridoids, lignansand squalene. *Food and Chemical Toxicology*, *38*(8), pp.647-659.

Pandita, D., Kumar, S., Poonia, N. and Lather, V., 2014. Solid lipid nanoparticles enhance oral bioavailability of resveratrol, a natural polyphenol. *Food research international*, *62*, pp.1165-1174.

Papaneophytou, C.P. and Kontopidis, G., 2014. Statistical approaches to maximize recombinant protein expression in Escherichia coli: a general review. *Protein expression and purification*, *94*, pp.22-32.

Paravastu, A.K., Leapman, R.D., Yau, W.M. and Tycko, R., 2008. Molecular structural basis for polymorphism in Alzheimer's β-amyloid fibrils. *Proceedings of the National Academy of Sciences*, *105*(47), pp.18349-18354.

Pardo-Moreno, T., González-Acedo, A., Rivas-Domínguez, A., García-Morales, V., García-Cozar, F.J., Ramos-Rodríguez, J.J. and Melguizo-Rodríguez, L., 2022. Therapeutic approach to Alzheimer's disease: current treatments and new perspectives. *Pharmaceutics*, *14*(6), p.1117.

Park, J.S., Lee, J., Jung, E.S., Kim, M.H., Kim, I.B., Son, H., Kim, S., Kim, S., Park, Y.M., Mook-Jung, I. and Yu, S.J., 2019. Brain somatic mutations observed in Alzheimer's disease associated with aging and dysregulation of tau phosphorylation. *Nature communications*, *10*(1), p.3090.

Pastore, A., Salvadori, S. and Temussi, P.A., 2007. Peptides and proteins in a confined environment: NMR spectra at natural isotopic abundance. *Journal of peptide science: an official publication of the European Peptide Society*, *13*(5), pp.342-347.

Patel, S., Chavhan, S., Soni, H., Babbar, A.K., Mathur, R., Mishra, A.K. and Sawant, K., 2011. Brain targeting of risperidone-loaded solid lipid nanoparticles by intranasal route. *Journal of drug targeting*, *19*(6), pp.468-474.

Peña, A., Sánchez, N.S., Padilla-Garfias, F., Ramiro-Cortés, Y., Araiza-Villanueva, M. and Calahorra, M., 2023. The Use of Thioflavin T for the Estimation and Measurement of the Plasma Membrane Electric Potential Difference in Different Yeast Strains. *Journal of Fungi*, *9*(9), p.948.

Peng, Y., Hou, C., Yang, Z., Li, C., Jia, L., Liu, J., Tang, Y., Shi, L., Li, Y., Long, J. and Liu, J., 2016. Hydroxytyrosol mildly improve cognitive function independent of APP processing in APP/PS1 mice. *Molecular Nutrition & Food Research*, *60*(11), pp.2331-2342.

Pérez-Camino, M.C., Moreda, W. and Cert, A., 1996. Determination of diacylglycerol isomers in vegetable oils by solid-phase extraction followed by gas chromatography on a polar phase. *Journal of Chromatography A*, *721*(2), pp.305-314.

Perez-Martinez, P., Garcia-Rios, A., Delgado-Lista, J., Perez-Jimenez, F. and Lopez-Miranda, J., 2011. Mediterranean diet rich in olive oil and obesity, metabolic syndrome and diabetes mellitus. *Current pharmaceutical design*, *17*(8), pp.769-777.

Phan, H.T., Samarat, K., Takamura, Y., Azo-Oussou, A.F., Nakazono, Y. and Vestergaard, M.D.C., 2019. Polyphenols modulate alzheimer's amyloid beta aggregation in a structure-dependent manner. *Nutrients*, *11*(4), p.756.

Pickett, E.K., Herrmann, A.G., McQueen, J., Abt, K., Dando, O., Tulloch, J., Jain, P., Dunnett, S., Sohrabi, S., Fjeldstad, M.P. and Calkin, W., 2019. Amyloid beta and tau cooperate to cause reversible behavioral and transcriptional deficits in a model of Alzheimer's disease. *Cell reports*, *29*(11), pp.3592-3604.

Pickhardt, M., Larbig, G., Khlistunova, I., Coksezen, A., Meyer, B., Mandelkow, E.M., Schmidt, B. and Mandelkow, E., 2007. Phenylthiazolyl-hydrazide and its derivatives are potent inhibitors of τ aggregation and toxicity in vitro and in cells. *Biochemistry*, *46*(35), pp.10016-10023.

Pinto, J., Paiva-Martins, F., Corona, G., Debnam, E.S., Oruna-Concha, M.J., Vauzour, D., Gordon, M.H. and Spencer, J.P., 2011. Absorption and metabolism of olive oil secoiridoids in the small intestine. *British Journal of Nutrition*, *105*(11), pp.1607-1618.

Pinto-Hernandez, P., Castilla-Silgado, J., Coto-Vilcapoma, A., Fernández-Sanjurjo, M., Fernández-García, B., Tomás-Zapico, C. and Iglesias-Gutiérrez, E., 2023. Modulation of microRNAs through lifestyle changes in Alzheimer's disease. *Nutrients*, *15*(17), p.3688.

Pirisi, F.M., Cabras, P., Cao, C.F., Migliorini, M. and Muggelli, M., 2000. Phenolic compounds in virgin olive oil. 2. Reappraisal of the extraction, HPLC separation, and quantification procedures. *Journal of agricultural and food chemistry*, *48*(4), pp.1191-1196.

Pitt, J., Roth, W., Lacor, P., Smith III, A.B., Blankenship, M., Velasco, P., De Felice, F., Breslin, P. and Klein, W.L., 2009. Alzheimer's-associated Aβ oligomers show altered structure, immunoreactivity and synaptotoxicity with low doses of oleocanthal. *Toxicology and applied pharmacology*, *240*(2), pp.189-197.

Pizarro, M.L., Becerra, M., Sayago, A., Beltrán, M. and Beltrán, R., 2013. Comparison of different extraction methods to determine phenolic compounds in virgin olive oil. *Food Analytical Methods*, *6*, pp.123-132.

Pokrzywa, M., Pawełek, K., Kucia, W.E., Sarbak, S., Chorell, E., Almqvist, F. and Wittung-Stafshede, P., 2017. Effects of small-molecule amyloid modulators on a Drosophila model of Parkinson's disease. *PLoS One*, *12*(9), p.e0184117.

Porat, Y., Abramowitz, A. and Gazit, E., 2006. Inhibition of amyloid fibril formation by polyphenols: structural similarity and aromatic interactions as a common inhibition mechanism. *Chemical biology & drug design*, *67*(1), pp.27-37.

Pranitha, D., Parthiban, N., Dinakaran, S., Ghosh, S. and Banji, D.S., 2011. Solid state nuclear magnetic resonance spectroscopy-A review. *Asian J. Pharm. Clin. Res*, *4*, pp.9-14.

Prokop, S., Miller, K.R. and Heppner, F.L., 2013. Microglia actions in Alzheimer's disease. *Acta neuropathologica*, *126*, pp.461-477.

Pu, F.F., Yin, S., Chen, H.Y., Dai, Z., Qian, T.X., Wang, C.C., Xu, H. and Wang, X.Y., 2015. Oleuropein improves long term potentiation at perforant path-dentate gyrus synapses in vivo. *Chinese Herbal Medicines*, *7*(3), pp.255-260.

Pu, S., Gong, C. and Robertson, A.W., 2020. Liquid cell transmission electron microscopy and its applications. *Royal Society open science*, *7*(1), p.191204.

Qin, C., Hu, S., Zhang, S., Zhao, D., Wang, Y., Li, H., Peng, Y., Shi, L., Xu, X., Wang, C. and Liu, J., 2021. Hydroxytyrosol acetate improves the cognitive function of APP/PS1 transgenic mice in ERβ-dependent manner. *Molecular Nutrition & Food Research*, *65*(3), p.2000797.

Qosa, H., Mohamed, L.A., Batarseh, Y.S., Alqahtani, S., Ibrahim, B., LeVine III, H., Keller, J.N. and Kaddoumi, A., 2015. Extra-virgin olive oil attenuates amyloid-β and tau pathologies in the brains of TgSwDI mice. *The Journal of Nutritional Biochemistry*, *26*(12), pp.1479-1490.

Querfurth, H.W. and LaFerla, F.M., 2010. Alzheimer's disease. *New England Journal of Medicine*, *362*(4), pp.329-344.

Race, B., Jeffrey, M., McGovern, G., Dorward, D. and Chesebro, B., 2017. Ultrastructure and pathology of prion protein amyloid accumulation and cellular damage in extraneural tissues of scrapie-infected transgenic mice expressing anchorless prion protein. *Prion*, *11*(4), pp.234-248.

Rahman, M.M. and Lendel, C., 2021. Extracellular protein components of amyloid plaques and their roles in Alzheimer's disease pathology. *Molecular Neurodegeneration*, *16*(1), p.59.

Rambaran, R.N. and Serpell, L.C., 2008. Amyloid fibrils: abnormal protein assembly. *Prion*, *2*(3), pp.112-117.

Ratha, B.N., Ghosh, A., Brender, J.R., Gayen, N., Ilyas, H., Neeraja, C., Das, K.P., Mandal, A.K. and Bhunia, A., 2016. Inhibition of insulin amyloid fibrillation by a novel amphipathic heptapeptide. *Journal of biological chemistry*, *291*(45), pp.23545-23556.

Rigacci, S., 2015. Olive oil phenols as promising multi-targeting agents against Alzheimer's disease. *Springer International Publishing. Natural compounds as therapeutic agents for amyloidogenic diseases*, pp.1-20.

Rigacci, S., Guidotti, V., Bucciantini, M., Nichino, D., Relini, A., Berti, A. and Stefani, M., 2011. Aβ (1-42) aggregates into non-toxic amyloid assemblies in the presence of the natural polyphenol oleuropein aglycon. *Current Alzheimer Research*, *8*(8), pp.841-852.

Robinson, J.L., Lee, E.B., Xie, S.X., Rennert, L., Suh, E., Bredenberg, C., Caswell, C., Van Deerlin, V.M., Yan, N., Yousef, A. and Hurtig, H.I., 2018. Neurodegenerative disease concomitant proteinopathies are prevalent, age-related and APOE4-associated. *Brain*, *141*(7), pp.2181-2193.

Rodríguez-López, P., Lozano-Sanchez, J., Borrás-Linares, I., Emanuelli, T., Menéndez, J.A. and Segura-Carretero, A., 2020. Structure–biological activity relationships of extra-virgin olive oil phenolic compounds: Health properties and bioavailability. *Antioxidants*, *9*(8), p.685.

Rodríguez-López, P., Lozano-Sánchez, J., Borras-Linares, I., Emanuelli, T., Menendez, J.A. and Segura-Carretero, A., 2021. Polyphenols in olive oil: The importance of phenolic compounds in the chemical composition of olive oil. In *Olives and Olive Oil in Health and Disease Prevention* (pp. 111-122). Academic press.

Rodríguez-Morató, J., Xicota, L., Fitó, M., Farré, M., Dierssen, M. and De la Torre, R., 2015. Potential role of olive oil phenolic compounds in the prevention of neurodegenerative diseases. *Molecules*, *20*(3), pp.4655-4680.

Rogaev, E.I., Sherrington, R., Rogaeva, E.A., Levesque, G., Ikeda, M., Liang, Y., Chi, H., Lin, C., Holman, K., Tsuda, T. and Mar, L., 1995. Familial Alzheimer's disease in kindreds with missense mutations in a gene on chromosome 1 related to the Alzheimer's disease type 3 gene. *Nature*, *376*(6543), pp.775-778.

Rosero-Moreano, M., 2018, November. New Trends in Chemical Analysis of Disinfection By. In *Disinfection* (p. 55-77). BoD–Books on Demand. London, UK: IntechOpen.

Rovellini, P., Cortesi, N. and Fedeli, E., 1997. Analysis of flavonoids from Olea europaea by HPLC-UV and HPLC-electrospray-MS.

Ruan, C., Kong, J., He, X., Hu, B. and Zeng, X., 2022. Interaction between polyphenols and amyloids: from the view of prevention of protein misfolding disorders related diseases. *Food Materials Research*, *2*(1), pp.1-15.

Ruan, Z., Pathak, D., Venkatesan Kalavai, S., Yoshii-Kitahara, A., Muraoka, S., Bhatt, N., Takamatsu-Yukawa, K., Hu, J., Wang, Y., Hersh, S. and Ericsson, M., 2021. Alzheimer's disease brain-derived extracellular vesicles spread tau pathology in interneurons. *Brain*, *144*(1), pp.288-309.

Rubinski, A., Franzmeier, N., Neitzel, J., Ewers, M. and Alzheimer's Disease Neuroimaging Initiative (ADNI), 2020. FDG-PET hypermetabolism is associated with higher tau-PET

in mild cognitive impairment at low amyloid-PET levels. *Alzheimer's research & therapy*, *12*, pp.1-12.

Rubió, L., Serra, A., Macià, A., Piñol, C., Romero, M.P. and Motilva, M.J., 2014. In vivo distribution and deconjugation of hydroxytyrosol phase II metabolites in red blood cells: a potential new target for hydroxytyrosol. *Journal of functional foods*, *10*, pp.139-143.

Ruiz-Aracama, A., Goicoechea, E. and Guillén, M.D., 2017. Direct study of minor extra-virgin olive oil components without any sample modification. 1H NMR multisupression experiment: A powerful tool. *Food Chemistry*, *228*, pp.301-314.

Ryan, T.M., Friedhuber, A., Lind, M., Howlett, G.J., Masters, C. and Roberts, B.R., 2012. Small amphipathic molecules modulate secondary structure and amyloid fibril-forming kinetics of Alzheimer disease peptide Aβ1–42. *Journal of Biological Chemistry*, *287*(20), pp.16947-16954.

Sadigh-Eteghad, S., Sabermarouf, B., Majdi, A., Talebi, M., Farhoudi, M. and Mahmoudi, J., 2015. Amyloid-beta: a crucial factor in Alzheimer's disease. *Medical principles and practice*, *24*(1), pp.1-10.

Sagar Aryal., 2024, https://microbenotes.com/high-performance-liquid-chromatography-hplc/ [Accessed 16 August 2024].

Salis, C., Papageorgiou, L., Papakonstantinou, E., Hagidimitriou, M. and Vlachakis, D., 2020. Olive oil polyphenols in neurodegenerative pathologies. *GeNeDis 2018: Genetics and Neurodegeneration*, pp.77-91.

Santangelo, C., Filesi, C., Varì, R., Scazzocchio, B., Filardi, T., Fogliano, V., D'archivio, M., Giovannini, C., Lenzi, A., Morano, S. and Masella, R., 2016. Consumption of extra-virgin olive oil rich in phenolic compounds improves metabolic control in patients with type 2 diabetes mellitus: A possible involvement of reduced levels of circulating visfatin. *Journal of endocrinological investigation*, *39*, pp.1295-1301.

Sarkar, A., Angeline, M.S., Anand, K., Ambasta, R.K. and Kumar, P., 2012. Naringenin and quercetin reverse the effect of hypobaric hypoxia and elicit neuroprotective response in the murine model. *Brain research*, *1481*, pp.59-70.

Satapathy, M.K., Yen, T.L., Jan, J.S., Tang, R.D., Wang, J.Y., Taliyan, R. and Yang, C.H., 2021. Solid lipid nanoparticles (SLNs): an advanced drug delivery system targeting brain through BBB. *Pharmaceutics*, *13*(8), p.1183.

Saunders, J.C., Young, L.M., Mahood, R.A., Jackson, M.P., Revill, C.H., Foster, R.J., Smith, D.A., Ashcroft, A.E., Brockwell, D.J. and Radford, S.E., 2016. An in vivo platform for identifying inhibitors of protein aggregation. *Nature chemical biology*, *12*(2), pp.94-101.

Scarmeas, N., Luchsinger, J.A., Schupf, N., Brickman, A.M., Cosentino, S., Tang, M.X. and Stern, Y., 2009. Physical activity, diet, and risk of Alzheimer disease. *Jama*, *302*(6), pp.627-637.

Scarmeas, N., Stern, Y., Mayeux, R., Manly, J.J., Schupf, N. and Luchsinger, J.A., 2009. Mediterranean diet and mild cognitive impairment. *Archives of neurology*, *66*(2), pp.216-225.

Schachter, A.S. and Davis, K.L., 2000. Alzheimer's disease. *Dialogues in clinical neuroscience*, *2*(2), pp.91-100.

Schägger, H. and Von Jagow, G., 1987. Tricine-sodium dodecyl sulfate-polyacrylamide gel electrophoresis for the separation of proteins in the range from 1 to 100 kDa. *Analytical biochemistry*, *166*(2), pp.368-379.

Scheltens, P., De Strooper, B., Kivipelto, M., Holstege, H., Chételat, G., Teunissen, C.E., Cummings, J. and van der Flier, W.M., 2021. Alzheimer's disease. *The Lancet*, *397*(10284), pp.1577-1590.

Schneider, A., Araujo, G.W., Trajkovic, K., Herrmann, M.M., Merkler, D., Mandelkow, E.M., Weissert, R. and Simons, M., 2004. Hyperphosphorylation and aggregation of tau in experimental autoimmune encephalomyelitis. *Journal of Biological Chemistry*, *279*(53), pp.55833-55839.

Schneider, C.A., Rasband, W.S. and Eliceiri, K.W., 2012. NIH Image to ImageJ: 25 years of image analysis. *Nature methods*, *9*(7), pp.671-675.

Scoditti, E., Calabriso, N., Massaro, M., Pellegrino, M., Storelli, C., Martines, G., De Caterina, R. and Carluccio, M.A., 2012. Mediterranean diet polyphenols reduce inflammatory angiogenesis through MMP-9 and COX-2 inhibition in human vascular endothelial cells: a potentially protective mechanism in atherosclerotic vascular disease and cancer. *Archives of biochemistry and biophysics*, *527*(2), pp.81-89.

Selkoe, D.J. and Hardy, J., 2016. The amyloid hypothesis of Alzheimer's disease at 25 years. *EMBO molecular medicine*, *8*(6), pp.595-608.

Selkoe, D.J., 2002. Alzheimer's disease is a synaptic failure. *Science*, *298*(5594), pp.789-791.

Sepporta, M.V., Fuccelli, R., Rosignoli, P., Ricci, G., Servili, M., Morozzi, G. and Fabiani, R., 2014. Oleuropein inhibits tumour growth and metastases dissemination in ovariectomised nude mice with MCF-7 human breast tumour xenografts. *Journal of functional foods*, *8*, pp.269-273.

Servili, M., Baldioli, M., Selvaggini, R., Miniati, E., Macchioni, A. and Montedoro, G., 1999. High-performance liquid chromatography evaluation of phenols in olive fruit, virgin olive oil, vegetation waters, and pomace and 1D-and 2D-nuclear magnetic resonance characterization. *Journal of the American Oil Chemists' Society*, *76*, pp.873-882.

Shahidi, F. and Naczk, M., 1996. Food phenolics: Sources, chemistry, effects, applications. *(No Title)*.

Shankar, G.M., Li, S., Mehta, T.H., Garcia-Munoz, A., Shepardson, N.E., Smith, I., Brett, F.M., Farrell, M.A., Rowan, M.J., Lemere, C.A. and Regan, C.M., 2008. Amyloid-β protein dimers isolated directly from Alzheimer's brains impair synaptic plasticity and memory. *Nature medicine*, *14*(8), pp.837-842.

Sharoar, M.G., Thapa, A., Shahnawaz, M., Ramasamy, V.S., Woo, E.R., Shin, S.Y. and Park, I.S., 2012. Keampferol-3-O-rhamnoside abrogates amyloid beta toxicity by modulating monomers and remodeling oligomers and fibrils to non-toxic aggregates. *Journal of biomedical science*, *19*, pp.1-13.

Sheppard, O. and Coleman, M., 2020. Alzheimer’s disease: etiology, neuropathology and pathogenesis. *Exon Publications*, pp.1-21.

Sheridan, R.P., Maiorov, V.N., Holloway, M.K., Cornell, W.D. and Gao, Y.D., 2010. Drug-like density: a method of quantifying the “bindability” of a protein target based on a very large set of pockets and drug-like ligands from the Protein Data Bank. *Journal of chemical information and modeling*, *50*(11), pp.2029-2040.

Sherrington, R., Rogaev, E.I., Liang, Y.A., Rogaeva, E.A., Levesque, G., Ikeda, M., Chi, H., Lin, C., Li, G., Holman, K. and Tsuda, T., 1995. Cloning of a gene bearing missense mutations in early-onset familial Alzheimer's disease. *Nature*, *375*(6534), pp.754-760.

Shi, X., Lin, X., Hu, R., Sun, N., Hao, J. and Gao, C., 2016. Toxicological differences between NMDA receptor antagonists and cholinesterase inhibitors. *American Journal of Alzheimer's Disease & Other Dementias®*, *31*(5), pp.405-412.

Shipton, O.A., Leitz, J.R., Dworzak, J., Acton, C.E., Tunbridge, E.M., Denk, F., Dawson, H.N., Vitek, M.P., Wade-Martins, R., Paulsen, O. and Vargas-Caballero, M., 2011. Tau protein is required for amyloid β-induced impairment of hippocampal long-term potentiation. *Journal of Neuroscience*, *31*(5), pp.1688-1692.

Sierra, C.F.E., 2019. Fundamentals of transmission electron microscopy, the technique with the best resolution in the world. *screen*, *9*, p.10.

Singh, R., 2014. *Membrane technology and engineering for water purification: application, systems design and operation. Second edition.* Butterworth-Heinemann.

Singla, R.K., Dubey, A.K., Garg, A., Sharma, R.K., Fiorino, M., Ameen, S.M., Haddad, M.A. and Al-Hiary, M., 2019. Natural polyphenols: Chemical classification, definition of classes, subcategories, and structures. *Journal of AOAC International*, *102*(5), pp.1397-1400.

Sipe, J.D., Benson, M.D., Buxbaum, J.N., Ikeda, S.I., Merlini, G., Saraiva, M.J. and Westermark, P., 2016. Amyloid fibril proteins and amyloidosis: chemical identification and clinical classification International Society of Amyloidosis 2016 Nomenclature Guidelines. *Amyloid*, *23*(4), pp.209-213.

Sipe, J.D., Benson, M.D., Buxbaum, J.N., Ikeda, S.I., Merlini, G., Saraiva, M.J. and Westermark, P., 2010. Amyloid fibril protein nomenclature: 2010 recommendations from the nomenclature committee of the International Society of Amyloidosis. *Amyloid*, *17*(3-4), pp.101-104.

Sofi, F., Abbate, R., Gensini, G.F. and Casini, A., 2010. Accruing evidence on benefits of adherence to the Mediterranean diet on health: an updated systematic review and meta-analysis. *The American journal of clinical nutrition*, *92*(5), pp.1189-1196.

Sofi, F., Macchi, C., Abbate, R., Gensini, G.F. and Casini, A., 2013. Mediterranean diet and health. *Biofactors*, *39*(4), pp.335-342.

Sotiropoulos, I., Galas, M.C., Silva, J.M., Skoulakis, E., Wegmann, S., Maina, M.B., Blum, D., Sayas, C.L., Mandelkow, E.M., Mandelkow, E. and Spillantini, M.G., 2017. Atypical, non-standard functions of the microtubule associated Tau protein. *Acta neuropathologica communications*, *5*, pp.1-11.

Souto, E.B. and Müller, R.H., 2006. Applications of lipid nanoparticles (SLN and NLC) in food industry. *Journal of Food Technology, 4*(1),90–95.

Spires-Jones, T.L. and Hyman, B.T., 2014. The intersection of amyloid beta and tau at synapses in Alzheimer's disease. *Neuron*, *82*(4), pp.756-771.

Spires-Jones, T.L., Attems, J. and Thal, D.R., 2017. Interactions of pathological proteins in neurodegenerative diseases. *Acta neuropathologica*, *134*, pp.187-205.

Sreerama, N. and Woody, R.W., 2000. Estimation of protein secondary structure from circular dichroism spectra: comparison of CONTIN, SELCON, and CDSSTR methods with an expanded reference set. *Analytical biochemistry*, *287*(2), pp.252-260.

Sreerama, N. and Woody, R.W., 2004. Computation and analysis of protein circular dichroism spectra. *Methods in enzymology*, *383*, pp.318-351.

Sreerama, N. and Woody, R.W., 2004. On the analysis of membrane protein circular dichroism spectra. *Protein science*, *13*(1), pp.100-112.

Stalikas, C.D., 2007. Extraction, separation, and detection methods for phenolic acids and flavonoids. *Journal of separation science*, *30*(18), pp.3268-3295.

Stamer, K., Vogel, R., Thies, E., Mandelkow, E. and Mandelkow, E.M., 2002. Tau blocks traffic of organelles, neurofilaments, and APP vesicles in neurons and enhances oxidative stress. *The Journal of cell biology*, *156*(6), pp.1051-1063.

Stefani, M. and Rigacci, S., 2013. Protein folding and aggregation into amyloid: the interference by natural phenolic compounds. *International journal of molecular sciences*, *14*(6), pp.12411-12457.

Stefani, M. and Rigacci, S., 2014. Beneficial properties of natural phenols: highlight on protection against pathological conditions associated with amyloid aggregation. *BioFactors*, *40*(5), pp.482-493.

Stefani, M., 2008. Protein folding and misfolding on surfaces. *International journal of molecular sciences*, *9*(12), pp.2515-2542.

Stein, T.D. and Crary, J.F., 2020, August. Chronic traumatic encephalopathy and neuropathological comorbidities. In *Seminars in neurology* (Vol. 40, No. 04, pp. 384-393). Thieme Medical Publishers.

Stewart, K.L., Hughes, E., Yates, E.A., Akien, G.R., Huang, T.Y., Lima, M.A., Rudd, T.R., Guerrini, M., Hung, S.C., Radford, S.E. and Middleton, D.A., 2016. Atomic details of the interactions of glycosaminoglycans with amyloid-β fibrils. *Journal of the American Chemical Society*, *138*(27), pp.8328-8331.

St-Laurent-Thibault, C., Arseneault, M., Longpre, F. and Ramassamy, C., 2011. Tyrosol and hydroxytyrosol two main components of olive oil, protect N2a cells against amyloid-β-induced toxicity. involvement of the NF-κB signaling. *Current Alzheimer Research*, *8*(5), pp.543-551.

Stringer, K.A., McKay, R.T., Karnovsky, A., Quémerais, B. and Lacy, P., 2016. Metabolomics and its application to acute lung diseases. *Frontiers in immunology*, *7*, p.44.

Suárez, M., Macià, A., Romero, M.P. and Motilva, M.J., 2008. Improved liquid chromatography tandem mass spectrometry method for the determination of phenolic compounds in virgin olive oil. *Journal of Chromatography A*, *1214*(1-2), pp.90-99.

Subasinghe, S., Unabia, S., Barrow, C.J., Mok, S.S., Aguilar, M.I. and Small, D.H., 2003. Cholesterol is necessary both for the toxic effect of Aβ peptides on vascular smooth muscle cells and for Aβ binding to vascular smooth muscle cell membranes. *Journal of neurochemistry*, *84*(3), pp.471-479.

Swarbrick, J., 2013. *Encyclopedia of Pharmaceutical Technology: Volume 6*. CRC press.

Tabanez, M., Santos, I.R., Ikebara, J.M., Camargo, M.L., Dos Santos, B.A., Freire, B.M., Batista, B.L., Takada, S.H., Squitti, R., Kihara, A.H. and Cerchiaro, G., 2023. The Impact of Hydroxytyrosol on the Metallomic-Profile in an Animal Model of Alzheimer's Disease. *International Journal of Molecular Sciences*, *24*(19), p.14950.

Targuma, S., Njobeh, P.B. and Ndungu, P.G., 2021. Current applications of magnetic nanomaterials for extraction of mycotoxins, pesticides, and pharmaceuticals in food commodities. *Molecules*, *26*(14), p.4284.

Tasioula-Margari, M. and Tsabolatidou, E., 2015. Extraction, separation, and identification of phenolic compounds in virgin olive oil by HPLC-DAD and HPLC-MS. *Antioxidants*, *4*(3), pp.548-562.

Telmoudi, A., Rezig, L., Mahmoudi, I., Mnif, W., Algarni, Z. and Chouaibi, M., 2024. Nanoncapsulation of tyrosol using natural biopolymers: optimization, characterization and physical stability of nanoparticles. *Journal of Food Measurement and Characterization*, *18*(3), pp.1804-1824.

Thal, D.R., Ghebremedhin, E., Rüb, U., Yamaguchi, H., Del Tredici, K. and Braak, H., 2002. Two types of sporadic cerebral amyloid angiopathy. *Journal of Neuropathology & Experimental Neurology*, *61*(3), pp.282-293.

Thal, D.R., Rüb, U., Orantes, M. and Braak, H., 2002. Phases of Aβ-deposition in the human brain and its relevance for the development of AD. *Neurology*, *58*(12), pp.1791-1800.

Townsend, D., 2016. *Molecular level characterisation of apolipoprotein AI aggregation leading to fibrils comprising of both α-helical and β-sheet structures*. Lancaster University (United Kingdom).

Townsend, D., Fullwood, N.J., Yates, E.A. and Middleton, D.A., 2020. Aggregation kinetics and filament structure of a tau fragment are influenced by the sulfation pattern of the cofactor heparin. *Biochemistry*, *59*(41), pp.4003-4014.

Townsend, D., Hughes, E., Akien, G., Stewart, K.L., Radford, S.E., Rochester, D. and Middleton, D.A., 2018. Epigallocatechin-3-gallate remodels apolipoprotein AI amyloid fibrils into soluble oligomers in the presence of heparin. *Journal of Biological Chemistry*, *293*(33), pp.12877-12893.

Trejo-Lopez, J.A., Yachnis, A.T. and Prokop, S., 2022. Neuropathology of Alzheimer's disease. *Neurotherapeutics*, *19*(1), pp.173-185.

Tripoli, E., Giammanco, M., Tabacchi, G., Di Majo, D., Giammanco, S. and La Guardia, M., 2005. The phenolic compounds of olive oil: structure, biological activity and beneficial effects on human health. *Nutrition research reviews*, *18*(1), pp.98-112.

Tsolaki, M., Lazarou, E., Kozori, M., Petridou, N., Tabakis, I., Lazarou, I., Karakota, M., Saoulidis, I., Melliou, E. and Magiatis, P., 2020. A randomized clinical trial of greek high phenolic early harvest extra virgin olive oil in mild cognitive impairment: The MICOIL pilot study. *Journal of Alzheimer's Disease*, *78*(2), pp.801-817.

Tzekaki, E.E., Papaspyropoulos, A., Tsolaki, M., Lazarou, E., Kozori, M. and Pantazaki, A.A., 2021. Restoration of BMI1 levels after the administration of early harvest extra virgin olive oil as a therapeutic strategy against Alzheimer's disease. *Experimental Gerontology*, *144*, p.111178.

Van der Lee, M. and Van den Pol, E., 2015, April. Chromatographic Separation of Surfactants in Chemical EOR. In *IOR 2015-18th European Symposium on Improved Oil Recovery* (pp. cp-445). European Association of Geoscientists & Engineers.

Vassilaki, M., Aakre, J.A., Syrjanen, J.A., Mielke, M.M., Geda, Y.E., Kremers, W.K., Machulda, M.M., Alhurani, R.E., Staubo, S.C., Knopman, D.S. and Petersen, R.C., 2018. Mediterranean diet, its components, and amyloid imaging biomarkers. *Journal of Alzheimer's Disease*, *64*(1), pp.281-290.

Vaz, M. and Silvestre, S., 2020. Alzheimer's disease: Recent treatment strategies. *European journal of pharmacology*, *887*, p.173554.

Vazquez Roncero, A., 1978. Polyphenols in olive oil and their influence on the characteristics of oil. *Revue Française des Corps Gras*, *25*, pp.21-26.

Vazquez Roncero, A., Del Valle, C.J. and Del Valle, L.J., 1976. Phenolic Compounds in Olives. III. Polyphenols in Olive Oil. *Grasas Aceites*, *27*, pp.185-191.

Vázquez, A., 1973. Determination de los polifenoles totalen en aceite de Olivia. *Grass Aceites*, *24*, pp.350-357.

Velander, P., Wu, L., Henderson, F., Zhang, S., Bevan, D.R. and Xu, B., 2017. Natural product-based amyloid inhibitors. *Biochemical pharmacology*, *139*, pp.40-55.

Viegas, C., Patrício, A.B., Prata, J.M., Nadhman, A., Chintamaneni, P.K. and Fonte, P., 2023. Solid lipid nanoparticles vs. nanostructured lipid carriers: a comparative review. *Pharmaceutics*, *15*(6), p.1593.

Viola, K.L. and Klein, W.L., 2015. Amyloid β oligomers in Alzheimer's disease pathogenesis, treatment, and diagnosis. *Acta neuropathologica*, *129*(2), pp.183-206.

Visioli, F., Rodríguez-Pérez, M., Gómez-Torres, Ó., Pintado-Losa, C. and Burgos-Ramos, E., 2022. Hydroxytyrosol improves mitochondrial energetics of a cellular model of Alzheimer's disease. *Nutritional Neuroscience*, *25*(5), pp.990-1000.

Vrabec, R., Blunden, G. and Cahlíková, L., 2023. Natural alkaloids as multi-target compounds towards factors implicated in Alzheimer's disease. *International Journal of Molecular Sciences*, *24*(5), p.4399.

Vrancx, C., Vadukul, D.M., Suelves, N., Contino, S., D'Auria, L., Perrin, F., van Pesch, V., Hanseeuw, B., Quinton, L. and Kienlen-Campard, P., 2021. Mechanism of cellular formation and in vivo seeding effects of hexameric β-amyloid assemblies. *Molecular neurobiology*, *58*, pp.6647-6669.

Walker, J.M., Fudym, Y., Farrell, K., Iida, M.A., Bieniek, K.F., Seshadri, S., White III, C.L., Crary, J.F. and Richardson, T.E., 2021. Asymmetry of hippocampal tau pathology in primary age-related tauopathy and Alzheimer disease. *Journal of Neuropathology & Experimental Neurology*, *80*(5), pp.436-445.

Walker, J.M., Richardson, T.E., Farrell, K., Iida, M.A., Foong, C., Shang, P., Attems, J., Ayalon, G., Beach, T.G., Bigio, E.H. and Budson, A., 2021. Early selective vulnerability of the CA2 hippocampal subfield in primary age-related tauopathy. *Journal of Neuropathology & Experimental Neurology*, *80*(2), pp.102-111.

Walker, L.C., 2020. Aβ plaques. *Free neuropathology*, *1*, pp.1-31.

Wallace, B.A., Wallace, B.A. and Janes, R.W. eds., 2009. *Modern techniques for circular dichroism and synchrotron radiation circular dichroism spectroscopy* (Vol. 1). IOS press.

Walsh, D.M., Thulin, E., Minogue, A.M., Gustavsson, N., Pang, E., Teplow, D.B. and Linse, S., 2009. A facile method for expression and purification of the Alzheimer's disease-associated amyloid β-peptide. *The FEBS journal*, *276*(5), pp.1266-1281.

Wang, Q., Ning, L., Niu, Y., Liu, H. and Yao, X., 2015. Molecular mechanism of the inhibition and remodeling of human islet amyloid polypeptide (hIAPP1–37) oligomer by resveratrol from molecular dynamics simulation. *The Journal of Physical Chemistry B*, *119*(1), pp.15-24.

Wang, S., Moustaid-Moussa, N., Chen, L., Mo, H., Shastri, A., Su, R., Bapat, P., Kwun, I. and Shen, C.L., 2014. Novel insights of dietary polyphenols and obesity. *The Journal of nutritional biochemistry*, *25*(1), pp.1-18.

Wang, X., Yu, J. and Zhang, X., 2022. Dietary polyphenols as prospective natural-compound depression treatment from the perspective of intestinal microbiota regulation. *Molecules*, *27*(21), p.7637.

Wani, T.A., Masoodi, F.A., Gani, A., Baba, W.N., Rahmanian, N., Akhter, R., Wani, I.A. and Ahmad, M., 2018. Olive oil and its principal bioactive compound: Hydroxytyrosol–A review of the recent literature. *Trends in Food Science & Technology*, *77*, pp.77-90.

Weinbrenner, T., Fitó, M., Saez, G.T., Rijken, P., Tormos, C., Coolen, S., De La Torre, R. and Covas, M.I., 2004. Bioavailability of phenolic compounds from olive oil and oxidative/antioxidant status at postprandial state in healthy humans. *Drugs under experimental and clinical research*, *30*(5-6), pp.207-212.

Westermark, P., 2012. Amyloid fibril protein nomenclature: 2012 recommendations from the nomenclature committee of the international society of amyloidosis. Amyloid: The International Journal of Experimental and Clinical Investigation: *The Official Journal of the International Society of Amyloidosis, 17*(3–4), pp.101–4.

White, L.R., Edland, S.D., Hemmy, L.S., Montine, K.S., Zarow, C., Sonnen, J.A., Uyehara-Lock, J.H., Gelber, R.P., Ross, G.W., Petrovitch, H. and Masaki, K.H., 2016. Neuropathologic comorbidity and cognitive impairment in the Nun and Honolulu-Asia Aging Studies. *Neurology*, *86*(11), pp.1000-1008.

Whitmore, L. and Wallace, B.A., 2008. Protein secondary structure analyses from circular dichroism spectroscopy: methods and reference databases. *Biopolymers: Original Research on Biomolecules*, *89*(5), pp.392-400.

Wu, C., Lei, H., Wang, Z., Zhang, W. and Duan, Y., 2006. Phenol red interacts with the protofibril-like oligomers of an amyloidogenic hexapeptide NFGAIL through both hydrophobic and aromatic contacts. *Biophysical journal*, *91*(10), pp.3664-3672.

Xu, G., Ulm, B.S., Howard, J., Fromholt, S.E., Lu, Q., Lee, B.B., Walker, A., Borchelt, D.R. and Lewis, J., 2022. TAPPing into the potential of inducible tau/APP transgenic mice. *Neuropathology and Applied Neurobiology*, *48*(3), p.e12791.

Xue, C., Lin, T.Y., Chang, D. and Guo, Z., 2017. Thioflavin T as an amyloid dye: fibril quantification, optimal concentration and effect on aggregation. *Royal Society open science*, *4*(1), p.160696.

Yan, J.J., Cho, J.Y., Kim, H.S., Kim, K.L., Jung, J.S., Huh, S.O., Suh, H.W., Kim, Y.H. and Song, D.K., 2001. Protection against β-amyloid peptide toxicity in vivo with long-term administration of ferulic acid. *British journal of pharmacology*, *133*(1), pp.89-96.

Yan, J.J., Jung, J.S., Kim, T.K., Hasan, M.A., Hong, C.W., Nam, J.S. and Song, D.K., 2013. Protective effects of ferulic acid in amyloid precursor protein plus presenilin-1 transgenic mouse model of Alzheimer disease. *Biological and Pharmaceutical Bulletin*, *36*(1), pp.140-143.

Yang, Y., Bai, L., Li, X., Xiong, J., Xu, P., Guo, C. and Xue, M., 2014. Transport of active flavonoids, based on cytotoxicity and lipophilicity: An evaluation using the blood–brain barrier cell and Caco-2 cell models. *Toxicology in Vitro*, *28*(3), pp.388-396.

Yasuhara, O., Muramatsu, H., Kim, S.U., Muramatsu, T., Maruta, H. and McGeer, P.L., 1993. Midkine, a novel neurotrophic factor, is present in senile plaques of Alzheimer disease. *Biochemical and Biophysical Research Communications*, *192*(1), pp.246-251.

Yorulmaz, A., Poyrazoglu, E.S., Ozcan, M.M. and Tekin, A., 2012. Phenolic profiles of Turkish olives and olive oils. *European Journal of Lipid Science and Technology*, *114*(9), pp.1083-1093.

Yoshiyama, Y., Higuchi, M., Zhang, B., Huang, S.M., Iwata, N., Saido, T.C., Maeda, J., Suhara, T., Trojanowski, J.Q. and Lee, V.M.Y., 2007. Synapse loss and microglial activation precede tangles in a P301S tauopathy mouse model. *Neuron*, *53*(3), pp.337-351.

Youdim, K.A., Dobbie, M.S., Kuhnle, G., Proteggente, A.R., Abbott, N.J. and Rice-Evans, C., 2003. Interaction between flavonoids and the blood–brain barrier: in vitro studies. *Journal of neurochemistry*, *85*(1), pp.180-192.

Zagoskina, N.V., Zubova, M.Y., Nechaeva, T.L., Kazantseva, V.V., Goncharuk, E.A., Katanskaya, V.M., Baranova, E.N. and Aksenova, M.A., 2023. Polyphenols in plants: Structure, biosynthesis, abiotic stress regulation, and practical applications. *International Journal of Molecular Sciences*, *24*(18), p.13874.

Zanetti, O., Solerte, S.B. and Cantoni, F., 2009. Life expectancy in Alzheimer's disease (AD). *Archives of gerontology and geriatrics*, *49*, pp.237-243.

Zaware, B.B., Gilhotra, R. and Chaudhari, S.R., 2018. A Review On Therapeutic Potential Of Caesalpinia crista. *RESEARCH JOURNAL OF PHARMACEUTICAL BIOLOGICAL AND CHEMICAL SCIENCES*, *9*(5), pp.555-566.

Zdravkovic, S., 2017. *Solid phase extraction: Realizing the advantages of an underutilized technique* [online]. Available online: https: //www.ppdi.com/Blog/2017/May/Solid-phase-extraction- [Accessed 6 January 2024].

Zhang, H., Wei, W., Zhao, M., Ma, L., Jiang, X., Pei, H., Cao, Y. and Li, H., 2021. Interaction between Aβ and tau in the pathogenesis of Alzheimer's disease. *International journal of biological sciences*, *17*(9), p.2181.

Zhang, W., Falcon, B., Murzin, A.G., Fan, J., Crowther, R.A., Goedert, M. and Scheres, S.H., 2019. Heparin-induced tau filaments are polymorphic and differ from those in Alzheimer's and Pick's diseases. *elife*, *8*, p.e43584.

Zheng, A., Li, H., Xu, J., Cao, K., Li, H., Pu, W., Yang, Z., Peng, Y., Long, J., Liu, J. and Feng, Z., 2015. Hydroxytyrosol improves mitochondrial function and reduces oxidative stress in the brain of db/db mice: Role of AMP-activated protein kinase activation. *British Journal of Nutrition*, *113*(11), pp.1667-1676.

Zheng, W.H., Bastianetto, S., Mennicken, F., Ma, W. and Kar, S., 2002. Amyloid β peptide induces tau phosphorylation and loss of cholinergic neurons in rat primary septal cultures. *Neuroscience*, *115*(1), pp.201-211.

Zimmermann, M., Atmanene, C., Xu, Q., Fouillen, L., Van Dorsselaer, A., Bonnet, D., Marsol, C., Hibert, M., Sanglier-Cianferani, S., Pigault, C. and McNamara, L.K., 2010.

Homodimerization of the death-associated protein kinase catalytic domain: development of a new small molecule fluorescent reporter. *PLoS One*, *5*(11), p.e14120.
Zott, B., Simon, M.M., Hong, W., Unger, F., Chen-Engerer, H.J., Frosch, M.P., Sakmann, B., Walsh, D.M. and Konnerth, A., 2019. A vicious cycle of β amyloid–dependent neuronal hyperactivation. *Science*, *365*(6453), pp.559-565.
Zupo, R., Castellana, F., Crupi, P., Desantis, A., Rondanelli, M., Corbo, F. and Clodoveo, M.L., 2023. Olive oil polyphenols improve HDL cholesterol and promote maintenance of lipid metabolism: a systematic review and meta-analysis of randomized controlled trials. *Metabolites*, *13*(12), p.1187.

Appendix 1

Table S4.1. An intensive review up to date summarises most of components have been identified in olive oil products from different geographic areas of the world including their chemical formulas, structures and mass.

Chemical name	Chemical formula	Mass
Hydroxytyrosol, [(3, 4dihydroxyphenyl) ethanol] or 3, 4-DHPEA.	$C_8H_{10}O_3$	154.062994
3, 4-dihdroxyphenyl-ethanol-glucoside or Hydroxytyrosol 1-O-glucoside.	$C_{14}H_{20}O_8$	316.115818
Vanillyl alcohol.	$C_8H_{10}O_3$	154.0630
Dimethoxyphenol.	$C_8H_{10}O_3$	154.0630
3, 4-dihydroxyphenylglycol.	$C_8H_{10}O_4$	170.0579
Dihydroxytyrosol.	$C_8H_{10}O_4$	170.0579
Tyrosol, [(*p*-hydroxyphenyl) ethanol], *p*-HPEA or 3-hydroxyphenyl- ethanol 2-(4-hydroxyphenyl) ethanol 4-hydroxyphenyl- ethanol.	$C_8H_{10}O_2$	138.06808
Tyrosol-Glucoside (Salidroside).	$C_{14}H_{20}O_7$	300.120903
Dihydroxyphenilacetic acid or 3, 4-Dihydroxyphenylacetic acid (dopac) **(3, 4-OH)**, (3, 4-DHPAA).	$C_8H_8O_4$	168.042259
Vanillin, (4-hydroxy-3-methoxy benzaldeyde).	$C_8H_8O_3$	152.047344
Oxidized hydroxytyrosol.	$C_8H_8O_3$	152.047344
(*p*-Hydroxyphenyl acetic acid) or 4-Hydroxyphenyl acetic acid **(4-OH) (Hydroxyphenylacetic acids)**.	$C_8H_8O_3$	152.047344

Akasbi, M., Shoeman, D.W. and Csallany, A.S., 1993. High-performance liquid chromatography of selected phenolic compounds in olive oils. Journal of the American Oil Chemists' Society, 70(4), pp.367-370.

Baiano, A.N.T.O.N.I.E.T.T.A., Gambacorta, G., Terracone, C.A.R.M.E.L.A., Previtali, M.A., Lamacchia, C.A.R.M.E.L.A. and La Notte, E.N.N.I.O., 2009. Changes in phenolic content and antioxidant activity of Italian extra-virgin olive oils during storage. Journal of food science, 74(2), pp.C177-C183.

Baldioli, M., Servili, M., Perretti, G. and Montedoro, G.F., 1996. Antioxidant activity of tocopherols and phenolic compounds of virgin olive oil. Journal of the American Oil Chemists' Society, 73(11), pp.1589-1593.

Becerra-Herrera, M., Sánchez-Astudillo, M., Beltrán, R. and Sayago, A., 2014. Determination of phenolic compounds in olive oil: New method based on liquid–liquid micro extraction and ultra high performance liquid chromatography-triple–quadrupole mass spectrometry. LWT-Food Science and Technology, 57(1), pp.49-57.

Bendini, A., Bonoli, M., Cerretani, L., Biguzzi, B., Lercker, G. and Toschi, T.G., 2003. Liquid–liquid and solid-phase extractions of phenols from virgin olive oil and their separation by chromatographic and electrophoretic methods. Journal of Chromatography A, 985(1-2), pp.425-433.

Bendini, A., Cerretani, L., Carrasco-Pancorbo, A., Gómez-Caravaca, A.M., Segura-Carretero, A., Fernández-Gutiérrez, A. and Lercker, G., 2007. Phenolic molecules in virgin olive oils: a survey of their sensory properties, health effects, antioxidant activity and analytical methods. An overview of the last decade Alessandra. Molecules, 12(8), pp.1679-1719.

Boskou, D. ed., 2008. Olive oil: minor constituents and health. CRC press.

Brenes, M., García, A., García, P. and Garrido, A., 2000. Rapid and complete extraction of phenols from olive oil and determination by means of a coulometric electrode array system. Journal of agricultural and food chemistry, 48(11), pp.5178-5183.

Capriotti, A.L., Cavaliere, C., Crescenzi, C., Foglia, P., Nescatelli, R., Samperi, R. and Laganà, A., 2014. Comparison of extraction methods for the identification and quantification of polyphenols in virgin olive oil by ultra-HPLC-QToF mass spectrometry. Food chemistry, 158, pp.392-400.

Christophoridou, S., Dais, P., Tseng, L.H. and Spraul, M., 2005. Separation and identification of phenolic compounds in olive oil by coupling high-performance liquid chromatography with postcolumn solid-phase extraction to nuclear magnetic resonance spectroscopy (LC-SPE-NMR). Journal of Agricultural and Food Chemistry, 53(12), pp.4667-4679.

de Fernandez, M.D.L.A., SotoVargas, V.C. and Silva, M.F., 2014. Phenolic compounds and antioxidant capacity of monovarietal olive oils produced in Argentina. Journal of the American Oil Chemists' Society, 91(12), pp.2021-2033.

De la Torre-Carbot, K., Jauregui, O., Gimeno, E., Castellote, A.I., Lamuela-Raventós, R.M. and López-Sabater, M.C., 2005. Characterization and quantification of phenolic compounds in olive oils by solid-phase extraction, HPLC-DAD, and HPLC-MS/MS. Journal of agricultural and food chemistry, 53(11), pp.4331-4340.

Fanali, C., Della Posta, S., Vilmercati, A., Dugo, L., Russo, M., Petitti, T., Mondello, L. and De Gara, L., 2018. Extraction, analysis, and antioxidant activity evaluation of phenolic compounds in different Italian extra-virgin olive oils. Molecules, 23(12), p.3249.

Farré, M., Picó, Y. and Barceló, D., 2019. Direct analysis in real-time high-resolution mass spectrometry as a valuable tool for polyphenols profiling in olive oil. Analytical methods, 11(4), pp.472-482.

Ferro, M.D., Santos, S.A., Silvestre, A.J. and Duarte, M.F., 2019. Chromatographic separation of phenolic compounds from extra virgin olive oil: Development and validation of a new method based on a biphenyl HPLC column. International Journal of Molecular Sciences, 20(1), p.201.

Fuentes Pérez, E., Paucar, F., Tapia, F., Ortiz Viedma, J., Jiménez Patiño, P.A. and Romero Palacios, N., 2018. Effect of the composition of extra virgin olive oils on the differentiation and antioxidant capacities of twelve monovarietals.

García-Villalba, R., Carrasco-Pancorbo, A., Vázquez-Martín, A., Oliveras-Ferraros, C., Menéndez, J.A., Segura-Carretero, A. and Fernández-Gutiérrez, A., 2009. A 2-D-HPLC-CE platform coupled to ESI-TOF-MS to characterize the phenolic fraction in olive oil. Electrophoresis, 30(15), pp.2688-2701.

Gilbert-López, B., Valencia-Reyes, Z.L., Yufra-Picardo, V.M., García-Reyes, J.F., Ramos-Martos, N. and Molina-Díaz, A., 2014. Determination of polyphenols in commercial extra virgin olive oils from different origins (Mediterranean and South American countries) by liquid chromatography–electrospray time-of-flight mass spectrometry. Food analytical methods, 7(9), pp.1824-1833

Gilbert-López, B., Valencia-Reyes, Z.L., Yufra-Picardo, V.M., García-Reyes, J.F., Ramos-Martos, N. and Molina-Díaz, A., 2014. Determination of polyphenols in commercial extra virgin olive oils from different origins (Mediterranean and South American countries) by liquid chromatography–electrospray time-of-flight mass spectrometry. Food analytical methods, 7(9), pp.1824-1833.

Gómez Caravaca, A.M., Carrasco Pancorbo, A., Cañabate Díaz, B., Segura Carretero, A. and Fernández Gutiérrez, A., 2005. Electrophoretic identification and quantitation of compounds in the polyphenolic fraction of extra-virgin olive oil. Electrophoresis, 26(18), pp.3538-3551.

Gutfinger, T., 1981. Polyphenols in olive oils. Journal of the American Oil Chemists' Society, 58(11), pp.966-968.

Liberatore, L., Procida, G., d'Alessandro, N. and Cichelli, A., 2001. Solid-phase extraction and gas chromatographic analysis of phenolic compounds in virgin olive oil. Food Chemistry, 73(1), pp.119-124.

Lozano-Sánchez, J., Bendini, A., Quirantes-Piné, R., Cerretani, L., Segura-Carretero, A. and Fernández-Gutiérrez, A., 2013. Monitoring the bioactive compounds status of extra-virgin olive oil and storage by-products over the shelf life. Food Control, 30(2), pp.606-615.

Manai-Djebali, H., Krichène, D., Ouni, Y., Gallardo, L., Sánchez, J., Osorio, E., Daoud, D., Guido, F. and Zarrouk, M., 2012. Chemical profiles of five minor olive oil varieties grown in central Tunisia. Journal of Food Composition and Analysis, 27(2), pp.109-119.

Mateos, R., Espartero, J.L., Trujillo, M., Rios, J.J., León-Camacho, M., Alcudia, F. and Cert, A., 2001. Determination of phenols, flavones, and lignans in virgin olive oils by solid-phase extraction and high-performance liquid chromatography with diode array ultraviolet detection. Journal of Agricultural and Food Chemistry, 49(5), pp.2185-2192.

Montedoro, G., Servili, M., Baldioli, M. and Miniati, E., 1992. Simple and hydrolyzable phenolic compounds in virgin olive oil. 1. Their extraction, separation, and quantitative and semiquantitative evaluation by HPLC. Journal of Agricultural and Food Chemistry, 40(9), pp.1571-1576.

Montedoro, G., Servili, M., Baldioli, M. and Miniati, E., 1992. Simple and hydrolyzable phenolic compounds in virgin olive oil. 2. Initial characterization of the hydrolyzable fraction. Journal of Agricultural and Food Chemistry, 40(9), pp.1577-1580.

Montedoro, G., Servili, M., Baldioli, M., Selvaggini, R., Miniati, E. and Macchioni, A., 1993. Simple and hydrolyzable compounds in virgin olive oil. 3. Spectroscopic characterizations of the secoiridoid derivatives. Journal of Agricultural and Food Chemistry, 41(11), pp.2228-2234.

Naushad, M. and Khan, M.R., 2014. Ultra performance liquid chromatography mass spectrometry: evaluation and applications in food analysis. CRC Press.

Negro, C., Aprile, A., Luvisi, A., Nicolì, F., Nutricati, E., Vergine, M., Miceli, A., Blando, F., Sabella, E. and De Bellis, L., 2019. Phenolic profile and antioxidant activity of Italian monovarietal extra virgin olive oils. Antioxidants, 8(6), p.161.

Oliveras-López, M.J., Innocenti, M., Giaccherini, C., Ieri, F., Romani, A. and Mulinacci, N., 2007. Study of the phenolic composition of spanish and italian monocultivar extra virgin olive oils: Distribution of lignans, secoiridoidic, simple phenols and flavonoids. Talanta, 73(4), pp.726-732.

Olmo-García, L., Polari, J.J., Li, X., Bajoub, A., Fernández-Gutiérrez, A., Wang, S.C. and Carrasco-Pancorbo, A., 2018. Deep insight into the minor fraction of virgin olive oil by using LC-MS and GC-MS multi-class methodologies. Food chemistry, 261, pp.184-193.

Owen, R.W., Giacosa, A., Hull, W.E., Haubner, R., Spiegelhalder, B. and Bartsch, H., 2000. The antioxidant/anticancer potential of phenolic compounds isolated from olive oil. European Journal of Cancer, 36(10), pp.1235-1247.

Owen, R.W., Mier, W., Giacosa, A., Hull, W.E., Spiegelhalder, B. and Bartsch, H., 2000. Identification of lignans as major components in the phenolic fraction of olive oil. Clinical Chemistry, 46(7), pp.976-988.

Papadopoulos, G. and Boskou, D., 1991. Antioxidant effect of natural phenols on olive oil. Journal of the American Oil Chemists' Society, 68(9), pp.669-671.

Pirisi, F.M., Cabras, P., Cao, C.F., Migliorini, M. and Muggelli, M., 2000. Phenolic compounds in virgin olive oil. 2. Reappraisal of the extraction, HPLC separation, and quantification procedures. Journal of Agricultural and Food Chemistry, 48(4), pp.1191-1196.

Pizarro, M.L., Becerra, M., Sayago, A., Beltrán, M. and Beltrán, R., 2013. Comparison of different extraction methods to determine phenolic compounds in virgin olive oil. Food Analytical Methods, 6(1), pp.123-132.

Ricciutelli, M., Marconi, S., Boarelli, M.C., Caprioli, G., Sagratini, G., Ballini, R. and Fiorini, D., 2017. Olive oil polyphenols: A quantitative method by high-performance liquid-chromatography-diode-array detection for their determination and the assessment of the related health claim. Journal of Chromatography A, 1481, pp.53-63.

Rodríguez-López, P., Lozano-Sanchez, J., Borrás-Linares, I., Emanuelli, T., Menéndez, J.A. and Segura-Carretero, A., 2020. Structure–Biological Activity Relationships of Extra-Virgin Olive Oil Phenolic Compounds: Health Properties and Bioavailability. Antioxidants, 9(8), p.685.

Schneider, S., 2016. Quality Analysis of Extra Virgin Olive Oils—Part 6 Nutritive Benefi ts—Phenolic Compounds in Virgin Olive Oil. Agilent Technology Application Note.

Servili, M. and Montedoro, G., 2002. Contribution of phenolic compounds to virgin olive oil quality. European Journal of Lipid Science and Technology, 104(9-10), pp.602-613.

Servili, M., Esposto, S., Fabiani, R., Urbani, S., Taticchi, A., Mariucci, F., Selvaggini, R. and Montedoro, G.F., 2009. Phenolic compounds in olive oil: antioxidant, health and organoleptic activities according to their chemical structure. Inflammopharmacology, 17(2), pp.76-84.

Suárez, M., Macià, A., Romero, M.P. and Motilva, M.J., 2008. Improved liquid chromatography tandem mass spectrometry method for the determination of phenolic compounds in virgin olive oil. Journal of Chromatography A, 1214(1-2), pp.90-99.

Tasioula-Margari, M. and Okogeri, O., 2001. Isolation and characterization of virgin olive oil phenolic compounds by HPLC/UV and GC-MS. Journal of Food Science, 66(4), pp.530-534.

Tasioula-Margari, M. and Tsabolatidou, E., 2015. Extraction, separation, and identification of phenolic compounds in virgin olive oil by HPLC-DAD and HPLC-MS. Antioxidants, 4(3), pp.548-562.

Tripoli, E., Giammanco, M., Tabacchi, G., Di Majo, D., Giammanco, S. and La Guardia, M., 2005. The phenolic compounds of olive oil: structure, biological activity and beneficial effects on human health. Nutrition research reviews, 18(1), pp.98-112.

Tsimidou, M., Lytridou, M., Boskou, D., Pappa-Louisi, A., Kotsifaki, F. and Petrakis, C., 1996. On the determination of minor phenolic acids of virgin olive oil by RP-HPLC. GRASAS Y ACEITES-SEVILLA-, 47, pp.151-157.

Tsimidou, M., Papadopoulos, G. and Boskou, D., 1992. Determination of phenolic compounds in virgin olive oil by reversed-phase HPLC with emphasis on UV detection. Food Chemistry, 44(1), pp.53-60.

Tsimidou, M., Papadopoulos, G. and Boskou, D., 1992. Phenolic compounds and stability of virgin olive oil—Part I. Food Chemistry, 45(2), pp.141-144.

Syringic acid.	$C_9H_{10}O_5$	198.052823
Cinnamic acid.	$C_9H_8O_2$	148.052429
Ferulic acid.	$C_{10}H_{10}O_4$	194.057909
Vanillic acid.	$C_8H_8O_4$	168.042259
Methyl caffeate.	$C_{10}H_{10}O_4$	194.057910
p-Coumaric acid **4-OH**.	$C_9H_8O_3$	164.047344
o-Coumaric acid **2-OH**.	$C_9H_8O_3$	164.047344
m-Coumaric acid or *m*-Hydroxycinnamic acid.	$C_9H_8O_3$	164.047344
Caffeic acid.	$C_9H_8O_4$	180.042259
Caffeic acid 3-glucoside.	$C_{15}H_{18}O_9$	342.095082
Hydroxycaffeic acid.	$C_9H_8O_5$	196.037173
Gentisic acid **(2, 5-OH)**.	$C_7H_6O_4$	154.026609
Gallic acid.	$C_7H_6O_5$	170.021523
Sinapinic acid.	$C_{11}H_{12}O_5$	224.068473

Akasbi, M., Shoeman, D.W. and Csallany, A.S., 1993. High-performance liquid chromatography of selected phenolic compounds in olive oils. Journal of the American Oil Chemists' Society, 70(4), pp.367-370.

Baldioli, M., Servili, M., Perretti, G. and Montedoro, G.F., 1996. Antioxidant activity of tocopherols and phenolic compounds of virgin olive oil. Journal of the American Oil Chemists' Society, 73(11), pp.1589-1593.

Becerra-Herrera, M., Sánchez-Astudillo, M., Beltrán, R. and Sayago, A., 2014. Determination of phenolic compounds in olive oil: New method based on liquid–liquid micro extraction and ultra high performance liquid chromatography-triple–quadrupole mass spectrometry. LWT-Food Science and Technology, 57(1), pp.49-57.

Bendini, A., Bonoli, M., Cerretani, L., Biguzzi, B., Lercker, G. and Toschi, T.G., 2003. Liquid–liquid and solid-phase extractions of phenols from virgin olive oil and their separation by chromatographic and electrophoretic methods. Journal of Chromatography A, 985(1-2), pp.425-433.

Bendini, A., Cerretani, L., Carrasco-Pancorbo, A., Gómez-Caravaca, A.M., Segura-Carretero, A., Fernández-Gutiérrez, A. and Lercker, G., 2007. Phenolic molecules in virgin olive oils: a survey of their sensory properties, health effects, antioxidant activity and analytical methods. An overview of the last decade Alessandra. Molecules, 12(8), pp.1679-1719.

Boskou, D. ed., 2008. Olive oil: minor constituents and health. CRC press.

Brenes, M., García, A., García, P. and Garrido, A., 2000. Rapid and complete extraction of phenols from olive oil and determination by means of a coulometric electrode array system. Journal of agricultural and food chemistry, 48(11), pp.5178-5183.

Capriotti, A.L., Cavaliere, C., Crescenzi, C., Foglia, P., Nescatelli, R., Samperi, R. and Laganà, A., 2014. Comparison of extraction methods for the identification and quantification of polyphenols in virgin olive oil by ultra-HPLC-QToF mass spectrometry. Food chemistry, 158, pp.392-400.

Christophoridou, S., Dais, P., Tseng, L.H. and Spraul, M., 2005. Separation and identification of phenolic compounds in olive oil by coupling high-performance liquid chromatography with postcolumn solid-phase extraction to nuclear magnetic resonance spectroscopy (LC-SPE-NMR). Journal of Agricultural and Food Chemistry, 53(12), pp.4667-4679.

de Fernandez, M.D.L.A., SotoVargas, V.C. and Silva, M.F., 2014. Phenolic compounds and antioxidant capacity of monovarietal olive oils produced in Argentina. Journal of the American Oil Chemists' Society, 91(12), pp.2021-2033.

De la Torre-Carbot, K., Jauregui, O., Gimeno, E., Castellote, A.I., Lamuela-Raventós, R.M. and López-Sabater, M.C., 2005. Characterization and quantification of phenolic compounds in olive oils by solid-phase extraction, HPLC-DAD, and HPLC-MS/MS. Journal of agricultural and food chemistry, 53(11), pp.4331-4340.

Fanali, C., Della Posta, S., Vilmercati, A., Dugo, L., Russo, M., Petitti, T., Mondello, L. and De Gara, L., 2018. Extraction, analysis, and antioxidant activity evaluation of phenolic compounds in different Italian extra-virgin olive oils. Molecules, 23(12), p.3249.

Ferro, M.D., Santos, S.A., Silvestre, A.J. and Duarte, M.F., 2019. Chromatographic separation of phenolic compounds from extra virgin olive oil: Development and validation of a new method based on a biphenyl HPLC column. International Journal of Molecular Sciences, 20(1), p.201.

Fuentes Pérez, E., Paucar, F., Tapia, F., Ortiz Viedma, J., Jiménez Patiño, P.A. and Romero Palacios, N., 2018. Effect of the composition of extra virgin olive oils on the differentiation and antioxidant capacities of twelve monovarietals.

García-Villalba, R., Carrasco-Pancorbo, A., Vázquez-Martín, A., Oliveras-Ferraros, C., Menéndez, J.A., Segura-Carretero, A. and Fernández-Gutiérrez, A., 2009. A 2-D-HPLC-CE platform coupled to ESI-TOF-MS to characterize the phenolic fraction in olive oil. Electrophoresis, 30(15), pp.2688-2701.

Gilbert-López, B., Valencia-Reyes, Z.L., Yufra-Picardo, V.M., García-Reyes, J.F., Ramos-Martos, N. and Molina-Díaz, A., 2014. Determination of polyphenols in commercial extra virgin olive oils from different origins (Mediterranean and South American countries) by liquid chromatography–electrospray time-of-flight mass spectrometry. Food analytical methods, 7(9), pp.1824-1833

Gilbert-López, B., Valencia-Reyes, Z.L., Yufra-Picardo, V.M., García-Reyes, J.F., Ramos-Martos, N. and Molina-Díaz, A., 2014. Determination of polyphenols in commercial extra virgin olive oils from different origins (Mediterranean and South American countries) by liquid chromatography–electrospray time-of-flight mass spectrometry. Food analytical methods, 7(9), pp.1824-1833.

Gutfinger, T., 1981. Polyphenols in olive oils. Journal of the American Oil Chemists' Society, 58(11), pp.966-968.

Liberatore, L., Procida, G., d'Alessandro, N. and Cichelli, A., 2001. Solid-phase extraction and gas chromatographic analysis of phenolic compounds in virgin olive oil. Food Chemistry, 73(1), pp.119-124.

Lozano-Sánchez, J., Bendini, A., Quirantes-Piné, R., Cerretani, L., Segura-Carretero, A. and Fernández-Gutiérrez, A., 2013. Monitoring the bioactive compounds status of extra-virgin olive oil and storage by-products over the shelf life. Food Control, 30(2), pp.606-615.

Manai-Djebali, H., Krichène, D., Ouni, Y., Gallardo, L., Sánchez, J., Osorio, E., Daoud, D., Guido, F. and Zarrouk, M., 2012. Chemical profiles of five minor olive oil varieties grown in central Tunisia. Journal of Food Composition and Analysis, 27(2), pp.109-119.

Mateos, R., Espartero, J.L., Trujillo, M., Rios, J.J., León-Camacho, M., Alcudia, F. and Cert, A., 2001. Determination of phenols, flavones, and lignans in virgin olive oils by solid-phase extraction and high-performance liquid chromatography with diode array ultraviolet detection. Journal of Agricultural and Food Chemistry, 49(5), pp.2185-2192.

Montedoro, G., Servili, M., Baldioli, M. and Miniati, E., 1992. Simple and hydrolyzable phenolic compounds in virgin olive oil. 1. Their extraction, separation, and quantitative and semiquantitative evaluation by HPLC. Journal of Agricultural and Food Chemistry, 40(9), pp.1571-1576.

Montedoro, G., Servili, M., Baldioli, M. and Miniati, E., 1992. Simple and hydrolyzable phenolic compounds in virgin olive oil. 2. Initial characterization of the hydrolyzable fraction. Journal of Agricultural and Food Chemistry, 40(9), pp.1577-1580.

Montedoro, G., Servili, M., Baldioli, M., Selvaggini, R., Miniati, E. and Macchioni, A., 1993. Simple and hydrolyzable compounds in virgin olive oil. 3. Spectroscopic characterizations of the secoiridoid derivatives. Journal of Agricultural and Food Chemistry, 41(11), pp.2228-2234.

Naushad, M. and Khan, M.R., 2014. Ultra performance liquid chromatography mass spectrometry: evaluation and applications in food analysis. CRC Press.

Olmo-García, L., Polari, J.J., Li, X., Bajoub, A., Fernández-Gutiérrez, A., Wang, S.C. and Carrasco-Pancorbo, A., 2018. Deep insight into the minor fraction of virgin olive oil by using LC-MS and GC-MS multi-class methodologies. Food chemistry, 261, pp.184-193.

Papadopoulos, G. and Boskou, D., 1991. Antioxidant effect of natural phenols on olive oil. Journal of the American Oil Chemists' Society, 68(9), pp.669-671.

Pirisi, F.M., Cabras, P., Cao, C.F., Migliorini, M. and Muggelli, M., 2000. Phenolic compounds in virgin olive oil. 2. Reappraisal of the extraction, HPLC separation, and quantification procedures. Journal of Agricultural and Food Chemistry, 48(4), pp.1191-1196.

Pizarro, M.L., Becerra, M., Sayago, A., Beltrán, M. and Beltrán, R., 2013. Comparison of different extraction methods to determine phenolic compounds in virgin olive oil. Food Analytical Methods, 6(1), pp.123-132.

Ricciutelli, M., Marconi, S., Boarelli, M.C., Caprioli, G., Sagratini, G., Ballini, R. and Fiorini, D., 2017. Olive oil polyphenols: A quantitative method by high-performance liquid-chromatography-diode-array detection for their determination and the assessment of the related health claim. Journal of Chromatography A, 1481, pp.53-63.

Rodríguez-López, P., Lozano-Sanchez, J., Borrás-Linares, I., Emanuelli, T., Menéndez, J.A. and Segura-Carretero, A., 2020. Structure–Biological Activity Relationships of Extra-Virgin Olive Oil Phenolic Compounds: Health Properties and Bioavailability. Antioxidants, 9(8), p.685.

Schneider, S., 2016. Quality Analysis of Extra Virgin Olive Oils—Part 6 Nutritive Benefi ts—Phenolic Compounds in Virgin Olive Oil. Agilent Technology Application Note.

Servili, M. and Montedoro, G., 2002. Contribution of phenolic compounds to virgin olive oil quality. European Journal of Lipid Science and Technology, 104(9-10), pp.602-613.

Servili, M., Esposto, S., Fabiani, R., Urbani, S., Taticchi, A., Mariucci, F., Selvaggini, R. and Montedoro, G.F., 2009. Phenolic compounds in olive oil: antioxidant, health and organoleptic activities according to their chemical structure. Inflammopharmacology, 17(2), pp.76-84.

Suárez, M., Macià, A., Romero, M.P. and Motilva, M.J., 2008. Improved liquid chromatography tandem mass spectrometry method for the determination of phenolic compounds in virgin olive oil. Journal of Chromatography A, 1214(1-2), pp.90-99.

Tasioula-Margari, M. and Okogeri, O., 2001. Isolation and characterization of virgin olive oil phenolic compounds by HPLC/UV and GC-MS. Journal of Food Science, 66(4), pp.530-534.

Tasioula-Margari, M. and Tsabolatidou, E., 2015. Extraction, separation, and identification of phenolic compounds in virgin olive oil by HPLC-DAD and HPLC-MS. Antioxidants, 4(3), pp.548-562.

Tripoli, E., Giammanco, M., Tabacchi, G., Di Majo, D., Giammanco, S. and La Guardia, M., 2005. The phenolic compounds of olive oil: structure, biological activity and beneficial effects on human health. Nutrition research reviews, 18(1), pp.98-112.

Tsimidou, M., Lytridou, M., Boskou, D., Pappa-Louisi, A., Kotsifaki, F. and Petrakis, C., 1996. On the determination of minor phenolic acids of virgin olive oil by RP-HPLC. GRASAS Y ACEITES-SEVILLA-, 47, pp.151-157.

Tsimidou, M., Papadopoulos, G. and Boskou, D., 1992. Determination of phenolic compounds in virgin olive oil by reversed-phase HPLC with emphasis on UV detection. Food Chemistry, 44(1), pp.53-60.

Tsimidou, M., Papadopoulos, G. and Boskou, D., 1992. Phenolic compounds and stability of virgin olive oil—Part I. Food Chemistry, 45(2), pp.141-144.

Elenolic acid.	$C_{11}H_{14}O_6$	242.079038
Elenolic acid- glucoside.	$C_{17}H_{25}O_{11}$	405.1397
Deoxyelenoic acid.	$C_{11}H_{15}O_5$ $C_{11}H_{14}O_5$	227.0919 226.0841
Hydroxyelenoic acid, Hydroxylated form of elenolic acid, Hydroxy-EA.	$C_{11}H_{14}O_7$	258.0740
Decarboxymethyl elenolic acid.	$C_9H_{12}O_4$	184.073559
Hydroxy decarboxymethyl elenolic acid.	$C_9H_8O_3$	164.0473
Dihydroxy-EA (UK6, UK7).	$C_{11}H_{16}O_6$	244.0947
Licodione.	$C_{11}H_{12}O_8$	272.0532
α-Arbutin.	$C_{12}H_{16}O_7$	272.0896
Pentamethoxy benzoic acid.	$C_{12}H_{16}O_7$	272.0896
Erigerosido.	$C_{11}H_{14}O_8$	274.0689

Bendini, A., Cerretani, L., Carrasco-Pancorbo, A., Gómez-Caravaca, A.M., Segura-Carretero, A., Fernández-Gutiérrez, A. and Lercker, G., 2007. Phenolic molecules in virgin olive oils: a survey of their sensory properties, health effects, antioxidant activity and analytical methods. An overview of the last decade Alessandra. Molecules, 12(8), pp.1679-1719.

Boskou, D. ed., 2008. Olive oil: minor constituents and health. CRC press.

Capriotti, A.L., Cavaliere, C., Crescenzi, C., Foglia, P., Nescatelli, R., Samperi, R. and Laganà, A., 2014. Comparison of extraction methods for the identification and quantification of polyphenols in virgin olive oil by ultra-HPLC-QToF mass spectrometry. Food chemistry, 158, pp.392-400.

Christophoridou, S., Dais, P., Tseng, L.H. and Spraul, M., 2005. Separation and identification of phenolic compounds in olive oil by coupling high-performance liquid chromatography with postcolumn solid-phase extraction to nuclear magnetic resonance spectroscopy (LC-SPE-NMR). Journal of Agricultural and Food Chemistry, 53(12), pp.4667-4679.

Fanali, C., Della Posta, S., Vilmercati, A., Dugo, L., Russo, M., Petitti, T., Mondello, L. and De Gara, L., 2018. Extraction, analysis, and antioxidant activity evaluation of phenolic compounds in different Italian extra-virgin olive oils. Molecules, 23(12), p.3249.

Farré, M., Picó, Y. and Barceló, D., 2019. Direct analysis in real-time high-resolution mass spectrometry as a valuable tool for polyphenols profiling in olive oil. Analytical methods, 11(4), pp.472-482.

Fuentes Pérez, E., Paucar, F., Tapia, F., Ortiz Viedma, J., Jiménez Patiño, P.A. and Romero Palacios, N., 2018. Effect of the composition of extra virgin olive oils on the differentiation and antioxidant capacities of twelve monovarietals.

García-Villalba, R., Carrasco-Pancorbo, A., Vázquez-Martín, A., Oliveras-Ferraros, C., Menéndez, J.A., Segura-Carretero, A. and Fernández-Gutiérrez, A., 2009. A 2-D-HPLC-CE platform coupled to ESI-TOF-MS to characterize the phenolic fraction in olive oil. Electrophoresis, 30(15), pp.2688-2701.

Gilbert-López, B., Valencia-Reyes, Z.L., Yufra-Picardo, V.M., García-Reyes, J.F., Ramos-Martos, N. and Molina-Díaz, A., 2014. Determination of polyphenols in commercial extra virgin olive oils from different origins (Mediterranean and South American countries) by liquid chromatography–electrospray time-of-flight mass spectrometry. Food analytical methods, 7(9), pp.1824-1833

Gómez Caravaca, A.M., Carrasco Pancorbo, A., Cañabate Díaz, B., Segura Carretero, A. and Fernández Gutiérrez, A., 2005. Electrophoretic identification and quantitation of compounds in the polyphenolic fraction of extra-virgin olive oil. Electrophoresis, 26(18), pp.3538-3551.
Lozano-Sánchez, J., Bendini, A., Quirantes-Piné, R., Cerretani, L., Segura-Carretero, A. and Fernández-Gutiérrez, A., 2013. Monitoring the bioactive compounds status of extra-virgin olive oil and storage by-products over the shelf life. Food Control, 30(2), pp.606-615.
Mateos, R., Espartero, J.L., Trujillo, M., Rios, J.J., León-Camacho, M., Alcudia, F. and Cert, A., 2001. Determination of phenols, flavones, and lignans in virgin olive oils by solid-phase extraction and high-performance liquid chromatography with diode array ultraviolet detection. Journal of Agricultural and Food Chemistry, 49(5), pp.2185-2192.
Montedoro, G., Servili, M., Baldioli, M. and Miniati, E., 1992. Simple and hydrolyzable phenolic compounds in virgin olive oil. 1. Their extraction, separation, and quantitative and semiquantitative evaluation by HPLC. Journal of Agricultural and Food Chemistry, 40(9), pp.1571-1576.
Montedoro, G., Servili, M., Baldioli, M. and Miniati, E., 1992. Simple and hydrolyzable phenolic compounds in virgin olive oil. 2. Initial characterization of the hydrolyzable fraction. Journal of Agricultural and Food Chemistry, 40(9), pp.1577-1580.
Montedoro, G., Servili, M., Baldioli, M., Selvaggini, R., Miniati, E. and Macchioni, A., 1993. Simple and hydrolyzable compounds in virgin olive oil. 3. Spectroscopic characterizations of the secoiridoid derivatives. Journal of Agricultural and Food Chemistry, 41(11), pp.2228-2234.
Negro, C., Aprile, A., Luvisi, A., Nicolì, F., Nutricati, E., Vergine, M., Miceli, A., Blando, F., Sabella, E. and De Bellis, L., 2019. Phenolic profile and antioxidant activity of Italian monovarietal extra virgin olive oils. Antioxidants, 8(6), p.161.
Olmo-García, L., Polari, J.J., Li, X., Bajoub, A., Fernández-Gutiérrez, A., Wang, S.C. and Carrasco-Pancorbo, A., 2018. Deep insight into the minor fraction of virgin olive oil by using LC-MS and GC-MS multi-class methodologies. Food chemistry, 261, pp.184-193.
Pirisi, F.M., Cabras, P., Cao, C.F., Migliorini, M. and Muggelli, M., 2000. Phenolic compounds in virgin olive oil. 2. Reappraisal of the extraction, HPLC separation, and quantification procedures. Journal of Agricultural and Food Chemistry, 48(4), pp.1191-1196.
Tripoli, E., Giammanco, M., Tabacchi, G., Di Majo, D., Giammanco, S. and La Guardia, M., 2005. The phenolic compounds of olive oil: structure, biological activity and beneficial effects on human health. Nutrition research reviews, 18(1), pp.98-112.

Benzoic acid.	**$C_7H_6O_2$**	122.036779
Hydroxybenzoic acid.	**$C_7H_6O_3$**	138.0317
3-Hydroxybenzoic acid **3-OH**.	**$C_7H_6O_3$**	138.031694
p-Hydroxybenzoic acid, 4-Hydroxybenzoic **4-OH**.	**$C_7H_6O_3$**	138.031694
Dihydroxybenzoquinone.	**$C_6H_4O_4$**	140.0110
3-Methoxybenzoic acid (3-MBA).	**$C_8H_8O_3$**	152.047344
3, 4-Dihydroxybenzoic acid, protocatechuic acid (PA) and Dihydroxybenzoic acid.	**$C_7H_6O_4$**	154.026609
4-Hydroxy-3-methoxyphenylacetic acid.	**$C_9H_{10}O_4$**	182.0579
Homovanillic acid.	**$C_9H_{10}O_4$**	182.0579
3-(3, 4-Dihydroxyphenyl) propanoic acid, dihydrocaffeic acid (DHCA).	**$C_9H_{10}O_4$**	182.057909

Akasbi, M., Shoeman, D.W. and Csallany, A.S., 1993. High-performance liquid chromatography of selected phenolic compounds in olive oils. Journal of the American Oil Chemists' Society, 70(4), pp.367-370.
Becerra-Herrera, M., Sánchez-Astudillo, M., Beltrán, R. and Sayago, A., 2014. Determination of phenolic compounds in olive oil: New method based on liquid–liquid micro extraction and ultra high performance liquid chromatography-triple–quadrupole mass spectrometry. LWT-Food Science and Technology, 57(1), pp.49-57.
Bendini, A., Bonoli, M., Cerretani, L., Biguzzi, B., Lercker, G. and Toschi, T.G., 2003. Liquid–liquid and solid-phase extractions of phenols from virgin olive oil and their separation by chromatographic and electrophoretic methods. Journal of Chromatography A, 985(1-2), pp.425-433.
Bendini, A., Cerretani, L., Carrasco-Pancorbo, A., Gómez-Caravaca, A.M., Segura-Carretero, A., Fernández-Gutiérrez, A. and Lercker, G., 2007. Phenolic molecules in virgin olive oils: a survey of their sensory properties, health effects, antioxidant activity and analytical methods. An overview of the last decade Alessandra. Molecules, 12(8), pp.1679-1719.
Boskou, D. ed., 2008. Olive oil: minor constituents and health. CRC press.

Capriotti, A.L., Cavaliere, C., Crescenzi, C., Foglia, P., Nescatelli, R., Samperi, R. and Laganà, A., 2014. Comparison of extraction methods for the identification and quantification of polyphenols in virgin olive oil by ultra-HPLC-QToF mass spectrometry. Food chemistry, 158, pp.392-400.

Farré, M., Picó, Y. and Barceló, D., 2019. Direct analysis in real-time high-resolution mass spectrometry as a valuable tool for polyphenols profiling in olive oil. Analytical methods, 11(4), pp.472-482.

Gutfinger, T., 1981. Polyphenols in olive oils. Journal of the American Oil Chemists' Society, 58(11), pp.966-968.

Liberatore, L., Procida, G., d'Alessandro, N. and Cichelli, A., 2001. Solid-phase extraction and gas chromatographic analysis of phenolic compounds in virgin olive oil. Food Chemistry, 73(1), pp.119-124.

Lozano-Sánchez, J., Bendini, A., Quirantes-Piné, R., Cerretani, L., Segura-Carretero, A. and Fernández-Gutiérrez, A., 2013. Monitoring the bioactive compounds status of extra-virgin olive oil and storage by-products over the shelf life. Food Control, 30(2), pp.606-615.

Montedoro, G., Servili, M., Baldioli, M. and Miniati, E., 1992. Simple and hydrolyzable phenolic compounds in virgin olive oil. 1. Their extraction, separation, and quantitative and semiquantitative evaluation by HPLC. Journal of Agricultural and Food Chemistry, 40(9), pp.1571-1576.

Montedoro, G., Servili, M., Baldioli, M. and Miniati, E., 1992. Simple and hydrolyzable phenolic compounds in virgin olive oil. 2. Initial characterization of the hydrolyzable fraction. Journal of Agricultural and Food Chemistry, 40(9), pp.1577-1580.

Montedoro, G., Servili, M., Baldioli, M., Selvaggini, R., Miniati, E. and Macchioni, A., 1993. Simple and hydrolyzable compounds in virgin olive oil. 3. Spectroscopic characterizations of the secoiridoid derivatives. Journal of Agricultural and Food Chemistry, 41(11), pp.2228-2234.

Naushad, M. and Khan, M.R., 2014. Ultra performance liquid chromatography mass spectrometry: evaluation and applications in food analysis. CRC Press.

Olmo-García, L., Polari, J.J., Li, X., Bajoub, A., Fernández-Gutiérrez, A., Wang, S.C. and Carrasco-Pancorbo, A., 2018. Deep insight into the minor fraction of virgin olive oil by using LC-MS and GC-MS multi-class methodologies. Food chemistry, 261, pp.184-193.

Papadopoulos, G. and Boskou, D., 1991. Antioxidant effect of natural phenols on olive oil. Journal of the American Oil Chemists' Society, 68(9), pp.669-671.

Rodríguez-López, P., Lozano-Sanchez, J., Borrás-Linares, I., Emanuelli, T., Menéndez, J.A. and Segura-Carretero, A., 2020. Structure–Biological Activity Relationships of Extra-Virgin Olive Oil Phenolic Compounds: Health Properties and Bioavailability. Antioxidants, 9(8), p.685.

Schneider, S., 2016. Quality Analysis of Extra Virgin Olive Oils—Part 6 Nutritive Benefi ts—Phenolic Compounds in Virgin Olive Oil. Agilent Technology Application Note.

Servili, M. and Montedoro, G., 2002. Contribution of phenolic compounds to virgin olive oil quality. European Journal of Lipid Science and Technology, 104(9-10), pp.602-613.

Servili, M., Esposto, S., Fabiani, R., Urbani, S., Taticchi, A., Mariucci, F., Selvaggini, R. and Montedoro, G.F., 2009. Phenolic compounds in olive oil: antioxidant, health and organoleptic activities according to their chemical structure. Inflammopharmacology, 17(2), pp.76-84.

Tsimidou, M., Papadopoulos, G. and Boskou, D., 1992. Determination of phenolic compounds in virgin olive oil by reversed-phase HPLC with emphasis on UV detection. Food Chemistry, 44(1), pp.53-60.

Tsimidou, M., Papadopoulos, G. and Boskou, D., 1992. Phenolic compounds and stability of virgin olive oil—Part I. Food Chemistry, 45(2), pp.141-144.

(+)-Taxifolin.	$C_{15}H_{12}O_7$	304.0583
Apigenin.	$C_{15}H_{10}O_5$	270.0528
Luteolin.	$C_{15}H_{10}O_6$	286.0477
Altenuene (mycotoxin).	$C_{15}H_{16}O_6$	292.0947
(+)-Pinoresinol.	$C_{20}H_{22}O_6$	358.1416
Matairesinol.	$C_{20}H_{22}O_6$	358.1416
(+)-1-Acetoxypinoresinol.	$C_{22}H_{24}O_8$	416.1471
(+)-1-Hydroxypinoresinol.	$C_{20}H_{22}O_7$	374.1366

Baiano, A.N.T.O.N.I.E.T.T.A., Gambacorta, G., Terracone, C.A.R.M.E.L.A., Previtali, M.A., Lamacchia, C.A.R.M.E.L.A. and La Notte, E.N.N.I.O., 2009. Changes in phenolic content and antioxidant activity of Italian extra-virgin olive oils during storage. Journal of food science, 74(2), pp.C177-C183.

Becerra-Herrera, M., Sánchez-Astudillo, M., Beltrán, R. and Sayago, A., 2014. Determination of phenolic compounds in olive oil: New method based on liquid–liquid micro extraction and ultra high performance liquid chromatography-triple–quadrupole mass spectrometry. LWT-Food Science and Technology, 57(1), pp.49-57.

Bendini, A., Bonoli, M., Cerretani, L., Biguzzi, B., Lercker, G. and Toschi, T.G., 2003. Liquid–liquid and solid-phase extractions of phenols from virgin olive oil and their separation by chromatographic and electrophoretic methods. Journal of Chromatography A, 985(1-2), pp.425-433.

Bendini, A., Cerretani, L., Carrasco-Pancorbo, A., Gómez-Caravaca, A.M., Segura-Carretero, A., Fernández-Gutiérrez, A. and Lercker, G., 2007. Phenolic molecules in virgin olive oils: a survey of their sensory properties, health effects, antioxidant activity and analytical methods. An overview of the last decade Alessandra. Molecules, 12(8), pp.1679-1719.

Boskou, D. ed., 2008. Olive oil: minor constituents and health. CRC press.

Brenes, M., García, A., García, P. and Garrido, A., 2000. Rapid and complete extraction of phenols from olive oil and determination by means of a coulometric electrode array system. Journal of agricultural and food chemistry, 48(11), pp.5178-5183.

Capriotti, A.L., Cavaliere, C., Crescenzi, C., Foglia, P., Nescatelli, R., Samperi, R. and Laganà, A., 2014. Comparison of extraction methods for the identification and quantification of polyphenols in virgin olive oil by ultra-HPLC-QToF mass spectrometry. Food chemistry, 158, pp.392-400.

Christophoridou, S., Dais, P., Tseng, L.H. and Spraul, M., 2005. Separation and identification of phenolic compounds in olive oil by coupling high-performance liquid chromatography with postcolumn solid-phase extraction to nuclear magnetic resonance spectroscopy (LC-SPE-NMR). Journal of Agricultural and Food Chemistry, 53(12), pp.4667-4679.

de Fernandez, M.D.L.A., SotoVargas, V.C. and Silva, M.F., 2014. Phenolic compounds and antioxidant capacity of monovarietal olive oils produced in Argentina. Journal of the American Oil Chemists' Society, 91(12), pp.2021-2033.

De la Torre-Carbot, K., Jauregui, O., Gimeno, E., Castellote, A.I., Lamuela-Raventós, R.M. and López-Sabater, M.C., 2005. Characterization and quantification of phenolic compounds in olive oils by solid-phase extraction, HPLC-DAD, and HPLC-MS/MS. Journal of agricultural and food chemistry, 53(11), pp.4331-4340.

Del, C.M., Ritelli, E., Procida, G.I.U.S.E.P.P.E., Murmura, F. and Cichelli, A., 2006. Characterization of extra virgin olive oils obtained from different cultivars. Pomologia Croatica: Glasilo Hrvatskog agronomskog društva, 12(1), pp.29-41.

Fanali, C., Della Posta, S., Vilmercati, A., Dugo, L., Russo, M., Petitti, T., Mondello, L. and De Gara, L., 2018. Extraction, analysis, and antioxidant activity evaluation of phenolic compounds in different Italian extra-virgin olive oils. Molecules, 23(12), p.3249.

Fuentes Pérez, E., Paucar, F., Tapia, F., Ortiz Viedma, J., Jiménez Patiño, P.A. and Romero Palacios, N., 2018. Effect of the composition of extra virgin olive oils on the differentiation and antioxidant capacities of twelve monovarietals.

Gilbert-López, B., Valencia-Reyes, Z.L., Yufra-Picardo, V.M., García-Reyes, J.F., Ramos-Martos, N. and Molina-Díaz, A., 2014. Determination of polyphenols in commercial extra virgin olive oils from different origins (Mediterranean and South American countries) by liquid chromatography–electrospray time-of-flight mass spectrometry. Food analytical methods, 7(9), pp.1824-1833

Gilbert-López, B., Valencia-Reyes, Z.L., Yufra-Picardo, V.M., García-Reyes, J.F., Ramos-Martos, N. and Molina-Díaz, A., 2014. Determination of polyphenols in commercial extra virgin olive oils from different origins (Mediterranean and South American countries) by liquid chromatography–electrospray time-of-flight mass spectrometry. Food analytical methods, 7(9), pp.1824-1833.

Gómez Caravaca, A.M., Carrasco Pancorbo, A., Cañabate Díaz, B., Segura Carretero, A. and Fernández Gutiérrez, A., 2005. Electrophoretic identification and quantitation of compounds in the polyphenolic fraction of extra-virgin olive oil. Electrophoresis, 26(18), pp.3538-3551.

Lozano-Sánchez, J., Bendini, A., Quirantes-Piné, R., Cerretani, L., Segura-Carretero, A. and Fernández-Gutiérrez, A., 2013. Monitoring the bioactive compounds status of extra-virgin olive oil and storage by-products over the shelf life. Food Control, 30(2), pp.606-615.

Manai-Djebali, H., Krichène, D., Ouni, Y., Gallardo, L., Sánchez, J., Osorio, E., Daoud, D., Guido, F. and Zarrouk, M., 2012. Chemical profiles of five minor olive oil varieties grown in central Tunisia. Journal of Food Composition and Analysis, 27(2), pp.109-119.

Mateos, R., Espartero, J.L., Trujillo, M., Rios, J.J., León-Camacho, M., Alcudia, F. and Cert, A., 2001. Determination of phenols, flavones, and lignans in virgin olive oils by solid-phase extraction and high-performance liquid chromatography with diode array ultraviolet detection. Journal of Agricultural and Food Chemistry, 49(5), pp.2185-2192.

Naushad, M. and Khan, M.R., 2014. Ultra performance liquid chromatography mass spectrometry: evaluation and applications in food analysis. CRC Press.

Negro, C., Aprile, A., Luvisi, A., Nicolì, F., Nutricati, E., Vergine, M., Miceli, A., Blando, F., Sabella, E. and De Bellis, L., 2019. Phenolic profile and antioxidant activity of Italian monovarietal extra virgin olive oils. Antioxidants, 8(6), p.161.

Oliveras-López, M.J., Innocenti, M., Giaccherini, C., Ieri, F., Romani, A. and Mulinacci, N., 2007. Study of the phenolic composition of spanish and italian monocultivar extra virgin olive oils: Distribution of lignans, secoiridoidic, simple phenols and flavonoids. Talanta, 73(4), pp.726-732.

Olmo-García, L., Polari, J.J., Li, X., Bajoub, A., Fernández-Gutiérrez, A., Wang, S.C. and Carrasco-Pancorbo, A., 2018. Deep insight into the minor fraction of virgin olive oil by using LC-MS and GC-MS multi-class methodologies. Food chemistry, 261, pp.184-193.

Owen, R.W., Giacosa, A., Hull, W.E., Haubner, R., Spiegelhalder, B. and Bartsch, H., 2000. The antioxidant/anticancer potential of phenolic compounds isolated from olive oil. European Journal of Cancer, 36(10), pp.1235-1247.

Owen, R.W., Mier, W., Giacosa, A., Hull, W.E., Spiegelhalder, B. and Bartsch, H., 2000. Identification of lignans as major components in the phenolic fraction of olive oil. Clinical Chemistry, 46(7), pp.976-988.

Pirisi, F.M., Cabras, P., Cao, C.F., Migliorini, M. and Muggelli, M., 2000. Phenolic compounds in virgin olive oil. 2. Reappraisal of the extraction, HPLC separation, and quantification procedures. Journal of Agricultural and Food Chemistry, 48(4), pp.1191-1196.

Pizarro, M.L., Becerra, M., Sayago, A., Beltrán, M. and Beltrán, R., 2013. Comparison of different extraction methods to determine phenolic compounds in virgin olive oil. Food Analytical Methods, 6(1), pp.123-132.

Ricciutelli, M., Marconi, S., Boarelli, M.C., Caprioli, G., Sagratini, G., Ballini, R. and Fiorini, D., 2017. Olive oil polyphenols: A quantitative method by high-performance liquid-chromatography-diode-array detection for their determination and the assessment of the related health claim. Journal of Chromatography A, 1481, pp.53-63.

Rodríguez-López, P., Lozano-Sanchez, J., Borrás-Linares, I., Emanuelli, T., Menéndez, J.A. and Segura-Carretero, A., 2020. Structure–Biological Activity Relationships of Extra-Virgin Olive Oil Phenolic Compounds: Health Properties and Bioavailability. Antioxidants, 9(8), p.685.

Schneider, S., 2016. Quality Analysis of Extra Virgin Olive Oils—Part 6 Nutritive Benefi ts—Phenolic Compounds in Virgin Olive Oil. Agilent Technology Application Note.

Servili, M. and Montedoro, G., 2002. Contribution of phenolic compounds to virgin olive oil quality. European Journal of Lipid Science and Technology, 104(9-10), pp.602-613.

Servili, M., Esposto, S., Fabiani, R., Urbani, S., Taticchi, A., Mariucci, F., Selvaggini, R. and Montedoro, G.F., 2009. Phenolic compounds in olive oil: antioxidant, health and organoleptic activities according to their chemical structure. Inflammopharmacology, 17(2), pp.76-84.

Suárez, M., Macià, A., Romero, M.P. and Motilva, M.J., 2008. Improved liquid chromatography tandem mass spectrometry method for the determination of phenolic compounds in virgin olive oil. Journal of Chromatography A, 1214(1-2), pp.90-99.

Tasioula-Margari, M. and Tsabolatidou, E., 2015. Extraction, separation, and identification of phenolic compounds in virgin olive oil by HPLC-DAD and HPLC-MS. Antioxidants, 4(3), pp.548-562.

Tripoli, E., Giammanco, M., Tabacchi, G., Di Majo, D., Giammanco, S. and La Guardia, M., 2005. The phenolic compounds of olive oil: structure, biological activity and beneficial effects on human health. Nutrition research reviews, 18(1), pp.98-112.

1-Phenyl-6, 7-dihydroxy-isochroman.	$C_{15}H_{14}O_3$	242.094294
1-(3'-Methoxy-4'-hydroxy) phenyl6, 7-dihydroxy-isochroman.	$C_{16}H_{16}O_5$	288.099774
Tyrosyl acetate.	$C_{10}H_{12}O_3$	180.078645
Hydroxytyrosol acetate.	$C_{10}H_{12}O_4$	196.073559
Hydroxytyrosol acyclodihydroelenolate.	$C_{19}H_{26}O_8$	382.162770
Homovanillyl alcohol or Homovanillic alcohol.	$C_9H_{12}O_3$	168.078644

Becerra-Herrera, M., Sánchez-Astudillo, M., Beltrán, R. and Sayago, A., 2014. Determination of phenolic compounds in olive oil: New method based on liquid–liquid micro extraction and ultra high performance liquid chromatography-triple–quadrupole mass spectrometry. LWT-Food Science and Technology, 57(1), pp.49-57.

Bendini, A., Cerretani, L., Carrasco-Pancorbo, A., Gómez-Caravaca, A.M., Segura-Carretero, A., Fernández-Gutiérrez, A. and Lercker, G., 2007. Phenolic molecules in virgin olive oils: a survey of their sensory properties, health effects, antioxidant activity and analytical methods. An overview of the last decade Alessandra. Molecules, 12(8), pp.1679-1719.

Boskou, D. ed., 2008. Olive oil: minor constituents and health. CRC press.

Capriotti, A.L., Cavaliere, C., Crescenzi, C., Foglia, P., Nescatelli, R., Samperi, R. and Laganà, A., 2014. Comparison of extraction methods for the identification and quantification of polyphenols in virgin olive oil by ultra-HPLC-QToF mass spectrometry. Food chemistry, 158, pp.392-400.

Christophoridou, S., Dais, P., Tseng, L.H. and Spraul, M., 2005. Separation and identification of phenolic compounds in olive oil by coupling high-performance liquid chromatography with postcolumn solid-phase extraction to nuclear magnetic resonance spectroscopy (LC-SPE-NMR). Journal of Agricultural and Food Chemistry, 53(12), pp.4667-4679.
Lozano-Sánchez, J., Bendini, A., Quirantes-Piné, R., Cerretani, L., Segura-Carretero, A. and Fernández-Gutiérrez, A., 2013. Monitoring the bioactive compounds status of extra-virgin olive oil and storage by-products over the shelf life. Food Control, 30(2), pp.606-615.
Mateos, R., Espartero, J.L., Trujillo, M., Rios, J.J., León-Camacho, M., Alcudia, F. and Cert, A., 2001. Determination of phenols, flavones, and lignans in virgin olive oils by solid-phase extraction and high-performance liquid chromatography with diode array ultraviolet detection. Journal of Agricultural and Food Chemistry, 49(5), pp.2185-2192.
Naushad, M. and Khan, M.R., 2014. Ultra performance liquid chromatography mass spectrometry: evaluation and applications in food analysis. CRC Press.
Olmo-García, L., Polari, J.J., Li, X., Bajoub, A., Fernández-Gutiérrez, A., Wang, S.C. and Carrasco-Pancorbo, A., 2018. Deep insight into the minor fraction of virgin olive oil by using LC-MS and GC-MS multi-class methodologies. Food chemistry, 261, pp.184-193.
Rodríguez-López, P., Lozano-Sanchez, J., Borrás-Linares, I., Emanuelli, T., Menéndez, J.A. and Segura-Carretero, A., 2020. Structure–Biological Activity Relationships of Extra-Virgin Olive Oil Phenolic Compounds: Health Properties and Bioavailability. Antioxidants, 9(8), p.685.
Schneider, S., 2016. Quality Analysis of Extra Virgin Olive Oils—Part 6 Nutritive Benefi ts—Phenolic Compounds in Virgin Olive Oil. Agilent Technology Application Note.
Servili, M., Esposto, S., Fabiani, R., Urbani, S., Taticchi, A., Mariucci, F., Selvaggini, R. and Montedoro, G.F., 2009. Phenolic compounds in olive oil: antioxidant, health and organoleptic activities according to their chemical structure. Inflammopharmacology, 17(2), pp.76-84.
Tasioula-Margari, M. and Tsabolatidou, E., 2015. Extraction, separation, and identification of phenolic compounds in virgin olive oil by HPLC-DAD and HPLC-MS. Antioxidants, 4(3), pp.548-562.

Ligstroside.	**$C_{25}H_{32}O_{12}$**	524.1894
Oleuropein or 3, 4-DHPEA-Elenolic acid glucoside or Oleuropein glucoside. Oleuropein (OLE) is an ester of hydroxytyrosol (3, 4-DHPEA) and the elenolic acid glucoside.	**$C_{25}H_{32}O_{13}$**	540.184291
Oleuropein aglycone or 3, 4-dihydroxyphenylethanol−elenolic acid or 3, 4-DHPEA-EA (Ol Agl).	**$C_{19}H_{22}O_{8}$**	378.131468
Keto oleuropein aglycone.	**$C_{19}H_{20}O_{9}$**	392.1107
Hydroxy oleuropein aglycone **(**Hydroxy-Ol Agl).	**$C_{19}H_{22}O_{9}$**	394.1264
10-Hydroxy oleuropein aglycone **(**10-H-Ol Agl).	**$C_{19}H_{22}O_{9}$**	394.1264
Dihydroxy oleuropein aglycone (Dihydroxy-Ol Agl).	**$C_{19}H_{22}O_{10}$**	410.1213
Methyl oleuropein aglycone (Methyl 3, 4-DHPEA-EA).	**$C_{20}H_{24}O_{8}$**	392.1471
Methyl decarboxymethyl oleuropein aglycone.	**$C_{18}H_{22}O_{6}$**	334.141638
Hydroxydecarboxymethyl oleuropein aglycone (Hydroxy D-Ol Agl).	**$C_{17}H_{20}O_{7}$**	336.1209
Hydroxymethyl–decarboxymethyl Ligstroside aglycone.	**$C_{17}H_{18}O_{7}$**	334.1053
Hydroxymethyl decarboxymethyl ligstroside aglycone.	**$C_{18}H_{22}O_{6}$**	334.1416
[(+/-)-Oleocanthal], Decarboxymethyl ligstroside aglycon (*p*-HPEA-EDA).	**$C_{17}H_{20}O_{5}$**	304.131074

Ligstroside aglycon (Lig Agl) or (*p*-HPEA-EA).	$C_{19}H_{22}O_7$	362.1366
Dehydro-ligstroside aglycone.	$C_{19}H_{20}O_7$	360.1209
Dehydro-oleuropein aglycone.	$C_{19}H_{20}O_8$	376.1158
Keto ligstroside aglycone.	$C_{19}H_{20}O_8$	376.1158
Aldehydic form of oleuropein aglycone (3, 4-DHPEA-EA). Dialdehydic form of carboxymethyl oleuropein aglycone.	$C_{17}H_{19}O_6$	319.1182
Ligstroside aglycone. Dialdehydic form of carboxymethyl ligstroside aglycone.	$C_{17}H_{19}O_5$	303.1232
Dialdehydic form of decarboxymethyl oleuropein aglycone (3, 4-DHPEA-EDA) or Deacetoxyoleuropein aglycone.	$C_{17}H_{20}O_6$	320.1260
Hydroxy decarboxymethyl ligstroside aglycone (Hydroxy D-Lig Agl).	$C_{17}H_{20}O_6$	320.1260

Baiano, A.N.T.O.N.I.E.T.T.A., Gambacorta, G., Terracone, C.A.R.M.E.L.A., Previtali, M.A., Lamacchia, C.A.R.M.E.L.A. and La Notte, E.N.N.I.O., 2009. Changes in phenolic content and antioxidant activity of Italian extra-virgin olive oils during storage. Journal of food science, 74(2), pp.C177-C183.

Baldioli, M., Servili, M., Perretti, G. and Montedoro, G.F., 1996. Antioxidant activity of tocopherols and phenolic compounds of virgin olive oil. Journal of the American Oil Chemists' Society, 73(11), pp.1589-1593.

Becerra-Herrera, M., Sánchez-Astudillo, M., Beltrán, R. and Sayago, A., 2014. Determination of phenolic compounds in olive oil: New method based on liquid–liquid micro extraction and ultra high performance liquid chromatography-triple–quadrupole mass spectrometry. LWT-Food Science and Technology, 57(1), pp.49-57.

Bendini, A., Bonoli, M., Cerretani, L., Biguzzi, B., Lercker, G. and Toschi, T.G., 2003. Liquid–liquid and solid-phase extractions of phenols from virgin olive oil and their separation by chromatographic and electrophoretic methods. Journal of Chromatography A, 985(1-2), pp.425-433.

Bendini, A., Cerretani, L., Carrasco-Pancorbo, A., Gómez-Caravaca, A.M., Segura-Carretero, A., Fernández-Gutiérrez, A. and Lercker, G., 2007. Phenolic molecules in virgin olive oils: a survey of their sensory properties, health effects, antioxidant activity and analytical methods. An overview of the last decade Alessandra. Molecules, 12(8), pp.1679-1719.

Boskou, D. ed., 2008. Olive oil: minor constituents and health. CRC press.

Brenes, M., García, A., García, P. and Garrido, A., 2000. Rapid and complete extraction of phenols from olive oil and determination by means of a coulometric electrode array system. Journal of agricultural and food chemistry, 48(11), pp.5178-5183.

Capriotti, A.L., Cavaliere, C., Crescenzi, C., Foglia, P., Nescatelli, R., Samperi, R. and Laganà, A., 2014. Comparison of extraction methods for the identification and quantification of polyphenols in virgin olive oil by ultra-HPLC-QToF mass spectrometry. Food chemistry, 158, pp.392-400.

Christophoridou, S., Dais, P., Tseng, L.H. and Spraul, M., 2005. Separation and identification of phenolic compounds in olive oil by coupling high-performance liquid chromatography with postcolumn solid-phase extraction to nuclear magnetic resonance spectroscopy (LC-SPE-NMR). Journal of Agricultural and Food Chemistry, 53(12), pp.4667-4679.

de Fernandez, M.D.L.A., SotoVargas, V.C. and Silva, M.F., 2014. Phenolic compounds and antioxidant capacity of monovarietal olive oils produced in Argentina. Journal of the American Oil Chemists' Society, 91(12), pp.2021-2033.

De la Torre-Carbot, K., Jauregui, O., Gimeno, E., Castellote, A.I., Lamuela-Raventós, R.M. and López-Sabater, M.C., 2005. Characterization and quantification of phenolic compounds in olive oils by solid-phase extraction, HPLC-DAD, and HPLC-MS/MS. Journal of agricultural and food chemistry, 53(11), pp.4331-4340.

Fanali, C., Della Posta, S., Vilmercati, A., Dugo, L., Russo, M., Petitti, T., Mondello, L. and De Gara, L., 2018. Extraction, analysis, and antioxidant activity evaluation of phenolic compounds in different Italian extra-virgin olive oils. Molecules, 23(12), p.3249.

Farré, M., Picó, Y. and Barceló, D., 2019. Direct analysis in real-time high-resolution mass spectrometry as a valuable tool for polyphenols profiling in olive oil. Analytical methods, 11(4), pp.472-482.

Ferro, M.D., Santos, S.A., Silvestre, A.J. and Duarte, M.F., 2019. Chromatographic separation of phenolic compounds from extra virgin olive oil: Development and validation of a new method based on a biphenyl HPLC column. International Journal of Molecular Sciences, 20(1), p.201.

Fuentes Pérez, E., Paucar, F., Tapia, F., Ortiz Viedma, J., Jiménez Patiño, P.A. and Romero Palacios, N., 2018. Effect of the composition of extra virgin olive oils on the differentiation and antioxidant capacities of twelve monovarietals.

García-Villalba, R., Carrasco-Pancorbo, A., Vázquez-Martín, A., Oliveras-Ferraros, C., Menéndez, J.A., Segura-Carretero, A. and Fernández-Gutiérrez, A., 2009. A 2-D-HPLC-CE platform coupled to ESI-TOF-MS to characterize the phenolic fraction in olive oil. Electrophoresis, 30(15), pp.2688-2701.

Gilbert-López, B., Valencia-Reyes, Z.L., Yufra-Picardo, V.M., García-Reyes, J.F., Ramos-Martos, N. and Molina-Díaz, A., 2014. Determination of polyphenols in commercial extra virgin olive oils from different origins (Mediterranean and South American countries) by liquid chromatography–electrospray time-of-flight mass spectrometry. Food analytical methods, 7(9), pp.1824-1833.

Gilbert-López, B., Valencia-Reyes, Z.L., Yufra-Picardo, V.M., García-Reyes, J.F., Ramos-Martos, N. and Molina-Díaz, A., 2014. Determination of polyphenols in commercial extra virgin olive oils from different origins (Mediterranean and South American countries) by liquid chromatography–electrospray time-of-flight mass spectrometry. Food analytical methods, 7(9), pp.1824-1833.

Gómez Caravaca, A.M., Carrasco Pancorbo, A., Cañabate Díaz, B., Segura Carretero, A. and Fernández Gutiérrez, A., 2005. Electrophoretic identification and quantitation of compounds in the polyphenolic fraction of extra-virgin olive oil. Electrophoresis, 26(18), pp.3538-3551.

Gutfinger, T., 1981. Polyphenols in olive oils. Journal of the American Oil Chemists' Society, 58(11), pp.966-968.

Liberatore, L., Procida, G., d'Alessandro, N. and Cichelli, A., 2001. Solid-phase extraction and gas chromatographic analysis of phenolic compounds in virgin olive oil. Food Chemistry, 73(1), pp.119-124.

Lozano-Sánchez, J., Bendini, A., Quirantes-Piné, R., Cerretani, L., Segura-Carretero, A. and Fernández-Gutiérrez, A., 2013. Monitoring the bioactive compounds status of extra-virgin olive oil and storage by-products over the shelf life. Food Control, 30(2), pp.606-615.

Manai-Djebali, H., Krichène, D., Ouni, Y., Gallardo, L., Sánchez, J., Osorio, E., Daoud, D., Guido, F. and Zarrouk, M., 2012. Chemical profiles of five minor olive oil varieties grown in central Tunisia. Journal of Food Composition and Analysis, 27(2), pp.109-119.

Mateos, R., Espartero, J.L., Trujillo, M., Rios, J.J., León-Camacho, M., Alcudia, F. and Cert, A., 2001. Determination of phenols, flavones, and lignans in virgin olive oils by solid-phase extraction and high-performance liquid chromatography with diode array ultraviolet detection. Journal of Agricultural and Food Chemistry, 49(5), pp.2185-2192.

Montedoro, G., Servili, M., Baldioli, M. and Miniati, E., 1992. Simple and hydrolyzable phenolic compounds in virgin olive oil. 1. Their extraction, separation, and quantitative and semiquantitative evaluation by HPLC. Journal of Agricultural and Food Chemistry, 40(9), pp.1571-1576.

Montedoro, G., Servili, M., Baldioli, M. and Miniati, E., 1992. Simple and hydrolyzable phenolic compounds in virgin olive oil. 2. Initial characterization of the hydrolyzable fraction. Journal of Agricultural and Food Chemistry, 40(9), pp.1577-1580.

Montedoro, G., Servili, M., Baldioli, M., Selvaggini, R., Miniati, E. and Macchioni, A., 1993. Simple and hydrolyzable compounds in virgin olive oil. 3. Spectroscopic characterizations of the secoiridoid derivatives. Journal of Agricultural and Food Chemistry, 41(11), pp.2228-2234.

Naushad, M. and Khan, M.R., 2014. Ultra performance liquid chromatography mass spectrometry: evaluation and applications in food analysis. CRC Press.

Negro, C., Aprile, A., Luvisi, A., Nicolì, F., Nutricati, E., Vergine, M., Miceli, A., Blando, F., Sabella, E. and De Bellis, L., 2019. Phenolic profile and antioxidant activity of Italian monovarietal extra virgin olive oils. Antioxidants, 8(6), p.161.

Oliveras-López, M.J., Innocenti, M., Giaccherini, C., Ieri, F., Romani, A. and Mulinacci, N., 2007. Study of the phenolic composition of spanish and italian monocultivar extra virgin olive oils: Distribution of lignans, secoiridoidic, simple phenols and flavonoids. Talanta, 73(4), pp.726-732.

Olmo-García, L., Polari, J.J., Li, X., Bajoub, A., Fernández-Gutiérrez, A., Wang, S.C. and Carrasco-Pancorbo, A., 2018. Deep insight into the minor fraction of virgin olive oil by using LC-MS and GC-MS multi-class methodologies. Food chemistry, 261, pp.184-193.

Owen, R.W., Giacosa, A., Hull, W.E., Haubner, R., Spiegelhalder, B. and Bartsch, H., 2000. The antioxidant/anticancer potential of phenolic compounds isolated from olive oil. European Journal of Cancer, 36(10), pp.1235-1247.

Owen, R.W., Mier, W., Giacosa, A., Hull, W.E., Spiegelhalder, B. and Bartsch, H., 2000. Identification of lignans as major components in the phenolic fraction of olive oil. Clinical Chemistry, 46(7), pp.976-988.

Pirisi, F.M., Cabras, P., Cao, C.F., Migliorini, M. and Muggelli, M., 2000. Phenolic compounds in virgin olive oil. 2. Reappraisal of the extraction, HPLC separation, and quantification procedures. Journal of Agricultural and Food Chemistry, 48(4), pp.1191-1196.

Pizarro, M.L., Becerra, M., Sayago, A., Beltrán, M. and Beltrán, R., 2013. Comparison of different extraction methods to determine phenolic compounds in virgin olive oil. Food Analytical Methods, 6(1), pp.123-132.
Ricciutelli, M., Marconi, S., Boarelli, M.C., Caprioli, G., Sagratini, G., Ballini, R. and Fiorini, D., 2017. Olive oil polyphenols: A quantitative method by high-performance liquid-chromatography-diode-array detection for their determination and the assessment of the related health claim. Journal of Chromatography A, 1481, pp.53-63.
Rodríguez-López, P., Lozano-Sanchez, J., Borrás-Linares, I., Emanuelli, T., Menéndez, J.A. and Segura-Carretero, A., 2020. Structure–Biological Activity Relationships of Extra-Virgin Olive Oil Phenolic Compounds: Health Properties and Bioavailability. Antioxidants, 9(8), p.685.
Schneider, S., 2016. Quality Analysis of Extra Virgin Olive Oils—Part 6 Nutritive Benefi ts—Phenolic Compounds in Virgin Olive Oil. Agilent Technology Application Note.
Servili, M. and Montedoro, G., 2002. Contribution of phenolic compounds to virgin olive oil quality. European Journal of Lipid Science and Technology, 104(9-10), pp.602-613.
Servili, M., Esposto, S., Fabiani, R., Urbani, S., Taticchi, A., Mariucci, F., Selvaggini, R. and Montedoro, G.F., 2009. Phenolic compounds in olive oil: antioxidant, health and organoleptic activities according to their chemical structure. Inflammopharmacology, 17(2), pp.76-84.
Suárez, M., Macià, A., Romero, M.P. and Motilva, M.J., 2008. Improved liquid chromatography tandem mass spectrometry method for the determination of phenolic compounds in virgin olive oil. Journal of Chromatography A, 1214(1-2), pp.90-99.
Tasioula-Margari, M. and Tsabolatidou, E., 2015. Extraction, separation, and identification of phenolic compounds in virgin olive oil by HPLC-DAD and HPLC-MS. Antioxidants, 4(3), pp.548-562.
Tripoli, E., Giammanco, M., Tabacchi, G., Di Majo, D., Giammanco, S. and La Guardia, M., 2005. The phenolic compounds of olive oil: structure, biological activity and beneficial effects on human health. Nutrition research reviews, 18(1), pp.98-112.

Oleacein (mycophenolic acid).	$C_{17}H_{20}O_6$	320.125988
Rutin.	$C_{27}H_{30}O_{16}$	610.153385
Hydroxydecarboxymethyl elenolic acid.	$C_9H_{12}O_5$	200.0685
Dialdehydic decarboxymethyl elenolic acid.	$C_9H_{12}O_4$	184.0736
Butylated hydroxytoluene (BHT).	$C_{15}H_{24}O$	220.1827
(3,4-DHPEA-AC) Hydroxytyrosol Acetate 4-(acetoxyethyl)1,2dihydroxybenzene.	$C_{10}H_{12}O_4$	196.0736
Hydroxytyrosol ester of methyl malate.	$C_{13}H_{16}O_7$	284.0896
3, 4-dihydroxyphenylglycol (DHPG).	$C_8H_{10}O_4$	170.0579
Azeleic acid.	$C_9H_{16}O_4$	188.1049
Abscisic acid.	$C_{15}H_{20}O_4$	264.1362
Licodione.	$C_{15}H_{12}O_5$	272.0685
Chrysoeriol.	$C_{15}H_8O_7$	300.0270
Methyl aloeresin.	$C_{20}H_{24}O_9$	408.1420
2, 3, 5-Trihydroxy-1, 4-benzoquinone.	$C_6H_4O_5$	156.0059
Proto-catechuic acid.	$C_7H_6O_6$	186.0164
Quinic acid.	$C_7H_{12}O_6$	192.0634
Dehydrocamphenic acid.	$C_9H_{12}O_6$	216.0634

Becerra-Herrera, M., Sánchez-Astudillo, M., Beltrán, R. and Sayago, A., 2014. Determination of phenolic compounds in olive oil: New method based on liquid–liquid micro extraction and ultra high performance liquid chromatography-triple–quadrupole mass spectrometry. LWT-Food Science and Technology, 57(1), pp.49-57.
Capriotti, A.L., Cavaliere, C., Crescenzi, C., Foglia, P., Nescatelli, R., Samperi, R. and Laganà, A., 2014. Comparison of extraction methods for the identification and quantification of polyphenols in virgin olive oil by ultra-HPLC-QToF mass spectrometry. Food chemistry, 158, pp.392-400.
Christophoridou, S., Dais, P., Tseng, L.H. and Spraul, M., 2005. Separation and identification of phenolic compounds in olive oil by coupling high-performance liquid chromatography with postcolumn solid-phase extraction to nuclear magnetic resonance spectroscopy (LC-SPE-NMR). Journal of Agricultural and Food Chemistry, 53(12), pp.4667-4679.

de Fernandez, M.D.L.A., SotoVargas, V.C. and Silva, M.F., 2014. Phenolic compounds and antioxidant capacity of monovarietal olive oils produced in Argentina. Journal of the American Oil Chemists' Society, 91(12), pp.2021-2033.
Farré, M., Picó, Y. and Barceló, D., 2019. Direct analysis in real-time high-resolution mass spectrometry as a valuable tool for polyphenols profiling in olive oil. Analytical methods, 11(4), pp.472-482.
García-Villalba, R., Carrasco-Pancorbo, A., Vázquez-Martín, A., Oliveras-Ferraros, C., Menéndez, J.A., Segura-Carretero, A. and Fernández-Gutiérrez, A., 2009. A 2-D-HPLC-CE platform coupled to ESI-TOF-MS to characterize the phenolic fraction in olive oil. Electrophoresis, 30(15), pp.2688-2701.
Gutfinger, T., 1981. Polyphenols in olive oils. Journal of the American Oil Chemists' Society, 58(11), pp.966-968.
Lozano-Sánchez, J., Bendini, A., Quirantes-Piné, R., Cerretani, L., Segura-Carretero, A. and Fernández-Gutiérrez, A., 2013. Monitoring the bioactive compounds status of extra-virgin olive oil and storage by-products over the shelf life. Food Control, 30(2), pp.606-615.
Manai-Djebali, H., Krichène, D., Ouni, Y., Gallardo, L., Sánchez, J., Osorio, E., Daoud, D., Guido, F. and Zarrouk, M., 2012. Chemical profiles of five minor olive oil varieties grown in central Tunisia. Journal of Food Composition and Analysis, 27(2), pp.109-119.
Negro, C., Aprile, A., Luvisi, A., Nicolì, F., Nutricati, E., Vergine, M., Miceli, A., Blando, F., Sabella, E. and De Bellis, L., 2019. Phenolic profile and antioxidant activity of Italian monovarietal extra virgin olive oils. Antioxidants, 8(6), p.161.
Olmo-García, L., Polari, J.J., Li, X., Bajoub, A., Fernández-Gutiérrez, A., Wang, S.C. and Carrasco-Pancorbo, A., 2018. Deep insight into the minor fraction of virgin olive oil by using LC-MS and GC-MS multi-class methodologies. Food chemistry, 261, pp.184-193.
Papadopoulos, G. and Boskou, D., 1991. Antioxidant effect of natural phenols on olive oil. Journal of the American Oil Chemists' Society, 68(9), pp.669-671.
Pizarro, M.L., Becerra, M., Sayago, A., Beltrán, M. and Beltrán, R., 2013. Comparison of different extraction methods to determine phenolic compounds in virgin olive oil. Food Analytical Methods, 6(1), pp.123-132.
Suárez, M., Macià, A., Romero, M.P. and Motilva, M.J., 2008. Improved liquid chromatography tandem mass spectrometry method for the determination of phenolic compounds in virgin olive oil. Journal of Chromatography A, 1214(1-2), pp.90-99.

Cumaric acid.	$C_9H_{16}O_4$	188.1049
p-HPEA-AC: 4-(acetoxyethyl)-1 hydroxybenzene.	$C_{10}H_{12}O_3$	180.0786
Gibberellic acid.	$C_{19}H_{22}O_6$	346.1416
Resveratrol.	$C_{14}H_{12}O_3$	228.0786
Hydrated product of the dialdehydic form of decarboxymethyl-elenolic acid.	$C_9H_{14}O_5$	202.0841
Decarboxylated form of hydroxy-elenolic acid.	$C_{10}H_{14}O_5$	214.0841
Aldehydic form of decarboxymethyl-elenolic acid.	$C_{10}H_{16}O_5$	216.0998
Syringaresinol.	$C_{22}H_{26}O_8$	418.162768
Methyl acetal of the aglycone of ligstroside (Ligstroside aglycone methyl acetal).	$C_{20}H_{24}O_7$	376.152205
10-Hydroxyoleuropein.	$C_{25}H_{32}O_{14}$	556.179206
Elenolic acid glucoside.	$C_{17}H_{25}O_{11}$	405.139690
11-methyl oleoside.	$C_{17}H_{24}O_{11}$	404.131862
Diosmetin.	$C_{16}H_{12}O_6$	300.063388
Glepidotin C.	$C_{19}H_{22}O_3$	298.156895
Succinicacid.	$C_6H_8O_7$	192.027005
8-Prenyldihydrokaempferol 7-glucosi.	$C_{26}H_{30}O_{11}$	518.178815
Diprenylisoflavone derivative.	$C_{26}H_{28}O_5$	420.193675
Alpinumisoflavone derivative.	$C_{26}H_{26}O_4$	402.183110
Xanthonic acid.	$C_{15}H_{22}O_4$	266.151810
Capric acid.	$C_{10}H_{20}O_2$	172.146330
Oleuropeic acid.	$C_{10}H_{16}O_3$	184.109945

Tetrahydroxy–isoflavanone.	$C_{15}H_{12}O_6$	288.063390
Myristic acid.	$C_{14}H_{28}O_2$	228.208930
Oxodecanoic acid.	$C_{10}H_{18}O_3$	186.125595
Trimethoxyhydrocinnamic acid.	$C_{12}H_{16}O_5$	240.099775
Zinniol.	$C_{15}H_{22}O_4$	266.151810
2, 3-Dinor-8-iso prostaglandin F1-α.	$C_{18}H_{32}O_5$	328.224975
Dihydroxy-palmitic acid.	$C_{16}H_{32}O_4$	288.230060
Prenylflavones derivative.	$C_{30}H_{32}O_7$	504.214805
Prenylflavones derivative.	$C_{29}H_{28}O_6$	472.188590
Prenylflavones derivative.	$C_{30}H_{32}O_8$	520.209720
Trihydroxy-octadecenoic acid.	$C_{18}H_{34}O_5$	330.240625
Ostruthin.	$C_{19}H_{22}O_3$	298.156895
Vanillic acid, heptyl ester.	$C_{15}H_{22}O_4$	266.151810
Methyl luteoline.	$C_{16}H_{12}O_6$	300.063390
Demethyloleuropein.	$C_{24}H_{30}O_{13}$	526.168641
Clorogenic acid.	$C_{16}H_{18}O_9$	354.095082
Catechin.	$C_{15}H_{14}O_6$	290.079040
Naringenin.	$C_{15}H_{12}O_5$	272.068475
Quercetin.	$C_{15}H_{10}O_7$	302.042654
Maslinic acid.	$C_{30}H_{48}O_4$	472.355260
Betulinic acid.	$C_{30}H_{48}O_3$	456.360345
Linolenic acid.	$C_{18}H_{30}O_2$	278.224580
Oleanolic acid.	$C_{30}H_{48}O_3$	456.360345
Linoleic acid.	$C_{18}H_{32}O_2$	280.240230
Erythrodiol.	$C_{30}H_{50}O_2$	442.381080
Uvaol.	$C_{30}H_{50}O_2$	442.381080
Oleic acid.	$C_{18}H_{34}O_2$	282.255880
β+γ-tocopherol.	$C_{28}H_{46}O_2$	414.349780
α-tocopherol.	$C_{29}H_{48}O_2$	428.365430

Baldioli, M., Servili, M., Perretti, G. and Montedoro, G.F., 1996. Antioxidant activity of tocopherols and phenolic compounds of virgin olive oil. Journal of the American Oil Chemists' Society, 73(11), pp.1589-1593.

Capriotti, A.L., Cavaliere, C., Crescenzi, C., Foglia, P., Nescatelli, R., Samperi, R. and Laganà, A., 2014. Comparison of extraction methods for the identification and quantification of polyphenols in virgin olive oil by ultra-HPLC-QToF mass spectrometry. Food chemistry, 158, pp.392-400.

Christophoridou, S., Dais, P., Tseng, L.H. and Spraul, M., 2005. Separation and identification of phenolic compounds in olive oil by coupling high-performance liquid chromatography with postcolumn solid-phase extraction to nuclear magnetic resonance spectroscopy (LC-SPE-NMR). Journal of Agricultural and Food Chemistry, 53(12), pp.4667-4679.

de Fernandez, M.D.L.A., SotoVargas, V.C. and Silva, M.F., 2014. Phenolic compounds and antioxidant capacity of monovarietal olive oils produced in Argentina. Journal of the American Oil Chemists' Society, 91(12), pp.2021-2033.

De la Torre-Carbot, K., Jauregui, O., Gimeno, E., Castellote, A.I., Lamuela-Raventós, R.M. and López-Sabater, M.C., 2005. Characterization and quantification of phenolic compounds in olive oils by solid-phase extraction, HPLC-DAD, and HPLC-MS/MS. Journal of agricultural and food chemistry, 53(11), pp.4331-4340.

Fuentes Pérez, E., Paucar, F., Tapia, F., Ortiz Viedma, J., Jiménez Patiño, P.A. and Romero Palacios, N., 2018. Effect of the composition of extra virgin olive oils on the differentiation and antioxidant capacities of twelve monovarietals.

García-Villalba, R., Carrasco-Pancorbo, A., Vázquez-Martín, A., Oliveras-Ferraros, C., Menéndez, J.A., Segura-Carretero, A. and Fernández-Gutiérrez, A., 2009. A 2-D-HPLC-CE platform coupled to ESI-TOF-MS to characterize the phenolic fraction in olive oil. Electrophoresis, 30(15), pp.2688-2701.

Gilbert-López, B., Valencia-Reyes, Z.L., Yufra-Picardo, V.M., García-Reyes, J.F., Ramos-Martos, N. and Molina-Díaz, A., 2014. Determination of polyphenols in commercial extra virgin olive oils from different origins (Mediterranean and South American countries) by liquid chromatography–electrospray time-of-flight mass spectrometry. Food analytical methods, 7(9), pp.1824-1833

Gilbert-López, B., Valencia-Reyes, Z.L., Yufra-Picardo, V.M., García-Reyes, J.F., Ramos-Martos, N. and Molina-Díaz, A., 2014. Determination of polyphenols in commercial extra virgin olive oils from different origins (Mediterranean and South American countries) by liquid chromatography–electrospray time-of-flight mass spectrometry. Food analytical methods, 7(9), pp.1824-1833.

Gutfinger, T., 1981. Polyphenols in olive oils. Journal of the American Oil Chemists' Society, 58(11), pp.966-968.

Lozano-Sánchez, J., Bendini, A., Quirantes-Piné, R., Cerretani, L., Segura-Carretero, A. and Fernández-Gutiérrez, A., 2013. Monitoring the bioactive compounds status of extra-virgin olive oil and storage by-products over the shelf life. Food Control, 30(2), pp.606-615.

Negro, C., Aprile, A., Luvisi, A., Nicolì, F., Nutricati, E., Vergine, M., Miceli, A., Blando, F., Sabella, E. and De Bellis, L., 2019. Phenolic profile and antioxidant activity of Italian monovarietal extra virgin olive oils. Antioxidants, 8(6), p.161.

Olmo-García, L., Polari, J.J., Li, X., Bajoub, A., Fernández-Gutiérrez, A., Wang, S.C. and Carrasco-Pancorbo, A., 2018. Deep insight into the minor fraction of virgin olive oil by using LC-MS and GC-MS multi-class methodologies. *Food chemistry*, *261*, pp.184-193.

Tasioula-Margari, M. and Okogeri, O., 2001. Isolation and characterization of virgin olive oil phenolic compounds by HPLC/UV and GC-MS. Journal of Food Science, 66(4), pp.530-534.

Tripoli, E., Giammanco, M., Tabacchi, G., Di Majo, D., Giammanco, S. and La Guardia, M., 2005. The phenolic compounds of olive oil: structure, biological activity and beneficial effects on human health. Nutrition research reviews, 18(1), pp.98-112.

Table S4.1 continued. The main phenolic compounds and their chemical structures in olive oil products.

Phenyl alcohols	
Compound	**Chemical Structure**
Tyrosol [(*p*-hydroxyphenyl) ethanol] or *p*-HPEA	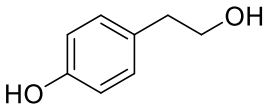
Hydroxytyrosol [(3,4-dihydroxyphenyl) ethanol] or 3,4-DHPEA	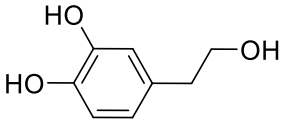
Benzoic and derivatives acids	
Compound	**Chemical Structure**
3-Hydroxybenzoic acid	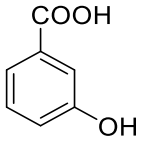
p- Hydroxybenzoic acid	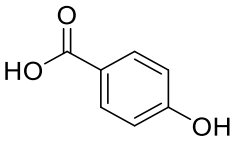
3,4-Dihydroxybenzoic acid	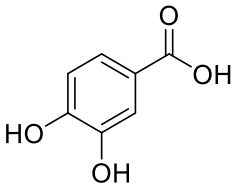
Gentisic acid	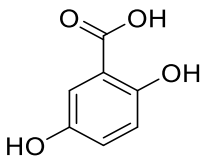

Vanillic acid	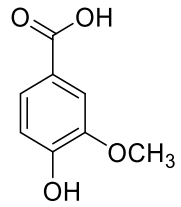
Gallic acid	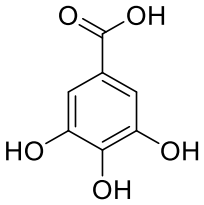
Syringic acid	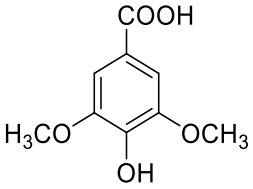
Cinnamic acids and derivatives	
Compound	**Chemical Structure**
p-Coumaric acid	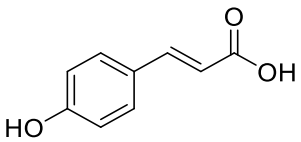
o-Coumaric acid	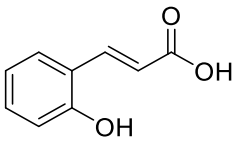
Caffeic Acid	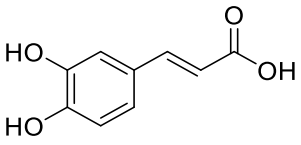

Ferulic Acid	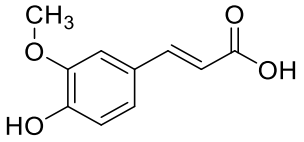
Sinapinic Acid	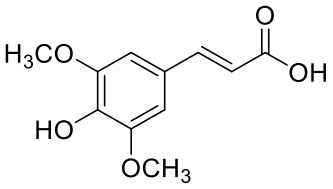
Other phenolic acids and derivatives	
Compound	**Chemical Structure**
p-Hydroxyphenylacetic acid	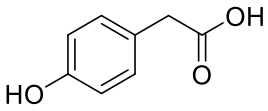
3,4-Dihydroxyphenylacetic acid	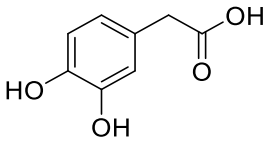
4-Hydroxy-3-methoxyphenylacetic acid	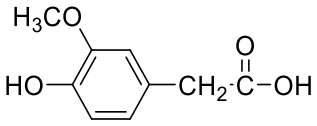
3-(3,4-Dihydroxyphenyl) propanoic acid	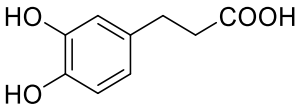

Secoiridoids	
Compound	**Chemical Structure**
Oleuropein	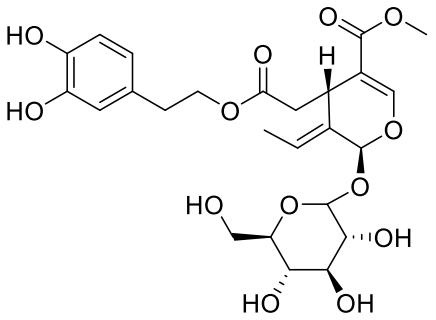
Ligstroside	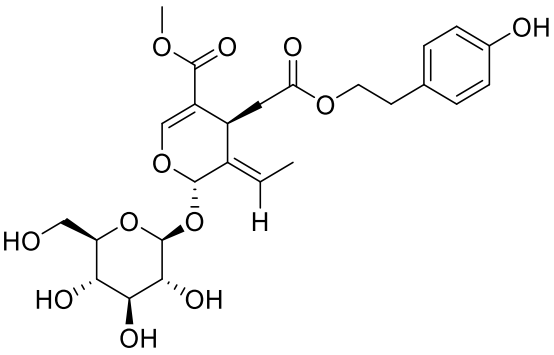
Secoiridoid Derivates: **Dialdehydic forms of secoiridoids**	
Compound	**Chemical Structure**

Decarboxymethyloleuropein aglycon (3,4-DHPEA-EDA)	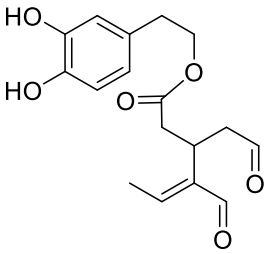
Decarboxymethyl ligstroside aglycon (*p*-HPEA-EDA)	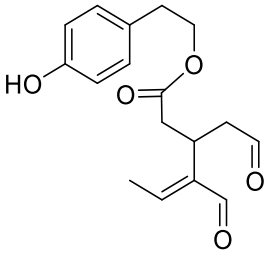
Secoiridoid Aglycons	
Compound	**Chemical Structure**
Oleuropein aglycon or 3,4-DHPEA-EA ((Aldehydic form of oleuropein aglycon))	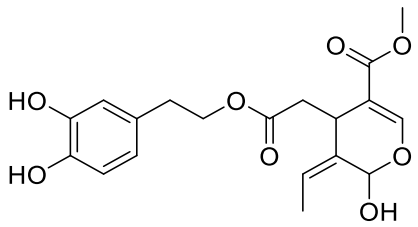
Ligstroside aglycon or *p*-HPEA-EA ((Aldehydic form ligstroside aglycon))	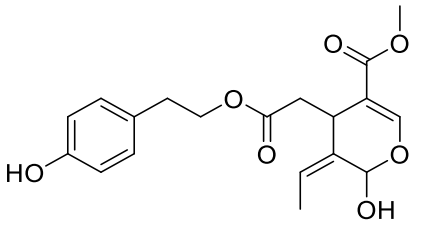

Flavonoids	
Compound	**Chemical Structure**
Apigenin	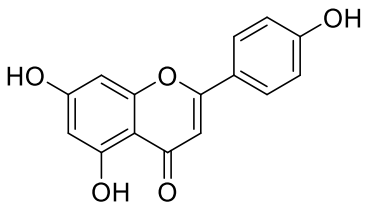
Luteolin	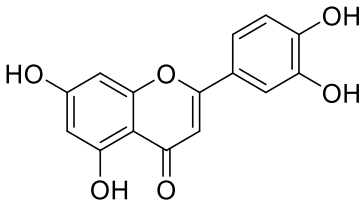
(+)-Taxifolin	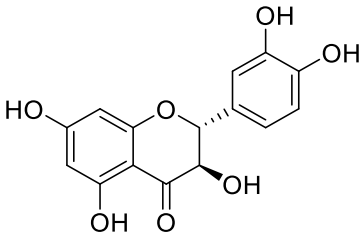

Lignans	
Compound	**Chemical Structure**
(+)-Pinoresinol	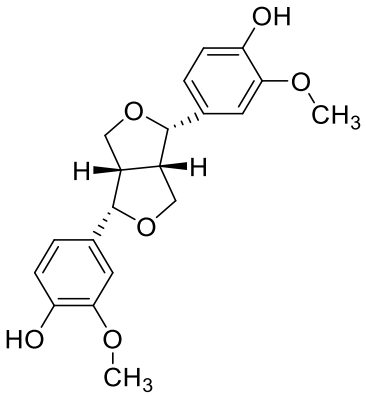
(+)-1-Acetoxypinoresinol	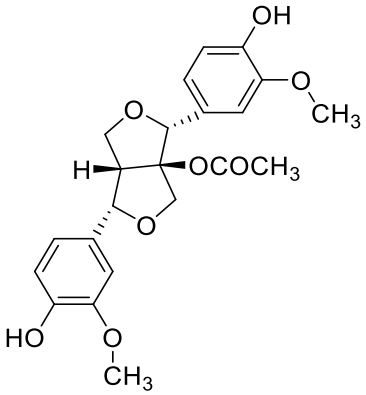
(+)-1-Hydroxypinoresinol	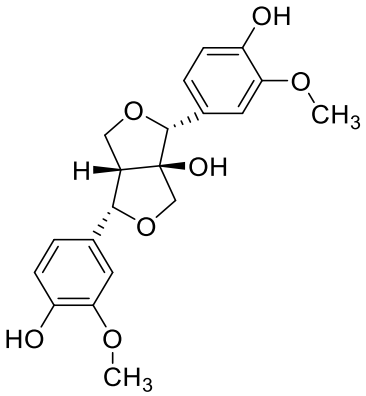

Hydroxyisochromans	
Compound	**Chemical Structure**
1-Phenyl-6,7-dihydroxyisochroman	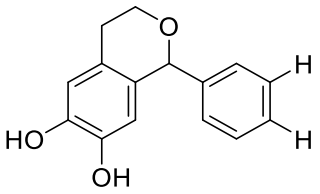
1-(3'-Methoxy-4'-hydroxy) phenyl-6,7-dihydroxyisochroman	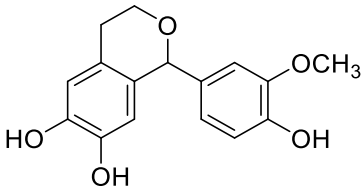

Bendini, A., Cerretani, L., Carrasco-Pancorbo, A., Gómez-Caravaca, A.M., Segura-Carretero, A., Fernández-Gutiérrez, A. and Lercker, G., 2007. Phenolic molecules in virgin olive oils: a survey of their sensory properties, health effects, antioxidant activity and analytical methods. An overview of the last decade Alessandra. Molecules, 12(8), pp.1679-1719.

Naushad, M. and Khan, M.R., 2014. Ultra performance liquid chromatography mass spectrometry: evaluation and applications in food analysis. CRC Press.

Omar, S.H., 2010. Oleuropein in olive and its pharmacological effects. Scientia pharmaceutica, 78(2), pp.133-154.

Rodríguez-López, P., Lozano-Sanchez, J., Borrás-Linares, I., Emanuelli, T., Menéndez, J.A. and Segura-Carretero, A., 2020. Structure–Biological Activity Relationships of Extra-Virgin Olive Oil Phenolic Compounds: Health Properties and Bioavailability. *Antioxidants*, *9*(8), p.685.

Suárez, M., Macià, A., Romero, M.P. and Motilva, M.J., 2008. Improved liquid chromatography tandem mass spectrometry method for the determination of phenolic compounds in virgin olive oil. Journal of Chromatography A, 1214(1-2), pp.90-99.

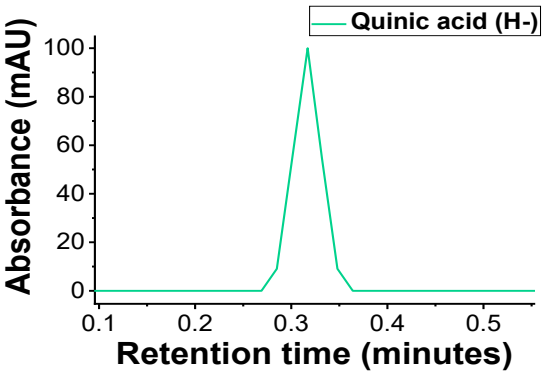
Quinic acid (H-)
Absorbance (mAU)
Retention time (minutes)

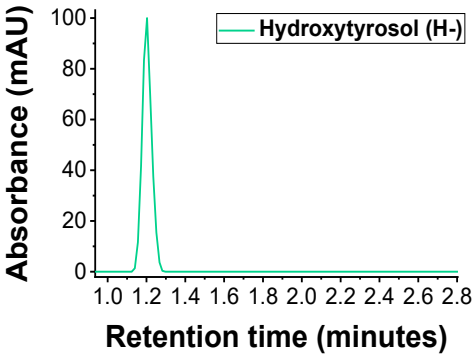
Hydroxytyrosol (H-)
Absorbance (mAU)
Retention time (minutes)

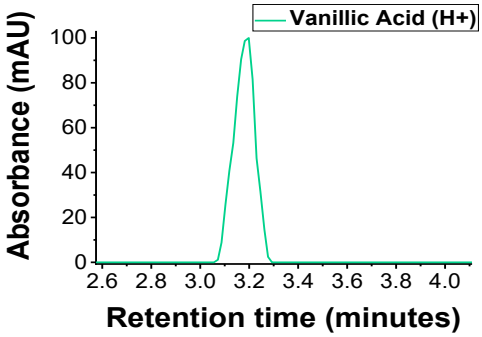
Vanillic Acid (H+)
Absorbance (mAU)
Retention time (minutes)

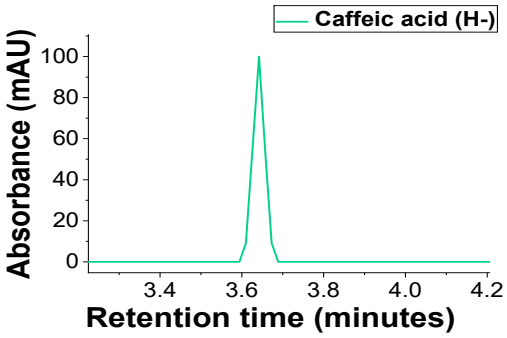
Caffeic acid (H-)
Absorbance (mAU)
Retention time (minutes)

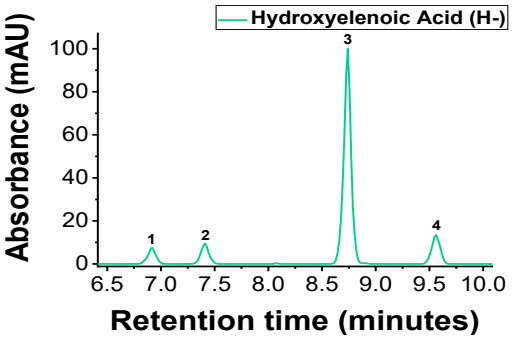
Hydroxyelenoic Acid (H-)
1
2
3
4
Absorbance (mAU)
Retention time (minutes)

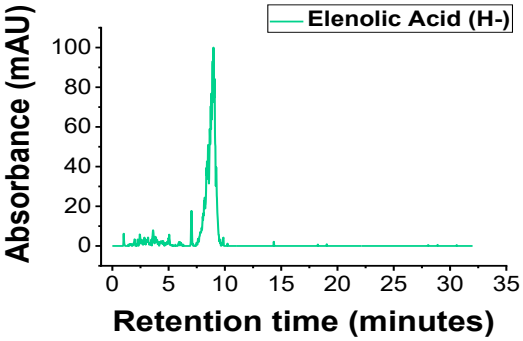
Elenolic Acid (H-)
Absorbance (mAU)
Retention time (minutes)

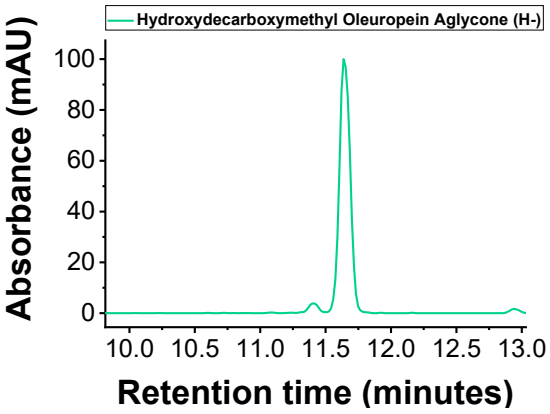
Hydroxydecarboxymethyl Oleuropein Aglycone (H-)
Absorbance (mAU)
Retention time (minutes)

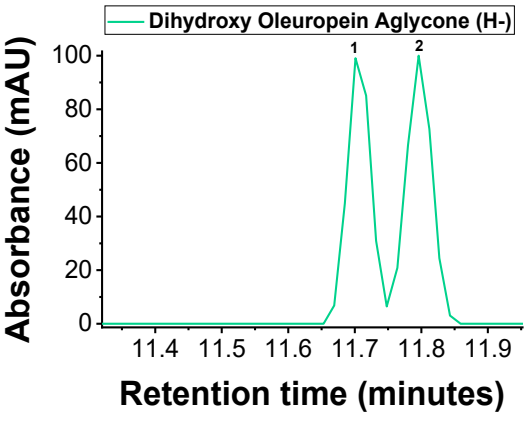
Dihydroxy Oleuropein Aglycone (H-)
1
2
Absorbance (mAU)
Retention time (minutes)

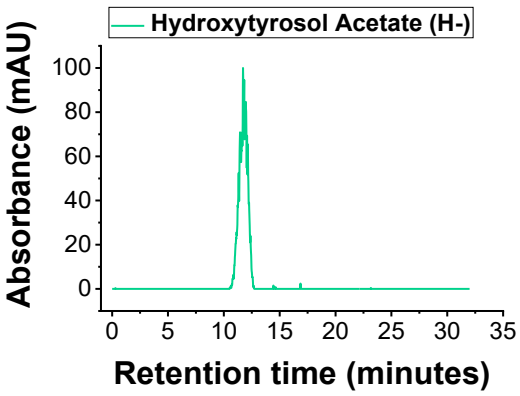
Hydroxytyrosol Acetate (H-)
Absorbance (mAU)
Retention time (minutes)

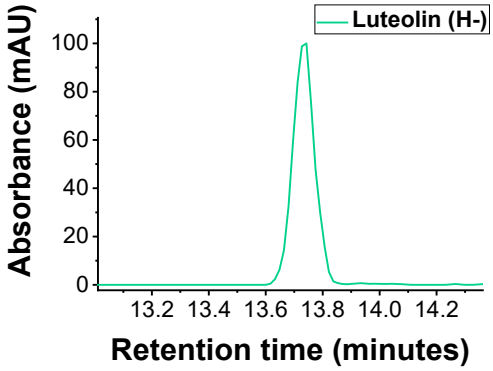
Luteolin (H-)
Absorbance (mAU)
Retention time (minutes)

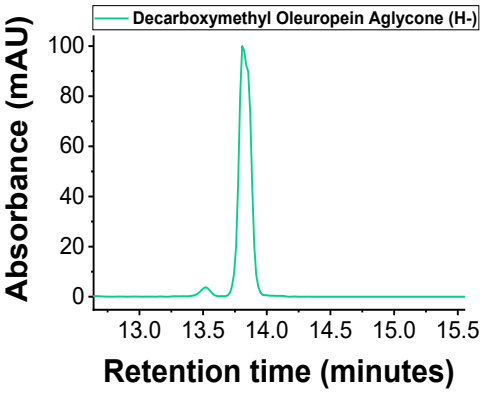
Decarboxymethyl Oleuropein Aglycone (H-)
Absorbance (mAU)
Retention time (minutes)

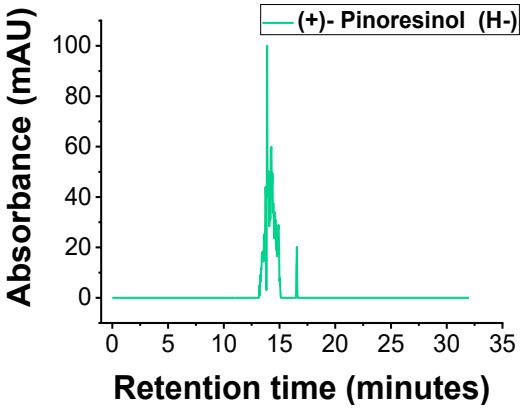
(+)- Pinoresinol (H-)
Absorbance (mAU)
Retention time (minutes)

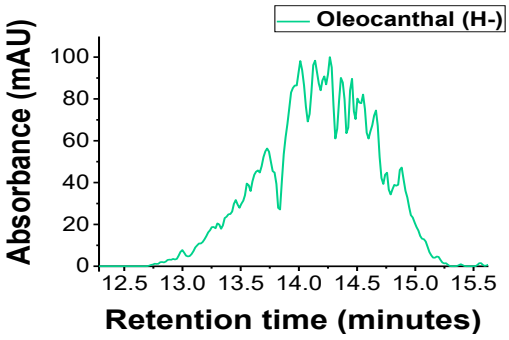
Oleocanthal (H-)
Absorbance (mAU)
Retention time (minutes)

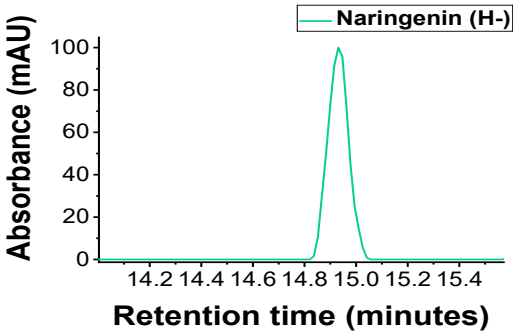
Naringenin (H-)
Absorbance (mAU)
Retention time (minutes)

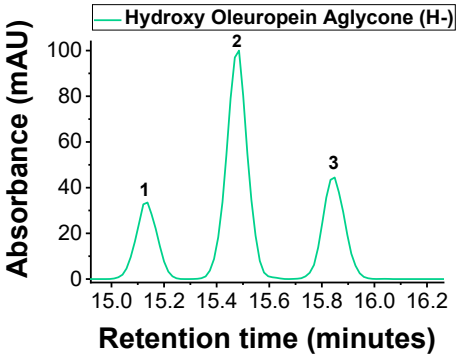
Hydroxy Oleuropein Aglycone (H-)
1
2
3
Absorbance (mAU)
Retention time (minutes)

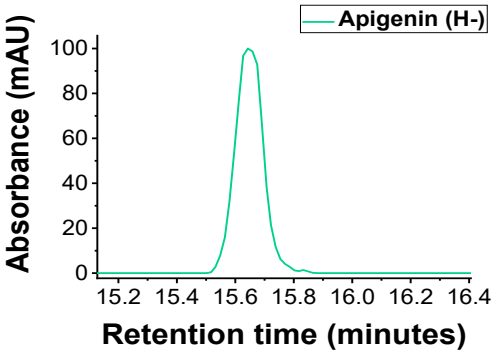
Apigenin (H-)
Absorbance (mAU)
Retention time (minutes)

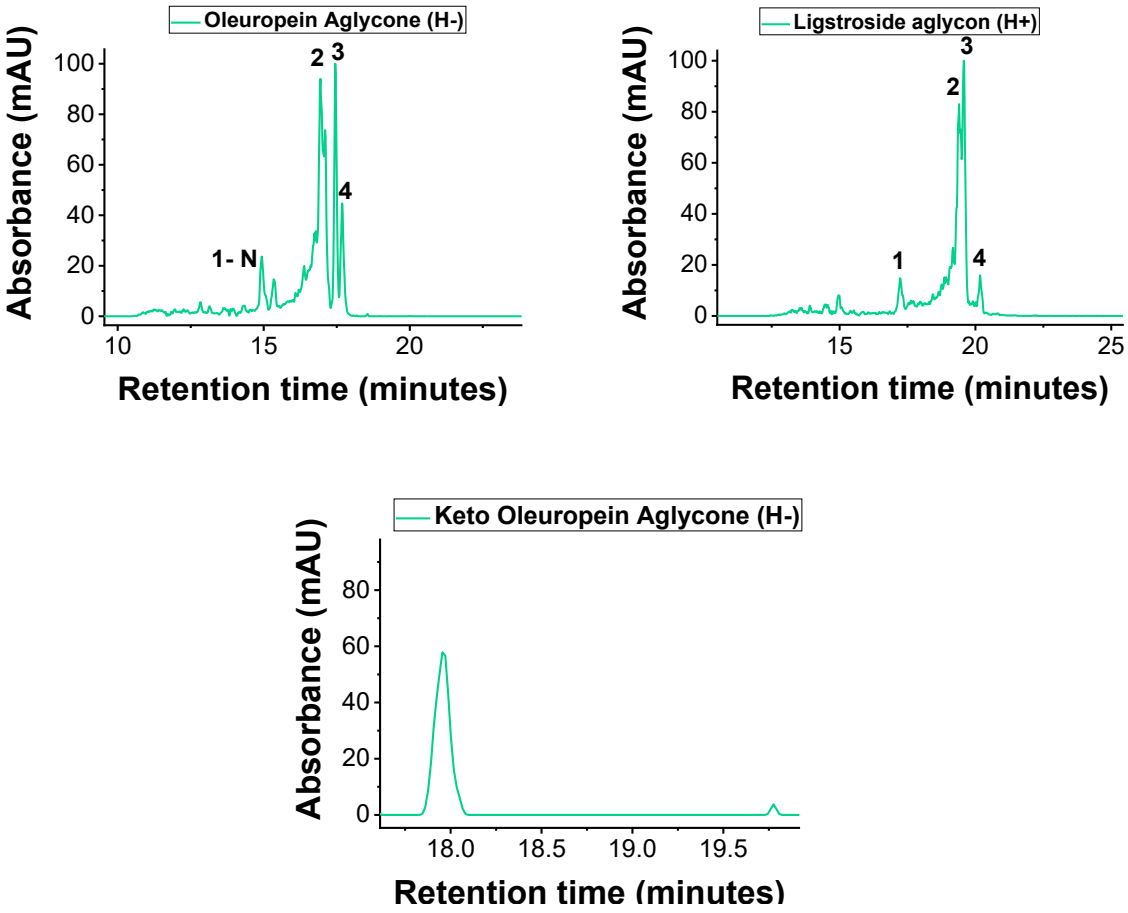

Figure S4.1. Ion chromatograms for individual phenolic compounds detected from Greek EVOO by LC-MS (individual peak detection and retention time).

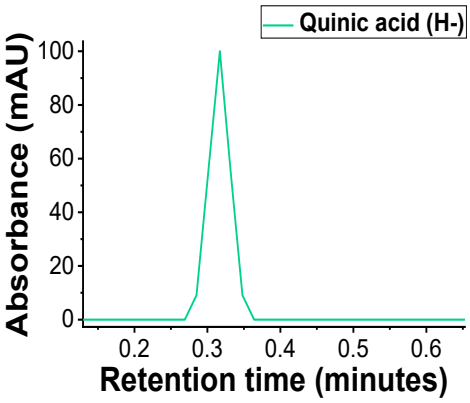
Quinic acid (H-)
Absorbance (mAU)
Retention time (minutes)

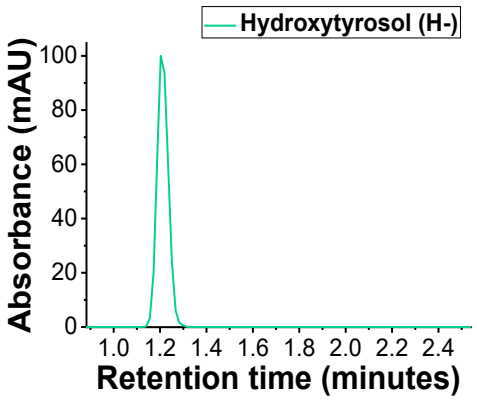
Hydroxytyrosol (H-)
Absorbance (mAU)
Retention time (minutes)

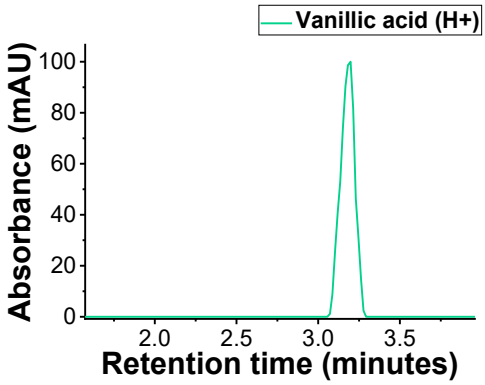
Vanillic acid (H+)
Absorbance (mAU)
Retention time (minutes)

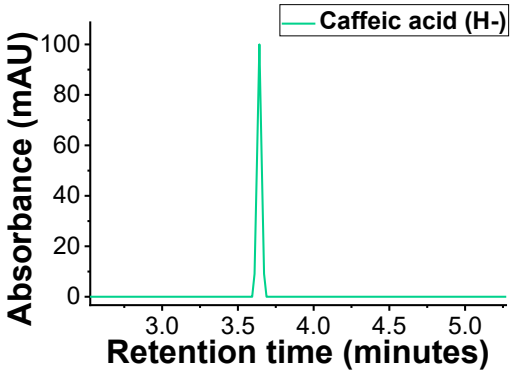
Caffeic acid (H-)
Absorbance (mAU)
Retention time (minutes)

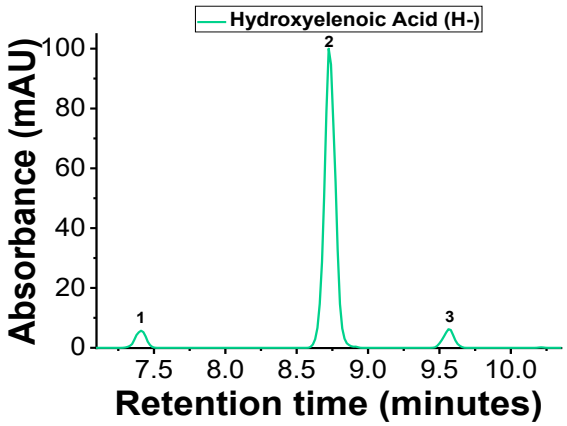
Hydroxyelenoic Acid (H-)
1
2
3
Absorbance (mAU)
Retention time (minutes)

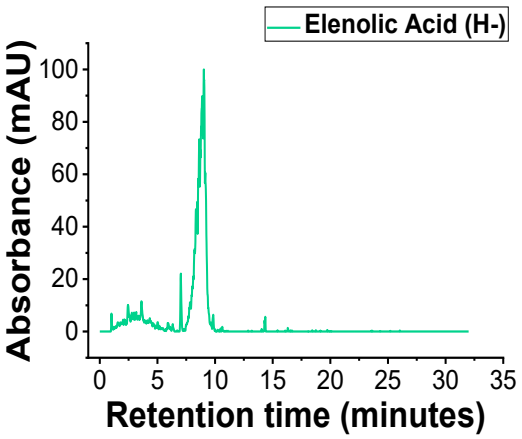
Elenolic Acid (H-)
Absorbance (mAU)
Retention time (minutes)

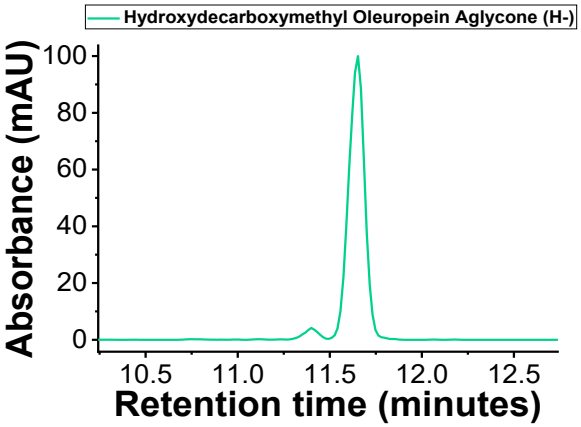
Hydroxydecarboxymethyl Oleuropein Aglycone (H-)
Absorbance (mAU)
Retention time (minutes)

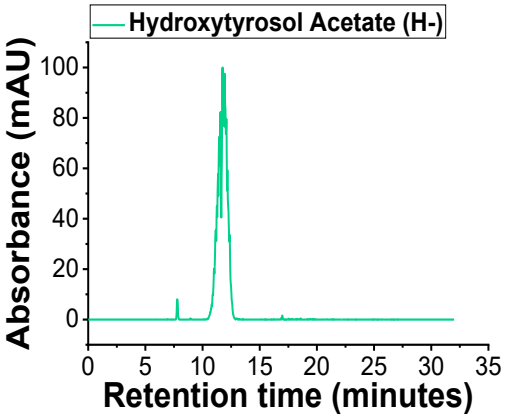
Hydroxytyrosol Acetate (H-)
Absorbance (mAU)
Retention time (minutes)

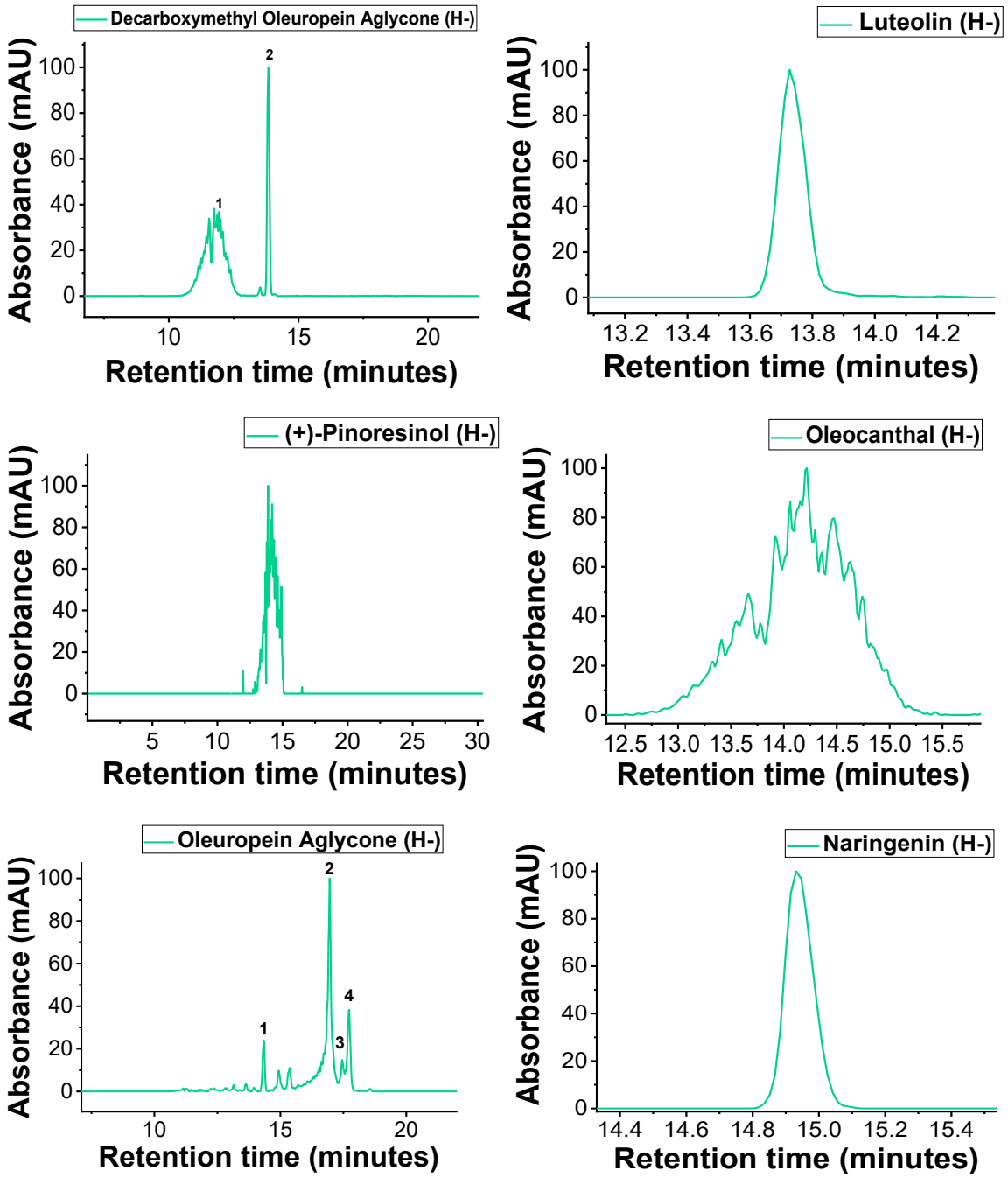
Decarboxymethyl Oleuropein Aglycone (H-)
Absorbance (mAU)
Retention time (minutes)
1
2
Luteolin (H-)
(+)-Pinoresinol (H-)
Oleocanthal (H-)
Oleuropein Aglycone (H-)
3
4
Naringenin (H-)

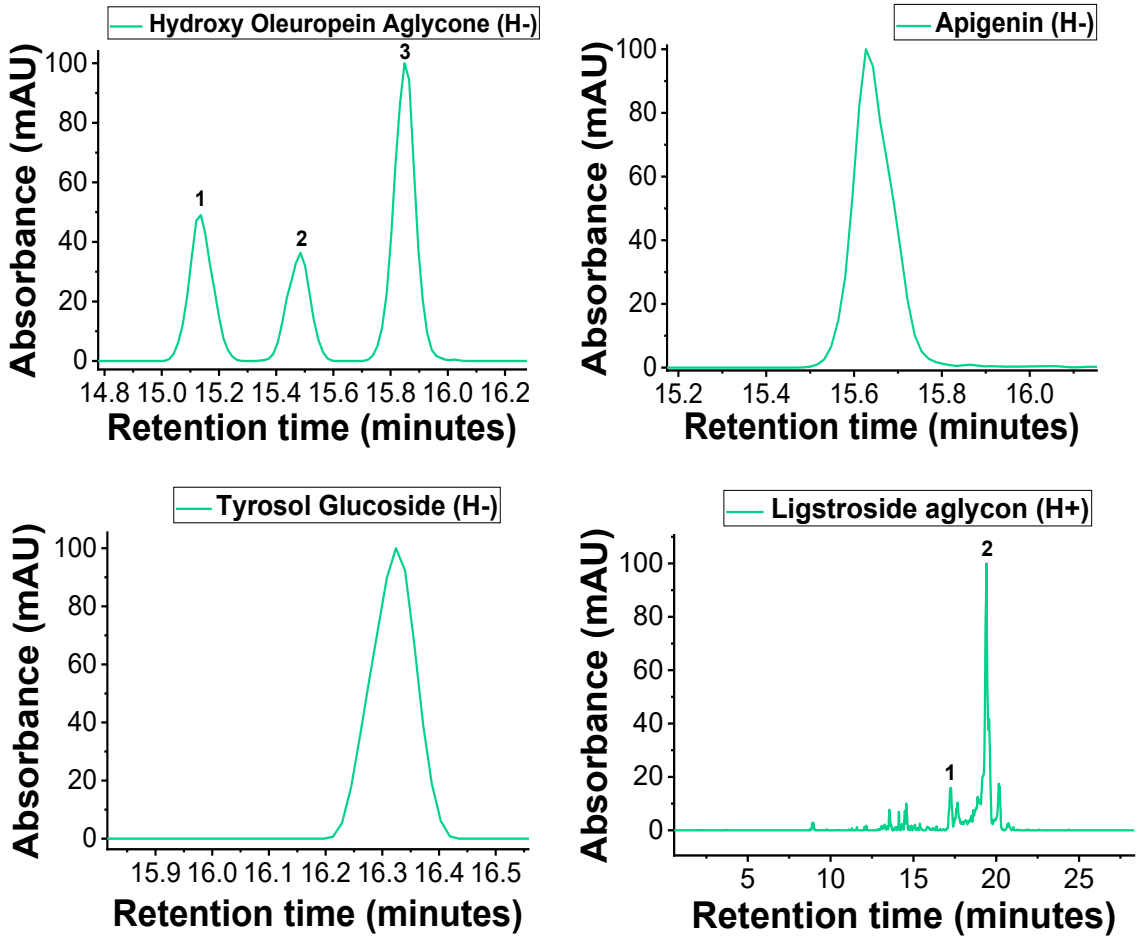

Figure S4.2. Ion chromatograms for individual phenolic compounds detected from Saudi EVOO by LC-MS (individual peak detection and retention time).

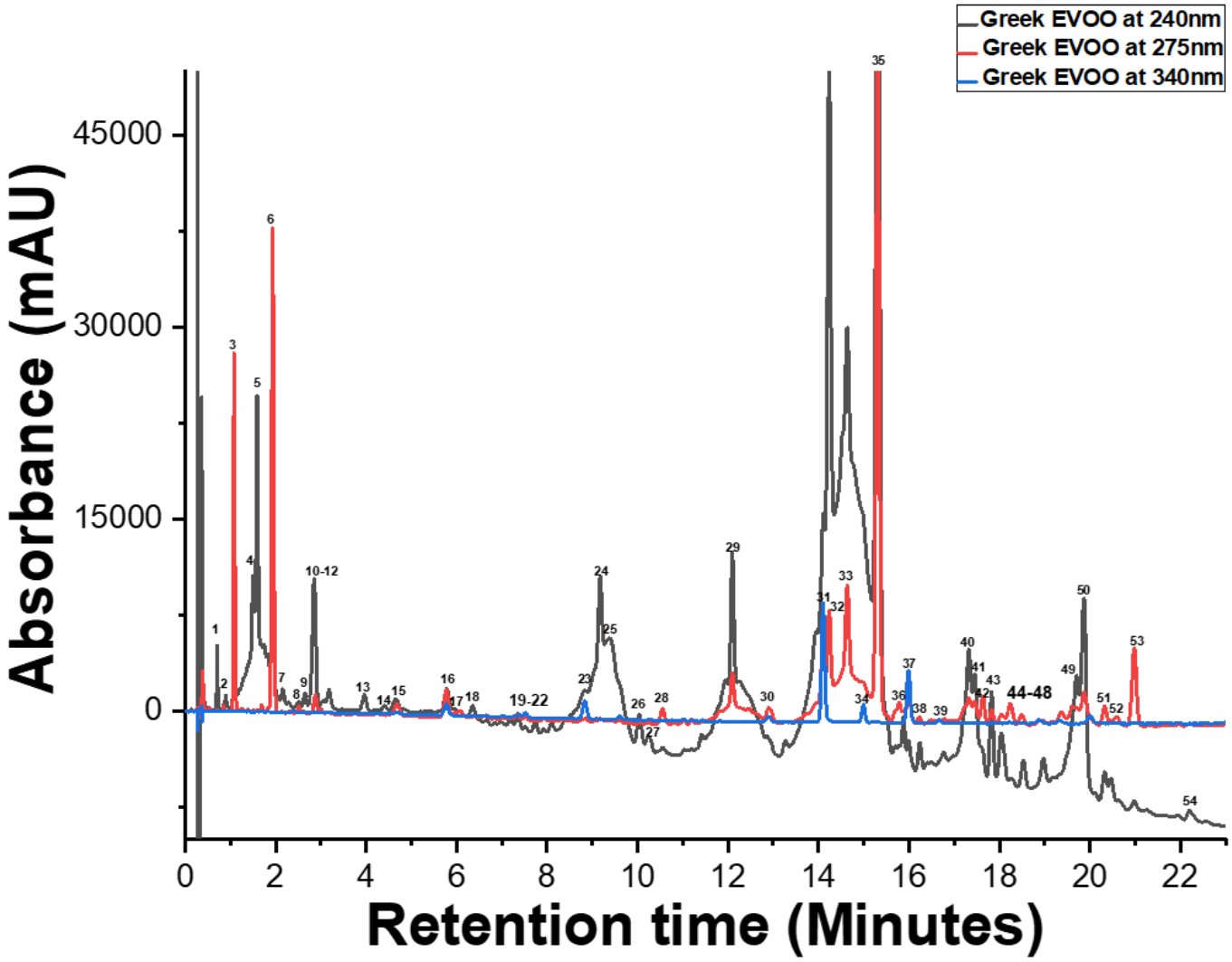

Figure S4.3. Greek EVOO alternative representation of the reverse-phase HPLC chromatogram as shown in **Figure 4.11**.

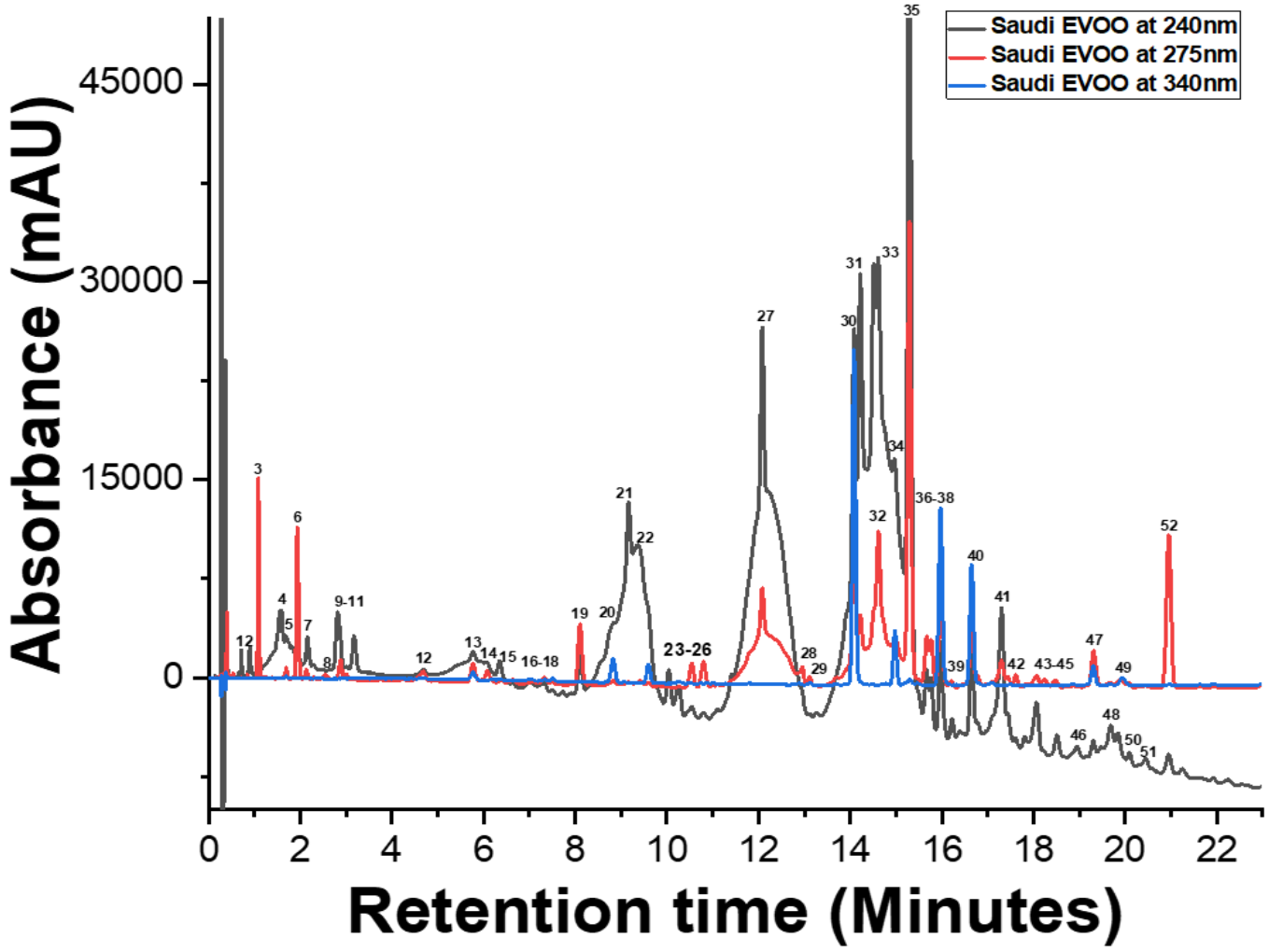

Figure S4.4. Saudi EVOO alternative representation of the reverse-phase HPLC chromatogram as shown in **Figure 4.11**.

Table S4.2. Retention time and area contribution from the integration of the HPLC spectra acquired from the Greek EVOO crude extract at 275 nm.

RT	Area	Area%	S/N	$Width_{50\%}$	Height
0.231	1542	0.154	5.71	0.055	381
0.363	10951	1.093	18.64	0.043	1244
0.536	5308	0.530	12.90	0.000	861
0.707	6037	0.603	10.47	0.000	699
0.846	6007	0.600	14.81	0.000	988
1.081	64433	6.431	402.96	0.032	26891
1.238	5882	0.587	11.16	0.000	745
1.383	3217	0.321	9.64	0.000	643
1.500	2712	0.271	8.24	0.000	550
1.592	2863	0.286	8.56	0.000	571
1.690	4574	0.457	14.17	0.079	946
1.933	129575	12.932	568.47	0.050	37935
2.131	2561	0.256	5.48	0.000	365
2.306	3531	0.352	5.75	0.000	384
2.511	4050	0.404	10.40	0.089	694
2.632	2092	0.209	4.61	0.000	308
2.876	8834	0.882	23.43	0.080	1564
3.003	2180	0.218	6.56	0.000	437
3.144	1172	0.117	2.70	0.000	180
4.247	600	0.060	1.37	0.100	91
4.681	7553	0.754	13.98	0.121	933
5.772	14707	1.468	32.80	0.104	2189
5.984	2849	0.284	6.37	0.000	425
6.081	3436	0.343	8.03	0.000	536
6.383	714	0.071	1.74	0.093	116
6.653	2422	0.242	4.10	0.134	273
7.332	1904	0.190	4.91	0.093	328
7.521	954	0.095	3.01	0.079	201
7.929	1349	0.135	3.40	0.092	227
8.096	903	0.090	1.32	0.121	88
8.341	894	0.089	2.79	0.078	186
8.840	1879	0.188	3.57	0.118	238
9.178	1255	0.125	3.08	0.085	206
9.440	493	0.049	1.20	0.108	80
9.588	786	0.078	2.19	0.090	146
10.218	742	0.074	1.50	0.132	100
10.552	8590	0.857	18.43	0.107	1230
10.815	919	0.092	2.19	0.102	146
11.027	2119	0.211	5.93	0.079	396
11.196	1517	0.151	5.25	0.068	350

	11.424	1111	0.111	1.90	0.000	127
	11.808	9087	0.907	12.35	0.000	824
	12.094	45846	4.576	56.63	0.099	3779
	12.456	11438	1.142	13.18	0.000	879
	12.897	7433	0.742	14.10	0.136	941
	13.257	370	0.037	1.37	0.067	91
	14.101	26915	2.686	81.69	0.077	5451
	14.234	31284	3.122	93.00	0.081	6206
	14.636	35954	3.588	101.10	0.084	6747
	14.984	932	0.093	2.57	0.086	171
	15.308	277604	27.707	783.46	0.082	52282
	15.784	12469	1.244	21.84	0.000	1458
	15.991	19534	1.950	42.63	0.091	2845
	16.226	2585	0.258	7.27	0.087	485
	16.787	681	0.068	2.33	0.072	156
	16.968	725	0.072	1.28	0.000	85
	17.322	20136	2.010	27.87	0.000	1860
	17.452	10880	1.086	24.22	0.000	1616
	17.633	10916	1.089	30.14	0.086	2012
	17.826	5542	0.553	15.70	0.082	1048
	18.045	5780	0.577	10.37	0.000	692
	18.235	11464	1.144	22.89	0.123	1528
	18.490	5273	0.526	11.12	0.117	742
	18.892	4032	0.402	4.99	0.199	333
	19.168	1840	0.184	3.61	0.000	241
	19.368	9352	0.933	14.66	0.172	978
	19.613	11536	1.151	21.47	0.000	1433
	19.704	8024	0.801	20.36	0.000	1359
	19.870	25648	2.560	38.14	0.154	2545
	20.324	10363	1.034	22.41	0.108	1495
	20.591	7831	0.782	10.14	0.226	676
	20.979	42761	4.268	91.00	0.110	6072
	22.200	1301	0.130	2.51	0.121	167
	23.053	1183	0.118	2.18	0.134	145
	Total	1001933		100.000	192344	

Table S4.3. Retention time and area contribution from the integration of the HPLC spectra acquired from the Saudi EVOO crude extract at 275 nm.

RT	Area	Area%	S/N	$Width_{50\%}$	Height
0.227	1496	0.146	5.58	0.057	356
0.389	9691	0.948	76.67	0.014	4886
0.536	1402	0.137	6.63	0.034	423
0.844	507	0.050	4.41	0.025	281
1.079	30628	2.997	229.43	0.031	14622
1.236	600	0.059	2.40	0.043	153
1.376	274	0.027	1.77	0.037	113
1.496	268	0.026	1.57	0.044	100
1.688	3157	0.309	13.16	0.046	839
1.932	37545	3.674	179.44	0.050	11436
2.129	2674	0.262	11.18	0.058	713
2.294	806	0.079	3.14	0.063	200
2.537	3074	0.301	5.71	0.135	364
2.873	7638	0.747	23.77	0.076	1515
2.998	2021	0.198	6.75	0.000	430
3.176	353	0.035	0.87	0.107	56
4.676	7322	0.716	11.37	0.156	725
5.766	9486	0.928	22.49	0.103	1434
6.078	7304	0.715	13.47	0.109	858
6.379	863	0.084	2.45	0.088	156
6.633	1764	0.173	4.26	0.104	271
7.315	3196	0.313	7.69	0.094	490
7.502	966	0.095	2.69	0.000	172
7.912	638	0.062	1.60	0.000	102
8.103	28559	2.795	72.32	0.096	4609
8.325	655	0.064	2.37	0.068	151
8.831	2330	0.228	4.69	0.112	299
9.158	1950	0.191	3.86	0.121	246
9.407	3604	0.353	5.74	0.153	366
9.591	1876	0.184	4.65	0.110	297
9.814	606	0.059	1.44	0.114	92
10.269	752	0.074	2.07	0.097	132
10.540	12526	1.226	28.84	0.105	1838
10.798	12535	1.227	29.87	0.104	1904
11.000	207	0.020	0.78	0.058	50
11.105	456	0.045	2.26	0.051	144
12.080	186497	18.249	107.88	0.181	6875
12.950	2443	0.239	11.04	0.058	704
13.117	2559	0.250	9.04	0.072	576
13.256	180	0.018	0.89	0.048	57

	13.709	1037	0.101	2.70	0.095	172
	14.084	75411	7.379	236.99	0.076	15104
	14.220	14999	1.468	47.54	0.000	3030
	14.618	48927	4.787	116.30	0.089	7412
	14.978	7308	0.715	16.30	0.109	1039
	15.293	179067	17.522	531.55	0.082	33876
	15.673	20032	1.960	55.05	0.000	3508
	15.768	16076	1.573	51.27	0.000	3267
	15.974	51483	5.038	142.49	0.087	9081
	16.209	2537	0.248	7.13	0.091	455
	16.464	1515	0.148	3.51	0.000	224
	16.651	32384	3.169	85.26	0.089	5434
	16.779	3309	0.324	12.08	0.000	770
	17.104	1017	0.099	3.18	0.000	203
	17.303	14236	1.393	28.83	0.112	1837
	17.443	3030	0.297	9.66	0.000	616
	17.615	3906	0.382	13.14	0.076	837
	17.856	2208	0.216	4.01	0.000	255
	18.069	7429	0.727	13.96	0.140	889
	18.239	5109	0.500	9.79	0.000	624
	18.475	4335	0.424	8.85	0.125	564
	18.680	582	0.057	0.90	0.000	57
	18.874	1950	0.191	2.54	0.216	162
	19.311	21693	2.123	43.93	0.110	2800
	19.677	4928	0.482	6.57	0.000	419
	19.890	6810	0.666	8.81	0.242	561
	20.089	2113	0.207	6.05	0.000	385
	20.449	2671	0.261	2.80	0.246	178
	20.954	83636	8.184	181.05	0.113	11538
	21.616	778	0.076	1.49	0.116	95
	21.947	992	0.097	2.43	0.106	155
	23.007	1794	0.176	3.75	0.111	239
	24.263	1283	0.126	3.01	0.105	192
	25.936	1390	0.136	2.17	0.000	138
	26.190	2666	0.261	4.11	0.000	262
	26.400	1501	0.147	2.87	0.000	183
	26.800	425	0.042	0.99	0.108	63
	Total	1021973		100.000165654		

Greek EVOO **Saudi EVOO**

(c) **Vanillic acid**

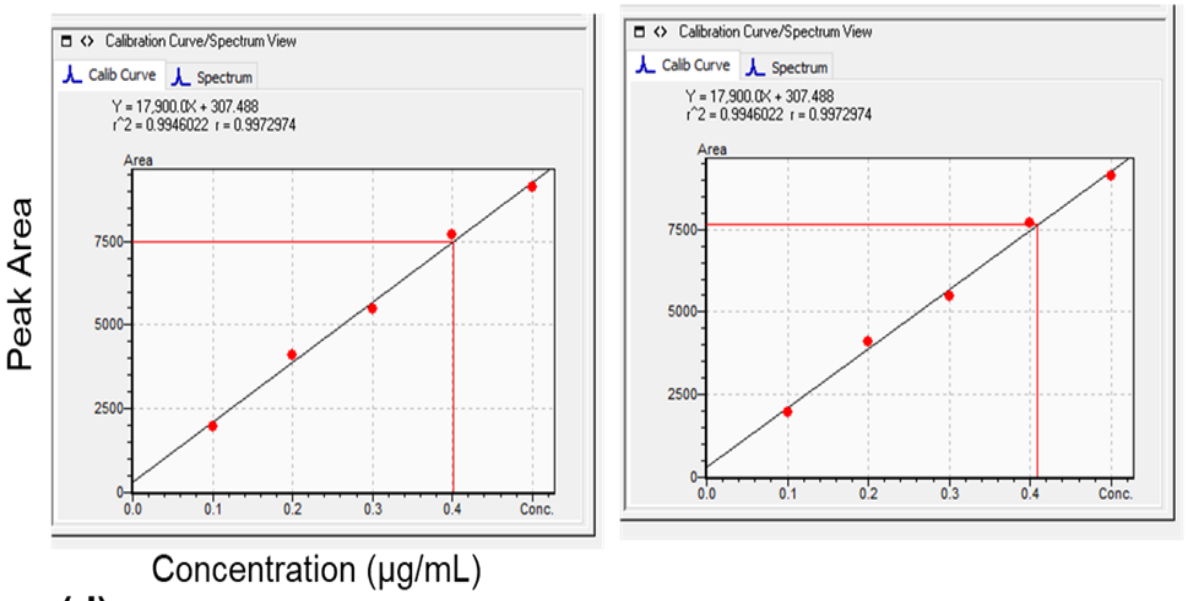

(d) **Caffeic acid**

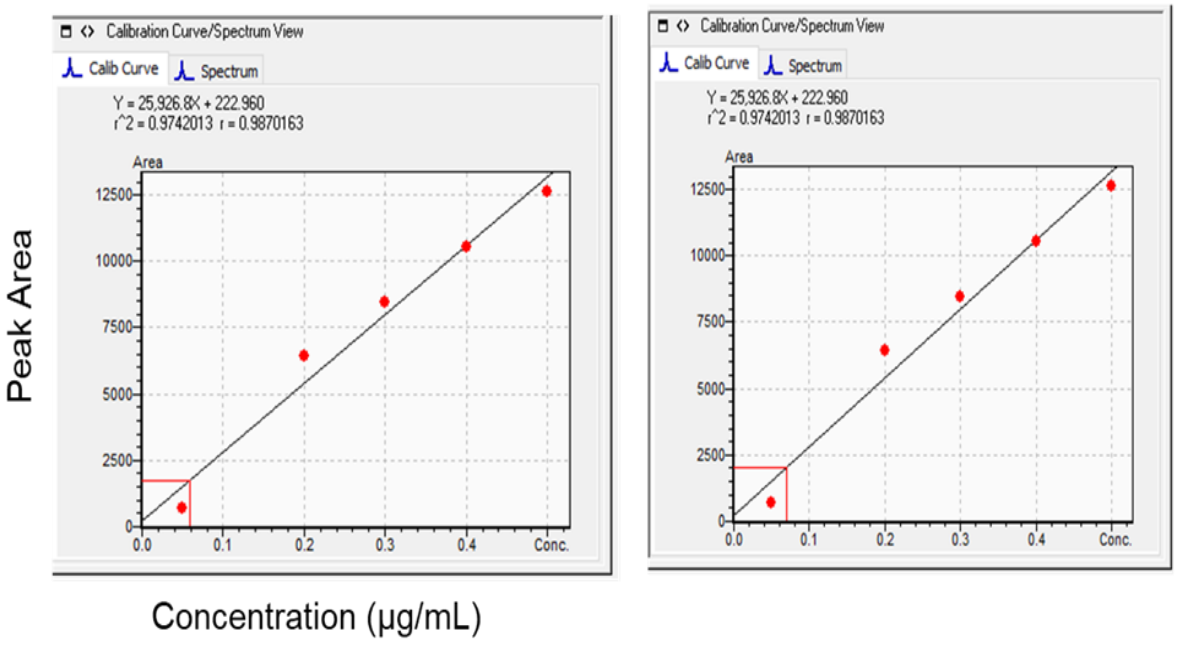

(e)

P-Coumaric acid

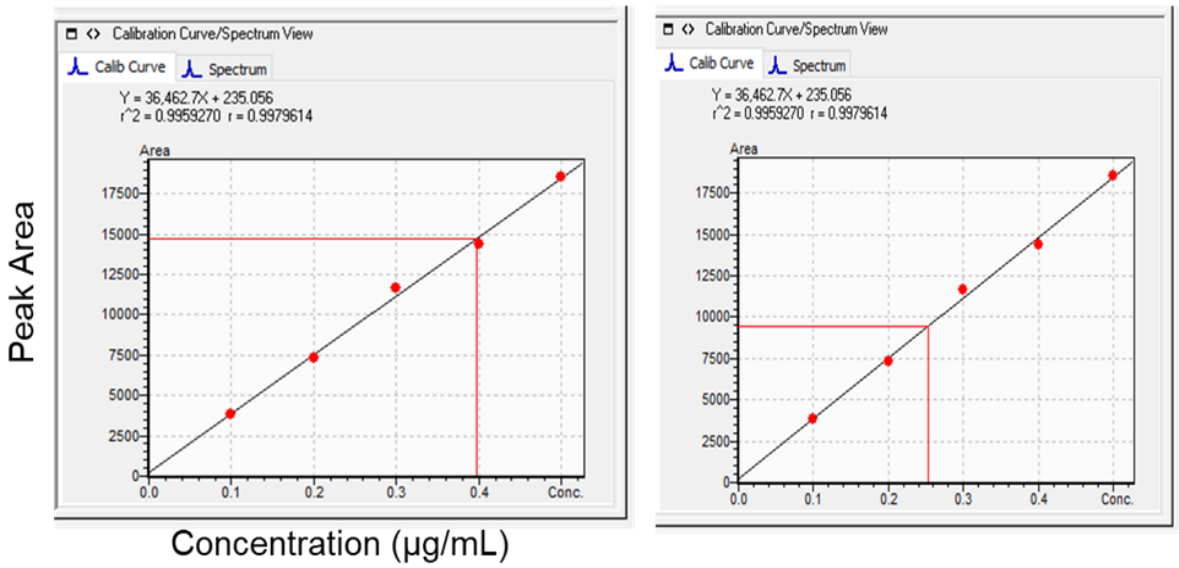

(f)

Ferulic acid

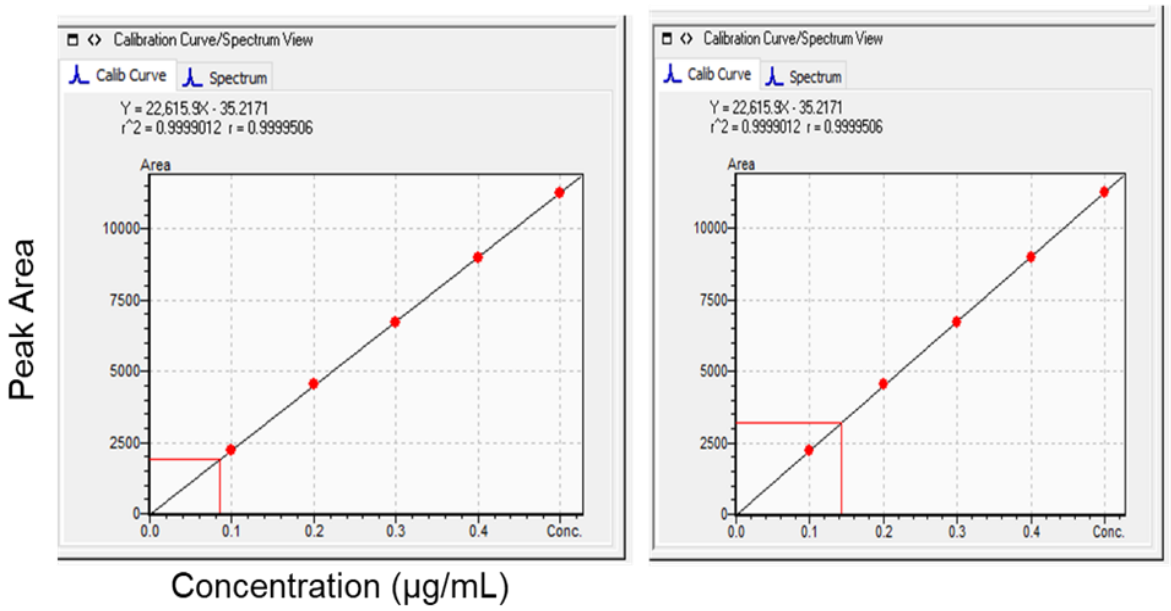

(g)

Oleuropein

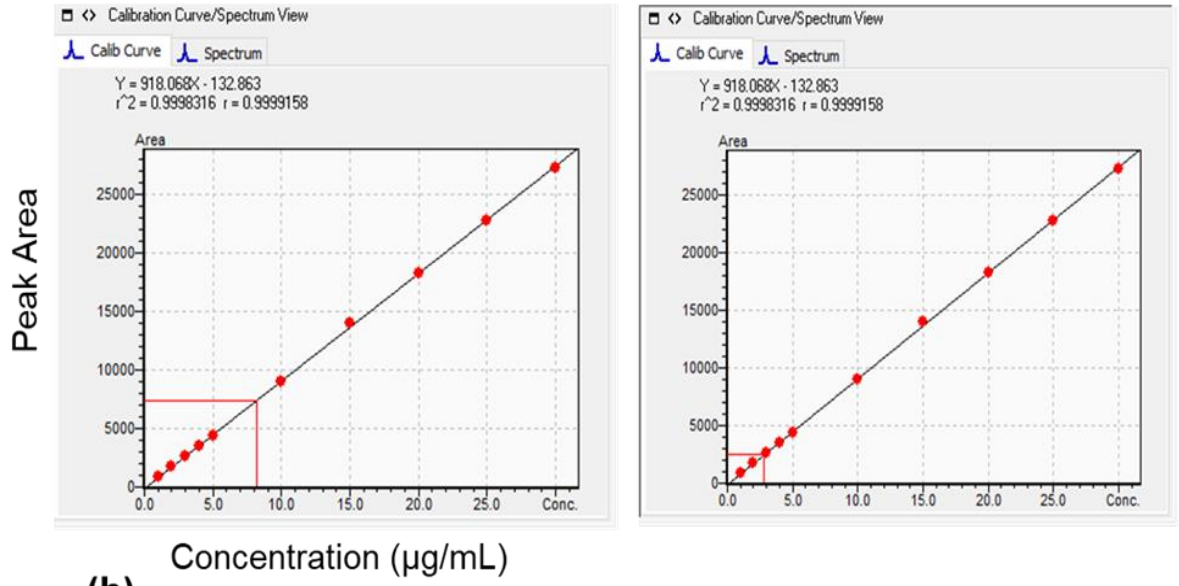

(h)

Luteolin

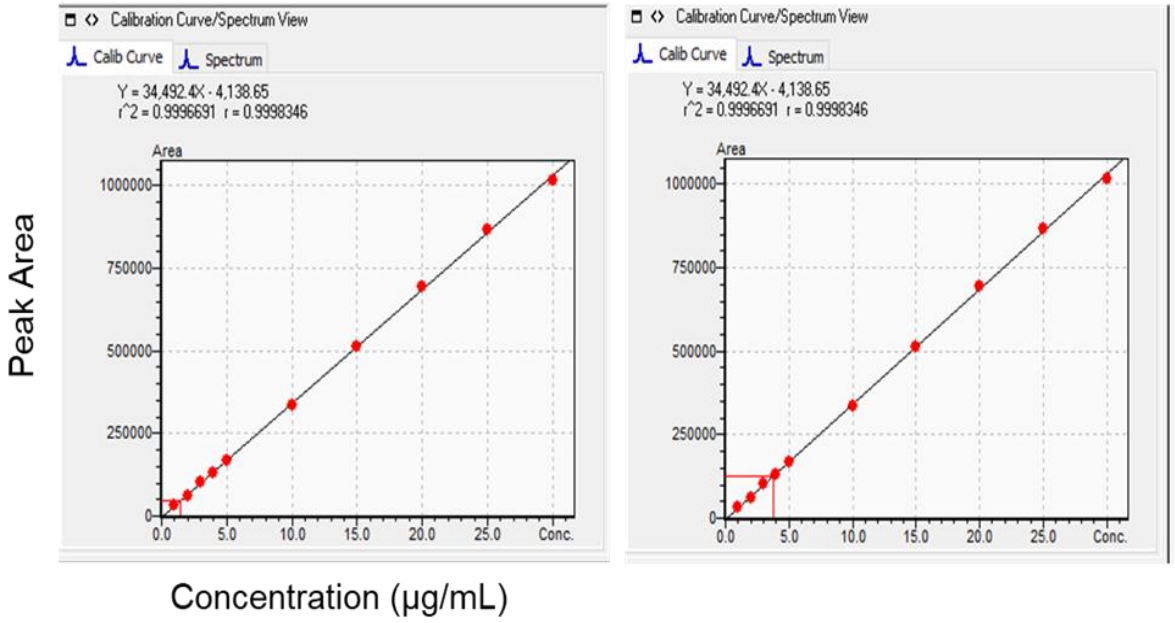

(i)

(+)-Pinoresinol

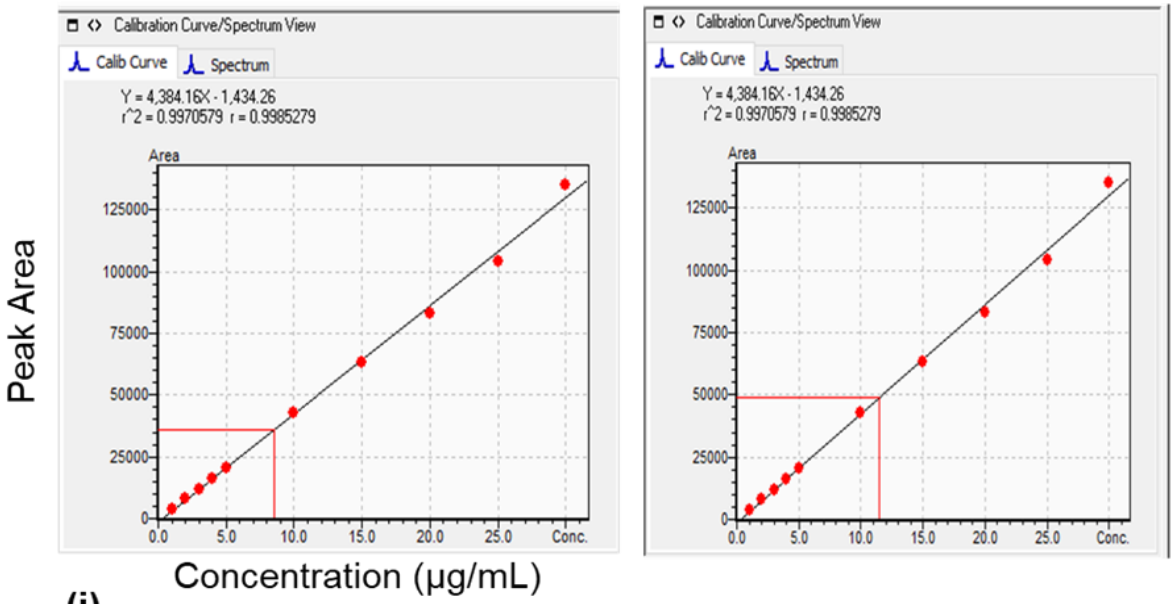

(j)

Naringenin

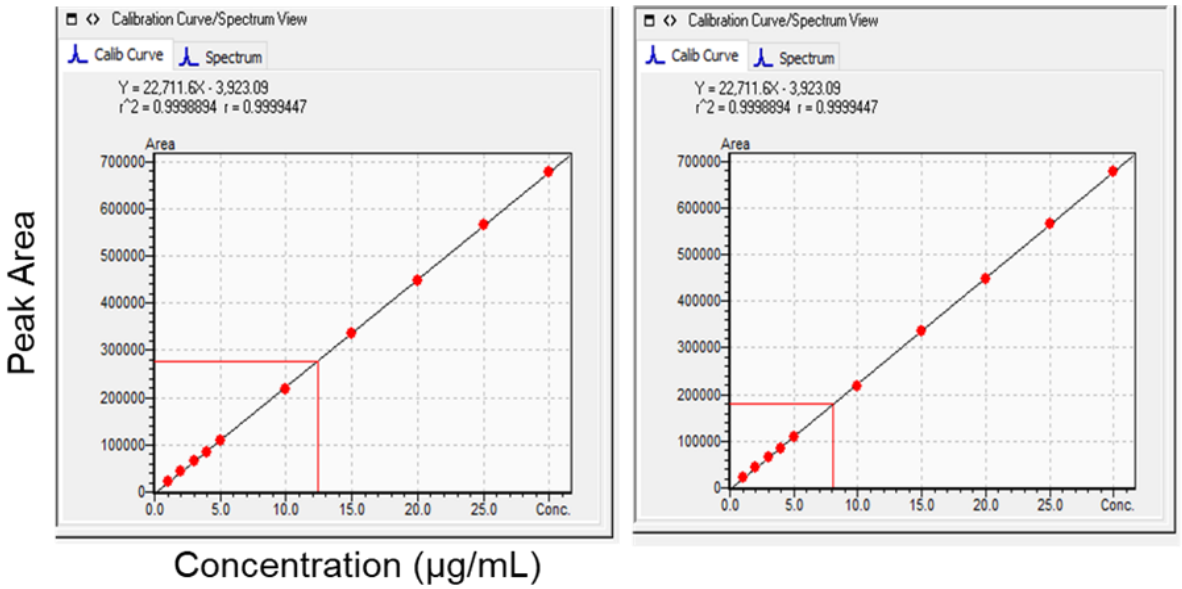

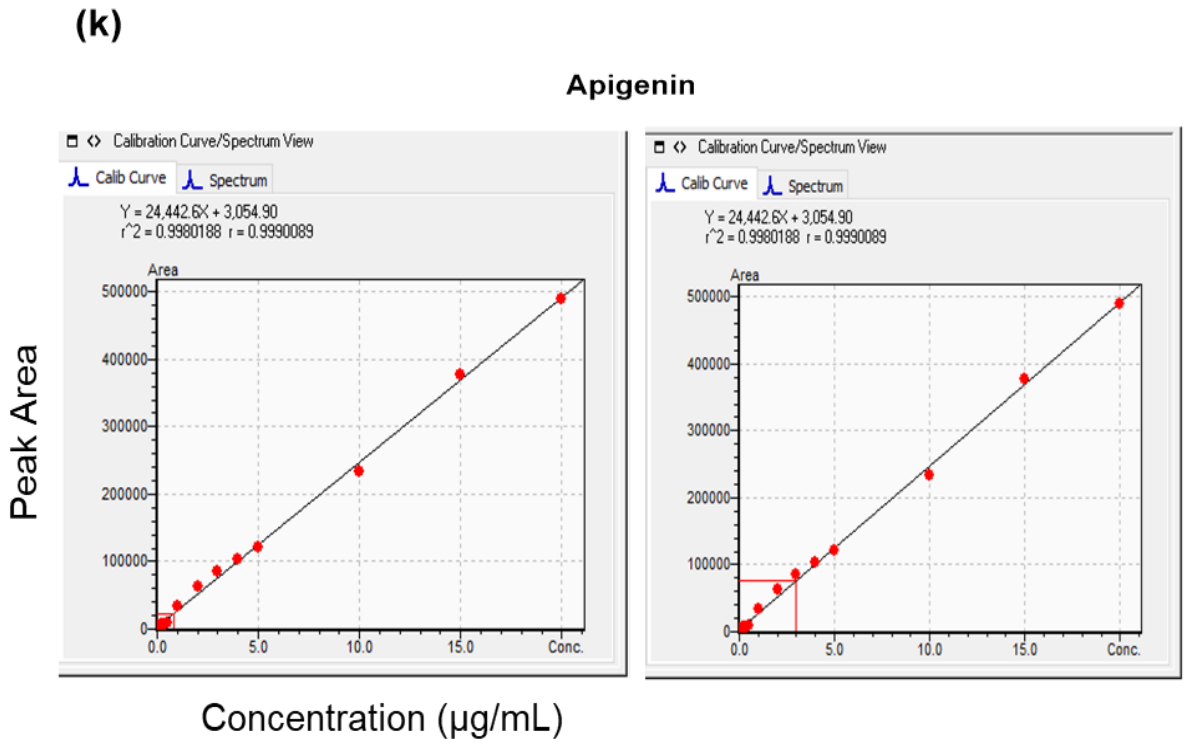

Figure S4.5. The calibration curves of some phenolic compounds extracted from Greek and Saudi EVOOs. These include vanillic acid, caffeic acid, *p*-coumaric acid, ferulic acid, cinnamic acid, oleuropein, luteolin, (+)-pinoresinol, naringenin and apigenin respectively.

Appendix 2

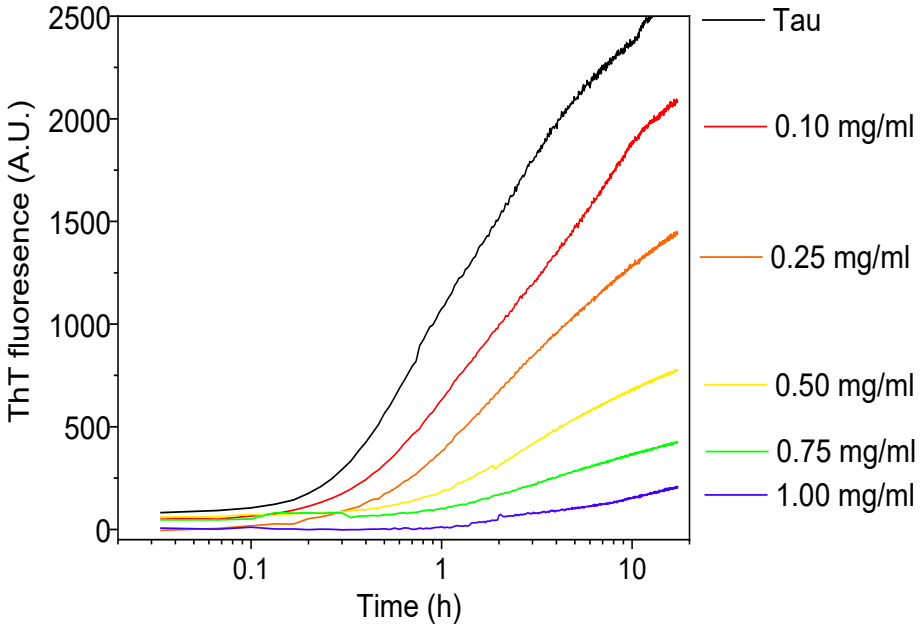

Figure S5.1. Reproduction of figure 5.3 (a) of the main text on a logarithmic time scale.

Table S5.1. Output from the ICM Pro (Molsoft) pocket finder algorithm for 6QJH (Tau).

	Volume (A)	Area (A)	Hydrophobicity[1]	Buriedness[2]	Merck's Drugable[3]	Radius	Nonsphericity[4]
1	749	570	0.6565	0.8927	1.194	5.634	1.429
2	341.6	285.3	0.57	0.7932	0.0261	4.337	1.207
3	191	219.3	0.4816	0.7651	-0.7145	3.573	1.367
4	131.3	189.2	0.4279	0.6006	-1.761	3.153	1.514
5	130.4	148.2	0.7312	0.7984	-0.2981	3.146	1.192
6	114.5	154	0.4964	0.7818	-0.9929	3.012	1.351
7	110.3	148.6	0.5198	0.6818	-1.362	2.975	1.336
8	106.7	130.7	0.6757	0.705	-0.9408	2.942	1.202

[1]Fraction of the pocket surface in contact with hydrophobic protein residues.

[2]Solvent accessible surface of the pocket divided the accessible surface covered by the shell. Values of 0.5 (open) to 1 (buried).

[3]Merck's drug like density score where >0.5 is considered druggable.

[4]Area of pocket / area of perfect sphere. Value of 1 is a sphere.

Table S5.2. Output from the ICM Pro (Molsoft) pocket finder algorithm for 2LMQ (Amyloid beta Aβ).

	Volume (A)	Area (A)	Hydrophobicity[1]	Buriedness[2]	Merck's Drugable[3]	Radius	Nonsphericity[4]
1	857	877.5	0.6182	0.6827	0.3793	5.893	2.011
2	590.1	549.9	0.741	0.8376	0.9928	5.203	1.616
3	571.3	736.5	0.5312	0.6352	-0.3048	5.147	2.212
4	566.3	545.4	0.8024	0.885	1.289	5.132	1.648
5	549.7	632.1	0.6167	0.7617	0.3591	5.082	1.948
6	533.5	524.6	0.6127	0.7438	0.2576	5.031	1.649
7	342.9	369.3	0.6151	0.8795	0.4711	4.342	1.559
8	308.7	350.5	0.5405	0.7861	-0.1437	4.193	1.587
9	301.8	264.5	0.5847	0.7987	-0.01011	4.161	1.216
10	212.7	276.3	0.5612	0.5965	-1.119	3.703	1.604
11	170.8	172	0.4704	0.7155	-1.018	3.442	1.156
12	130.2	134.5	0.7712	0.9852	0.527	3.144	1.083
13	104.5	131.7	0.7263	0.8599	-0.2306	2.922	1.228

[1]Fraction of the pocket surface in contact with hydrophobic protein residues.

[2]Solvent accessible surface of the pocket divided the accessible surface covered by the shell. Values of 0.5 (open) to 1 (buried).

[3]Merck's drug like density score where >0.5 is considered druggable.

[4]Area of pocket / area of perfect sphere. Value of 1 is a sphere.

Table S5.3. Results of Aβ40 docking. ICM Pro (Molsoft) predicted binding energies for compounds docked to the amyloid beta filament (PDB 2LMQ). The overall binding energy is summarised as ICM Pro's grid docking energy value.

Compound	ICM Grid Docking Energy	H- Bond Energy	Electrostatic Energy	Hydrophobic Potential Energy	VdW Potential Energy	Binding Pocket
Thioflavin T	-18.15	0.00	-0.4002	-5.294	-72.44	5
Ouinic Acid	-3.092	-3.897	-6.317	-0.4296	-34.39	6
Tyrosol	-30.64	-4.06	-4.038	-0.5834	-39.12	6
Hydroxytyrosol	-29.23	-3.826	-3.498	-0.5948	-40.73	6
Coumaric acid	-28.21	-2.487	-5.04	-0.1735	-42.19	6
Elenolic acid	-31.25	-2.354	-1.92	-1.777	-47.57	6
Ferulic acid	-20.44	-2.639	-4.04	-0.6087	-46.09	6
Hydroxydecarboxymethyl oleuropein aglycone	-44.49	-2.738	-4.455	-2.48	-71.75	6
Pinoresinol	1.022	-0.01035	-1.238	-5.578	-77.04	5
Luteolin	- 23.83	-0.9489	-1.775	-3.559	-60.67	5
Oleocanthal	-44. 2	-2.911	-4.308	-2.802	-65.54	6
Decarboxymethyl oleuropein aglycone	-46.33	-1.763	-3.13	-3.196	-71.48	6
Hydroxy Oleuropein Aglycone	-57.17	-4.469	-6.962	-3.551	-73.4	6
Apigenin	- 23.63	-1.252	-4.849	-1.333	-57. 28	6

Oleuropein Aglycone (3, 4-DHPEA-EA)	-45.05	-0.02881	-1.152	-4.975	-81.32	5
Hydroxytyrosol Acetate (3,4-DHPEA-AC)	-35.7	-1.508	-2.797	-1.866	-50.76	6
Tyrosol Glucoside (Salidroside)	-14.34	-4.65	-3.206	-1.625	-63.4	6
Oleuropein Glucoside	-15.46	-2.863	-2.558	-5.323	-86.21	1
Vanillic Acid	-17.2	-0.01612	-1.799	-1.628	-44.35	5
Gibberellic acid	29.4	-1.595	-3.381	-4.806	-54.49	1
Caffeic acid	-28.42	-2.205	-5.568	-0.09351	-43.94	6
Cinnamic acid	-25.27	-0.01044	-3.152	-1.989	-41.38	5

*All energies are given in kcal/mol.

Table S5.4. Results of tau docking. ICM Pro (Molsoft) predicted binding energies for compounds docked to the tau filament (PDB 6QJH). The overall binding energy is summarised as ICM Pro's grid docking energy value.

Compound	ICM Grid Docking Energy	H- Bond Energy	Electrostatic Energy	Hydrophobic Potential Energy	VdW Potential Energy	Binding Pocket
Thioflavin T	-1.267	0.00	-0.1734	-4.222	-56.3	2
Ouinic Acid	7.005	-8.525	-7.411	0.338	-20.39	3
Tyrosol	-20.91	-2.14	-3.181	-1.647	-31.33	1
Hydroxytyrosol	-19.24	-0.3309	-1.864	-1.764	-33.86	2
Coumaric acid	-20.39	-1.619	-1.725	-1.487	-36.85	2
Elenolic acid	-22.84	-1.115	0.04751	-2.3	-42.82	2
Ferulic acid	-2.248	-3.385	-5.369	-2.126	-24.57	6
Hydroxydecarboxymethyl oleuropein aglycone	-24.94	-2.475	-3.361	-3.322	-50.86	2
Pinoresinol	27.18	-4.139	-2.504	-2.043	-43.11	4
Luteolin	-3.341	-3.158	-3.151	-1.05	-38.78	3
Oleocanthal	-30.75	-6.598	-2.954	-2.187	-52.73	1
Decarboxymethyl oleuropein aglycone	-24.68	-3.744	-2.552	-1.909	-50.49	1
Hydroxy Oleuropein Aglycone	-30.87	-3.097	-3.638	-3.985	-52.66	2
Apigenin	-11.87	-1.808	-0.2094	-3.049	-47.39	2

Oleuropein Aglycone (3, 4-DHPEA-EA)	-24.93	-3.028	-1.518	-4.164	-54.66	2
Hydroxytyrosol Acetate (3,4-DHPEA-AC)	-24.55	-1.32	-0.6199	-2.222	-41.23	2
Tyrosol Glucoside (Salidroside)	9.185	-6.855	-6.476	-0.3413	-35.09	4
Oleuropein Glucoside	13.4	-6.798	-3.717	-3.033	-54.27	4
Vanillic Acid	-5.332	-1.258	-1.514	-1.413	-34.14	2
Gibberellic acid	51.01	-2.939	-1.608	-1.011	-39.96	3
Caffeic acid	-19.9	-2.229	-2.135	-1.708	-36.9	2
Cinnamic acid	-19.09	-1.408	-1.342	-1.578	-35.65	2

*All energies are given in kcal/mol.

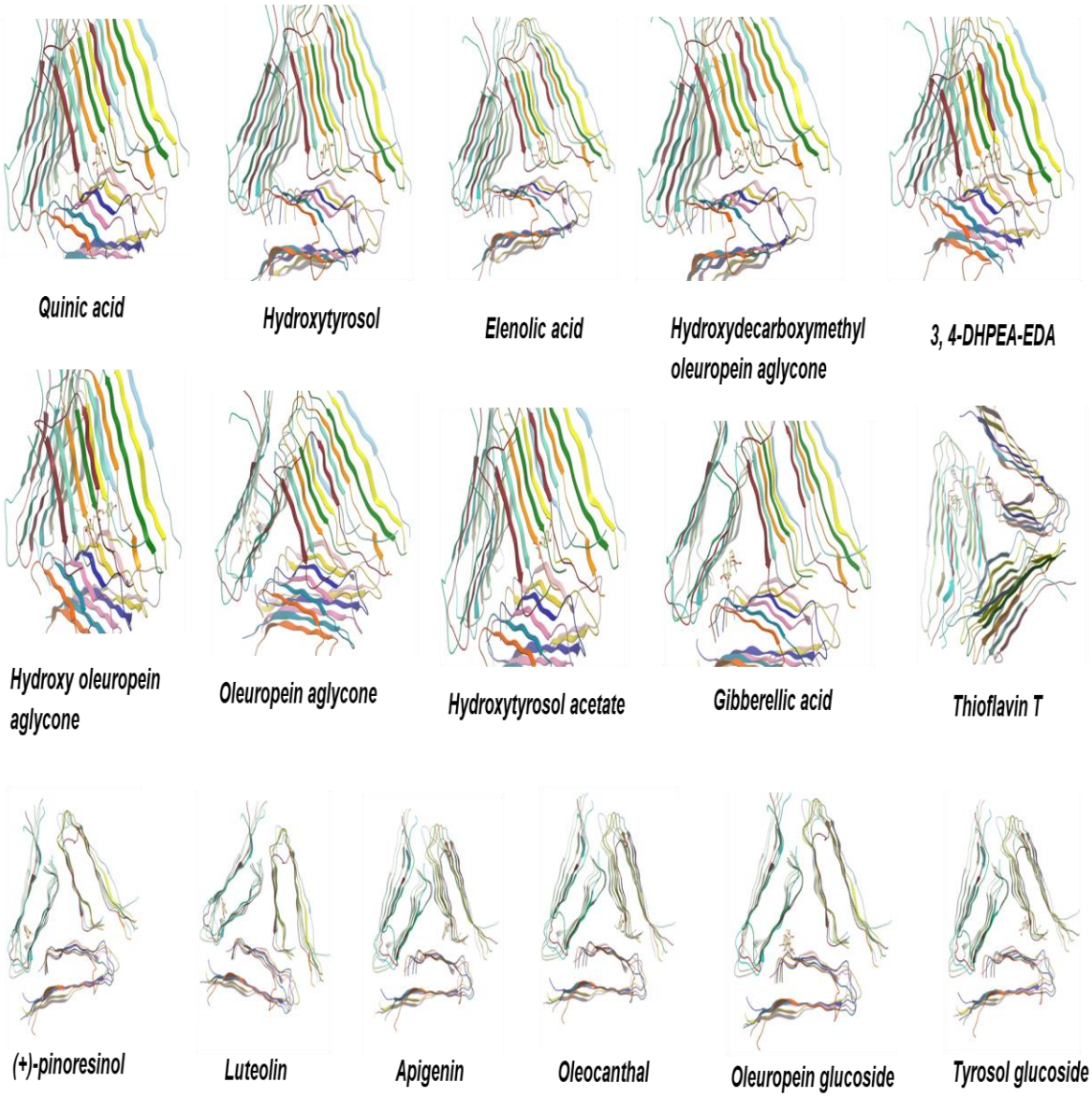

Figure S5.2. Docking sites for EVOO phenols on the solid-state NMR-derived 3-fold symmetry structural model of Aβ40 (PDB 2LMQ), predicted using the ICM Pro software.

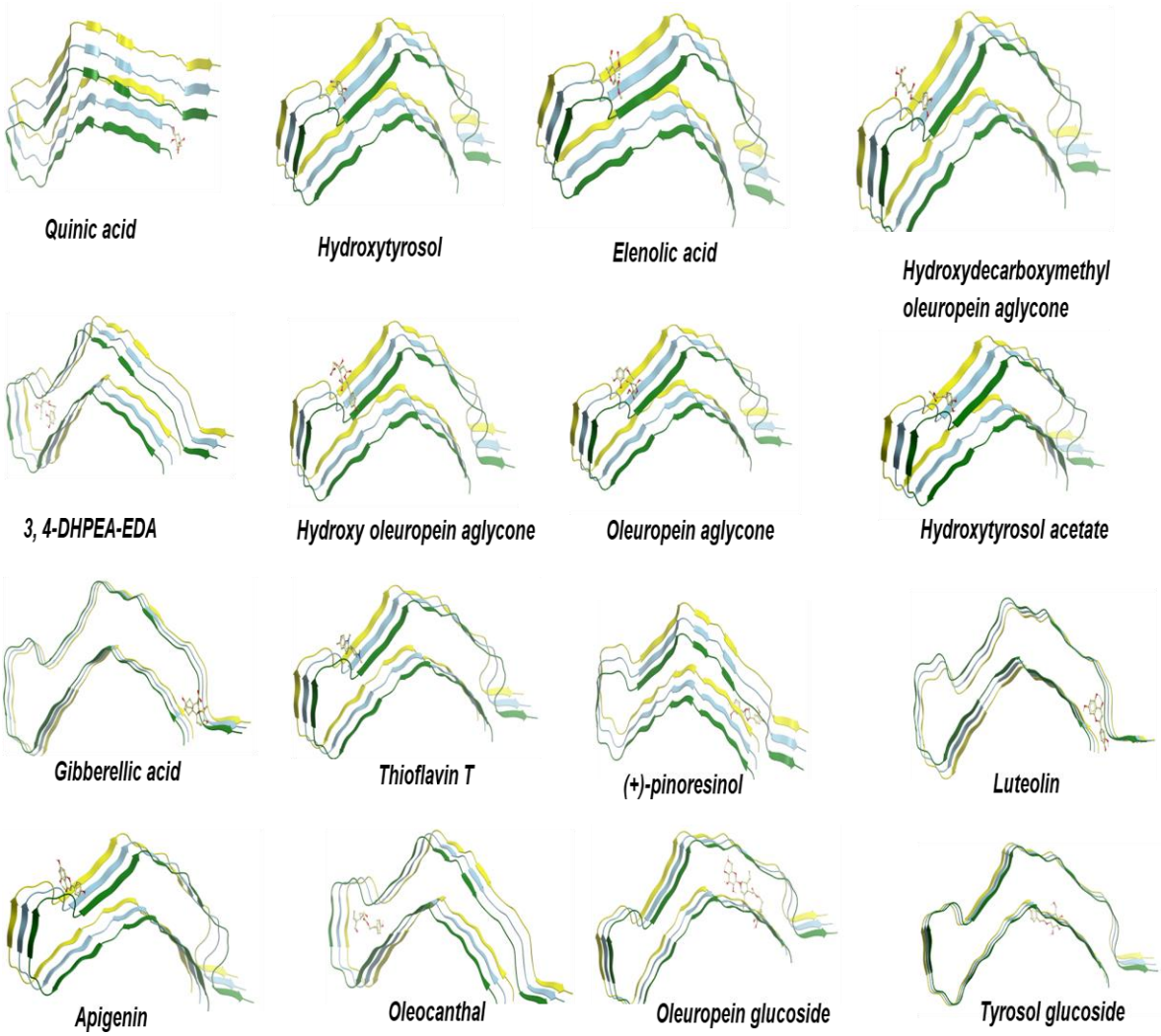

Figure S5.3. Docking sites for EVOO phenols on the cryo-EM structure of heparin-induced 2N4R tau snake filaments (PDB 6QJH), predicted using the ICM Pro software.

Appendix 3

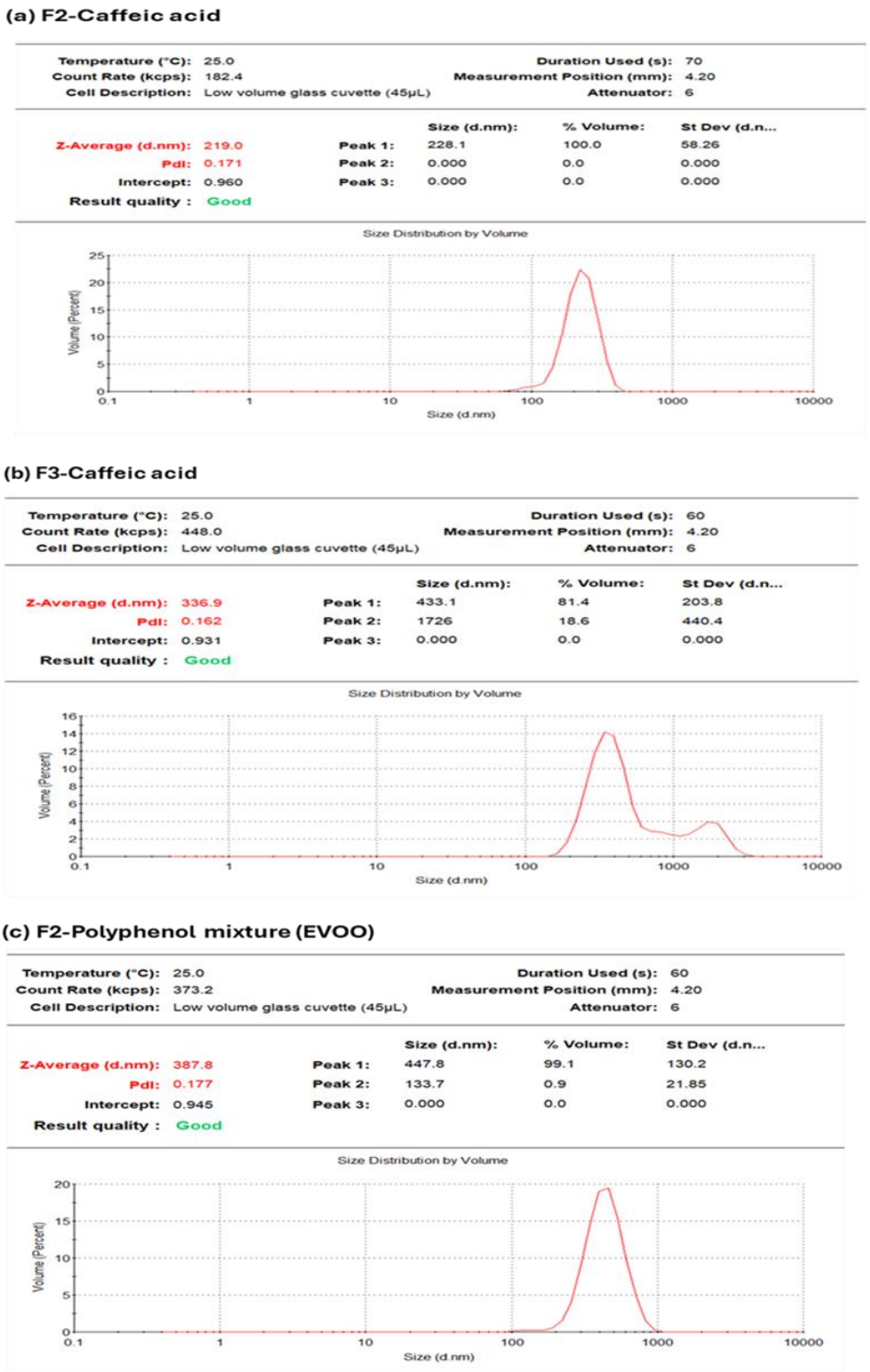

Figure S6.1. Chromatograms obtained from DLS analysis for all SLN formulations. (a) F2 caffeic acid SLNs. (b) F3 caffeic acid SLNs. (c) F2 polyphenol SLNs. (This figure is related to **Table 6.2** and **Table 6.3**).

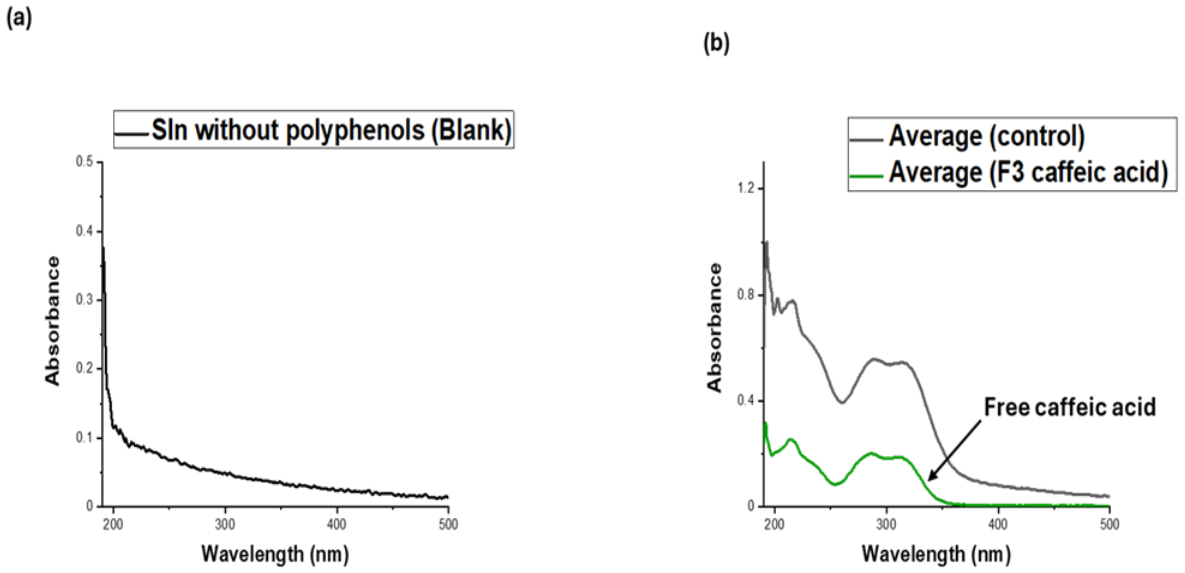

Figure S6.2. UV-Vis absorbance of entrapment efficiency of caffeic acid SLNs to separate nanoparticles from free caffeic acid. (a) Blank SLN formulation without polyphenols. (b) the caffeic acid SLN formulation F3 using 200 mg of stearic acid. (This figure is related to **Table 6.2** and **Figure 6.9**).

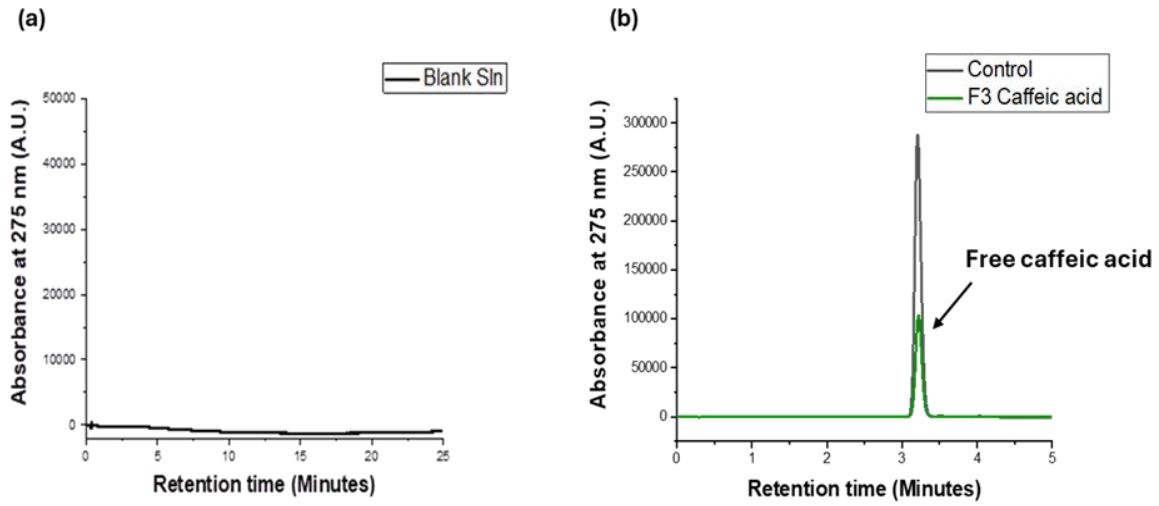

Figure S6.3. HPLC chromatogram analysis at 275 nm of entrapment efficiency of caffeic acid SLN to separate nanoparticles from free caffeic acid. (a) blank SLN formulation without caffeic acid. (b) the formulation **F3** of caffeic acid SLN using 200 mg of stearic acid. (This figure is related to **Table 6.2** and **Figure 6.11**).

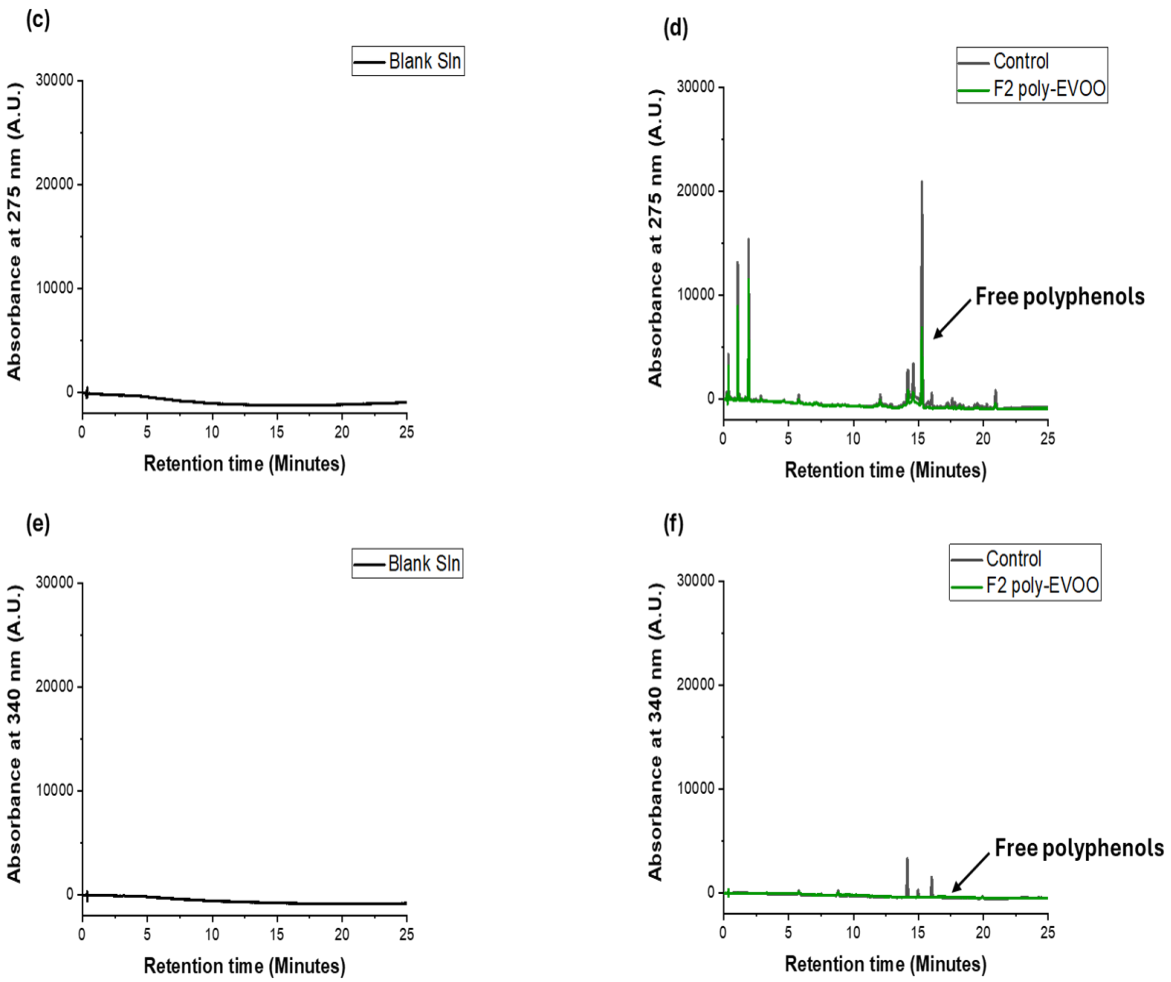

Figure S6.4. HPLC analysis at 275 nm and 340 nm of entrapment efficiency of Greek polyphenols mixture in solid lipid nanoparticles using F2 formulation of SLN. (c and d) HPLC chromatograms at 275 nm (top). (e and f) HPLC chromatograms at 340 nm (bottom). (This figure is related to **Table 6.3** and **Figure 6.12**).

.

Table S6.1. UV-Vis analysis and calculation of entrapment efficiency of caffeic acid formulations in solid lipid nanoparticles at 275 nm measured in triplicated and taken the average.

SLN sample formulation	(1) Absorbance at 275 nm	(2) Absorbance at 275 nm	(3) Absorbance at 275 nm	Average at 275 nm	Standard deviation	EE%
Control (Only caffeic acid)	0.494	0.484	0.482	0.486	0.00643	-
Formulation of SLN (F1- caffeic acid)	n.d.	n.d.	n.d.	n.d.	n.d.	n.d.
Formulation of SLN (F2- caffeic acid)	0.179	0.181	0.182	0.180	0.00153	63
Formulation of SLN (F3- caffeic acid)	0.171	0.171	0.173	0.171	0.00115	64.8

n.d.: not detected F: Formulation of SLN EE%: Entrapment Efficiency %

Table S6.2. UV-Vis analysis and calculation of entrapment efficiency of Greek polyphenols mixture in solid lipid nanoparticles using F2 formulation of SLN at 275 nm measured in triplicated and taken the average.

SLN sample formulation	(1) Absorbance at 275 nm	(2) Absorbance at 275 nm	(3) Absorbance at 275 nm	Average at 275 nm	Standard deviation	EE%
Control (Only phenolic mixtures)	0.304	0.317	0.316	0.312	0.00723	-
Formulation of SLN (F2- phenolic mixtures)	0.045	0.045	0.046	0.045	0.000577	85.6

Table S6.3. HPLC analysis and calculation of entrapment efficiency of caffeic acid formulations in solid lipid nanoparticles at 275 nm.

SLN Sample	Peak	Retention time (min)	Compound	Wavelength λ (nm)[b]	Control area	Sample area	EE%
F2- caffeic	1	3.2	Caffeic acid	275	1721183	647536	62.4%
F3- caffeic	1	3.2	Caffeic acid	275	1721183	607710	64.7%

F: Formulation of SLN EE%: Entrapment Efficiency %

Table S6.4. HPLC analysis and calculation of entrapment efficiency of Greek polyphenols mixture in solid lipid nanoparticles using F2 formulation of SLN at 240 nm, 275 nm and 340 nm.

Retention time (min)	Compound	Wavelength λ (nm)[b]	Control area	Sample area	EE%
0.3	Unkown	275	3802	2706	28.8
1.0	Hydroxytyrosol	275	26170	17778	32.0
1.2	Unknown	275	1229	880	28.4
1.9	Tyrosol	275	50872	38408	24.5
2.9	Vanillic acid	275	2418	1353	44.0
3.0	Caffeic acid	275	533	200	62.5
5.7	*p*-Coumaric acid	275	6548	2560	60.9
7.7	Unknown	240	1741	1539	11.6
8.1	Unknown	240	3855	2659	31.0
8.9	Unknown	340	3429	1525	55.5
9.2	Unknown	240	65107	52940	18.7
9.3	Unknown	240	43696	34217	21.7
9.5	Unknown	240	28954	14971	48.3
9.9	Unknown	240	4176	3014	27.8
12.1	Unknown	240	66304	43998	33.6
14.1	Luteolin	340	19687	0	100
14.2	Unknown	275	34119	11914	65.1
14.6	(+)-Pinoresinol	275	48146	26756	44.4
15.0	Unknown	340	3854	713	81.5
15.3	Naringenin	275	121810	44035	63.8
15.8	Unknown	275	2697	636	76.4
16.0	Apigenin	340	11300	0	100
17.2	Unknown	275	2111	912	56.8
17.3	Unknown	275	2135	1123	47.4
17.6	Unknown	275	4173	387	90.7
17.8	Unknown	275	2811	1027	63.5
18.0	Unknown	275	1242	208	83.3
18.2	Unknown	275	2882	1222	57.6
18.4	Unknown	275	1760	865	50.9
18.9	Unknown	240	4097	1419	65.4
19.3	Unknown	275	3156	754	76.1
19.5	Unknown	275	5415	1498	72.3
19.6	Unknown	240	29228	6403	78.1
19.9	Unknown	275	3108	518	83.3
20.0	Unknown	340	1695	293	82.7
20.3	Unknown	275	3364	388	88.5
20.5	Unknown	275	1173	523	55.4
20.9	Unknown	275	12710	3996	68.6
22.2	Unknown	240	2167	0	100
22.6	Unknown	240	648	0	100

EE%: Entrapment Efficiency %

Data below shows experiments carried on in triplicate measurements.

F2-Caffeic acid

Temperature (°C):	25.0		Duration Used (s):	70
Count Rate (kcps):	182.4		Measurement Position (mm):	4.20
Cell Description:	Low volume glass cuvette (45µL)		Attenuator:	6

		Size (d.nm):	% Volume:	St Dev (d.n...
Z-Average (d.nm):	220.4	Peak 1:	221.6	100.0	68.56
PdI:	0.208	Peak 2:	0.000	0.0	0.000
Intercept:	0.960	Peak 3:	0.000	0.0	0.000
Result quality :	Good				

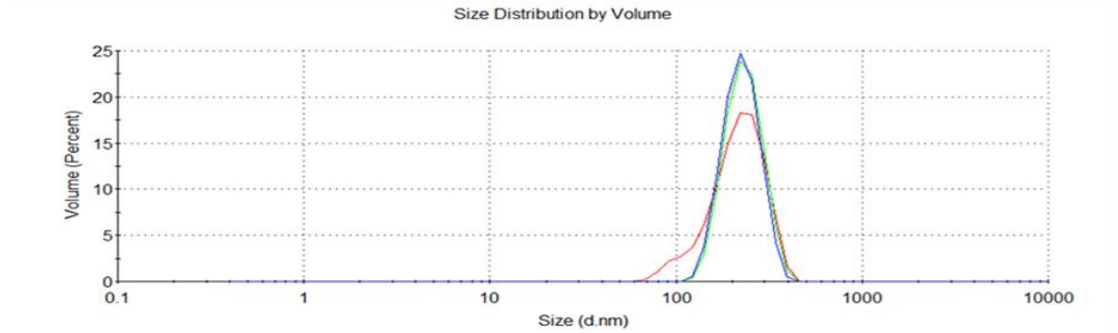

F2-Polyphenol mixture (EVOO)

Temperature (°C):	25.0		Duration Used (s):	60
Count Rate (kcps):	366.3		Measurement Position (mm):	4.20
Cell Description:	Low volume glass cuvette (45µL)		Attenuator:	6

		Size (d.nm):	% Volume:	St Dev (d.n...
Z-Average (d.nm):	384.7	Peak 1:	460.8	97.7	131.7
PdI:	0.180	Peak 2:	130.3	2.3	20.40
Intercept:	0.940	Peak 3:	0.000	0.0	0.000
Result quality :	Good				

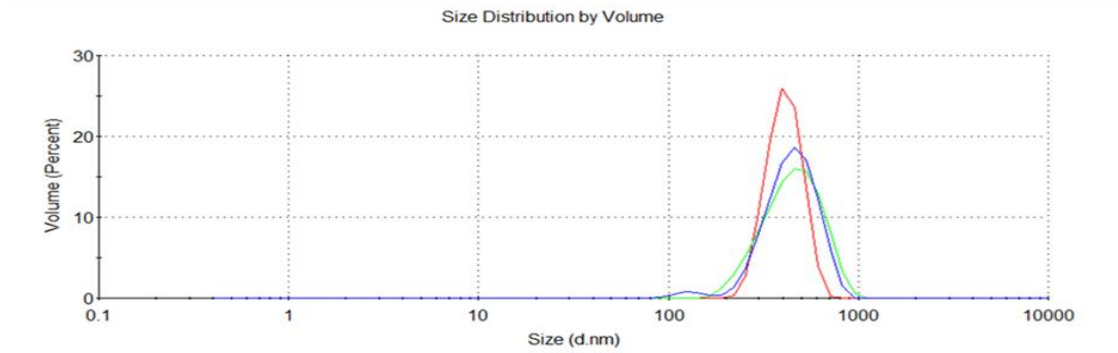

Figure S6.5. DLS data in in triplicate measurements for SLN formulations. (This figure is related to **Table 6.2** and **Table 6.3**).

Table S6.5. Zeta potential in triplicate measurements of formulations F2 using 100 mg stearic acid and F3 using 200 mg steric acid of caffeic acid and polyphenol mixture-EVOO SLNs.

Sample Name	T (°C)	Zeta Potential (mV)	Average	Standard deviation
F2- Caffeic acid 1	25	-8.43		
F2- Caffeic acid 2	24.9	-8.23	-8.49333	0.30006
F2- Caffeic acid 3	24.9	-8.82		
F3- Caffeic acid 1	25	-8.11		
F3- Caffeic acid 2	24.9	-8.27	-8.2	0.08185
F3- Caffeic acid 3	24.9	-8.22		
F2- poly EVOO 1	25	-12.7		
F2- poly EVOO 2	25	-13.3	-12.93333	0.32146
F2- poly EVOO 3	25	-12.8		

Poly: Polyphenols F: Formulation of SLN

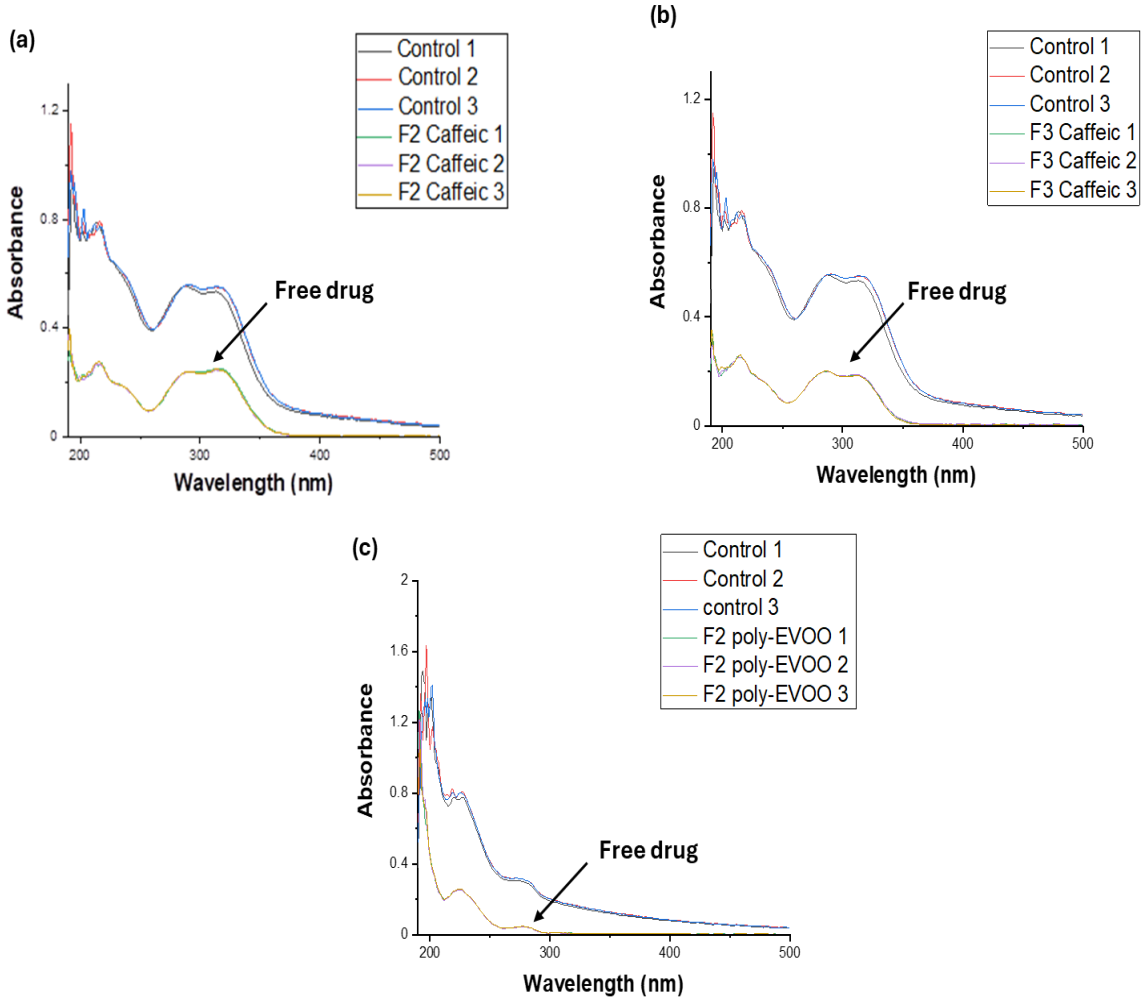

Figure S6.6. UV-Vis absorbance of entrapment efficiency of caffeic and EVOO SLNs to separate nanoparticles from free caffeic acid and phenolic mixture in triplicate measurements. (a and b, top) F2 using 100 mg stearic acid and F3 using 200 mg stearic acid for SLN formulations (F2 and F3) of caffeic acid. (c, bottom) F2 using 100 mg stearic acid for SLN formulation (F2) of polyphenols mixture derived from Greek EVOO.

Table S6.6. Shows stability of SLNs after 8 months storge in room temperature measuring (particle size and (Pdi) in triplicate).

Sample Name	Particle size (nm)	Average	Standard deviation	PI	Average	Standard deviation
F2- Caffeic acid 1	628.2			0.27		
F2- Caffeic acid 2	634.9	628.96667	5.58957	0.268	0.27367	0.00814
F2- Caffeic acid 3	623.8			0.283		
F3- Caffeic acid 1	595.9			0.287		
F3- Caffeic acid 2	585.3	594.36667	8.40555	0.281	0.29667	0.02214
F3- Caffeic acid 3	601.9			0.322		
F2- poly EVOO 1	650.4			0.392		
F2- poly EVOO 2	699.4	674.16667	24.5329	0.374	0.39367	0.02055
F2- poly EVOO 3	672.7			0.415		

Poly: Polyphenols F: Formulation of SLN

Table S6.7. The fluorescence of phenolic mixture (EVOO) SLNs samples measured using plate reader, fluorescence measurements with excitation at 482 nm and emission at 515 nm, were taken from triplicate samples on a Molecular Devices Flexstation 3 Microplate Reader (Molecular Devices).

Samples	Run 1	Run 2	Run 3	Mean	Standard deviation
SLNs labelled with fluorescent probe C16	5431.6	5291.8	5329.9	5351.1	72.2
SLNs labelled with fluorescent probe C16 + polyphenols (EVOO)	2059.8	2014.4	1991.3	2021.8	34.8
SLNs unlabelled + polyphenols (EVOO)	33.891	31.686	32.446	32.6	1.1

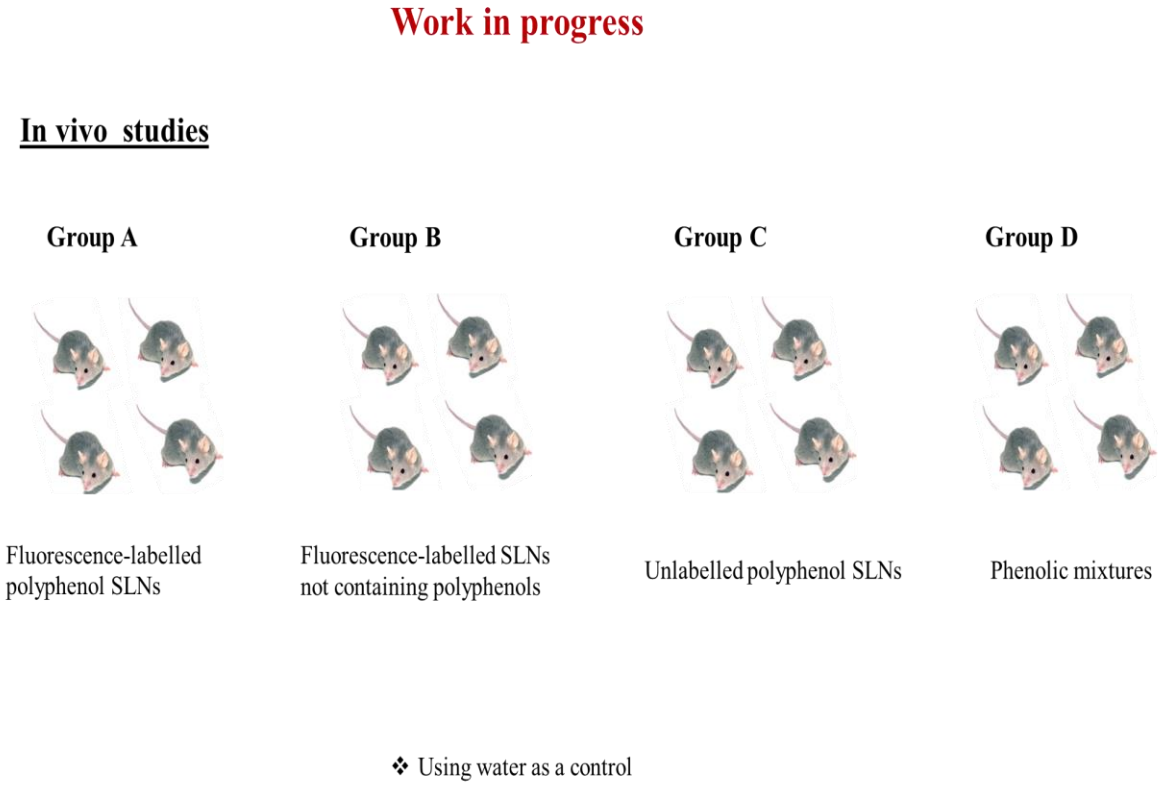

Figure S7.1. Animal experiment: different groups of four mice each has been treated once a day for 7 days with a 100 µL solution containing 250 µg SLNs.